BBRC

Bioscience Biotechnology Research Communications

VOLUME-12 NUMBER-1 (Jan-Mar 2019)
Print ISSN: 0974-6455
Online ISSN: 2321-4007
CODEN: BBRCBA
www.bbrc.in
University Grants Commission (UGC)
New Delhi, India Approved Journal

An International Peer Reviewed Open Access Journal For Rapid Publication

Published By:
Society for Science & Nature (SSN)
Bhopal India
Indexed by Thomson Reuters, Now Clarivate Analytics USA
ISI ESCI SJIF=4.186
Online Content Available: Every 3 Months at www.bbrc.in

SOCIETY
FOR SCIENCE AND NATURE
SCIENCE FOR LIFE

Registered with the Registrar of Newspapers for India under Reg. No. 498/2007
Bioscience Biotechnology Research Communications
VOLUME-12 NUMBER-1 (Jan-Mar 2019)

Continued Inside Cover

Printed By:
Society For Science & Nature Bhopal India
C-52, HB Colony, Koh-e-Fiza
Bhopal - 462001, INDIA

ISSN 0974-6455
9 770974 645002

Registered with the Registrar of Newspapers for India under Reg. No. 498/2007
Bioscience Biotechnology Research Communications
VOLUME-12 NUMBER-1 (Jan-Mar 2019)

Continued From Back Cover

Bioscience Biotechnology Research Communications
(Abbreviation: Biosc. Biotech. Res. Comm.)
University Grants Commission (UGC) Ministry of HRD Government of India approved Journal.

About the Journal

Bioscience Biotechnology Research Communications, BBRC is a broad based internationally indexed official publication of Society for Science & Nature (SSN) since 2008. The international journal publishes peer reviewed original research papers, exciting reviews and short communications in basic and applied areas of life sciences and the upcoming state of the art technologies, including Biology and Medicine on a fast track. The young editorial team of BBRC tries hard to provide a high quality flawless format of scientific communication for the popularization and advancement of science, worldwide. During these years hundreds of peer reviewed research papers of very high quality have been published in BBRC and authors like Kiran Shaw Majumdar of Biocon, Bangalore have contributed to BBRC helping it achieve high readership in a short span of time. Reviewing the published research articles, it becomes evident that on an average, about 7 papers out of 10 are subjected to healthy revisions in BBRC making quality reading. We owe this achievement to our reverend reviewers! We hope the standards set by BBRC will improve further making this international journal unique and easily accessible to the scientific fraternity across the globe. In its tenth year of successful existence as a scholarly publication, BBRC has now become an open access Thomson Reuters ISI ESC/Clarivate Analytics USA Indexed journal also approved by University Grants Commission (UGC) Ministry of Human Resource Development, Government of India, New Delhi and has a NAAS-2018, Government of India, Indian Council of Agricultural Research (ICAR) New Delhi rating of 4.38 and SJIF 4.196.

Scope of the Journal

The journal offers an international peer reviewed fast track platform, encouraging contributions from research students, faculty members and academicians from developing countries. Manuscripts in the following areas of Bioscience and Biotechnology are considered for rapid publication:

- Biology, Botany, Zoology, Ecology and Aquaculture
- Biophysics, Molecular Biology, Genetics and Genetic Engineering
- Biotechnology, Bioinformatics, Proteomics and Nanotechnology
- Microbiology, Pathology, Immunology and Diagnostics
- Physiology, Endocrinology, Biochemistry and Biochemical Engineering
- Environmental Sciences, Toxicology & Environmental Engineering
- Biology and Medicine including Nutrition.
- Diseases, Pharmaceutical Sciences and Public Health.

On Piracy, Pilferage and Other Human Academic Malpractice

Bioscience Biotechnology Research Communications strongly advocates the policy of outrightly condemning and reporting of any academic malpractice with regard to manipulation, copying, pilfering or pirating of any research material or data in practice and writing thereof. It is the duty of all our revered contributors of BBRC to kindly verify the authenticity of their scientific text in all of their manuscripts with regard to standard of scientific research done worldwide. Our reviewers are also being requested to report any of such discrepancies immediately so as to curb this malady. Any case of any kind of piracy detected, will be liable for legal action as per prevailing laws. Articles found with any form of plagiarism will be liable for immediate retraction from the issue after proper confirmation, following standard publication norms.

On Ethical and Animal Welfare Issues

Bioscience Biotechnology Research Communications requires that the experimental conditions under which human and animal assays and tests are performed are as per standard protocols used worldwide. Studies on animals must comply with the prevailing standards of animal welfare according to Indian Council of Medical Research Guidelines in India and likewise following similar condition following elsewhere. Authors must make it clear that the procedures they used were as humane as possible and have been complied with the guidelines. Studies involving human subjects must be carried out with the formal approval of the relevant Ethical Committee and evidence of such approval must be provided along with the submission.

Published by:
Society For Science & Nature (SSN)
Bhopal, India.

Bioscience Biotechnology Research Communications
International Open Access Peer Reviewed Journal For Rapid Publication
(Indexed in Leading National and International Scientific Citation Agencies
Approved by University Grants Commission (UGC) New Delhi)
(NAAS 2019 Journal Score – 4.31 SJIF 2018 4.196)
Visit us at: http://www.bbrc.in

Honorary Advisory and Editorial Board:

CONTENTS

BBRC
Bioscience Biotechnology Research Communications

VOLUME 12 • NUMBER 1 • JAN-MAR 2019

ORIGINAL RESEARCH ARTICLES

Biosci. Biotech. Res. Comm. Vol 12 No (1) (2019)

BBRC
Bioscience Biotechnology
Research Communications

OBITUARY

Obituary for Prof. Mir Athar Ali
MA (English, Urdu and Persian) BT LLB

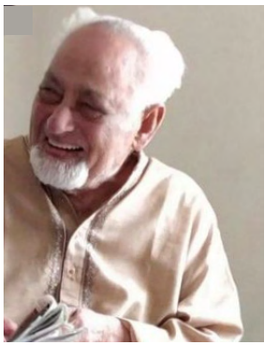

Your life and thought will continue to inspire us

It's incredibly painful to write this obituary for Prof. Mir Athar Ali, the founder of *Bioscience Biotechnology Research Communications*, who bid farewell on1st January 2019. He left for his heavenly abode at the age of 95 with his wit, humour and intellect all afresh. To write about him is a hard task, a living legend, a teacher by birth a friend, philosopher and guide for decades. He was a lover of nature, an analytical scientist, due to the fact that he served for most of his life in Science and Agriculture Colleges of Shri Shivaji Education Society Maharashtra, where his colleagues came from various disciplines of Science.

Na Sataishki Tamanna, na Silahki Parwah" (No desire for any praise, no care for any reward). This was the simple philosophy of a man who dedicated his entire life for education. Prof. Mir Athar Ali, son of Dr Mir Gauhar Ali got his basic school education in the early 1930s from the prestigious British based Government Mohammedan High School established in 1866 in Amravati India.Prof Ali had outstanding teachers of international repute who were real hard task masters, a proof of those classic school periods which made him remember till his last time, hundreds of idioms, phrases and couplets of famous poets and philosophers. He often said, **'what is open is fair,'** which many a times affected him, but never hada regret.

He almost had The Oxford University's English Language Dictionary memorised, unbelievable, Almighty's Grace! Though Prof. Ali was a hardcore student of literature, he had a natural talent for nature and experimental sciences, from repairing radios, transistors, bicycles, his old scooter, the Italian *Lambretta*. He always used to assemble old items, followed the concept of best from waste about 70 years ago, trying is hands in dairy sciences, agriculture, gardening and landscape development. On the witty side, his betterhalf, Mrs. Sidiqua Begum, MA from the then Robertson College, fondly used to call him 'Uncle Podger,' for his spread up of tools and leftovers, which she used to clean up later!

Prof. Ali obtained his first Master's degree in English Literature from Nagpur University, almost seven decades ago in the late 1940s, followed by two more MAs in Urdu and Persian and BT in Education from the famous Spencer's Training College Jabalpur, the 1889 founded college of India. He was a triple MA in those pre partition days. He continued his quest for education, earning degree in Law, obtaining the latter professional degree after his retirement in 1985, when he fought and successfully won his own legal cases, setting an example of how a teacher of principles can turn into a brilliant lawyer, when in dire need. His outstanding arguments in impeccable English in the High Court and the Honourable Supreme Court even left the Learned Judges in awe! Some of them used to address him with respectful humour, a tribute to a petitioner who fought for justice.

Thinking of him, we recall the words of Pierre de Coubertin: "The most important thing in life is not the triumph but the struggle. The essential thing is not to have conquered but to have fought well." He lived a life fighting for what he believed is right and just.
Prof. Ali believed that education is the best medium to inculcate high morals and social values among all of us. He had a firm belief that students can become ambassadors par excellence of goodwill for the community, state and the country. He envisioned an institution where students would learn an approach especially suited to con-

fronting many of the hugely complex challenges of life that face us. He founded AIHMS New Delhi for all over development and well-being of needy students. A man of Herculean intellectual and organizational capabilities, hestrived hard to create to bring about real and lasting improvement in the lives of the poor and needy.

Being a self-made man, Sir Ali strongly believed in himself and strived hard to diligently follow his principles throughout his life. All along he was a staunch fighter and committed guardian of his values. Nothing stopped him from expressing what he believed in. His dynamism, foresight and commitment to perfection will endure in our minds for many years. He left many of his dreams unfulfilled and many of his admirers desperate. To many of us he will always be a great source of moral and personal inspiration. Even though he is with us today no more, the legacy he left behind will remain immortal forever.

We the entire team of *Bioscience Biotechnology Research Communications* pray that his soul rest in eternal peace!

Medical
Communication

Biosci. Biotech. Res. Comm. 12(1): 1-6 (2019)

BBRC
Bioscience Biotechnology
Research Communications

A study on awareness and practices of physicians about diabetic retinopathy in primary-care centers Hail, Saudi Arabia

Abdulsalam Eisa Mazyad Alshammari[1], Eman Murdi Abdullah Alshammari[1], Abdulaziz Moqbel Fale Alshammari[1], Mohd. Saleem[1] and Md. Jahoor Alam[2]*

[1]*College of Medicine, University of Hail, Hail, KSA*
[2]*College of Applied Medical Sciences, University of Hail, Hail, Kingdom of Saudi Arabia*

ABSTRACT

The present study was aimed to assess the level of awareness of knowledge, awareness and practices of physicians in Primary-Care Centers Hail, Saudi Arabia. Cross-sectional and descriptive responses were obtained by using a semi-structured multi-point questionnaire that was prepared in English as well as in Arabic. It consisted of open and closed-ended questions. The data were analyzed using SPSS tool. A total of 62 subjects were included in the study. More than one third of subjects were <40 years of age with mean age of 44.26±11.00 ranging from 26-72 years. Majority viewed that diabetic type 1 patient should visit an ophthalmologist after diagnosis (82.3%). Retinal vascular disease was reported as the most common eye disease associated with diabetic retinopathy (66.1%). About one third of the subjects adapted direct (hand-held) ophthalmoscope and a dilated fundus exam for evaluating diabetic retinopathy each constituting 33.9% and 32.3% respectively. Journals were the main source of knowledge about diabetic retinopathy (72.6%). This study displays the need for hands on training of physicians about detection of diabetic retinopathy by direct use of ophthalmoscopes. Barriers for ophthalmoscope examination as perceived need to be further addressed and evaluated.

KEY WORDS: DIABETIC RETINOPATHY, KNOWLEDGE, AWARENESS, PRACTICES, PHYSICIANS

ARTICLE INFORMATION:

Corresponding Author: jahooralam@gmail.com
Received 12th Jan, 2019
Accepted after revision 12th March, 2019
BBRC Print ISSN: 0974-6455
Online ISSN: 2321-4007 CODEN: USA BBRCBA
Thomson Reuters ISI ESC / Clarivate Analytics USA
NAAS Journal Score 2019: 4.31 SJIF: 4.196

Online Contents Available at: http//www.bbrc.in/
DOI: 10.21786/bbrc/12.1/1

INTRODUCTION

The prevalence of diabetes mellitus (DM) is increasing globally in both developed and developing countries (Rani et al., 2008). It is estimated that the number of patients with DM will be doubled by 2025 (Rathmann and Giani, 2004). It has been reported that Saudi Arabia with a high prevalence of 24% was ranked 7th out of the top 10 countries for the prevalence of DM among people aged 20-79 years. Worldwide, DM being a leading cause of blindness due to its ocular complications (Sami et al, 2018). Diabetic retinopathy (DR) is the most common microvascular complication of diabetes. It is the foremost cause of blindness in working aged people as well as patients aged 55 years or older (Bunce and Wormald, 2006). DR is considered a significant blinding disease. It is included in the disease control strategy of the VISION 2020 initiative. It has been estimated that 84.5% of people with DM who have had the disease for >20 years will develop DR (UKPDS, 1998; Fong et al, 2004). In a national study in Saudi Arabia, the prevalence of DR was found to be 19.7%,whereas other studies suggested a prevalence ranging from 16.7% to 31%. Both type 1 and type 2 DM can lead to DR. DR is classified into two types: nonproliferative and proliferative. The former type may cause impaired vision if the macula is affected. Proliferative DR can also result in blindness, and it is more serious (Sami et al, 2018).

Knowledge about DM and DR along with their health impacts and treatments may be considered vital in motivating people to pursue appropriate eye care. Therefore, it may assist in dealing with visual impairment (Huang et al, 2013; Wang et al, 2008; Muecke et al, 2008). Despite the well-documented importance and magnitude of the issue in the literature, limited studies have explored the knowledge about DR among the patients with DM. Worldwide, studies have focused on prevalence, screening and the effects of DR. DM and DR are continuously growing problems in the Saudi population and cause socioeconomic burdens for the healthcare system (Çetin et al, 2013; Seneviratne and Prathapan, 2016).

The health burden due to DM in Saudi Arabia is predicted to rise to catastrophic levels, unless a wide-ranging epidemic control program/multidisciplinary approach is incorporated, with great emphasis laid on advocating a healthy diet, including exercise and active lifestyles, and weight control. To properly manage DM in Saudi Arabia, a multidisciplinary approach is required in which the general health practitioners play an important role (Al Ghamdi et al, 2017). The present study was aimed to assess the level of awareness of knowledge, awareness and practices of physicians in Primary-Care Centers Hail, Saudi Arabia.

MATERIAL AND METHODS

The study was a cross-sectional and descriptive. This study was conducted to assess the KAP of practitioners toward DR in Primary-Care Centers Hail, Saudi Arabia. Responses were obtained by using a semi-structured multi-point questionnaire that was prepared in English and Arabic. It consisted of open and closed-ended questions. To ensure clarity of the final questionnaire, a pilot study was conducted. The final questionnaires were consisted demographic data and general questions about the respondents as well as questions on knowledge & awareness levels. It did not include personal details of the respondent. The written consent from respondent is taken before handover the survey questionnaire. Also an ethical committee approval was taken from the ethical committee of the institute before starting this work.The collected data were coded and entered on a spreadsheet. Statistical analysis was performed using version 16.0. version (SPSS Inc., Chicago) statistical software.

RESULTS

A total of 62 subjects were included in the study. More than one third of subjects were <40 years of age with mean age of 44.26±11.00 ranging from 26-72 years. About half of the subjects were males (51.6%). More than half of the subjects were Sudanese (54.8%). Majority of the subjects were general practitioner (72.6%). More than one third of subjects were practicing for 10-20 years (46.8%) (Table 1).

Table 2 depicts the distribution of subjects according to knowledge about diabetic retinopathy. Majority viewed that diabetic type 1 patient should visit an ophthalmologist after diagnosis (82.3%). About one third of the subjects opined that patient should visit an ophthalmologist immediately after diagnosis and every year (33.9%). Majority of the subjects viewed that type 2 patient should visit an ophthalmologist following diagnosis (98.4%). Majority of the subjects also viewed that after type 2 diabetes diagnosis, patient should visit an ophthalmologist immediately after diagnosis (79%). More than half of subjects viewed that type 2 diabetic patient should visit an ophthalmologist every one year (58.1%).

Retinal vascular disease was reported as the most common eye disease associated with diabetic retinopathy (66.1%). Cataract was reported as the second most common eye disease associated with diabetic retinopathy (53.2%). Retinal detachment was reported as the third most common eye disease associated with diabetic retinopathy (45.2%). Uncontrolled diabetes was reported as the most common risk for diabetic retinopathy (58.1%). Long duration of diabetes was reported as the second most

Table 1. Demographic profile of subjects

Demographic profile	No. (n=62)	%
Age in years		
<40	24	38.7
41-50	19	30.6
>50	19	30.6
Mean±SD (Range)	44.26±11.00 (26-72)	
Gender		
Male	32	51.6
Female	30	48.4
Nationality		
Saudi	4	6.5
Egyptian	13	21.0
Sudanese	34	54.8
Syrian	4	6.5
Jordanian	1	1.6
Indian	2	3.2
Pakistani	4	6.5
Medical specialty		
Family medicine	15	24.2
General Practitioner	45	72.6
Others	2	3.2
Experience in years		
<10	17	27.4
10-20	29	46.8
21-30	10	16.1
>30	6	9.7
Mean ±SD (Median)	15.84±9.68 (15.00)	

common risk for diabetic retinopathy (43.5%). Diabetic with HTN was reported as the third most common risk for diabetic retinopathy (37.1%). Decrease visual acuity was the most common symptom of diabetic retinopathy (62.9%) (Table 3). About one third of the subjects adapted direct (hand-held) ophthalmoscope and a dilated fundus exam for evaluating diabetic retinopathy each constituting 33.9% and 32.3% respectively. The percentage of the other methods was less than 10% (Fig. 1).

Table 4 shows the distribution of subjects according to signs and treatment of retinopathy. Neovascularization was reported as the most common early signs of diabetic retinopathy (41.9%). Micro-aneurysms was reported as the second most common early signs of diabetic retinopathy (19.4%). Intra vitreous anti-VEGF (37.1%) was the most common treatment choice among the subjects. More than half of subjects referred both people who were asymptomatic and only if they reported symptoms of vision loss (62.9%) (Table 4).

Majority of the subjects had knowledge about using ophthalmoscope (77.4%) and 46.8% did eye examination to a diabetic patient. Majority of subjects referred all diabetic patients to an ophthalmologist (75.8%). More than half of subjects followed-up referred patients (64.5%). More than one third of patients were involved in the diabetic retinopathy public awareness programs to educate the public in the past one-year (40.3%)

Table 2. Distribution of subjects according to knowledge about diabetic retinopathy

Knowledge about	No. (n=62)	%
Diabetic type 1 patient should visit an ophthalmologist after diagnosis		
Yes	51	82.3
No	9	14.5
Do not know	2	3.2
How soon after type 1 diabetes diagnosis should a patient visit an ophthalmologist?		
Immediately after diagnosis	21	33.9
One year after diagnosis	15	24.2
Two years after diagnosis	2	3.2
Five years after diagnosis	20	32.3
Do not know	4	6.5
How regular should a type 1 diabetic patient visit an ophthalmologist?		
Every 5 years	15	24.2
Every 2 years	4	6.5
Every year	21	33.9
Based on ophthalmologist screening assessment	20	32.3
Do not know	2	3.2
Should a diabetic type 2 patient visit an ophthalmologist following diagnosis		
Yes	61	98.4
No	1	1.6
How soon after type 2 diabetes diagnosis should a patient visit an ophthalmologist?		
Immediately after diagnosis	49	79.0
One year after diagnosis	8	12.9
Two years after diagnosis	2	3.2
Five years after diagnosis	2	3.2
Do not know	1	1.6
How regular should a type 2 diabetic patient visit an ophthalmologist		
Every 5 years	4	6.5
Every 2 years	1	1.6
Every 1 year	36	58.1
Based on ophthalmologist screening assessment	20	32.3
Do not know	1	1.6

Table 3. Distribution of subjects according to knowledge about eye diseases associated with Diabetic Retinopathy

	No. (n=62)	%
Knowledge about eye diseases associated with Diabetic Retinopathy*		
Pterygium	9	14.5
Glaucoma	15	24.2
Retinal vascular disease	41	66.1
Cataract	33	53.2
Macular degeneration	25	40.3
Trachoma	2	3.2
Vitreous hemorrhage	18	29.0
Conjunctivitis	6	9.7
Retinal detachment	28	45.2
Macular edema	16	25.8
All the above	9	14.5
None of the above	0	0.0
Don't know	0	0.0
Which of the following increase risk for Diabetic Retinopathy?*		
Pregnancy	2	3.2
Uncontrolled diabetes	36	58.1
Long duration of diabetes	27	43.5
Hyperthyroidism	3	4.8
Diabetics with HTN	23	37.1
All the above	23	37.1
None of the above	0	0.0
Don't know	0	0.0
Which of the following is early symptom of diabetic retinopathy?*		
Pain	5	8.1
Photosensitivity	8	12.9
Decrease visual acuity	39	62.9
Blindness	2	3.2
All the above	12	19.4
No symptoms	8	12.9
Don't know	2	3.2

*Multiple responses

Table 4. Distribution of subjects according to signs and treatment of retinopathy

	No. (n=62)	%
Which of the following is early signs of diabetic retinopathy?*		
Neovascularization	26	41.9
Retinal swelling	4	6.5
Vitreous hemorrhage	2	3.2
Fatty exudates	8	12.9
Micro-aneurysms	12	19.4
Papilloedema	7	11.3
All the above	18	29.0
None of the above	0	0.0
Don't know	4	6.5
Treatment choice for patients with Diabetic Retinopathy?*		
LASIK	10	16.1
Vitrectomy	2	3.2
Laser photocoagulation	23	37.1
Intravitreous anti-VEGF	12	19.4
Intravitreous corticosteroids	2	3.2
All the above	10	16.1
None of the above	0	0.0
Don't know	14	22.6
Routinely referred for eye examinations?*		
Referral of people who were asymptomatic	13	21.0
Only if they report symptoms of vision loss	7	11.3
All the above	39	62.9
None of the above .	5	8.1
Don't know	1	1.6

*Multiple response

(Table-5). Journals was the main source of knowledge about diabetic retinopathy (72.6%) followed by Radio/TV (40.3%), Seminars, meetings, symposiums (38.7%), senior medical personal (12.9%), books (11.3%) and newspaper & internet (8.1%) (Fig.2).

DISCUSSION

Geographically, Hail is considered to be a broad health area compared to other areas in Saudi Arabia with almost equal practice for rural and urban situations which makes it a good representative of the Saudi community.In the present study, more than one third of subjects were <40 years of age with mean age of 44.26±11.00ranging from 26-72 years. About half of the subjects were males (51.6%). More than half of the subjects were Sudanese (54.8%). Majority of the subjects were general practitioner (72.6%). More than one third of subjects were practicing for 10-20 years (46.8%).

Majority of the subjects were general practitioner (72.6%) and more than one third of subjects were practicing for 10-20 years (46.8%) in this study. Al Ghamdi et al (2017) reported that most of the physician had short periods of practice and were more specialized in discipline rather than family medicine and only one third had special training in diabetes and DR management.

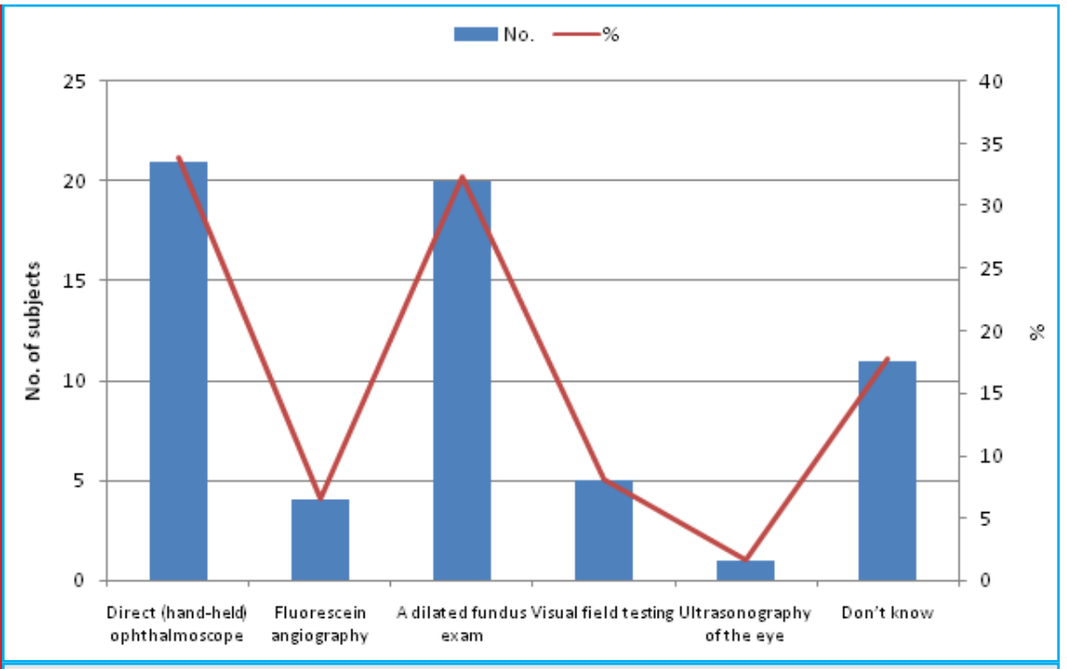

FIGURE 1. Distribution of subjects according to the best method for evaluating diabetic retinopathy

The majority of the physicians had adequate knowledge about DR and followed national and international guidelines for its management. Most of the physician were well aware about consequences of DR. They knew that the ideal method of examination was ophthalmoscopy. However, this was not practiced by many. Here, there was a disparity between knowledge level and practice pattern. The gap between knowledge and practice in DR screening has been reported (Sparrow et al, 1993). This study neither elucidated the barriers that block the phy-

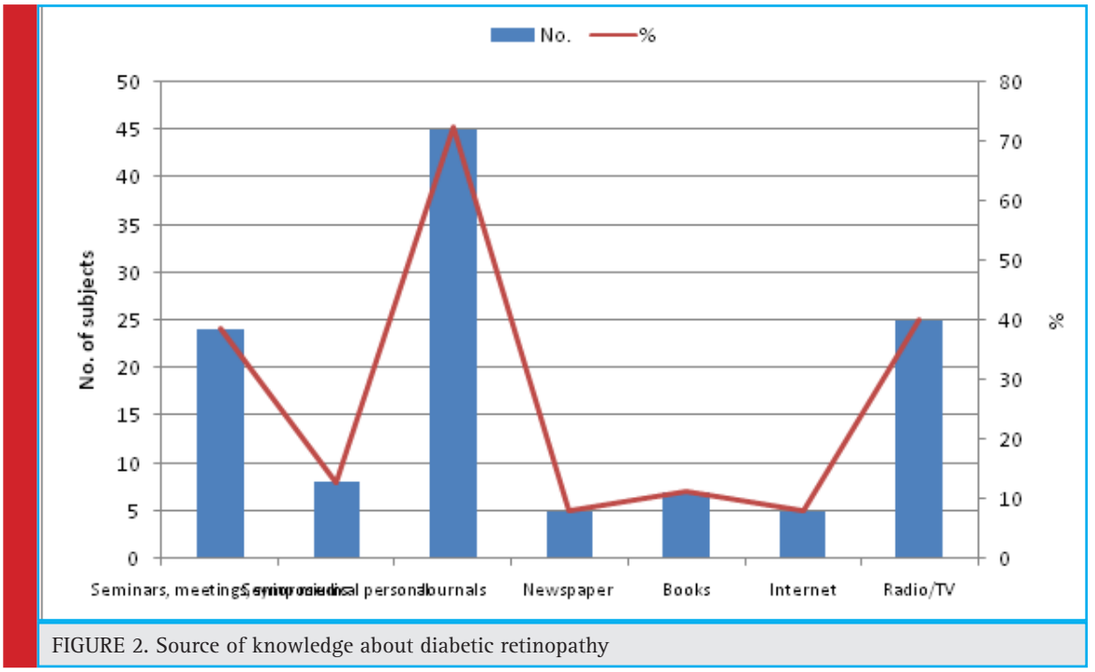

FIGURE 2. Source of knowledge about diabetic retinopathy

Table 5. Distribution of subjects according to practices of retinopathy patients

	No. (n=62)	%
Knowledge about how to use the ophthalmoscope?		
Yes	48	77.4
No	14	22.6
Did eye examination to a diabetic patient?		
Yes	29	46.8
No	33	53.2
Type of diabetic patients referred to an ophthalmologist?		
Type 1	5	8.1
Type 2	2	3.2
Long duration diabetics	5	8.1
All diabetics	47	75.8
If they develop any eye problem	3	4.8
Followed-up the patients referred to the specialists?		
Yes	40	64.5
No	22	35.5
Involved in diabetic retinopathy public awareness programs to educate the public in the past one-year?		
Yes	25	40.3
No	37	59.7

sician from putting their knowledge into practice, or the ways to close this evidence-practice gap.

Although a significant percentage of the physician had limited knowledge about the importance of diabetic retinopathy risk factors. Lack of hands on training courses could be an important reason and that needs to be investigated. Ophthalmoscopes are considered basic equipment that is regularly supplied by the Ministry of Health to primary health care practice. Shortage in ophthalmoscopes in PHCs reflects some lacunae in health care system. Individual practitioners can consider getting their own ophthalmoscope, which will greatly improve the quality of their work. Once the infrastructure is available, it need not be a problem for the physician to put their knowledge into practice.

CONCLUSION

This study displays the need for hands on training of physician about detection of DR by direct use of ophthalmoscopes. Barriers for ophthalmoscope examination as perceived need to be further addressed and evaluated. Furthermore, It is of great importance to improve the screening facilities at the primary health care setting. This study also suggested that all stakeholders including policymakers and especially health providers should prioritize building awareness. In addition, all available and feasible resources should be channeled towards reducing the burden of diabetic retinopathy.

REFERENCES

Rani, P, Raman, R, Subramani, S. (2008) Knowledge of diabetes and diabetic retinopathy among rural populations in India, and the influence of knowledge of diabetic retinopathy on attitude and practice. Rural Remote Health; 8: 838.

Rathmann, W, Giani, G. (2004) Global prevalence of diabetes: estimates for the year 2000 and projections for 2030. Diabetes Care; 27: 2568–2569.

Sami H. Alzahrani, Marwan A. Bakarman, Saleh M. Alqahtani et al. (2018) Awareness of diabetic retinopathy among people with diabetes in Jeddah, Saudi Arabia. TAEM; 9 (4).

Bunce, C, Wormald, R. (2006) Leading causes of certification for blindness and partial sight in England & Wales. BMC Public Health; 6: 58.et

UK Prospective Diabetes Study (UKPDS) Group. (1998) Effect of intensive blood-glucose control with metformin on complications in overweight patients with type 2 diabetes (UKPDS 34). Lancet; 352: 854–865.

Fong, DS, Aiello, L, Gardner, TW. (2004) Retinopathy in diabetes. Diabetes Care; 27(Suppl. 1): S84–S87.

Huang, OS, Zheng, Y, Tay, WT. (2013) Lack of awareness of common eye conditions in the community. Ophthalmic Epidemiol; 20: 52–60.

Wang, S, Tikellis, G, Wong, N. (2008) Lack of knowledge of glycosylated hemoglobin in patients with diabetic retinopathy. Diabetes Res Clin Pract ; 81: e15–e17.

Muecke, JS, Newland, HS, Ryan, P. (2008) Awareness of diabetic eye disease among general practitioners and diabetic patients in Yangon, Myanmar. Clin Exp Ophthalmol; 36: 265–273.

Çetin, EN, Zencir, M, Fenkçi, S. (2013) Assessment of awareness of diabetic retinopathy and utilization of eye care services among Turkish diabetic patients. Prim Care Diabetes; 7: 297–302.

Seneviratne, B, Prathapan, S. (2016) Knowledge on diabetic retinopathy among diabetes mellitus patients attending the Colombo South Teaching Hospital, Sri Lanka. J US China Med Sci; 13: 35–46.

Al Ghamdi A, Rabiu M, Al Qurashi AM, Al Zaydi M, Al Ghamdi AH, Gumaa SA, Althomali TA, Al Ghamdi AN. (2017) Knowledge, attitude and practice pattern among general health practitioners regarding diabetic retinopathy Taif, Kingdom of Saudi Arabia. Saudi J Health Sci; 6:44-51

Sparrow JM, McLeod BK, Smith TD, Birch MK, Rosenthal AR. (1993) The prevalence of diabetic retinopathy and maculopathy and their risk factors in the non-insulin-treated diabetic patients of an English town. Eye (Lond); 7(Pt 1):158-63.

Ecological
Communication

Biosci. Biotech. Res. Comm. 12(1): 7-16 (2019)

BBRC
Bioscience Biotechnology
Research Communications

Evaluation of soil biological activity by a vertical profile and erosion catena

Fedor Lisetskii[1]*, Denis Vladimirov[2] and Vladimir Cherniavskih[3]

[1]*Federal and Regional Centre for Aerospace and Surface Monitoring of the Objects and Natural Resources, Belgorod State National Research University, Belgorod, Russian Federation*
[2]*Institute of Earth Sciences, Belgorod State National Research University, Belgorod, Russian Federation*
[3]*Department of Biology, Belgorod State National Research University, Belgorod, Russian Federation*

ABSTRACT

The differentiation of soil fertility vertically and its territorial distribution on the slopes have a genetic origin. The main aim of the study was to establish a link between the level of effective soil fertility and its biological activity in two dimensions. The degree interaction between the cellulose decomposition activity and the yield of barley on separate layers of the southern Chernozem was established. The erosion catena demonstrates that the cellulose decomposition intensity in non-eroded and moderately eroded soils was determined by the differences in magnitude and variation soil water reserves in individual soil layers. The results showed that the microbiological activity of the soil reflecting the intensity of the transformation process of organic matter and the degree of nutrients availability in the yield is likely to act as the sensitive indicator of hydrothermal conditions. In addition, according to the research results, the effective fertility of individual soil layers both in the vertical dimension and in the topographic gradient was evident.

KEY WORDS: CELLULOSE-DECOMPOSING MICROORGANISMS, SOIL FERTILITY, CATENA, SOIL EROSION

INTRODUCTION

Most abiotic factors and, particularly, air and soil humidity and temperature, concentration and migration of chemical elements and compounds in the soil and ultimately soil fertility tends to change regularly along hillslope gradient. Studies of vegetation patterns along a vertical gradient have shown that microtopography driven soil moisture has an important role in the formation of vegetation patterns (Deák et al., 2014) and soil-plant cover (Lisetskii et al., 2014a). Effective fertility is mostly materialized through microorganism activity;

ARTICLE INFORMATION:

Corresponding Author: liset@bsu.edu.ru
Received 10th Dec 2018
Accepted after revision 21st Feb 2019
BBRC Print ISSN: 0974-6455
Online ISSN: 2321-4007 CODEN: USA BBRCBA
Thomson Reuters ISI ESC / Clarivate Analytics USA
NAAS Journal Score 2019: 4.31 SJIF: 4.196

Online Contents Available at: http//www.bbrc.in/
DOI: 10.21786/bbrc/12.1/2

therefore, there is a direct link between soil fertility and its biological activity. This applies to natural changes in fertility and microbiota activity conditions both by vertical measurement in profile and by topographic gradient. About 65% of the world's land is subject to water erosion and 28% – to deflation (Webb et al., 2006). In intensive agriculture in semi- arid regions the area of eroded soils increased, on the slopes with eroded soils, the humus content decreased (Prudnikova and Savin, 2015, Haddad et al., 2018; Upton et al., 2018).

Erosion on slope soils changes not only soil profile morphology, the OM content (Lisetskii, 2008), the texture of soils at different degrees of erosion on slopes with free runoff became coarser by one gradation (Gabbasova et al., 2016), but also the complex of physico-chemical properties, (Volungevicius et al., 2018) and content chemical elements useful for plants (Zelenskaya et al., 2018), which ultimately affects soil formation speed and soil loss tolerance value (Shtompel et al., 1998). During prolonged ploughing of chernozems as compared with a pasture or virgin, the number, size, and biomass of bacterial cells and microfungi biomass decrease (Polyanskaya et al., 2016). The aim of this study was to determine changes in the morphological, physical and chemical properties of soils caused by their agrogenic transformation.

The main soil fertility factor is the organic matter (OM) contained in it. The intensity of plant residues decomposition OM in the soil can be judged by its biological activity, which reflects the related complex of biological processes. For the entire life of soil, the main source of energy is cellulose, which, for example, amounts to 57% in winter wheat straw. Cellulose mineralization synthesizes compounds, which are essential for plant growth, humification processes and soil microorganism vital activities. The cellulose-decomposing group of bacteria decomposing plant residues release oxidative enzymes into the environment, which causes humus synthesis to run more intensively using decay products of these residues (Zakharov, 1978). It is not always possible to assess the level of fertility of individual layers of soil profile by number of nutrients available to the plants. Therefore, it is necessary to search for such indicators of soil fertility that correlate with yields. It was previously found (Tikhomirova, 1970; Zakharov, 1978; Yemtsev and Mishustin, 2005; Ulrich et al., 2008; Widhiya et al., 2016; Haddad et al., 2018; Upton et al., 2018), that the complex of soil conditions required for the vital activity of aerobic microorganisms, which decompose cellulose, coincide with the conditions of crop formation.

Cellulolytic soil activity can be used as an indicator of the vital functions of cellulose decomposing microorganisms, and conditions for formation of cultivated plant yield. It is known that cellulose constitutes the bulk of plant residues, and the role of cellulose-destroying microorganisms is significant, since they are producers of biologically active substances, which replenish the pool of these compounds in the OM soil. For example, many types of cellulolytic bacteria (genus *Cellulomonas*, *Cellvibrio*, *Bacillus*, *Myxococcus*, *Pseudomonas*, *Flavobacterium* and others) synthesize amino acids, growth agents, vitamins, pigments and oxidative enzymes which are involved in redox processes of plant residue humification (Kozlov et al., 2017). When cellulose is decomposed, the cellulolytic microorganisms release a significant amount of mucus involved in soil conditioning as well as pigments of various nature directly involved in humus synthesis (Zavarzin, 2014).

The need for environmental conditions varies in different cellulose-destroying microorganisms; therefore, it is common for different types of soils to have certain groups of cellulose-destroying microorganisms (Yemtsev and Mishustin, 2005). Semiarid regions with obvious shortage of sediments are characterized by formation of soil conditions in the presence of moisture redistribution along hillslope gradient, and they are significantly changed when using irrigation. The aims of the study were to establish a link between the level of effective fertility based on irrigation soils profile and cellulolytic activity and to identify differences in the rate of organic matter destruction in soils with varying erosion index on erosion catena.

MATERIALS AND METHODS

Study area: The study area is a part of the southern steppe subzone located seaside and characterized by a weakly dissected surface. Here landscapes are formed in the conditions of hot summer, dry warm autumn and moderately warm wet winter. Average annual air temperature (at the nearest weather station (Odessa)) is10.2 °C. The average air temperature in summer varies from 19.4 °C (June) to 22.2 °C (July). The average annual amount of precipitation (since 1894) was 386 mm. Evaporation value is 800 mm, humidity factor is 0.48 and i.e. the correction exceeds precipitation 1.5–2 times. The century-old precipitation trend is characterized by alternation of wet and dry periods (with a reduction to 310–320 mm per year). Heliothermal cycles with major periods of 11 and 10 years which are part of a lower-frequency natural periodicity (Ivanov and Lisetskii, 1995), consist in the region covered by our study of 3–4 year phases of change in the amount of heat and moisture.

The studies were carried out on the following two test areas: irrigation land on a relatively flat watershed (Pir) and non-irrigated agrolandscapes (boghara) with slopes characterized by active soil erosion (Pboh). The Pir test area is a Loess Plateau with a slight eastward slope.

Belyaevka region (Ukraine). Medium-steppe subzone. Lower Dniester irrigation system (Shkodogorsky array). It was built in 1964. The irrigation area exceeds 37 thou. ha. Groundwater occurs at a depth of 2–5 m. The source of irrigation is the water of the Dniester River. Dominating soils are Southern heavy loam solonetz Chernozem. Humus horizon thickness is 55 cm. Corg is 1.79%. It boils from HCl starting with 70 cm and demonstrates vigorous boiling from 78 cm.

The Pboh test area is a gently undulating loess plain (slopes of steepness<2° occupy 39%) which belongs to a very dry and moderately hot agro-climatic zone. Share of eroded soils (Southern heavy loam Chernozem) is 28%, including moderately eroded soils, which occupy 29% of the total area of eroded soils. We examined the erosion catena on the slope of western exposition with average slope of 2° (experience 3).

Data used: Problem-solving was based on the research program, which included four experiments.

Experiments 1A and 1B included a field experiment on assessment of biological activity with southern irrigation (1A) Chernozem layers (within the genetic horizons) and a vegetation experiment with the same layers to assess the level of effective fertility (1B). The results of these experiments complemented each other. Experiment 1A was carried out in the field to determine differences in the rate of cellulose (%) decomposition in individual layers of irrigated southern Chernozem. Oats and peas planting. Oat phase gives rise to booting (fifth sheet, height 47 cm). A cellophane film of 3x6 cm in size was put into a nylon mesh with mesh size of 0.25 mm and vertically attached to the soil (3-fold repeatability). Experiment 1B was conducted in a phytotron with separate soil layers. We cultivated Odessa-82, a recognized spring barley variety, by 14 plants per a vessel with capacity of 2520 cm^3. Since individual soil layers had different moisture content (from 43 to 62%), the moisture in the soil was maintained using gravimetric method at from 25.9% to 37.4%.

The phytotron-maintained average temperature and relative humidity values (according to thermograph and hygrograph records) were 21–25° and 55–65% respectively between seeding and barley earing periods (90 days). We equalized the illumination conditions by periodic vessel rearrangement. For the vegetation experiment, we followed the previous recommendation that for options with transitional horizons (AB, BC) a sufficient number of repetitions at a probability level of 0.95 should be considered as 4–6-fold repeatability, and for options with other horizons reliable results can be obtained when using 3–4 vessels. This made it possible to conduct more reasonable analysis of the mean options with due account for marginal error of difference of the means. Due to different option repeatability in the experiments, the non-equivalence of contrast of means was taken into account when assessing significance of particular differences.

Experiment 2 was carried out in the field to assess differences in linen fabric decomposition for 2 periods of biotest exposure in layers 0–10 and 10–20 cm under fallow conditions. As for the experiment location, it was the western exposure ravine slope near water divide, where the southern unwashed Chernozem (depth of horizon A is 32 cm, humus horizon thickness is (A+AB) 50 cm) was present. Experiment 3 was conducted in the field on the erosion catena. Objects under study: 1) Medium loamy non-eroded at the water divide Southern Chernozem, depth of horizon A is 32 cm, humus horizon thickness is (A+AB) is 53 cm; 2) Medium-eroded Chernozem 270 m down the slope. Soil moisture and bulk density were monitored at the depths of 10 and 20 cm for 459 days using 22 observation periods. The experiment was carried out for two calendar years in the same periods of exposure (August – October). The initial phase of the experiment ran under the stubble of winter wheat (minor cultivation), and since September processes took place in winter wheat rhizosphere, then after the wheat was plowed in May corn was sown and harvested for silage, and in September the plowing was done.

Methods: Activity of microflora destroying cellulose in individual layers of the ploughing horizon was determined by the rate of pure linen fabric decomposition since flax fibers consist of cellulose for 80% and impurities in the form of minerals and lignin for 20%. Decomposing cellulose with simple communities of microorganisms (1–2 species) is significantly more sensitive to the soil conditions than plant residues, and its usage provides more accurate results due to uniformity of chemical composition of biotests. The method of "applications" is objective enough to assess the intensity of microbiological activity in different layers of the soil profile and to compare agricultural technologies, including the use of irrigation. The method of applications use is modified (Mirchink, 1988), but it is based on the assessment of intensity of linen fabric decomposition by the difference in dry weight before and after exposure. Biotesting was carried out using squares of linen fabric size 10×10 cm, which was covered with a nylon mesh with mesh size of 0.25 mm and laid horizontally in the soil at depths of 10 and 20 cm in order to preserve defragmented material after decomposition. In addition, we used chemically pure cellulose film in the applications method. The bags removed with films were washed from soil particles first with tap water and then with distilled water. The loss of film weight was determined using analytical scales, and then we calculated the average percent-

age (%) of decomposition for each examined layer and computed the average percentage for examined layers in each option of the experiment. We used the Euclidean distance calculation to make cumulative comparison of soil layers by parameters, such as humidity (%), bulk density (t m^{-3}) and soil moisture reserve (mm). Chemical analyses of soils included the following standard procedures: Corg content, by Tyurin's method and CO_2 by acidometry. The determination of cation exchange capacity (CEC) in calcareous soils was performed using EDTA–Na_2.

RESULTS AND DISCUSSION

Microbiological activity of irrigation soil

Soil irrigation results in increased number of certain groups of microorganisms: algae, nitrifiers, denitrifiers, but less actinomycetes, aerobic organisms, which decompose cellulose (Table 1).

An increase in erosion resistance of steppe soils during irrigation is explained largely due to growth by higher numbers of algae, fungi, aerobic cellulose-degrading microorganisms, and oligonitrophiles, in particular (Lisetskii et. al., 2018). Our results (Table 1) showed that irrigation had maximum effect on the number of groups, such as denitrifiers, eutrophic plants, anaerobic bacteria and nitrifiers. Under comparable conditions, sunflower and wheat have no advantages due to irrigation in terms of the number of microorganisms (with the exception of algae).

During three periods of vegetation it was natural in May–June for biological activity to show a decrease within meter-deep layer in certain layers of irrigation Chernozem, except for the upper part of carbonate horizon B1 (Table 2), which is associated with its chemical properties.

Due to increased duration of irrigation reclamation in seven arid zones of Ukraine, it becomes relevant to study transformation tendencies in soil fertility profile distribution under irrigation impact. In response to 35 years of irrigation the soil is reported to have humus profile extension by 9 cm as compared to bogharic soil (Lisetskii, 1988), and increased humus reserve within one meter thick layer. The experiment revealed the existence of more clear horizon-oriented differences in effective fertility than in the non-irrigated Southern Chernozem. For example, the subsurface layer fertility decreased dramatically (F_{20-34} is 0.49). The results of dispersion analysis of barley grain yield obtained from individual layers of Southern Chernozem in experiment 1B showed that at the level F_{01} there were proven differences of effective fertility between all layers, except for layers to 50–64 and 64–75 cm that can be combined (Table 3). The relative (%) evaluation of effective fertility is determined by the ratio of grain yield for each tested layer (i) to ploughing layer yield (denoted by F_i).

Features of effective fertility profile distribution in irrigated soil are closely interrelated with microbiological activity. As shown by our two-year observations in the most important vegetation period (May-July), this is facilitated by absence of significant horizon-oriented differences in the moisture content of a meter-thick layer of soil. On average, over three periods of microbiological tests exposure (May-June), the subsurface and underlying horizons of irrigated Chernozem showed decreased cellulolytic activity of soils in proportion to the reduced level of effective fertility (Figure 1). It is noteworthy that as for potential fertility (Table 3), the 75–100 cm layer is less fertile than layers to 50–64 and 64–75 cm, but it appeared that this layer demonstrated higher cellulolytic activity and yield.

The results in Figure 1 show that the statistical dependence is virtually proportional: cellulolytic activ-

Table 1. The change in the number of microorganisms in the soil with irrigation in a layer of 0-20 cm

Indicators	Units of measure	With irrigation		No irrigation	
		sunflower	winter wheat	sunflower	winter wheat
Soil moisture	%	20.53	18.32	15.21	17.72
Eutrophic plants, total	million /1 g. soil	12.30	13.80	13.20	13.5
Actinomycetes	million /1 g. soil	3.50	4.80	5.40	5.50
Fungi	thousand / 1 g. soil	57.80	68.90	54.30	70.40
Nitrifiers	million /1 g. soil	2.46	2.07	2.26	1.70
Denitrifiers	million /1 g. soil	0.85	1.30	0.64	1.05
Decompose cellulose:					
– aerobic	thousand / 1 g. soil	1.93	2.85	3.46	3.13
– anaerobic		1.33	0.93	1.00	0.92
Algae	thousand / 1 g. soil	98.40	S	N/F	N/F

Note: N/F, Not Found; S, Sporadic.

Table 2. The degree of transformation of cellulose (%) in separate layers of southern (irrigated) Chernozem (experiments 1A)

Horizon	Layers, cm	Periods of transformation of cellulose*			
		1	2	3	Average
Aar	0–20	24.01±1.66	32.38±3.13	40.37±4.65	32.26±5.03
A	20–34	23.19±1.07	29.16±2.67	35.12±2.72	29.16±3.58
AB1	34–50	20.45±0.80	22.51±1.09	21.59±0.54	21.52±0.89
$B1_{ca}$	50–75	9.27±0.28	18.74±1.02	19.60±0.78	15.87±2.94
$B2_{ca}$. C_{ca}	75–100	15.05±0.25	21.74±1.08	17.38±0.92	18.06±1.84

Note: * Periods: 1 – 14.05–29.05 (the beginning of tubulation heading stage, fruiting peas); 2 – 29.05–13.06 (heading-flowering stage, fruiting peas); 3 – 13.06–28.06 (flowering-kernel milk stage, fruiting- wither peas).

Table 3. Chemical properties of individual layers of irrigation Southern Chernozem and the results of vegetation experience (1B)

Horizon	Layers, cm	Humus,%	CEC, cmol kg^{-1}	share Ca in CEC,%	Grain harvest (G), g/vessel[a]	F_i,%
Aar	0–20	2.86	25.77	85.8	1.677±0.05	100
A	20–34	2.03	25.27	87.1	0.827±0.17*	49
AB1	34–50	2.15	24.27	84.9	0.448±0.15*	27
$B1_{ca}$	50–64	1.62	22.45	87.0	0.148±0.06*	5
$B1_{ca}$	64–75	1.51	21.15	86.5	0.089±0.02	
$B2_{ca}$, C_{ca}	75–100	1.15	20.57	84.1	0.277±0.06*	17

Note: [a]An asterisk indicates significant differences in grain yield between two adjacent variants (* P <0.01).

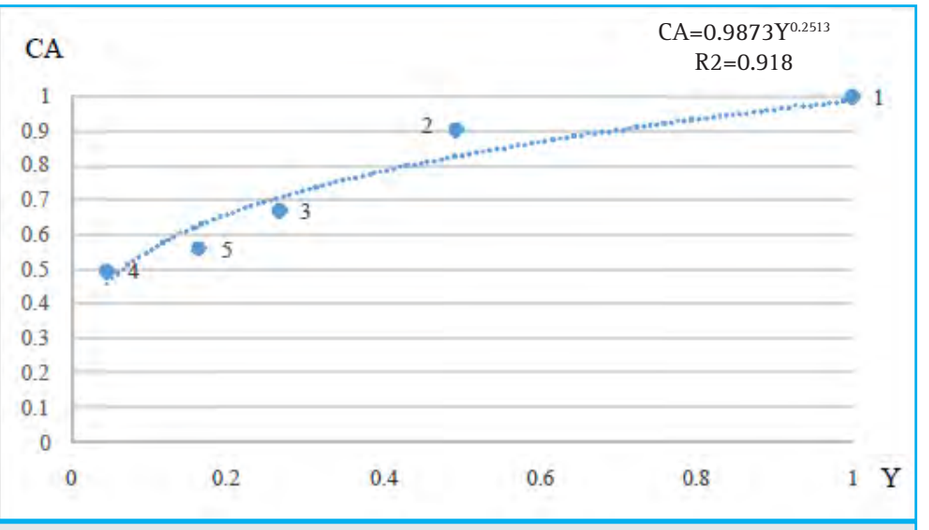

FIGURE 1. The dependence of the normalized values of cellulolytic activity (CA) on the yield of barley (Y) on separate layers of the southern Chernozem (figures are relative to the arable horizon). The numbers 1, 2, 3, 4, 5 denote layers 0–20, 20–34, 34–50, 50–75, 75–100 cm, respectively

Table 4. Chemical properties of individual layers of fallow southern Chernozem

Layers, cm	Humus	$CaCO_3$	CEC, cmol kg^{-1}			
	%		Ca	Mg	K	Na
0–10	2.59	4.63	21.70	4.0	0.09	0.07
10–20	2.56	5.93	19.80	3.6	0.10	0.07

ity tends to grow by 18% with increased yield by each 20%. Therefore, microbiological soil activity can act as an indicator of effective fertility of individual layers of soil profile. It shows the intensity of organic matter transformation process and the degree of possible materialization of available nutrients in the crop. However, the microbiota activity is ahead of those pedogenesis processes, which determine effective soil fertility.

Biotesting of in layer 0–20 cm fallow land

Fallow lands can significantly restore the lost soil fertility even for a short period. The results of experiment 2 showed that in fallow condition the chemical parameters of virgin soil were virtually achieved, except for carbonate content, which obviously requires longer time (Table 4).

In the 0 to 20 cm layer of the Chernozems the basal respiration rate and the content of the microbial biomass were minimal in the soil irrigated for 40 years without fertilizer and maximal in the fallow ones (120 yrs) (Prikhod'ko et al., 2013).Our results (Table 5) show that the intensity of microbiological processes can vary vertically under the influence of differences in moisture content even in 10 centimeter soil layers.

The experiments demonstrated that the differentiation of the ploughing horizon into different in terms of effective fertility parts occurred after 2.5–3 months (Il'ina, 1980). And as for fallow land, as in our experiment, any change in hydrothermal conditions (decrease in average soil moisture from 23 to 14% and in-layer to 0–20 cm soil moisture reserve on 17 mm in the second month as compared to the first month) is followed by multidirectional biological activity, when maintaining minor differences in humus and carbonates content and the composition of cation exchange (Table 5). In the first month, the linen fabric decomposition proportion was slightly higher in the upper 10 cm layers as compared to the lower ones, but in two months, vice versa, cellulose destruction processes were more intense in 10–20 cm layer than in the upper 10 cm soil layers. This is due to the more soil moisture in the 10–20 cm layer as compared with the upper 10 cm during the second period of exposure (from 32 to 62 days).

Dynamics of moisture content and microbiota activity in erosion catena soils

Experiment 3 was conducted on the erosion catena in agrolandscape, which distinguishes this experiment from experiment 2. With the research territory, being significantly eroded (about 60%), the percentage of moderately eroded soils is 13–14% (Lisetskii et al., 2014 b). Due to erosion, the slope soils lose OM and become less fertile (Table 6). The content of available cellulose in the form of surface residues on any moderately eroded soil is 55–60% of its amount on any non-eroded soil (Lisetskii, 1992).

The variability of indicators of microbocenosis conditions of steppe soils correlated with the dynamics of the climate (Kashirskaya et al., 2018). During the first year of experiment the climatic conditions changed as follows: during the second period (30–60 days) the air temperature was 2.3°C higher than the long-term average annual normal temperature, and it corresponded to the normal value at the beginning and at the end of the experiment; the precipitation was lower than the normal level in the first and second 30 days on 10 and 22.4 mm respectively, but in the third month precipita-

Table 5. Changing the conditions of moisture and the results of the decomposition of linen fabric for two periods of biotest exposure in fallow southern Chernozem

Indicators	Layers, cm	32 days (Aug. Sept)	62 days (Aug. Sept)
Soil moisture,%	0–10	24.68	12.04
	10–20	22.45	14.05
Soil moisture reserve, mm	0–10	28.88	16.01
	10–20	27.84	17.00
Deal decomposition (%) in the layer	0–10	30.31±2.55	46.82±3.12
	10–20	28.44±2.39	56.76±3.30
	0–20	29.38±2.47	51.79±2.19

Table 6. Chemical properties of soil erosion catena

Depth, cm	Humus	$CaCO_3$	CEC, cmol kg^{-1}			
	%		Ca	Mg	K	Na
Unwashed soil						
10	2.46	6.13	23.70	4.40	0.12	0.08
20	2.52	5.75	23.50	4.00	0.09	0.08
Moderately washed soil						
10	2.24	2.68	20.60	4.00	0.09	0.07
20	2.22	6.82	19.90	3.60	0.09	0.07

tion indicator was by 30.8 mm more. The second year (starting from the eighth observation period) was very dry: if temperatures were close to the normal range, the moisture deficit increased from 18.8 and 28.8 to 36 mm in each of three months (August – October, 16–21 timing of observations). Naturally, this was mostly repeated in soil moisture dynamics (Figure 2). Moderately eroded soil had more severe moisture deficit.

On average, during the observation period (1 year and 3 months), the soil moisture reserve in the 0-20 cm layer was by 4 mm higher in unwashed soil as compared to the moderately washed soil. However, these soils (0–10 and 10–20 cm) have different layer-by-layer moisture characteristics. If the second layer of unwashed soil was more compacted than the upper one and had more moisture content and reserves, the lower layer of the moderately washed soil had lower moisture content, density and soil moisture reserve than the 0–10 cm layer. The Euclidean distance calculations make it possible for separate soil layer parameters to be considered as individual ones, and based on that to determine resulting differences of the investigated soil layers. The results obtained show that the unwashed and moderately washed soils have the greatest differences in terms of amount and variations of soil moisture reserves in individual soil layers. On average, during 22 observation periods (for 459 days) the soil moisture reserves were by 10% more in non-eroded Chernozem as compared to the moderately eroded one (Figure 2).

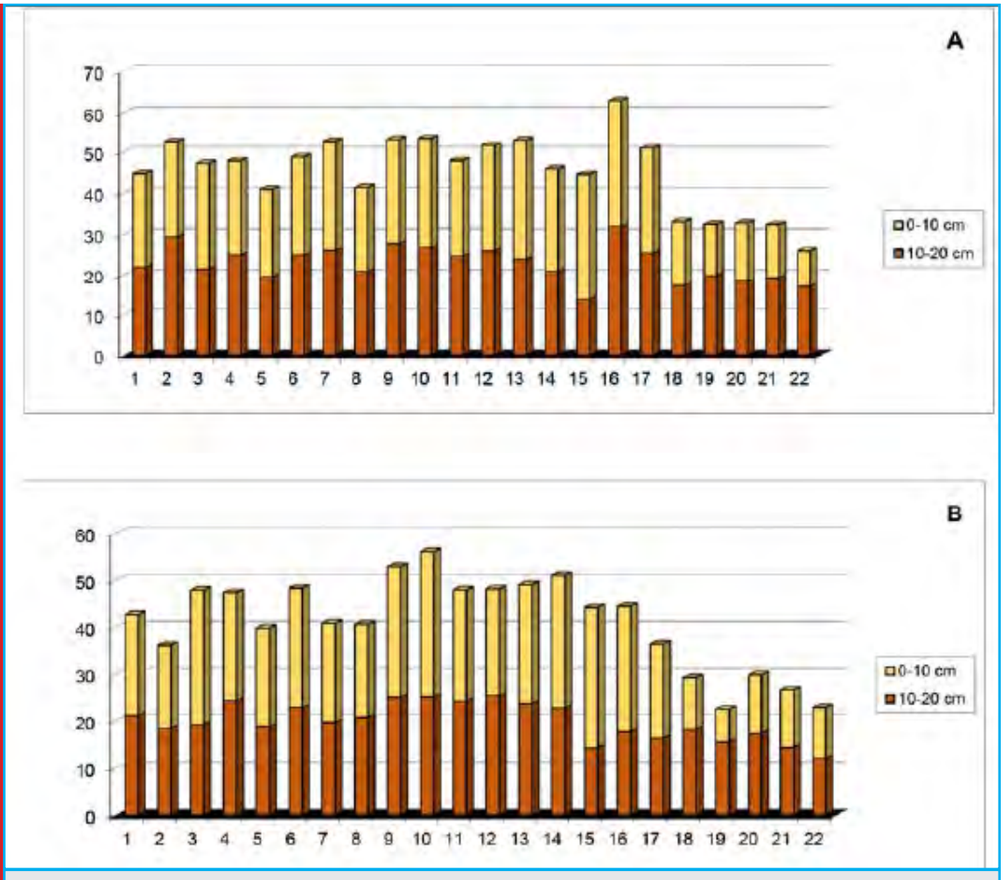

FIGURE 2. Dynamics of soil moisture reserves (mm) for 22 periods of observations every 21 days in the layers of southern Chernozem not eroded (A) and moderately eroded (B)

Table 7. The intensity of the decomposition of cellulose, depending on the duration of exposure, the degree of erosion of the soil and its depth

Exposure time, days	Depth, cm	Soil erosion		Difference (H–Cp)
		Unwashed soil	Moderately washed soil	
1st year				
30	10	25.85	23.75	2.1
	20	6.06	14.77	-8.7
	difference	15.96	19.26	-3.3
60	10	53.90	58.63	-4.7
	20	24.32	42.56	-18.2
	average	39.11	50.60	-11.5
91	10	74.94	64.55	10.4
	20	45.25	57.80	-12.6
	average	60.10	61.18	-1.1
	difference			-5.3
2nd year				
30	10	24.08	26.52	-2.4
	20	21.56	25.63	-4.1
	average	22.82	26.08	-3.3
60	10	26.44	34.52	-8.1
	20	51.55	39.68	11.9
	average	39.00	37.10	1.9
90	10	64.11	54.35	9.8
	20	55.72	42.03	13.7
	average	59.92	48.19	11.7
	difference			3.5

The results of two-year experiment on cellulose (Table 7) decomposition showed that in the first year the rate of cellulose decomposition was more often higher in the ploughing horizon of the moderately washed soil than in the unwashed one. Therefore, over 3 months of decomposition this difference reached 5%, although the total amount of cellulose destruction became almost the same in the ploughing horizons in both soils: 60–61%. However, decomposition that is more active occurred at a depth of 20 cm in moderately washed soil rather than at a depth of 10 cm, and in the unwashed soil – vice versa. During the second year of the experiment, we could observe similar situation as in the previous year only at the beginning of the decomposition process, then the decomposition rate was higher in unwashed soil, which ultimately resulted in higher transformation rate. In addition, after 3 months the degree of organic matter decomposition in the 0–20 cm layer of moderately washed soil was inferior to that of unwashed one by 11%.

For two years of experiments, during the biotest exposure periods the soil moisture reserve differences were greater between non-eroded and moderately eroded soils in the second year rather than in the first one: 28 and 11% respectively. This reflected in the differences in cellulose decomposition rate (Table 7).

Comparison of data on rate of decomposition in the fallow land (Table 5) and in winter wheat sowing (Table 7) showed that over 60 days the biological activity of the unwashed soil (0–20 cm) was higher by 13% in the fallow land than in the agrocenosis. These features are confirmed by earlier studies as well. The rate of OM destruction is lower in winter wheat due to the less favorable moisture conditions for development and functioning of cellulose-destroying microorganisms (Val'kov and Kargaltsev, 1982).

Earlier (Mirchink, 1988) it was suggested that one can judge about "the total intensity of microbiological processes in general" by the degree of biotests decay. Indeed, our results have shown that in agricultural landscapes the degree of cellulose microorganism activity depends on differences in hydrothermal conditions as well as the entire set of soil fertility resources.

CONCLUSION

Distribution of soil fertility by vertical profile and based on erosion catena is genetically related, since long-

term erosion action involves lower soil layers into the ploughing horizon. However, anthropogenic pedogenesis changes the living conditions of microorganisms in the processed horizon. It turned out that the size and variation of soil moisture reserve in individual layers of non-eroded and moderately eroded soil on erosion catena were the most important parameters for microbiological activity among the hydrothermal parameters. Soil conditions, which are essential for the vital activities of cellulose-decomposing microorganisms, are largely similar to the conditions that ensure crop formation. The study results have shown that microbiological soil activity, which reflects the intensity of organic matter transformation process and the degree of possible materialization of available nutrients in the crop can act as a sensitive indicator of hydrothermal conditions and effective fertility of individual soil layers both in vertical measurement and by topographic gradient.

We associate prospects for further studies with an increase in the number of soil objects on the erosion catena (from weakly to highly eroded) and evaluation of the transformation of microbiological activity due to differences in the hydrothermal regime, which are caused by the exposure of the slopes, especially for the northern and southern slopes.

ACKNOWLEDGEMENTS

The work was done in the framework of the implementation of the base part of the state assignment of the Ministry of Education and Science of the Russian Federation for the Belgorod State National Research University on 2017–2019 years (Project No. 5.4711.2017/6.7).

REFERENCES

Deák, B., Valkó, O., Alexander, C., Mücke, W., Kania, A., Tamás, J. and Heilmeier H. (2014). Fine-scale vertical position as an indicator of vegetation in alkali grasslands – case study based on remotely sensed data. Flora, 209: 693–697. https://doi.org/10.1016/j.flora.2014.09.005

Gabbasova, I.M., Suleimanov, R.R., Komissarov, M.A., Garipov, T.T., Sidorova, L.V., Khaziev, F.K., Khabirov, I.K., Fruehauf, M. and Liebelt P. (2016). Temporal changes of eroded soils depending on their agricultural use in the southern Cis-Ural region. Eurasian Soil Sci., 49(10): 1204–1210. https://doi.org/10.1134/S1064229316100070

Haddad, S.A., Lemanowicz, J. and Abd El-Azeim, M.M. (2018). Cellulose decomposition in clay and sandy soils contaminated with heavy metals. Int. J Env Sci and Technology: 1–16. https://doi.org/10.1007/s13762-018-1918-1

Il'ina, L.V. (1980). Differentiation of the arable layer of gray forest soil and the ways of its regulation. Proceedings of the Gorky Agricultural Institute, 142: 16–23. (in Russian)

Ivanov, I.V. and Lisetskii, F.N. (1995). Manycentury periodicity of solar-activity and soil formation. Biofizika, 40(4): 905–910.

Kashirskaya, N.N., Khomutova, T.E., Kuznetsova, T.V., Shishlina, N.I. and Borisov, A.V. (2018). Dynamics of Chemical and Microbiological Soil Properties in the Desert-Steppe Zone of the Southeast Russian Plain during the Second Part of the Holocene (4000 BC-XIII century AC). Arid Ecosystems, 8(1): 38–46. https://doi.org/10.1134/S2079096118010055

Kozlov, A.V., Kulikova, A.H. and Uromova, I.P. (2017). Biological activity of the cespitose-podsolic soil and productivity agrophytocenosis in dependence from use of high-siliceous breeds as soil conditioners. NAUCH VED BELGORO EN, 39(11): 155–166.

Lisetskii, F.N. (1988). Profile distribution of fertility in soils of the Ukrainian steppe and changes in it as a result of erosion processes. Pochvovedenie, 4: 68–76.

Lisetskii, F.N. (1992). Periodization of antropogenically determined evolution of steppe ecosystems. SOV J ECOL, 23(5): 281–287.

Lisetskii, F.N. (2008). Agrogenic transformation of soils in the dry steppe zone under the impact of antique and recent land management practices. Eurasian Soil Sci., 41(8): 805–817.

Lisetskii, F.N., Goleusov, P.V., Moysiyenko, I.I. and Sudnik-Wojcikowska, B. (2014 a). Microzonal distribution of soils and plants along the catenas of mound structures. CONTEMP PROBL ECOL, 7(3): 282–293. https://doi.org/10.1134/s1995425514030111

Lisetskii, F.N., Pavlyuk, Ya.V., Kirilenko, Zh.A. and Pichura, V.I. (2014 b). Basin organization of nature management for solving hydroecological problems. RUSS METEOROL HYDRO, 39(8): 550–557. https://doi.org/10.3103/s106837391408007x

Lisetskii, F.N., Zemlyakova, A.V. and Kirichenko, A.D. (2018). Variability of microbiota under diverse conditions of soil moistening. BIOL BULL, 45(4): 337–344. https://doi.org/10.1134/S106235901804009X

Mirchink, T.G. (1988). Soil microbiology. Moscow: MGU. 220 p. (in Russian)

Polyanskaya, L.M., Prikhod'ko, V.E., Lomakin, D.G. and Chernov, I.Yu. (2016). The number and biomass of microorganisms in ancient buried and recent chernozems under different land uses. Eurasian Soil Sci., 49(10): 1122–113. https://doi.org/10.1134/S1064229316100100

Prikhod'ko, V.E., Cheverdin, Yu.I. and Titova, T.V. (2013). Changes in the organic matter forms in chernozems of the Kamennaya Steppe under Different Land Uses, Locations,and Hydromorphism Degrees. Eurasian Soil Sci., 46(12): 1166–1176. https://doi.org/10.1134/S1064229313120065

Prudnikova, E.Y. and Savin, I.Y. (2015). Satellite assessment of dehumification of arable soils in Saratov region. Eurasian Soil Sci., 48(5): 533–539. https://doi.org/10.1134/S1064229315050075

Shtompel, Y.A., Lisetskii, F.N., Sukhanovskii, Y.P. and Srtelnikova, A.V. (1998). Soil loss tolerance of brown forest soils of northwestern Caucasus under intensive agriculture. Eurasian Soil Sci., 31(2): 185–190.

Tikhomirova, L.D. 1970. A method for determining effective soil fertility. Patent number: 338196. Patent Assignee: Experimental Design Bureau of the Siberian Scientific Research Institute of Agriculture. Inventor: Tikhomirova, L.D. http://www.findpatent.ru/patent/33/338196.html

Ulrich, A., Klimke, G. and Wirth, S. (2008). Diversity and activity of cellulose-decomposing bacteria, isolated from a sandy and a loamy soil after long-term manure application. Microbial Ecology, 55(3): 512–522. https://doi.org/10.1007/s00248-007-9296-0

Upton, R.N., Bach, E.M. and Hofmockel, K.S. (2018). Belowground response of prairie restoration and resiliency to drought. Agriculture Ecosystems & Environment, 266: 122–132. https://doi.org/10.1016/j.agee.2018.07.021

Val'kov, V.F. and Kargaltsev, V.I. (1982). Biological activity of typical chernozem and its change under the influence of fertilizers in crop rotation. Agrochemistry, 4: 64–69. (in Russian)

Volungevicius, J., Amaleviciute, K., Feiziene, D., Feiza, V., Slepetiene, A., Liaudanskienė, I., Versuliene, A. and Vaisvalavicius, R. (2018). The effects of agrogenic transformation on soil profile morphology, organic carbon and physico-chemical properties in Retisols of Western Lithuania. ARCH AGRON SOIL SCI, 64(13): 1910–1923. https://doi.org/10.1080/03650340.2018.1467006

Webb, N.P., McGowan, H.A., Phinn, S.R. and McTainsh G.H. (2006). AUSLEM (Australian Land Erodibility Model): a tool for identifying wind erosion hazard in Australia. Geomorphology, 78(3-4): 179–200. https://doi.org/10.1016/j.geomorph.2006.01.012

Widhiya, E.W. and Suharjono Ardiyati, T. (2016). Potency of bacterial consortium from apple crops as production of indole acetic acid (IAA). Int. J. ChemTech Res., 9(6): 718–724.

Yemtsev, V.T. and Mishustin, E.N. (2005). Microbiology. 5th ed. Moscow: Drofa. 445 p. (in Russian)

Zakharov, I.S. (1978). Formation of humus substances by cellulose-destroying microorganisms. Chisinau: Shtiintsa. 115 p. (in Russian)

Zavarzin, G.A. (2014). Lectures on naturalists' microbiology. Moscow: Nauka. 348 p. (in Russian)

Zelenskaya, E., Pichura, V. and Domaratsky, Y. (2018). Priorities of agroecological monitoring of the composition of soil trace elements taking into account the peculiarities of its formation over time. J ENG APPL SCI, 13(14): 5807–5813. https://doi.org/10.3923/jeasci.2018.5807.5813

Biotechnological Communication

Biosci. Biotech. Res. Comm. 12(1): 17-25 (2019)

BBRC Bioscience Biotechnology Research Communications

Experimental protection of ESBL producing *Salmonella typhi* bacteremic induced mice model by φGRCST; a therapeutic approach

Rahul Narasanna,[1] Manjunath Chavadi,[1] Liyakat Ahmed,[2] Syed Sannauallah[2] and Kelmani Chandrakanth[1]*

[1]*Department of Biotechnology Gulbarga University Kalaburagi*
[2]*Luqman College of Pharmacy, Gulbarga, Karnataka 585101, India*

ABSTRACT

Salmonella typhi specific bacteriophage i.e. φGRCST exhibited potential bacteriolytic activity against n=4, ESBL producing S. typhi isolates in vitro. The φGRCST possesses an icosahedral head with 50 nm size and contractile tail belongs to Myoviridae Vi01-like family. The experimental outcome of in vivo studies in BALB/c mice induced with S. typhi bacteraemia treated with 1.5×10^7 PFU φGRCST showed 100% survival with zero causality was recorded. On contrary, only 67% and 83% survival rate was observed in the group of mice which received standard antibiotic ciprofloxacin. The IgG and IgM titres of anti-phage GRCST antibodies were detected, with increased 4100 fold, 600 fold respectively. This result demonstrates that the antibodies elicited by φGRCST are non-neutralizing.

KEY WORDS: BALB/C MICE, ESBL, φGRCST, IN VIVO, IGG, IGM, SALMONELLA TYPHI

INTRODUCTION

The Viruses or Bacteriophage which infects bacteria were discovered in 1915 by Frederick Twort. The era of "bacteriophage" was begun with the seminal publication by Felix D'Herelle in 1917, demonstrating "un bacteriophage obligatoire" means "a bacteriophage mandatory". Total of 13 microbiologists worked together integrate the applications of phages in the field of medicine. Till date, over 6000 various bacteriophages were discovered, which includes 6196 bacterial and 88 archaeal viruses, identified morphologically and classification was accomplished (Ackermann et al., 2012). Morphologically, the majority of these phages consisting contractile tail

ARTICLE INFORMATION:

Corresponding Author: ckelmani@gmail.com
Received 4th Jan, 2019
Accepted after revision 20th March, 2019
BBRC Print ISSN: 0974-6455
Online ISSN: 2321-4007 CODEN: USA BBRCBA
Thomson Reuters ISI ESC / Clarivate Analytics USA
NAAS Journal Score 2019: 4.31 SJIF: 4.196

Online Contents Available at: http//www.bbrc.in/
DOI: 10.21786/bbrc/12.1/3

with polyhedral, filamentous or pleomorphic head types. The classification of phages so far has been achieved significantly based on their genetic content (DNA vs. RNA), their morphology, and their limited host range i.e. specific host (Deghorain et al., 2012).

Increasing case studies of antimicrobial resistance and relented discoveries and development have propelled the researchers to search for an alternative therapy has led to the revitalization of bacteriophage (phage) studies in the Western world. Recently, WHO Listed, a global priority pathogens consist of 12 bacterial species categorized into critical, high and medium priority based on their level of resistance and availability of therapeutics pathogens (Tacconelli et al., 2018). While this is a contentious figure (De Kraker et al., 2016), it nonetheless highlights the serious problem we face regarding therapeutic options for multi-drug resistant (MDR) bacterial infections (Bassetti et al., 2017).

Phage therapy; obligatory lytic phages were employed to kill the specific bacterial hosts, without causing damage to human host cells and nullifying the impact on commensal bacteria. Rapid evolving of phage therapy has resulted in resolving life-threatening clinical cases. Currently, antibiotic alternative facing the regulations and policies surrounding clinical use and application beyond compassionate cases (Furfaro et al., 2018).

In the year 1919, phage therapy was the first time practiced in human beings at the hospital des Enfants Malades in Paris, France, when D'Herelle successfully treated many children's who were suffering from severe dysentery by using phages as a therapeutics, he has isolated these infective phages in Pasteur Institute, from stools of soldiers (Sulakvelidze et al., 2005).

Salmonella bacteria are often health hazards, associated with a million food borne illnesses per year in the US. Bacteriophages have been specifically used to identify *Salmonella* species and may also be useful in therapy and prophylaxis of *Salmonella* infections. The phage FelixO1 was first used in 1943 by Felix and Callow as part of a "phage-typing" system for the identification *Salmonella typhi* (Anderson et al., 1953).

First commercial phage produced by Theodore Mazure, in which contains, cocktails—Bacté-Coli-Phage, Bacté-Intesti-Phage, Bacté-Dysentérie-Phage, Bacté-Pyo-Phage and Bacté-Rhino-Phage (Abedon et al., 2011). Henri de Montclos, chief clinical microbiologist at Pasteur Institute of Lyon, for 10 years, his research team has produced first anti-staphylococcal vaccines and therapeutic phages in the year early 1990s. The bacteriophages were administered to treat the "acute colitis" due to infections of *Shigella* or *Salmonella* in Georgia (Mikeladze et al., 1936). Potential administration of Bacté-Pyo-Phage and Bacté-Intesti-Phage, undiluted resulted in drastic reduction of mortality rate from 85% to 20%.

Therapeutic application of bacteriophage started in Eastern Europe and the former Soviet Union, currently it's been applied widespread as a part of health care systems. However, the efficiency of phage therapy is investigated according to rigorous scientific standards and presented a list of key criteria for consideration and reporting of phage therapy studies (Kutter et al., 2010; Abedon, 2017; Villarroel et al., 2017). Information critical to the success of clinical trials includes the adequate characterization and selection of phages as well as of the subjects (humans) and the target bacteria., in addition to that, the choice of appropriate disease targets for phage therapy (Harper, 2018). On the other hand, it may be that broad-host range phages are more common than is currently believed, due in part to biases in phage isolation methods (De Jonge et al., 2018); this disparity deserves much further research.

However, recent research and its outcomes suggest that bacteriophage therapy is the appropriate treatment to cure *Salmonella* associated infections. Majorly typhoid fever was treated with bacteriophages by Tsouloukidze *et al.*, 1936 (Tsulukidze et al., 1936); who successfully treated twenty patients suffering from peritonitis due to intestinal perforations in typhoid fever (Abedon et al., 2011). There are some published reports of successful treatment against Salmonella-associated disease with prophylactic phage therapy in treating Russian soldiers suffering from dysentery during and after World War II (Kutter et al., 2009). The reports suggest that, it has been already practiced in broiler chickens. The bacteriophages were able to reduce *S. enteritidis* counts on chicken skin at refrigeration temperature and short contact time (Atterbury et al., 2007). In addition, the decrease of *S. enteritidis* count on artificially-contaminated chicken skin after phage treatment corresponded to the reduction achieved by chemical agents commonly used in the poultry industry. A significant breakthrough is, bacteriophages were used as biocontrol agents in Pigs to control the infection, according to the study conducted by Albino *et al.*, 2014; and the outcome of the study was a significant reduction in the colonization of *Salmonella* in pigs administered with pool of bacteriophages (Albino et al., 2014)

MATERIALS AND METHODS

Phage Isolation, Production, and Titration

ESBL resistant strain *S. typhi* BST 51 was used to specific host isolate bacteriophage from raw sewage samples. The sewage sample was collected from various places of Kalaburagi. The sample was filtered with sewage was filtered with filter paper, and subsequently 40 ml of sewage was added to the 10 ml of 10X LB broth, inoculated

with *S. typhi* BST 51 strain and incubated for 18-24 hr. The media was centrifuged at 10000 rpm for 10 min and the supernatant was collected and subsequently filtered using a 0.2 µm syringe filter (Melo et al., 2014b).

Screening of GRCST (G: Gulbarga, R: Rahul, C: Chandrakanth Kelmani, S: *Salmonell*a, T: *Typhi*) bacteriophage was accomplished by plaque assay method i.e. agar overlay technique. The LB agar plates were prepared, 0.1 ml of supernatant was serially diluted in 0.9 ml of LB media from 10^1 -10^{10} in 1.5 ml eppendorf tubes 0.5 ml of test culture *S. typhi* BST 51 with 0.1 O. D was equally distributed to another set of 10 eppendorf and labelled for each dilution tubes subsequently 0.1 ml serially diluted filtrate was added to the respective tubes containing 0.5 ml of *S. typhi* BST51 bacterial culture labelled with respective dilution, incubated for 10-15 min. Each labelled tube was taken and uniformly mixed with LB soft agar containing 0.6% agar in a molten state at a temperature of 40 ^{0}C- 45 ^{0}C. Thereafter soft agar was overlaid on LB hard agar plates containing 2% agar and kept for incubation at 18-24 hr. Plaque formation on agar plates indicates bacteriophage positive (Mazzocco et al., 2009; Kropinski et al., 2009).

Phage purification and storage

An isolated colony of *S. typhi B*ST 51 strain was inoculated into the LB broth, the culture was allowed to attain an OD of 0.1, and then infected with φGRCST of 2X10^7 PFU, the culture was co-cultivated for 18 hr at 37 ^{0}C in a shaking incubator (240 rpm). Polyethylene glycol-8000 (PEG) or NaCl was added to the lysate to a final concentration of 20% or 0.5 M respectively and incubated at 1 hr at 4 ^{0}C. After centrifugation at 10,000 rpm (16 min at 4 ^{0}C) in a sorvall RC5B centrifuge, polyethylene glycol (PEG-8000) was added to the supernatant to a final concentration of 10%. The lysate was incubated overnight at 4 ^{0}C with gentle stirring. Polyethylene glycol-precipitated phage was collected by centrifugation at 15,000 rpm for 20 min. The resulting pellets were resuspended in 3 ml of SM phage buffer (20 mM Tris-HCL [PH 7.4], 100 mM NaCl, 10 mM $MgSO_4$), filtered through 0.2 µm bacterial filters and phage filtrate was recovered and dialyzed against phage buffer. Purified phage GRCST was stored in aliquots of phage buffer at- 20 ^{0}C (Sambrook and Russell, 2001)).

Transmission Electron Microscopy

The morphology of φGRCST particles was observed by transmission electron microscopy, as previously described (Melo et al., 2014b). A drop of Purified phage GRCST suspension was fixed with fixative. Samples were dehydrated with series of ethanol series, passed through a "transition solvent" such as propylene oxide and then infiltrated and embedded in a liquid resin such as epoxy and LR White resin. The processed suspension was applied to a Farmvar carbon coated grid for 5 min; subsequently stained with 2% uranyl acetate. The grids were examined in a Transmission Electron Microscope at 200kv (2000X – 1500000 X) (Ayache et al., 2010).

ANIMAL EXPERIMENT

Selection of Animals

Disease free, healthy and active BALB/c mice breed were selected for *in vivo* studies. Both female and male mice were chosen for the experimental purpose with animals weighing in the range of 20-30 gm. Animals were obtained from Sri Venkateswara Enterprises, Bangalore, approved by the institute of Animal Ethics Committee (237/99/CPCSEA). Animals were nourished under controlled climate conditions and fed with standard pellet (VRK Nutrition and Solutions, Sangli, Maharashtra, India Ltd.), and provided sufficient amount of potable water for drinking. Animals were kept for 10 days before experimentation to acclimatize for laboratory conditions. The animals were housed and the entire experiment was carried out in Luqman Pharmacy College, Kalaburagi).

Selection of pathogen and induction of bacteraemia

Salmonella typhi BST 51 (Blood *Salmonella typhi* 51) selected for induction of typhoid fever in experimental mice. *S. typhi* BST 51 strain has been chosen based on its resistance power to n=7, antibiotics and exhibited a high range of MIC to cefetoxime and also capable of producing ESBL. The selected pathogen was inoculated in LB broth, after 8-12 hr incubation, growth reached 0.2 O.D. Thereafter it was serially diluted in 0.1M PBS and CFU (Colony forming units) was calculated. Subsequently, 10^7-10^9 CFU was administered to experimental mice intraperitoneal to determine the MLD (Minimum Lethal Dose).

Efficacy of bacteriophage in challenged BALB/c mice

Experimental animals (BALB/c) mice were divided into six groups and each group consist of 6 animals each. The doses were fixed and prepared in PBS and administered intraperitoneal (i.p). Mice from the group I received only PBS as a control, Group II animals administered with *S. typhi* BST 51 (2×10^9 CFU) diluted in PBS, Group III animals administered with only GRCST phage (1.5×10^7 PFU) to check the lethality of phage on Mice. Group IV animals (Mice) represents **(Test group)**, Group V and VI animals represent **(Standard)** challenged with *S. typhi* **BST 51 (2×10^9 CFU)** by intraperitoneal injection to induce typhoid. Thereafter, 20 mins induction, Group IV (Test) Mice received a **φGRCST (1.5×10^7 PFU),** and similarly Group V and VI animals received standard ciprofloxacin

Table 1. Group wise distribution of mice with intraperitoneal administration with various inducing agents

	Groups	
Control	Group I	Mice+PBS
Control	GroupII	Mice + *S. typhi* BST 51 (2×10^9 CFU)
Control	Group III	Mice + phage GRCST (1.5×10^7 PFU)
Test	Group IV	Mice + *S. typhi* BST 51 (2×10^9 CFU) + φ GRCST (1.5×10^7 PFU)
Standard	Group V	Mice + *S. typhi* BST 51 (2×10^9 CFU) + Ciprofloxacin (1mg/ml)
Standard (Multiple doses)	Group VI	Mice + *S. typhi* BST 51 (2×10^9 CFU) + Ciprofloxacin (1mg/ml)

antibiotic substituting bacteriophage. **In Group VI** ciprofloxacin were administered in multiple doses, daily up to 7 days. All the six groups were kept in hygienic condition with a continuous supply of food and water for 14 days. The significant observation made and results were recorded (Table 1).

Determination of immunologic response against φGRCST in mice

Introduction of bacteriophage in human body as a therapeutic agent cause significant stimulation of humoral immunity subsequently leads to production of antibodies. According to previous reports it is a potent antigen causes no toxic effect on health of humans. During experiment BALB/c mice were treated with φGRCST (1.5×10^7 PFU) through i.p injection. At various time point, mice blood was collected from optic vein and subsequently subjected for ELISA (Enzyme Linked Immunosorbent Assay) for the detection of antibody titres of IgG and IgM antibody in serum of experimental mice described by Biswas *et al.*, 2002.

ELISA is a semi-quantitative method used to determine the concentration of primary antibody in serum in antigen coated wells. In ELISA detection was done based on positive enzyme-substrate reaction makes change in colour.

RESULTS

Isolation and Morphology of Salmonella typhi specific φGRCST

The plaque formation indicates the presence of *S. typhi* specific bacteriophage i.e. φGRCST (Fig 1). TEM results revealed that φGRCST (G: Gulbarga, R: Rahul, C: Chandrakanth Kelmani, S: *Salmonell*a, T: *Typhi*) possesses an icosahedral head with 50 nm size and contractile tail as shown in figure belongs to *Myoviridae* Vi01-like family (Fig 2).

Broad Host Range Screening

In order to investigate the broad host specificity of φGRCST exhibited potential bacteriolytic activity against n=4 **(BST 43, BST 94, BST 130, BST 141),** ESBL

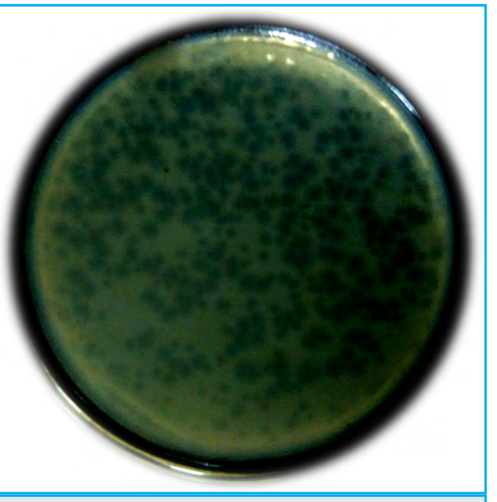

FIGURE 1. Plaques of φGRCST against *S. typhi* BST 51 isolate

producing *S. typhi* isolates among n=9 selected isolates. The plaque formation was observed against (n=4) tested isolates (Fig 3 and Table 2)

ANIMAL EXPERIMENTS

Experimental induction of *S. typhi* BST 51 strain in BALB/c mice and determination of Minimum Lethal dose (MLD)

No causality was reported in the first group mice, which received 1XPBS and were proactive and healthy. Consequently, only 83 % of mice survived in group II mice which received until the 7th day of experimentation. However, we observed the 100% mortality in III group on day 7 but in contrast, 100% mortality was recorded on 4th day itself in group IV. Based on the observation 2×10^9 CFU was determined as MLD (Fig 4)

Treatment and rescue of experimentally challenged BALB/c mice with φGRCST

The comparative study was carried out to evaluate the efficacy of phage GRCST with Standard antibiotic (cip-

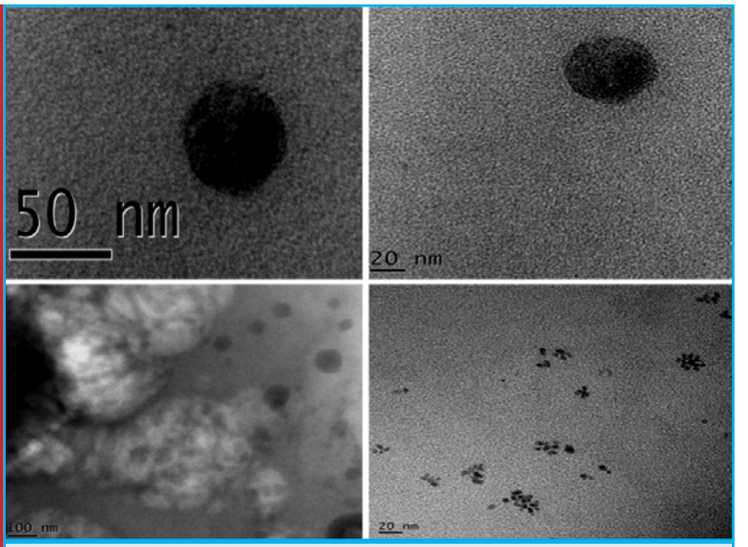

FIGURE 2. Transmission Electron Microscopic images of φGRCST Scale bars represent 50 nm.

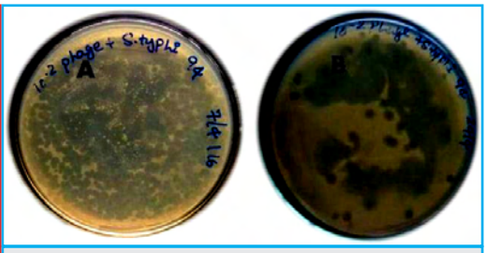

FIGURE 3. Plates showing the clear lysis of MDR *S. typhi* BST 94 isolate by φGRCST

rofloxacin). The observation made on daily basis up to 14 days and data was recorded and represented in the graph. According to the observation made, there was 100% rescue was accomplished challenged BALB/c mice treated with 1.5×10^7 PFU φGRCST, comparatively 67% and 83% survival rate was observed in the group of mice which received standard antibiotic ciprofloxacin in a single dose and in multiple doses for treatment. The multiple doses were given on daily basis and results obtained were represented in statistical graph (Fig 5).

The host immune response against phage GRCST in BALB/c mice

The blood was collected from the optical vein of BALB/c mice (n=6) and serum was separated, both IgG, IgM titres of anti-phage GRCST antibodies were detected, subsequently increased with 4100 fold, 600 fold respectively in both the cases (Fig 6 and Fig 7). Incubation of phage GRCST with an excess of mice anti-phage GRCST antibodies did not interfere with phage's capacity to lyse susceptible bacteria. This result demonstrates that the antibodies elicited by φGRCST are non-neutralizing.

Table 2. Bacteriolytic activity of φGRCST against MDR *S. typhi* isolates

S. typhi **isolates**	**Bacteriophage**	**Plaque formation**	**Growth inhibition**
BST 42	Φ GRCST	Negative	Negative
BST 43	Φ GRCST	Positive	Positive
BST 48	Φ GRCST	Negative	Negative
BST 51	Φ GRCST	Positive	Positive
BST 72	Φ GRCST	Negative	Negative
BST 94	Φ GRCST	Positive	Positive
BST 103	Φ GRCST	Negative	Negative
BST 107	Φ GRCST	Negative	Negative
BST 130	Φ GRCST	Positive	Positive
BST 141	Φ GRCST	Positive	Positive

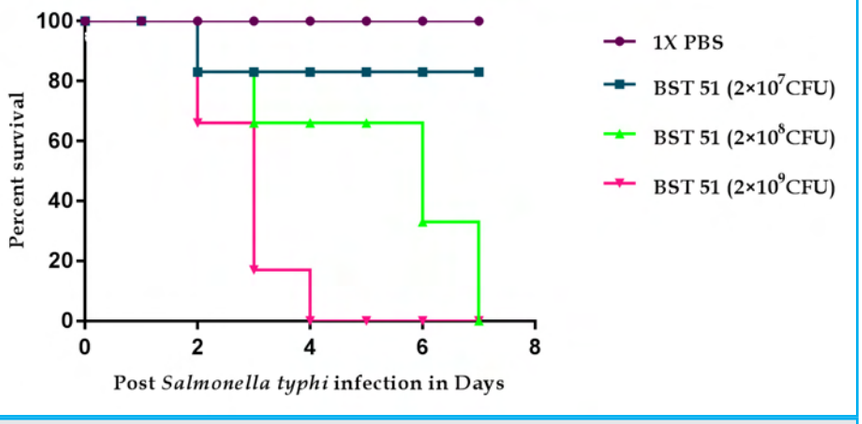

FIGURE 4. Determination of the MLD of *S. typhi* BST 51 in BALB/c mice n=6 in each group were infected intraperitoneal (I.p) with serially diluted bacterial suspensions of S. typhi BST 51. The percentage Survival was determined upto 7 days.

No significant difference was found in BALB/c mice IgG and IgM titres against φGRCST. The anaphylactic reactions were negative, and no changes in animal behaviour, no significant changes in the body temperature or no other side effects were observed in both the groups.

DISCUSSION

Over the years, application of phages as therapeutic alternatives or complements to antibiotic therapy has been evaluated extensively (Viertel et al., 2014) and has even been listed by the US National Institute of Allergy and Infectious Diseases as one important approach to combat antibiotic resistance (Reardon, 2014)

In the present study, the isolated φGRCST effectively infective to MDR S. *typhi* BST 51 strain (ESBL producing isolate) from sewage sample. *In vitro* experiments showed remarkable antibacterial activity against the *S. typhi* BST 51; plaque formation indicates the presence of bacteriophage. The broad host range study of φGRCST, demonstrated the efficiency of φGRCST potentially lysed n=4 (44.44%), ESBL producing *S. typhi* isolates (Table 2). The positive plaque formation was observed in all (n=4) *S. typhi* strains (Fig 2). Similarly, host range screening was carried out by Wang et al., 2016; with Phage 5460 potentially lysed 12 out of 18 *P. mirabilis* strains (67%), three out of six *P. vulgaris* strains and one tested *P. penneri* strain; while phage 5461 killed all (100%) of the *Proteus* spp. tested.

Transmission Electron Microscopic (TEM) study of φGRCST revealed that our phage belongs to *Myoviridae* family. The phages which exhibit tail were classified in the order Caudavirales (dsDNA) (Ackermann et al., 2006). This study was concentrated on the bacteriophage in the field of therapeutics, which act against MDR *S. typhi*, the characteristic feature φGRCST possesses an icosahedral head with size 50 nm with contractile tails consisting of a sheath with a central tube (Fig 2); it belongs to *Myoviridae Vi01*-like family of phages containing *S. typhi*-specific Vi01 (Hooton et al., 2011).

In vivo studies conducted in the BALB/c mice model (weighing from 20-30 gms) for the experimental examination of the efficacy of φGRCST. The mice models were showed the effective of prevention of infection caused by antibiotic-resistant bacteria (Wang et al., 2006; Capparelli et al., 2007; Vinodkumar et al., 2008). In the present study, successfully experimented the *in vivo* efficacy of φGRCST against *S. typhi* BST 51 infected mice model and obtained moderate results.

The minimum lethal dose (MLD) was determined by intraperitoneal administration of 2×10^7 CFU, 2×10^8 CFU and 2×10^9 CFU bacterial dose. Total of 100% survival rate was recorded in 1X PBS induced mice. Only 83% survival rate was observed in mice received 2×10^7 CFU bacterial dosage. The comparative study was carried out to evaluate the efficacy of φGRCST with standard antibiotic (ciprofloxacin). The 100% rescue was accomplished in challenged BALB/c mice treated with 1.5×10^7 PFU phage GRCST, comparatively, 67% and 83% survival rate was observed in the group of mice which received standard antibiotic ciprofloxacin in a single dose and in multiple doses for treatment. The multiple doses were given on daily basis (Fig 4). Relatively, the similar kind of experiment was conducted on *S. paratyphi B* infected mice and successfully rescued by treating with phage Φ1 (Wang et al., 2006).

The therapeutic effect of φGRCST was successfully achieved *in vivo*, the given phage (1.5×10^7 PFU) administered along with saline showed no side effects on health

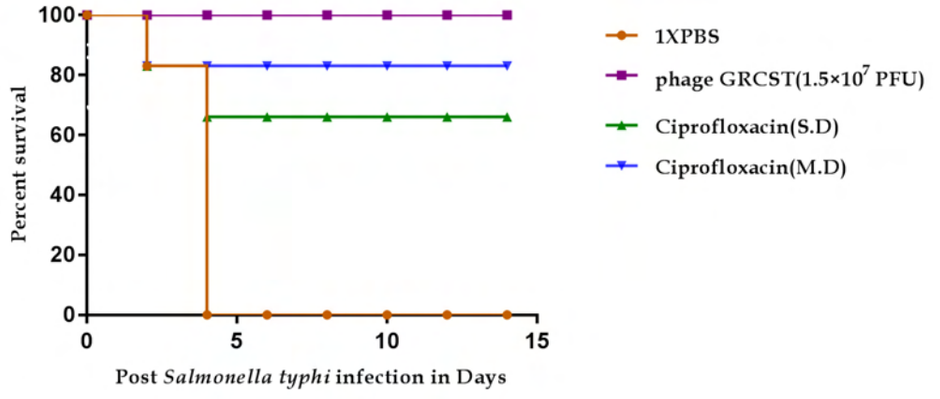

FIGURE 5. The protection efficacy of phage therapy with ciprofloxacin (single and multiple doses) treatment of BALB/c mice.

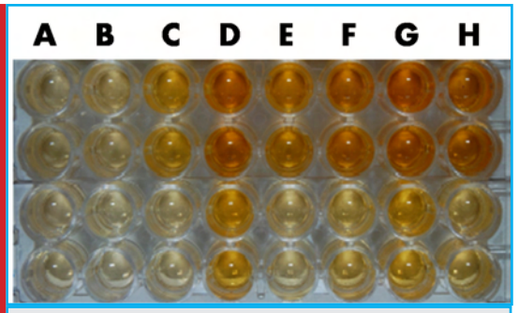

FIGURE 6. ELISA of IgG antibody titre in φGRCST immunized mice from *S. typhi*. A: Serum sample taken from control induced with 1X PBS B-F: Serum of mice treated with phage GRCST

and behavior of the experimental animals. Thus, phage rescue experiments could be conducted by without bias (Uchiyama et al., 2008).

The immunology of phages has been a subject debate over the years. The potential induced phages in; in vivo, subsequently lead to the humoral immune responses ultimately results in the inactivation of phage virion particles. There were some early assumptions; Kucharewica-Krukowska and Slopek, 1987, phage therapy in both animals and patients subsequently affect the patients immunity, by stimulating the immune system and subsequent production of anti-phage antibodies production of neutralizing antibodies, rapid emergence of phage-resistant bacterial strains (Stent, 1963; Lederberg, 1996; Cairns et al., 2009) and efficacy of phages only when

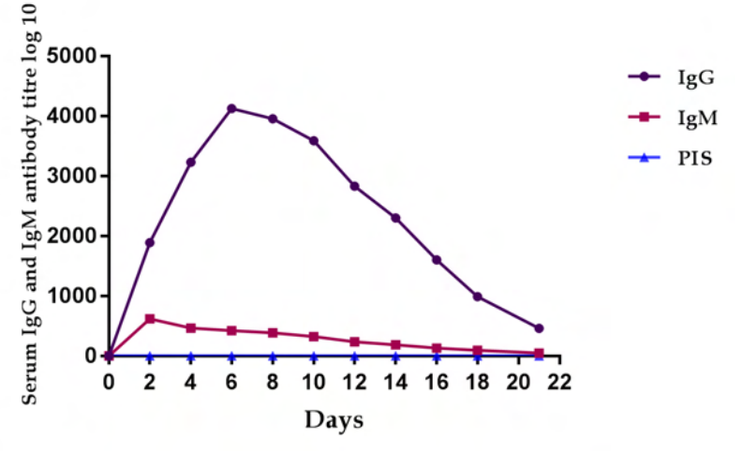

FIGURE 7. The raised antibody titre level (IgG and IgM) against φGRCST in BALB/c mice

administered shortly after bacterial infection (Bull et al., 2002); are the most frequent criticisms of the clinical use of phages. Recently, similar kind of studies were conducted by Wang et al., (2016); comparatively results obtained were very much similar to the activity of Phage SLPW showed a broad host range and high efficiency of plating against various types of S. aureus. Phage SLPW remained stable under a various temperatures or pH range. Further, it efficiently lysed MRSA strains in vitro and in vivo. Intraperitoneal phage administration at 1 h post-infection cured the mice and reduced the bacterial expression of inflammatory cytokines in mice (Wang et al., 2016).

Titre of IgG and IgM was well measured BALB/c mice after a single dose of φGRCST induction, the background titre was increased significantly with 4100 fold, and 600 fold respectively (Fig 6 and Fig 7). Incubation of phage GRCST with an excess of mice anti-phage GRCST antibodies did not interfere with phage's capacity to lyse susceptible bacteria. This result demonstrates that the antibodies elicited by phage GRCST are non-neutralizing. The similar kind of immune response study was conducted in phageϕ1 against Salp572 (*S. paratyphi B*) with an elevated level of mice anti-ϕ1 antibodies did not interfere with phage's capacity to lyse phage-susceptible bacteria. This result demonstrates that the antibodies elicited by phageϕ1 are non-neutralizing (Capparelli et al., 2010). This study clearly emphasizes that mice does produce antibodies against induced phages but they are non-neutralizing. Indeed, Gorski *et a*l., 2006 (Górski, et al., 2007); have provided enough evidence of a positive impact of phages on immune system functioning and have explored potential phage anti-tumour properties mediated through observed shifts in levels of various cytokines as a consequence of interactions between extra decorative head proteins with surface proteins of certain immune-system cells (Budynek et al., 2010). The immune response to φGRCST was not associated with anaphylaxis or other adverse immunological reactions. The anaphylactic reactions were negative, and no changes in animal behavior, no significant changes in the body temperature or no other side effects were observed in both the group

CONCLUSION

The bacteriophage therapy will serve for better perspective, with minimum side effects. The present investigation attempted to find and characterize a bacteriophage infective against the multidrug resistant and ESBL producing *S. typhi*. Our explored phage was lytic against many MDR *S. typhi* isolates, it's *in vivo* efficacy proved as an excellent therapeutic agent. The significant outcome of our conducted study a single dose of 1.5×10^7 PFU of phage GRCST successfully eliminated bacteria from mice circulatory system without influencing the host immune system and rescued infected mice, compare to antibiotics failed to rescue all infected mice. Hence, we conclude that our explored φGRCST is clinically more efficient than earlier reported; further characterization like whole genome sequencing and identification and cloning of genes coding for bacterial lysis of the φGRCST may prove as an excellent alternative therapeutic agent. Based on our observations of this study, phage therapy can be used as an alternative therapy for those patients not responding to antibiotic treatment.

CONFLICT OF INTEREST

The authors declare of no conflict of interest in conducting this study.

REFERENCES

Abedon, S. T., Kuhl, S. J., Blasdel, B. G., & Kutter, E. M. (2011). Phage treatment of human infections. Bacteriophage, 1(2), 66-85.

Ackermann, H. W. (2012). Bacteriophage electron microscopy. Adv. Virus Res, 82, 1-32.

Ackermann, H.W. (2006). Classification of bacteriophages. In The Bacteriophages, Ed.Calendar R, Oxford University Press, ISBN 0-19-514850-9, New York, USA, pp. 8–16

Albino, L. A., Rostagno, M. H., Húngaro, H. M., & Mendonça, R. C. (2014). Isolation, characterization, and application of bacteriophages for *Salmonella spp*. biocontrol in pigs. Foodborne pathogens and disease, 11(8), 602-609.

Anderson, E. S., & Felix, A. (1953). The Vi type-determining phages carried by *Salmonella typhi*. Microbiology, 9(1), 65-88.

Atterbury, R. J., Van Bergen, M. A. P., Ortiz, F., Lovell, M. A., Harris, J. A., De Boer, A., & Barrow, P. A. (2007). Bacteriophage therapy to reduce *Salmonella* colonization of broiler chickens. Applied and environmental microbiology, 73(14), 4543-4549.

Ayache, J., Beaunier, L., Boumendil, J., Ehret, G., & Laub, D. (2010). Sample preparation handbook for transmission electron microscopy: techniques (Vol. 2). Springer Science & Business Media.

Bassetti, M., Poulakou, G., Ruppe, E., Bouza, E., Van Hal, S. J., and Brink,A. (2017). Antimicrobial resistance in the next 30 years, humankind,bugs and drugs: a visionary approach. Intensive Care Med. 43, 1464–1475. doi: 10.1007/s00134-017-4878-x

Biswas, B., Adhya, S., Washart, P., Paul, B., Trostel, A. N., Powell, B., ... & Merril, C. R. (2002). Bacteriophage therapy rescues mice bacteremic from a clinical isolate of vancomycin-resistant *Enterococcus faecium*. Infection and immunity, 70(1), 204-210.

Budynek, P., Dabrowska, K., Skaradzinski, G., Górski, A. (2010). Bacteriophages and cancer. Arch.Microbiol. 192:315–320.

Bull, J. J., Levin, B. R., DeRouin, T., Walker, N., & Bloch, C. A. (2002). Dynamics of success and failure in phage and anti-

biotic therapy in experimental infections. BMC microbiology, 2(1), 1.

Cairns, B. J., Timms, A. R., Jansen, V. A., Connerton, I. F., & Payne, R. J. (2009). Quantitative models of in vitro bacteriophage–host dynamics and their application to phage therapy. PLoS Pathog, 5(1), e1000253.

Capparelli, R., Nocerino, N., Iannaccone, M., Ercolini, D., Parlato, M., Chiara, M., & Iannelli, D. (2010). Bacteriophage therapy of *Salmonella enterica*: a fresh appraisal of bacteriophage therapy. Journal of Infectious Diseases, 2011(1), 52-61.

Capparelli, R., Parlato, M., Borriello, G., Salvatore, P., & Iannelli, D. (2007). Experimental phage therapy against *Staphylococcus aureus* in mice. Antimicrobial agents and chemotherapy, 51(8), 2765-2773.

Chanishvili, N., Sharp, R.A. (2009). Literature Review of the Practical Application of Bacteriophage Research. Tbilisi, Georgia: Eliava Institute.

De Jonge, P. A., Nobrega, F. L., Brouns, S. J. J., and Dutilh, B. E. (2018). Molecular and evolutionary determinants of bacteriophage host range. Trends Microbiol.7:1352. doi: 10.1016/j.tim.2018.08.006

De Kraker,M. E., Stewardson, A. J., and Harbarth, S. (2016). Will 10 million people die a year due to antimicrobial resistance by 2050? PLoS Med. 13:e1002184. doi: 10.1371/journal.pmed.1002184

Deghorain M, Bobay LM, Smeesters PR, Bousbata S, Vermeersch M, Perez-Morga D, Drèze PA, Rocha EP, Touchon M, Van Melderen L (2012) Characterization of novel phages isolated in coagulase-negative *staphylococci* reveals evolutionary relationships with *Staphylococcus aureus* phages. J Bacteriol 194:5829–5839

Furfaro, L.L., Payne, M.S. and Chang, B.J., 2018. Bacteriophage therapy: Clinical trials and regulatory hurdles. Frontiers in cellular and infection microbiology, 8.

Górski, A., Borysowski, J., Miedzybrodzki, R., & Weber-Dabrowska, B. (2007). Bacteriophages in medicine (pp. 125-158). Caister Academic Press.

Harper, D. R. (2018). Criteria for selecting suitable infectious diseases for phage therapy. Viruses 10:E177. doi: 10.3390/v10040177

Hooton, S. P., Timms, A. R., Rowsell, J., Wilson, R., & Connerton, I. F. (2011). *Salmonella Typhimurium*-specific bacteriophage ΦSH19 and the origins of species specificity in the Vi01-like phage family. Virology journal, 8(1), 1.

Kropinski, A. M., Mazzocco, A., Waddell, T. E., Lingohr, E., and Johnson, R. P. (2009). Enumeration of bacteriophages by double agar overlay plaque assay. Methods Mol. Biol. 501, 69–76. doi: 10.1007/978-1-60327-164-6_7

Kutter EM. Bacteriophage therapy: past and present. In: Schaecter M, editor. Encyclopedia of Microbiology. Oxford: Elsevier; 2009. pp. 258–266.

Lederberg, J. (1996). Smaller fleas... ad infinitum: therapeutic bacteriophage redux. Proceedings of the National Academy of Sciences, 93(8), 3167-3168.

Mazzocco, A., Waddell, T. E., Lingohr, E., & Johnson, R. P. (2009). Enumeration of bacteriophages by the direct plating plaque assay. Bacteriophages: Methods and Protocols, Volume 1: Isolation, Characterization, and Interactions, 77-80.

Melo, L. D., Sillankorva, S., Ackermann, H. W., Kropinski, A. M., Azeredo, J., and Cerca, N. (2014b). Isolation and characterization of a new *Staphylococcus epidermidis* broad-spectrum bacteriophage. J. Gen. Virol. 95(Pt 2), 506–515. doi: 10.1099/vir.0.060590-0

Mikeladze, C., Nemsadze, E., Alexidze, N., Assanichvili, T. (1936). On the treatment of typhoid fever and acute colitis by d'Herelle bacteriophage. La Médecine. 1936; 17:33–38. (Fre).

Reardon, S. (2014). Phage therapy gets revitalized. Nature 510, 15–16. doi: 10.1038/510015a

Sambrook, J., and Russell, D. W. (2001). Molecular Cloning: A Laboratory Manual, 3rd Edn. New York, NY: Cold Spring Harbor Laboratory Press

Stent, G. S. (1963). Molecular biology of bacterial viruses. Molecular biology of bacterial viruses.

Sulakvelidze, A., Barrow, P. (2005). Phage therapy in animals and agribusiness. In: Kutter E, Sulakvelidze A, eds. Bacteriophages: Biology and Application. Boca Raton, FL: CRC Press, 335-80.

Tacconelli, E., Carrara, E., Savoldi, A., Harbarth, S., Mendelson, M., Monnet, D.L., et al. (2018). Discovery, research, and development of new antibiotics: the WHO priority list of antibiotic-resistant bacteria and tuberculosis. Lancet Infect Dis. 18, 318–327. doi: 10.1016/S1473-3099(17)30753-3

Tsulukidze, A. (1936). Sur l'application du bacteriophage dans la peritonite par perforation au cours de la fievre typhoide. La Médecine, 17(Suppl), 41-2.

Uchiyama, J., Rashel, M., Maeda, Y., Takemura, I., Sugihara, S., Akechi, K., ... & Matsuzaki, S. (2008). Isolation and characterization of a novel *Enterococcus faecalis* bacteriophage φEF24C as a therapeutic candidate. FEMS Microbiology letters, 278(2), 200-206.

Vinodkumar, C. S., Kalsurmath, S., & Neelagund, Y. F. (2008). Utility of lytic bacteriophage in the treatment of multidrug-resistant *Pseudomonas aeruginosa* septicemia in mice. Indian Journal of Pathology and Microbiology, 51(3), 360.

Vinogradov, E., and Perry, M. B. (2000). Structural analysis of the core region of lipopolysaccharides from *Proteus mirabilis* serotypes O6, O48 and O57. Eur. J. Biochem. 267, 2439–2446. doi: 10.1046/j.1432-1327.2000. 01262.x

Wang, J., Hu, B., Xu, M., Yan, Q., Liu, S., Zhu, X., & Li, Q. Q. (2006). Use of bacteriophage in the treatment of experimental animal bacteremia from imipenem-resistant *Pseudomonas aeruginosa*. International journal of molecular medicine, 17(2), 309-318.

Wang, Z., Zheng, P., Ji, W., Fu, Q., Wang, H., Yan, Y., & Sun, J. (2016). SLPW: A virulent bacteriophage targeting methicillin-resistant *Staphylococcus aureus* in vitro and in vivo. Frontiers in microbiology, 7, 934.

Medical
Communication

Biosci. Biotech. Res. Comm. 12(1): 26-35 (2019)

BBRC
Bioscience Biotechnology
Research Communications

Anticancer and antibacterial potential of MDR *Staphylococcus aureus* mediated synthesized silver nanoparticles

Mohd Haseeb[1], Mohd Sajid Khan[2], Abu Baker[2], Imran Khan[2], Iram Wahid[2] and M.S. Mohamed Jaabir*

[1]*Department of Biotechnology, National College, (Autonomous), Tiruchirappalli, Tamil Nadu, India*
[2]*Department of Biosciences, Integral University Lucknow, Uttar Pradesh India*

ABSTRACT

The increasing cases of resistance, low efficacy and high toxicity of antibiotics and anticancer agents have led to the discovery of nanoparticles as potent antimicrobial and anticancer agents to combat the threat of Multi Drug Resistance (MDR) and to minimize the side effects of drugs. The synthesized silver nanoparticles (SAgNPs) (synthesized using MDR *Staphylococcus aureus*) were characterized to confirm synthesis, shape, size, hydrodynamic diameter, colloidal stability and surface functionalization, by UV-visible spectroscopy, TEM, DLS, zeta potential test and FTIR respectively. SAgNPs were found to have spherical shape with a size of 15 nm. Hydrodynamic diameter of nanoparticles was found to be 88.65 nm and the value of zeta potential was recorded to be -24.03 mV. The antimicrobial and anticancer potential of SAgNPs was performed against normal & MDR strains of *S. aureus* and human colon cancer cell line (HCT-116), respectively.. The MICs of SAgNPs against normal and MDR *S. aureus* strains were found to be 0.025 µg/ml & 0.053 µg/ml, respectively. Similarly, IC50 against HCT-116 cell line was found to be 0.069 µg/ml by MTT Assay. DAPI analysis confirmed the interaction of SAgNPs with DNA in order to initiate apoptosis for killing cancer cells.

KEY WORDS: ANTICANCER; DAPI; DLS; MDR; MTT; SAGNPS

ARTICLE INFORMATION:

Corresponding Author: mohamedjaabir@nct.ac.in
Received 2nd Jan, 2019
Accepted after revision 7th March, 2019
BBRC Print ISSN: 0974-6455
Online ISSN: 2321-4007 CODEN: USA BBRCBA
Thomson Reuters ISI ESC / Clarivate Analytics USA
NAAS Journal Score 2019: 4.31 SJIF: 4.196

Online Contents Available at: http//www.bbrc.in/
DOI: 10.21786/bbrc/12.1/4

INTRODUCTION

Toxicity, high cost of the drugs used in the treatment of cancer and microbial diseases, rise in the cases of antibiotic resistance due to frequent use of antibiotics have forced researchers to look for alternatives in medicine and therapeutics. Side effects of chemotherapeutic drugs due to poor specificity towards targets and high dose requirements have also made it necessary for nano-medicine to address the issue and look for other efficient and cost effective molecules bearing high degree of efficacy for the target cells **(Riehemann *et al.*, 2009)**.

Inorganic nanoparticles are being widely used throughout the world due to their incredible yet, potential applications. Among the metal NPs, Silver nanoparticles (AgNPs) in particular have attracted considerable attention in various fields and have been used as therapeutic agent (Shrivastava *et al.*, 2009), as catalyst (Christopher *et al.*, 2011) antimicrobial and anti-inflammatory agents (El-Chaghaby, and Ahmad, 2011; Veerasamy *et al.*, 2011), as a strong cytotoxic agent against cancer cell lines (Jacob *et al.*, 2012) . Silver and silver ions have been used since a long time as strong antimicrobial and anti-inflammatory agents. Nano-silver or silver nanoparticles (AgNPs) have shown promising results against the antibiotic resistant bacteria (Yah and Simate, 2015). AgNPs have also been investigated for their antimicrobial potential against Multi Drug Resistant MDR strains of several pathogenic microbes (Alshaye *et al.*, 2017). The role of AgNPs in diagnostic and probing of cancer has also been reported earlier in a research study (Huang *et al.*, 2017).

In literature, several chemical and physical methods have been used for the synthesis of AgNPs, but these methods utilize large amount of toxic chemicals and extreme conditions like high temperature and are not economical. The green synthesis approaches are a solution to this problem and are more ecofriendly, simple, reliable, reproducible and non-toxic. Recently, researchers have exploited microorganism as a production tool for the biosynthesis of inorganic metallic nanoparticles, such as silver, cadmium, gold and sulfide (Hassaan *et al.*, 2018; Elsalam *et al.*, 2018).

The bacterial synthesis seems to be advantageous because of minimal utilization of toxic chemicals and sustainability of large scale production. Many reports have shown that numerous bacterial strains of Staphylococcus aureus, Bacillus cereus, Bacillus subtilis, Escherichia coli, Bacillus licheniformis, Enterobacter cloacae, Klebsiella pneumonia, Lactobacillus acidophilus, and Pseudomonas aeroginosa, are capable of synthesizing nanoparticles (NPs) (Ghiuă *et al.*, 2018; Muthulakshmi *et al.* 2018; Fatemi *et al.*, 2018).

Biosynthetic methods can be categorized into two groups, on the basis of location of synthesis i.e. intracellular and extracellular synthesis. The extracellular synthesis of nanoparticles is simple and economical because of the simplicity in its procedure for not only synthesis but also of recovery and purification as well, under large scale production **(Singh *et al.*, 2018).** All these reasons make the bacteria a potential source for the extracellular synthesis of AgNPs avoiding the use of toxic and hazardous chemicals.

Novel technologies are being developed to overcome the challenges imposed by bacteria and cancer cells, the resistance associated with the regular use of antibiotics through MDR phenomenon and to minimize the side effects of the drugs used in chemotherapy **(Mohammed *et al.*, 2018).**

The current study aims to address the issues of MDR resistance of bacteria *S. aureus* an uses AgNPs as a tool against cancer cells. Here, AgNPs were synthesized extracellularly from bacteria MDR *S. aureus*, characterized by UV-vis spectroscopy, Transmission Electron Microscopy (TEM), Zeta potential value, Dynamic Light Scattering (DLS), Fourier Transformed Infra Red (FTIR), and subsequently tested against normal and MDR *S. aureus* as well as against cancer cell lines HCT-116

MATERIALS & METHODS

All the chemicals and media were purchased from Sigma Aldrich (St. Louis, USA) and HiMedia, India. The multidrug resistant (MDR) and normal strain of *Staphylococcus aureus* (NCIM 2079) were obtained from NCIM, Pune, India.

Synthesis of AgNPs

The MDR strain of *S. aureus* (NCIM 2079) was used for the synthesis of AgNPs. Bacterial strain was maintained on nutrient agar at 37° C. The bacterial cultures (OD600- 0.60) were transferred to Erlenmeyer flasks containing 250 ml nutrient broth and incubated at 37°C on a rotary shaker (180 rpm) for 6-8 hrs. The bacterial cells were collected by centrifugation (6000 g, 10 min at 10°C), washed extensively with sterile distilled water under aseptic conditions and used for further studies. Two different reactions were carried out by incubating *S. aureus* (NCIM 2079) cells (wet weight-5gm) in 100ml sterile distilled water containing 1mM AgNO3 in two different 500ml Erlenmeyer flasks for 6-8 hrs at rotatory shaker (180 rpm) at 37°C. The monitoring of the bacteria mediated reduction of silver ions was accomplished by the visual color change and UV–visible spectrum analysis for the reaction mixture.

At the end of synthesis, the unbound proteins were removed by Precipitation with 100% (v/v) volumes of absolute ethanol and the AgNPs were collected for further characterization.

Characterization Of AgNPs

The AgNPs synthesized using *S.aureus* (NCIM 2079) were characterized by UV-Vis Spectroscopy, Dynamic Light Scattering, Zeta potential analysis, TEM and FTIR for the confirmation of synthesis, size, shape, stability, surface functionalization and identification.UV-Vis spectrophotometer measurements were performed on a Shimadzu dual-beam spectrophotometer (model UV-1601 PC) operated at a resolution of 1nm.

Transmission Electron Microscopy (TEM) measurements were performed to analyze the size and morphology. Samples were prepared by drying a drop of AgNPs solution on carbon coated TEM copper grids followed by measurements on (TEM) FEI Company, TecnaiTM G2 Spirit BioTWIN operated at an accelerating voltage of 80kV. The study was done Indian Institute of Toxicological Research (IITR), Lucknow, India. Dynamic Light Scattering (DLS) was used to analyze the mean particle size (MPS) of biosynthesized AgNPs using dynamic light scattering particle size analyzer (Zetasizer Nano-ZS, Model ZEN3600, Malvern Instrument Ltd, Malvern, UK). The samples were taken in a DTS0112-low volume disposable sizing cuvette of 1.5 ml capacity. The sample powder was dissolved to a concentration of 0.5% (w/v) in deionised water and sonicated for 1 min before analysis. After filtering through a syringe filter of 0.4µm pore size, solution was centrifuged at 5000 rpm for 30min and measured for its particle size. Mean particle size was the average of triplicate measurements for a single sample. Zeta potential of AgNPs was determined to measure the charge, as the metal nanoparticles are normally charged or carry charge of capping agents. This analysis was done in Zetasizer Nano-ZS, (Malvern Instrument Ltd. and Malvern, UK).Fourier-transform infrared spectroscopy analysis (FTIR) was used to identify capped biomolecules over the surface of as synthesized AgNPs was done by FT-IR (Perkin Elmer Spectrum, Jasco- 6100). For the analysis, silver nanoparticles were dried, grounded with KBr pellets and analyzed in the wavelength range of 4000 to 400 cm^{-1}.

The antibacterial activity of *AgNPs* was determined against MDR strain of *Staphylococcus aureus* (NICM 2079), and Normal Strains of *Staphylococcus aureus* (NICM 2079). The bacterial cells ($OD_{600\text{-}0.60}$) were allowed to grow in nutrient broth for 24 hours and kept in a shaker incubator at 180 rpm for 24 hrs at 37ºC. Bacterial lawns were prepared using 100 ml of cultured broth. Agar well diffusion method (Khan *et al.*, 2011) was used to determine preliminary antibacterial activity of biosynthesized AgNPs. Plates were prepared by pouring around 25 ml of sterile Mueller Hinton Agar (MHA) media in sterilized petridishes. Different strains of bacterial culture chosen for the study was swabbed using sterilized cotton swab. Sterilized gel puncture was used to make wells of 5 mm diameter. Two wells were made in each plate, with each one containing distilled water (for control) and the other was loaded with synthesized silver nanoparticles. The plates were left for 24 hr incubation at 37ºC. The inhibition was examined by identifying the clear zone around the well.

The minimum inhibitory concentration (MIC) of the synthesized AgNPs was determined by double diffusion method (Sarker *et al.*, 2007). The MIC_{50} was determined by broth dilution, performed on a 96 flat-bottom well plate. The medium used in the plates were prepared at double the final strength to allow for a 50% dilution once the inoculum is added. This approach allowed the inoculum to be prepared in distilled water, which permitted the absorbance to be determined using a spectrophotometer without interference from colored media. All the bacterial strains were allowed to grow till mid-logrithmic phase. Culture was subsequently harvested by centrifugation, washed with 1mM sodium Phosphate buffer (SPB) at pH 7.4, and diluted to 2×10^5 colony forming units (CFU)/ml in Saline phosphate buffer. About 90 µL of Mueller-Hinton broth was used in 96 well- microtitre plates to serially dilute the silver nanoparticles in desired concentrations. Bacterial suspension of 95×10^4 CFU/ well was used as inoculum. Inoculated Microtitre wells were incubated overnight at 37º C. The MIC_{50} was determined by taking lowest concentration of AgNPs at which the bacterial growth was inhibited. The numbers of colonies were determined by agar plate count method as discussed by Morones *et al.*, (2005).The minimum bactericidal concentration (MBC) is the lowest concentration of an antibacterial agent required to kill a particular bacterium. It can be determined from broth dilution minimum inhibitory concentration (MIC) tests by sub culturing to agar plates that do not contain the test agent.

Cell viability and IC_{50} value determination of AgNPs against cancer line HCT-116

The biosynthesized silver nanoparticles were tested against the Human colon cancer cell line HCT-116. The anticancer activity of synthesized silver NPs was determined by MTT (3-[4, 5-dimethylthiazol-2-yl]-2, 5-diphenyltetrazolium bromide) assay and nuclear degradation was checked by DAPI (4', 6-diamino-2-phenylindiole) toxicology assays. For this, the cells were treated with varying concentration of AgNPs and the effect was analyzed by MTT assay and DAPI.

To determine the effect of Ag nanoparticles on cancer cells, MTT assay was performed. For this the HCT 116 cells were plated in 96 well plate with each well seeded with 1 X 10^4 cells. The plate was incubated for 24 hours in CO_2 incubator. After incubation, cells were treated with Ag NP of various concentrations in triplicate with

untreated cells as the positive control and incubated for 48 hours. After this, media was removed and wells were loaded with 50µl of 3-(4, 5-dimethylthiazol-2-yl)-2, 5-diphenyltetrazolium bromide (MTT) dye (5mg/ml in PBS) and fresh culture media. Then the plate was incubated for 4 hours. Formosan crystals formed during the process were dissolved by adding 100µl of DMSO (Dimethyl sulfoxide) and incubated for one hour. The reduced MTT was quantified by measuring optical density at 570 nm in ELISA reader.

The Percentage inhibition of the cells was calculated using the formula

$$X = 100 - (A\ test - A\ blank) / (A\ control - A\ blank) \times 100$$

Where, X- Percentage inhibition, A test – absorbance of the test sample, A blank – absorbance of blank and A control – absorbance of the control sample. The IC50 value was calculated from the data obtained.

The Apoptotic effect of Ag NP on the cell line was determined by nuclear fluorescent staining by DAPI. For this the cells were seeded in 96 well plate and treated with the Ag NP as mentioned above. Then media was removed and cells were washed with PBS and fixed with 4% para formaldehyde for 10 minutes. Then the staining with DAPI was performed along with permeabilizing buffer to fix the stain into the cells. After staining, the cell imaging was obtained under fluorescence microscope. The cells showing fragmented and condensed nuclei were considered as the apoptotic cells.

RESULTS AND DISCUSSION

Nanoparticles synthesis was observed as the color of reaction mixture changed from light yellow to dark brown, a characteristic color change associated with formation of silver nanoparticles. UV-Vis, spectroscopy is simple and sensitive techniques for characterization of colloidal suspension and requires very short period of time for measurement (Tomaszewska *et al.*, 2013). In UV-Vis, spectroscopy, the measurement of intensity of light passing through the sample is done, as the optical properties of metal nanoparticles are due to collective oscillation of conduction electrons, excited by electromagnetic radiation (Singh *et al.*, 2018).

The UV-Vis spectrum in our results shows the maximum absorbance peak around 430 nm, thereby confirming the synthesis of AgNPs in the sample.

Transmission Electron Microscopy (TEM) was used to visualize the shape and to determine the size distribution of synthesized AgNPs (fig.2.). TEM images were obtained using JEOL 3010, operating at 200 kV accelerating voltage. The TEM analysis was performed at Indian Institute of Toxicological Research (IITR), Lucknow, India. The high resolution images for topographical studies revealed the structure and morphology of synthesized silver nanoparticles (AgNPs) and average size was found to be 15 nm.

Gomaa and Zakaria (2017) have reported similarly in the synthesis of spherical shaped AgNPs with an average size of 17 nm using *Staphylococcus aureus* and *Escherichia coli*.

Dynamic light scattering (DLS) based on the laser diffraction method with multiple scattering technique was chosen to determine the size of AgNPs. DLS is a method which is dependent upon the interaction of light with particles in suspension. It is typically used to measure the particles size distribution in the range of 2 nm to 500 nm (Tomaszewska *et al.*, 2013). In DLS measurement the scattered light passing through the colloidal suspen-

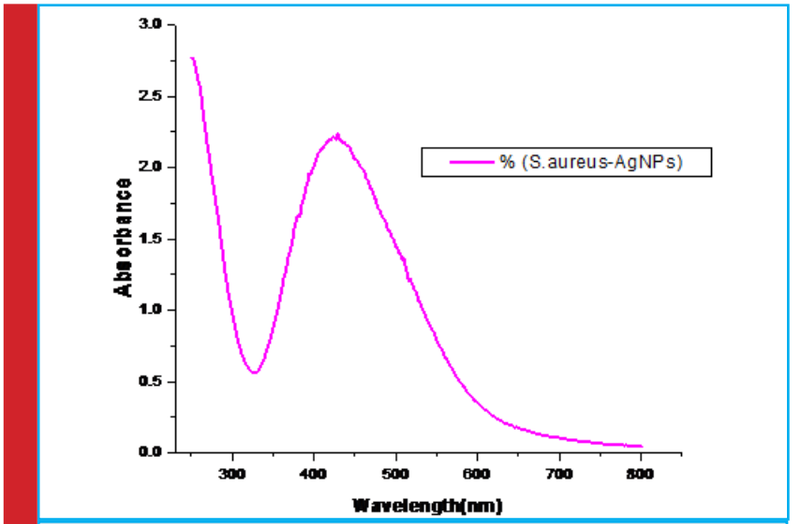

FIGURE 1. UV-Visible Spectrum of Synthesized Silver Nanoparticles

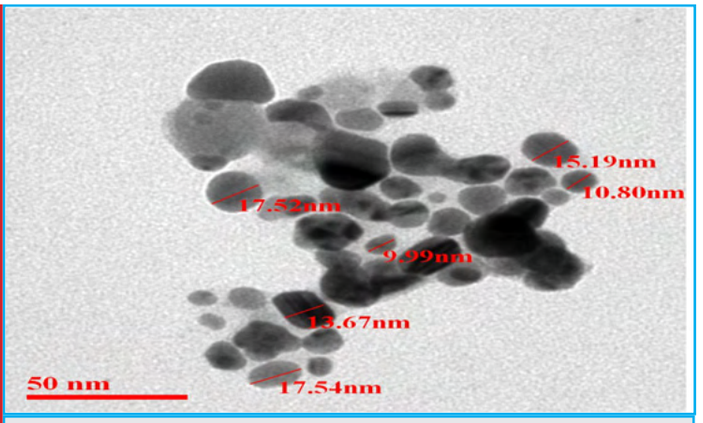

FIGURE 2. TEM image (taken at magnification of 110000x) Showing the Shape, Internal Structure and Size of AgNPs

sion relies on Rayleigh scattering from the particles in suspension (Fissan *et al.*, 2014). Next, the hydrodynamic size of the particles is determined by analyzing the modulation of intensity of scattered light as function of time (Dieckmann *et al.*, 2009). DLS revealed the Z-average value to be 88.65 nm. Similar results were obtained in another research in which average diameter silver NPs was found to be 87.46 nm in the aqueous colloidal suspension of AgNPs. (Singh *et al.*, 2018).

The determination of Zeta potential is considered as an effective simplest, and most straight forward method to predict the stability and understand surface properties of the nanoparticles. Zeta potential is a measure of the colloidal stability of the nanoparticles in a solution (Saeb *et al.*, 2014). The shielding or exposure of charged groups or concentration, distribution, ionization and adsorption of nano-particles can also be estimated from zeta potential (Guilatt *et al.,* 2004).

Information with reference to the concentration, distribution, exposure or shielding of charged moieties; ionization and adsorption could be inferred from the analysis of zeta potential. In the present study, the zeta potential of the synthesized AgNPs was found to be -24.3 mV, which confirmed that the AgNPs were highly stable in colloidal suspension. Similar observation were also recorded in which zeta potential value was measured to be -25.5 mV (Singh *et al.*, 2018).

FTIR of the synthesized AgNPs is performed to spot the position of various functional groups of the capping agent and their vibration patterns. The FTIR results of the sample states that the position of Amide I(C=O) bond is 1637 cm-1 with transmittance of 10.75%, O-H(Stretch) is 3583.13 cm-1 with transmittance of 9.19%, C-O(Stretch) is 1082.41 cm-1 with transmittance of 16.19% and Alkyne (Stretch) bond 2097.88 cm-1 with transmittance of 33.17%.

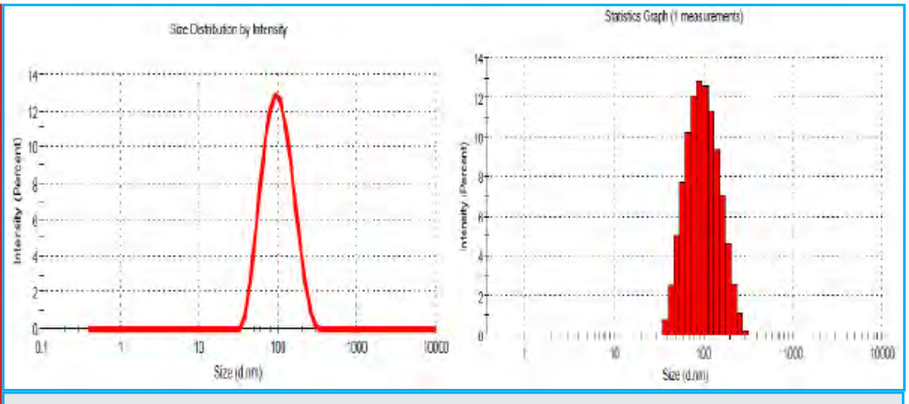

FIGURE 3. DLS Curve (Z-value-88.65 nm) of the AgNPs synthesized using MDR *S.aureus* bacteria.

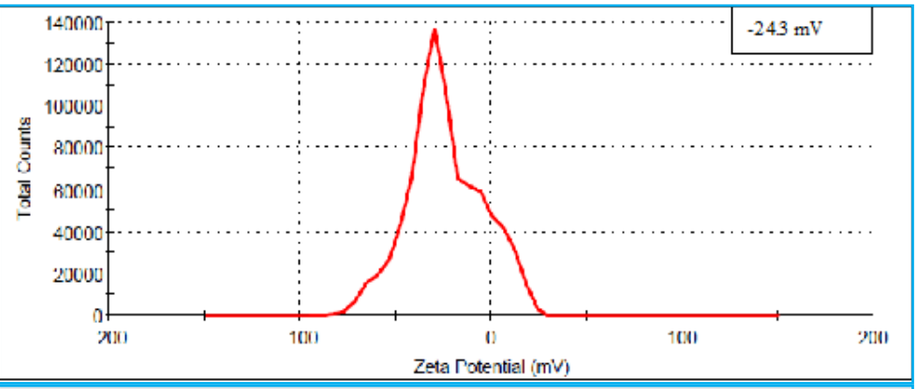

FIGURE 4. Curve representing the Zeta potential (-24.3 mV) of the AgNPs synthesized

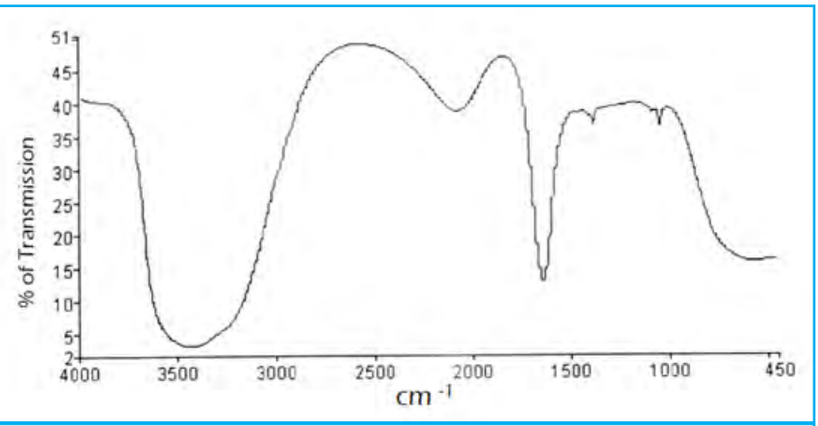

FIGURE 5. The FTIR Spectraof the AgNPs synthesized using MDR *S.aureus* bacteria.

Antibacterial activity of AgNPs against normal and MDR strains

The AgNPs synthesized using MDR *S.aureus* was tested for its antibacterial potential, against normal strains of *S.aureus*. The same was tested against strains of MDR *S.aureus* as well. The antimicrobial potential was tested by agar well diffusion method, MIC and MBC.

In general MIC is defined as the minimum amount of drug required to inhibit the growth of bacteria to 70%-80%. MIC_{50} is defined as the minimum amount of drug required to inhibit the growth of bacteria to 50%. The clear zone of inhibition around the inoculated area confirmed the antibacterial potential of as the synthesized AgNPs. MIC and MBC concentrations were calculated

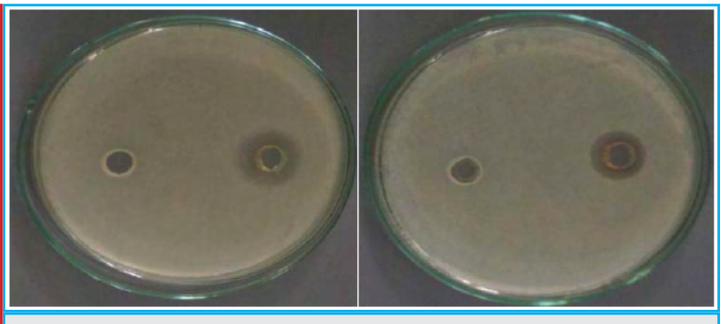

FIGURE 6. Plates showing the zone of inhibition of AgNPs against- a) Normal strain of *S.aureus*, b) MDR *S. aureus*

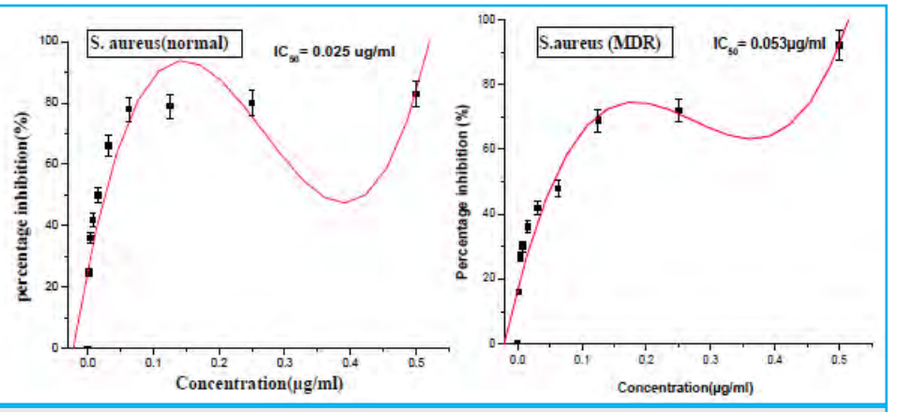

FIGURE 7. Curve representing the MIC of AgNPs against a) Normal strain of *S.aureus*. b) MDR *S.aureus*

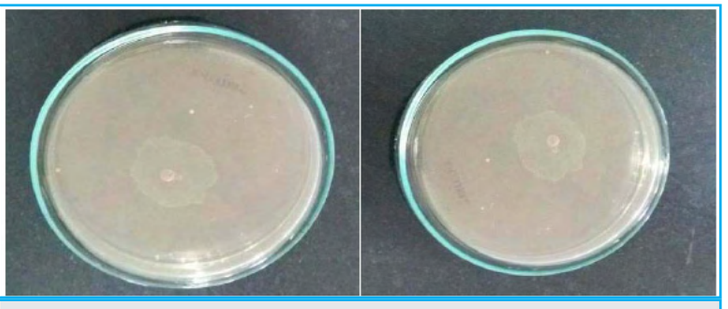

FIGURE 8. Plates showing MBC of AgNPs against: a) MDR strain of *S.aureus* and b: *S.aureus* (Normal strain)

under varying concentrations of the AgNPs synthesized using MDR *S.aureus*. The Zone of inhibition of AgNPs against normal strain and MDR strains of *S.aureus* were found to be 2.8 cm and 2.5 cm respectively (figure no. 6a and 6b). The Minimum inhibitory concentration of AgNPs against normal strain and MDR strains of *S.aureus* were found to be 0.025 µg/ml and 0.053 µg/ml for respectively. The lowest concentration with no visible growth indicating 99.5% killing of the inoculum was found to be double the value of MIC, (see figure 8 a and b).

Anticancer activity against HCT-116

To evaluate the sensitivity of colon cancer cells to the AgNPs, human colon cancer cell line HCT-116 was treated with different doses (0.01–10 µg/ml) of AgNPs

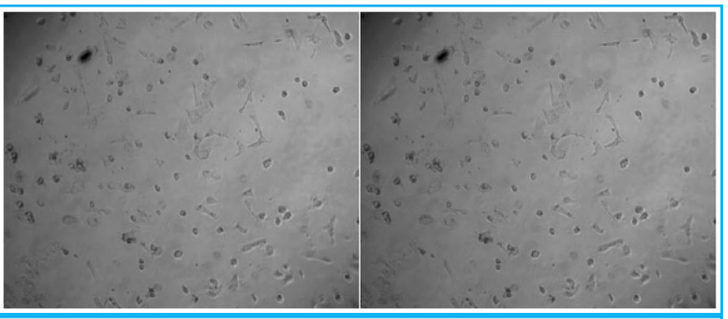

FIGURE 9. Imagesof human colon cancer cell line HCT-116 (Taken at magnification of 10x): a) untreated cells b) cells treated with AgNPs.

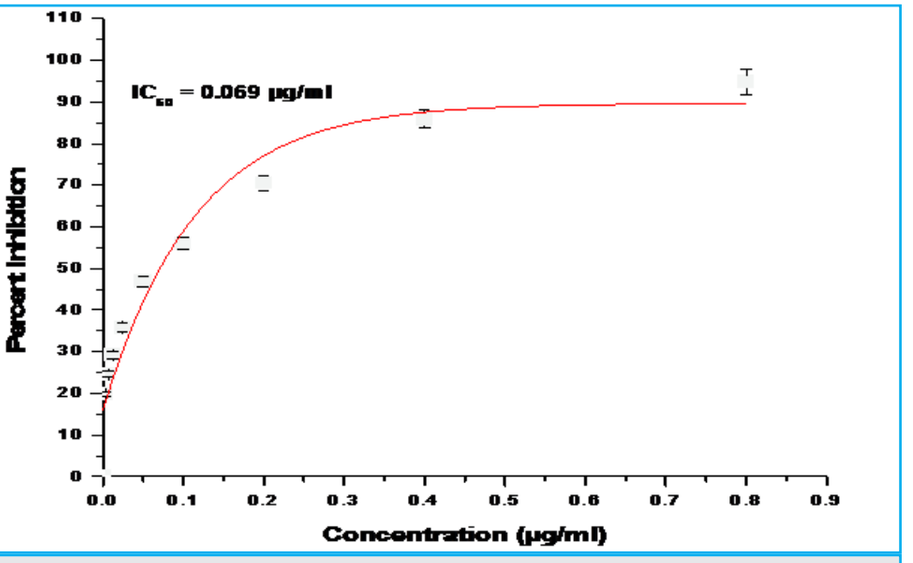

FIGURE 10. Graph showing the IC_{50} of AgNPs against Human coloncancer cell lines HCT-116

synthesized using MDR *S.aureus* for 24 and 48 h followed by MTT assay (Fig. 9 a and 9b). MTT is a dye which is reduced to formazon crystals during metabolism, cellular mechanism of MTT reduction into formazan is understood, involving reaction with NADH or similar reducing molecules that transfer electrons to MTT Viable cells with active metabolism convert MTT into a purple colored formazan product with an absorbance maximum near 570 nm. When cells die, they lose the ability to convert MTT into formazan, thus color formation serves as a useful and convenient marker of only the viable cells. So, the intensity of the colored product is measured which is directly proportional to the number of viable cells in the culture **(Präbst *et al.*, 2017).** The MTT analysis was done to assess the activity of mitochondrial succinate dehydrogenase **(Singh *et al.*, 2018).**

Here, the decrease in the MTT reduction could be due to decrease in cell viability which in turn can be attributed to cytotoxic activity of silver nanoparticles. Our results shows that AgNPs at a concentration of 0.069 µg/ml reduced growth of human colon cancer cells by 50%, after 24 h of treatment. Similar pattern of results with more pronounced cytotoxic effect was observed after 48 h of treatment thus proving AgNPs to be more anti-proliferative and cytotoxic for colon cancer cells. Similar findings have been reported in earlier studies, (Singh *et al.*, 2018; Patra *et al.*, 2018).

AgNPs induced nuclear condensation in HCT-116 cells: Apoptosis is characterized by changes in cellular morphology such nuclear fragmentation, degradation of DNA, condensation of chromatin, apoptotic body formation and membrane blabbing (Sheikh *et al.,* 2018). In order to confirm apoptosis in AgNPs treated colon cancer cells, DAPI nuclear staining was performed. DAPI (4', 6-diamidino-2-phenylindole) is a fluorescent stain which preferably binds to AT rich regions of DNA.

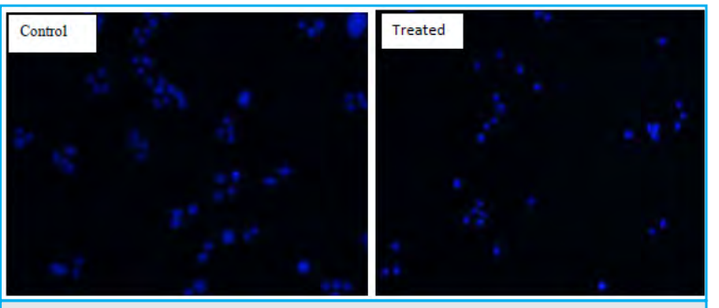

FIGURE 11. Representing DAPI Images of Human Colon cancer cell line HCT-116 (taken at a magnification of 20x): Control cells, on left and Cells treated with AgNPs, on right.

The fluorescence intensity of DAPI increases to approximately 20 times when DAPI is bound to DNA. As the ell permeability is compromised due to apoptosis; DAPI enters easily inside the cell where its binding to DNA produces a strong blue color (Baharara *et al.,* 2018).

After treatment with AgNPs for 24 h, significant nuclear changes in colon cancer cells were observed via DAPI staining. As apparent from photomicrographs, AgNPs induced nuclear condensation and fragmentation in colon cancer cells in a dose dependent manner, whereas the control cells exhibited normal cell morphology. The results were evident that AgNPs induced apoptosis in colon cancer cells in a time and dose-dependent manner. Our results are in agreement with several other researches published earlier (Gurunathan *et al.,* 2018; Baharara *et al.,* 2018; Kishore *et al*., 2018).

CONCLUSION

In this study, MDR strain of *S. aureus* was used to synthesize silver NPs, with the goal to inhibit the MDR strains of *S.aureus* as well as normal strain of *S.aureus* to assess its anticancer potential.The synthesized NPs were found to be spherical in shape and approximately 15 nm in size. The NPs were found to form a stable suspension with a zeta potential value of -24.03 m. These particles were found to be capped by extracellular bacterial proteins (confirmed by FTIR). The minimum inhibitory concentrations were found to be 0.025 µg/ml for *S.aureus* (normal) and 0.053 µg/ml for *S.aureus* (MDR), respectively. These nanoparticles were also found to be substantially effective against human colon cancer cell lines HCT-116, with an IC_{50} value of 0.069 µg/ml. Further optimization is needed in order to assess the anticancer properties of as synthesized AgNPs.

ACKNOWLEDGEMENTS

Authors acknowledge the support of National College (Autonomous) for providing all the necessary facilities to carry out this research work.

REFERENCES

Alshaye, N.A., Elobeid, M.M., Alkhalifah, D.H. and Mohammed, A.E., (2017). Characterization of Biogenic Silver Nanoparticles by Salvadora persica Leaves Extract and its Application Against Some MDR Pathogens E. coli and S. aureus. Research Journal of Microbiology, 12, pp.74-81.

Baharara, J., Ramezani, T., Hosseini, N. and Mousavi, M., (2018). Silver Nanoparticles Synthesized Coating with *Zataria multiflora* Leaves Extract Induced Apoptosis in HeLa Cells Through p53 Activation. Iranian journal of pharmaceutical research: IJPR, 17(2), p.627.

Christopher, P., Xin, H. and Linic, S., (2011). Visible-light-enhanced catalytic oxidation reactions on plasmonic silver nanostructures. Nature chemistry, 3(6), p.467.

Dieckmann, Y., Cölfen, H., Hofmann, H. and Petri-Fink, A., (2009). Particle size distribution measurements of manganese-doped ZnS nanoparticles. Analytical chemistry, 81(10), pp.3889-3895.

Elsalam, S.S.A., Taha, R.H., Tawfeik, A.M., El-Monem, M.O.A. and Mahmoud, H.A., (2018). Antimicrobial Activity of Bio and Chemical Synthesized Cadmium Sulfide Nanoparticles. Egyptian Journal of Hospital Medicine, 70(9).

El-Chaghaby, G.A. and Ahmad, A.F., (2011). Biosynthesis of silver nanoparticles using *Pistacia lentiscus* leaves extract and investigation of their antimicrobial effect. Oriental Journal of Chemistry, 27(3), p.929.

Fatemi, M., Mollania, N., Momeni-Moghaddam, M. and Sadeghifar, F., (2018). Extracellular biosynthesis of magnetic iron oxide nanoparticles by *Bacillus cereus* strain HMH1: Characterization and in vitro cytotoxicity analysis on MCF-7 and 3T3 cell lines. Journal of biotechnology, 270, pp.1-11.

Fissan, H., Ristig, S., Kaminski, H., Asbach, C. and Epple, M., (2014). Comparison of different characterization methods for nanoparticle dispersions before and after aerosolization. Analytical Methods, 6(18), pp.7324-7334.

Ghiuă, I., Cristea, D., Croitoru, C., Kost, J., Wenkert, R., Vyrides, I., Anayiotos, A. and Munteanu, D., (2018). Characterization and antimicrobial activity of silver nanoparticles, biosynthesized using *Bacillus* species. Applied Surface Science, 438, pp.66-73.

Gomaa, E.Z., (2017). Silver nanoparticles as an antimicrobial agent: A case study on *Staphylococcus aureus* and *Escherichia coli* as models for Gram-positive and Gram-negative bacteria. The Journal of general and applied microbiology, 63(1), pp.36-43.

Gurunathan, S., Qasim, M., Park, C., Yoo, H., Kim, J.H. and Hong, K., (2018). Cytotoxic Potential and Molecular Pathway Analysis of Silver Nanoparticles in Human Colon Cancer Cells HCT116. International journal of molecular sciences, 19(8), p.2269.

Hassaan, M.A. and Hosny, S., (2018). Green Synthesis of Ag and Au Nanoparticles from Micro and Macro Algae-Review. International Journal of Atmospheric and Oceanic Sciences, 2(1), p.10.

Huang, Y., Fan, C.Q., Dong, H., Wang, S.M., Yang, X.C. and Yang, S.M., (2017). Current applications and future prospects of nanomaterials in tumor therapy. International journal of nanomedicine, 12, p.1815.

Jacob, S.J.P., Finub, J.S. and Narayanan, A., (2012). Synthesis of silver nanoparticles using *Piper longum* leaf extracts and its cytotoxic activity against Hep-2 cell line. Colloids and Surfaces B: Biointerfaces, 91, pp.212-214.

Kishore, M., Abdulqader, A.T., Ahmad, H.S. and Hanumantharao, Y., (2018). Anticancer and antibacterial potential of green silver nanoparticles synthesized from *Maytenus senega-*

lensis (L.) leaf extract and their characterization. Drug Invention Today, *10*(4).

Mohammed, A.E., Al-Qahtani, A., Al-Mutairi, A., Al-Shamri, B. and Aabed, K.F., (2018). Antibacterial and Cytotoxic Potential of Biosynthesized Silver Nanoparticles by Some Plant Extracts. Nanomaterials (Basel, Switzerland), 8(6).

Morones, J.R., Elechiguerra, J.L., Camacho, A., Holt, K., Kouri, J.B., Ramírez, J.T. and Yacaman, M.J., (2005). The bactericidal effect of silver nanoparticles. Nanotechnology, 16(10), p. 2346.

Muthulakshmi, K., Uma, C., Sivagurunathan, P., Yoganathan, K. and Satheeshkumar, S., (2018). Extracellular, biosynthesis of silver nanoparticles using *Enterobacter cloacae* (mk163462) and their antibacterial activity against certain multidrug resistant pathogens. Journal of Pharmacognosy and Phytochemistry, 7(6), pp.741-747.

Patra, N., Kar, D., Pal, A. and Behera, A., 2018. Antibacterial, anticancer, anti-diabetic and catalytic activity of bio-conjugated metal nanoparticles. Advances in Natural Sciences: Nanoscience and Nanotechnology, 9(3), p.035001.

Präbst, K., Engelhardt, H., Ringgeler, S. and Hübner, H., (2017). Basic colorimetric proliferation assays: MTT, WST, and resazurin. Cell Viability Assays: Methods and Protocols, pp.1-17.

Rabinovich-Guilatt, L., Couvreur, P., Lambert, G., Goldstein, D., Benita, S. and Dubernet, C., (2004). Extensive surface studies help to analyse zeta potential data: the case of cationic emulsions. Chemistry and Physics of Lipids, 131(1), pp.1-13.

Riehemann, K., Schneider, S.W., Luger, T.A., Godin, B., Ferrari, M. and Fuchs, H., (2009). Nanomedicine—challenge and perspectives. Angewandte Chemie International Edition, 48(5), pp.872-897.

Saeb, A., Alshammari, A.S., Al-Brahim, H. and Al-Rubeaan, K.A., (2014). Production of silver nanoparticles with strong and stable antimicrobial activity against highly pathogenic and multidrug resistant bacteria. The Scientific World Journal, 2014.

Sarker, S.D., Nahar, L. and Kumarasamy, Y., (2007). Microtitre plate-based antibacterial assay incorporating resazurin as an indicator of cell growth, and its application in the in vitro antibacterial screening of phytochemicals. Methods, 42(4), pp.321-324.

Sheikh, E., Bhatt, M.B. and Tripathi, M., (2018). Bio-based synthesised and characterized monodispersed *Curcuma longa* silver nanoparticles induce targeted anticancer activity in breast cancer cells. Pharmacognosy Magazine, *14*(57), p.340.

Shrivastava, S., Bera, T., Singh, S.K., Singh, G., Ramachandrarao, P. and Dash, D., (2009). Characterization of antiplatelet properties of silver nanoparticles. ACS nano, 3(6), pp.1357-1364.

Singh, H., Du, J., Singh, P. and Yi, T.H., (2018). Ecofriendly synthesis of silver and gold nanoparticles by *Euphrasia officinalis* leaf extract and its biomedical applications. Artificial cells, nanomedicine, and biotechnology, *46*(6), pp.1163-1170.

Singh, H., Du, J., Singh, P. and Yi, T.H., (2018). Extracellular synthesis of silver nanoparticles by *Pseudomonas sp*. THG-LS1. 4 and their antimicrobial application. Journal of pharmaceutical analysis, 8(4), pp.258-264.

Singh, H., Du, J., Singh, P. and Yi, T.H., (2018). Role of green silver nanoparticles synthesized from *Symphytum officinale* leaf extract in protection against UVB-induced photoaging. Journal of Nanostructure in Chemistry, 8(3), pp.359-368.

Sudheer Khan, S., Bharath Kumar, E., Mukherjee, A. and Chandrasekaran, N., (2011). Bacterial tolerance to silver nanoparticles (SNPs): *Aeromonas punctata* isolated from sewage environment. Journal of basic microbiology, 51(2), pp.183-190.

Tomaszewska, E., Soliwoda, K., Kadziola, K., Tkacz-Szczesna, B., Celichowski, G., Cichomski, M., Szmaja, W. and Grobelny, J., (2013). Detection limits of DLS and UV-Vis spectroscopy in characterization of polydisperse nanoparticles colloids. Journal of Nanomaterials 13, p.60.

Veerasamy, R., Xin, T.Z., Gunasagaran, S., Xiang, T.F.W., Yang, E.F.C., Jeyakumar, N. and Dhanaraj, S.A., 2011. Biosynthesis of silver nanoparticles using mangosteen leaf extract and evaluation of their antimicrobial activities. Journal of Saudi Chemical Society, 15(2), pp.113-120.

Yah, C.S. and Simate, G.S., 2015. Nanoparticles as potential new generation broad spectrum antimicrobial agents. DARU Journal of Pharmaceutical Sciences, 23(1), p.43.

Zweifel, U.L. and Hagstrom, A., 1995. Total counts of marine bacteria include a large fraction of non-nucleoid-containing bacteria (ghosts). Applied and Environmental Microbiology, 61(6), pp.2180-2185.

Medical
Communication

Biosci. Biotech. Res. Comm. 12(1): 36-45 (2019)

BBRC
Bioscience Biotechnology
Research Communications

Investigations on the development of biodegradable nanoparticles for anti-cancer drug

Seyed Goodarz Fallah Vahdati

Department of Doctoral Pharmacy, Mazandaran University of Medical Sciences (Mazums) Sari, Iran

ABSTRACT

In this research study, it has been attempted to synthesize mPEG-PCL dual copolymers and use their nanoparticles for tamoxifen anticancer drug delivery. Tamoxifen is a non-steroidal anti-estrogen that also has weak estrogenic effects. Tamoxifen is used to treat breast cancer and infertility dependent on oligomenorrhea or secondary amenorrhea. This drug inhibits estradiol receptors and, using it, ovulation involves the occupation of estrogen receptors and eliminates the inhibitory effect of the hormone and thereby stimulates the release of the gonadotrophin-releasing hormone from the hypothalamus. In order to increase the local concentration of tamoxifen in Estrogen Receptor (ER) positive breast cancer, we have prepared and characterized nanoparticle formulation using methoxy poly (ethylene glycol) –Poly (ε-caprolactone) (mPEG-PCL). In this study, PEG-PCL copolymers were synthesized from mPEG and ε-caprolactone (ε-CL) using $Sn(oct)_2$ as catalyst by ring opening polymerization. The copolymers were prepared and characterized by ^{1}H-NMR, FTIR, DSC and GPC. From the results, it was clear that nanoparticles showed sustained release behavior for a long period of time. These results suggest that the nanostructure of mPEG-PCL nanoparticles can be used as a promising candidate for sustained release of tamoxifen.

KEY WORDS: NANOPARTICLES, MPEG-PCL, TAMOXIFEN, CONTROLLED DRUG DELIVERY

INTRODUCTION

Nanotechnology has enormous potential in various fields, used in the development of insecticides, pharmaceuticals (Manjili et al, 2018), and electronics. Nowadays, nanoparticles have found widespread use that can be mentioned in several ways: dermal delivery, as antimicrobial and anticancer agents, carries peptide and protein medications such as insulin, as well as carriers of anti-inflammatory and respiratory drugs. Also, some biodegradable polymer-derived drug delivery systems, such as nanoparticles delivering anticancer agents, are

ARTICLE INFORMATION:

Corresponding Author: g.vahdati@aftermail.ir
Received 27th Dec 2018
Accepted after revision 25th March 2019
BBRC Print ISSN: 0974-6455
Online ISSN: 2321-4007 CODEN: USA BBRCBA
Thomson Reuters ISI ESC / Clarivate Analytics USA
NAAS Journal Score 2019: 4.31 SJIF: 4.196

Online Contents Available at: http//www.bbrc.in/
DOI: 10.21786/bbrc/12.1/5

commercially available (Sajadi Tabassi, 2012). PCL-PEG-PCL is a thermo- sensitive copolymer which is more flexible than PCL-PEG diblock copolymer for drug loading and drug delivery, (Kesente, 2017, Zamani et al, 2018).

Biodegradable polymeric materials are ideal carrier systems for biomedical applications. Features like controlled and sustained delivery, improved drug pharmacokinetics, reduced side effects and safe degradation make the use of these materials very attractive in a lot of medical fields, with dermatology included (Bunker, 2012). Biodegradable polymers have several advantages over non-biodegradable polymers for controlled drug delivery. It does not require surgical use after use, which is the most important advantage in a drug that has no surgical complications. Natural and synthetic biodegradable polymers have good properties, such as biocompatibility, biodegradability and high mechanical resistance. They have a negligible toxicity, and their destruction is non-toxic. Due to their mechanical properties, they are suitable for a wide range of specifications. Natural biodegradable polymers such as gelatin, albumin, chitosan, hyaluronic acid, and biodegradable synthetic polymers such as Poly(ε-caprolactone) PCL, PEO, and aliphatic thermoplastic polyester, such as Poly(lactic acid) and poly(lactid-co-glycolid), are fully investigated for drug delivery systems, (Verhoef, 2013).

Polyethylene glycol is a non-ionic polyether that has excellent biocompatibility. Ethylene oxide is non-toxic and approved by the FDA. Polyethylene glycol is a neutral polymer with end hydroxyl groups that has poor hydrogen bands, PEG molecules can be added to drug carriers through a number of different routes, including covalently.When PEG is covalently attached to the protein, it is biologically stored, and when linked to covalently, PEG can help solubilize other molecules. PEG is soluble in water and a few organic solvents. One of the biggest benefits of PEG for drug delivery systems is its ability to stay long in the body (Jenkins et al, 2016). Poly (ethylene glycol) (PEG) has been used on the outer surface of polymeric micelles, due to its beneficial characteristics of pharmacokinetic of the micelles; i.e., long-circulating characteristics and significant tumor accumulation. Considering its properties such as nontoxicity, hydrophilicity, solubility in water and organic solvents, and absence of antigenicity and immunogenicity, PEG could be used for many clinical applications (Kelley et al, 2016).

Polycaprolactone is an aliphatic polyester and its monomeric form ε-caprolactone is a biodegradable and biodegradable, non-toxic polymer having a semi-crystalline structure and a melting point of about 59-64° C, hydrophobic, as well as a low glass transition temperature of about -60 °C, is also synthesized by loop polymerization, (Danafar et al, 2012).

Copolymers are in fact polymers that are polymerized by two or more different monomers and have different properties of homopolymers. Today, due to the various properties of copolymers, attention has been paid to their application in various fields, especially drug delivery. Among these copolymers, it can be noted that mPEG-PCL copolymers can, due to the duality, create a variety of polymer particles by varying the proportion of hydrophobic to hydrophilic. The obvious properties of these copolymers are their biodegradability, which in the body turns into nontoxic absorbent metabolites. These properties have made these polymers a lot of potential for applications in areas of nanotechnology, tissue engineering and drug chemistry. The nanoparticles obtained by these copolymers, due to their core-shell property, have the potential to store the drug in the nucleolar nucleus (PCL) and the shell (PEG) has a dual role in particle stabilization and bioassay distribution. This copolymer is used to create drug carrier systems, slow release. Copper mPEG-PCL is used with dual-mode behavior to form core-shell core membranes. This polymer carrier, as a carrier of hydrophobic drugs, increases circulation time in the blood and reduces the absorption of nanoparticles by the liver, (Rychter et al, 2018).

Copolymer PCL-PEG-PCL was synthesized by loop polymerization method at 120 ° C and 24 hours by Keng-Lun Chang et al (Rychter et al, 2018). Then, the copolymer nanoparticles were used as a lauric acid carrier for the treatment of acne vulgaris. The size of the nanoparticles was about 24-24 nm. Hiremath in a research paper, prepared polyacroclactone injectable microspheres loaded with tamoxifen by solvent evaporation and in the presence of surfactant (PVA) for the treatment of breast cancer. They produced microspheres with a percentage of surfactant 0.4% and 0.8% with varying levels of tamoxifen and pcl. When 0.4% PVA was used, the mean size of 44-48 nm and the loading rate of the drug in microspheres were higher compared with 0.8% PVA was used, the size of the microspheres was 26-28 nm and the drug loading was lower than the first one. This is due to the reduction in the tension between the organic phase and the blue phase during the fabrication of nanoparticles and the increase in viscosity in the final blue phase.

Copolymer mPEM-PCL was synthesized by Wichuda et al (2011) using methoxypoly (ethylene glycol) and poly (caprolactone) and the Sn (Oct) 2 catalyst, and the nanoparticles of this copolymer were prepared using nanotube and without any surfactant preparation. Became According to TEM analysis, spherical nanoparticles have a smooth surface. The mean particle size and glass transition temperature decreased and the melting temperature significantly increased with increasing mPEG / PCL ratio. Authors have reviewed the two drugs Ibuprofen

and Indomethacin in PCL-PEG-PCL triloclopropylmer nanoparticles and the effect of nicotinic acid on the production of nanoparticles. Increasing the amount of nicotinic acid increases the particle size and increases the hydrophobicity of the polymer, increasing drug loading for both drugs compared to nicotine-free nanoparticles. Shakiba et al (2017) in a study to achieve the controlled release of ATRA, PCL-PEG-PCL copolymer with average molecular weight of 5.34 kDa was synthesized. The nanosized micelles were prepared from copolymer by nano-precipitation method. In the case of 10% drug to polymer ratio, more than 80% of the drug was released within 3 days, whereas for ratio of 2% more than 90% of the drug was released within 3 h. The cytotoxic study performed by MTT assay showed that H1299 survival percent decreased significantly (P≤0.05) after exposure to drug-loaded micelles, while no proliferation inhibition effect was observed by either free ATRA or blank PCL-PEG-PCL micelles.

Gavasane and Pawar (2014) believed that polymers are becoming increasingly important in the field of drug delivery. The pharmaceutical applications of polymers range from their use as binders in tablets to viscosity and flow controlling agents in liquids, suspensions and emulsions. Polymers are classified as biodegradable and nonbiodegradable. Biodegradable polymers have been widely used in biomedical applications because of their known biocompatibility and biodegradability. The present communication gives an overview of the different biodegradable polymers that are currently being used in the development of controlled drug delivery system.

MATERIALS AND METHODS

Stannous 2-ethyl-hexanoate [Sn (Oct) 2], Dichloromethane, Petroleum ether, Chloroform, Ethanol, Methanol, Acetone, ε-Caprolactone, Methoxyethylene glycol, Tetrahydrofuran, Methoxyethylene oxide, Calcium Hydride, PVA, all of which were used with high purity from Merck and Sigma, and also tamoxifen citrate from Iran Hormone Inc. The copolymer of mPEG-PCL was synthesized by loop-polymerization of caproclactone-free monomer in the presence of dry methoxy-polyethylene glycol as a primer and catalysts of tinctanate (reaction 1).

In this way, the amount of 3 g of mPEG (MW = 5000) is introduced into a balloon of a span and dried under vacuum and at a temperature of 80 ° C for 24 hours.

The 6 g is taken from a monomeraproclactone in a balloon for 1 week in its calcium hydrogen hydride after the end of the desired period by the Buchner funnel and the vacuum pump. mPEG and caprolactone in a spatula, then add the Sn $(oct)_2$ catalyst at 0.01 milloles per mMEG of mPEG hydroxyl group to the contents of the balloon. Then the vacuum balloon is placed in the bath of oil. Under nitrogen atmosphere and magnetic stirring, the reaction temperature was adjusted to 150 ° C and the reaction time was allowed for 12 hours. Then cool the system, dissolve the copolymer into chloroform, and dissolve in cold ether. Collect the precipitate with filter paper and dry it.

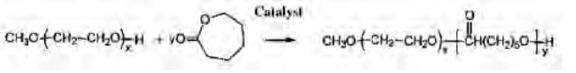

Reaction (1) mPEG-PCL Copolymer Synthesis Route

Analysis of copolymers mPEG-PCL

^{1}HNMR has been used to determine the copolymer structure of mPEG-PCL. ^{1}HNMR spectra were taken with Bruker 400MHz device at 25 ° C. Dieter chloroform (CDCL3) has been used as solvent and tri-methyl ketone (TMS) as the internal standard. The spectra taken in (CDCL3) were used to determine the molecular weight of synthetic copolymers by using sub-surface integration of various chemical groups. The ratio of lactone to ethylene glycol in synthetic copolymer can be calculated using Equation 1.

$$PCL:EO=\frac{\frac{Ia}{3}}{\frac{Ie}{4}}=1.33\times\frac{Ia}{Ie} \quad (1)$$

In this equation, Ia is the integral of the subliminal surface associated with PCL, which appears in the range of 1.5-1.6 ppm in the spectrum, and Ie is the integral of the PEG methylene group substrate, which is about 3.6-3.7 ppm, is observed.

When the PCL / EO ratio is synthesized in copolymer, PCL polymerization degree is calculated by considering the degree of polymerization of PEG starting from Equation 2. Finally, the molecular mass of copolymer is obtained using equation 3.

$$DP_{PCL}=DP_{PEG}\times PCL/EO \quad (2)$$

$$M_{n(mPEG-PCL)}=(DP_{PCL}\times M_{W\,PCL})+(DP_{PEG}\times M_{W\,EO}) \quad (3)$$

FT-IR Infrared Spectroscopy

To confirm the mPEG-PCL copolymer formation, the FT -IR spectrum has been used. The FT-IR spectra of various specimens were recorded using a Bruker spectrometer (FT-IR).

Gel Permeation Chromatography (GPC)

The average molecular mass and mPEG-PCL copolymer molecular mass distribution are analyzed by chromatographic gel analysis. For the GPC analysis, the German Knauer machine was used. The sample was completely dissolved in pure tetrahydrofuran and, after

being injected into the column, and compared with the calibration graph, drawn using standard polystyrene; the molecular mass and the synthesized PolyDispersity copolymer were calculated.

Differential Scaling Calorimeter (DSC)

DSC analysis was used to study the thermal behavior of mPEG-PCL copolymers and their nanoparticles. The samples were heated at a temperature of 10 °C / min and measured in a range of 25-200 °C using a Mettler Toledo, Star SW 9.30, manufactured by England.

Analysis of the morphology of nanoparticles by Scanning Electron Microscopy (SEM)

SEM (Scanning Electron Miroscopy) is used to capture specimens. In this way, a layer of gold is placed on the sample and the electron beam is emitted. Then, they shrink two or three electron beam concentrating lenses so that when they come in contact with the specimen diameter it is between 10-2 nm. Then several pictures are taken from the sample. For SEM imaging, the XL30 was used as an XL series manufactured by Philips and Hitachi S4160 Cold Field Emission.

Study of drug release in vitro at pH = 40.5

To study drug release, place 10 mg of suspension of nanoparticles in 2 ml of buffer and place in a 12000 cut off bag and place it in a container containing 13 ml phosphate buffer (pH = 4.50). Place the bag containing the dialysis bag in a 37-°C chiccroncobacterial device and remove 1 ml from the outer solution of the dialysis bag at specified times, and replaced with fresh buffer, and the amount of drug released by the UV spectrophotometer measured at 250 nm wavelengths. Each of the measurements is repeated three times, and the average of these three data is used to calculate the amount of drug released.

RESULTS AND DISCUSSION:

Investigating the FT-IR spectrum of the mPEG-PCL copolymer

In Fig. 1, the FT-IR spectrum of mPEG-PCL is shown. From the mPEG-PCL Copolymer FT-IR spectrum, it can be seen that the absorption band at the frequency of 1108 cm^{-1} and 1240 is related to the tensile bond (C-O). The sharp and severe absorbing strip at a frequency of 1722 cm^{-1} shows the existence of steric carbonyl groups (C = O), indicating the formation of mPEG-PCL copolymer. Methylene hydrone ($-CH_2-$) adsorb two C-H adsorbents, which are related to the symmetric and asymmetric adsorbent adsorption, which absorbs the first in 2869 cm^{-1} and the second in 2943 cm^{-1}

Investigating the ^{1}HNMR spectrum of mPEG-PCL copolymer

After reviewing the raw materials used in synthesis to confirm the synthesis of copolymer, the structure. As

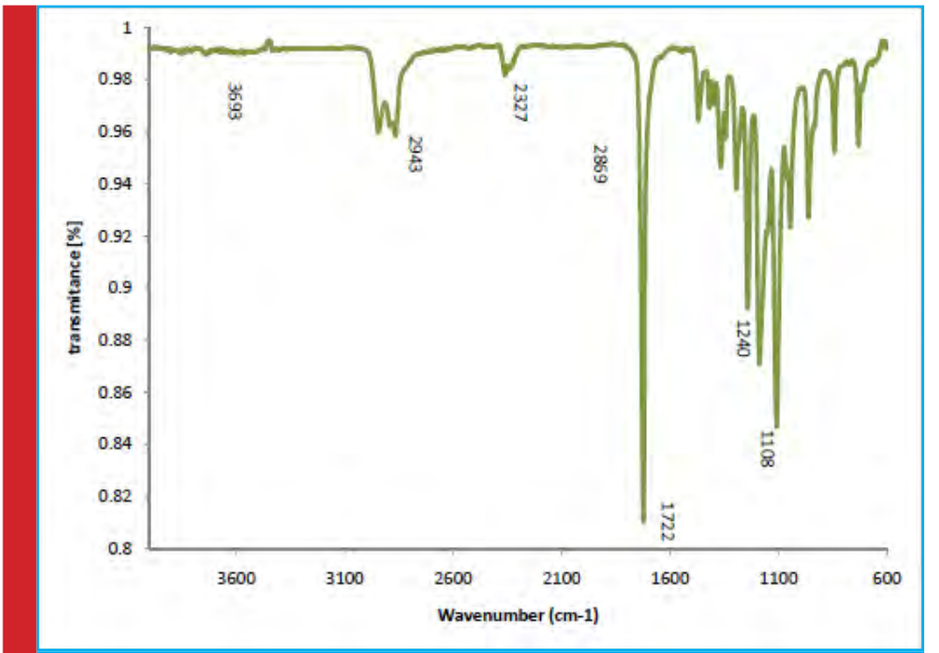

FIGURE 1. FT-IR spectrum of mPEG-PCL copolymer

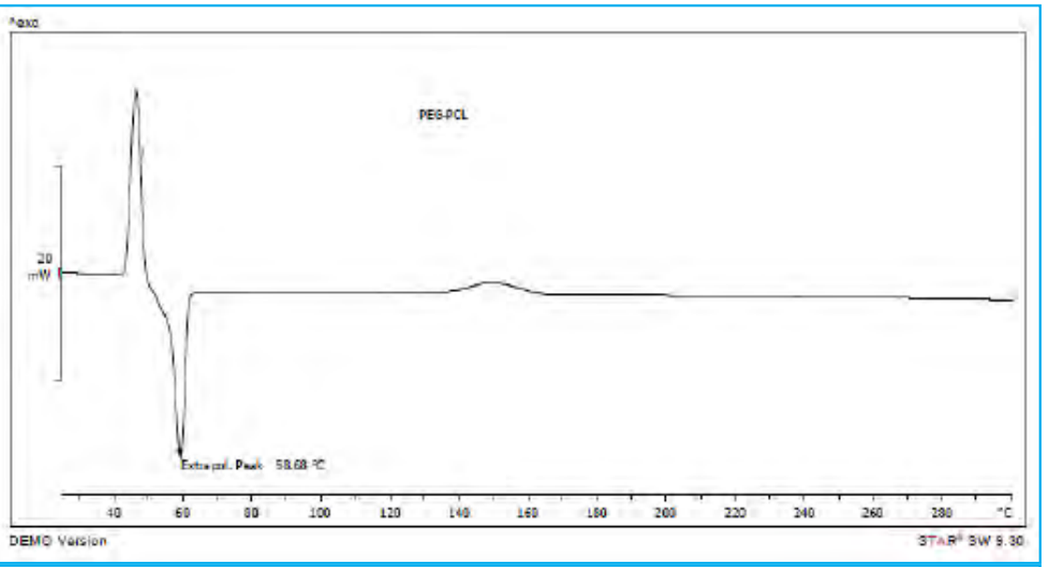

FIGURE 2. The DSC Spectrum of Mpeg-PCL copolymer, it appears in the peak temperature range at 40.3 °C, which can be attributed to the crystallization temperature of PEG.

can be seen, the peak in the area of 3.38 ppm and 3.64 is related to the methoxy group and the methyl group PEG. Peak 1.3 ppm (2H, g), 1.6 ppm (4H, f), 2.2 ppm (2H, e), ppm 4.06 (2H, h) 3.4 ppm (3H,a) respectively corresponding to group -$(CH_2)_3$-,(- $(CH_2)_2$-$OCCH_2$-) - and (-CH_2OOC-) caprolactone. The weight of the molecular weight calculated with ^{1}HNMR is 21000 g / mol.

Investigating the Differential scanning calorimeter (DSC) spectrum of mPEG-PCL copolymer

Thermal analysis can be defined as measuring the properties of a polymer sample against temperature variations. The most important and final factor in the study of polymers is to measure and measure their thermal stability. Usually weight loss is used to measure thermal stability. Weight variations are recorded against a rise in temperature or against a rise in time at constant temperature. Differential Schematic Thermometry (DSC) is a method in which the difference in thermal energy input to the sample and reference material is measured as a function of temperature. The mPEG-PCL copolymer DSC shows in Fig. 2, the peak of the sample is in the range of 67.42 °C, which is a thermoforming courier. Previous studies have shown that PEG and PCL hemopolymers, both of which are semi-crystalline polymers, have a melting point of 62 °C and 60 °C, respectively. However, in the copolymer spectrum, the thermal event belongs to the melting point of PEG and PCL. In addition, it appears in the peak temperature range at 40.3 °C, which can be attributed to the crystallization temperature of PEG.

Investigating the GPC spectrum associated with mPEG-PCL copolymer

The molecular mass of the weighted mass and molecular weight distribution of mPEG-PCL copolymer is investigated by analysis of gel chromatography. The sample is dissolved in the tetrahydrofuran and, after being injected into the column, and compared to the calibration graph compiled using standard polystyrene, the molecular mass and the synthesized poly-dispersed copolymer are calculated. The molecular mass distribution diagram is indicated in Fig. 3, which represents a peak at 7.02 seconds after sampling. After placing this time on the Exell chart, the value of mPEG = 5000 g / mol is the mass of the molecular weight of 24663 g/ mol.

Analysis and measuring the size of the nanoparticles

At this stage, after preparing the nanoparticles, the size of the nanoparticles prepared from the DLS sample was taken. According to the measurement of the size of the nanoparticles (Fig. 4), the mean particle size without drug loading was 184.4 nm with PDI = 0.418 obtained.

The average size of the polymer nanoparticles that was loaded onto the drug was investigated by the particle size chart, shown in Fig. 5. According to the size chart of nanoparticles, the average nanoparticle size of 151.7% was obtained with PDI = 0.328. Due to the lack of drug-loading nanoparticles at 184.4 nm, drug loading has not significantly changed the size of the nanoparticles, which can be a reason for absorbing the drug into nanoparticles.

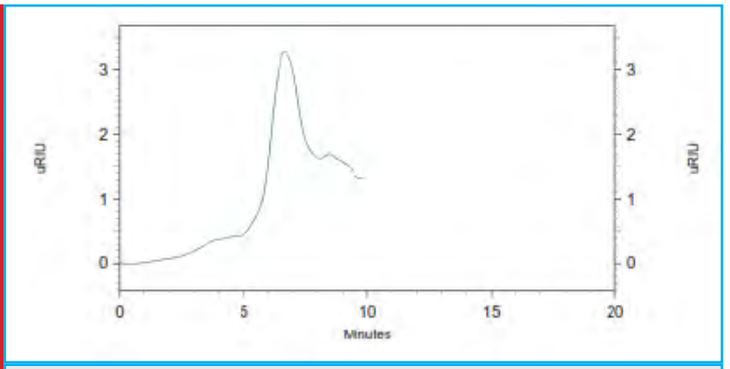

FIGURE 3. GPC Spectra of Mpeg-PCL copolymer, which represents a peak at 7.02 seconds after sampling.

SEM Analysis of Polymer Nanoparticles Loaded with Tamoxifen

The morphology of nanoparticles was investigated using SEM and its images are depicted in Fig. 6.After the preparation of nanoparticles loaded with tamoxifen, a SEM photo was taken, depicted in Figure 6. The SEM image shows that nanoparticles have a spherical shape and approximately one shape with a size of 234 nm. As can be seen, the average size of nanoparticles from a photographed image is well-matched with the size of the DLS.

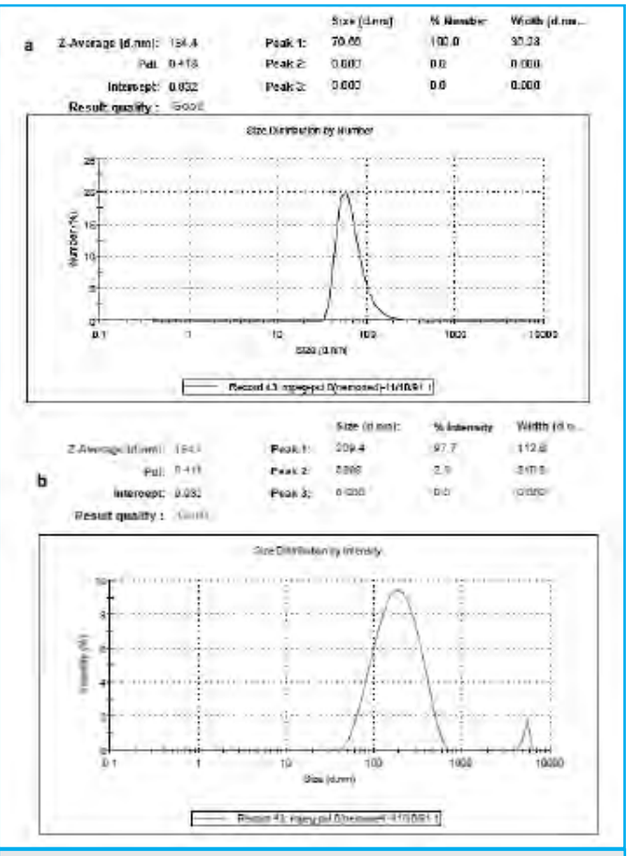

FIGURE 4. The curve of the size of polymerized nanoparticles synthesized without loading the drug, a) numerically, b) in intensity

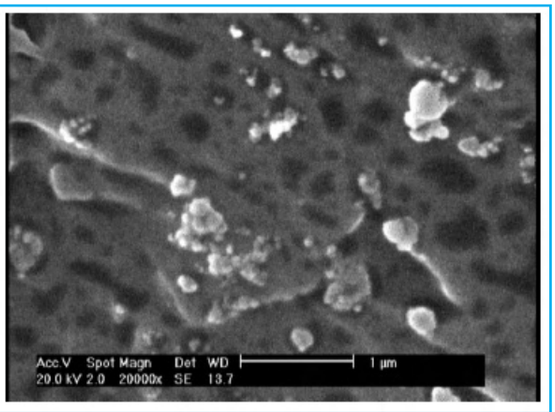

FIGURE 6.

FT-IR spectra of polymeric nanoparticles mPE-PCL loaded with tamoxifen

Regarding the structure of tamoxifen citrate (Fig. 7) and the FT-IR spectrum, the average absorption bands in 1590 cm^{-1} and 1471 cm^{-1} are related to the aromatic ring group. Absorption band in 2828 cm^{-1} of the unsaturated stretch C-H_3 group, absorption band of 2960 cm^{-1} of the CH_3 group. The 1217 cm^{-1} band represents the tensile C-O group, and the 1300 cm^{-1} band represents the C-N stretching group. The band in the 703 cm-1 region of the

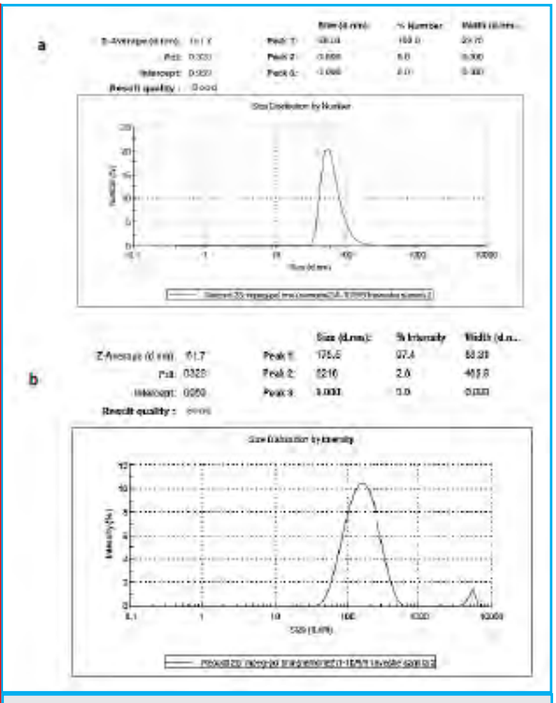

FIGURE 5. The size of nanoparticles loaded with tamoxifen (a) in numerical order b) in intensity

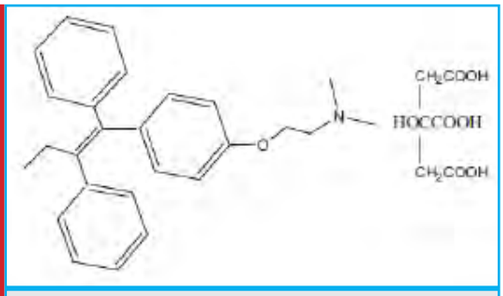

FIGURE 7. The structure of tamoxifen citrate

Ortho substrate and the 3010 cm^{-1} band represents the OH strain group (Fig. 8)

Comparison of the range of nanoparticles loaded with the mPEG-PCL copolymer spectrum and tamoxifen spectrum showed drug loading in nanoparticles. The existence of a band of 1602 cm^{-1} shows the aromatic ring in both of the two spectra of tamoxifen and nanoparticles. The 1728 cm^{-1} band in two spectra of copolymer and nanoparticles represents the carbonyl tensile group. The 1300 cm^{-1} band is available in two spectra of tamoxifen and nanoparticles that specify the C-N group. The C = O group has a tensile strength of 1217 cm^{-1} in two spectra of tamoxifen and nanoparticles. The presence of bands of 2868 cm^{-1} and 2940 cm^{-1} in two spectra of copolymers and nanoparticles, indicating methylene tensile CH groups. The results from the following spectrum (Figure 9) showed that tamoxifen drug was loaded onto polymer nanoparticles.

DSC spectrum of tamoxifen citrate

The DSC for tamoxifen shows that the peak from the specimen is in the range of 145.43 °C, which is a thermosetting peak and represents the melting point of tamoxifen citrate (Figure 10).

Tamoxifen measurement

Figure 11 shows the tamoxifen curve at a maximum wavelength of 250 nm. Which shows very good linear citizenship of the concentration of tamoxifen with its adsorption in an organic environment. The linear equa-

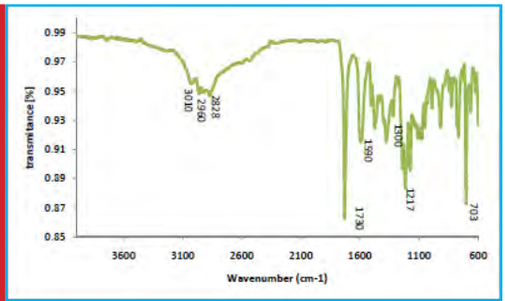

FIGURE 8. FT-IR spectrum of tamoxifen citrate

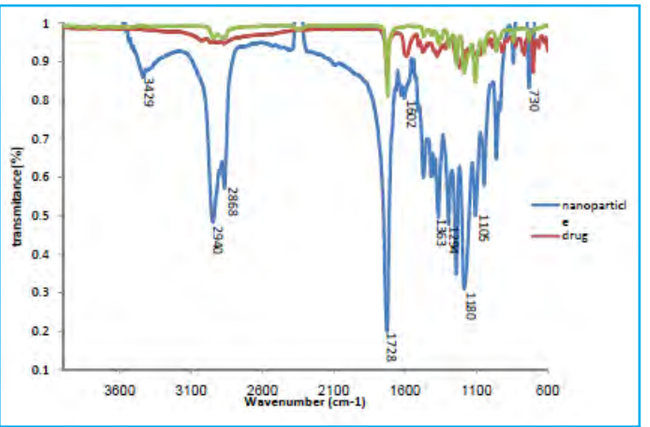

FIGURE 9. FT-IR Spectrum of Nanoparticles

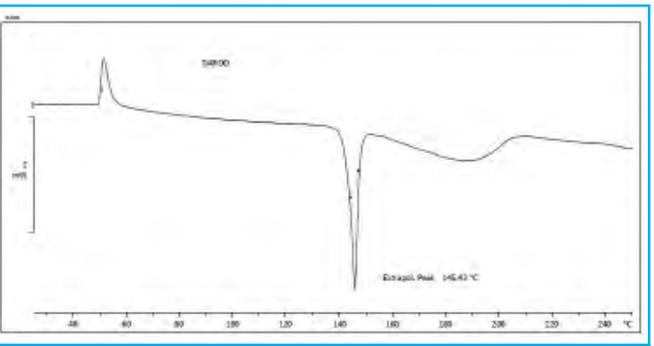

FIGURE 10. DSC spectrum of tamoxifen citrate

tion obtained from this graph has been used to estimate the concentration of tamoxifen in assessing the drug loading rate in the drug release analysis.

Determination of tamoxifen loading and encapsulation in mPEG-PCL copolymer micelles according to the calcification curve of tamoxifen

According to the following calculations, the amount of drug loaded and encapsulated was 12.909% and 70.025%, respectively. The reason for loading the drug in tamoxifen in the hydrophobic nucleus of the nanoparticles (the PCL portion) is the hydrophobic nature of the drug.

$$\%DL = \frac{14.005}{108.49\ mg\,(drug+polymer)} \times 100 = 12.909$$

$$\%EE = \frac{14.005}{20mg(\ drug)} \times 100 = 70.025$$

According to the following calculations, if the percentage of precipitation of nanoparticles loaded with

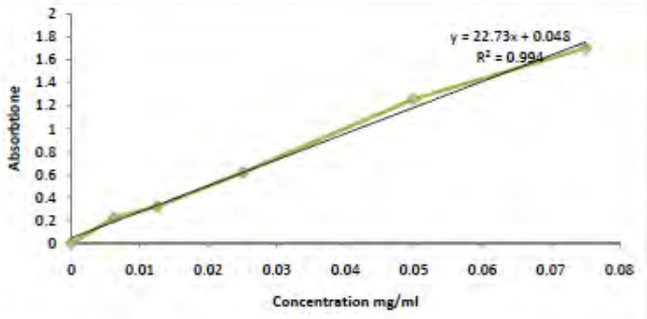

FIGURE 11. Calibration curve for tamoxifen citrate at γ = 250 nm

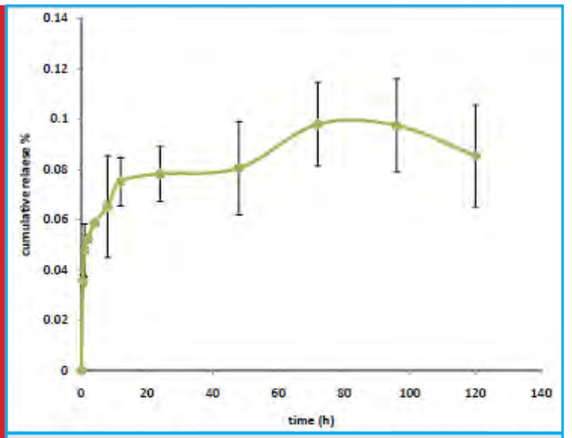

FIGURE 12. The graph of drug release from nanoparticles at pH = 7.40 contains tween 80

tamoxifen is 100%, the theoretical loading of the drug should be about 16.66%.

$$DL = \frac{20}{120mg\,(drug+polymer)} \times 100 = 16.66\,\%$$

Based on the results obtained and the proximity of theoretical and empirical results, the degree of encapsulation of the drug in nanoparticles is determined. The mPEG-PCL nanoparticles show a high ability to encapsulate tamoxifen.

Reviewing the drug release pattern from nanoparticles synthesized at pH = 7.40

Figure 13 shows the release of tamoxifen from nanoparticles of mPEG-PCL in a phosphate buffer with pH = 7.40 contain thiamine. Tamoxifen citrate is a highly hydrophobic drug. Therefore, phosphate buffer containing 0.01 (w / v) Tween 80 was used to increase the solubility of the drug. According to the chart, in the first 72 hours, 9.82% of the tamoxifen drug was released from the nanoparticles.

In this research work, it was first mPEG-PCL polymer in the laboratory synthesized. Subsequently, nanoparticles containing tamoxifen were prepared by a single emulsion method, after which the size and surface profile of them were evaluated. Finally, drug release from nanoparticles was investigated at various pH levels. In this collaborative research, mPEG-PCL copolymer was synthesized with a mPEG / PCL ratio of 1.3, and its structure and composition were confirmed by ^{1}HNMR and FT-IR. The thermal behavior of copolymer synthesized by DSC was investigated and the molecular mass of the copolymer synthesized by GPC was determined. In the FT-IR spectrum, the mPEG-PCL copolymer exhibits a sharp absorption band at a frequency of 1722 cm^{-1}, which confirms the presence of carbonyl steary groups (C = O) and shows a severe peak in 2963 cm^{-1} representing ethylene groups of PEG that can confirm copolymer synthesis. The results of mPEG-PCL copolymer synthesis showed that the copolymer was completely synthesized. The DSC of mPEG-PCL copolymer indicates that the sample courtesy is in the range of 67.42 ° C, which is a thermosetting peak and represents the melting point of PCL and PEG.

The polymer was used to make biodegradable nanoparticles based on polyethylene glycol and polycaprolactone. Copolymer micelles mPEG-PCL were prepared by single emulsion method and tamoxifen drug was loaded. The particle size was about 151.7 nm and particle zeta potential was 13.9 mv. The drug loading efficiency in nanoparticles and the drug release profile in vitro were measured by UV spectroscopy.

The results showed that the loading and encapsulated drug was 12% and 70%, respectively, indicating high drug loading in nanoparticles. Data from drug release from nanoparticles in different environments also showed that the drug was controlled and released from nanoparticles over a long period of time. Overall, it can be concluded from the current research that pharmaceutical-containing mPEG-PCL nanoparticles can be considered as a good option for controlled release and tamoxifen in the treatment of cancer. Generally, the results of this research work provide valuable information for the development of new pharmaceutical systems and the production of high-strength polymers and a higher volume-to-volume ratio in the structure of nano-materials, especially mPEG-PCL-based nanoparticles.

REFERENCES

Alex Bunker (2012). Poly (Ethylene Glycol) in Drug Delivery, Why Does it Work, and Can We do Better? All Atom Molecular Dynamics Simulation Provides Some Answers. Physics Procedia. Volume 34, 2012, Pages 24-33.

Chao. C, Ming. H, Chun. H. (2011) The Nanoparticles for Combating Acne Vulgairs: In-vitro Efficacy of Lauric Acid- Loaded PCL-PEG-PCL on Propion bactrium acne, International Conference on Nanotechnology and Biosensors, IPCBEE 2 (2011) IACSIT Press, Singapore.

Chen, Y., Chen, X., Chen, Y., Wei, H., Lin, S., Tian, H. Gu, X. (2018). Preparation, characterisation, and controlled release of sex pheromone-loaded MPEG-PCL diblock copolymer micelles for Spodoptera litura (Lepidoptera: Noctuidae). PLoS ONE, 13(9), e0203062. http://doi.org/10.1371/journal.pone.0203062

Danafar H, Rostamizadeh K, Davaran S, Hamidi M. Preparation and characterization of PLA-PEG-PLA tri-block copolymer polymersomes as a novel carrier for lisinopril. Res Pharm Sci. 2012;7(5):S398.

Ebrahim Shakiba, Saeedeh Khazaei, Marziyeh Hajialyani, Bandar Astinchap, Ali Fattahi (2017). Preparation and in vitro characterization of retinoic acid-loaded poly(ε-caprolactone)-

poly(ethylene glycol)-poly(ε-caprolactone) micelles . Research in Pharmaceutical Sciences, December 2017; 12(6): 465-478

Gavasane AJ, Pawar HA (2014) Synthetic Biodegradable Polymers Used in Controlled Drug Delivery System: An Overview. Clin Pharmacol Biopharm 3:121.doi:10.4172/2167-065X. 1000121

Hiremath. G.J, kusm. D.V. Tamoxifev. Loaded poly(ε-caprolactone) based injectable microspheres for breast cancer, International Journal of Pharmacy and Pharmaceutical Sciences. 2 (2010) 0975-1491.

Jenkins SI, Weinberg D, Al-Shakli AF, Fernandes AR, Yiu HHP, Telling ND, Roach P, Chari DM (2016). 'Stealth' nanoparticles evade neural immune cells but also evade major brain cell populations: Implications for PEG-based neurotherapeutics. J Control Release. 2016 Feb 28;224:136-145. doi: 10.1016/j.jconrel.2016.01.013. Epub 2016 Jan 11.

Kesente, M., Kavetsou, E., Roussaki, M., Blidi, S., Loupassaki, S., Chanioti, S., Detsi, A. (2017). Encapsulation of Olive Leaves Extracts in Biodegradable PLA Nanoparticles for Use in Cosmetic Formulation. Bioengineering, 4(3), 75. http://doi.org/10.3390/bioengineering4030075

Manjili H K, Malvandi H, Mousavi M S, Attari E, Danafar H. In vitro and in vivo delivery of artemisinin loaded PCL–PEG–PCL micelles and its pharmacokinetic study. Artificial cells, nanomedicine, and biotechnology. 2018; 46(5), 926–936. 10.1080/21691401.2017.1347880

Gou M, Wei X, Men K, Wang B, Luo F, Zhao X, Wei Y, Qian Z PCL/PEG copolymeric nanoparticles: potential nanoplatforms for anticancer agent delivery. Curr Drug Targets. 2011 Jul 1; 12(8):1131-50.

Rancan, F., Blume-Peytavi, U., & Vogt, A. (2014). Utilization of biodegradable polymeric materials as delivery agents in dermatology. Clinical, Cosmetic and Investigational Dermatology, 7, 23–34. http://doi.org/10.2147/CCID.S39559

Rychter M, Baranowska-Korczyc A, Milanowski B, Jarek M, Maciejewska BM, Coy EL, Lulek J (2018). Cilostazol-Loaded Poly(ε-Caprolactone) Electrospun Drug Delivery System for Cardiovascular Applications. Pharm Res. 2018 Jan 16;35(2):32. doi: 10.1007/s11095-017-2314-0.

Sajadi Tabassi SA, Khodaverdi E, Hadizadeh F, Rashid R. Preparation of hydrogels based on inclusion complexes of the triblock copolymer PCL-PEG-PCL with ε-cyclodextrin (ε-CD). Res Pharm Sci. 2012;7(5):S975.

Syed A.A. Rizvia Ayman M. Saleh (2016). Applications of nanoparticle systems in drug delivery technology. Saudi Pharmaceutical Journal. Volume 26, Issue 1, January 2018, Pages 64-70

Suksiriworaponga. J, Sriphab. K, Kreuterc. J, Junyapraserta. V.B, (2012) Functionalized (poly(-caprolactone))2-poly(ethylene glycol) nanoparticles with grafting nicotinic acid as drug carriers, International Journal of Pharmaceutics. 423 562-570.

Verhoef, J. J. F., & Anchordoquy, T. J. (2013). Questioning the Use of PEGylation for Drug Delivery. Drug Delivery and Translational Research, 3(6), 499–503.

Wichuda. N, Mangkorn. S-A, Yodthong. B. (2011) Biodegradable Blend Nanoparticles of Amphiphilic Diblock Copolymers Prepared by Nano-Precipitation Method, Journal of Biomaterials and Nanobiotechnology. 2 561-566.

Biotechnological Communication

Biosci. Biotech. Res. Comm. 12(1): 46-53 (2019)

BBRC Bioscience Biotechnology Research Communications

Overlap extension PCR to anneal multiple DNA fragments for high-throughput double stranded RNAi vector construction

K. Prasad Babu[1,3]*, M. Manamohan[3] and M. Krishna Reddy[2]

[1]*Division of Biotechnology, IIHR-ICAR, Hessaraghatta Lake Post, Hessaraghatta, Bangalore, India-560089*
[2]*Division of Plant Pathology, IIHR-ICAR, Hessaraghatta Lake Post, Hessaraghatta, Bangalore, India-560089*
[3]*Department of Biotechnology, Centre for post-graduate studies, Jain university, Bangalore, India*

ABSTRACT

RNA interference is a sequence dependent gene silencing mechanism with huge potential in agriculture. Virus disease management has become a daunting task due to the lack of availability of resistant cultivars. In this scenario, RNAi mediated viral resistance has acquired importance. RNAi can be employed to silence the viral genes conferring virus resistance. Transformation of the host with an RNAi vector synthesizing hairpin RNA is a prerequisite. It is highly desirable to develop multiple virus resistance due to the fact that, viruses counter the host RNAi by employing silencing suppressors there by leading to resistance breakdown. This can be addressed by targeting all the commonly infecting viruses along with viral slicing suppressors. This increases the complexity of RNAi vector construction as multiple fragments are involved to develop an ihp construct. OE(Overlap-Extension)-PCR is the method of choice due to its several advantages such as no extraneous sequences are incorporated unlike as in restriction based fragment joining and it is also simple and economical compared to other methods. In this experiment, we demonstrate the use of OE-PCR in the construction of an intron containing hairpin RNA synthesizing vector targeting seven genes from four viruses viz. that commonly to tomato and chilli for imparting multiple virus resistance viz. capsicum chlorosis virus, groundnut bud necrosis virus, cucumber mosaic virus and chilli veinal mottle virus. Seven viral gene fragments were joined together in to 1.64kb fragment by OE-PCR. The complete stretch was assembled into the pBI121 and mobilized in to Agrobacterium for transformation.

KEY WORDS: OVERLAP PCR, RNA INTERFERENCE, VIRUS RESISTANCE, AGROBACTERIUM

ARTICLE INFORMATION:

Corresponding Author: prasu8050655414@gmail.com
Received 29th Dec, 2018
Accepted after revision 26th March, 2019
BBRC Print ISSN: 0974-6455
Online ISSN: 2321-4007 CODEN: USA BBRCBA
Thomson Reuters ISI ESC / Clarivate Analytics USA
NAAS Journal Score 2019: 4.31 SJIF: 4.196

Online Contents Available at: http//www.bbrc.in/
DOI: 10.21786/bbrc/12.1/6

INTRODUCTION

Tomato (*Solanum lycopersicum* L.) and chilli (*Capsicum annum*) are commercially important vegetable crops grown globally. Virus management in these crops has been challenging in recent years due to intensive cultivation and spurt in the insect vectors population resulting in virus disease outbreak (Sastrosiswojo 1995; Umamaheswaran *et al*., 2003). Viral diseases caused by some major viruses like Tospovirus, Cucumovirus and Potyvirus results in immense economic loss in these crops productivity. Tospoviruses (capsicum chlorosis virus and groundnut bud necrosis virus) are negative single-stranded RNA virus, belongs to *Bunyaviridae* family and containing three genomic segments L, M and S, transmitted by thrips (Haan *et al*., 1990, 1991, Krishna Reddy *et al*., 2008). Cucumovirus (cucumber mosaic virus-CMV) is a positive sense single-stranded RNA virus belonging to family *Bromoviridae* (Palukaitis *et al*., 1992). Potyvirus (ChiVMV-chilli veinal mottle virus), belongs to the family *Potyviridae*, is a single molecule which is linear, positive-sense, single-stranded RNA (ssRNA). Potyvirus and cucumovirus are transmitted by insect vector aphids in a non-persistent manner (Berger *et al*., 2005). Current virus disease management involves prophylactics, roguing and insect vector control. Non availability of the resistance gene pools in most of the cultivated crops poses a serious hurdle in resistant breeding. In this regard RNA interference is highly promising in imparting virus resistance (Simon-Mateo and García 2011, Duan *et al*., 2012; Li *et al*., 2106; Jia *et al*., 2017).

RNA interference is a natural antiviral defense system, degrades the RNA molecules in a sequence-specific manner and it is activated in response to double-stranded RNA formed during viral replication (Voinnet *et al*., 2001). RNAi mediated gene silencing involves, formation of double-stranded RNA, so called “hairpin” RNA (hpRNA), formed by annealing of the reverse complementary sequence at one half of the RNA, which is recognized by and activates plant RNAi machinery leading to the degradation the viral RNA, finally plants recovering from viral infection. The expression of virus-specific dsRNA as hairpin structures renders the plants resistant against virus infection (Bonfim *et al*., 2007). In plants, intron-mediated hairpin RNA (ihpRNA) by incorporating an intron as a spacer sequence between the sense and antisense fragments results in higher gene silencing efficiency in the transgenic plants (Wesley *et al.,* 2001). Moreover, field level virus resistance is achieved by targeting multiple viruses in a single chimeric construct (Bucher *et al*., 2006; Zhang *et al*., 2011; Thu *et al.,* 2016; Hameed *et al.,* 2017).

Therefore, a cost efficient, high-throughput system for designing and making of ihpRNA constructs is in great demand. To achieve broad spectrum resistance, there is a need to target multiple virus genes, to join these fragments the selection of restriction enzymes may not be possible in case multiple fragment splicing due to the limited choice and incompatibility of restriction enzymes and also the introduction of extraneous non-target sequences might interfere with the silencing efficiency. Due to these difficulties, OE-PCR is the method of choice to join multiple fragments.

OE-PCR is a technique used to synthesize artificial genes, joining one or more DNA segments together to form a new genetic combination (Li *et al*., 2008) The OE-PCR was first described by (Higuchi *et al*., 1988). The basic principle of OE-PCR is that individual DNA fragments are designed to have a short stretch of their 3’ ends to be complimentary and these overlaps are extended in PCR to splice the two fragments in to one (Harton *et al.,* 1989), the initial PCR fragments then generate overlap gene fragments that can be used as new templates for another PCR to form a full length fragment (Heckman et al., 2007; Wäneskog and Bjerling 2014; Hussain and Chong 2016).

Targeting multiple viruses is important in aiming for RNAi based robust and durable resistance. In this study, RNAi gene construct against broad spectrum of viruses was designed based on the conserved sequences from four different viruses commonly infesting tomato and chilli *viz.,* Capsicum chlorosis virus-nucleocapsid (CaCV-N), Groundnut bud necrosis virus-Nucleocapsid and Non-structural proteins (GBNV-N and NSs), Cucumber mosaic virus-2b and Coat protein (CMV-2b and CP) and Chilli veinal mottle virus-helper component proteinase and coat protein (ChiVMV HC-Pro and CP). We used OE-PCR to join all seven fragments in a single stretch to construct hpRNAi-MVR binary vector for plant transformation to impart multiple virus resistance in tomato and chilli. This is the first report by using OE-PCR for joining seven gene fragments in ihpRNA construct for plant virus resistance.

MATERIALS AND METHODS

Selection of target gene sequences for dsRNA construct

Based on the literature survey, we have selected major virus diseases affecting tomato and chilli in Southern India, viz. GBNV, CaCV, CMV, ChiVMV diseases have caused a drastic yield loss in India. To develop broad spectrum ihpRNA vector, we have selected the above four viruses, from these 7 crucial genes were selected to express hairpin RNA in transgenic plants. The sequences

of these genes were retrieved from GenBank at the National Center for Biotechnology Information (NCBI) (http://www.ncbi.nlm.nih.gov/BLAST/). BioEdit-multiple sequence alignment using Clustal W (Hall 1999) was carried out and highly conserved regions were selected for dsRNA design from the alignment of about 100-150 viral sequences reported. The selected conserved regions of CaCV-N gene (255bp), GBNV-N gene (255bp) and GBNV-NSs gene (261bp) from Tospovirus, CMV 2b (232bp) and CMV CP gene (214bp) from Cucumovirus and ChiVMV HC-Pro (209bp) and ChiVMV-CP (221bp) from Potyvirus respectively. The detailed GenBank accession for the selected genes included in the (table 1). Off-target effect minimization was carried out using dscheck and Genome BLAST analysis to select highly conserved regions.

Overlap Primer designing and amplification of desired gene fragments

The clones of viral genes were obtained from the Division of Plant pathology, ICAR-IIHR, Bengaluru. The overlap primers were designed for the individual fragments of fragment S1, S2, S3, S4, S5 and S6 and it generates overhang region of 10-15bp to join the next fragment. No restriction enzymes were incorporated between these fragments. Restriction sites of *Bam*H1/*Sac*1 and *Sex*A1 were added in 5' region of S1 fragment and 3' region of S7 fragment to form ihpRNA construct forming sense: Intron: Antisense orientation. All individual fragments were amplified using PCR. All PCR reactions were carried out in 25µl reaction contains 50ng of template, the PCR mix contains 1x Phusion HF buffer 3% DMSO, 200 µM DNTPs, 0.5 µM PCR primers and 1U Phusion® High-Fidelity DNA Polymerase (NEB, USA). The PCR conditions were as follows: initial denaturation for 30 seconds at 98 °C, followed by 35 cycles of denaturation 10 seconds at 98 °C, 30 seconds at 55 °C annealing, 10 seconds at 72 °C extension and the final extension 30 minutes at 72 °C.

The amplified products were purified using NucleoSpin® Gel and PCR Clean-up kit (Macherey-Nagel, Germany), and ligated into PTZ57R/T cloning vector by using T4 DNA ligase (Thermo scientific, USA). The ligated products were transformed in to *E.coli* (DH5α) using heat shock method. The transformed clones were sequenced by Sanger Sequencing method (Eurofins Genomics India Pvt Ltd, Bangalore). The confirmed clones were used further for overlap PCR.

Joining of fragments by Overlap PCR:

Three rounds of overlap PCR were carried out to join all 7 fragments. The PCR parameters for the modified Overlap PCR is as follows: PCR was carried out in a 50µl reaction contains 50ng of purified individual fragments, the PCR mix contains 1x Phusion HF buffer 3% DMSO, 200 µM DNTPs, 0.5 µM PCR primers and 1U Phusion® High-Fidelity DNA Polymerase (NEB, USA) the PCR mix contains no primers. The overlap PCR as follows: initial denaturation for 1 minute at 98 °C followed by extension at 72 °C for 15 minutes, pause/hold the programme at 72 °C or place the tubes in ice, then add the end primers and resume the programme followed by 35 cycles of denaturation for 10 seconds at 98 °C, annealing for 30 seconds at 60 °C, extension for 30s/kb at 72 °C and final extension for 30 minutes at 72 °C. The above PCR conditions were followed to join all fragments.

In First round of overlap PCR, the fragments of S1+S2 were joined by using F1 and R2 primers, S4+S5 fragments were joined by using F4 and R5 primers and the fragments of S6+S7 were joined by using F6 and R7 primers respectively. An aliquot of all post PCR products were confirmed on agarose gel, the confirmed products were purified by NucleoSpin® Gel and PCR Clean-up kit (Macherey-Nagel, Germany). The **Second round** overlap PCR was carried out by joining the fragments of S1+S2 with S3 using F1 and R3 primers and fragments of S4+S5 with S6+S7 were joined using F4 and R7 primers. An aliquot of post PCR products was used for confirmation of amplification and the rest was used for purification. Likewise, **the final** round PCR was continued by joining the fragments of S1+S2+S3 with S4+S5+S6+S7 using F1 and R7 primers (Fig 1 and 2). The *Bam*H1/*Sac*1 restriction sites were incorporated in the F1 primer and *Sex*A1 restriction site were incorporated in R7 primer, used to form Sense and Antisense fragments. A complete stretch 1.647kb fragment was purified and ligated in to PTZ57R/T cloning vector (Thermo scientific, USA) using T4 DNA ligase (Thermo scientific, USA) and the ligated product was transformed in *E.coli* (DH5α cells). Plasmids were isolated using alkaline lysis method and three clones were sequenced for confirmation of the fragments joined by OE-PCR.

The complete stretch containing all three fragments of 7 genes in sense and antisense orientation interspersed by PDS intron was released using *Bam*H1 and *Sac*I restriction sites, this fragment was purified and ligated into the binary vector pBI121 between CaMV 35S promoter and NOS terminator using *Bam*H1 and *Sac*I sites. The ligation of sense-intron-antisense fragments in pBI121 binary vector were confirmed by restriction digestion using *Bam*HI and *Sac*I. The resulting plasmid was designated as hpRNAi-MVR. The RNAi expression cassette (hpRNAi-MVR) was electroporated into *Agrobacterium tumefaciens* strain EHA105, the electroporated cells were grown on selectable antibiotics kanamycin 100mg l^{-1} and rifampicin 25mg l^{-1} containing

Table 1. List of primers used in this study F1 primers containing Bam H1/Sac1 restriction sites indicated in italics. Overlap regions indicated in bold letters. R7 primer containing SexA1 restriction site indicated in italics.

Primer Name	Primer sequence (5' –> 3')	Segment size in bp
F1	AGTGAggatccAGTGGAAAGTATAAGTTCTGTG	
F1	AGTGAgagctcAGTGGAAAGTATAAGTTCTGTG	
R1	TTGACACCTTCTCCAGAGAAACCAATACATAACATATCC	255
F2	TTCTCTGGAGAAGGTGTCAA	
R2	TGAAGGTCCAGTCATCTGGATTTGGTTATGCATTGTGAA	261
F3	CAGATGACTGGACCTTCAA	
R3	CCGTCGATTCTTCTTGTGAGCCAGAGGGAATATAATTGGT	255
F4	CTCACAAGAAGAATCGACGG	
R4	GCGACAGGACTCTAATCATTACCAGCGAACCAATCCG	232
F5	TTAGAGTCCTGTCGCAACAG	
R5	TGTTGCTCTTCCACCAGCTTCTTATCGAACTCAGTG	214
F6	GGTGGAAGAGCAACAAGCGA	
R6	AAGGTTAACAACAGCCCACGCTTTCCCCATATGA	209
F7	GCTGTTGTTAACCTTGAACACCT	
R7	AGATaccwggtTCCATCATAACCCAATAACC	221

LB media and the clones were confirmed by PCR and Restriction digestion. Glycerol stocks were prepared for the confirmed clones and stored in -80 °C for further use.

RESULTS AND DISCUSSION

PCR amplification of seven individual fragments by using proof reading Phusion DNA Polymerase yielded the expected amplicon sizes as assessed by agarose gel electrophoresis and sequencing. The expected amplicon sizes were CaCV-N gene 255bp, GBNV-NSs gene 261bp, GBNV-N gene 255bp, CMV-2b gene 232bp, CMV-CP gene 214bp, ChiVMV-HC pro gene 209bp and ChiVMV-CP gene 221bp respectively.

Overlap extension PCR was carried in 3 successive rounds of PCR reactions to efficiently complete the joining of all the seven fragments (Fig. 1).

In first round of OE-PCR, the S1+S2, S4+S5 and S6+S7 fragments were successfully joined separately

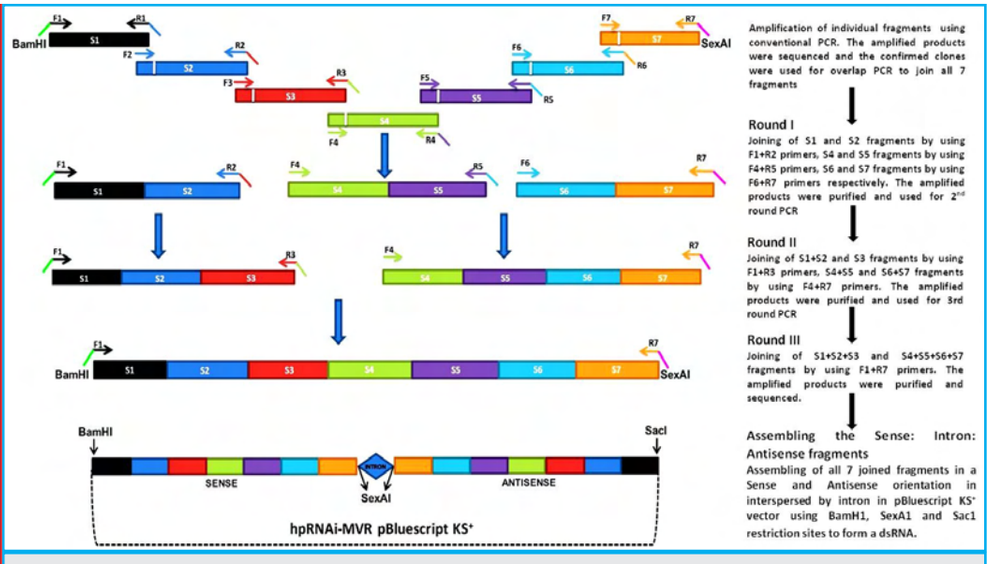

FIGURE 1. Overview of overlap extension PCR method

with the expected size if about 516bp, 446bp and 430bp. The amplified PCR products were purified and these eluted products were subsequently used for next round of OE-PCR. In second round OE-PCR, S1+S2+S3 and S4+S5+S6+S7 were joined successfully and the fragment sizes were 771bp and 876bp. Third round OE-PCR, assembled all seven fragments by combining fragments obtained from the second round OE-PCR. The size of the final fragment was about 1647bp. Sequencing revealed that there were no errors or mutations/ mismatches after at splicing of all the 7 fragments (Fig. 2).

The amplicon represents the results of final round overlap PCR, for sense fragment, *Bam*H1 forward primer

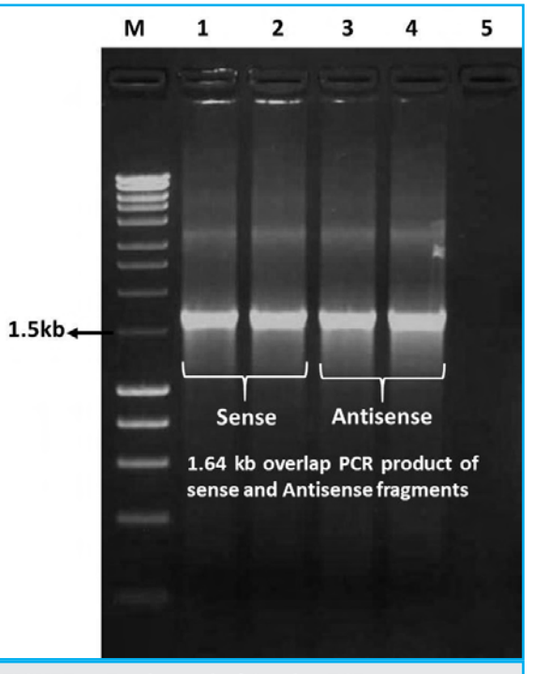

FIGURE 2. Final round of Overlap PCR.

and SexA1 reverse primer (F1+R7) were used and for Antisense fragment *Sac*1 forward primer and SexA1 reverse primer (F1+R7) were used. The gel picture depicts that the expected amplicons of both sense and antisense fragments. M. HyperLadder 1kb; 1, 2. Final overlap PCR product of Sense fragment of about 1.64kb; 3,5. Final overlap PCR product of Antisense fragment of about 1.64kb; 5. No template control (NTC).

To form dsRNA, the complete stretch of 1.647kb fragment in sense and antisense orientation with the intervening 0.25kb of pds intron were ligated and cloned, the plasmids were purified and the orientation of sense, intron and antisense fragments was confirmed by respective restriction digestion and release of fragment of expected size (Fig. 3).

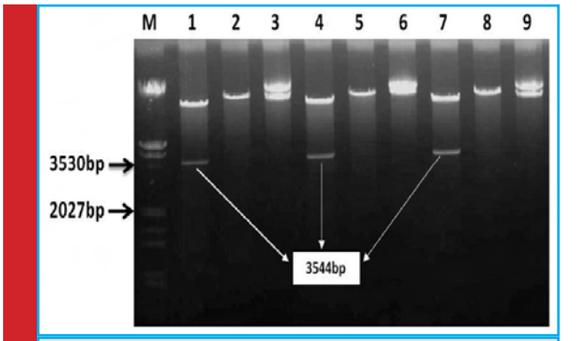

FIGURE 3. Restriction digestion of hpRNAi-MVR binary vector to confirm the stretch of Sense, Antisense and Intron fragments:
M : Lambda DNA/EcoRI+HindIII Marker
Lane 1,4,7 : Digested the hpRNAi-MVR binary vector with BamH1 and Sac1 restriction enzymes to confirm the complete stretch of Sense, Antisense and Intron fragments.
Lane 2,5,8 : Digestion of hpRNAi-MVR binary vector with BamH1
Lane 3,6,9 : hpRNAi-MVR binary vector un digested

DISCUSSION

Biotic stresses like viral diseases pose serious threat to crop production and estimated economic loss ranks second only to the other pathogens (Simon-Mateo and Garcia 2011). Efficient virus diseases control measures are not available and current virus management strategy in most cases are limited to insect vector control and roguing. Development of virus disease resistant lines is highly desirable and RNAi has a direct bearing in the development of genetically engineered virus resistant crops (Chicas and Macino 2001). Imparting virus resistance has been proven effective in various plant species by using hpRNAi constructs (Ammara *et al.,* 2015; Jia *et al.,* 2017; Kumar *et al.,* 2017).

Towards this, in this experiment we have developed a gene construct targeting multiple viruses commonly infecting two important Solancaeous crops, chilli and tomato by employing OE-PCR. Targeting single virus may not be sufficient as most often, the viral infections are mixed under field conditions, to overcome this problem, and also to minimize the resistance breakdown by a mechanism employed by viruses to overcome host induced viral gene silencing, known as "suppression of silencing" targeting multiple gene segments of virus including the respective silencing suppressors could therefore result in more durable and robust virus resistance to broad spectrum of virus infections under field conditions. In this regard, we have selected viral silencing suppressors like NSs gene for Tospovirus (Goswami

et al., 2012; Zhai *et al*., 2014), 2b gene for Cucumovirus (Du *et al*., 2014; Nemes *et al*., 2014) and HC-Pro gene for Potyvirus (Torres-Barcelo *et al*., 2010; Sahana *et al*., 2014) for broad spectrum virus resistance. The viral suppressors plays an important role, it protects the viral genome against RNA silencing and acts as RNA silencing suppressor (Lakatos *et al*., 2006). Hc-Pro gene from potyvirus blocks PTGS at tissue level, CMV 2b from cucumovirus prevents systemic silencing (Brigneti *et al*., 1998). NSs gene from tospovirus regulates the suppression of the viral movement and host defense mechanism (Lokesh *et al.,* 2010). Many researchers have reported resistance to multiple virus infections (Bucher *et al*., 2006; Zhang *et al*., 2011; Thu *et al.,* 2016; Hameed *et al.,* 2017). In this experiment, we have selected seven fragments to target seven viral genes, and this renders the development of gene construct a tedious and complex task as the commonly employed restriction digestion and ligation of fragments gets unwieldy as the number of fragments to be joined is more. Thus, we have employed OE-PCR successfully to accomplish the assembly of hpRNAi construct.

Splicing of two fragments of DNA, referred as overlap extension PCR established by (Yolov *et al.,* 1990), this method has many advantages like joining of many fragments of about 10.8kb using *pfu* proofreading polymerase (Shevchuk *et al.,* 2004). Majority of commercial kits and long PCR protocols are mainly based on Taq polymerase thus cannot be used for overlap extension PCR, because Taq leaves a single A-overhang at 3' region. This leads to disrupt the primer binding at overlap regions during overlap extension PCR (Sambrook *et al.,* 2001). The overlap extension PCR has many applications like, joining of 26 synthetic oligos of 54nt of about 969bp with 5 rounds of sequential overlap extension PCR (Zhang *et al.,* 2013). Many modified methods of OE-PCR have been applied in many genetic engineering areas, such as fusion of long length DNA fragments (Fujii *et al.,* 2013; Engel *et al.,* 2013), assembly of longer gene fragments (Benders *et al.,* 2010; You *et al.,* 2012).

Here, we developed a broad spectrum, multiple virus resistant hpRNAi-MVR vector by targeting 7 genes from 4 common virus groups for both tomato and chilli crops viz., CaCV N gene, PBNV N and NSs genes from Tospovirus, CMV 2b and CP gene from cucumovirus and HC-Pro and Polyprotein from ChiVMV. We have successfully employed the overlap extension PCR method to splice multiple gene fragments without using any restriction sites and adaptors etc. as the addition of non-specific sequences in the gene construct would have affected the RNAi efficacy due to its sequence dependence. The use of OE-PCR is highly desirable in the development of RNAi constructs involving splicing of multiple fragments. Simplified and efficient gene construct assembly for RNAi would aid in the development of virus resistant crops in avoiding crop yield loss.

CONCLUSION

Seamless joining of multiple fragments to create single fragment without using any restriction sites or ligase is a critical step in RNAi. Here, we demonstrated the application of overlap extension PCR to join seven viral gene fragments to develop hpRNAi-MVR construct useful for imparting virus disease resistance in both tomato and chilli. Virus diseases drastically reduce the crop yield and quality and are difficult to manage and only the long term solution to this is to develop virus resistant crop lines. Development of broad spectrum hpRNAi construct for commonly infecting viruses is one of the important aspects. Here, we developed an hpRNAi-MVR vector that is useful in developing multiple virus resistant tomato and chilli employing OE-PCR. Demonstrate that OE-PCR is a method of choice in RNAi gene construct for virus resistance as it is simple, fast and economical, can join multiple fragments in less time. This approach can be employed in developing gene constructs for durable, multiple virus resistance in other important crops.

ACKNOWLEDGEMENT

We are thankful to ICAR-IIHR, which provided the facility to carry out this research work. This is the part of Ph.D. dissertation work of first author.

REFERENCES

Ammara U., Mansoor S., Saeed M., Amin I., Briddon R.W. and Al-Sadi A.M. (2015). RNA interference-based resistance in transgenic tomato plants against Tomato yellow leaf curl virus-Oman (TYLCV-OM) and its associated betasatellite. Virology journal, 12(1): 38.

Benders G.A., Noskov V.N., Denisova E.A., Lartigue C., Gibson D.G., Assad-Garcia N., Chuang R.Y., Carrera W., Moodie M., Algire M.A., Phan Q., Alperovich N., Vashee S., Merryman C., Venter J.C., Smith H.O., Glass J.I., Hutchison C.A. (2010). Cloning whole bacterial genomes in yeast. Nucleic Acids Research, 38 (8): 2558–2569.

Berger P.H., Adams M.J., Barnett O.W., Brunt A.A., Hammond J., Hill J.H., Jordan R.L., Kashiwazaki S., Rybicki E., Spence N., Stenger D.C., Ohki S.T., Uyeda I., van Zaayen A., Valkonen J., Vetten H.J Family potyviridae. In: Fauquet C.M., Mayo M.A., Maniloff J., Dessel Berger U., Ball L. (eds) (2005). Virus taxonomy eighth report of the international committee on taxonomy of virus. Elsevier, Academic Press, London, 385–396.

Bonfim K., Faria J.C., Nogueira E.O., Mendes E.A. and Aragao F.J. (2007). RNAi-mediated resistance to Bean golden mosaic

virus in genetically engineered common bean (*Phaseolus vulgaris*). Molecular Plant-Microbe Interactions, 20 (6): 717-726.

Brigneti G., Voinnet O., Li W.X., Ji L.H., Ding S.H. and Baulcombe D.C. (1998). Viral pathogenicity determinants are suppressors of transgene silencing in *Nicotiana benthamiana*. EMBO Journal, 17: 6739–6746.

Bucher E., Lohuis D., van Poppel P.M., Geerts-Dimitriadou C., Goldbach R. and Prins M. (2006). Multiple virus resistance at a high frequency using a single transgene construct. Journal of General Virology, 87 (12): 3697-3701.

Chicas A. and Macino G. (2001). Characteristics of post transcriptional gene silencing. EMBO reports, 2 (11): 992-996.

De Haan P., Kormelink R., de Oliveira Resende R., Van Poelwijk F., Peters D. and Goldbach R. (1991). Tomato spotted wilt virus L RNA encodes a putative RNA polymerase. Journal of General Virology, 72 (9): 2207-2216.

De Haan P., Wagemakers L., Peters D. and Goldbach R. (1990). The S RNA segment of tomato spotted wilt virus has an ambisense character. Journal of General Virology, 71 (5): 1001-1007.

Du Z., Chen A., Chen W., Liao Q., Zhang H., Bao Y., Roossinck M.J. and Carr J.P. (2014). Nuclear-cytoplasmic partitioning of the Cucumber mosaic virus 2b protein determines the balance between its roles as a virulence determinant and RNA silencing suppressor. Journal of virology, JVI-00284.

Duan C.G., Wang C.H. and Guo H.S. (2012). Application of RNA silencing to plant disease resistance. Silence, 3 (1): 5.

Engel H., Gutiérrez-Fernández J., Flückiger C., Martínez-Ripoll M., Mühlemann K., Hermoso J.A., Hilty M., Hathaway L.J. (2013) Heteroresistance to fosfomycin is predominant in *Streptococcus pneumoniae* and depends on the murA1 gene. Antimicrobial Agents, 57 (6): 2801–2808.

Fujii W., Kano K., Sugiura K., Naito K. (2013). Repeatable construction method for engineered zinc finger nuclease based on overlap extension PCR and TA-cloning. PloS one, 8 (3): e59801.

Goswami S., Sahana N., Pandey V., Doblas P., Jain R.K., Palukaitis P., Canto T. and Praveen S. (2012). Interference in plant defense and development by non-structural protein NSs of Groundnut bud necrosis virus. Virus research, 163 (1): 368-373.

Hall T.A. (1999). BioEdit: a user-friendly biological sequence alignment editor and analysis program for Windows 95/98/NT. In Nucleic acids symposium series, 41 (41): 95-98.

Hameed A., Tahir M.N., Asad S., Bilal R., Van Eck J., Jander G. and Mansoor S. (2017). RNAi-mediated simultaneous resistance against three RNA viruses in potato. Molecular biotechnology, 59 (2-3): 73-83.

Heckman K.L., Pease L.R. (2007). Gene splicing and mutagenesis by PCR-driven overlap extension. Nat Protocols, 2: 924–932.

Higuchi R. (1988). A general method of in vitro preparation and specific mutagenesis of DNA fragments: study of protein and DNA interactions. Nucleic Acids Research, 16: 7351–7367.

Horton R.M., Hunt H.D., Ho S.N., Pullen J.K. and Pease L.R. (1989). Engineering hybrid genes without the use of restriction enzymes: gene splicing by overlap extension. Gene, 77 (1): 61-68.

Hussain H., and Chong N.F.M. (2016). Combined overlap extension PCR method for improved site directed mutagenesis. BioMed research international (doi.org/10.1155/2016/8041532).

Jia R., Zhao H., Huang J., Kong H., Zhang Y., Guo J., Huang Q., Guo Y., Wei Q., Zuo J. and Zhu Y.J. (2017). Use of RNAi technology to develop a PRSV-resistant transgenic papaya. Scientific Reports, 7 (1): 12636.

Krishnareddy M., Rani R.U., Kumar K.A., Reddy K.M. and Pappu H.R. (2008). Capsicum chlorosis virus (Genus Tospovirus) infecting Chili pepper (*Capsicum annuum*) in India. Plant disease, 92 (10): 1469-1469.

Kumar S., Tanti B., Patil B.L., Mukherjee S.K., Sahoo L. (2017). RNAi-derived transgenic resistance to Mungbean yellow mosaic India virus in cowpea. PLoS ONE, 12 (10): e0186786.

Lakatos L., Csorba T., Pantaleo V., Chapman E.J., Carrington J.C., Liu Y.P., Dolja V.V., Calvino L.F., Lopez., Moya J.J. and Burgyan J. (2006). Small RNA binding is a common strategy to suppress RNA silencing by several viral suppressors. The EMBO journal, 25 (12): 2768-2780.

Li X., Qiu Y., Shen Y., Ding C., Liu P., Zhou J. and Ma Z. (2008). Splicing together different regions of a gene by modified polymerase chain reaction-based site-directed mutagenesis. Analytical biochemistry, 373 (2): 398-400.

Li L.I., Cheng G.U., Biao W.A., Tong Z.H., Yang L.E., DAI Y.H., Wen H.E., LIANG C., WANG X.F. (2016). RNAi-mediated transgenic rice resistance to Rice stripe virus. Journal of integrative agriculture, 15(11):2539-49.

Lokesh B., Rashmi P.R., Amruta B.S., Srisathiyanarayanan D., Murthy M.R. and Savithri H.S. (2010). NSs encoded by groundnut bud necrosis virus is a bifunctional enzyme. PLoS One, 5 (3): e9757.

Manamohan M., Chandra G.S., Asokan R., Deepa H., Prakash M.N. and Kumar N.K. (2013). One-step DNA fragment assembly for expressing intron-containing hairpin RNA in plants for gene silencing. Analytical biochemistry, 433 (2): 189-191.

Nemes K., Gellert A., Balazs E. and Salanki K. (2014). Alanine scanning of Cucumber mosaic virus (CMV) 2B protein identifies different positions for cell-to-cell movement and gene silencing suppressor activity. PloS one, 9 (11): e112095.

Palukaitis P., Roossinck M.J., Dietzgen R.G. and Francki R.I. (1992). Cucumber mosaic virus. In Advances in virus research. Academic Press, 41: 281-348.

Sahana N., Kaur H., Jain R.K., Palukaitis P., Canto T. and Praveen S. (2014). The asparagine residue in the FRNK box of potyviral helper-component protease is critical for its small RNA binding and subcellular localization. Journal of General Virology, 95 (5): 1167-1177.

Sambrook J. and Russel D.W. (2001). Molecular Cloning: A Laboratory Manual. Cold Spring Harbor Laboratory Press, Cold Spring Harbor, NY.

Simon-Mateo C. and Garcia J.A. (2011). Antiviral strategies in plants based on RNA silencing. Biochimica et Biophysica Acta (BBA)-Gene Regulatory Mechanisms, 1809 (11): 722-731.

Thu L.T.M., Thuy V.T.X., Duc L.H., Son L.V., Ha C.H. and Mau C.H. (2016). RNAi-mediated resistance to SMV and BYMV in transgenic tobacco. Crop Breeding and Applied Biotechnology, 16 (3): 213-218.

Torres-Barcelo C., Daros J.A. and Elena S.F. (2010). HC-Pro hypo-and hyper suppressor mutants: differences in viral siRNA accumulation in vivo and siRNA binding activity in vitro. Archives of virology, 155 (2): 251-254.

Voinnet O. (2001). RNA silencing as a plant immune system against viruses. Trends Genetics, 17: 449–459.

Shevchuk N.A., Bryksin, A.V., Nusinovich, Y.A., Cabello, F.C., Sutherland, M., Ladisch S. (2004). Construction of long DNA molecules using long PCR-based fusion of several fragments simultaneously. Nucleic Acids Research, 32 (12): e19.

Waneskog M and Bjerling P. (2014). Multi-fragment site-directed mutagenic overlap extension polymerase chain reaction as a competitive alternative to the enzymatic assembly method. Analytical biochemistry, 444: 32-37.

Wesley S.V., Helliwell, C.A., Smith, N.A., Wang, M.B., Rouse, D.T, et al. (2001). Construct design for efficient, effective and high-throughput gene silencing in plants. Plant Journal, 27: 581–590.

Yolov AA., Shabarova, ZA. (1990).Constructing DNA by polymerase recombination. Nucleic Acids Res, 18(13): 3983–3986.

You C, Zhang XZ, Zhang YHP. (2012). Simple cloning via direct transformation of PCR product (DNA Multimer) to *Escherichia coli* and *Bacillus subtilis*. Applied and environmental microbiology, 78(5): 1593–1595.

Zhai, Y., Bag, S., Mitter, N., Turina, M. and Pappu, H.R. (2014). Mutational analysis of two highly conserved motifs in the silencing suppressor encoded by tomato spotted wilt virus (genus Tospovirus, family Bunyaviridae). Archives of virology, 159(6): 1499-1504.

Zhang, X., Sato, S., Ye, X., Dorrance, A.E., Morris, T.J., Clemente, T.E. and Qu, F. (2011). Robust RNAi-based resistance to mixed infection of three viruses in soybean plants expressing separate short hairpins from a single transgene. Phytopathology, 101(11): 1264-1269.

Sastrosiswojo, S. (1995). Integrated pest management in vegetable production. Symposium on Small Scale vegetable production and Horticultural Economics in Developing Countries. ISHS Acta Horticulturae, 369.

Umamaheswaran, K., Jain, R. K., Bhat, A. I. and Ashwai, Y. S.9. (2003). Biological and molecular characterization of Tospovirus isolate from tomato and its relationship with other Tospovirus. Indian Phytopathology, 56: 168-173.

Medical
Communication

Biosci. Biotech. Res. Comm. 12(1): 54-59 (2019)

BBRC
Bioscience Biotechnology
Research Communications

Prevalence and pathogenesis of otosclerosis: A review

Rania Abdulfattah Sharaf

Department of Speech Language Pathology and Audiology, National Guard Health Affairs, Ministry of National Guard, Riyadh Saudi Arabia

ABSTRACT

The current review is aimed to provide an overview of etio-pathogenesis of otosclerosis. Otosclerosis affects bony labyrinth resulting a progressive conductive hearing loss, a sensorineural hearing loss, or a mixed-type hearing loss. It is a hereditary localized disease of the otic capsule typified by new bone formation that is composed of different fibrillar and cellular pattern. The abnormal new bone produces ankylosis of the stapes footplate resulting in conductive deafness. The onset of the hearing loss due to otosclerosis is usually between 15 and 40 years of age. Otosclerosis is a disease of adult onset affecting more women than men in the world. The previous study also has identified the link of otosclerosis with the family history. Additionally, women at an earlier age reported greater severity of otosclerosis symptoms compared to men. Despite the numerous theories suggested, the etiology of otosclerosis has remained obscure. Since histopathological inner ear changes due to otosclerosis is important, this review will provide an updated overview of prevalence and etio-pathological changes in otosclerosis.

KEY WORDS: OTOSCLEROSIS, HEARING LOSS, OTOSPONGIOSIS, COCHLEAR LESIONS

INTRODUCTION

Otosclerosis is a disease of the bony labyrinth, which is characterized by fixation of the footplate of the stapes secondary to abnormal bone formation (Quesnel et al., 2018; Guild, 1994; Schuknecht, 1993). The area of the labyrinthine capsule immediately in front of the footplate of the stapes called “fissula antefenestrum” is the site of predilection for otosclerosis. Other frequent sites include the border of the round window and even the footplate of the stapes (Mansour et al., 2018; Guild, 1994; Schuknecht, 1993).

Virolainen (1972) reports that otosclerosis is usually bilateral. It is a hereditary localized disease of the otic capsule typified by new bone formation that is composed of different fibrillar and cellular pattern (Sho-

ARTICLE INFORMATION:

Corresponding Author: rania2222@hotmail.com
Received 27th Dec, 2018
Accepted after revision 21st Feb, 2019
BBRC Print ISSN: 0974-6455
Online ISSN: 2321-4007 CODEN: USA BBRCBA
Thomson Reuters ISI ESC / Clarivate Analytics USA
NAAS Journal Score 2019: 4.31 SJIF: 4.196

Online Contents Available at: http//www.bbrc.in/
DOI: 10.21786/bbrc/12.1/7

man et al., 2014; Guild, 1994; Schuknecht, 1993). The abnormal new bone produces ankylosis of the stapes footplate resulting in conductive deafness (Henriques et al., 2016; Guild, 1994; Schuknecht, 1993). Other part of the labyrinth may be involved resulting in sensorineural deafness and vestibular abnormalities (Ciuman, 2013; Smyth, 1997).

"Otospongiosis" is the other term for this condition and is preferred by many European otologists, as the abnormal new bone is highly vascular (Bittermann, 2014; Causse and colleague, 1984). However, in UK, the term "otosclerosis" is commonly used, which refers to the final inactive stage where there is sclerotic hard bone (Virolainen, 1972). According to Smyth (1997) neither of these terms is strictly correct.

Despite the numerous theories suggested, the etiology of otosclerosis has remained obscure. Delayed physiological development, inflammatory processes, cartilaginous deposits in the region of the fissula antefenestrum, disturbances in the blood supply, mechanical stimuli, etc. have all been described as possible cause of otosclerosis (Batson and Rizzolo, 2017; Cureoglu et al., 2006) (Figure 1). It is therefore possible that there are constitutional, local and activating factors, which could be responsible for the development of the otosclerotic foci either individually or jointly (Virolainen, 1972). This review aimed to provide an overview of prevalence and etio-pathogenesis of otosclerosis.

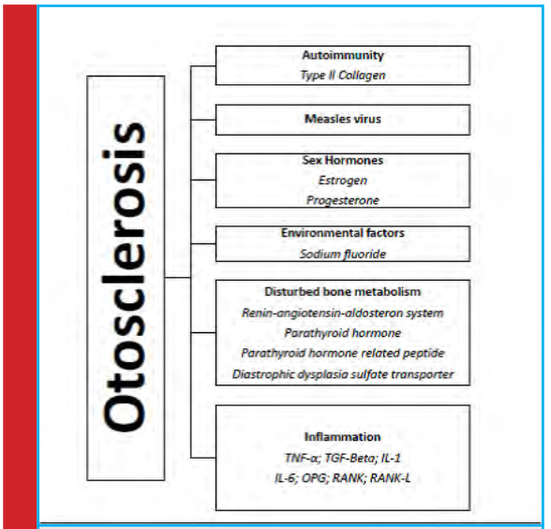

FIGURE 1. Etiopathogenetic factors of otosclerosis (Karosi & Sziklai, 2010)

REVIEW OF LITERATURE ON OTOSCLEROSIS

In the past years the study of otosclerosis has principally been devoted to the histochemistry of otosclerotic foci (Abdel-Ghany et al., 2014). A significant elevation in the activity of alkaline phosphatase and an equally significant fall in the activity of lactic acid dehydrogenase has been described (Moumoulidis et al., 2007). Some changes in the matrix of the otosclerotic bone have also been shown, for instance in the number and construction of the polysaccharides (Virolainen, 1972; Ziff, 2014).

Otosclerosis is a disease of adult onset affecting more women than men in the world (Crompton et al., 2019). The previous study also has identified the link of otosclerosis with the family history (Crompton et al., 2019). Additionally, women at an earlier age reported greater severity of otosclerosis symptoms compared to men (Crompton et al., 2019). Clinical manifestation of otosclerosis is more evident in White Europeans and people of Indian origin (Lin et al., 2007).

In additional to typical conductive hearing loss, patients suffering from otosclerosis also often have perceptive hearing loss (Cureoglu et al., 2010; Venail et al., 2007). Cochlear lesions are considered to be due to secretions from the active otosclerotic foci, which have found their way into the endolymph (Makarem and Linthicum, 2008). Vestibular disturbances even appear in patients suffering from otosclerosis (de Vilhena et al., 2016). These may be derived from otosclerotic vascular changes due to the disease or from biochemical changes in the inner ear fluids (Ciuman, 2013).

Because hearing loss is the dominant feature of otosclerosis, these patients have not been examined for the other disorders associated with otosclerosis as carefully as for hearing (Declau et al., 2007). Unsteadiness and or dizziness have been frequently observed in these patients (Yetişer, 2018). Abnormal electronystagmographic findings have been reported in otosclerotics (Gupta and Mundra, 2015). Further studies of these changes would throw additional light on the general view about otosclerosis (Purohit, 2014).

OCCURRENCE OF OTOSCLEROTIC FOCI

It's important to distinguish between clinical, non-clinical or histological otosclerosis; the latter is about 10 times more common than the former (Smyth, 1997; McElveen and Kutz, 2018). In 1940, first study revealed histological otosclerosis on the temporal bones in 12% of 200 autopsies (Virolainen, 1972). In 1944, Guild demonstrated histological otosclerosis in only 8.3% of 482 African races but much less in the wider population around 1%. A recent histological study reported lack of evidence for nonotosclerotic stapes fixation in people undergoing stapedectomy (Quesnel et al., 2016).

Otosclerosis is usually bilateral, however the frequency of histological unilateral otosclerosis ranges between 13% and 30% (Foster and Backous, 2018; Quesnel et al., 2018). The area of the labyrinthine capsule immediately

in front of the footplate of the stapes called 'fissula antefenestrum' is the site of predilection for otosclerosis; other frequent sites may include border of the round window and even the footplate of the stapes around the cochlea, the internal auditory canal or less often around the semicircular canal (Michaels and Soucek, 2011).

The focus nearly always originates in the endochondral layer of the labyrinthine capsule, extending in many cases into the periosteal layer as far as the mucosa of the tympanic cavity, and into the endosteal layer of the labyrinth (Naumann et al., 2005). Where the focus reaches the mucoperiosteum of the tympanum and the endosteum of the labyrinth, these show varying degrees of fibrous thickening and increased vascularity (Makarem et al., 2010).

Virolainen (1972) quotes Seligman and Shambaugh (1951) that assessment of 2086 post-operative surgery of ear revealed that cochlear nerve involvement is present twice as often when otosclerotic foci are situated in the horizontal semicircular canal, compared with the frequency of the involvement when the canal is not affected. Histological otosclerosis is at any rate quite frequently asymptomatic (Declau et al., 2007). In a previous review of Ménière's disease, the lateral semicircular canal was found at autopsy to be full of otosclerotic bone (Oberman et al., 2017).

PATHOLOGICAL CHANGES IN OTOSCLEROSIS

Otosclerosis is a disease of the bony labyrinthine capsule, frequently developing in areas where embryonic cartilage persists (Bloch, 2012; Babcock et al., 2018). The pathological process is characterized by resorption of the normal bone, often around the blood vessels, and by the replacement of normal bone with cellular fibrous connective tissue (Rudic et al., 2015). Areas undergoing active resorption are extensively vascularised (Rudic et al., 2015). Focus may contain areas at different stages of activity that can be described as active intermediate and inactive final stage (Karosi & Sziklai, 2010). Karosi et al., (2011) reported that the activity of alkaline phosphatase increases in the focus.

The term "otospongiosis" refers to the active phase of the disease, which is characterized by the presence of vascular space containing highly cellular fibroses tissue, mononuclear histiocytes together with osteocytes and osteoclasts (Parahy and Linthicum, 1984; Uppal et al., 2010). These cells contain many enzymes, which are released in to the surrounding tissues resulting in its absorption (Ziff, 2014). The term "otosclerosis" refers to the final stage of highly mineralized bone with a mosaic appearance (Quesnel et al., 2013). Osteoclasts have disappeared but osteocytes and/or osteoblasts may still be seen in the peripheral areas (Quesnel et al., 2013).

Previous study had suggested that some enzyme serve as the initiating factor of decalcification (Purohit & Hermans, 2014). Another study suggested that the focus shows alkaline phosphates during the first phase and the whole of secondary phase until the bone is completely calcified, alkaline phosphatase will then disappear (Gronowicz et al., 2014). Some studies observed the presence of abnormal accumulation of mucopolysaccharides in to the otosclerosis focus (Ricci, 1962; Ribári et al., 1991). A recent study reported higher level of total oxidant status and oxidative stress index in patients with otosclerosis (Baysal et al., 2017). Additionally, reactive oxygen species could be developed in otosclerotic foci (Rudic et al., 2015).

PERILYMPH CHANGES IN OTOSCLEROSIS

The perilymph has an extra-cellular character with low potassium, glucose, amino acid, and high sodium concentration (Palmer et al., 2016). The blood-labyrinthine barrier permeability has been slightly increased in ears of patients with Ménière's disease (Tagaya et al., 2011). Additionally, the blood-labyrinthine barrier permeability is also increased in other diseases, for instance sudden deafness (Sugiura et al., 2006; Yoshida et al., 2008), labyrinthine invasion of cholesteatoma (Sone et al., 2007; Sone et al., 2012), vestibular schwannoma (Yamazaki et al., 2009), and relapsing polychondritis (Kato et al., 2014). Endolymphatic hydrops (EHs) is often seen in patients with otosclerosis, and preoperative EH was one of the risk factor for inner ear disturbances following stapes surgery (Mukaida et al., 2015). Furthermore, increased permeability of the blood-labyrinthine barrier and endolymphatic hydrops could also causes sensorineural hearing loss in otosclerosis (Mukaida et al., 2015). A recent study assessed and compared cochlear lymph signal intensity in patients with otosclerosis, Ménière's disease, and healthy individuals (Naganawa et al., 2016). The results of this study indicated an increased cochlear lymph signal intensity ratio in patients with otosclerosis than Ménière's disease or healthy individuals (Naganawa et al., 2016). Many studies has been reported an association of EH with otosclerosis (Franklin et al., 1990; Yoon et al., 1990; Shea et al., 1994); however, there is a lack of understanding about the mechanism for the development of EH in patients with otosclerosis (Mukaida et al., 2015).

CONCLUSIONS

The histological and pathological changes of otosclerosis is still not fully explained. To enhance a better understanding of the pathogenesis of otosclerosis, it is vital to use modern biologic methods to examine pathological changes in human temporal bones with otosclerosis.

REFERENCES

Abdel-Ghany, A. F., Osman, N. M., & Botros, S. M. (2014). Correlation between the size, CT density of otosclerotic foci, and audiological tests in cases of otosclerosis. The Journal of International Advanced Otology, 10(2), 156.

Babcock, T. A., & Liu, X. Z. (2018). Otosclerosis: From Genetics to Molecular Biology. Otolaryngologic Clinics of North America, 51(2), 305-318.

Batson, L., & Rizzolo, D. (2017). Otosclerosis: an update on diagnosis and treatment. Journal of the American Academy of PAs, 30(2), 17-22.

Baysal, E., Gulsen, S., Aytac, I., Celenk, F., Ensari, N., Taysi, S., ... & Kanlikama, M. (2017). Oxidative stress in otosclerosis. Redox Report, 22(5), 235-239.

Bittermann, A. J. (2014). The treatment of patients with otosclerosis. From expert opinion to evidence-based practice (Vol. 67). Utrecht University.

Bloch, S. L. (2012). On the biology of the bony otic capsule and the pathogenesis of otosclerosis. Danish medical journal, 59(10), B4524-B4524.

Bretlau, P., & Jørgensen, M. B. (1968). Otosclerosis in the lateral semi-circular canal. The Journal of Laryngology & Otology, 82(1), 65-67.

Causse, J. R., & Causse, J. B. (1984). Otospongiosis as a genetic disease. Early detection, medical management, and prevention. The American journal of otology, 5(3), 211-223.

Causse, J. R., Uriel, J., Berges, J., Shambaugh, J. G., Bretlau, P., & Causse, J. B. (1982). The enzymatic mechanism of the otospongiotic disease and NaF action on the enzymatic balance. The American journal of otology, 3(4), 297-314.

Ciuman, R. R. (2013). Inner ear symptoms and disease: Pathophysiological understanding and therapeutic options. Medical science monitor: international medical journal of experimental and clinical research, 19, 1195.

Crompton, M., Cadge, B. A., Ziff, J. L., Mowat, A. J., Nash, R., Lavy, J. A., ... & Dawson, S. J. (2019). The Epidemiology of Otosclerosis in a British Cohort. Otology & Neurotology, 40(1), 22-30.

Cureoglu, S., Baylan, M. Y., & Paparella, M. M. (2010). Cochlear otosclerosis. Current opinion in otolaryngology & head and neck surgery, 18(5), 357.

Cureoglu, S., Schachern, P. A., Ferlito, A., Rinaldo, A., Tsuprun, V., & Paparella, M. M. (2006). Otosclerosis: etiopathogenesis and histopathology. American journal of otolaryngology, 27(5), 334-340.

de Vilhena, D., Gambôa, I., Duarte, D., & Lopes, G. (2016). Vestibular disorders after stapedial surgery in patients with otosclerosis. International journal of otolaryngology, 2016.

Declau, F., Van Spaendonck, M., Timmermans, J. P., Michaels, L., Liang, J., Qiu, J. P., & Van De Heyning, P. (2007). Prevalence of histologic otosclerosis: an unbiased temporal bone study in Caucasians. In Otosclerosis and Stapes Surgery (Vol. 65, pp. 6-16). Karger Publishers.

Foster, M. F., & Backous, D. D. (2018). Clinical Evaluation of the Patient with Otosclerosis. Otolaryngologic Clinics of North America, 51(2), 319-326.

Franklin, D. J., Pollak, A., & Fisch, U. (1990). Ménière's symptoms resulting from bilateral otosclerotic occlusion of the endolymphatic duct: an analysis of a causal relationship between otosclerosis and Ménière's disease. The American journal of otology, 11(2), 135-140.

Gronowicz, G., Richardson, Y. L., Flynn, J., Kveton, J., Eisen, M., Leonard, G., ... & Parham, K. (2014). Differences in otosclerotic and normal human stapedial osteoblast properties are normalized by alendronate in vitro. Otolaryngology–Head and Neck Surgery, 151(4), 657-666.

Guild, S. R. (1944). Histologic otosclerosis. Ann Otol Rhinol Laryngol, 53(1045), 71.

Gupta, S. K., & Mundra, R. K. (2015). Electronystagmography a very useful diagnostic tool in cases of vertigo. Indian Journal of Otolaryngology and Head & Neck Surgery, 67(4), 370-374.

Henriques, V., Teles, R., Sousa, A., Estevão, R., Rodrigues, J., Gomes, A., ... & Fernandes, F. (2016). Abnormal Congenital Location of Stapes' Superstructure: Clinical and Embryological Implications. Case reports in otolaryngology, 2016.

Karosi, T., & Sziklai, I. (2010). Etiopathogenesis of otosclerosis. European archives of oto-rhino-laryngology, 267(9), 1337-1349.

Karosi, T., Csomor, P., Szalmás, A., Kónya, J., Petkó, M., & Sziklai, I. (2011). Osteoprotegerin expression and sensitivity in otosclerosis with different histological activity. European archives of oto-rhino-laryngology, 268(3), 357-365.

Kato, M., Katayama, N., Naganawa, S., & Nakashima, T. (2014). Three-dimensional fluid-attenuated inversion recovery magnetic resonance imaging findings in a patient with relapsing polychondritis. The Journal of Laryngology & Otology, 128(2), 192-194.

Lin, C. Y., Yang, Y. C., Leon Guo, Y., Wu, C. H., Chang, C. J., & Wu, J. L. (2007). Prevalence of hearing impairment in an adult population in southern Taiwan. International journal of audiology, 46(12), 732-737.

Makarem, A. O., Hoang, T. A., Lo, W. W., Linthicum, F. H., & Fayad, J. N. (2010). Cavitating otosclerosis: clinical, radiological and histopathological correlations. Otology & neurotology: official publication of the American Otological Society, American Neurotology Society [and] European Academy of Otology and Neurotology, 31(3), 381.

Makarem, A., & Linthicum, F. H. (2008). Cochlear otosclerosis and endolymphatic hydrops. Otology & neurotology: official publication of the American Otological Society, American Neurotology Society [and] European Academy of Otology and Neurotology, 29(4), 571.

Mansour, S., Magnan, J., Nicolas, K., & Haidar, H. (2018). Otosclerosis. In Middle Ear Diseases (pp. 1-83). Springer, Cham.

McElveen, J. T., & Kutz, J. W. (2018). Controversies in the Evaluation and Management of Otosclerosis. Otolaryngologic Clinics of North America, 51(2), 487-499.

Michaels, L., & Soucek, S. (2011). Origin and growth of otosclerosis. Acta oto-laryngologica, 131(5), 460-468.

Moumoulidis, I., Axon, P., Baguley, D., & Reid, E. (2007). A review on the genetics of otosclerosis. Clinical otolaryngology, 32(4), 239-247.

Mukaida, T., Sone, M., Yoshida, T., Kato, K., Teranishi, M., Naganawa, S., & Nakashima, T. (2015). Magnetic resonance imaging evaluation of endolymphatic hydrops in cases with otosclerosis. Otology & Neurotology, 36(7), 1146-1150.

Naganawa, S., Kawai, H., Taoka, T., Suzuki, K., Iwano, S., Satake, H., ... & Ikeda, M. (2016). Cochlear lymph fluid signal increase in patients with otosclerosis after intravenous administration of gadodiamide. Magnetic Resonance in Medical Sciences, mp-2015.

Naumann, I. C., Porcellini, B., & Fisch, U. (2005). Otosclerosis: incidence of positive findings on high-resolution computed tomography and their correlation to audiological test data. Annals of Otology, Rhinology & Laryngology, 114(9), 709-716.

Oberman, B. S., Patel, V. A., Cureoglu, S., & Isildak, H. (2017). The aetiopathologies of Ménière's disease: a contemporary review. Acta Otorhinolaryngologica Italica, 37(4), 250.

Palmer, J. C., Lord, M. S., Pinyon, J. L., Wise, A. K., Lovell, N. H., Carter, P. M., ... & Green, R. A. (2016, August). Understanding the cochlear implant environment by mapping perilymph proteomes from different species. In 2016 38th Annual International Conference of the IEEE Engineering in Medicine and Biology Society (EMBC) (pp. 5237-5240). IEEE.

Parahy, C., & Linthicum Jr, F. H. (1984). Otosclerosis and otospongiosis: clinical and histological comparisons. The Laryngoscope, 94(4), 508-512.

Purohit, B., & Hermans, R. (2014). Imaging in otosclerosis: A pictorial review. Insights into imaging, 5(2), 245-252.

Quesnel, A. M., Ishai, R., & McKenna, M. J. (2018). Otosclerosis: temporal bone pathology. Otolaryngologic Clinics of North America, 51(2), 291-303.

Quesnel, A. M., Ishai, R., Cureoglu, S., Linthicum, F., Lopez, I. A., Nadol Jr, J. B., & McKenna, M. J. (2016). Lack of evidence for nonotosclerotic stapes fixation in human temporal bone histopathology. Otology & neurotology: official publication of the American Otological Society, American Neurotology Society [and] European Academy of Otology and Neurotology, 37(4), 316.

Quesnel, A. M., Moonis, G., Appel, J., O'malley, J. T., McKenna, M. J., Curtin, H. D., & Merchant, S. N. (2013). Correlation of computed tomography with histopathology in otosclerosis. Otology & neurotology, 34(1), 22.

Ribári, O., Pereplica, M., & Sziklai, I. (1991). Oversulfated mucopolysaccharides in the otosclerotic bone. Acta oto-laryngologica, 111(2), 362-365.

Ricci, V. (1962). Histochemical research on the otosclerotic focus. Considerations on the pathogenesis of otosclerosis and its classification among the" mesenchmopathies". Minerva otorinolaringologica, 12, 575.

Rudic, M., Keogh, I., Wagner, R., Wilkinson, E., Kiros, N., Ferrary, E., ... & Zarkovic, N. (2015). The pathophysiology of otosclerosis: review of current research. Hearing research, 330, 51-56.

Sakihara, Y., Parving, A. (1999). Clinical otosclerosis, prevalence estimates and spontaneous progress. Acta oto-laryngologica, 119(4), 468-472.

Schuknecht, H.F. (1993). Disorders of bone. In: Schuknecht HF, editor. Pathology of the ear. 2nd ed. Philadelphia7 Lea & Febiger; p. 365- 414.

Seligman, E., & Shambaugh Jr, G. E. (1951). XXXVI Otosclerosis of the Osseous Horizontal Semicircular Canal. Annals of Otology, Rhinology & Laryngology, 60(2), 375-381.

Shea, J. J., Ge, X., & Orchik, D. J. (1994). Endolymphatic hydrops associated with otosclerosis. The American journal of otology, 15(3), 348-357.

Shoman, N. M., Samy, R. N., & Choo, D. I. (2014). Congenital Malformations of the Ear. In Congenital Malformations of the Head and Neck (pp. 23-66). Springer, New York, NY.

Smyth, G. D. L. (1997). Otosclerosis. Scott-Brown's Otolaryngology-Otology, London, 1-14.

Sone, M., Mizuno, T., Sugiura, M., Naganawa, S., & Nakashima, T. (2007). Three-dimensional fluid-attenuated inversion recovery magnetic resonance imaging investigation of inner ear disturbances in cases of middle ear cholesteatoma with labyrinthine fistula. Otology & Neurotology, 28(8), 1029-1033.

Sone, M., Yoshida, T., Naganawa, S., Otake, H., Kato, K., Sano, R., ... & Nakashima, T. (2012). Comparison of computed tomography and magnetic resonance imaging for evaluation of cholesteatoma with labyrinthine fistulae. The Laryngoscope, 122(5), 1121-1125.

Sugiura, M., Naganawa, S., Teranishi, M., & Nakashima, T. (2006). Three-dimensional fluid-attenuated inversion recovery magnetic resonance imaging findings in patients with sudden sensorineural hearing loss. The Laryngoscope, 116(8), 1451-1454.

Tagaya, M., Yamazaki, M., Teranishi, M., Naganawa, S., Yoshida, T., Otake, H., ... & Nakashima, T. (2011). Endolymphatic hydrops and blood–labyrinth barrier in Meniere's disease. Acta oto-laryngologica, 131(5), 474-479.

Uppal, S., Bajaj, Y., & Coatesworth, A. P. (2010). Otosclerosis 2: the medical management of otosclerosis. International journal of clinical practice, 64(2), 256-265.

Venail, F., Lavieille, J. P., Meller, R., Deveze, A., Tardivet, L., & Magnan, J. (2007). New perspectives for middle ear implants: first results in otosclerosis with mixed hearing loss. The Laryngoscope, 117(3), 552-555.

Virolainen, E. (1972). Vestibular disturbances in clinical otosclerosis. Acta Oto-Laryngologica, 74(sup306), 5-34.

Yamazaki, M., Naganawa, S., Kawai, H., Nihashi, T., Fukatsu, H., & Nakashima, T. (2009). Increased signal intensity of the cochlea on pre-and post-contrast enhanced 3D-FLAIR in patients with vestibular schwannoma. Neuroradiology, 51(12), 855.

Yetişer, S. (2018). Bilateral vestibulopathy due to severe cochlear otosclerosis: a well-known condition without any favorable solution. Turkish archives of otorhinolaryngology, 56(3), 174.

Yoon, T. H., Paparella, M. M., & Schachern, P. A. (1990). Otosclerosis involving the vestibular aqueduct and Meniere's disease. Otolaryngology—Head and Neck Surgery, 103(1), 107-112.

Yoshida, T., Sugiura, M., Naganawa, S., Teranishi, M., Nakata, S., & Nakashima, T. (2008). Three-dimensional fluid-attenuated inversion recovery magnetic resonance imaging findings and prognosis in sudden sensorineural hearing loss. The Laryngoscope, 118(8), 1433-1437.

Ziff, J. L. (2014). A molecular and genetic analysis of otosclerosis [Doctoral dissertation, University College London (University of London)].

Medical
Communication

Biosci. Biotech. Res. Comm. 12(1): 60-65 (2019)

BBRC
Bioscience Biotechnology
Research Communications

Mitigation of radiation-induced pneumonitis in mice using alpha-tocopherol and nano-micelle curcumin

Piman Ameni Asl[1], Hana Saffar[2], Masoud Najafi[3], Ramezan Ali Taheri[1], Ali Qazvini[4,5] and Mohammad Reza Nourani[1]*

[1]*Nanobiotechnology Research Centre, Baqiyatallah University of Medical Sciences, Tehran, Iran*
[2]*Clinical and Anatomical Pathologist at Tehran University of Medical Sciences, Imam Khomeini Hospital Complex, Tehran, Iran*
[3]*Radiology and Nuclear Medicine Department, School of Paramedical Sciences, Kermanshah University of Medical Sciences, Kermanshah, Iran*
[4]*Chemical Injuries Research Center, Baqiatallah University of Medical Sciences, Tehran, Iran*
[5]*Department of Pulmonology, Faculty of Medicine, Baqiyatallah University of Medical Sciences, Tehran, Iran*

ABSTRACT

Pneumonitis is one of the most common consequences of exposure to high doses of ionizing radiation in lung tissue. It is associated with acute inflammation and infiltration of inflammatory cells, leading to massive release of several inflammatory mediators. Some studies have reported a risk for pneumonitis following exposure to a radiation disaster. In this experimental study, we aimed to evaluate possible mitigatory effect of alpha-tocopherol and nano-micelle curcumin on radiation pneumonitis in mice. 30 male mice were divided into 6 groups, including control, alpha-tocopherol or nano-micelle curcumin treatment, radiation, and radiation plus alpha-tocopherol or nano-micelle curcumin. Treatments were initially performed 1 day after irradiation and continued for 1 month. Irradiation was performed with 18 Gy using a cobalt-60 gamma rays source. After 8 weeks, mice were sacrificed and the lung tissues were removed for histopathological evaluation. Our study showed that pneumonitis was associated with was able to reduce inflammatory cells infiltration, edema, vascular and alveolar damage. Treatment with alpha-tocopherol could attenuated inflammation markers, while it could not mitigate vascular and alveolar damage. By contrast, nano-micelle curcumin was able to reduce inflammation, and vascular and alveolar damage. This study revealed that treatment with alpha-tocopherol or nano-micelle curcumin can mitigate radiation-induced pneumonitis in mice. These findings may pave the way to mitigation of radiation toxicity after a radiation disaster such as nuclear explosion or radiological events.

KEY WORDS: RADIATION; LUNG; PNEUMONITIS; ALPHA-TOCOPHEROL; NANO-MICELLES CURCUMIN

ARTICLE INFORMATION:

Corresponding Author: r.nourani@yahoo.com
Received 27th Dec, 2018
Accepted after revision 12th Feb, 2019
BBRC Print ISSN: 0974-6455
Online ISSN: 2321-4007 CODEN: USA BBRCBA
Thomson Reuters ISI ESC / Clarivate Analytics USA
NAAS Journal Score 2019: 4.31 SJIF: 4.196

Online Contents Available at: http//www.bbrc.in/
DOI: 10.21786/bbrc/12.1/8

INTRODUCTION

Pneumonitis is the most common frequent side effect of high dose ionizing radiation in lung tissue. It is characterized by acute inflammation in the arisen from inflammatory cells infiltration and thereby the release of several inflammatory mediators. A high dose of ionizing radiation has been shown to induce massive cell death followed by release of cytokines, inflammatory mediators, and reactive oxygen and nitrogen species (ROSs and RNSs, respectively). Chronic increased level of cytokines and production of free radicals lead to alveolar, vascular, bronchiolar damage, thereby interrupting normal function of lungs. This phenomenon may be observed in patients with various types of cancer in thoracic area such as non-small cell lung carcinoma (NSCLC), breast cancer, bronchial cancer, and etc. Moreover, mortality has been shown in association with lung injury among radioactive iodine- treated thyroid cancer patients with metastasis in the lungs, (Kwa et al. 1998, Rodrigues et al. 2004, Tsoutsou Koukourakis 2006, Hebestreit et al. 2011 and Najafı et al., 2018).

In addition to cancer patients, a body of evidence have suggested that pneumonitis may occur among people who were already exposed to acute ionizing radiation during nuclear or radiological disaster. Although bone marrow and gastrointestinal tract toxicity are the most common culprits for death following a radiation disaster, some studies have proposed that during whole body exposure to ionizing radiation, lung tissue may receive more than 7-8Gy; while lower parts of body may be affected by non-lethal doses, (Christofidou-Solomidou et al. 2011; Christofidou-Solomidou et al. 2017 and Yahyapour et al., 2018a).

Fortunately, stem cell therapy is able to prevent death caused by hematopoietic and gastrointestinal tract toxicity that occur following exposure to an acute radiation dose greater than 8Gy (Lataillade et al. 2007). Although this worthwhile therapeutic strategy can prevent early death, organ failure in lung following exposure to radiation is likely to occur. Additionally, there is piece of evidence indicating death caused by lung toxicity among people who were exposed to Chernobyl nuclear station explosion, (Deas et al. 2017; Yahyapour et al. 2018c).

Experimental studies have proposed that treatment with some antioxidants and immunomodulatory agents may mitigate radiation injury in radiosensitive organs. So, identification of mitigatory effect of low toxic antioxidants and flavonoids may be useful for to address the possible radiation disasters. Curcumin is a well-known herbal agent with potent anti-inflammatory and antioxidant effects. Previous studies have shown considerable protective effect of curcumin against toxicity of ionizing radiation, (Jurenka 2009, Cho et al. 2013; Patil et al. 2015 Yahyapour et al. 2018b Bagheri et al. 2018).

One of the most important concerns about the curcumin is its low absorption in gastric owing to high lipophilicity. This issue has been tackled in nano-micelle form of curcumin (Li et al. 2015). Consequently, more efficiency can be achieved with the same dose following treatment with nano-micelle form of curcumin. Alpha-tocopherol is another antioxidant that was used for mitigation of lung pneumonitis in the current study. It has shown a potent antioxidant effect which is able to protect and mitigate radiation toxicity (Ferreira et al. 2004; Singh et al. 2010). In this study, we aimed to illustrate possible mitigatory effect of nano-micelle form of curcumin and alpha-tocopherol on radiation-induced pneumonitis.

MATERIAL AND METHODS

Experimental design

All 30 male mice, purchased from Razi institute, Tehran, Iran; were kept under standard condition (temperature = 25C, humidity=55%, 12h light/12h dark). Then, they were divided into 6 groups (5mice in each). 1) G1 (control): mice who did not receive any drug or irradiation, and were taken only anesthesia drugs in a similar dose as other groups; 2) G2 (irradiation): mice who were irradiated locally in chest area, 3) G3 (alpha-tocopherol treatment): those received 200mg/kg/day alpha-tocopherol, 4) G4 (curcumin treatment): mice in this group were received 100mg/kg/day nano-micelle form of curcumin, 5) G5 (radiation plus alpha-tocopherol): mice were exposed to gamma rays, and after 24h, treatment with alpha-tocopherol was started, and 6) G6 (radiation plus curcumin): mice were exposed to gamma rays, and after 24h, treatment with nano-micelle form of curcumin was started. Finally, all mice were sacrificed 8weeks after irradiation and then the lung tissues were removed for histological evaluation.

Irradiation and drug administration

Alpha-tocopherol soft gel capsule was obtained from Nature Made and dissolved in olive oil. Each mouse orally received 1ml containing 6mg alpha-tocopherol (equal 200mg/kg). Then, treatment with alpha-tocopherol was started 1day after irradiation with the procedure of 5-time per week for 4 weeks. Nano-micelle form of curcumin was purchased from Exir Nano Sina, Mashahd, Iran, and was dissolved in water at a concentration of 1mg/ml. As mice drink 3 milliliter water daily which was equal to 100mg per kg per day. Treatment was started 24h after irradiation and continued for 1 month. Then, Irradiation was performed using a cobalt-60 source. Before this, mice were anesthetized using a combination of ketamine and xylazine (). After that, they were exposed to gamma rays source at supine position with

Table 1. Histopathological results of pneumonitis incidence following mice lung exposure to ionizing radiation and mitigation by alpha-tocopherol and nano-micelle curcumin.

	Macrophage infiltration	Lymphocyte infiltration	Neutrophil infiltration	Vascular thickening	Alveolar thickening	Edema and thrombosis
Control	0±00	0.50±0.50	0±00	0±00	0±00	0±00
Alpha-tocopherol	0±00	0.66±0.47	0±00	0±00	0±00	0±00
Curcumin	0±00	0.33±0.47	0±00	0.66±47	0±00	0±00
Radiation	3.0±00	3.0±00	3.0±00	2.0±00	1.66±47	1±00
Radiation plus Alpha-tocopherol	0.6±0.49	1.2±0.40	0.40±0.48	1.4±0.80	1.4±0.80	0.6±0.49
Radiation plus Curcumin	1.0±1.41	1.0±0.81	0.33±0.47	0.33±0.47	0.33±0.47	0±00

a distance of 80cm. subsequently, irradiation of chest was done at a dose of 60cGy/min and other parts of the mice's body were shielded using lead block.

Histopathological evaluation

Following fixation of lung tissues, all samples were embedded into a block of paraffin. Then, they were cut by microtome to pieces with 4-micron thickness. Resultant lung pieces were located on the slides to be stained. Each slide was stained using hematoxylin and eosin (H&E). The stained slides were evaluated for morphological changes by a histopathologist. Pneumonitis markers including infiltration of inflammatory cells and alveolar and vascular damages were detected. All these procedures were performed in the pathology unit of Imam Khomeini hospital, Tehran University of Medical Sciences, Tehran, Iran.

Statically analyses

Results of histopathological evaluation were reported as grade 0 to3. Changes in each groups were calculated as mean ± standard deviation. Mann-Whitney test was used to evaluate the significance in the groups (SPSS V16).

RESULTS

Histopathological evaluations showed a significant increase in pneumonitis markers following exposure to radiation. a drastic increase was also shown in the infiltration of inflammatory cells including macrophages,

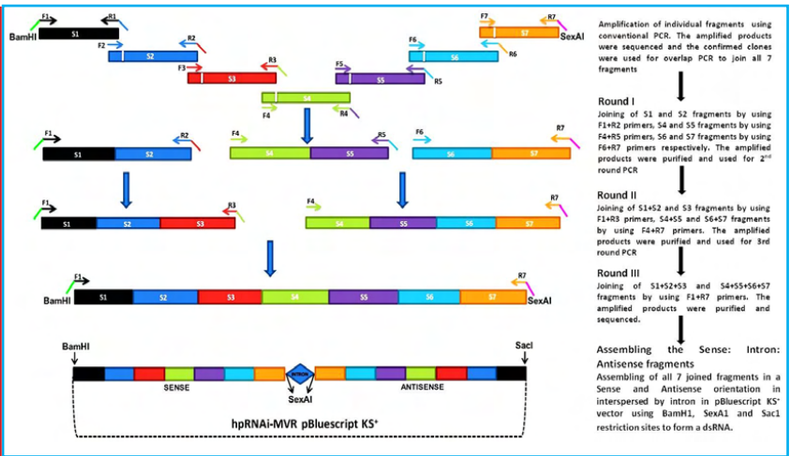

FIGURE 1. Histopathological evaluation of radiomitigatory effects of alpha-tocopherol and nano-micelle curcumin on radiation-induced pneumonitis. Irradiation cause severe infiltration of macrophages, neutrophils and lymphocytes; as well as vascular and alveolar thickening, and edema. However, treatment with nano-micelle curcumin or alpha-tocopherol attenuated these markers significantly. A: Control; B: Nano-micelle curcumin; C: alpha-tocopherol; D: Radiation; E: Radiation + Nano-micelle curcumin; F: Radiation + alpha-tocopherol (H&E staining, ×100).

lymphocytes and neutrophils (p=0.008). Treatment with alpha-tocopherol caused significant amelioration of these inflammatory cells (p value of 0.018, 0.014, and 0.018 for mitigation of macrophages, lymphocytes, and neutrophils, respectively). When mice were treated with alpha-tocopherol after irradiation, only a low infiltration of lymphocytes observed, with infiltration of macrophages and neutrophils being similar to that in control group. Irradiation also lead to a moderate vascular thickening (p=0.008) and a mild alveolar thickening (p=0.01) and edema (p=0.008). However, treatment with alpha-tocopherol failed mitigate these parameters. Treatment with alpha-tocopherol alone did not cause any toxicity, and lung morphology in this group was similar to that in control group.

Treatment with curcumin nano-micelle has a potent mitigatory effect on radiation-induced pneumonitis. However, treatment with neither nano-micelle curcumin nor alpha-tocopherol led to significant change in morphological properties of mice lung tissue. On the other hand, treatment with nano-micelle curcumin after irradiation could significantly attenuate infiltration of lymphocytes (p=0.037) and neutrophils (p=0.037), however, the difference in infiltration of macrophages wasn't significant. administration of this drug also led to a remarkable attenuation of vascular thickening (p=0.037), edema, and thrombosis (p=0.025). However, difference in alveolar thickening between radiation group and radiation plus nano-micelle curcumin was not significant.

DISCUSSION

As previously mentioned, radiation-induced pneumonitis is the acute response of lung tissue which leads to respiratory impairments, and also may cause death in a few months. As results of this study showed, lung exposure to ionizing radiation caused severe infiltration of macrophages, lymphocytes and neutrophils, all of which resulting from massive DNA damage and cell death which in turn lead to the release of chemokines and recruitment of circulatory cells into the injured area (Mukaida et al. 1998). These cells are able to produce massive free radicals via a phenomenon named respiratory burst. Production of free radicals activates several signaling pathways, including redox reactions by pro-oxidant enzymes, that lead to chronic oxidative stress (Yahyapour et al. 2018d). Also, they are capable of releasing several pro-inflammatory and pro-fibrotic cytokines. Interactions between oxidative stress and inflammatory cytokines plays a key role in development of late effects of radiotherapy and radiation disaster. targeting these interactions has been proposed as a strategy for mitigation of radiation injury (Farhood et al. 2018). With respect to the results, post irradiation-chronic inflammation causes alveolar and vascular injury, edema, and thrombosis.

To date, some agents have been proposed for mitigation of radiation-induced lung injury in animal models. Targeting COX-2 by celecoxib has been shown to alleviate pneumonitis and increase survival following local chest irradiation (Hunter et al. 2013). renin-angiotensin system also has been proposed as a target for mitigation of lung pneumonitis (Medhora et al. 2012). Ghosh et al. showed that administration of captopril or losartan (which are angiotensin inhibitor) mitigates radiation pneumonitis and increases survival through the improved breathing, amelioration of vascular injury, and reduction of infiltration of inflammatory cells (Ghosh et al. 2009; Molthen et al. 2012). Similar results have been obtained with antioxidants. Mahmood et al. showed that treatment with genistein and/or Eukarion (EUK)-207, which have antioxidant effects, can mitigate the release of inflammatory cytokines such as IL-1α, IL-1β, IL-6 and TNF-α, and reduce oxidative stress and activity of macrophages (Mahmood et al. 2011). BIO 300, a nanosuspension of genistein has shown similar results (Jackson et al. 2017). These studies show pivotal role of both free radical production and elevated activity of inflammatory mediators in development of radiation-induced pneumonitis.

In current study we aimed to detect possible mitigatory effects of two natural anti-inflammation and antioxidant agents. Curcumin demonstrated potent anti-inflammatory properties. However, it has low absorbance in intestine which may reduce its efficiency. In recent years, several studies have used other forms of curcumin with high absorbance. For instance, Nano-micelle curcumin is a low cost form of curcumin with easy absorbance. Results of this study showed that treatment with nano-micelle curcumin can strongly mitigate inflammation, infiltration of inflammatory cells, thrombosis, and vascular and alveolar injury. Mitigatory effect of nano-micelle curcumin may be mediated by suppression of inflammatory mediators such as NF-kB which in turn leads to reduced release of inflammatory cytokines. Additionally, curcumin has antioxidant properties and is able to reduce activity of pro-oxidant enzymes such as COX-2 and iNOS.

Alpha-tocopherol was another agent we used for mitigation of lung pneumonitis. Treatment with Alpha-tocopherol reduced the serum level of cytokines such as G-CSF, IL-10, IL-6, IL-12, and FLT3 in peripheral blood mononuclear cells (PBMCs) (Singh et al. 2014). Moreover, it was shown to mitigate intestinal injury following exposure to radiation through suppression of apoptosis and enhancement of cell proliferation (Singh et al. 2013). This study showed that post-exposure treatment with alpha-

tocopherol can mitigate infiltration of macrophages, lymphocytes and neutrophils. However, differences for alveolar and vascular was not significant. It is possible that longer follow-up or treatment with higher dose of alpha-tocopherol would be beneficial for a remarkable mitigation of radiation-induced lung pneumonitis.

CONCLUSION

This study showed that treatment with alpha-tocopherol or nano-micelle curcumin could mitigate radiation-induced pneumonitis in mice. However, alpha-tocopherol could not mitigate alveolar and vascular injury. Owing to the low toxicity of these agents, longer treatment or higher doses of alpha-tocopherol would be more effective. These findings may pave the way to mitigation of radiation toxicity after a radiation disaster such as nuclear explosion or radiological events.

DECLARATIONS

Acknowledgments

Not Applicable

Funding

Baqiyatallah University of Medical Sciences.

Availability of data and materials

All the relevant data and materials are presented in this article.

Authors' contributions

All authors were involved in this project.

Ethics approval

This study was approved by the Ethical Committee of the Baqiyatallah University of Medical Sciences on Animal Care.

Consent for publication

Not applicable.

Competing interests

The authors declare that they have no competing interests.

REFERENCES

Bagheri, Hamed, et al. (2018), Protection Against Radiation-Induced Micronuclei in Rat Bone Marrow Erythrocytes by Curcumin and Selenium L-Methionine (2018).

Cho, Y. J., et al. (2013), Curcumin attenuates radiation-induced inflammation and fibrosis in rat lungs, Korean J Physiol Pharmacol, 17 (4), 267-74.

Christofidou-Solomidou, M., et al. (2017), Radiation Mitigating Properties of Intranasally Administered KL4 Surfactant in a Murine Model of Radiation-Induced Lung Damage', Radiat Res, 188 (5), 491-504.

Christofidou-Solomidou, M., et al. (2011), Dietary flaxseed administered post thoracic radiation treatment improves survival and mitigates radiation-induced pneumonopathy in mice, BMC Cancer, 11, 269.

Deas, S. D., Huprikar, N., and Skabelund, A. (2017), Radiation exposure and lung disease in today's nuclear world, Curr Opin Pulm Med, 23 (2), 167-72.

Farhood, B., et al. (2018), Intercellular communications-redox interactions in radiation toxicity; potential targets for radiation mitigation J Cell Commun Signal.

Ferreira, Paulo Renato, et al. (2004), Protective effect of alpha-tocopherol in head and neck cancer radiation-induced mucositis: A double-blind randomized trial, Head & Neck: Journal for the Sciences and Specialties of the Head and Neck, 26 (4), 313-21.

Ghosh, S. N., et al. (2009) Renin-Angiotensin system suppression mitigates experimental radiation pneumonitis, Int J Radiat Oncol Biol Phys, 75 (5), 1528-36.

Hebestreit, Helge, et al. (2011) Pulmonary fibrosis in youth treated with radioiodine for juvenile thyroid cancer and lung metastases after Chernobyl', European journal of nuclear medicine and molecular imaging, 38 (9), 1683.

Hunter, N. R., et al. (2013) Mitigation and treatment of radiation-induced thoracic injury with a cyclooxygenase-2 inhibitor, celecoxib Int J Radiat Oncol Biol Phys, 85 (2), 472-6.

Jackson, I. L., et al. (2017) BIO 300, a nanosuspension of genistein, mitigates pneumonitis/fibrosis following high-dose radiation exposure in the C57L/J murine model', Br J Pharmacol, 174 (24), 4738-50.

Jurenka, Julie S (2009) Anti-inflammatory properties of curcumin, a major constituent of Curcuma longa: a review of preclinical and clinical research', Alternative medicine review, 14 (2).

Kwa, Stefan LS, et al. (1998) Radiation pneumonitis as a function of mean lung dose: an analysis of pooled data of 540 patients International Journal of Radiation Oncology* Biology* Physics, 42 (1), 1-9.

Lataillade, JJ, et al. (2007) New approach to radiation burn treatment by dosimetry-guided surgery combined with autologous mesenchymal stem cell therapy'.

Li, Jinglei, et al. (2015) Modified curcumin with hyaluronic acid: combination of pro-drug and nano-micelle strategy to address the curcumin challenge', Food Research International, 69, 202-08.

Mahmood, J., et al. (2011) Mitigation of radiation-induced lung injury by genistein and EUK-207', Int J Radiat Biol, 87 (8), 889-901.

Medhora, Meetha, et al. (2012) Radiation damage to the lung: mitigation by angiotensin converting enzyme (ACE) inhibitors Respirology (Carlton, Vic.), 17 (1), 66-71.

Molthen, R. C., et al. (2012) Mitigation of radiation induced pulmonary vascular injury by delayed treatment with captopril Respirology, 17 (8), 1261-8.

Mukaida, Naofumi, Harada, Akihisa, and Matsushima, Kouji (1998) Interleukin-8 (IL-8) and monocyte chemotactic and activating factor (MCAF/MCP-1), chemokines essentially involved in inflammatory and immune reactions Cytokine & growth factor reviews, 9 (1), 9-23.

Najafi, M., et al. (2018) Mechanisms of inflammatory responses to radiation and normal tissues toxicity: clinical implications Int J Radiat Biol, 94 (4), 335-56.

Patil, KarthiKeya, et al. (2015) Use of Curcumin Mouthrinse in Radio-Chemotherapy Induced Oral Mucositis Patients: A Pilot Study Journal of clinical and diagnostic research: JCDR, 9 (8), ZC59-62.

Rodrigues, George, et al. (2004) Prediction of radiation pneumonitis by dose–volume histogram parameters in lung cancer—a systematic review Radiotherapy and oncology, 71 (2), 127-38.

Singh, V. K., et al. (2013) Alpha-tocopherol succinate-mobilized progenitors improve intestinal integrity after whole body irradiation Int J Radiat Biol, 89 (5), 334-45.

Singh, Vijay K, Brown, Darren S, and Kao, Tzu-Cheg (2010) Alpha-tocopherol succinate protects mice from gamma-radiation by induction of granulocyte-colony stimulating factor', International journal of radiation biology, 86 (1), 12-21.

Singh, Vijay K., et al. (2014) Alpha-tocopherol succinate- and AMD3100-mobilized progenitors mitigate radiation combined injury in mice Journal of Radiation Research, 55 (1), 41-53.

Tsoutsou, Pelagia G and Koukourakis, Michael I (2006), 'Radiation pneumonitis and fibrosis: mechanisms underlying its pathogenesis and implications for future research', International Journal of Radiation Oncology Biology Physics, 66 (5), 1281-93.

Yahyapour, R., et al. (2018a) Targeting of Inflammation for Radiation Protection and Mitigation Curr Mol Pharmacol, 11 (3), 203-10.

Yahyapour, R., et al. (2018b) Radiation protection and mitigation by natural antioxidants and flavonoids; implications to radiotherapy and radiation disasters, Curr Mol Pharmacol.

Yahyapour, R., et al. (2018c), 'Radiation-induced inflammation and autoimmune diseases', Mil Med Res, 5 (1), 9.

Yahyapour, R., et al. (2018d), Reduction-oxidation (redox) system in radiation-induced normal tissue injury: molecular mechanisms and implications in radiation therapeutics, Clin Transl Oncol, 20 (8), 975-88.

Biotechnological Communication

Biosci. Biotech. Res. Comm. 12(1): 66-72 (2019)

BBRC Bioscience Biotechnology Research Communications

Isolation, phenotypic and molecular characterization of *Burkholderia* sp. (strain, PCS1) from maize fields exhibiting starch hydrolysis ability

Priya Chatterjee, Paromita Roy, Paramita Mandal and Soumendranath Chatterjee*

Department of Zoology, The University of Burdwan, Burdwan, 713104, India

ABSTRACT

The starch hydrolysing bacteria have important role in plant nutrient uptake. The aim of the present study is to isolate and characterize bacteria that are able to degrade starch from the rhizospheres of maize plants. Isolation and characterization were performed in the laboratory. The bacterial isolate (PCS1) was non-pathogenic and found to be positive for catalase, lipid hydrolysis and nitrogen fixation. The PCS1 also fermented sucrose, xylose, dextrose, galactose and mannose. The PCS1 strain showed halo-zone on starch medium and starch degrading index was found to be 2.14. The 16S rRNA gene sequence and phylogenetic tree analysis revealed that the PCS1 belonged to one of the strains of *Burkholderia cepacia* complex.

KEY WORDS: AMYLASE; PHYLOGENETIC ANALYSIS; RHIZOSPHERE; STARCH DEGRADING INDEX

INTRODUCTION

A wide range of ecological niches have been occupied by the members of the genus *Burkholderia* sp. ranging from soils to the respiratory tract of humans (van Elsas *et al*., 2002; Coenye and Vandamme, 2003; Salles *et al*., 2002, 2004; Janssen, 2006). Beside free-living rhizospheric association with plants, some of the *Burkholderia* strains and species are also epiphytic and endophytic, including obligate endosymbionts and phytopathogen (Coenye and Vandamme, 2003; Janssen, 2006). The research studies on maize rhizosphere have shown that the *Burkholderia* are the predominant bacterial groups in maize of Italian agricultural fields (Hebbar *et al*., 1992; Ramette *et al*., 2005). In addition, Viallard *et al*. (1998) have shown that the species *B. graminis* and *B. cepacia* genomovar III are

ARTICLE INFORMATION:

Corresponding Author: soumen.microbiology@gmail.com
Received 2nd Jan 2019
Accepted after revision 28th March 2019
BBRC Print ISSN: 0974-6455
Online ISSN: 2321-4007 CODEN: USA BBRCBA
Thomson Reuters ISI ESC / Clarivate Analytics USA
NAAS Journal Score 2019: 4.31 SJIF: 4.196

Online Contents Available at: http//www.bbrc.in/
DOI: 10.21786/bbrc/12.1/9

abundant in maize fields of France. The most abundant isolates belonged to the genus *Burkholderia*. Silva *et al.* (2016) studied the soils of the Amazon basin and found that *Burkholderia* spp. associated with the maize plants carry *nifH* genes and able to synthesize indole-3-acetic acid (IAA) and solubilize calcium phosphate. Recently, Correa-Galeote (2018) have shown that the cultivation history is the main driver of endophytic colonization of *Burkholderia* spp. in maize plants

Bevivino *et al.* (1998) evaluated the metabolic and molecular profiles for some traits associated with biocontrol and plant growth promoting (PGP) activity in *Burkholderia cepacia* population. They showed that the *B. cepacia* strains displayed a wide antibiosis against the phytopathogenic fungi. Further studies on maize rhizosphere have shown the association of other species such as *Burkholderia unamae* (Caballero-Mellado *et al.*, 2004) and *B. silvatlantica* (Perin *et al.*, 2006a). The *Burkholderia vietnamiensis* was first described in the rice rhizosphere in Vietnam (Tran Van *et al.*, 1994; Gillis *et al.*, 1995) along with other *Burkholderia* species from the rhizosphere of maize and coffee in Mexico (Estrada-de Los Santos *et al.*, 2001).

Several novel diazotrophic bacterial species belonging to the genus *Burkholderia* that may form both epiphytic and endophytic populations with the maize roots are known to be associated with N_2 fixation such as *B. vietnamiensis* (Estrada-de Los Santos *et al.*, 2001; Estrada *et al.*, 2002), *Burkholderia tropica* (Reis *et al.*, 2004) and *Burkholderia cenocepacia* (Balandreau *et al.*, 2001). Kost *et al.* (2014) demonstrated oxalotrophy as one of the vital traits of the genus *Burkholderia phytofirmans*. So far, the studies were focused on the diversity of *Burkholderia* spp. in maize soils, N_2 fixing ability and plant growth promotion traits. The starch solubilising ability of *Burkholderia* spp. from maize roots is still not reported from any part of India. The objective of the present research work is to identify and characterization of *Burkholderia* spp. associated with maize rhizosphere capable of starch solubilization.

MATERIALS AND METHODS

The research work was carried out in the Crop Research and Seed Multiplication Farm (CRSMF) of the University of Burdwan, West Bengal, located in the eastern part of India (latitude, 87°50'37.35' E and longitude, 23°15'7.29'N and average altitude of 30m above mean sea level) using one variety of *Zea mays* L. (var. *RE-55, Royal England*).The soil samples were collected at the depth of 10 cm using soil auger from the rhizosphere of maize plants in sterile polythene bags and were taken to the Microbiology and Parasitology Laboratory of the University of Burdwan for bacterial analysis. The soil was air-dried and diluted up to 10^{-3} using sterile distilled water. From this dilution 100µl portion was mixed with sterile nutrient agar medium (NA) (peptone: beef extract: NaCl: agar at 5:3:3:1 g l^{-1}) and was distributed in 5 sterilized plates. The plates were incubated at 30 ± 0.1 °C in the BOD incubator for 24 hours to obtain isolated colonies. The colonies were observed on the incubated plates and the most abundant colonies (S1) were purified on NA plates. The bacterial isolate was maintained on the NA slants at 4 ± 0.1° C for subsequent characterization and identification. The morphological characters such as shape, size, colour, margin and opacity of the isolated colonies were determined. The bacteria was streaked on different media including starch (Starch Agar, Himedia, India) and free-living nitrogen-fixing media (Mannitol, 10 g l^{-1}; K_2HPO_4, 0.5 g l^{-1}; $MgSO_4$. $7H_2O$, 0.2 g l^{-1}; NaCl, 0.2 g l^{-1}; $MnSO_4.4H_2O$, trace; $FeCl_3$, trace; Agar powder 10 g l^{-1}) and plates were kept at 30 ± 0.1 °C in the BOD incubator. After 24 hours, standard microbiological methods were followed for morphological and biochemical characterization of the isolate (Holt *et al.*, 1994; Sneath and Holt, 2001; Forbes *et al.*, 2007).

The Gram staining was performed using Gram staining kit (Himedia, India). Motility test was done by stabbing the bacteria into SIM agar (Czaban *et al.*, 2007). The biochemical properties such as catalase, citrate utilization, nitrate reduction, indole production, Methyl-Red (MR), Voges-Proskauer (VP), urease, oxidase, and carbohydrate metabolism (acid-gas production) tests were performed. The pathogenicity test was done on Blood Agar and by DNase test (Benson *et al.*, 2012). Carbohydrate fermentation test was performed using the sugar discs of maltose, adonitol, fructose, inositol, mannose sucrose, raffinose, dextrose, cellobiose, galactose, rhamnose, xylose, melibiose, lactose, salicin, ducitol, sorbitol, mannitol, trehalose and arabinose (Azmi *et al.*, 2014).

In addition, the qualitative determination of enzymes such as starch hydrolysis, lipid hydrolysis, protein hydrolysis (gelatine) tests were also performed. The starch plates were flooded with Grams Iodine after 24 hours of incubation. The ability of the bacteria to degrade starch was described by Starch Degrading Index (SDI), which is the ratio of the total diameter of clear zone and colony diameter (Nusrat and Rahman, 2007). The sensitivity analysis of the isolate to the recommended doses of antibiotics was done following Brown *et al.* (2004). The strain was tested for tetracycline (tcn), amoxicillin (amx), gentamycin (gen), ciprofloxacin (cip), azithromycin (azi), nalidixic acid (nal), ofloxacin (ofx), neomycin (nm), rifampicin (rif), bacitracin (bac), chloramphenicol (chl), kanamycin (kan), erythromycin (ery), ampicillin (amp), penicillin (pcn) and doxycycline (dox). The zone interpretation was done following CLSI (2011).

Genomic DNA isolation kit was used to isolate the genomic DNA of the bacterial strain from the pure cul-

ture pellet (DNA-Xpress TM Kit, Himedia-MB501). The rDNA fragment was amplified by PCR and the product was sequenced by Genetic Analyzer (ABI 3130, Genetic Analyzer) bidirectionally using the forward and reverse primer. The bacterial 16S rDNA fragment was amplified with primers 8F (5'-AGA GTT TGA TCC TGG CTC AG-3') and 1492R (5'-ACG GCT ACC TTG TTA CGA CTT-3'). The following PCR cycling conditions were used in the study: 94°C for 300 s; followed by 36 cycles of 94°C for 30 s, 58°C for 60 s, and 72°C for 60 s; and then a final elongation step at 72°C for 7 minutes.

RESULTS AND DISCUSSION

The colony of the bacterial isolate (PCS1) was white, round with an average diameter of 6mm, opaque and flat (Fig. 1). The Gram staining of the bacteria showed rod-shaped and Gram-negative properties of this strain. The motility test of the strain indicated non-motile character. The bacterial isolate (PCS1) showed a positive result for catalase and negative for MR, VP, citrate reductase, nitrate reductase and indole production (Table 1). The Triple Sugar Iron (TSI) showed yellow slant and yellow butt, and also gas production. The pathogenicity test in Blood Agar and DNase agar showed no halo-zone formation. The carbohydrate fermentation results are shown in the Table 2. The strain (PCS1) was able to ferment sucrose, xylose, dextrose, galactose and mannose. The bacteria responded positively to the lipid hydrolysis and negatively to the protein (gelatine) hydrolysis test. The bacterial strain (PCS1) was able to grow on nitrogen-free medium.The starch hydrolysis test showed a positive result for the bacteria. The SDI calculated from the halo zone and colony ratio, which was found to be 2.14 in the present study.The bacterial strain was found to be sensitive to the recommended doses of the antibiotics used in the study except ampicillin and penicillin, which showed with no zone formation. The results of the zone of inhibition exhibited by the strain is shown in Fig. 2. Based on the morphological, biochemical and phylogenetic tree analysis, the PCS1 isolate was identified as one of the strains of *Burkholderia cepacia* complex. The restriction map of the 16S rRNA gene sequence of PCS1is shown in Fig. 3. The molecu-

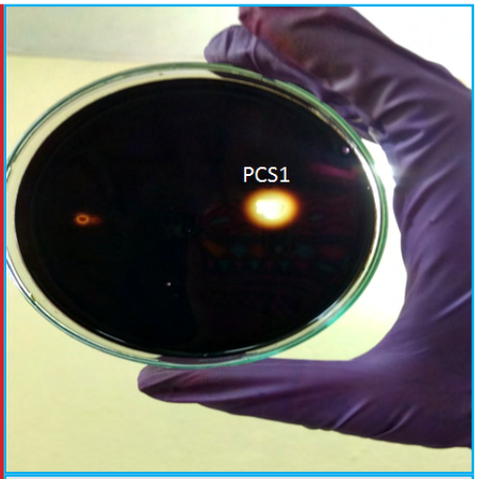

FIGURE 1. Halo-zone surrounding the PCS1 colony on starch agar plate.

Table 1. Biochemical test of PCS1 strain

Test	Results
Catalase	Positive
Indole	Negative
Citrate	Negative
MR	Negative
VP	Negative
TSI	Positive
Oxidase	Negative
Nitrate	Negative
Lipid hydrolysis	Positive
Protein (gelatine) hydrolysis	Negative
Starch hydrolysis	Positive

Table 2. Carbohydrate fermentation ability of PCS1

Carbohydrate	Response
Maltose	Negative
Adonitol	Negative
Fructose	Negative
Inositol	Negative
Mannose	Positive
Sucrose	Positive
Raffinose	Negative
Dextrose	Positive
Cellobiose	Negative
Galactose	Positive
Rhamnose	Negative
Xylose	Positive
Melibiose	Negative
Lactose	Negative
Salicin	Negative
Ducitol	Negative
Sorbitol	Negative
Mannitol	Negative
Trehalose	Negative
Arabinose	Negative

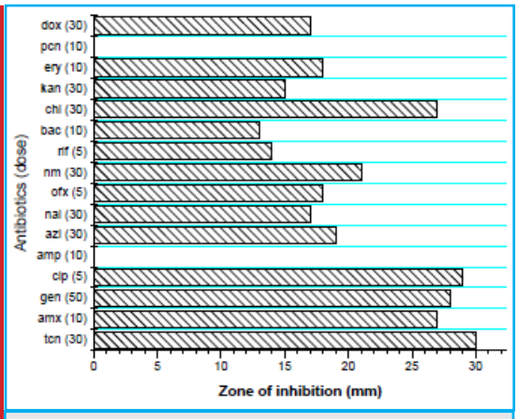

FIGURE 2. The sensitivity of PCS1 strain to the antibiotics.The size of zone of inhibition (mm) is represented in the X-axis. No zone formation is observed against penicillin (pcn) and ampicillin (amp). The antibiotics with recommended doses, in bracket are represented in Y-axis.

lar percentage of GC and AT content were 59.20% and 40.80 % respectively. The phylogenetic tree showed that the PCS1 was branched with *Burkholderia cepacia* ATCC 55792 (AY741359) (Fig. 4).

The bacterial communities are harboured by plant roots and shoots. In the rhizosphere, the root exudates are known to be the source of carbon and energy for the bacterial population. The secretion of root exudates varies with plant species and growth phases. These exudates are of highly diverse chemical nature ranging from small carboxylates to complex phenolic compounds. These exudates are utilized as substrates by the bacterial groups colonized in the rhizosphere. Brito *et al.* (2018) isolated *Burkholderia ambifaria* from the rhizoplane of the maize plants and showed that colonization of this bacterial isolate is responsible for an increase in shoot growth, root and root hair. The amylase is secreted extra-cellularly by starch degrading rhizobacteria and facilitate other different organic matters for plants to easily absorb and manufacture their food (Cordeiro *et al.*, 2003).

Smits *et al.* (1996) advocated that the rhizobacteria often show the high value of the starch degrading index, which belongs to Gram-positive and spore-forming bacterial groups; and the enzyme production from the microorganism is directly correlated to the time period of incubation. Another finding on starch degradability by amylase was shown by Wang *et al.* (2016), the authors observed that the ability to hydrolyse starch by amylase is independent of the diameter of the colony formed by Gram-negative, non-spore forming rhizobacteria. The calculated SDI value of PCS1 is quite high in comparison to some other gram-negative bacteria. The strains of *Burkholderia* spp. are capable of producing amylase enzymes to degrade starch into a soluble form and promote the maize plant growth. Dida (2018) studied the SDI of *Bacillus* spp. from the rhizosphere of various plants in Ethiopia and reported that the SDI falls between 1.23 and 2.15. The present findings in relation to SDI is comparable with *Bacillus* spp..

Draghi *et al.* (2014) reported two strains of *Burkholderia cordobensis* namely LMG 27620T and LMG 27621 from Argentina. They observed that the strains were well capable of starch hydrolysis. The DNA G+C content of the strain PCS1 was 59.20 mol %, which is within the range reported for members of genus *Burkholderia* (59-69.9 mol %; Gillis *et al.*, 1995). The present results are in agreement with the research works of Draghi *et al.* (2014) and Lim *et al.* (2012). The results of carbon compound utilization by the PCS1 strain of *Burkholderia cepacia* are corroborated with the findings of Yabuuchi *et al.* (1992).

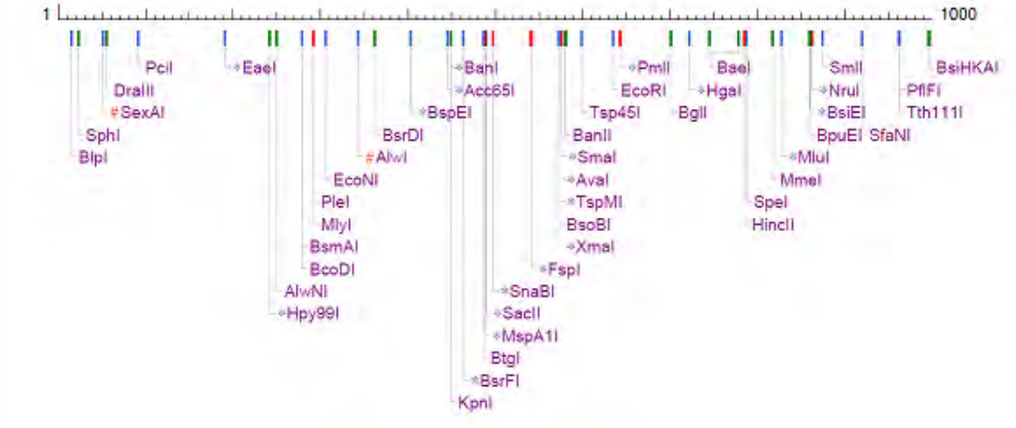

FIGURE 3. The figure showing the restriction map of the 16S rRNA gene sequence of the isolate PCS1.

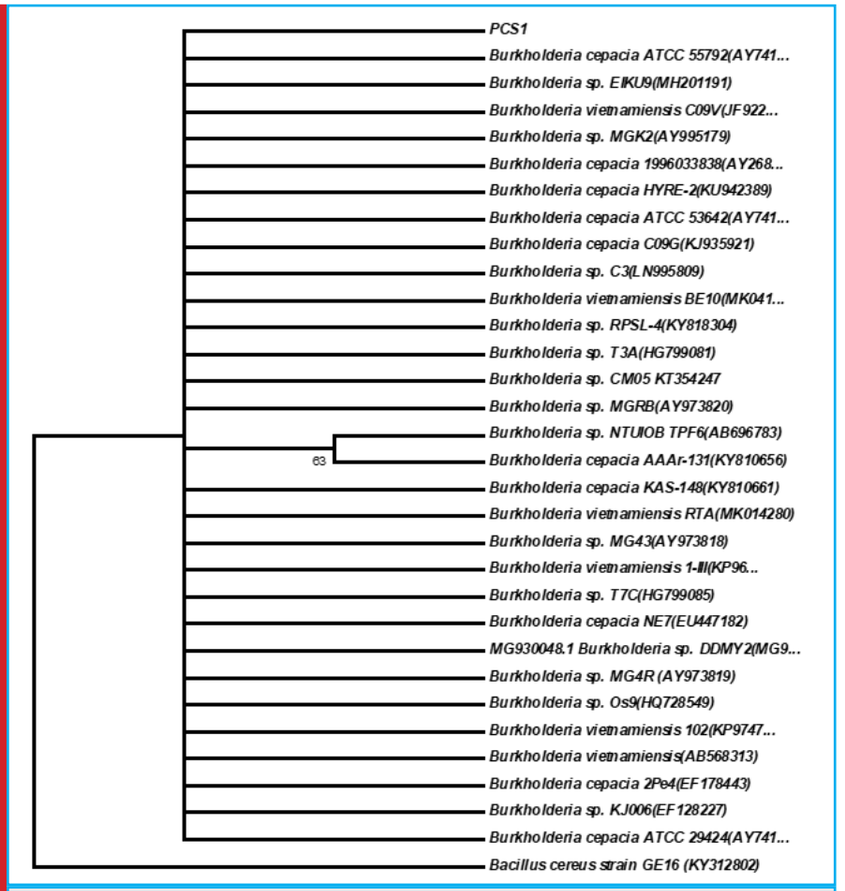

FIGURE 4. The neighbourhood joining tree of the PCS1 strain based on 16S rRNA gene sequence

Dalmastri *et al.* (1999) studied the effect of soil type, maize cultivar and root localization on the genetic diversity of *Burkholderia cepacia* populations and found that the degree of genetic diversity was regulated strictly by the soil types. Salles *et al.* (2004) added that the distribution of *Burkholderia* spp. in soil is attributed to the land use history of that area beside the maize cultivar and soil type. It is probably due to the soil type and maize cultivar, which were responsible for the deviation of the characteristics of the novel strain, PCS1 from the other strains of *Burkholderia cepacia*, reported from other parts of the world.

CONCLUSION

In addition to nitrogen fixation in soils, *Burkholderia* spp. also exhibit starch degrading property that is beneficial to maize plants. The DNA G+C content and the carbohydrate fermentation abilities of the novel strain, PCS1 supports the properties of the genus *Burkholderia*. The phylogenetic tree showed the clustering of PCS1 with *Burkholderia cepacia*. It can be said that the variation of the strains from the other strains of *Burkholderia* were due to the type of soil and maize cultivar used in the study.

ACKNOWLEDGEMENTS

The first author is thankful to the Department of Zoology, The University of Burdwan for giving all sorts of laboratory facilities to conduct this research. Thanks are due to the agricultural scientists of the Department of Agriculture, Govt. of West Bengal and scientists of CRSMF, The University of Burdwan for extending the help to carry out the research.

REFERENCES

Azmi, S.A., Catterjee, S.N., Saha, N.C. (2014). Phenotypic and molecular characterization of bubble eye gold fish pathogenic ampicillin resistant *Bacillus* sp(GF1). Int. J. of Pharma. Bio. Sci., 4: 342-351.

Balandreau, J., Viallard, V., Cournoyer, B., Coenye, T., Laevens, S., Vandamme, P. (2001). *Burkholderia cepacia* genomovar III is a common plant-associated bacterium. Appl. Environ. Microbiol., 67: 982–985.

Benson, D.A., Karsch-Mizrachi, I., Clark, K., Lipman, D.J., Ostell, J., Sayers, E.W. (2012). GenBank. Nucleic Acids Res., 40: 48-53.

Bevivino, A., Dalmastri, C., Tabacchioni, S., Chiarini, L., Belli, M.L., Piana, S., Materazzo, A., Vandamme, P., Manno, G. (2002). *Burkholderia cepacia* complex bacteria from clinical and environmental sources in Italy: genomovar status and distribution of traits related to virulence and transmissibility. J. Clin. Microbiol., 40: 846–851.

Brito, T.S., Buss, R.P.L.A., Carvalho, J.P.F.C., Eberling, T., Martinez, A.S., Vandeir Francisco Guimarães, V.F., Chaves, E.I.D.O. (2018). Growth promotion of *Burkholderia ambifaria* associated to nitrogen fertilization in the initial development of corn. J. Agric. Sci., 10(6): 123-135.

Brown, A. (2004). Benson's Microbiological applications: Laboratory Manual in General Microbiology. McGraw-Hill Science/Engineering/Math, New York.

Caballero-Mellado, J., Martinez-Aguilar, L., Paredes-Valdez, G., Estrada-de los Santos, P . (2004). *Burkholderia unamae* sp. nov, and N_2-fixing rhizospheric and endophytic species. Int. J. Syst. Evol. Microbiol., 54: 1165–1172.

CLSI (2011). Clincal Laboratory Standards Institute. Performance Standards for Antimicrobial Susceptibility Testing; Twenty-First Informational Supplement. Wayne, Pennsylvania, USA.

Coenye, T., Vandamme, P., Govan, J.R.W., Li Puma, J.J. (2001d). Taxonomy and identification of the *Burkholderia cepacia* complex. J. Clin. Microbiol., 39: 3427–3436.

Cordeiro, C.A.M., Martinas, M.L.L., Lucaino, A. (2003). Production and Properties of alpha amylase from thermophylic Bacillus species. Brazil J. Microbiol., 33: 1-3.

Correa-Galeote, D., Bedmar, E.J., Arone, G.J. (2018). Maize endophytic bacterial diversity as affected by soil cultivation history. Front. in Microbiol., 9: 484.

Czaban, J., Gajda, A., Wroblewska, B. (2007). The motility of bacteria from rhizosphere and different zones of winter wheat roots. Polish. J. of Environ. Stud., 16 (2): 301-308.

Dalmastri, C., Chiarini, L., Cantale, C., Bevivino, A., Tabacchioni, S. (1999). Soil type and maize cultivar affect the genetic diversity of maize root-associated *Burkholderia cepacia* populations. Microb. Ecol., 38: 273-284.

Draghi, W.O., Peeters, C., Cnockaert, M., Snauwaert, C., Wall, L.G., Zorreguieta, A., Vandamme, P. (2014). Burkholderia cordobensis sp. nov., from agricultural soils. Int. J. System. Evol. Microbiol., 64: 2003-2008.

Estrada, L.S.P., Bustillos-Cristales, R., Caballero-Mellado, J. (2001). *Burkholderia*, a genus rich in plant-associated nitrogen fixers with wide environmental and geographic distribution. Appl. Environ. Microbiol., 67: 2790–2798.

Estrada, L.S.P., Mavingui, P., Cournoyer, B., Fontaine, F., Balandreau, J., Caballero-Mellado, J. (2002). A N_2 -fixing endophytic *Burkholderia* sp. associated with maize plants cultivated in Mexico. Can. J. Microbiol., 48: 285–294.

Forbes, B.A., Sahm, D.F., Weissfeld, A.S. 2007. Bailey & Scott's Diagnostic Microbiology, Elsevier, Inc., St. Louis, MO, USA, 12th edition.

Gillis, M., Van, T., Bardin, R., Goor, M., Hebbar, P., Willems, A., Segers, P., Kersters, K., Heulin, T., Fernandez, M.P. (1995). Polyphasic taxonomy in the genus *Burkholderia* leading to an amended description of the genus and proposition of *Burkholderia vietnamiensis* sp. nov. for N_2-fixing isolates from rice in Vietnam. Int. J. Syst. Bacteriol., 4(5): 274–289.

Hebbar, P., Davey, A.G., Merrin, J., Dart, P.J. (1992). Rhizobacteria of maize antagonistic to *Fusarium moniliforme* , a soil borne fungal pathogen: colonisation of rhizosphere and roots. Soil Biol. Biochem., 24: 989–997.

Holt, J.G., Krieg, N.R., Sneath, P.H.A., Staley, J.T. and Williams, S.T. (1994). Bergey's Manual of Determinative Bacteriology (9th Int. ed.), Williams and Wilkins, Maryland, USA, pp. 565-596.

Janssen, P.H. (2006). Identifying the dominant soil bacteria taxa in libraries of 16S rRNA and 16S rRNA genes. Appl. Environ. Microbiol., 72: 1719–1728.

Jukes, T.H., Cantor, C.R. (1969). Evolution of protein molecules. In: Munro, H.N., (ed). Mammalian Protein Metabolism, New York. Academic Press.

Kost, T., Stopnisek, N., Agnoli, K., Eberl, L., Weisskopf, L. (2014). Oxalotrophy, a widespread trait of plant-associated *Burkholderia* species, is involved in successful root colonization of lupin and maize by *Burkholderia phytofirmans*. A Report, University of Zurich.

Krisle da Silva, K., Perin, L., Gomes, M.L., Barauna, A.C., Pereira, G.M.D., Mosqueria, C.A., Costa, I.B., O'hara, G., Zilli, J.E. (2016). Diversity and capacity to promote maize growth of bacteria isolated from the Amazon region. Act. Aamaz., 46(2): 111-118.

Lim, J.S., Choi, B.S., Choi, A.Y., Kim, K.D., Kim, D.I., Choi, I.Y., Ka, J.O. (2012). Complete genome sequence of the fenitrothion-degrading *Burkholderia* sp. strain YI23. J. Bacteriol., 194: 896.

Nusrat, A., Rahman, S.R. (2007). Comparative studies on the production of extracellular α-amylase by three mesophilic Bacillus isolates. Bangladesh J. of Microbiol., 24(2): 129-132.

Perin, L., Martinez-Aguilar, L., Paredes-Valdez, G., Baldani, J.I., Estrada-de Los Santos, P., Reis, V.M., Caballero-Mellado, J. (2006a). *Burkholderia silvatlantica* sp. nov., a diazotrophic bacterium associated with sugar cane and maize. Int. J. Syst. Evol. Microbiol., 56: 1931–1937.

Ramette, A., LiPuma, J.J., Tiedje, J.M. (2005). Species abundance and diversity of *Burkholderia* complex in the environment. Appl. Environ. Microbiol., 71: 1193–1201.

Reis, V.M., Estrada-de los Santos, P., Tenorio-Salgado, S. (2004). *Burkholderia tropica* sp. nov, a novel nitrogen-fixing , plant associated bacterium. Int. J. Syst. Evol. Microbiol., 54: 2155–2162.

Saitou, N., Nei, M. (I987). The neighbor-joining method: a new method for reconstructing phylogenetic trees. Mol. Biol., 4: 406-425.

Salles, J.F., De Souza, F.A., van Elsas, J.D. (2002). Molecular method to assess the diversit y of *Burkholderia* species in environmental samples. Appl. Environ. Microbiol., 68: 1595–1603.

Salles, J.F., van Veen, J.A., van Elsas, J.D. (2004). Multivariate analyses of *Burkholderia* species in soil: effect of crop and land use history. Appl. Environ. Microbiol., 70: 4012–4020.

Smits, J.P., Rinzema, J., Tramper, H., Van, M., Knol, W. (1996). Solid-state fermentation of wheat bran by *Trichoderma reesei* QM9414: substrate composition changes, C balance, enzyme production, growth and kinetics. Appl. Micro. Biotechnol., 46: 489-496.

Sneath, P.H.A., Holt. J.G. (2001). Bergey's Manual of Systematic Bacteriology (2nd ed.), Williams & Wilkins, Springer-Verlag, NY, USA, 1, pp. 64.

Tran Van, V., Mavingui, P., Berge, O., Balandreau, J., Heulin, T. (1994). Promotion de croissance du riz inocule par une bacteria fixatrice d'azote, *Burkholderia vietnamiensis* , isolee d'un sol-sulfat e acide du Vietnam Agronomie., 14 : 697–707.

Van Elsas, J.D., Garbeva, P. Salles, J. (2002). Effects of agronomical measures on the microbial diversity of soils as related to the suppression of soil-borne plant pathogens. Biodegradation, 13: 29–40.

Viallard, V., Poirier, I., Cournoyer, B., Haurat, J., Wiebkin, S., Ophel-Keller, K., Balandreau, J. (1998). *Burkholderia graminis* sp. nov.,a rhizospheric *Burkholderia* species, and reassessment of *Pseudomonas phenazinium* ,*Pseudomonas pyrrocinia* and *Pseudomonas glathei* as *Burkholderia*. Int. J. Syst. Bacteriol., 48: 549–563.

Wang, S., Lin, C., Liu, Y., Shen, Z., Jeyaseelan, J., Qin, W. (2016). Characterization of a starch-hydrolyzing α-amylase produced by *Aspergillus niger* WLB42 mutated by ethyl methane sulfonate treatment. Int. J. Biochem. Mol. B., 7(1): 1-10.

Yabuuchi, E., Kosako, Y., Oyaizu, H., Yano, I., Hotta, H., Hashimoto, Y., Ezaki, T. & Arakawa, M. (1992). Proposal of Burkholderia gen. nov. and transfer of seven species of the genus *Pseudomonas* homology group II to the new genus, with the type species *Burkholderia cepacia* (Palleroni and Holmes 1981) comb. nov. Microbiol. Immunol., 36: 1251–1275.

Pharmaceutical Communication

Biosci. Biotech. Res. Comm. 12(1): 73-79 (2019)

BBRC Bioscience Biotechnology Research Communications

Improved production of withanolides in adventitious root cultures of *Withania somnifera* by suspension culture method

Sindhu Rangaraju*, A.N. Lokesha and Chenna Reddy Aswath

Division of Floriculture and Medicinal Crops, ICAR-Indian Institute of Horticultural Research, Hesaraghatta Lake post, Bangalore-89

ABSTRACT

Jawahar Ashwagandha-20 (JA-20) and Arka Ashwagandha (AA) seeds were raised in *in vitro* conditions and phenotypic differences between the plants was recorded. The adventitious roots were derived from leaves of the two varieties in *in vitro* conditions. The effects of the strength of media and concentration and the combination of auxins (IAA and IBA) for adventitious roots multiplication using suspension culture were studied. After 30 days of suspension culture, root biomass was measured and HPLC analysis of major withanolides in leaves and adventitious roots was conducted. Arka Ashwagandha variety had higher total withanolide content of 1.621 mg/g, Withaferin A content of 1.362 mg/g and root yield of 4.066 g from 0.1g inoculum in 30 days compared to JA-20 which had total withanolide content of 1.156 mg/g, Withaferin A content of 0.930 mg/g on dry weight basis and root mass of 3.71g from 0.1g of inoculum in 30 days. The present study thus helps in the identification of an elite cultivar of Ashwagandha and development of a standard protocol for mass multiplication of adventitious root in hormone-free media. This is beneficial in the preparation of health supplements in terms of human health issues due to negligible residual effects of hormones in the final product.

KEY WORDS: ADVENTITIOUS ROOT CULTURE, ASHWAGANDHA, JA 20, IAA- INDOLE ACETIC ACID, IBA- INDOLE-3-BUTYRIC ACID

ARTICLE INFORMATION:

Corresponding Author: sindhurangaraju63@gmail.co.in
Received 9th Feb, 2019
Accepted after revision 12th March, 2019
BBRC Print ISSN: 0974-6455
Online ISSN: 2321-4007 CODEN: USA BBRCBA
Thomson Reuters ISI ESC / Clarivate Analytics USA
NAAS Journal Score 2019: 4.31 SJIF: 4.196

Online Contents Available at: http//www.bbrc.in/
DOI: 10.21786/bbrc/12.1/10

INTRODUCTION

Ashwagandha (*Withania somnifera Dunal*) is a medicinal crop of commercial importance, belongs to family *Solanacea*e, and is considered as an alternate to *Panax ginseng* in its therapeutic values (CSIR.,1976). It is used for curing a wide range of diseases in Ayurveda and other indigenous systems of medicine for over 5000 years (Akram *et al*., 2011). The herb has the highest value for its pharmacological activity in preparation of various Ayurvedic formulations. It is anti-stress, anti aging, and aids in recovering from neurodegenerative disorders (Bhattacharya *et al.,* 2002). It is a small, erect, branched, woody shrub that grows up to 1.50m tall. It is cultivated under rainfed condition in marginal soils by small and marginal farmers of Madhya Pradesh, Rajasthan, Gujarat, Andhra Pradesh, Karnataka, and other states. Apart from chemical constituents like alkaloids and withanolides, it also contains a variety of amino acids including aspartic acid, proline, tryptophan, tyrosine, cysteine, alanine, glycine, and a high amount of iron.

Withanolides are C-28 steroidal lactones (Alfonso *et al*., 1993). Major withanolides identified include Withanolide A, Withanoside IV and VI (Tohda *et al*., 2005), Withaferin A (Oh *et al*., 2008), Withanosides IV and V (Matsuda *et al*., 2001) and Withanoside B (Pramanick *et al*., 2008). Ashwagandha is available in the Western world as a dietary supplement. Its also known as “Indian Ginseng” and “Winter Cherry”. Withanolide A has strong neuro pharmacological properties of promoting outgrowth, synaptic reconstruction, and a potential to reconstruct neural networks (Kuboyama *et a*l., 2005; Tohda *et al*., 2005 a,b). Withaferin A inhibits angiogenesis (Mohan *et al*., 2004), metastasis (Misico *et al*., 2002). The major pharmacological activity of *Withania somnifera* is contributed to two major withanolides, Withaferin and Withaferin D (Gupta *et al.,* 2007, Sindhu *et al*., 2018).

Arka Ashwagandha is a variety identified at ICAR-Indian Institute of Horticulture Research, for high dry root yield and high total withanolide content. The variety has double the dry root yield (10 q/ha) than JA-20 (5.27q/ha). The other significant features are early vigor, field tolerance to bacterial wilt, late blight, leaf spot diseases and pests (*Epilachna* beetle, mites and aphids). It matures in 180 days and is characterized by desired root thickness and depth. The distinguishing features of the variety are lengthy tertiary branch, thick stem which has dense curved pubescence, lanceolate leaves with obtuse leaf tip, bigger fruit capsules and fruits. JA-20 is a released variety from MPKVV, Mandsaur, Madhya Pradesh used as a check in AICRP National trials and it yields about 5 q/ha.

Recent advances in tissue culture methodologies have improved secondary metabolite production across various medicinal plants. Selection of high bioactive producing lines, optimization of culture conditions, metabolic engineering, elicitation strategies and use of bioreactor culture systems has made the production of useful metabolites *in vitro* at a shorter duration of time (Sarin *et al*., 2005). Plant-specific metabolites can be effectively obtained from organ and plant culture systems (Verpoorte *et al*., 2002). Plant cell and organ culture systems are promising methodologies as they aid in rapid proliferation of cells/organs, condensed biosynthetic cycles in comparison to field grown plants (Ramachandra Rao and Ravishankar, 2002, Thanh Tam et al., 2019).

Adventitious roots suspension cultures are found to be ideal for biomass accumulation in *Echinacea purpurea* (Wu *et al*., 2007) and *P. notoginseng* (Gao *et al*., 2005). Recent studies indicate that explant type and genotype affect the accumulation of bioactive compounds in adventitious root cultures of *Polygonum multiflorum* (Ho *et al.,*2019) Lack of post-harvest storage technology for roots (Govil *et al*., 1993; Singh and Kumar., 1998), excessive exploitation of natural resources, problems in field cultivation as it is dependent on monsoon, time consuming and laborious are reasons enough to multiply adventitious roots of *Withania somnifera* in suspension culture which meet the global market requirement of Ashwagandha.

MATERIALS AND METHODS

Seeds of *Withania somnifera* like JA-20 and Arka Ashwagandha were selected. Seed pretreatment was conducted as per our earlier reports (Sindhu *et al*., 2018), morphological and phenotypic examination of 30-day old plants was done. The adventitious roots were induced in these two varieties, which were then harvested from 10-day old leaf culture bottles supplemented with auxins. These roots were washed with sterile distilled water two times to remove the small traces of agar followed by treatment for 1 minute with 3% sodium hypochloride, then the traces of sodium hypochlorite from roots were removed by washing again with sterile distilled water. The roots were dried by blotting with sterile tissue paper. The known quantity of roots (100 mg) were weighed and transferred into 100 ml of full strength MS liquid media supplemented with different concentration and a combination of auxins in conical flasks with 3% sucrose concentration under 16 hours of photoperiod and placed in an orbital shaker at 90 rpm at 25°C. The mass of multiplied roots was observed after 30 days of inoculation and was compared with the control.

Extraction of bioactive principles from *W. somnifera:* The adventitious roots were extracted from the liquid medium and the *in vitro* leaves were taken washed using distilled water to remove the traces of medium, dried and powdered using pestle and mortar. Adventitious roots were

assessed for total withanolides and also different components that contribute to total withanolides whereas the leaves were assessed only for Withaferin A content. The analysis of bio actives was done using High Performance Liquid Chromatography method. One gram of dry root powder was extracted with methanol at 80^{0}C on a water bath and the residue was re-extracted twice with methanol, till the extract was colorless. The extracts were pooled and filtered through sample clarification kit and were subjected to analysis by HPLC with Photo Diode Array. Seven standards such as Withanoside IV, Withanoside V, Withaferin A, Withanolide A, Withanolide B, Withanone and Withanostramolide from Natural Remedies Pvt. Ltd, Bangalore were used to quantify the total amount of withaferin A present in leaf samples and withanolides in root samples. The chromatogram was recorded at 227 nm and later the contents of various withanolides were added to estimate the total withanolide and expressed as mg/g on a dry weight basis.

$$\frac{\text{Area of the sample x Standard Wt. (mg) x Sample dilution x Purity of standard}}{\text{Area of the standard x Standard dilution x sample weight (mg) x 100}} \times 100$$

Data Analysis:

All experiments were repeated thrice. Mean values of treatments were subjected to ANOVA and significant differences were separated by Duncan's Multiple Range Test. To determine significance at P<0.05SPSS (Windows version 75.1, SPSS Inc., Chicago) was used.

RESULTS AND DISCUSSION

1. Morphological comparison between two varieties of Ashwagandha.

In vitro plants were assessed for plant height using 1 mm ruler from base of the stem to apical meristem. Leaf shape was also observed.

Table 1. Phenotypic differences between Arka Ashwagandha and JA-20 in *in vitro* conditions.

Traits	Arka Ashwagandha	JA -20
Plant height (cm)	6.30	5.50
Number of roots	17	16
Leaf shape	Lanceolate	Ovate
Leaf base	Concave	Concave
Leaf tip	Obtuse	Acute

2. Influence of hormone supplementation on the proliferation of *Withania somnifera* adventitious roots in suspension culture

For large scale production of useful bioactive metabolites, the use of cell suspension cultures is favored due to its rapid growth cycles over other kinds of cell culture methods. Qualitative and quantitative analysis requires a considerable quantity of cells to determine growth responses and metabolism of phytochemicals, for these studies cell suspension cultures are found to be best suited (Vanishree *et al*., 2004).

In the current study, the establishment of adventitious root suspension culture of *Withania somnifera* was done for two varieties Arka Ashwagandha and JA-20 with different hormone supplementation on media and further the biomass accumulation and total withanolides were estimated. Significant phenotypic differences were recorded in the proliferation of root cultures in MS medium, supplemented with hormones and without hormones. In the hormone supplemented medium, the root biomass was higher, but there was no elongation of lateral roots. The suspension culture media with hormones gave rise to fluffy roots, with callus like exudates formed around the senescent root tissues and subsequently released into the medium which could not be further multiplied in suspension cultures whereas media without supplementation of hormones had normal roots

Table 2. Data represent mean ± standard error of five replications in three independent experiments, each with one explant per treatment. Values followed by the different letters are significant P<0.05 according to Duncan's Range Multiple Test. Data were scored after 30 days of culture. Growth Conditions: Media- Full MS liquid medium supplement with different hormone combinations, 3% sucrose, 16 hours photoperiod at 25±2°C.

Treatment	Combination of auxins mg/l		The quantity of root obtained in gram/100 ml of media after 30 days of culture		Remarks
	IAA	IBA	AA	JA-20	
Control	0.0	0.0	4.066±0.118f	3.718±0.150f	Normal roots
T1	0.25	0.75	8.340±0.098b	7.254±0.135b	Fluffy roots
T2	0.50	0.50	6.400±0.139c	6.248±0.072c	Fluffy roots
T3	0.75	0.25	5.640±0.083d	5.364±0.068d	Fluffy roots
T4	1.0	0.0	4.682±0.086e	4.098±0.114e	Fluffy roots
T5	0.0	1.0	9.612±0.088a	8.314±0.138a	Fluffy roots

Table 3. Data represent mean ± standard error of five replications in three independent experiments, each with one explant per treatment. Values followed by the different letters are significant P<0.05 according to Duncan's Range Multiple Test. Data were scored after 30 days of culture. Growth Conditions- Media- Full MS liquid medium supplement with different hormone combinations, 3% sucrose, 16 hours photoperiod at 25±2°C.

Treatment	Arka Ashwagandha	JA-20
Half MS	3.684±0.074b	3.520±0.073b
Full MS	4.066±0.066a	3.718±0.054a

with important factors of proliferation like lateral root formation, elongation of lateral roots which favored further multiplication of adventitious roots. Lateral root formation was essential for rapid growth and higher biomass production in *Rauwolfia serpentine L* (Pandey *et al*., 2010), thus indicating that phytohormone supplementation does not always enhance the regeneration frequency (Roychowdhury *et al*., 2013).

Genes involved in the synthesis of auxins are expressed in roots, which contribute to normal root growth and maintenance (Petersson *et al*., 2009). Auxin biosynthesis genes are expressed at root stem cell nice to increase the level of auxins (Stepanova *et al.,* 2008). Signaling pathways for other plant hormones also influence the auxin response in roots (Kuppusamy *et al*., 2008). Though there was higher root mass in media supplemented with hormones, considering lateral root formation, proliferation and morphology of roots, MS media without hormone supplementation was considered best.

3. Influence of media strength on proliferation of *Withania somnifera* adventitious roots in suspension cultures

Both half strength MS medium and full strength MS medium were found to be suitable for biomass production of adventitious roots in *Panax ginseng*, but highest secondary metabolite content was induced in full strength MS medium (Yu et al., 2000). Full strength MS medium supplemented with 2.0mg/l IBA under continuous agitation increased the biomass of root tissue in *Vernonia amygdalina* (Khalaffala *et al*., 2009). Several researchers have also reported cell suspension culture studies in *Withania somnifera* (Sivanandan *et al*., 2012b and Praveen *et al*., 2011), hence full strength media without hormone supplementation was considered best suited for adventitious root multiplication in suspension culture as it provides more nutrients and reduces the frequency of subculturing in both varieties of Ashwagandha.

Different types of roots obtained by hormone treatments in *Withania somnifera*.

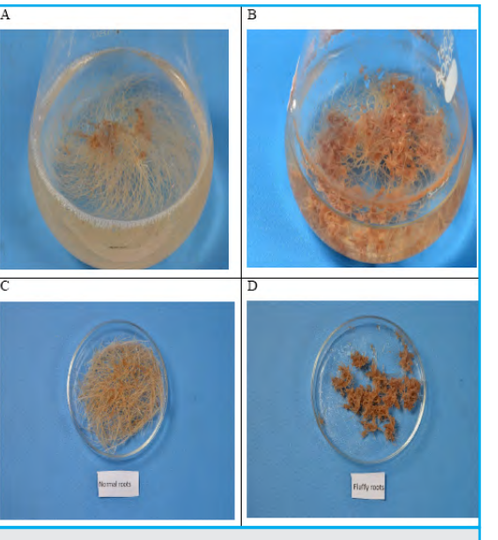

FIGURE 1. Different types of roots obtained in Arka Ashwagandha. A-Control, B-Hormone treated roots, C-Normal roots obtained after suspension culture in hormone-free medium, D-Fluffy roots obtained after suspension culture in hormone media.

4. Withanolides identified and total withanolide content in leaf and adventitious roots by HPLC analysis

HPLC analysis of *Withania somnifera* using methanolic extraction was reported by many researchers like Ganzera *et al*., (2003), Sangwan *et al*., (2004). The present study indicated that the roots had higher total withanolide content i.e., 1.621mg/g on a dry weight basis in Arka ashwagandha, compared to the total withanolide content in JA-20 root was 1.156 mg/g on a dry weight basis. Withanolide A which has a biological activity of sedative and hypnotic was 0.38mg/g on a dry weight basis in Arka Ashwagandha in comparison to JA 20

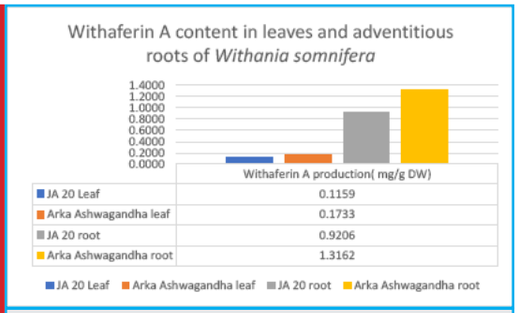

FIGURE 2. Withaferin A production in leaves and roots of *Withania somnifera* analyzed by HPLC.

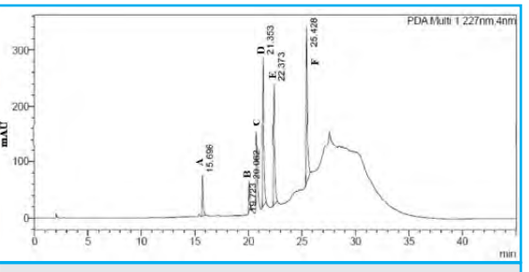

FIGURE 3. Standard HPLC chromatogram of *W. somnifera* root extracts. A. Withanoside IV, B. Withanoside V, C. Withaferin A, D. 12-Deoxy Withastramonolide, E. Withanolide A and F. Withanolide B.

which has 0.28mg/g on a dry weight basis. Madhavi *et al* (2012) reported a Withanolide A content of 136 µg/g dry weight in 120 days old hairy root culture and 13µg/g dry weight in 210 days old hairy root culture of *Withania somnifera,* Dewin *et al.,* (2010) reported Withanolide A content of 0.019 mg/g in *in vitro* roots of *Withania somnifera* which is much lesser than the Withanolide A content reported in the present study. The methanolic extract of *Withania somnifera* has GABA mimetic activity, anti-inflammatory and anti-stress properties (Mir *et al*., 2012).

Withaferin A contributes to most of the pharmacological activity of *Withania somnifera* with its antibacterial, antifungal, antiarthritic, antitumor and antibiotic properties. Dalavayi *et al*., (2006) identified Withaferin A in roots and leaves of Ashwagandha. The Withaferin A content in Arka Ashwagandha roots was identified to be 1.316mg/g on a dry weight basis compared to JA- 20 with a content of 0.926mg/g on a dry weight basis. The Withaferin A content in Arka Ashwagandha leaves was 0.1733mg/g on a dry weight basis compared to JA-20 leaves 0.116 mg/g on a dry weight basis.

Madhavi *et al* (2012) reported that Withaferin A was not detected in 120 day old hairy root cultures, whereas it was 136µg /g dry weight in 210 day old hairy root cultures of *Withania somnifera,* Sivanandan *et al* (2012) reported 0.85mg/g in 40 day old callus cultures of *Withania somnifera,* which is much lesser than the Withaferin A content reported in the present study. Dewir *et al* (2010) reported a Withaferin A content of 0.013 mg/g dry weight in *in vitro* roots, the present study indicates 100 times increased Withaferin A content.

CONCLUSION

This current study helps in the identification of an elite cultivar of *Withania somnifera* for mass production of withaferin A and total withanolides. Field cultivation of *Withania somnifera* is a laborious task, as the crop is prone to diseases like seed rot and blight, harvesting of roots is a tedious task. The provision for alternative sources of Ashwagandha through cell cultures and micropropagation must be encouraged as it reduces the heavy dependence on the wild population to fulfill the global demand of *Withania somnifera*. Adventitious root multiplication through suspension cultures in hormone free medium provide an easy way for mass production of useful withanolides and can be used by neutraceutical and pharmaceutical industries as there would not be traces of hormones in the end product.

Comparison of Withaferin A content between adventitious roots and *in vitro* leaves in *Withania somnifera*.

Table 4. Analysis of Withanolides in adventitious roots of *Withania somnifera* by HPLC Data represents mean ± standard error of three replications. Values followed by the different letters are significant P<0.05 according to Duncan's Range Multiple Test. Data were scored after 30 days of culture.

Variety	Withanoside IV	Withanoside V	Withaferin A	12-Deoxy withastromalide	Withanolide A	Withanolide B	Total Withanolides
	mg/g on dry weight basis						
Arka ashwagandha root	0.013±0.000[a]	0.025±0.001[b]	1.362±0.032[a]	0.181±0.004[a]	0.038±0.001[a]	0.003±0.000[a]	1.621±0.069[a]
JA-20 root	0.011±0.001[b]	0.037±0.003[a]	0.930±0.005[b]	0.173±0.004[b]	0.028±0.001[b]	0.002±0.000[b]	1.1558±0.013[b]

ACKNOWLEDGMENTS

This research was conducted at ICAR- Indian Institute of Horticulture Research and was funded by the Department of Science and Technology through DST Inspire fellowship. The first author also acknowledges Centre for postgraduate study, Jain University for conducting this research.

REFERENCES

Akram M, Mohiuddin E, Hannan A and Usmanghani K (2011) *Withania somnifera* (L.) Dunal (Pharmacology Activity), Pharmacognosy Journal, 2(18):77-78.

Alfonso D, Bernardinelle G and Kapetanidisn I (1993) Withanolides from *Lochoma coccinaum,* Phytochemistry, 34(2):517-521.

Bhattacharya SK, Bhattacharya D, Sairam K and Ghosal S (2002) Effect of *Withania somnifera* glycol-withanolides on a rat model of tardive dyskinesia, Phytomedicine 9(2):167-170.

Dalavayi S, Kulkarni SM, Itikala RL and Itikala S (2006). Determination of Withaferin A in two *Withania* species by RP-HPLC method. Indian Journal of Pharmaceutical Sciences. 68:253-256.

Dewir Y.H, Chakrabarty D, Lee S.-H, Hahn E.-J. and Paek K.-Y(2010) Indirect degeneration of *Withania somnifera* and comparative analysis of Withanolides in *in vitro* and green house plants. Biologia Plantarum 54(2):357-360,2010.

Sivanandhan G, Arun M, Mayavan S, Rajesh M, Jeyaraj M, Kapil Dev G, Manickavasagam M, Selvaraj N and Ganapathi A (2012b) Optimization of elicitation conditions with Methyl Jasmonate and Salicylic Acid to improve the productivity of Withanolides in the adventitious root cultures of *Withania somnifera*(L.)Dunal. Applied Biochem Biotechnol 168:681-696.

Ganzera M, Choudhary MI, Khan IA (2003) Quantitative HPLC analysis of Withanolides in *Withania somnifera*. Fitoter 74:68-76.

Gao X, Zhu C, Gao W, Jia W, Qui M, Zhang Y and Xiao P (2005) Induction and characterization of adventitious roots directly from the explants of *Panax notoginseng*, Biotechnology letters, 27(22):1771-1775.

Gould AR, Everett NP, Wang TL, Street HE (1981) Studies on the control of cell cycle in cultured plant cells: Effects of nutrient limitation and nutrient starvation. Protoplasma, 106 (1-2):1-13.

Govil JN, Singh VK and Shamima H (1993) In: Glimpses in plant research Vol. X medicinal plants: New Vistas of research (Part1) today and tomorrow printers and publishers, New Delhi India. 232-253.

Ho,TT.,Jeonh,CS.,Lee,H. et.al. (2019) Plant Cell Tiss Organ Cult (2019).https://doi.org/10.1007/s11240-018-01556-5.

Kuboyama T, Tohda C, Komastu K (2005)Neuritic regeneration and synaptic reconstruction induced by withanolide A. Br J Pharmacol 144:961-971.

Kuppuswamy KT, Walcher CL and Nemhausar JL (2008) Cross-regulatory mechanisms in hormone signaling. Plant Molecular Biology. 9(4)375-381.

Matsuda H, Murakami T, Kishi A, Yoshikawa M (2001) Structures of Withanolides I, II, III, IV, V, VI and VII, new withanolide glycosides from the roots of Indian *Withania somnifera* Dunal and inhibitory activity of tachyphylaxis to clonidine in isolated guinea pig ileum. Bioorganic and medicinal chemistry, 9(6):1499-1507.

Morano-Risueno MA, Van Norman JM, Moreno A, Zhang J, Ahnert SE and Benfey PN (2010) Oscillating gene expression determines competence for periodic *Arabidopsis* root branching. Science, 329 (5997): 1306-1311

Oh JH, Lee TJ, Kim SH, Choi YH, Lee SH, Lee JM, Kim YH, Park JW and Kwon TK (2008) Induction of apoptosis by Withaferin A in human leukemia U937 cells through downregulation of AKT phosphorylation. Apoptosis, 13(12):1494-504.

Pandey VP, Cherian E and Pathani G (2010) Effect of Growth Regulators and Culture conditions on Direct Root Induction of *Rauwolfia serpentine* L. (Apocynaceae) Benth by leaf explants. Tropical Journal of Pharmaceutical Research, 9(1):2734.

Petersson SV, Johansson AL, Kowalczyk M, Makovychuk A, Wang JY, Moritz T, Grebe M, Benfey PN, Sandberg G and Ljung K(2009) An auxin gradient and maximum in the *Arabidopsis* root affects shown by high-resolution cell-specific analysis of IAA distribution and synthesis. Plant cell 21(6):1659-1668.

Pramanick S, Roy A, Ghosh S, Majumdar HK and Mukhopadhyay S (2008) Withanolide Z, A new chlorinated withanolide from *Withania somnifera*, Planta Medica, 74(14):1745-48.

Praveen N and Murthy HN (2010) Production of Withanolide-A from adventitious root cultures of *Withania somnifera*. Acta Physiology Plantarum. 32(5): 1017-1022

Ramachandra Rao S, Ravishankar GA (2002) Plant cell cultures: chemical factories of secondary metabolites. Biotech Adv 20:10-153.

Roy Chowdhary D, Majumdhar A and Jha S (2013) *Agrobacterium rhizogenesis* mediated transformation in medicinal plants: Prospects and Challenges in biotechnology for medicinal plants. Springer Verlag Berlin Heidelberg, 41.

Sarin R (2005) Useful metabolites from plant tissue cultures. Biotechnology 4:79-93.

Sindhu Rangaraju, A.N. Lokesha and Chenna Reddy Aswath (2018) Standardization of various factors for production of adventitious roots in selected varieties of *Withania somnifera* and estimation of total withanolides content by High Performance Liquid Chromatography, Biosci. Biotech. Res. Comm. 11(3): 451-460.

Singh S and Kumar S (1998) In Withania somnifera: The Indian ginseng, *Ashwagandha*. Central Institute of medicinal and aromatic plants, Lucknow, India.

Thanh-Tam, Ho Choel-Sueng, Jeong Hyoshin, Lee So-Young Park (2019) Effect of explant- type and genotype on the accumulation of bioactive compounds in adventitious root cultures of *Polygonum multiflorum*, Plant cell tissue and organ culture:

Tohda C, Kuboyama T and Komatsu K (2005) Search for natural products related to regeneration of the neuronal network. Neurosignals, 14(1-2):34-45.

Vanisree M, Lee C, Lo S, Nalavade SM, Lin CY and Tsay H (2004) Studies on the production of some important secondary metabolites from medicinal plants by plant tissue cultures. Botanical buttelin of Academia Sinica, 45:1-22.

Verpoorte R, Contin A, Memelink J (2002). Biotechnology for the production of Plant secondary metabolites. Phytochem Rev 1:13-25.

Wu CH, Dewir YH, Hahn EJ and Peak KY (2006) Optimization of culturing conditions for the production of biomass and phenolics from adventitious roots of *Echinacea angustifolia*. Journal of Plant Biology, 49(3):193-199.

Wu CH, Murthy HN, Hahn EJ and Paek KY (2007) Large-Scale cultivation of adventitious roots of *Echinacea purpurea* in air lift bioreactors for the production of chichoric acid, chlorogenic acid and caftaric acid. Biotechnology Letters 29(8):1179-1182.

Yu KW, Hahn EJ and Paek KY (2000) Production of adventitious *ginseng* roots using Bioreactor. Korean Journal of Plant Tissue Culture 27:309-315.

Biotechnological Communication

Biosci. Biotech. Res. Comm. 12(1): 80-89 (2019)

BBRC Bioscience Biotechnology Research Communications

Molecular characterization and genetic diversity of Indian potato, (*Solanum tuberosum* L.) germplasms using microsatellite and RAPD markers

Manthan Kapuria[1,2], Darshan Dharajiya[1,3]*, Karen Pachchigar[1,4] and R. M. Chauhan[5]

[1]*Department of Plant Molecular Biology and Biotechnology, C. P. College of Agriculture (CPCA), Sardarkrushinagar Dantiwada Agricultural University (SDAU), Sardarkrushinagar-385506, Gujarat, India*
[2]*Shree P. M. Patel Institute of Integrated M. Sc. in Biotechnology, Anand-388001, Gujarat, India*
[3]*Department of Biotechnology, Mehsana Urban Institute of Sciences, Ganpat University, Ganpat Vidyanagar–384012, Gujarat, India*
[4]*College of Basic Science and Humanities, SDAU, Sardarkrushinagar-385506, Gujarat, India*
[5]*Centre of Seed Technology, S. D. Agricultural University, Sardarkrushinagar-385506, Gujarat, India*

ABSTRACT

Potato (*Solanum tuberosum* L.) is the fourth most important food crop in the world and an important vegetable crop. The genus *Solanum* consists of 220 tuber containing species of which seven tuber-bearing species is used for commercial cultivation. Potato is a self-pollinated crop with cross-pollination up to 2.54 percent. Use of molecular markers to determine genetic variation, genetic diversity and evolutionary relatedness is becoming more popular for the assessment of diversity among cultivars of crop species of from various geographical origins. In the present study, total 42 RAPD markers have been employed, out of which 21 primers were polymorphic with 66.95% average polymorphism and 0.783 average PIC value, indicating higher informativeness of primers. In the present study, total 25 SSR markers have been employed out of these only 4 potent SSR primers were polymorphic. For SSR markers, average polymorphism was 58.33% and mean PIC value was 0.712. The results of current study indicate that RAPD and SSR markers used in the study have very promising polymorphism and PIC values hence, seemed to be good for the molecular characterization and assessing genetic relationship among genotypes of potato.

KEY WORDS: POTATO (*SOLANUM TUBEROSUM* L.), MOLECULAR MARKERS, MICROSATELLITE, RAPD, SSR

ARTICLE INFORMATION:

Corresponding Author: darshanbiotech1@gmail.com
Received 24th Dec, 2018
Accepted after revision 1st March, 2019
BBRC Print ISSN: 0974-6455
Online ISSN: 2321-4007 CODEN: USA BBRCBA
Thomson Reuters ISI ESC / Clarivate Analytics USA
NAAS Journal Score 2019: 4.31 SJIF: 4.196

Online Contents Available at: http//www.bbrc.in/
DOI: 10.21786/bbrc/12.1/11

INTRODUCTION

Potato (*Solanum tuberosum* L.) originated from South America is one of the major vegetable crops of the world which is also the fourth most important food crop in the world, after maize, wheat, and rice (Ghebreslassie *et al*., 2016; Majeed and Muhammad, 2018). In India, it was introduced in early seventeenth century possibly by the Portuguese or by the Britishers (Pal and Nath, 1951; Kapuria *et al*., 2016). It is a source of low cost energy to the human diet hence, it is considered as an economy food (Pandey and Sarkar, 2005). Globally, the major potato growing nations are China, India, Russia, Ukraine and United States of America (Bradshaw, 2019). The genus *Solanum* consists of 220 tuber-containing species among which seven tuber bearing species exploited for commercial cultivation (Hawkes and Jackson, 1992). The most important feature in potato taxonomy is the variation in ploidy level. Potato is a self-pollinated crop and the level of cross-pollination is up to 2.54 percent (Kapuria *et al*., 2016; Wang *et al*., 2019).

Knowledge of the genetic diversity and relationships among the varieties/cultivars are very beneficial to recognize the gene pool, to recognize the gaps in germplasm collections and to improve effective conservation and management approaches. Use of DNA markers for the identification of genetic variation, genetic diversity and evolutionary relatedness can be useful in identifying genetic/population structure as well as diversity among cultivars from various geographical origins. Due to their simplicity, reliability and cost effectiveness, PCR based methods are in demand (Parita *et al*., 2018).

Different PCR based techniques have been developed during the last two decades, each with specific benefits and drawbacks. The random amplified polymorphic DNA (RAPD) marker system is rapid, simple and requires no prior sequence information in which one random 10-mer primer is used (Welsh and McClelland, 1990; Williams *et al*., 1990). The dominant nature of inheritance of RAPD is considered as its drawback. Among different classes of molecular markers, simple sequence repeats (SSR)/microsatellites which are tandem repeats of 1-6 nucleotide long DNA motifs gaining importance in plant breeding and genetics due to their co-dominant inheritance, multi-allelic nature, relative abundance, hyper variability, reproducibility, good genome coverage including organellar genomes, chromosome specific location, amenability to automation and high throughput genotyping (Oliveira *et al*., 2006; Walunjkar *et al*., 2013). The PCR based techniques have been used for DNA fingerprinting and genotyping in potato including RAPD (McGregor *et al*., 2000; Ghislain *et al*., 2006; Chimote *et al*., 2007; Rocha *et al*., 2010; Gorji *et al*., 2011; Onamu *et al*., 2016; Ayman *et al*., 2018), SSR (McGregor *et al*., 2000; Braun and Wenzel, 2004; Feingold *et al*., 2005; Ghislain *et al*., 2006; Chimote *et al*., 2007; Ghislain *et al*., 2009; Rocha *et al*., 2010; Favoretto *et al*., 2011; Maras *et al*., 2017; Ahmed *et al*., 2018; Tiwari *et al*., 2019), ISSR (McGregor *et al*., 2000; Bornet *et al*., 2002; Gorji *et al*., 2011; Vanishree *et al*., 2016) and AFLP (McGregor *et al*., 2000; Braun and Wenzel, 2004; Solano Solis *et al*., 2007; Jian *et al*., 2017). The present work was conducted to evaluate the phylogenetic relatedness of Indian potato genotypes using RAPD and SSR markers.

MATERIALS AND METHODS

Plant material used in the study

Plant material consisted of young leaves sampled from young plants of 15 diverse Indian potato germplasms (Table 1). They were grown in Botanical Garden, C.P. College of Agriculture, SDAU, Sardarkrushinagar, Gujarat, India.

Genomic DNA extraction and quantification

Genomic DNA was extracted from tender fresh leaves of each germplasm by using CTAB (Cetyl Trimethyl Ammonium Bromide) method described by Doyle and Doyle, (1990) with minor modifications. The quality and integrity of DNA were checked by electrophoresis using 0.8% agarose gel. The DNA samples were quantified on UV spectrophotometer (BioSpectrometer, Eppendorf, Germany). The stocks were diluted to a final concentration of 30 ng/µl of DNA and used for further work.

PCR amplification

RAPD analysis

Forty two primers were selected and used to ascertain polymorphism among diverse germplasms of potato. The

Table 1. Potato germplasms used in the present study

Sr. No.	Germplasm	Sr. No.	Germplasm	Sr. No.	Germplasm
1	DSP-7	6	DSP-287	11	Kufri Kundan
2	Kufri Chipsona-1	7	Kufri Pushkar	12	Kufri Khyati
3	JX-249	8	Kufri Jyoti	13	Kufri Bahar
4	MF-1	9	Kufri Sutlaj	14	Kufri Anand
5	MS/95-1309	10	Kufri Badshah	15	KCM

RAPD primers used in present study are UBC, OPA, OPB, OPC, OPH, OPG, OPW and OPX series and polymorphic primers used in the analysis are given in Table 2. PCR was carried out as method given by Yasmin *et al*., (2006) with minor modifications in a total reaction volume of 25 µl. The PCR mixture consisted of 1 X PCR buffer, 10 mM dNTPs, 2.0 mM $MgCl_2$, 1 U of Taq DNA polymerase, 20 pmol/µl Primer and 30 ng/µl DNA template. All amplifications were carried out on a eppendorf thermal cycler using PCR conditions initial denaturation at 94°C (4 min) one time, denaturation at 94 °C for 1min, annealing at Tm of primer for 45 sec and extension at 72°C for 2 min for 35 cycles with final extension of 72°C for 7 min.

SSR analysis

PCR was carried out as method given by Ghebreslassie *et al.,* (2016) with minor modifications in a total reaction volume of 25 µl. The PCR mixture consisted of 1 X PCR buffer, 10 mM dNTPs, 2.0 mM $MgCl_2$, 1 U Taq DNA polymerase, 20 pmol/µl of primer pair and 30ng/µl of template DNA. The polymorphic primers used in present study are given in Table 2. PCR conditions consisted of initial denaturation at 94°C (4 min) for first cycle only, denaturation at 94 °C for 30 sec, annealing at Tm of primer for 1 min and extension at 72°C for 1 min for 35 cycles with final extension of 72°C for 6 min.

Resolution of amplified products

The amplified products of RAPD and SSR were resolved on 1.5% and 3.0% agarose gel (Dharajiya *et al*., 2017). The gel was stained with ethidium bromide (10µl/100ml). The standard DNA marker (100 bp) was also run along with the samples. After electrophoresis, the gel was carefully taken out of the casting tray and photographed using AlphaEaseFC 4.0.0 Gel Documentation system (Alpha Innotech Corporation, USA).

Analysis of RAPD and SSR data

Data were scored for computer analysis on the basis of the presence (1) or absence (0) of the amplified DNA fragments. The data were entered into the binary matrix and subsequently analyzed using PAleontological STatistics (PAST) -Version 3.18 (Hammer *et al.,* 2001) was used for genetic diversity evaluation. Coefficients of similarity were calculated by using Jaccard's similarity co-efficient (Jaccard, 1908) and cluster analysis was performed by using the Un-weighted Pair Group Method with Arithmetic Mean (UPGMA) function of PAST version 3.18. The Relationship between the potato genotypes was graphically represented in the form of dendrograms by using the cluster analysis function of the software. In this method the dendrogram and similarity matrix were correlated to find the goodness-of-fit of the dendrogram constructed based on the similarity coefficients. The marker data were then standardized for Principal Component Analysis (PCA). The software program AlphaEaseFC version 6.0.0 developed by Alpha Innotech Corporation, USA was used for determining the Molecular Weight (MW) of bands separated on the gel. The Polymorphism Information Content (PIC) value for each locus was calculated on the basis of allele frequency by the formula given by Anderson *et al.,* (1993). The polymorphism percentage was calculated as per the method suggested by Smith *et al*., (1997).

RESULTS AND DISCUSSION

Molecular marker analysis

Total 42 RAPD primers were used for screening of 15 potato germplasms. Out of 42 primers, 21 were polymorphic which amplified a total of 116 reproducible DNA fragments. Out of total 116 DNA fragments, 79 fragments were polymorphic with the mean number of polymorphic bands per primer was 3.76. The size of amplified fragments varied from 140 to 2059 bp. The highest number of amplified bands (8) was exhibited by primer UBC 31 and UBC 34 whereas lowest number of amplified bands (3) was produced by primer OPW 4. The highest polymorphism (100%) was exhibited by two primer OPA 8 and OPB 18, while the lowest polymorphism (20.00 %) was evinced with OPW 8. The average polymorphism detected by the RAPD loci in the present investigation was 66.95 % (Table 2).

Out of 25 SSR primers used in the study, 4 were polymorphic which amplified a total of 18 reproducible fragments among which 11 fragments were polymorphic. The mean number of polymorphic bands was 2.75. The size of PCR amplified fragments varied from 125 to 1899 bp. The highest number of amplified band (6) was exhibited by primer STWIN12G and STCPKIN 3 and the lowest number of amplified bands (2) was exhibited by primer STPRINPSG. The highest polymorphism (66.66) was exhibited by two primers *viz*., STWIN12G and STCPKIN 3, while the lowest polymorphism (50.00%) was evinced with STPRINPSG and STACCS 3. The average polymorphism detected by the SSR loci in the present investigation was 58.33 % (Table 2).

The distribution of the primers used in the study according to the PIC values and per cent polymorphism is given in the Fig. 1. Most of the RAPD primers (11) have PIC value from 0.7 to 0.8 whereas two SSR primers have PIC value from 0.8 to 0.9. Most of the RAPD primers have per cent polymorphism more than 60 %. It indicates that these primers possess good importance in the diversity analysis in potato.

Table 2. Result of RAPD and SSR analysis in potato genotypes

Sr. No.	Primer name	TB	TPB	TMB	% P	PIC	AL (bp)
RAPD Primers							
1	UBC-34	8	6	2	75.00	0.852	228 to 1800
2	UBC 77	4	2	2	50.00	0.737	152 to 553
3	UBC 88	6	4	2	66.66	0.797	274 to 1888
4	UBC 31	8	4	4	50.00	0.858	309 to 2022
5	UBC 33	5	3	2	60.00	0.782	129 to 493
6	OPH 5	5	4	1	80.00	0.763	276 to 807
7	OPA 7	5	5	0	100.0	0.776	214 to 1227
8	OPA 6	7	4	3	57.14	0.848	140 to 827
9	OPB 18	5	5	0	100.0	0.786	201 to 586
10	OPB 10	4	3	1	75.00	0.732	430 to 1216
11	OPB 6	3	1	2	33.33	0.606	197 to 649
12	OPB 5	6	5	1	83.33	0.801	678 to 2059
13	OPA 19	6	4	2	66.66	0.822	172 to 677
14	OPA 12	5	4	1	80.00	0.790	143 to 638
15	OPA 8	7	7	0	100.0	0.846	154 to 560
16	OPA 3	6	4	2	66.66	0.785	260 to 1030
17	OPA 2	7	6	1	85.71	0.841	195 to 2047
18	OPW 8	5	1	4	20.00	0.776	369 to 1529
19	OPW 5	5	2	3	40.00	0.770	437 to 1526
20	OPW 4	3	2	1	66.66	0.660	824 to 1840
21	OPW 2	6	3	3	50.00	0.823	382 to 1101
Total		116	79	37	-	-	-
Mean		5.52	3.76	1.76	66.95	0.783	-
Range		3 to 8	1 to 7	0 to 4	20 to 100	0.606 to 0.858	143 to 2059
SSR Primers							
1	STACCS 3	4	2	2	50.00	0.709	272 to 529
2	STCPKIN 3	6	4	2	66.66	0.819	212 to 915
3	STPRINPSG	2	1	1	50.00	0.497	165 to 528
4	STWIN12G	6	4	2	66.66	0.821	125 to 1899
Total		18	11	7	-	-	-
Mean		4.5	2.75	1.75	58.33	0.712	-
Range		2 to 6	1 to 4	1 to 2	50.00 to 66.66	0.497 to 0.821	125 to 1899

TB: Total no. of Bands; TPB: Total no. of Polymorphic Bands; TMB: Total no. of Monomorphic Bands; PIC: Polymorphism Information Content; % P: Per cent Polymorphism; MW: Molecular Weight; AL: Amplicon Length; bp: base Pair

Construction of dendrogram

RAPD based dendrogram

Jaccard's co-efficients were used to compare set of variables and to generate similarity matrix. Jaccard's co-efficients for all genotypes as per RAPD analysis are shown in Table 3. Similarity indices were estimated on the basis of twenty one RAPD primers ranged from 0.56 (between DSP-287 and Kufri Chipsona-1) to 0.82 (between Kufri Kundan and Kufri Sutluj). UPGMA (unweighted pair-group method with arithmetic mean) dendrogram was prepared by using Jaccard's similarity co-efficients (Fig 2. (A)). The dendrogram clustered with the data generated by all primers and their amplicons grouped the 15 genotypes into two major clusters *i.e.,* Cluster A and Cluster B. Dendrogram showed two major clusters with co-efficient value 0.7564. The cluster A contained only one genotype, namely, Kufri Pushkar. The cluster B was

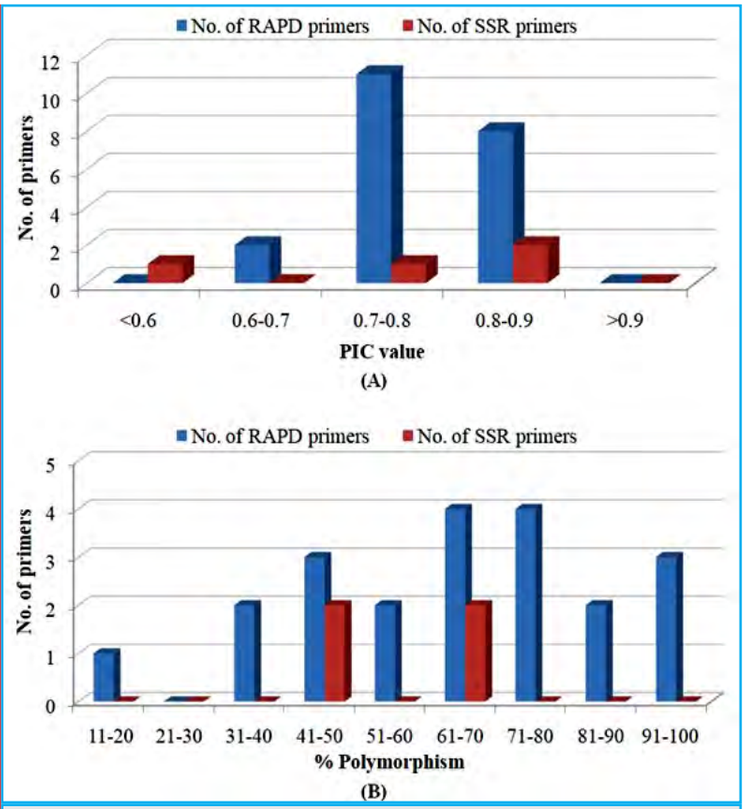

FIGURE 1. Distribution of RAPD and SSR primers according to (A) PIC values and (B) % polymorphism

further grouped in three clusters B1, B2 and B3. The cluster B1 contained 11 genotypes. The cluster B2 and B3 contains two and one genotype, respectively.

SSR based dendrogram

Jaccard's similarity co-efficients (Table 4) were estimated on the basis of four SSR primers, ranged from 0.47 (Kufri Badshah and Kufri Kundan with DSP-287) to 1.0 (between Kufri Kundan and Kufri Badshah). UPGMA dendrogram was prepared by using Jaccard's similarity co-efficients which was grouped into two main clusters *i.e.*, Cluster A and Cluster B (Fig 2. (B)). Dendrogram showed two major clusters with co-efficient value 0.8306. The cluster A was further divided into two clusters A1 and A2. The cluster A1 contained 6 genotypes and cluster A2 contained 8 genotypes. The cluster B was dividing into one group containing only one genotype DSP-287. Genotypes Kufri Badshah and Kufri Kundan had highest similarity.

Principle Component analysis (PCA)

In the PCA plot, derived from the RAPD genotyping data, it can be observed that Kufri Pushkar and Kufri Sutluj is placed farthest from Kufri Anand in the 1st coordinate (X-axis), while Kufri Bahar and MF-1 were placed farthest in the 2nd coordinate (Y-axis) (Fig. 3 (A)). Most of the varieties with moderately resistances were located in 1st coordinate right side in the plot including MF-1, DSP-287 and MS/95-1309 except Kufri Sutlaj.

In the PCA plot derived from the SSR genotyping data, it can be observed that DSP-287 and Kufri Sutluj is placed farthest from Kufri Anand in the 1st coordinate (X-axis), while Kufri Jyoti and DSP-287 were placed farthest in the 2nd coordinate (Y-axis) (Fig. 3 (B)). Varieties with moderately resistance located on the right side of 1st coordinate in the plot including the MF-1 and MS/95-1309 except Kufri Sutluj and DSP-287.

In potato, various studies have been previously reported at molecular level deciphering variation across accession and varieties. Center wise studies also have been performed that indicating within the center diversity. Previously, RAPD analysis has been employed in many literature for checking molecular polymorphism and allelic variation McGregor *et al.,* (2000), Yasmin *et al.,* (2006), Chimote *et al.,* (2007), Onamu *et al.*, (2016) and Ayman *et al.*, (2018). In the present study, total 42

Table 3. Jaccard's co-efficients for potato genotypes by RAPD analysis

	DSP-7	K. Chip-1	JX-249	MF-1	MS/95-1309	DSP-287	K. Pushkar	K. Jyoti	K. Sutlaj	K. Badshah	K. Kundan	K. Khyati	K. Bahar	K. Anand	KCM
DSP-7	1.000														
K. Chip-1	0.644	1.000													
JX-249	0.677	0.667	1.000												
MF-1	0.663	0.634	0.616	1.000											
MS/95-1309	0.663	0.670	0.737	0.670	1.000										
DSP-287	0.670	0.560	0.708	0.660	0.727	1.000									
K. Pushkar	0.663	0.598	0.582	0.586	0.670	0.626	1.000								
K. Jyoti	0.617	0.640	0.711	0.576	0.731	0.633	0.641	1.000							
K. Sutlaj	0.602	0.659	0.691	0.578	0.677	0.667	0.660	0.761	1.000						
K. Badshah	0.635	0.641	0.590	0.677	0.694	0.701	0.696	0.667	0.778	1.000					
K. Kundan	0.674	0.628	0.643	0.598	0.663	0.740	0.663	0.653	0.820	0.780	1.000				
K. Khyati	0.692	0.663	0.733	0.681	0.630	0.653	0.594	0.652	0.725	0.688	0.710	1.000			
K. Bahar	0.656	0.644	0.696	0.580	0.698	0.636	0.645	0.767	0.707	0.670	0.747	0.692	1.000		
K. Anand	0.699	0.600	0.702	0.653	0.687	0.694	0.570	0.714	0.643	0.677	0.698	0.717	0.816	1.000	
KCM	0.619	0.624	0.639	0.643	0.694	0.650	0.592	0.685	0.633	0.684	0.636	0.688	0.725	0.769	1.000

Table 4. Jaccard's co-efficients for potato genotypes by SSR analysis

	DSP-7	K. Chip-1	JX-249	MF-1	MS/95-1309	DSP-287	K. Pushkar	K. Jyoti	K. Sutlaj	K. Badshah	K. Kundan	K. Khyati	K. Bahar	K. Anand	KCM
DSP-7	1.000														
K. Chip-1	0.882	1.000													
JX-249	0.667	0.765	1.000												
MF-1	0.882	0.882	0.765	1.000											
MS/95-1309	0.824	0.824	0.706	0.938	1.000										
DSP-287	0.706	0.611	0.588	0.706	0.647	1.000									
K. Pushkar	0.588	0.688	0.786	0.688	0.625	0.500	1.000								
K. Jyoti	0.824	0.824	0.813	0.824	0.765	0.556	0.733	1.000							
K. Sutlaj	0.647	0.647	0.857	0.647	0.588	0.563	0.769	0.688	1.000						
K. Badshah	0.647	0.750	0.857	0.750	0.688	0.471	0.917	0.800	0.846	1.000					
K. Kundan	0.647	0.750	0.857	0.750	0.688	0.471	0.917	0.800	0.846	1.000	1.000				
K. Khyati	0.722	0.722	0.813	0.824	0.765	0.647	0.733	0.765	0.800	0.800	0.800	1.000			
K. Bahar	0.688	0.688	0.786	0.688	0.625	0.500	0.833	0.733	0.917	0.917	0.917	0.733	1.000		
K. Anand	0.824	0.722	0.706	0.824	0.765	0.750	0.625	0.667	0.800	0.688	0.688	0.875	0.733	1.000	
KCM	0.824	0.824	0.813	0.938	0.875	0.647	0.733	0.875	0.688	0.800	0.800	0.875	0.733	0.765	1.000

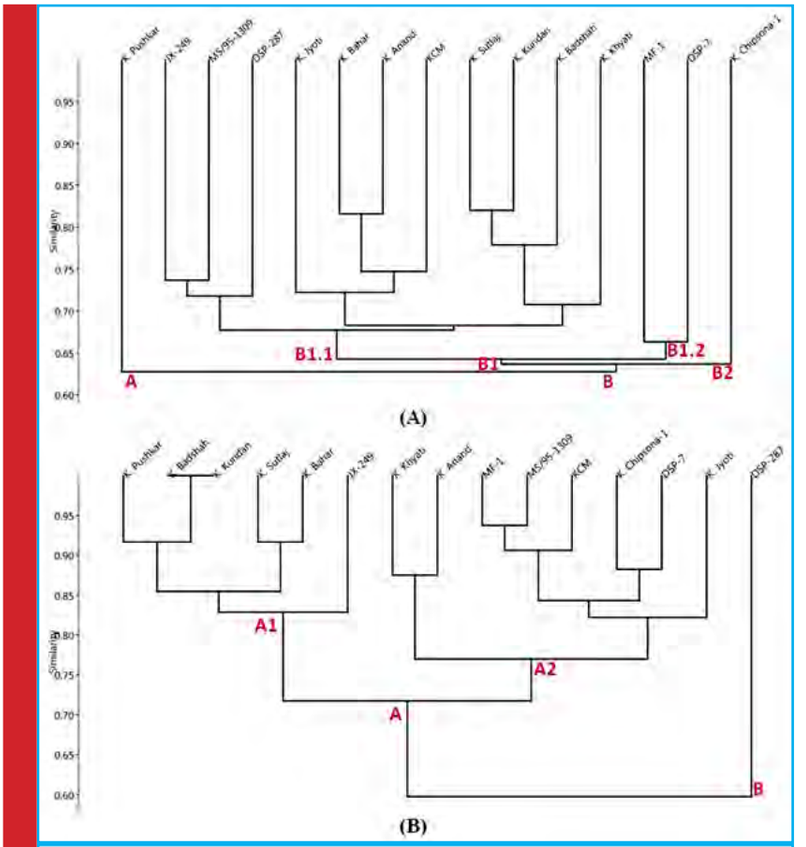

FIGURE 2. Dendrogram potato genotypes constructed from (A) RAPD and (B) SSR based Jaccard's similarity using UPGMA method

RAPD markers have been employed out of which 50% of primers accounts for mean polymorphism greater than 66.95% with PIC 0.783, indicating higher informativeness of primers. Previously, Chimote *et al.,* (2007), Gorji *et al*., (2011) and El Komy *et al.,* (2012) found mean polymorphism about 20%, 31% and 57.4% which was less then present result, indicating more superior polymorphic potential of primers used in the present study and its employment for further research by other in future. Moreover, Gorji *et al*., (2011) found 0.28 mean PIC value which was very less as compared to the mean PIC value of RAPD (0.78) in the present research. Recently, Onamu *et al*., (2018) used 19 RAPD markers for the assessment of genetic diversity among 35 potato accessions and reported 81.45% polymorphism which was higher as compare to the current investigation.

Among DNA markers, microsatellites have been chosen over RAPD because of their co-dominant behavior, multiallelism, reproducibility, and high level of polymorphism detected. In potato, few researchers such as Mc Gregor *et al*., (2000), Feingold *et al*., (2005), Ghislain *et al*., (2006), Chimote *et al*., (2007), Sharma and Nandineni, (2014), Maras *et al*., (2017), Ahmed *et al*., (2018) and Tiwari *et al*., (2019) have successfully used SSR markers. In the present study, total 25 SSR markers have been employed out of these only 4 potent SSR primers were polymorphic. Average polymorphism was 58.33% and mean PIC value was 0.712. Previously, Chimote *et al*., (2007) work with SSR marker for with general morphological character turns to only mean 19.5% polymorphism with almost same genotype indicating more superior polymorphic potential of our SSR marker and its employment for further research by other in future. While, Sharma and Nandineni, (2014) worked with different Kufri varieties by using same set of SSR markers their study revealed more polymorphism (80-90%) then the present study. Biniam *et al*., (2016) found that 97.8% SSR markers were highly polymorphic with an average PIC value of 0.87 which was very promising for the characterization of potato genotypes. In recent times, Duan *et al*., (2019) used 20 SSR markers for the analysis of genetic diversity among 217 potato cultivars and reported 97.99% polymorphism and 0.83 PIC value which were higher as compare to the current investiga-

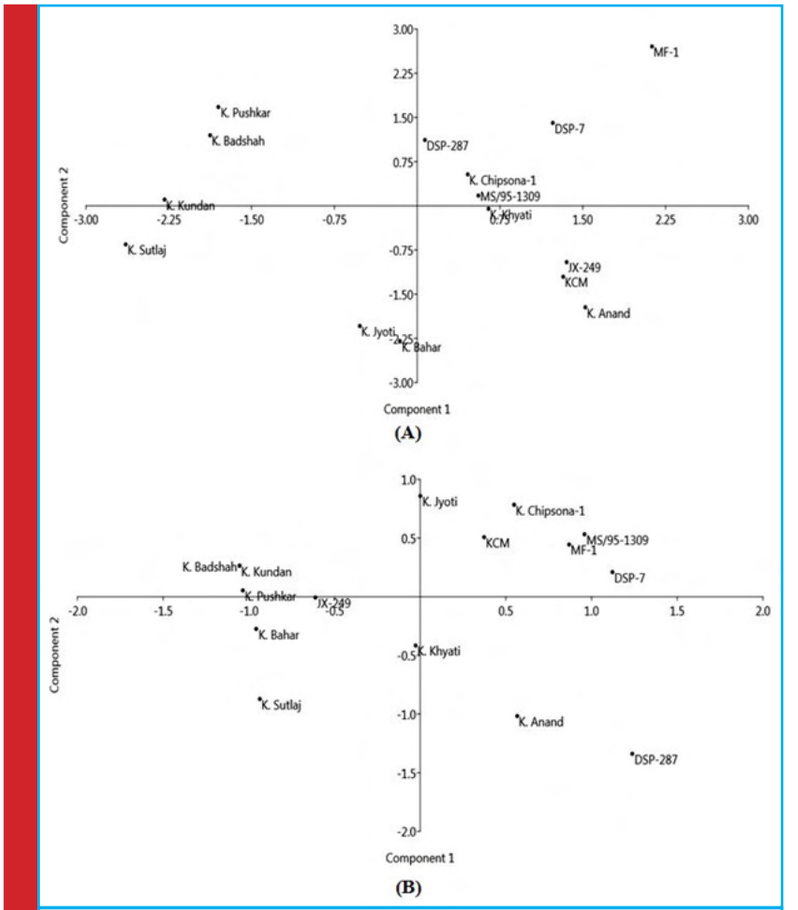

FIGURE 3. PCA analysis of potato genotypes based on (A) RAPD and (B) SSR analysis

tion. The molecular markers with high PIC values can be utilized for the diversity analysis in potato germplasms.

CONCLUSION

The results of current study indicate that RAPD and SSR markers used in the study seemed to be the good for the molecular assay for fingerprinting and assessing genetic relationship among genotypes of potato as they have very promising polymorphism and PIC values. These markers can be utilized for molecular breeding for the improvement of potato.

ACKNOWLEDGEMENT

The authors thank authorities of SDAU and staff of Potato Research Station, Deesa, Gujarat, India, for providing facilities to carry out the research work.

REFERENCES

Ahmed, S., Zhou, X., Pang, Y., Xu, Y., Tong, C., Bao, J. (2018) Genetic diversity of potato genotypes estimated by starch physicochemical properties and microsatellite markers. Food Chemistry 257: 368-375.

Anderson, J.A. (1993) Optimizing parental selection for genetic linkage maps. Genome 36: 181-186.

Ayman, E.F., Zakia, A., Mohamed, T., Sobieh, S., Salah, A. (2018) Molecular diversity analysis of two in vitro and irradiated potato varieties expressed by random amplified polymorphic DNA. Notulae Scientia Biologicae 10(1): 45-51.

Biniam, M.G., Githiri, S.M., Mehari, T., Kasili, R.W., Ghislain, M., Magembe, E. (2016) Genetic diversity assessment of farmers' and improved potato (*Solanum tuberosum*) cultivars from Eritrea using simple sequence repeat (SSR) markers. African Journal of Biotechnology 15(35): 1883-1891.

Bornet, B., Goraguer, F., Joly, G., Branchard, M. (2002) Genetic diversity in European and Argentinian cultivated potatoes

(*Solanum tuberosum* subsp. *tuberosum*) detected by inter-simple sequence repeats (ISSRs). Genome 45(3): 481-484.

Bradshaw, J.E. (2019) Improving the nutritional value of potatoes by conventional breeding and genetic modification. In Quality Breeding in Field Crops (pp. 41-84). Springer, Cham.

Braun, A., Wenzel, G. (2004) Molecular analysis of genetic variation in potato (*Solarium tuberosum* L.). I. German cultivars and advanced clones. Potato Research 47: 81-92.

Chimote, V.P., Pattanayak, D., Naik, P.S. (2007) Molecular and morphological divergence studies in Indian potato varieties. Indian Journal of Biotechnology 6: 216-223.

Dharajiya, D.T., Khadia, S.M., Pagi, N.K., Khatrani, T.J., Jasani, H.V., Khunt, A.D., Ravindrababu, Y. (2017) Modified method of high quality genomic DNA extraction from mungbean [*Vigna radiata* (L.) Wilczek] suitable for PCR based amplification. Indian Journal of Science and Technology 10(20): 1-7.

Doyle, J.J., Doyle, J.L., (1990) Isolation of plant DNA from fresh tissue. Focus 12: 13–15.

Duan, Y., Liu, J., Xu, J., Bian, C., Duan, S., Pang, W., Hu, J., Li, G., Jin, L. (2019) DNA fingerprinting and genetic diversity analysis with simple sequence repeat markers of 217 potato cultivars (*Solanum tuberosum* L.) in China. American Journal of Potato Research 96(1): 21-32.

El Komy, M.H., Saleh, A.A., Molan, Y.Y. (2012) Molecular characterization of early blight disease resistant and susceptible potato cultivars using random amplified polymorphic DNA (RAPD) and simple sequence repeats (SSR) markers. African Journal of Biotechnology 11(1): 37-45.

Favoretto, P., Veasey, E.A., Melo, P.C.T.D. (2011) Molecular characterization of potato cultivars using SSR markers. Horticulture Brasileria 29(4): 542-547.

Feingold, S., Lloyd, J., Norero, N., Bonierbale, M., Lorenzen, J. (2005) Mapping and characterization of new EST-derived microsatellites for potato (*Solanum tuberosum* L.). Theoretical and Applied Genetics 111(3): 456-466.

Ghebreslassie, B.M., Githiri, S.M., Mehari, T., Kasili, R.W., Ghislain, M., Magembe, E. (2016) Genetic diversity assessment of farmers' and improved potato (*Solanum tuberosum*) cultivars from Eritrea using simple sequence repeat (SSR) markers. African Journal of Biotechnology 15(35): 1883-1891.

Ghislain, M., Andrade, D., Rodríguez, F., Hijmans, R.J., Spooner, D.M. (2006) Genetic analysis of the cultivated potato *Solanum tuberosum* L. Phureja group using RAPDs and nuclear SSRs. Theoretical and Applied Genetics 113(8): 1515-1527.

Ghislain, M., Núnez, J., del Rosario Herrera, M., Pignataro, J., Guzman, F., Bonierbale, M., Spooner, D.M. (2009) Robust and highly informative microsatellite-based genetic identity kit for potato. Molecular Breeding 23(3): 377-388.

Gorji, A.M., Poczai, P., Polgar, Z., Taller, J. (2011) Efficiency of arbitrarily amplified dominant markers (SCoT, ISSR and RAPD) for diagnostic fingerprinting in tetraploid potato. American. Journal of Potato Research 88(3): 226-237.

Hammer, Ø., Harper, D.A.T., Ryan, P.D. (2001) PAST: palaeontological statistics software package for education and data analysis. Palaeontologia Electronica 4(1): 9.

Hawkes, J.G., Jackson, M.T. (1992) Taxonomic and evolutionary implications of the endosperm balance number hypothesis in potatoes. Theoretical and Applied Genetics 84: 180-185.

Jaccard, P. (1908) Nouvelles recherches sur la distribution florale. Bulletin de la Société vaudoise des sciences naturelles 44: 223-270.

Jian, W., Lu, H., Wang, R.Y., He, M.M., Liu, Q.C. (2017) Genetic diversity and population structure of 288 potato (*Solanum tuberosum* L.) germplasms revealed by SSR and AFLP markers. Journal of Integrative Agriculture 16(11): 2434-2443.

Kapuria, M., Dharajiya, D., Khatrani, T., Jasani, H., Chaudhari, S.M., Chauhan, R.M. (2016) Evaluation of Indian potato (*Solanum tuberosum* L.) germplasms against common scab caused by *Streptomyces scabies*. International Journal of Agriculture Sciences 8(19): 1336-1338.

Majeed, A., Muhammad, Z. (2018) Potato production in Pakistan: challenges and prospective management strategies–a review. Pakistan Journal of Botany 50(5): 2077-2084.

Maras, M., Sedlar, A., Reid, A., Božović, V., Jovović, Z., Meglič, V., Dolničar, P. (2017) Genetic diversity and redundancy among potato accessions in the Montenegrin collection as revealed by microsatellite markers. American Journal of Potato Research 94(4): 306-313.

McGregor, C.E., Lambert, C.A., Greyling, M.M., Louw, J.H., Warnich, L. (2000) A comparative assessment of DNA fingerprinting techniques (RAPD, ISSR, AFLP and SSR) in tetraploid potato (*Solanum tuberosum* L.) germplasm. Euphytica 113(2): 135-144.

Oliveira, E.J., Pádua, J.G., Zucchi, M.I., Vencovsky, R., Vieira, M.L.C. (2006) Origin, evolution and genome distribution of microsatellites. Genetics and Molecular Biology 29(2): 294-307.

Onamu, R., Legaria, J., Rodríguez, J.L., Sahagùn, J., Pèrez, J. (2016) Molecular characterization of potato (*Solanum tuberosum* L.) genotypes using random amplified polymorphic DNA (RAPD) and inter simple sequence repeat (ISSR) markers. African Journal of Biotechnology 15(22): 1015-1025.

Pal, B.P., Nath, P. (1951) Indian potato varieties. Indian Council Agricultural Research, New Delhi. Miscellaneous Bulletin. 62: 63.

Pandey, S.K., Sarkar, D. (2005) Potato in India: Emerging trends and challenges in the new millennium. Potato Journal 32(3-4): 93-104.

Parita, B., Kumar, S.N., Darshan, D., Karen, P. (2018) Elucidation of genetic diversity among ashwagandha [*Withania somnifera* (L.) Dunal] genotypes using EST-SSR markers. Research Journal of Biotechnology 13(10): 52-59.

Rocha, E.A., Paiva, L.V., Carvalho, H.H.D., Guimarães, C.T. (2010) Molecular characterization and genetic diversity of potato cultivars using SSR and RAPD markers. Crop Breeding and Applied Biotechnology 10(3): 204-210.

Sharma, V., Nandineni, M.R. (2014) Assessment of genetic diversity among Indian potato (*Solanum tuberosum* L.) collection using microsatellite and retrotransposon based marker systems. Molecular Phylogenetics and Evolution 73: 10-17.

Smith, J.S.C., Chin, E.C.L., Shu, H., Smith, O.S., Wall, S.J., Senior, M.L., Mitchell, S.E., Kresovich, S., Ziegle, J. (1997) An evaluation of the utility of SSR loci as molecular markers in maize (*Zea mays* L.): comparisons with data from RFLPs and pedigree Theoretical and Applied Genetics 95: 163-173.

Solano Solis, J., Morales Ulloa, D., Anabalón Rodríguez, L. (2007) Molecular description and similarity relationships among native germplasm potatoes (*Solanum tuberosum* ssp. *tuberosum* L.) using morphological data and AFLP markers. Electronic Journal of Biotechnology 10(3): 436-443.

Tiwari, J.K., Ali, N., Devi, S., Kumar, V., Zinta, R., Chakrabarti, S.K. (2018) Development of microsatellite markers set for identification of Indian potato varieties. Scientia Horticulturae 231: 22-30.

Vanishree, G., Patil, V.U., Kardile, H., Bhardwaj, V., Singh, R., Chakrabarti, S.K. (2016) DNA fingerprinting of Indian potato cultivars by inter simple sequence repeats (ISSRs) markers. Potato Journal 43(1): 70-77.

Walunjkar, B., Parihar, A., Chaurasia, P., Pachchigar, K., Chauhan, R.M. (2013) Genetic analysis of wild and cultivated germplasm of pigeonpea using random amplified polymorphic DNA (RAPD) and simple sequence repeats (SSR) markers. African Journal of Biotechnology 12(40): 5823-5832.

Wang, Y., Rashid, M., Li, X., Yao, C., Lu, L., Bai, J., Li, Y., Xu, N., Yang, Q., Zhang, L., Bryan, G.J. (2019) Collection and evaluation of genetic diversity and population structure of potato landraces and varieties in China. Frontiers in Plant Science 10: 139.

Yasmin, S., Islam, M.S., Kondoker, M., Nasiruddin, M., Alam, S. (2006) Molecular characterization of potato germplasm by random amplified polymorphic DNA markers. Biotechnology 5(1): 27-31.

Biotechnological Communication

Biosci. Biotech. Res. Comm. 12(1): 90-98 (2019)

BBRC Bioscience Biotechnology Research Communications

Histobiochemical and physicochemical characterization of mutant jute *Corchorus capsularis* CMU 013 with poorly developed fibre

Sanjoy Sadhukhan

Plant Molecular Biology Laboratory, Department of Botany, Raiganj University, Raiganj – 733134, Uttar Dinajpur, West Bengal, India

ABSTRACT

Jute, an important lingo-cellulosic rich natural bast fibre, is the second only after cotton in production. It is obtained from the plant belonging to Malvaceae. The advantages of the fibre lies in its properties i.e. environment-friendly, good insulating, antistatic properties, low thermal conductivity and moderate moisture regain.High lignin content of jute fibre hinders its utilization in textile industry and diversified value-added products. To make jute suitable for diverse use, especially in textiles, many efforts were made to modify its chemical composition and physicochemical characteristics. With the aim of developing jute fibre with reduced lignin content, the comparative histobiochemical and physicochemical parameters were studied between normal jute and a stable mutant jute line with decreased lignin content. An x-ray-induced mutant line (CMU 013) of jute (Corchorus capsularis) was histobiochemically and physico-chemically evaluated along with its normal parent (JRC 321). The anatomy and morphology of mutant jute differ from normal jute in regard to fibre formation and deposition of fibre forming materials. The primary and secondary vascular bundles are normal in both JRC 321 and CMU 013 but bast fibre formation is less pronounced in mutant jute. The percentage of lignin content is reduced from 19.27% (JRC 321 jute) to 8.627% and cellulose content increased from 48.237% (JRC 321 jute) to 6.397%. X-ray diffraction analysis revealed that the mutant jute has less rigidity and is brittle in nature. Histobiochemical evidence of jute stem of JRC 321 demonstrates that the bast fibre contains decent amount of cementing material, i.e. lignin which is validated by the biochemical analysis of the fibre. Deposition of the lignin was found to be prerequisite for generation of well-developed fibre as corroborated by SEM. The fragile nature of the fibre as seen

ARTICLE INFORMATION:

Corresponding Author: sanjoysadhukhan@gmail.com
Received 27th Dec, 2018
Accepted after revision 21st Feb, 2019
BBRC Print ISSN: 0974-6455
Online ISSN: 2321-4007 CODEN: USA BBRCBA
Thomson Reuters ISI ESC / Clarivate Analytics USA
NAAS Journal Score 2019: 4.31 SJIF: 4.196

Online Contents Available at: http//www.bbrc.in/
DOI: 10.21786/bbrc/12.1/12

in the SEM of CMU 013 jute was validated by the X-ray diffraction analysis and tensile strength. This mutant may serve as a model to understand the molecular mechanism that organizes the development of secondary wall thickening in jute bast fibre cells.

KEY WORDS: JUTE FIBRE, LIGNIN, MUTANT, SCANNING ELECTRON MICROSCOPY, FTIR SPECTROSCOPY, STRENGTH

INTRODUCTION

Jute, a lignocellulosic natural bast fibre obtained from the plant *Corchorus* sp. is a dicotyledonous annual crop belonging to the family Malvaceae. The fibre originates from the secondary phloem tissue of the stem. It consists of long extraxylary cells which mechanically support the phloem (Guerriero *et. al.* 2017), also known as bast fibre. The jute fibre is one of the most versatile natural fibres and it has considerable commercial significance for the generation of diversified value-added industrial products i.e. immense potentiality for industrial production of packaging, textiles, non-textile, construction, and agricultural sectors. Advantages of jute include environment-friendly, renewable resources (Gorshkova 2012), good insulating and antistatic properties, as well as having low thermal conductivity and moderate moisture regain. Of late, it has been well established that a score of value-added commercial products of great utility can be produced based on diverse utilization of jute fibre due to its high strength, high modulus, and high flexural rigidity. However, some problems have been encountered with the quality of jute fibre that figures as critical for their suitability for generation of its value-added textile industrial end products. Utilization of natural fibres including jute depends on its physical and chemical properties. An extensive comparative study has been made on different physical and chemical properties of different natural fibres (McGovern et al., 1983 and Young, 1993) and those properties have been found to be the basis of the historical utilization of the natural fibre. It has also been shown that strength, stiffness, and extensibility of jute fiber decrease with gradual removal of lignin. The deposition of lignin into cellulose and other cell wall materials might be one of the reasons behind the strength and stiffness of natural fiber like jute (Roy, 1953; Meredith 1956). Lignin is a secondary plant metabolite which hinders high-end industrial applications of several plant products including jute (Choudhary *et al* 2017).

Anatomical studies on jute fibre showed that the strength and fineness of the fibre are correlated with number of cells per bundle, length-breadth ratio of fibre cells and cross-sectional area of the fibre cells. The crystallinity of cellulose has a large influence on the mechanical properties of natural fibres. Jute bast fibres are composed of xylan with high degree of lignifications whereas flax, ramie and hemp bast fibres, have a high abundance of crystalline cellulose (Guerriero *et. al.* 2017). Fibres like jute, hemp, flax, and ramie have their cellulosic chains oriented nearly parallel to the fibre axis (in the range 7-12°), and they exhibit high strength in contrast to cotton fibre. Cotton fibres, with appreciably lower tensile strengths, are characterized by spiraled cellulose chains that are oriented approximately 30° to the fibre axis (Rials et al., 1997). Moisture content and fibre purity also influence the degree of crystallinity in jute and mesta fibres (Ray, 1969). X-ray diffraction and Fourier Transformed Infra-Red (FTIR) Spectroscopy are powerful tools to evaluate the structure of jute (Bera *et. al.* 2002). The bast fibre lignin is significantly different from that of the typical 'woody plant lignin' (Day *et. al.* 2005). Development of bast fibre in jute (*Corchorus* spp.) is a complex process involving differentiation of secondary phloem fibres from the cambium accompanied by lignification of the fibre cell wall (Kundu *et. al.* 2012). The formation of secondary phloem fibres starts long after the initiation of secondary xylem (Snegireva 2015).

In the present study, comparison between an induced mutant (CMU 013) of *Corchorus capsularis* having an altered form of bast fibre and a normal jute (JRC 321) plant was performed on the basis of the histobiochemical and physicochemical characters of jute fibres.

MATERIALS AND METHODS

Transverse sections of jute stems of 45 days after sowing (DAS) normal and mutant were prepared, dehydrated and stained with lignin-specific stain phloroglucinol-HCl (Srivastava 1966). The stained sections were observed and photographed using Leica DM LS optical microscope.Freehand transverse sections were prepared of jute stems of 60 days old both normal and mutant were prepared and dehydrated. The surface morphology of dry jute fibers of both cultivated and mutant varieties was evaluated by scanning electron microscopy using JEOL, JSM 5800, at the Central Research Facility, IIT Kharagpur. The images of scanning electron microscopy were taken at electron volt of 20 KeV.

Estimation of cellulose, hemicellulose, and lignin

For composition analysis, neutral detergent solution (NDS) and acid detergent solution (ADS) were used. Hemicellulose, cellulose, and lignin were estimated following the method (Sadasivam and Manickam 2008). For estimation of these components, the jute fibers were refluxed separately with NDS and ADS followed by washing the insoluble part with hot water and acetone in each case. The insoluble parts obtained after treatment with NDS and ADS are termed as Neutral Detergent Fiber (NDF) and Acid Detergent Fiber (ADF) respectively. The hemicellulose content of jute fibers was obtained as a difference of NDF and ADF. The cellulose content of jute fibers was obtained as the difference of ADF and residue after extraction of ADF with 72% sulphuric acid. The lignin content of jute fiber was obtained as the difference of residue after extraction of ADF with 72% sulphuric acid and ash obtained by igniting ADF. In typical procedure hemicellulose, lignin and cellulose of jute fiber were estimated as follows:

For determination of NDF about 1 g of jute fiber powder was taken in a round bottom flask to which 10 ml cold NDS, 2 ml decahydronaphthalene and 0.5 g sodium sulphate were added and refluxed for 1h. The solid residue was filtered in a sintered glass crucible (G-2) and washed with hot water followed by washing twice with acetone. The residue was collected, dried at 100°C for 8 h and stored after weighing in a desiccator. This residue was designated as NDF. For determination of ADF about 1g of jute fiber powder was taken in a round bottom flask to which 100ml of ADS were added. The content of the flask was heated to boiling in a controlled way to avoid foaming for 5 to 10 min followed by refluxing for 1h. The residue was filtered through sintered glass crucible (G-2), washed with hot water and acetone. The washed residue was then dried at 100°C for overnight. The dried residue was designated as ADF and was stored in a desiccator.

For determination of Acid Detergent Lignin (ADL), weighed amount of ADF was taken in a 100ml beaker to which 25 to 50ml 72% sulphuric acid and 1g asbestos fibre was added. The content of the beaker was continuously stirred for 3h. Then the content was diluted with distilled water and the residue was filtered through a preweighed Whatman No. 1 filter paper and washed with water to remove last traces of acid. The residue of the filter paper was dried at 100°C for 2 h. The weight of the residue after drying on filter paper was taken. The filter paper with the residue was transferred on a preweighed silica crucible, which was heated in a muffle furnace at 550°C for 3 h. The weight of ash was calculated after weighing the cold crucible with the ash. For obtaining % ADL, a blank test was performed by taking 1 g asbestos fibre following the same procedure as before. In this blank test, weights of two residues, one weight after drying on filter paper at 100°C for 2 h and the other weight after heating at 550°C for 3 h in a muffle furnace in an identical way: (Protocol adopted from, Sadasivam and Manickam 2008)

NDF = Hemicellulose + Cellulose + Lignin + Minerals
ADF = Cellulose + Lignin + Minerals
Hemicellulose = NDF - ADF
Cellulose = ADF - Residue after extraction with 72% H_2SO_4
Lignin = Residue after extraction with 72% H_2SO_4 - ash

The tensile strength of normal and mutant jute fibers was determined by subjecting the fibers to Hounsfield Universal tensile testing machine with the following parameters: load range =10.000N, extension range = 3.000mm, speed = 0.0500mm/min, temperature = 25°C, relative humidity = 70%. Clean and dry strands collected from the middle portion of the fiber reeds were used for the measurement after proper gripping through paper boards. Before testing, the specimens were kept in desiccators for 2 days. A stress-strain curve of the cultivated and mutant jute fibers was plotted.IR study of both normal and mutant jute fibers was done using a Nexus 870 Nicolet FTIR spectrophotometer (Edwards *et al*., (1997), Samal *et al*., (1995), Rana *et al*., (1997), Pan *et al*., (1999). Jute fibers were crushed with liquid nitrogen into a fine powder and dried in desiccators. An equal weight of both cultivated and mutant fibers was taken and made pellet with potassium bromide and subjected to IR spectrophotometer.

X-ray diffraction (XRD) analysis: XRD of dry jute fibres were carried out by Philips PW 1729 X-ray generator using Co target (γ=0.179 nm) at a scanning speed of 2° / min and the data recorded every 0.02° (2θ) for the angular range of 2θ = 10-50° (Varma *et al*., 1984).

RESULTS

Anatomical study of jute stems

The morphological differences of the mutant (CMU-013) having discontinuous fibre directed to study the developmental pattern in fibre formation in its stem compared to cultivated variety JRC 321. Thus, jute stem of 60 days old from both the JRC 321 and CMU 013 was sectioned transversely and stained with phloroglucinol-HCl and analyzed microscopically. It was revealed that the bast fibre (secondary phloem fibre) was poorly developed in CMU 013 (Figure 1) indicating a weaker deposition of the fibre forming components.The comparison was also studied by scanning electron microscopy (SEM) to measure the fiber-forming zone in both the CMU 013 and JRC

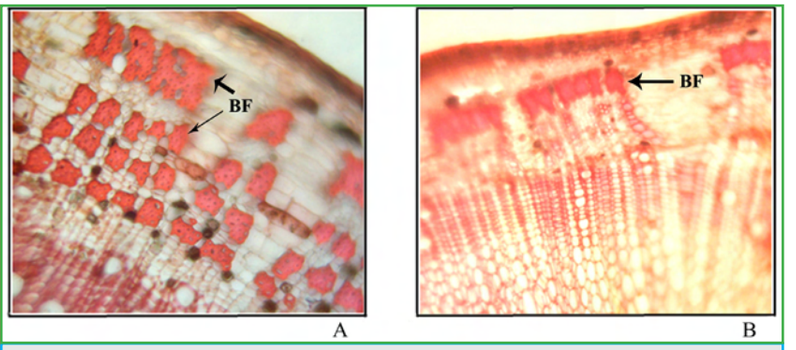

FIGURE 1. Anatomical differences of normal and mutant jute stems. Stem sections at 60 days after sowing (DAS) stained with phloroglucinol-HCl and viewed under optical microscope A: JRC 321 (40X magnification), B: CMU 013 (20X magnification). BF – Bast Fibre

321. It was found that the thickness of the bast cell wall in JRC 321 was 4.5 µm whereas it was 2.2 µm in case of CMU 013. Moreover, the diameter (3.65 µm) of the lumen in jute fibre of CMU 013 was found to be more than the JRC 321 (2.25 µm), which indicated further lack of deposition of the fibre forming components in CMU 013 (Figure 2).

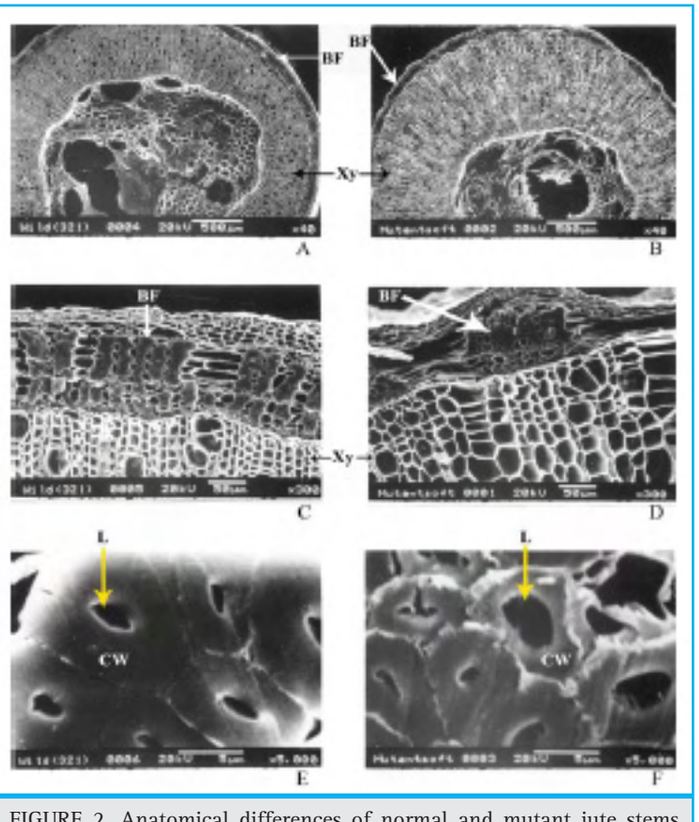

FIGURE 2. Anatomical differences of normal and mutant jute stems under SEM. A: JRC 321 and B: CMU 013 at x 40 respectively; C: JRC 321 and D: CMU 013 at x 300 respectively. E and F: Fibre cells of JRC 321 and CMU 013 at x 5000 respectively. BF – Bast Fibre, Xy – Xylem, CW – Cell Wall, L – Lumen of the fibre cell.

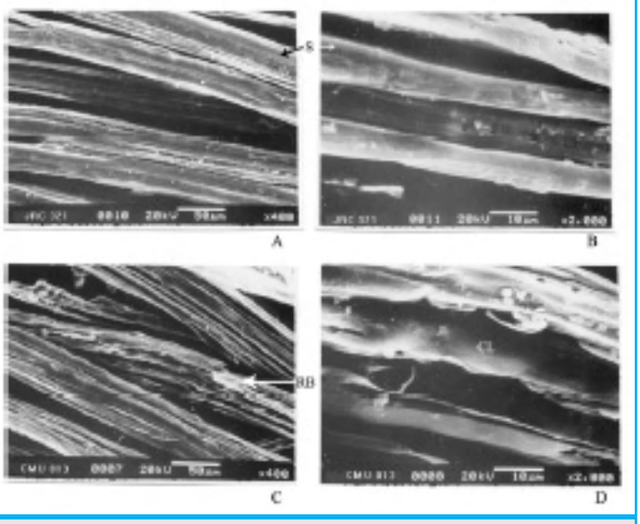

FIGURE 3. Surface morphology of the jute fibres of normal and mutant. A and B: normal JRC 321 at x 400 and x 2000 magnifications respectively. C and D: Mutant CMU 013 at x 400 and x 2000 magnifications respectively. S – Smooth surface, RB – Rough surface and Broken fibres, CL – 'Crater Like' Structures.

It was also observed from scanning electron micrograph that the surface morphology of the jute fibre isolated from CMU 013 was entirely different than that of JRC 321; the fiber of JRC 321 showed a smooth surface compared to that of the mutant CMU 013 having a rough surface and broken fibres. At a higher magnification, a crater-like structure was found to be present on the surface of the mutant jute fiber (Figure 3). Thus, it could be assumed that the fibre formation in the mutant is underdeveloped due to improper functions of the fibre forming elements.

The chemical components of cultivated and mutant jute fibers were estimated by gravimetric method. It was found that cultivated type fibers have more lignin and less cellulose compared to that of the mutant. Mutant has 28.42 % more cellulose than the cultivated fiber and whereas the cultivated fiber has 55 % more lignin than the mutant fiber.

The jute fibers of both the cultivated variety (JRC 321) and the mutant (CMU 013) were assessed for its tensile strength. The tensile strength of the jute fibers was measured by a Universal Tensile Testing Machine (Hounsfield) with a load cell 10,000 N, extension range = 30 mm, speed = 0.0500 mm/min, temperature of 25 °C and 70 % relative humidity. Clean and dry strands collected from the middle portion of the fiber reeds were used for the measurement. It was observed that the fibre of the cultivated variety showed to be stronger (tensile strength of 952.4 MPa) with an elongation percentage at break of 2.51 % than the mutant jute (tensile strength of 600.8 MPa) with an elongation percentage at break of 1.67 %. It was found that the jute fiber of JRC 321 covered a higher total area under the stress-strain curve compared to that of the mutant CMU 013 (Figure 4). This indicated that the jute fiber in the cultivated variety was stronger than that of the mutant. From a calculation of the area under the stress-strain plot it was found that the jute of the cultivated variety needs more energy than that of the mutant for breaking the fibre under a tensile load.

FTIR vibrational bands of the cultivated and mutant area are shown in Figure 5, and Table 2. In the mutant type of fibre shifting of H bonded –OH stretching frequency value to higher region indicates that intermolecular H-bonding decreases and whereas in case of cultivated type of fibre shifting of H bonded –OH stretching frequency value to lower region indicates that intermolecular H-bonding increases. Peaks at 2903.76 cm^{-1} and 2916.84 cm^{-1} correspond to C-H stretching in methyl and methylene groups (in cellulose and hemicellulose) in jute. Asymmetric C-O-C stretching bands at 1110.67 cm^{-1} and 1111.85 cm^{-1} indicates the presence of the chain of anhydroglucose ring, i.e., cellulose. The 1427.11 cm^{-1} and 1426.78 cm^{-1} may be due to the presence of lignin on both cultivated and mutant jute fibres.

The fibres of both the cultivated and mutant jute were subjected to analyze by X-ray diffraction study within the angular range of 10° - 50° to measure the percentage crystallinity of the fibre. It was revealed from figure 6 that the percentage crystallinity of the fibre in cultivated variety was found to be 20.53 % whereas that

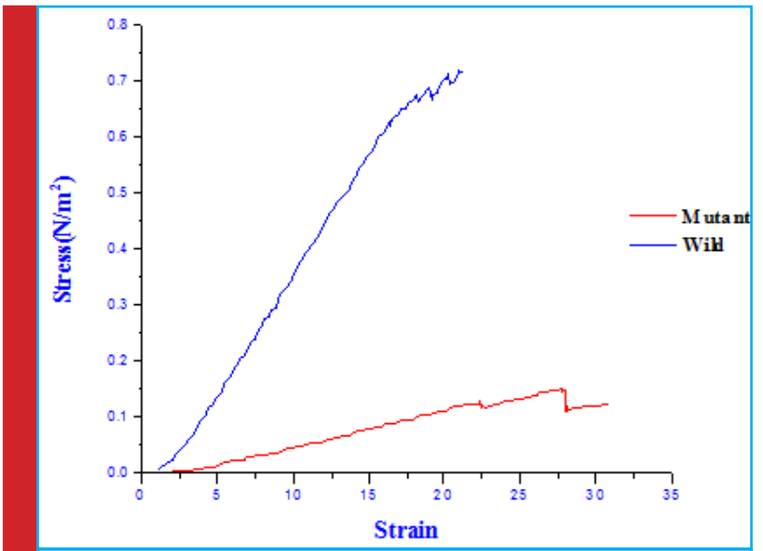

FIGURE 4. Stress-Strain curve of wild and mutant jute fibers.

of the mutant fibre was 13.9 % indicating more rigidity and brittle nature of the jute fibre in the cultivated variety.

DISCUSSION

The present study constitutes the first attempt to understand the physico-chemical differences between normal jute fibre and its mutant fibre. Jute (*Corchorus capsularis*) is the most important fibre producing crop in the world next to cotton in terms of yield. Anatomically, jute fibres, also known as bast fibres, are sclerenchyma cells with secondary cell wall thickening and are rigid in structure (Kundu, 1944; Fahn, 1990; Evert 2006, Crang *et. al.* 2018). Proper utilization of this fibre is hampered due to its coarse nature. Any attempt to improve the quality of the phloem fibre of jute would be valued for potential diversification of jute usage (Palit, 1999, 2001). Continuous attempts through breeding processes, X-ray induced mutation for generation of improved jute variety and also in improved retting process (Kharkwal et. al. 2004; Das *et. al.* 2018), to get the improved quality of jute fibres are being made without any significant outcome. Here, an induced mutant of *Corchorus capsularis*

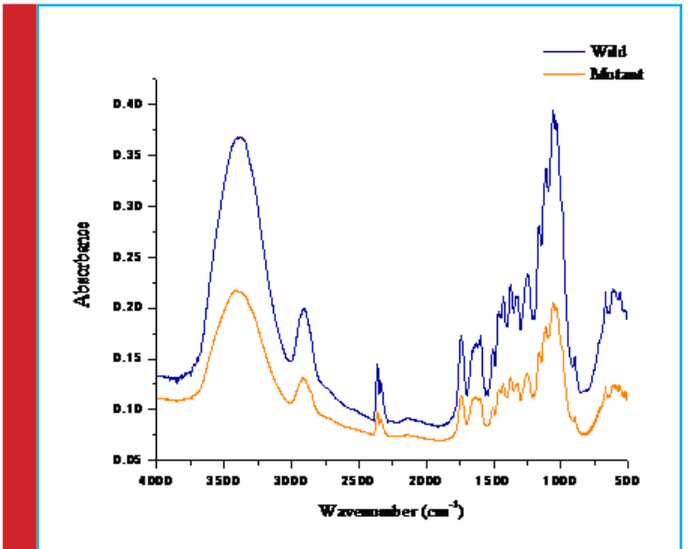

FIGURE 5. FTIR spectra of the JRC321 and CMU013 jute fibers.

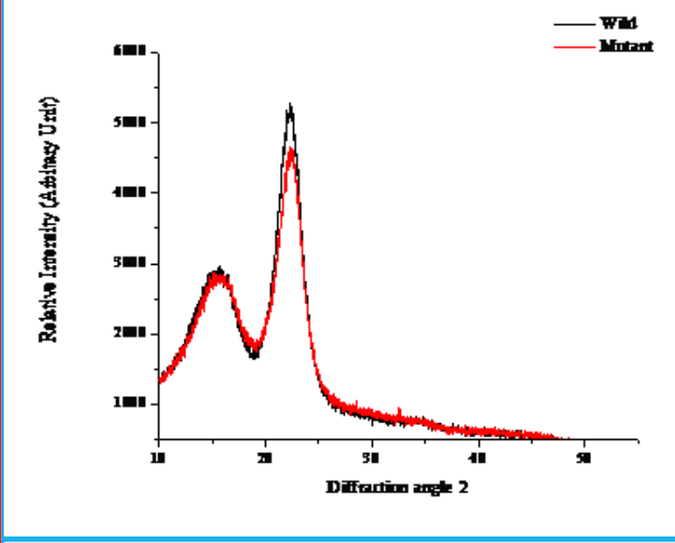

FIGURE 6. XRD of the wild and mutant jute fibers.

having an altered bast fibre was compared with a normal jute plant and identify some of the histobiochemical and physicochemical characters of jute fibres.

Histobiochemical evidence of jute stem of cultivated variety JRC 321 demonstrates that the development of the secondary cell wall in phloem was initiated at a particular stage of development of jute plant and matured well with deposition of cementing materials, particularly lignin (Figures 1 and 2) as evidenced in our previous studies (Samanta *et. al.* 2015). This deposition of the cementing materials was found to be prerequisite for generation of well-developed fibre revealed from the comparative study of the normal with mutant by SEM (Figures 3 and 4).

These data are supported by previous study of Meshram and Palit (2013) where the authors found that the cell wall thickness, strength of fibre and lignin content goes together and the high cellulose content results fibre fineness. Compositional analysis of the fibre forming components indicated that the fibre of normal jute contains 57% more lignin than mutant. The data are also supported by the earlier evidence that the secondary wall development and formation of compact group of the bast fibre cells involve deposition of lignin over the cellulose matrix (Priestley and Scott, 1936; Kundu et al., 1959; Preston, 1974; Grabber et al., 1991) though the presence of high amount of lignin was believed to be undesirable for fibre quality (Harlley, 1987). In contrast, the mutant fibre was found to contain a comparatively high amount of cellulose (Table 1) that could be expected to improve the quality and strength of the fibre. This observation was supported by another study in (*Corchorus olitorius* L.) mutant with low lignin (7.23%) in phloem fibre being compared to wild-type JRO 204 (13.7%) was identified and characterized (Choudhary *et al* 2017).

However, a contrary result was observed in continuity and tensile properties of the fibre. The fibre generated from mutant on retting was found to be discontinuous or fragmented. It is difficult to conclude whether this fragmented nature of fibre was due to less deposition of lignin or due to poor development of the cell wall. The fibre of the normal showed to be stronger (tensile strength of 952.4 MPa) with an elongation percentage at break of 2.512 % than the mutant jute (tensile strength of 600.8 MPa) with an elongation percentage at break of 1.676 % (Figure 4). This data was supported by a previous study in which the authors have used different natural fibres and studied the effect of fibre morphology on the tensile strength (Fidelisa *et. al.* 2013).

They found that the increased secondary cell-wall thickness causes increase in both the fiber strength and Young's modulus. This observation was further supported by the FTIR analysis and XRD analysis of both normal and mutant fibres (Figures 5 & 6). The XRD analysis of normal fibre revealed more crystallinity than

Table 1. Chemical composition of JRC 321 and CMU 013 jute fibers

Chemical components	Cellulose (%)	Hemicellulose (%)	Lignin (%)
Cultivated (JRC 321)	48.237	28.502	19.273
Mutant (CMU 013)	67.397	20.937	8.672

Table 2. Assignment of IR vibrational bands in JRC-321 (cultivated variety) and CMU-013 (mutant jute)

	JRC 321	CMU 013
Possible assignment of chemical groups	**cm^{-1}**	**cm^{-1}**
OH Stretching vibrations due to polymeric association	3382.98	3415.74
CH stretching in methyl and methylene groups (in cellulose and hemicellulose)	2903.76	2916.84
CN stretching bond	2360.14	2359.41
C=O stretching (in lignin and sugar aldehydes)	1737.95	1736.61
Aromatic skeletal vibrations	1596.15	1634.92
CC multiple band stretching aromatic	1503.64	1506.21
CH2 bending in lignin	1427.11	1426.78
Unsaturated nitrogen compound C-NO2 nitro compound	1371.89	1374.21
C-N vibrations, aromatic, primary	1321.43	1319.96
Ethers; Sulphur compound	1247.14	1246.08
S=O Stretching vibrations due to sulfonamides	1161.47	1162.63
C-O/C-C stretching	1110.67	1111.85
S=O Stretching vibrations due to sulfoxides	1058.16	1058.68
Alkene, distributed, cis	668.82	668.78

that in mutant. Due to higher crystallinity (20.53%) of normal, it is stronger than the mutant jute having lower crystallinity (13.9%), which supports the experimental observation of strength property. This result was supported by a previous study in which the authors found similar result (Saha *et. al.* 2010). Further to this, the higher crystallinity in JRC 321 fibre can be ascribed to the presence of more intermolecular H-bonding compared to that in mutant jute. FTIR analysis results (Figure 5 and Table 2) indicate the shifting of O-H stretching band from 3382.98 cm-1 in JRC321 to 3415.74 cm-1 in mutant. This confirms the influence of H-bonding on the higher crystalline nature of JRC 321.

CONCLUSION

It could be concluded that the molecular interaction of cellular components determines the fibre quality in jute in spite of the developmentally regulated synthesis of lignin only as evidenced earlier (Sengupta and Palit, 2004). Moreover, it could be expected that this interaction was genetically regulated as it was found to be hampered in the mutant. This mutant may serve as a model to understand the molecular mechanism that organizes the development of secondary wall thickening in jute bast fibre cells. The study will help in the development of desired jute fibre through genetic modifications.

ACKNOWLEDGEMENTS

Financial assistance in the form the grant support from the Department of Biotechnology, Government of India is acknowledged. Author would like to thank Dr. Jayanta Maity, Polymer and Textile Research Laboratory, Department of Chemistry, Sidho Kanho Birsha University for interpreting some of the data.

Strain is defined as the ratio of change in length to the original length and a ratio do not have any unit. But in the present study it was calculated in "**mm/mm**".

REFERENCES

Bera, A.K., Bandyopadhyay, S., Sen, S.K., Ghosh, S., Banerjee, A., (2002). Structural quality assessment of different cellulosic jute fibres by X-ray diffraction, Indian Journal of Fibre & Textile Research 27: 65-71.

Choudhary, S.B., Chowdhury, I., Singh, R.K., Pandey, S.P., Sharma, H.K., Anil Kumar, A., Karmakar, P.G., Kumari, N., Souframanien, J., Jambhulkar, S. J. (2017). Morphological, Histobiochemical and Molecular Characterisation of Low Lignin Phloem Fibre (*llpf*) Mutant of Dark Jute (*Corchorus olitorius* L.), Applied Biochemistry and Biotechnology. 183(3):980–992.

Crang, R., Lyons-Sobaski, S., Wise, R. (2018). Plant Anatomy: A Concept-Based Approach to the Structure of Seed Plants, 1st edn. Chapter 5:155-179. Springer.

Das, S., Majumdar, B., Saha, A.R., Sarkar, S., Jha, S.K. Sarkar, S.K., Saha, R. (2018). Comparative Study of Conventional and Improved Retting of Jute with Microbial Formulation, Proceedings of the National Academy of Sciences, India Section B: Biological Sciences. 88(4):1351–1357.

Day, A., Ruel, K., Neutelings, G., Crônier, D., David, H., Hawkins, S., Chabbert, B. (2005). Lignification in the flax stem: evidence for an unusual lignin in bast fibers, Planta. 222(2): 234–245.

Edwards, H.G.M., Farwell, D.W., Webster, D. (1997). FT Raman microscopy of untreated natural plant fibers, Spectrochimica Acta Part A, 53: 2383-2392.

Evert, R.F. (2006). Esau's plant anatomy, 3rd edn. John Wiley & Sons, Inc., Publication.

Fahn, A. (1990). Plant anatomy, 4th edn. Oxford: Pergamon Press.

Fidelisa, M.E.A., Pereira, T.V.C., Gomes, O. da Fonseca M., Silva, F. de Andrade., Filho, R.D.T. (2013). The effect of fiber morphology on the tensile strength of natural fibers, J Mater Res Technol. 2(2):149–157.

Gorshkova, T., Brutch, N., Chabbert, B., Deyholos, M., Hayashi, T., Lev-Yadun, S., Mellerowicz, E.J., Morvan, C., Neutelings, G., Pilate, G. (2012). Plant fibre formation: state of the art, recent and expected progress, and open questions, Crit Rev Plant Sci 31:201–228

Grabber, J.H., Jung, G.A., and Hill, R.R.Jr. (1991). Chemical composition of parenchyma and sclerenchyma cell walls isolated from orchardgrass and switchgrass, Crop Sci. 31: 1058–1065.

Guerriero, G., Behr, M., Legay, S., Mangeot-Peter, L., Zorzan, S., Ghoniem, M., Hausman, J.F. (2017). Transcriptomic profiling of hemp bast fibres at different developmental stages, Sci Rep. 7(1):4961.

Harlley, R.D. (1987). The chemistry of lignocellulosic materials from agricultural wastes in relation to processes for increasing their biodegradability, In Meer JM, van der Rijkens BA, Ferranti MP, eds. Degradation of lignocellulosics in ruminants and in industrial processes. London and New York: Elsevier Applied Science Publishers.

Kharkwal M.C., Pandey R.N., Pawar S.E. (2004). Mutation Breeding for Crop Improvement, In: Jain H.K., Kharkwal M.C. (eds) Plant Breeding. Springer, Dordrecht

Kundu B.C. (1944). Anatomy of jute stem with special reference to cambial activity and distribution of fibres in relation to leaf-trace system, Journal of Royal Asiatic Society, Bengal (Science) 10: 27–52.

Kundu, A., Sarkar D., Mandal, N.A., Sinha, M.K., Mahapatra, B.S. (2012) A secondary phloic (bast) fibre-shy (bfs) mutant of dark jute (*Corchorus olitorius* L.) develops lignified fibre cells but is defective in cambial activity, Plant Growth Regulation 67(1):45–55.

Kundu, B.C., Basak, K.C., and Sarkar, P.B. (1959). Jute in India (ed.) M.G. Kamath. The Indian central jute committee, Calcutta.

McGovern, J. N., Coffelt, D. E., Hurter, A. M., Ahuja, N. K., and Weidermann, A, (1983). Other fibres, in Pulp and Paper Manufacture, Vol. 3, Secondary Fibres and Agro-based Pulping, Hamilton F, Leopold B, Eds., TAPPI Press, Atlanta, Chapter IX.

Meredith R. (1956). Mechanical properties of Textile Fibres, Interscience Publisher, Inc., New York, Chaps. VI and VII.

Meshram, J.H., Palit, P. (2013) On the role of cell wall lignin in determining the fineness of jute fibre, Acta Physiologiae Plantarum 35(5):1565–1578.

Palit, P. (1999). Jute. In: Smith DL, Hamel C. eds. Crop yield, physiology and processes. Berlin: Springer-Verlag 271–286.

Palit, P., Sengupta, G., Datta, P., and Meshram, J. (2001). Lignin and lignification with special reference to its down regulation for the improvement of wood and bast fibre quality, Indian Journal of Plant Physiol. 6: 217–228.

Pan, N.C., Dey, A., Mahalanabish, K.K. (1999). Infrared spectra of bleached jute, Colourage 46(1): 15-19.

Preston, R.D. (1974). The physical biology of plant cell walls, London: Chapman and Hall.

Priestley, J.H., and Scott, L.I. (1936). Vascular anatomy of *Helianthus annus* L., Proceedings of the Leeds Philological and Literary Society Science Section 3: 159–173.

Rana, A.K., Basak, R.K., Mitra, B.C., Lawther, M., Banerjee, A.N. (1997). Studies of acetylation of jute using simplified procedure and its characterization, Journal Applied Polymer Science 64:1517- 1523.

Ray, P.K. (1969). On the degree of crystallinity in jute and mesta fibres in different states of purifications and moisture conditions, Journal Appl Polym Sci. 13(12): 2593-2600.

Rials T.G. (1997). Wolcott MP in Paper and Composites from Agro-Based Resources, Rowell RM, Young RA, Rowell JK, editors, Lewis Publishers, New York, P.73.

Roy, M.M. (1953). Mechanical properties of jute. II. The study of chemically treated fibres, Text Inst J. 44:T44.

Sadasivam S, Manickam A. (2008). Biochemical Methods, 3rd Edn., New Age International (P) Ltd. Publishers, New Delhi, pp 12-13, 208.

Saha, P., Manna, S., RoyChowdhury, S., Sen, R., Roy D., Adhikari, B. (2010). Enhancement of tensile strength of lignocellulosic jute fibers by alkali-steam treatment, Bioresource Technology. 101(9):3182-3187.

Samal, R.K., Mohanty, M., Panda, B.B. (1995). Effect of chemical modification on FTIR spectra: Physical and chemical behavior of jute-II, Journal of Polymer Materials 12(3): 235-240.

Samanta, P., Sadhukhan, S., Basu, A. (2015). Identification of differentially expressed transcripts associated with bast fibre development in *Corchorus capsularis* by suppression subtractive hybridization, Planta. 241(2):371-385.

Sengupta, G., and Palit, P. (2004). Characterization of lignified secondary phloem fibre-deficient mutant of jute (*Corchorus capsularis*), Annals of Botany 93: 211-220.

Snegireva, A., Chernova, T., Ageeva, M., Lev-Yadun, S., Gorshkova, T. (2015). Intrusive growth of primary and secondary phloem fibres in hemp stem determines fibre-bundle formation and structure, AoB Plants. 7: plv061

Srivastava LM. (1966). Histological studies on lignin, Tappi 49:173-183

Varma DS, Varma M, Varma IK. (1984). Coir Fibers: Part I: Effect of Physical and Chemical Treatments on Properties, Journal of Textile Research Inst 54:349.

Young, R. A. (1993). Kirk-Othmer Encyclopedia of Chemical Technology, 4th edition Vol.10, John Wiley and Sons, New York.

Microbiological
Communication

Biosci. Biotech. Res. Comm. 12(1): 99-107 (2019)

BBRC
Bioscience Biotechnology
Research Communications

Bacteriological profiling of toys and clothes of children from children's day care centre of Tarakeswar, Hooghly West Bengal, India

Raktima Bandyopadhyay[1], Sucharita Ghosh[2], Soumendranath Chatterjee[2] and Shyamapada Mandal[1]*

[1]*Laboratory of Microbiology and Experimental Medicine, Department of Zoology, University of Gour Banga, Malda, India and*
[2]*Parasitology and Microbiology Research Laboratory, Department of Zoology, University of Burdwan, Burdwan, India*

ABSTRACT

The antibiotic resistances of bacterial isolates from various sources have been reported worldwide. The present study stands for the isolation and characterization of the bacteria isolated from the toys and clothes of children collected from children's day care centre of Tarakeswar, Hooghly (WestBengal, India). Seven bacterial isolates (strain code: GUTY1, GUTY2, GUTY3, GUTY4, GUCL1, GUCL2 and GUCL3) were procured from the samples (toys and clothes) screened. Following conventional phenotypic and molecular characterization it was found that the children's clothes and toys were contaminated with different potential pathogenic bacteria. The isolates GUTY1 and GUCL1 were identified as *E. coli,* GUTY2 as *Aneurinibacillus* sp., GUCL3 and GUTY4 as *Bacillus cereus* where as GUTY3 as *Lysinibacillus* sp. and GUCL2 as *Staphylococcus aureus.* The disc diffusion susceptibility test revealed that the bacterial isolates had resistance to ampicillin only, or along with penicillin and/or rifampicin resistances.Thus, regular vigilance of antibiotic resistance of bacteria isolated from children's toys and clothes is imperatively needed in order to combat the bacterial infection to the children especially in our part of the globe.

KEY WORDS: TOYS AND CLOTHES, PATHOGENIC BACTERIA, 16S rRNA GENE, ANTIBIOTIC RESISTANCE, MAR INDEX

ARTICLE INFORMATION:

Corresponding Author: samtropmed@gmail.com
Received 12th Jan, 2019
Accepted after revision 22nd March, 2019
BBRC Print ISSN: 0974-6455
Online ISSN: 2321-4007 CODEN: USA BBRCBA
Thomson Reuters ISI ESC / Clarivate Analytics USA
Crossref Clarivate Analytics
NAAS Journal Score 2019: 4.31 SJIF: 4.196

Online Contents Available at: http//www.bbrc.in/
DOI: 10.21786/bbrc/12.1/13

INTRODUCTION

Working family members have to rely on childcare centers for providing a safe, healthy and caring environment for their children. Children are very susceptible to contagious diseases as they have not been exposed to many microbial infections and also have no resistance to them, or sometimes have not received required immunizations (ARCH, 1996; Myo clinic, 2006). Children have high hand to mouth activity and obtain infections at an earlier age. Various infections have been documented in children in the childcare centers (Van et al, 1996). They play and eat close together without having proper hygiene habits.Children having diapers are more susceptible to the spread of diarrheal diseases due to poor or inadequate handwashing, diaper changing and environmental sanitation measures (Van et al, 1991). These contributing factors create infections in childcare centers. In children's day care centre, children are commonly provided with toys and the safeties of these toys are usually not taken. Evidence has shown that belongings such as, toys and school-kits of children may easily be contaminated with microbes. Toys get passed from child to child and become contaminated through handling or by children putting their mouths to them, (Suviste, 1996, Agbulu et al 2015, Ali et al., 2016, Al-Easawi, et al., 2017 Johani et al., 2018).

Children are very much susceptible to microbial diseases. Frequently they suffer from bacterial infections like pneumonia, urinary tract infections, diarrhoea, and so many. Most of these diseases occur due to poor hygiene practices. It was noticed that the children at the study areas had been suffering from various types of food-borne and water-borne diseases. There are approximately 7000 newborn deaths every day, amounting to 46% of all child deaths under the age of 5-years (WHO, 2016). The current study has been undertaken to determine bacterial contamination of children's toys and clothes from West Bengal, India and to explore the bacterial antibiotic resistances.

MATERIALS AND METHODS

MICROBIOLOGICAL ANALYSIS

Ten toys were collected from a children day care centre of Tarakeswar, Hooghly (West Bengal state, India) with which the children seemed to play regularly. Ten cloth samples (socks and shirts) of children were randomly selected for the microbiological examination. Toys were kept in sterile plastic bags. In the laboratory, 0.1% peptone broth (sufficient to cover the toy) was poured into the bag and the toy was then rubbed from the outside of the bag to make sure that organisms were mixed with the broth. The broth was then shaken forcefully in the bag to make a uniform distribution of organisms, then serially diluted to 10^{-3} dilution and cultured following standard techniques (Maturin and Peeler, 2001). Ten clothes (socks and shirts) were selected for the microbiological examination. The area of clothes was swabbed using a sterile cotton swab, immersed in 0.1% peptone broth and used for culture.

Pour plating was done on nutrient agar for total bacterial count and on EMB agar for total coliform (TC) count. After pour plating Bacteria were isolated by sterile loop and streaked on nutrient agar plates and incubated at 30 ± 1 ^{o}C in a BOD incubator for 24 h to obtain the isolated colonies. Pure culture was maintained on agar slants for further characterization and identification. Three replications were made for each sample tested. Average colony forming unit (CFU) of coliform and total bacteria count per milliliter of broth was recorded for a specific toy or specific cloth. Total bacterial count and TC count were categorized as 'none detected', 'low' (between no CFU and $\leq10^{3}$ CFU/mL), 'moderate' ($>10^{3}$ CFU/mL and or 'high' ($\geq10^{5}$ CFU/mL).

DETERMINATION OF PHENOTYPIC IDENTITY OF ISOLATED BACTERIA

The shape, size, colour, margin and opacity of the isolated bacterial colonies were recorded. Phenotypic and biochemical characterization of the isolates were done following the standard protocol (Holt, 1984; Forbes et al., 2007). To study the bio-chemical properties, catalase, citrate utilization, nitrate reduction, indole production, methyl-red, Voges-Proskauer, urease, oxidase, and fermentation tests were done. For qualitative determination of enzymes, starch hydrolysis, lipase, protein hydrolysis, gelatin hydrolysis tests were done.

MOLECULAR CHARACTERIZATION OF BACTERIAL ISOLATES

The isolated bacteria from toys and clothes were identified both on the basis of 16S rRNA gene sequence analysis. Fingerprinting of the nucleotide was done following Lou and Golding (2007). The sequence data were aligned using the "ClustalW Submission Form" (http://www.ebi.ac.uk/clustalw) and analyzed by ClustalW (Thompson et al., 1994). Evolutionary distances were calculated using the method of Jukes and Cantor and the phylogenetic tree was prepared following the neighbor joining method (Saitou and Nei, 1987).

BACTERIAL ANTIBIOTIC SUSCEPTIBILITY AND MAR INDICES

The sensitivity of the bacterial isolates to antibiotics was tested following disc diffusion method (Bauer et

al., 1966), as mentioned earlier by Mandal et al (2011) and Mandal et al (2016). The antibiotic discs (Hi-Media, India): ampicillin (10-µg/disc), chloramphenicol (30-µg/disc), doxycycline (30-µg/disc), penicillin G (10 units/disc), levofloxacin (5 µg/ disc), nalidixic acid (30-µg/disc), and rifampicin (5-µg/disc), were used. Antibiotic susceptibility test results, in terms of zone diameter of inhibition, were interpreted following the criteria of CLSI (2013). The MAR indices for the isolated bacteria were calculated following standard methods (Maloo et al, 2014; Krumperman et al., 1983).

RESULTS AND DISCUSSION

The total bacteria count and TC count from the toys and clothes tested are shown in Table 1. The total bacteria count and TC count were categorized as 'none detected', 'low' (between no CFU and $\leq 10^3$ CFU/mL), 'moderate' ($>10^3$ CFU/mL and or 'high' ($\geq 10^5$ CFU/mL). Out of the 10 toys examined 3 were highly contaminated, 4 were moderately contaminated and the rest 3 had low contamination, while among 10 cloth samples tested, 2 were found highly contaminated, 3 were moderately contaminated and the rest 5 showed low bacterial contamination.

A total of 7 bacterial isolates (strain code: GUTY1, GUTY2, GUTY3 and GUTY4 from toy samples, and GUCL1, GUCL2 and GUCL3 from cloth samples) were procured from children's toys and clothes.The bacterial isolates GUTY1 and GUCL1 exhibited almost similar colony morphology and same biochemical properties: GUCL1 showed circular, creamy white and elevated colonies whereas GUTY1 formed spherical flat whitish colony; both were rod shaped. The bacteria were gram-negative non-spore forming, and were positive for catalase, methyl red (MR), indole, nitrate reduction, starch and gelatin hydrolysis but negative for citrate utilization, oxidase, urease, coagulase and Vogues-Proskauer (VP) test. The bacterial isolates: GUTY2 and GUTY3 formed circular, white and elevated colonies and were gram-positive spore forming rod shaped. The GUTY2 strain was positive for catalase, MR reaction, but negative for VP reaction, indole production, citrate activity, nitrate reduction, H_2S production, starch hydrolysis, gelatin hydrolysis, urease test, oxidase, coagulase test, lecithinase test, mannitol methyl red test.

The GUTY3 isolate was positive for catalase, indole, oxidase, nitrate reduction, starch and gelatin hydrolysis but negative for citrate utilization, methyl red and VP test. The bacterial isolate GUTY4 and GUCL3 showed

Table 1. The total bacteria count and total coli form count from children's toy and cloth samples

Sample	Bacterial count		Contamination status
	Total bacteria count (CFU/mL)	Total coliform count (CFU/mL)	
Toy 1	35×10^5	15×10^5	High
Cloth 1	21×10^2	11×10^2	Low
Toy 2	27×10^4	17×10^4	Moderate
Cloth 2	42×10^6	14×10^6	High
Toy 3	55×10^4	15×10^4	Moderate
Cloth 3	15×10^2	03×10^2	Low
Toy 4	12×10^2	07×10^2	Low
Cloth 4	11×10^4	34×10^4	Moderate
Toy 5	65×10^6	23×10^5	High
Cloth 5	5×10^2	5×10^2	Low
Toy 6	23×10^4	17×10^4	Moderate
Cloth 6	14×10^4	05×10^4	Moderate
Toy 7	14×10^4	05×10^4	Moderate
Cloth 7	22×10^2	16×10^2	Low
Toy 8	17×10^2	13×10^2	Low
Cloth 8	25×10^5	14×10^6	High
Toy 9	17×10^2	05×10^2	Moderate
Cloth 9	34×10^2	03×10^2	Low
Toy 10	27×10^6	07×10^5	High
Cloth 10	45×10^4	35×10^4	Moderate

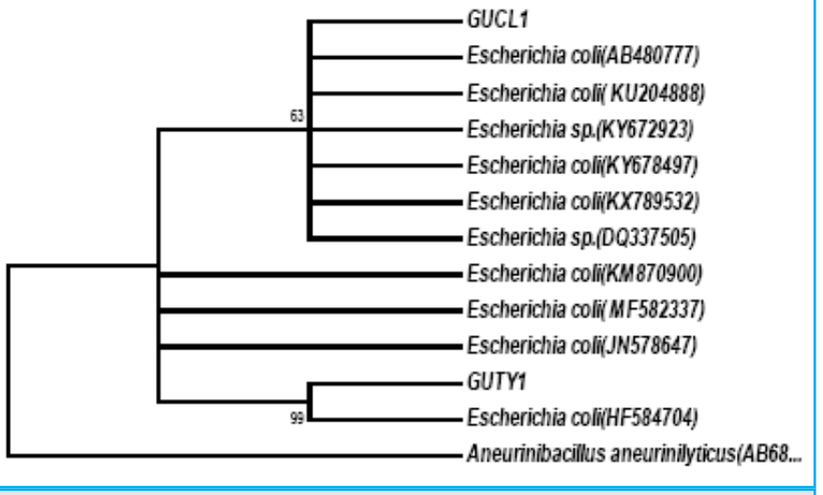

FIGURE 1. Phylogenetic tree constructed using partial 16S rRNA gene sequence of GUTY1 and GUCL1 with other neighboring 16S rRNA gene sequences retrieved from NCBI and RDP database.

more or less similar colony morphology. Both of them produced off-white, gummy and flat colonies with entire margin. GUCL3 formed spherical colonies where as GUTY4 formed circular colonies. Two bacterial isolates, GUTY4 and GUCL3, were spore forming gram-positive rod, and were positive for catalase, MR reaction, citrate activity, nitrate reduction, H_2S production, starch hydrolysis, gelatin hydrolysis, urease test, coagulase test, lecithinase test, and glucose-sucrose fermentation, but negative for VP reaction, indole production, oxidase and lactose fermentation. The GUCL2 isolate was non-spore forming gram-positive coccus, and positive for catalase test, oxidase test, H_2S production and lipid hydrolysis but negative for MR test, indole, nitrate reduction, citrate utilization, VP and urease tests as well as starch and gelatin hydrolysis. The microorganisms produced acid and/or gas from glucose but did not utilize lactose and mannitol.

The phylogenetic trees for 7 bacterial isolates, based on the partial 16S rRNA gene sequences, are represented in Figure 1 to Figure 5.The bacterium GUCL1 clustered with *E. coli* (AB480777, KU204888, KY672923, KY678497,

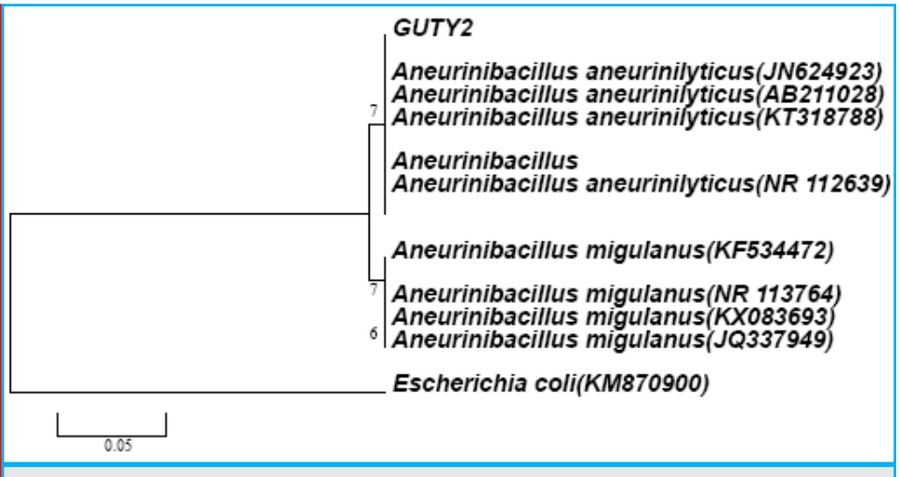

FIGURE 2. Phylogenetic tree constructed using partial 16S rRNA gene sequence of GUTY2 with other neighboring 16S rRNA gene sequences retrieved from NCBI and RDP database.

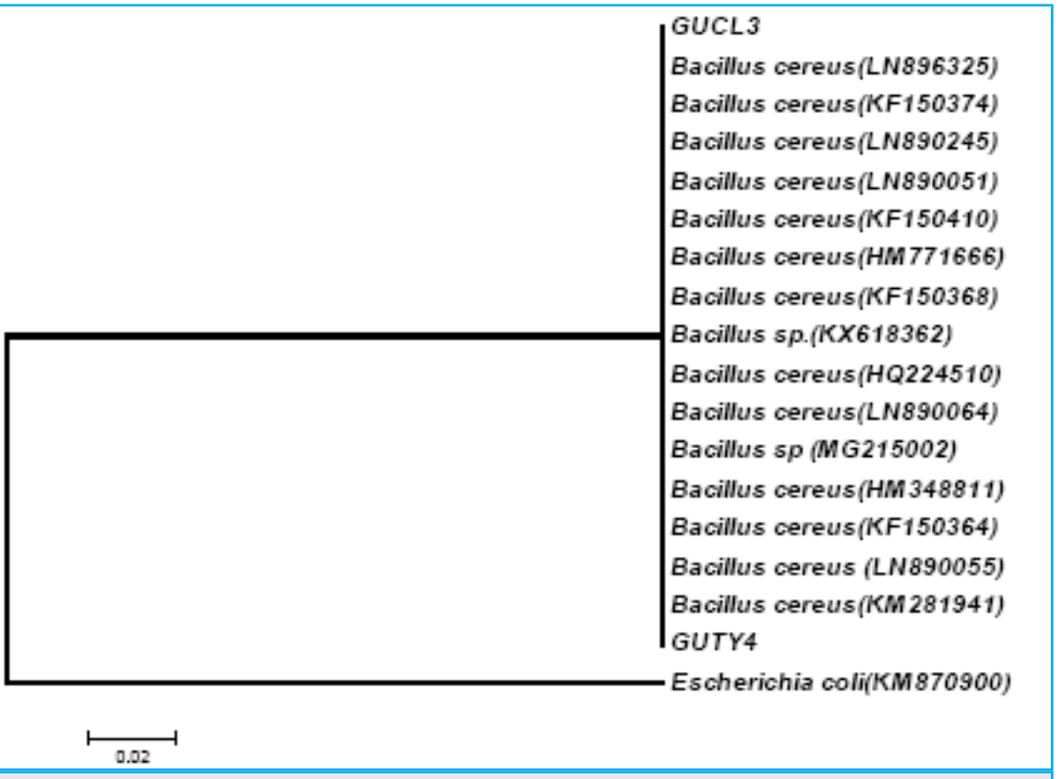

FIGURE 3. Phylogenetic tree constructed using partial 16S rRNA gene sequence of GUCL3 and GUTY4 with other neighboring 16S rRNA gene sequences retrieved from NCBI and RDP database.

KX789532, and DQ337505) with 63% bootstrap value and GUTY1 branched with *E.coli* (HF584704) with 99% bootstrap value (Figure 1).The GUTY2 isolate clustered with *Aneurinibacillus aneurinilyticus (*AB680012, JN624923, NR112639, AB211028, AB210964, and KT318788*)* and *Aneurinibacillus migulanus (*KF534472, NR113764, KX083693, and JQ337949),as represented in Figure 2.

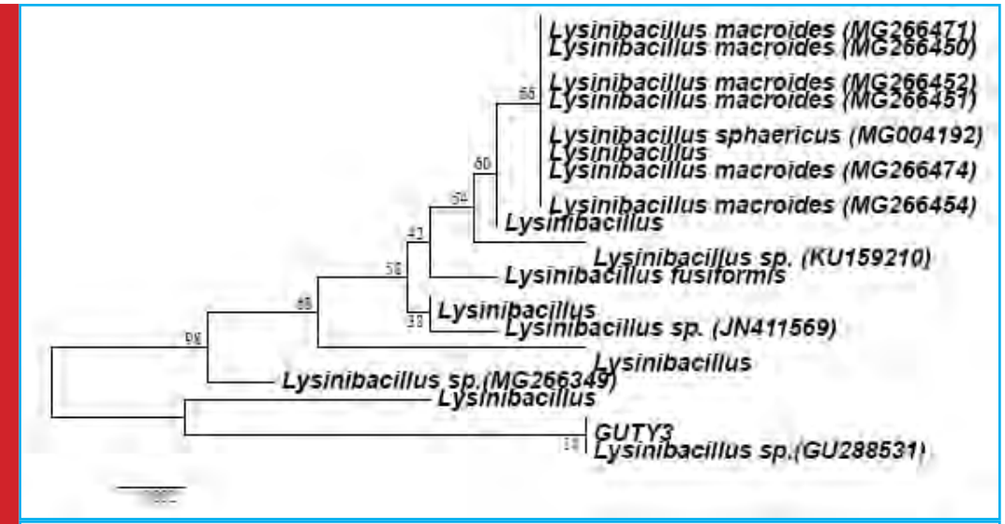

FIGURE 4. Phylogenetic tree constructed using partial 16S rRNA gene sequence of GUTY3 with other neighboring 16S rRNA gene sequences retrieved from NCBI and RDP database.

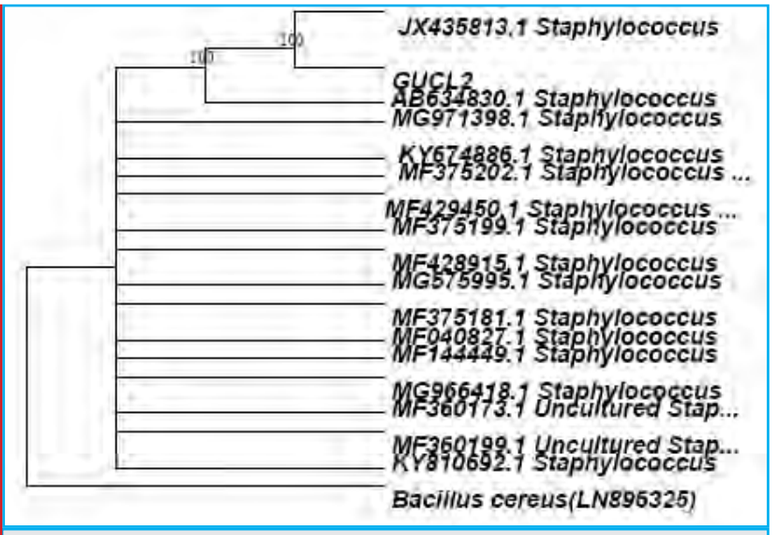

FIGURE 5. Phylogenetic tree constructed using partial 16S rRNA gene sequence of GUCL2 with other neighboring 16S rRNA gene sequences retrieved from NCBI and RDP database.

The bacterial isolates GUCL3 and GUTY4 (Figure 3) were clustered with *Bacillus cereus* (LN890051, KM281941, HQ224510, KF150364, HM771666, LN890245, KF150374, KF150368, LN890064, HM348811, LN890055, KF150410, and LN896325). The GUTY3 isolate branched with *Lysinibacillus* sp. (GU288531*)* with 100% bootstrap value (Figure 4). The GUCL2 strains (Figure 4) has been clustered with *Staphylococcus aureus* (JX435813). Therefore, on the basis of phenotypic characteristics and phylogenetic tree analysis of bacterial partial 16S rRNA gene sequence, GUTY1 and GUCL1 were identified as *E. coli*, GUTY2 as *Aneurinibacillus* sp., GUCL3 and GUTY4 both were identified as *Bacillus cereus* where as GUTY3 was identified as *Lysinibacillus* sp. and GUCL2 as *Staphylococcus aureus.*

The isolates *E.coli* GUTY1 and *E.coli* GUCL1 showed sensitivity to chloramphenicol, doxycycline, penicillin G, levofloxacin, nalidixic acid and rifampicin but resistant to ampicillin. The MAR index of *E.coli* (GUTY1 and GUCL1)isolates was 0.143. *Aneurinibacillus* sp. the GUTY2 isolate showed sensitivity to chloramphenicol, levofloxacin,doxycycline, rifampicin,nalidixic acid but resistance to ampicillin and penicillin; the MAR index for the strain was 0.285.The *Lysinibacillus sp*. GUTY3 isolate and *Bacillus cereus* GUTY4 and GUCL3 isolates showed resistance to ampicillin with MAR index of 0.143. The *Staphylococcus aureus* GUCL2 isolate had resistance to ampicillin, penicillin G and rifampicin with MAR index of 0.428.

The bacterial isolates from the toys and clothes were identified on the basis of their phenotypic as well as molecular characters. Phylogenetic studies or culture independent techniques usually provide a better scope of predictable bacterial diversity in child-care environments (Kelley et al., 2004; McManus and Kelley, 2005). The 16SrRNA gene has been used in phylogenetic studies as it is evolutionary stable and highly conserved (Weisburg et al., 1991). Besides these highly conserved primer binding sites, the 16S rRNA gene sequences have hypervariable regions for species-specific signature sequences which are very important for the characterization and identification of bacterial strains. The 16S rDNA based identification of bacteria potentially offers a useful alternative when phenotypic characterization methods fail (Deancourt et al., 2000; Lee et al., 2002). It is scientific and objective method of identification of microorganisms (Tang et al., 1998). Present investigation revealed the presence of both spore-forming (*B.cereus*, *Lysinibacillus sp*., *Aneurinibacillus sp*.) and non-spore forming bacteria (*E.coli* and *Staphylococcus aureus*) from toys provided to the children and also from the shirts or socks belonged to the children of the day-care centres.

The isolated bacteria had resistance either to ampicillin (*Bacillus cereus* GUTY4 and GUCL3) or to both the antibiotics: ampicillin and penicillin G (*E.coli* GUTY1 and *E. coli* GUCL1). Current study also showed the presence of *Staphylococcus aureus* GUCL2 which had resistance to three antibiotics: ampicillin, penicillin G and rifampicin. The spore-forming bacterial isolates also had resistance to several antibiotics. Present study revealed the presence of gram positive, spore-forming *Bacillus cereus* GUCL3 and *Bacillus cereus* GUTY4 having the ability to resist adverse or dry conditions and could be able to grow at a variable range of temperatures (Meer et al. 1991; Von Stetten et al. 1998; Nicholson, 2002;

Vilain et al, 2006). It has already been established as food-pathogens (Agata et al. 1995; Nester, 2004; Neely and Maley, 2000). The existence of *Staphylococcus* sp. was probably due to their colonization and survival on human skin and mucosa, without having any adverse effect (Kluytmans et al, 1997).

Similar bacterial diversity was reported by Lee et al. (2007). Microbial survival in clothes is determined by intrinsic factors including cloth properties or microbial features and also extrinsic factors comprising of environmental temperature, humidity etc. (Agbulu et al., 2010). Ivory and McCollum (1999) made an attempt to evaluate whether the presence of specific types of toys had any influence on the level of interactive play achieved by young children and concluded that cooperative play was significantly more common in the presence of social toys. McCrea et al (2000) screened coagulase-negative *Staphylococcus, Micrococcus* sp, *Bacillus* sp, methicillin-resistant *Staphylococcus aureus*, *Streptococcus* and coliforms from the toys provided to children in neonatal intensive care unit (NICU) cots and reported that toys may be reservoirs for potential infantile nosocomial sepsis. Avila-Aguero (2004) isolated coagulase-negative *Staphylococcus* sp.; *Bacillus* spp; *Staphylococcus aureus*; alpha-hemolytic *Streptococcus*; *Pseudomonas* spp; *Stenotrophomonas maltophilia*, and other gram-negative organisms from the toys provided to the children in a children hospital and concluded that toys could be contaminated with hazardous bacteria and afforded unnecessary risks for nosocomial infection.

Merriman et al (2002) reported that hard toys had relatively low levels of contamination in comparison to soft toys. According to Stauber *et al.,* (2013) faecal indicator bacterial levels on toys probably varied in respect to the water and sanitation conditions at home. Buttery *et al*. (1998) reported that nosocomial outbreak was associated with toys. The current study represents a take-home message that care should be taken for the cleaning and washing of socks and shirts/frocks of children on a regular basis. Toys in general provided to children in day-care centres pose an infectious risk and effective measures must be implemented to prevent the spread of infections via toys and other belongings, such as clothes.

CONCLUSION

From the present study it was found that the children's clothes and toys were contaminated with several kinds of bacteria (*Staphylococcus aureus*, *Bacillus cereus* and *E. coli*) having the capacity to cause severe illnesses, and such kinds of children's belonging might act as the vehicle of pathogenic bacteria in the community. From this point of view it is important to maintain proper hygiene of children. Parents should be more concern regarding this matter. The toys and clothes must be cleaned properly with disinfectants before everytime use. Overall, regular vigilance of drug resistant bacterial contaminants of children's belongings is an important and imperative task in order to combat life-threatening infection to children caused with such microbial pathogens.

AUTHOR CONTRIBUTION

Raktima Bandyopadhyay: performed experimental works and co-wrote the paper; Sucharita Ghosh: performed experimental works and co-wrote the paper; Soumendranath Chatterjee: characterized and analyzed the molecular identity of isolated bacteria; Shyamapada Mandal: designed the study and discussed the paper.

CONFLICTS OF INTEREST

There was no conflict of interest.

REFERENCES

Al-Easawi, N.A.F. and Emran, F.K., (2017). A Microbial Survey of Second Hand Clothe Samples Collected from Baghdad Market. Journal of Al-Nahrain University-Science, 20(3), pp.127-136.

Ali, S., Al-Harbi, M.M. and Rahman, S.R., (2016) Bacterial Isolates, Present On Surface Of Toys In Child Care Centers, In Al-Rass City, Al-Qassim Reigon. KSA.

ARCH National Resource Center for Respite and Crisis Care Services (1996). Preventing the spread of disease: Tips for providers. Retrieved November 10, 2006. From http://www.archrespite.org/ archfs42.htm.

Agata, N., Ohta, M., Mori, M., & Isobe, M. (1995). A novel dodecadepsipeptide, cereulide, is an emetic toxin of *Bacillus cereus*. FEMS microbiology letters, 129(1), 17-19.

Agbulu, C. O., Gberikon, G. M., & Ajine, B. O. (2015). Isolation and characterization of microorganisms associated with second hand female undergarments and children wear sold in Makurdi Metropolis. International Journal of Current Microbiology and Applied Sciences, 4(1), 716-724.

Avila-Aguero, M. L., German, G., Paris, M. M., Herrera, J. F., & Safe Toys Study Group. (2004). Toys in a pediatric hospital: Are they a bacterial source?. American journal of infection control, 32(5), 287-290.

Bauer AW, Kirby WMM, Skerris JC, Turuck M. (1966)Antibiotic susceptibility testing by a standard single diffusion method. American Journal of Clinical Pathology 45: 494-496.

Blumenstyk, G., & McCollum, K. (1999). 2 Reports Question Utility and Accessibility in Distance Education. Chronicle of Higher Education, 45(32), A31-A31.

Buttery, J. P., Alabaster, S. J., Heine, R. G., Scott, S. M., Crutchfield, R. A., & Garland, S. M. (1998). Multiresistant *Pseu-*

domonas aeruginosa outbreak in a pediatric oncology ward related to bath toys. The Pediatric infectious disease journal, 17(6), 509-513.

Drancourt, M., Bollet, C., Carlioz, A., Martelin, R., Gayral, J. P., & Raoult, D. (2000). 16S ribosomal DNA sequence analysis of a large collection of environmental and clinical unidentifiable bacterial isolates. Journal of clinical microbiology, 38(10), 3623-3630.

Francis, K. P., Mayr, R., von Stetten, F., Stewart, G. S., & Scherer, S. (1998). Discrimination of psychrotrophic and mesophilic strains of the *Bacillus cereus* group by PCR targeting of major cold shock protein genes. Applied and Environmental Microbiology, 64(9), 3525-3529.

Forbes BA, Sahm DF, Weissfeld AS. (2007) Bailey and Scott's Diagnostic of Microbiology 2007; 12th Edition, Mosby (Elsevier), USA.

Henze, A S.V., Bockmühl, D. and Höfer, D., (2015.) Fabric-skin models to assess infection transfer for impetigo contagiosa in a kindergarten scenario. European Journal of Clinical Microbiology & Infectious Diseases, 34(6), pp.1153-1160.

Holt JG. Bergey's manual of systematic bacteriology, Williams and Wilkins, Baltimore 1984.

Ibfelt, T., Engelund, E.H., Schultz, A.C. and Andersen, L.P., 2015. Effect of cleaning and disinfection of toys on infectious diseases and micro-organisms in daycare nurseries. Journal of Hospital Infection, 89(2), pp.109-115.

Johani, K., Abualsaud, D., Costa, D.M., Hu, H., Whiteley, G., Deva, A. and Vickery, K., (2018). Characterization of microbial community composition, antimicrobial resistance and biofilm on intensive care surfaces. Journal of infection and public health, 11(3), pp. 418-424.

Jukes TH and Cantor CR. (1969). Evolution of protein molecules. In: Munro HN, editor. Mammalian protein metabolism. New York. Academic Press.

Kelly, D., Campbell, J. I., King, T. P., Grant, G., Jansson, E. A., Coutts, A. G., ... & Conway, S. (2004). Commensal anaerobic gut bacteria attenuate inflammation by regulating nuclear-cytoplasmic shuttling of PPAR-γ and RelA. Nature immunology, 5(1), 104.

Kluytmans, J., Van Belkum, A., & Verbrugh, H. (1997). Nasal carriage of *Staphylococcus aureus:* epidemiology, underlying mechanisms, and associated risks. Clinical microbiology reviews, 10(3), 505-520.

Lee, P., Lee, S., Hong, S., & Chang, H. (2002). Isolation and characterization of a new succinic acid-producing bacterium, *Mannheimia succiniciproducens* MBEL55E, from bovine rumen. Applied microbiology and biotechnology, 58(5), 663-668.

Lee, M. K., Chiu, C. S., Chow, V. C., Lam, R. K., & Lai, R. W. (2007). Prevalence of hospital infection and antibiotic use at a university medical center in Hong Kong. Journal of Hospital Infection, 65(4), 341-347.

Lou M and Golding GB. (2007). Fingerprint: visual depiction of variation in multiple sequence alignments. Mol Ecol Notes, 7:908–914.

Mandal, MD., Mandal, S., and Pal, NK. Antibiotic resistance prevalence and pattern in environmental bacterial isolates. The Open Antimicrobial Agents Journal, 3, (2011), 45-52.

Mandal, S., Das, SN., Mandal, M., Plasmid mediated antibiotic and heavy metal co-resistance in bacterial isolates from Mahananda river water (Malda, India). Transl Med (Sunnyvale), 6, (2016) ,185. doi:10.4172/21611025.1000185

Maturin, L. J. (2001). Aerobic plate count. In: Bacteriological analytical manual online. http://www.cfsan.fda.gov/~ebam/bam-3.html

McCrea, K. W., Hartford, O., Davis, S., Eidhin, D. N., Lina, G., Speziale, P., & Höök, M. (2000). The serine-aspartate repeat (Sdr) protein family in *Staphylococcus epidermidis*. Microbiology, 146(7), 1535-1546.

McManus, C. J., & Kelley, S. T. (2005). Molecular survey of aeroplane bacterial contamination. Journal of applied microbiology, 99(3), 502-508.

Meer, R. R., Baker, J., Bodyfelt, F. W., & Griffiths, M. W. (1991). *Psychrotrophic bacillus* spp. in fluid milk products: a review. Journal of food protection, 54(12), 969-979.

Merriman, E., Corwin, P., & Ikram, R. (2002). Toys are a potential source of cross-infection in general practitioners' waiting rooms. Br J Gen Pract, 52(475), 138-140.

Mayo Clinic (2006). Children's illness: Top 5 causes of missed school. Retrieved December 15. 2006. http://mayoclinic.com/health/childrens-conditions/CC00059

NCCLS. Performance standards for antimicrobial disk susceptibility tests. 7th Ed. Approved standard National Committee for Clinical Laboratory Standards document M2- A7, 20(2002), NCCLS, Villanova, PA.

Neely, A. N., & Maley, M. P. (2000). Survival of Enterococci and Staphylococci on hospital fabrics and plastic. Journal of clinical microbiology, 38(2), 724-726.

Nester, Eugene, W., Anderson, DG., Roberts, CE., Pearsall, NN., (2004). Microbiology: A Human Perspective. McGraw-Hill Book Company, Inc., New York, U.S.A.

Nicholson, W. L. (2002). Roles of Bacillus endospores in the environment. Cellular and Molecular Life Sciences CMLS, 59(3), 410-416.

Saitou N and Nei M. (I987). The neighbor-joining method: a new method for reconstructing phylogenetic trees. Mol Biol, 4: 406-425.

Stauber, C. E., Walters, A., de Aceituno, A. M. F., & Sobsey, M. D. (2013). Bacterial contamination on household toys and association with water, sanitation and hygiene conditions in Honduras. International journal of environmental research and public health, 10(4), 1586-1597.

Suviste J. (1996). The toy trap uncovered. Nursing Times. 92(10): 56-60. 3.

Tang, D., Dowell, E. H., & Virgin, L. N. (1998). Limit cycle behavior of an airfoil with a control surface. Journal of Fluids and Structures, 12(7), 839-858.

Thompson JD, Higgins DG, Gibson TJ. (1994). Clustal W: improving the sensitivity of progressive multiple sequence alignment

through sequence weighting, positionspecific gap penalties and weight matrix choice. Nucleic Acids Res, 22: 4673-4680.

Van R, Chuan-Chuan W, Morrow A, Pickering L. (1991). The effect of diaper type and overclothing on fecal contamination in day-care centers. JAMA. 265: 1840-1844.

Van R, Morrow A, Reves R, Pickering L. (1996). Environmental contamination in child day-care centers. Am J Epidemiol 1991; 133: 460-470.

Vilain, S., Luo, Y., Hildreth, M. B., & Brözel, V. S. (2006). Analysis of the life cycle of the soil saprophyte *Bacillus cereus* in liquid soil extract and in soil. Applied and Environmental Microbiology, 72(7), 4970-4977.

Weisburg, W. G., Barns, S. M., Pelletier, D. A., & Lane, D. J. (1991). 16S ribosomal DNA amplification for phylogenetic study. Journal of Bacteriology, 173(2), 697-703.

Biotechnological Communication

Biosci. Biotech. Res. Comm. 12(1): 108-113 (2019)

BBRC Bioscience Biotechnology Research Communications

Application of Langmuir and Freundlich adsorption isotherms in screening suitable adsorbents and the role of FTIR in confirmation of *C-Phycocyanin* purification

Kethineni Chandrika[1], Sunkara Deviprasanth[2], Daram Pavan Kumar Reddy[2], Firdous Sultana[2] and Charishma Mandava[2]

[1]Associate Professor, Department of Biotechnology, Koneru Lakshmaiah Education Foundation, Vaddeswaram, Guntur, AP, India–522502

[2]Department of Biotechnology, Koneru Lakshmaiah Education Foundation, Vaddeswaram, Guntur, AP, India–522502–522502

ABSTRACT

Adsorption of C-Phycocyaninalong with its recovery and purity was tested with various adsorbents. Evaluation of experimental results shows that activated charcoal has a higher adsorption when compared to Graphite, Chitosan, and Sawdust and filter aid. Langmuir and Freundlich adsorption isotherms were taken into consideration to screen the best adsorbent. Although, Langmuir and Freundlich isotherms follow a similar sequence of ranking for adsorbents, Langmuir ranking had shown significant variation in 'qm' (Adsorption capacity) over the 'KF' (Binding constant) of Freundlich model. Nevertheless, both models predicted activated charcoal as the best adsorbent with the maximum specific adsorption. Discrete step optimization for Phycocyanin recovery and purification shows 1% activated charcoal retained 79.3% of CPC while adsorbing 64.8% of contaminant protein with 2.1 purity index. FTIR spectroscopic studies reveal that the C-PC after adsorption with 1% charcoal showed a significant reduction in the concentration of other components characteristic of the crude sample. Thus, this work suggests a quick and reliable way to screen adsorbents based on binding constants and FTIR studies.

KEY WORDS: ETHANOL FERMENTATION, MOLASSES, IMMOBILIZATION, ACTIVATORS, REDUCING SUGAR

ARTICLE INFORMATION:

Corresponding Author: kkchandrika@kluniversity.in
Received 2nd Jan, 2019
Accepted after revision 22nd March, 2019
BBRC Print ISSN: 0974-6455
Online ISSN: 2321-4007 CODEN: USA BBRCBA
Thomson Reuters ISI ESC / Clarivate Analytics USA
NAAS Journal Score 2019: 4.31 SJIF: 4.196

Online Contents Available at: http//www.bbrc.in/
DOI: 10.21786/bbrc/12.1/14

INTRODUCTION

C-Phycocyanin (C-PC), is a water-soluble protein pigment derived from the alga *Arthrospira platensis*. The pigment besides being a natural colorant is known as a potential antioxidant, anti-inflammatory agent. Studies also show C-PC is known for its platelet aggregation inhibitor. It has also shown to have hepato-protective and neuroprotective properties (Gupta, 2012). In pharmaceutical applications, the purity of C-PC should be (A620/A280) ≥ 4. Cosmetic and food industry requires a purity ratio of A620/A280 ≥ 2. On the other hand the analytical grade ('Medical' or 'Research' grade) prefers a purity ratio of 2.5-3.5 (Chaiklahan, 2011).

Phycocyanin is a protein complex which can be purified by a simple adsorption technique. Adsorption is a physical phenomenon in which one can notice an adhesion of atoms, ions and molecules on to a solid surface (Siegbahn, 1990). The adsorbate creates a film on the surface of the adsorbent. The process of adsorption can be explained with classical adsorption models such as the Langmuir and Freundlich isotherms. During a typical adsorption, before equilibrium, the amount of adsorbate on the adsorbent is a function of its pressure (if gas) or concentration (if liquid) at constant temperature. The amount of adsorbed material is the normalization of adsorbent mass, so that a comparison of different adsorbent material can be made during the screening of adsorbents. Freundlich and Langmuir isotherm models are useful tools for comparison of adsorption efficiency of the adsorbents.

A study (Alves, 2010) shows the adsorption of proteins such as bovine serum albumin, human serum albumin (HSA) and human fibronectin (HFN). In their study it was shown that albumin adsorption fits the Freundlich model. Several studies show enzyme (protein) adsorption onto the polymer particles (Tetsuya Yamamoto, 2017).

The recovery and yield of a desired product is important during extraction process. At present, several expensive unit operations are routinely adopted for purification of C-Phycocyanin. About 50-90% of the production costs are included in the purification steps. Common methods for extraction and purification of phycocyanin involve break up of cells using high pressure homogenization (Moraes, 2011), sonication (Furuki, 2003), freeze thawing, or enzymatic treatment; ammonium sulphate precipitation followed by procedures adopting hydrophobic (Bracewell, 2011). ion exchange, size exclusion (Jian-Feng, 2007), hydroxyapatite chromatography (Markov, 1974) and aqueous two phase extraction (Patil, 2007). In spite of the increased purity, these methods, however proven to be expensive and time consuming. In addition, some purification techniques may change the structural and functional properties of proteins, (Bermej, 2008 (Sikarwar, 2017).

Therefore, it is essential to develop a reliable economic process for the separation and purification of phycocyanin.The present work aims at process optimization for increased recovery and purity of phycocyanin using various adsorbent materials like Charcoal, Graphite, Chitosan, Saw dust and Filter aid in a minimum number of operations. The corresponding affinity of the adsorbent towards the protein was studied using Langmuir and Freundlich isotherm constants. (Finette, 1997)Considering the yield and purity index of the phycocyanin obtained after the each adsorption process with different adsorbent material, a suitable method has been developed which is more efficient and economically feasible.

MATERIALSAND METHODS

Phycocyanin extraction and estimation

Phycocyanin was extracted from spray dried *Spirulina platensis*. About 500mg of biomass was dissolved in 500mL of 50mM phosphate buffer (pH 6.8) or equal volume of distilled water in an Erlenmeyer flask (Borosil, India). About 20g of 0.65mm glass beads (Merck, India) and 0.25M $CaCl_2.2H_2O$ were weighed and pre-mixed with the biomass-solvent mixture. The extraction was done using a rotary shaker (Pharmacon, India) at 150 rpm for 30min. The lysed biomass was centrifuged (10,000 rpm, 10min at 10°C) and the supernatant was estimated for recovery and purity of phycocyanin using a double beam UV-Vis spectrophotomeer (Dynamica, Halo DB20). The peak for C-PC was identified at 620nm while the allophycocyanin was identified at 652 nm. The purity of C-PC was estimated by the absorbance index of A620/A280.The conc. of pigment (mg mL^{-1}) was estimated using the following equation adopted by (Moraes., 2011)

$$\frac{(O.D\,at\ 620nm - 0.474(OD\,at\ 652))}{5.34} \quad (1)$$

ADSORPTION STUDIES

The selected adsorbents for the present study are activated charcoal (Merck, India), Graphite (Ottokemi, India), Chitosan (Ottokemi, India), HyflosupercelFilter aid (Ottokemi, India) and Sawdust. The porous sawdust collected was washed with de-ionized water, air dried and sieved to a mesh size of 297 microns.

Batch adsorption experiments were carried out by adding 5% (wt/v) of each adsorbent material to 20mL of crude phycocyanin extract at five different concentrations (obtained by diluting the original crude extract (20%-100% (v/v)). The crude phycocyanin extract was

allowed to equilibrate with the adsorbent material for a contact time of 30 minutes on an orbital shaker at 150rpm and then centrifuged at 10,000rpm for 10minutes at 10°C. The corresponding phycocyanin concentration and the recovery after adsorption were calculated. The effect of various concentrations of charcoal (0.5, 1.0, 2.0, 5.0 % w/v) on the recovery and purity of phycocyanin after adsorption were also determined following the same protocol.

The equilibrium concentration (C_e) of the total protein in the supernatant collected was determined by Lowry's method (farina mujeeb., 2018) referring to the calibration curve of BSA standards. The equilibrium adsorption capacity (q_e) is obtained by dividing the amount of total protein adsorbed by the mass of the adsorbent material taken. The adsorption data was fitted into both Langmuir model (Eq. 2) and Freundlich model (Eq. 3). The maximum adsorption capacity (q_m) in Langmuir equation and the Binding constant (K_F) in Freundlich equation were determined accordingly. While 'n' being the Freundlich isotherm constant.These models were chosen to estimate the adsorption intensity of the sorbent towards the adsorbent

$$\frac{1}{q_e} = \frac{1}{q_m} + \frac{1}{C_e q_m b} \quad (2)$$

$$\ln q_e = \ln K_F + \frac{1}{n} \ln C_e \quad (3)$$

FTIR studies

Structural elucidation of Phycocyanin was made using Fourier transform – Infrared Spectroscopy, Spectrum Two™ was purchased from Perkin Elmer. (USA). The instrument uses LiTa03 (Lithium tantalite) pyroelectric infrared detector for scanning the samples. The CPC samples were applied on to a Calcium fluoride (CaF_2) glass windows for measuring the protein peakafter attaining equilibrium during adsorption process. All the spectra during analysis were smoothed and analysed by using Spectrum 10™ version 10.3.06 software.

RESULTS AND DISCUSSION

Batch adsorption experiments

The C-PC pigment recovery was made from the *S.platensis* dried biomass. The recovered extract was designated as 100% crude CPC solution. A series of dilutions was made and five different concentrations of the crude protein extract were generated to study the interaction of the crude CPC with different adsorbent materials- graphite, activated charcoal, filter aid, chitosan and sawdust. Table 1 enlists the adsorbents in the study and their physical properties with various isotherm constants. The methylene blue adsorption studies showed highest specific adsorption by activated charcoal followed by graphite, sawdust, filter aid and chitosan. The specific adsorption of protein in crude phycocyanin solution also revealed a similar order with maximum specific adsorption of protein being 10fold higher than chitosan (Sala, 2014).

Although, Langmuir and Freundlich isotherms follow a similar sequence of ranking for adsorbents, Langmuir ranking had shown significant variation in 'qm' (Adsorption capacity) over the 'KF' (Binding constant) of Freundlich model,both of which reveal the specific adsorption capacity of an adsorbentNevertheless, irrespective of the variation in the magnitude of constants in both cases, activated charcoal was shown to perform better than any of the adsorbent being adopted in the present study.

Table 1. Physical properties and isotherm constants for various adsorbents

S. No	Adsorbent	Physical properties		Langmuir Isotherm Constants# & regression			Freundlich Isotherm constants@& regression		
		Particle size (µm)	*specific adsorption (qm) (mg/g)	qm(g/g)	K(mL/g)	R 2	Kf(g/g)	n	R2
1.	Activated Charcoal	60	183.62	0.16	3978	0.99	0.60	4.35	0.99
2.	Graphite	50	134.0	0.14	2270	0.96	0.43	4.06	0.98
3.	Sawdust	297	80.2	0.02	113.2	0.99	0.39	1.30	0.99
4.	Filter aid	30	74.0	0.02	135.1	0.98	0.30	1.43	0.97
5.	Chitosan	300	50.3	0.02	163.7	0.99	0.25	1.43	0.99

*Methylene blue specific adsorption
#Langmuir constants:qmandK attained with phycocyanin-protein adsorption studies with various adsorbents
@Freundlich constants: 'n' and Kfattained with phycocyanin-protein adsorption studies with various adsorbents

Table 2. Partition profile of various concentrations of Crude Phycocyanin

S. No.	Dilution (%)	C-PC* (mg/mL)	Contaminant protein (mg/mL)	Total protein (mg/mL) (by Lowry's method)
1.	20%	0.074	0.436	0.51
2.	40%	0.144	0.756	0.9
3.	60%	0.199	1.241	1.44
4.	80%	0.266	1.754	2.02
5.	100%	0.33	1.9	2.23

*used in adsorption studies
*Crude Phycocyanin (total protein): defined by pigment-protein complex +contaminant protein

Comparison of the various adsorbent materials for phycocyanin recovery and yield

Phycocyanin, is essentially a protein –pigment complex. The adsorption of phycocyanin was attributed partly due to the protein complex associated with the pigment chromophore. The algal biomass also was shown to comprise 60% of total protein. Hence, during cell lysis and recovery of intracellular pigment-protein complex, supplemental protein contaminant (protein from biomass) (Rajakumar, 2015) is anticipated along with the crude total protein extract of phycocyanin.

The relative screening of the effective adsorbent material is based on the amount of adsorbed contaminant protein; the CPC recovered after adsorption and the purity index. Table 2 shows the total protein partition profile of the crude protein extract and Table 3 details the adsorption efficiency of the adsorbents during simultaneous CPC recovery and purification. In the initial batch adsorption studies, a higher purity index of 1.87 was observed with activated charcoal at a crude protein concentration of 100% (Table 4). Crude protein adsorption with activated charcoal exhibited a relatively higher purity index at all the five different concentrations when compared to the sorption studies with other adsorbents. Chitosan and Graphite are ranked in the next order for their purity index of the adsorbed phycocyanin (Minkova, 2003)

The importance of the current study lies in highlighting the proportion of the adsorbed contaminant protein. Data (Table 3) shows a significant proportion of the contaminant protein removal (84.95%) was observed with 5 % (w/v) activated charcoal at 60% concentration of the crude protein. Graphite was found to be next in its adsorption capacity of the contaminant protein (68.88%). Filter aid reported 64.46% contaminant protein removal at 80% crude protein concentration while sawdust reported 61.29% removal efficiency. Chitosan

Table 3. Adsorption studies at various concentrations of crude phycocyanin extract from *S. platensis*

Adsorbent	20%			40%			60%			80%			100%		
	Contaminant protein absorbed (%)	C-PC recovered after adsorption (%)	Purity Index	Contaminant protein absorbed (%)	C-PC recovered after adsorption (%)	Purity Index	Contaminant protein absorbed (%)	C-PC recovered after adsorption (%)	Purity Index	Contaminant protein absorbed (%)	C-PC recovered after adsorption (%)	Purity Index	Contaminant protein absorbed (%)	C-PC (%) recovered after adsorption	Purity Index
Graphite	62.52	83.78	0.32	54.87	10.34	0.63	67.30	65.82	0.74	87.88	76.24	0.87	68.10	50.00	0.75
Activated Charcoal	45.17	3.30	1.64	63.95	2.40	1.60	84.95	2.73	1.86	83.23	4.13	1.76	70.80	6.40	1.87
Chitosan	5.72	43.78	1.11	8.16	40.97	1.02	33.45	36.63	1.02	70.94	40.97	1.08	36.49	36.36	0.99
Filter aid	0.90	78.37	0.56	0.10	72.22	0.58	31.24	58.29	0.57	74.46	82.70	0.69	50.10	77.87	0.58
Sawdust	30.47	40.54	0.46	60.05	58.33	0.58	81.29	65.17	0.71	58.00	33.40	0.61	58.00	0.12	0.71

Table 4. Optimization of activated charcoal for selectiveremoval of crude protein from phycocyanin extract

S. No	Charcoal Concentration (%)	Contaminant Protein absorbed (%)	C-PC recovered After adsorption (%)	Purity Index
1.	0.5	57.80	87.20	1.62
2.	1.0	64.80	79.30	2.10
3.	2.0	53.50	63.43	2.37
4.	5.0	65.50	5.90	1.87

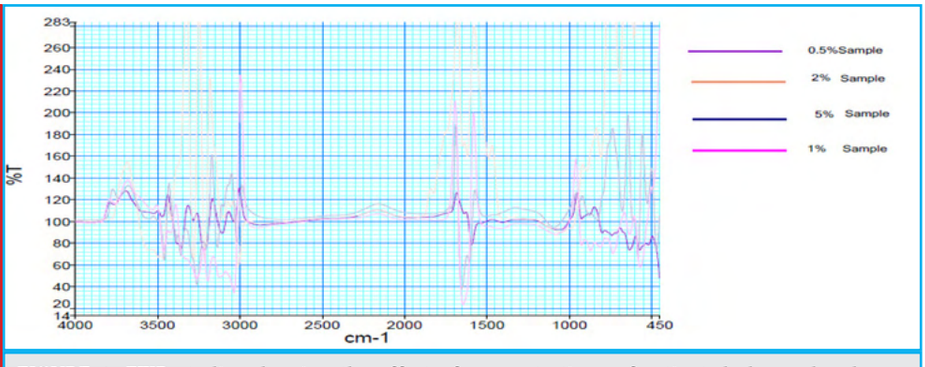

FIGURE 1. FTIR studies showing the effect of concentrations of activated charcoal adsorptionof pigment

reported 42.94% crude protein removal efficiency at 80% crude protein concentration.

The screening of the effective adsorbent for further study lies in its efficiency towards its CPC recovery and the relatively higher purity index after the adsorption experiment. On an average, the CPC recovery after the adsorption with activated charcoal was about 70%. Hence, the activated charcoal though reported lesser recovery of CPC compared to other adsorbents it was screened for further study due to its increased purity index and a higher percentage of contaminant protein removal. (Kethineni, 2018)

Discrete step optimization for Phycocyanin recovery and purification

At high concentration of activated charcoal (5%w/v), indiscriminate adsorption of protein (phycocyanin as well) was observed. However, a supplementary study on optimization of the concentration of activated charcoal for the CPC recovery is performed (Table 4). One percent activated charcoal retained 79.3% of CPC while adsorbing 64.8% of contaminant protein with 2.1 purity index. Nevertheless, a purity index of 2.37 was reported with 2% (w/v) activated charcoal with a CPC recovery of only 63.43%

FTIR spectra analysis of crude and adsorbed C-PC sample

The structural configuration of the Phycocyanin after adsorption at different concentrations of the charcoal as adsorbent were confirmed by FTIR spectra (Figure 1). On the FTIR spectra of crude C-PC, the peaks in the range of 3698.23-3460 cm-1 indicate the presence of O-H stretching vibrations and the peaks at 2932.99-2912.28 cm-1 represent the asymmetrical and symmetrical stretches of aliphatic CH2 groups. The frequency range from 1345.07-1250.18 are assigned to the C-O stretching, O-H bending vibrations and C-O asymmetric C-O-C stretching, which represent the presence of alcohols and esters. Peaks of 1133.11 and 1079.64 cm-1 represent symmetric C-H stretching vibration. The peak values of 677.39 and 640.22 cm-1 represent the stretch of S=O and S-O. The peaks at 537.21, 1650.72 and 3440.91 cm-1 in the FTIR spectra of crude C-PC are characteristic of phycocyanin, which are also present in the spectra of C-PC after adsorption with 1% charcoal. However, it can be seen that some peaks of C-PC crude sample disappear in the 1% charcoal adsorbed C-PC sample explaining the phenomena of increased purity index after adsorption. Thus, all the characteristic peaks of Phycocyanin observed in the crude C-PC sample is evident in the FTIR spectra of C-PC after adsorption with 1% charcoal with a significant reduction in the concentration of other components characteristic of the crude sample. Furthermore, the spectra also provide a fingerprint of the adsorbed Phycocyanin in the sample.

CONCLUSION

Process intensification approach in the recovery and purification of phycocyanin in the minimum number of operations is proposed. Basing on the scalability and economic feasibility, the activated charcoal (powder) at 1% was chosen to be the material of choice for simultaneous recovery and purification of phycocyanin. Amidst the high value and low volume nature of the targeted product, the recovery and specific yield of cyanobacterial phycocyanin from Spirulina platensis dried biomass showed the suitability of the biomass in various adsorption operations in optimizing the product extraction for maximum pigment recovery. The adsorption phenomena are further confirmed by the FTIR studies.

REFERENCES

Gupta, N.K., (2012) Effects of C-Phycocyanin on the representative genes of tumor development in mouse skin exposed to 12-O-tetradecanoyl-phorbol-13-acetate. Environmental toxicology and pharmacology, vol. 34(3), pages 941-948.

Chaiklahan, R., (2011) Separation and purification of phycocyanin from Spirulina sp. using a membrane process. Bioresource technology, vol. 102(14), pages 7159-7164.

Siegbahn, K. (1990). From X-ray to electron spectroscopy and new trends. Journal of Electron Spectroscopy and Related Phenomena, vol. 51, pages 11–36.

Alves, C., Reis, R. and Hunt, J. (2010). The competitive adsorption of human proteins onto natural-based biomaterials. Journal of The Royal Society Interface, vol. 7(50), pages 1367-1377.

Tetsuya yamamoyo., (2017). In-situ adsorption of polymer particles on multiwall. Carbon nanotubes using Colloidal techniques. Colloid and interface ScienceCommunication, vol. 20, pages 1-4.

Sikarwar, V.S., Zhao, M., (2017). Progress in biofuel production from gasification. Progress in Energy and Combustion Science, vol. 61, pages 189–248.

Moraes,C.C., (2011) C-phycocyanin extraction from Spirulina platensis wet biomass. Brazilian Journal of Chemical Engineering, vol. 28(1), pages 45-49.

Furuki (2003) Rapid and selective extraction of phycocyanin from Spirulina platensis adopting with ultrasonic cell disruption. Journal of Applied Phycology, vol. 15(4) pages 319-324.

Bracewell D.G. (2011). Ammonium sulphate precipitation followed by procedures adopting hydrophobic. Dual salt precipitation for the recovery from EscherichiacoliBiotechnical,vol. 27(5), pages 1306-1314.

Jian-Feng, N., (2007). Large-scale recovery of C-phycocyanin from Spirulina platensis using expanded bed adsorption chromatography. Journal of Chromatography B, vol. 850(1), pages 267-276.

Markov, G. G., & (1974). Hydroxyapatite column chromatography in procedures for isolation of purified DNA. Analytical Biochemistry, vol. 59(2), pages 555–563.

Patil, G., Raghavarao, K. (2007). Aqueous two-phase extraction for purification of C-phycocyanin. Biochemical Engineering Journal, vol. 34(2), pages 156-164.

Bermejo, P., (2008). Iron-chelating ability and antioxidant properties of phycocyanin isolated from a protean extract of Spirulinaplatensis. Food Chemistry, vol. 110(2), pages 436-445.

Finette, G., (1997). Comparative studies on the isothermal characteristics of proteins adsorbed under batch equilibrium conditions to ion-exchange, immobilised metal ion affinity and dye affinity matrices with different ionic strength and temperature conditions. Journal of Chromatography, vol. 763(1-2), pages 71–90.

Sala, L., Figueira, F., Cerveira, (2014). Kinetics and adsorption isotherm of C-phycocyanin from Spirulina platensis on ion-exchange resins. Brazilian Journal of Chemical Engineering, vol. 31(4), pages 1013-1022

Gangl, D., Zedler, J., Rajakumar, P., Martinez, E., Riseley, A., Włodarczyk, A., Purton, S., Sakuragi, Y., Howe, C., Jensen, P. and Robinson, C. (2015). Biotechnological exploitation of microalgae. Journal of Experimental Botany, vol. 66(22), pages. 6975-6990.

Minkova, K., Tchernov, A., Tchorbadjieva, M., Fournadjieva, S., Antova, R. and Busheva, M. (2003). Purification of C-phycocyanin from Spirulina (Arthrospira) fusiformis. Journal of Biotechnology, vol. 102(1), pages 55-59

Kethineni, C., Choragudi, S., Kokkiligadda, S., Jaswanthi, N. and Ronda, S. (2018). Development of Sequential Processes for Multiple Product Recovery from Microalgae. Industrial Biotechnology, vol 14(2), pages 95-106

Biotechnological Communication

Biosci. Biotech. Res. Comm. 12(1): 114-123 (2019)

BBRC Bioscience Biotechnology Research Communications

Upgradation of tannase production by *Klebsiella pneumoniae* KP715242 through heat, UV, NTG and MMS induced mutagenesis for enhanced tannase activity

Mukesh Kumar[1]*, Rajesh[2], Vivek Srivastava[3] and Raj Kumar Salar[4]

[1]*Department of Biotechnology, Ambala College of Engineering and Applied Research, Devsthali-133101, Ambala, Haryana, India*
[2]*Department of Biotechnology, Maharishi Markandeshwar University Sadopur Ambala -134007, Haryana, India*
[3]*Department of Botany and Biotechnology, Dayanand College, Hisar, 125001, Haryana, India*
[4]*Department of Biotechnology, Chaudhary Devi Lal University, Sirsa-125055, Haryana, India*

ABSTRACT

In the present study, a tannin acyl hydrolase producer bacterium *Klebsiella pneumoniae* (GenBank Accession Number KP715242) isolated from the soil was used for enhanced tannase production. An attempt was carried out to develop an efficient tannase producing strain by subjecting this parent strain (*K. pneumoniae* KP715242) to various mutagenic agents viz. heat, UV irradiations, NTG (N-methyl-N-nitro-N-nitrosoguinidine) and MMS (methyl methane sulfonate). Two most efficiently growing colonies per treatment were selected at 5–10% survival rate for each treatment. These mutants were assessed for enzyme production under submerged fermentation at preoptimized culture conditions i.e. 5.2 pH, 34.97°C temperature, 103.34 rpm agitation speed and 91.34 h of incubation time. Among these, the maximum tannase production (0.075 U/ml) was observed for the mutant U2. The most efficient mutant strain U2 had nearly 1.15 fold more enzyme activity as compared to the wild type strain (0.065 U/ml) after 90 h of incubation time under similar culture conditions. The maximum enzyme production in this mutant strain was 0.063 U/mL after an incubation time of 75 h as compared to wild type strain that had an incubation period of 90 h for a maximum enzyme activity of 0.065 U/mL. The results indicated that the mutated strain U2 exhibited higher tannase activity as well as less incubation as compared to the wild type strain.

KEY WORDS: KLEBSIELLA PNEUMONIAE, METHYL METHANE SULFONATE, MUTAGENESIS, N-METHYL-N-NITRO-N-NITROSOGUINIDINE, STRAIN IMPROVEMENT, TANNASE

ARTICLE INFORMATION:

Corresponding Author: mukesh.biotech@gmail.com
Received 22nd Dec 2018
Accepted after revision 21st March 2019
BBRC Print ISSN: 0974-6455
Online ISSN: 2321-4007 CODEN: USA BBRCBA
Thomson Reuters ISI ESC / Clarivate Analytics USA
NAAS Journal Score 2019: 4.31 SJIF: 4.196

Online Contents Available at: http//www.bbrc.in/
DOI: 10.21786/bbrc/12.1/15

INTRODUCTION

Tannins are water soluble polyphenolic compounds of varying molecular weights. These are extensively dispersed in the plant kingdom and are the fourth most abundant plant component after cellulose, hemicellulose and lignin. Tannins own several imperative biological properties, like defense against fungal, bacterial, and viral diseases. Tannins defend the susceptible parts of the plants from microbial attack by deactivating the attacking microbial extracellular enzymes (Aguilar and Sanchez, 2001). Tannins interact promptly with proteins and other molecules to make them indigestible, and adversely affect the nutritive value of animal food (Bhat *et al*., 1993). High concentration of tannic acid in soil has several detrimental effects like plant vegetation, cropping systems and low production yield. Moreover, tannin also causes various nutritional and processing problems like protein indigestibility, inhibition of enzymatic reactions and essential microbial processes such as those necessary for beer brewing. These undesirable properties of tannin are responsible for reduced voluntary feed intake, inefficient digestion and low animal productivity (Jana *et al*., 2014).

Tannin acyl hydrolase (tannase) causes the degradation of hydrolysable tannins because of its hydrolyzing ability for the ester and the depside bond with subsequent release of glucose, gallic acid and several galloyl esters of glucose (Haslam and Stangroom, 1996; Govindarajan *et al*., 2019). Tannase belongs to the esterase superfamily and has been shown to be intracellular as well as extracellular (Aguilar *et al*., 2007; Banerjee and Mahapatra, 2012). This enzyme has found numerous potential in different industrial aspects like food, brewing, beverages and, pharmaceuticals. It has been profoundly used for the preparation of instant tea, clarification of various fruit juices with other beverages and more importantly in the gallic acid production (Belmares *et al*., 2004; Mohapatra *et al*., 2009; Madeira *et al*., 2011; Chavez-Gonzalez *et al*., 2012, Ghosh and Mandal, 2015; Fathy *et al*., 2018; Aharwar *et al*., 2018).

Tannase has been reported to be present in plants, animals and microorganisms, with maximum production from the latter. It is synthesized by various microbes like bacteria, fungi, and yeast. However, maximum research work has been done in case of fungi. Nevertheless, fungal applications at commercial level are largely discouraged owing to its rather low growth rate coupled with relatively complex genome. On the other hand, growth potential of bacteria is very high and are comparatively easier to be handled at the genomic level. Apart from this, the bacteria also owe the ability to endure extreme temperature conditions, thereby exhibiting greater thermo-stability (Kumar *et al*., 2015). Moreover, bacterial tannase can also degrade and hydrolyze natural tannins and tannic acid very efficiently (Deschamps *et al*., 1983).

Production of tannase from microorganisms can be achieved through different methods like liquid surface, submerged (Smf), solid state fermentation (SSF) and modified solid-state fermentation (Belmares *et al*., 2004). Submerged fermentation is usually considered as more valuable because of easiness of sterilization, and process control to engineer in these systems (Mahapatra *et al*., 2005; Jana, 2013; Govindarajan *et al*., 2019). In view of the immense potential of tannase, large number of efforts have been carried out to make the production and purification of this enzyme more efficient. These efforts include the exploration of novel sources of tannase (Mahapatra and Banerjee, 2009; Chhokar *et al*., 2010; Zakipour *et al*., 2013) search of new and more effective fermentation systems (Purohit *et al*., 2006), statistical optimization of different culture conditions (Raaman *et al*., 2010; Aharwar *et al*., 2018), development of more efficient procedures for purification and recovery of tannase and enhanced tannase production through mutagenesis and recombinant microorganism (Curiel *et al*., 2009; Liu *et al*., 2018).

The present study represents a part of these efforts with an aim to produce a more efficient tannase producing mutant bacterial strain. In this study, we have made an attempt to enhance tannase production by different mutagenic approaches from culture of *Klebsiella pneumoniae* KP715242

MATERIALS AND METHODS

ISOLATION AND IDENTIFICATION OF TANNASE PRODUCING BACTERIAL STRAIN

A number of soil samples collected from different regions of Ambala, India were screened for the isolation of tannase positive bacterial strains. Each soil sample (1.0 gm) was suspended in 50 ml minimal medium containing K_2HPO_4:0.5g/l, KH_2PO_4:0.5g/l, $MgSO_4$:2.0g/l, $CaCl_2$: 1.0g/l and NH_4Cl: 3.0g/l supplemented with 1% tannic acid (pH 5.5) and incubated at 37°C on rotary shaker at 150 rpm for 24 hours (Osawa, 1990). A portion of each culture was transferred to fresh medium and cultured again under same conditions until pure cultures were obtained. The strains were maintained on nutrient agar slants in refrigerator at 4°C by regular transfer. All the pure isolates were assessed for tannic acid degradation using through visual reading method and zone of hydrolysis (Kumar *et al*., 2015a).

Bacterial strain with maximum tannase activity (TAH 10) was identified on the basis of its morphological,

physiological, biochemical characteristics and 16S rRNA gene sequence.

TANNASE ASSAY

For the tannase assay, 200 µl enzyme solution was mixed with 300µl of 1.0% (w/v) tannic acid prepared in 0.2 M acetate buffer of pH 5.5. The mixture was incubated for 40 minutes at 40°C, thereafter the reaction was stopped by the addition of 3.0 ml bovine serum albumin (1 mg/mL) that caused the precipitation of the residual tannic acid. The heat denatured enzyme was used as a control and was processed in similar way. The reaction mixture containing tubes were centrifuged at 7,000 x *g* for 10 minutes followed by the dissolution of the precipitates in 3.0 ml of SDS–triethanolamine (1% w/v) solution. Thereafter, 1.0 ml of $FeCl_3$ reagent (0.13 M) was added and the mixture was incubated for 15 minutes to get the color stabilized. The enzyme activity was measured by reading the absorbance of both the sample and control tubes at 530 nm against the blank (without tannic acid). One unit of the tannase was defined as the amount of enzyme, which is able to hydrolyze 1 mM of substrate tannic acid in 1 minute under assay conditions (Mondal *et al.*, 2001; Kumar *et al.*, 2016).

FORMULATION OF CELL SUSPENSION

For the preparation of the cell suspension, a small portion of 24 hours grown culture of *K. pneumoniae* was added in 50 mL nutrient broth followed by subsequent incubation at 37 °C for 12 hours under shaking conditions (110 rpm). A cell biomass pellet was obtained by centrifuging 10 ml inoculated broth at 9000 x g for 10 min at 4°C. The cell suspension (approximately 10^{7-8} cells/ml) was prepared by dissolving this pellet in 10 ml sterilized saline and was used for further studies.

HEAT INDUCED MUTAGENESIS

In order to carry out heat induced mutagenesis, 1.0 ml of cell suspension was transferred to a sterilized test tube and was heated at 60 °C for different time intervals ranging from 20 to 70 minutes. The cell suspension was serially diluted to obtain a final dilution of 10^{-6}/ml. After the dilution, 100 µl of heat treated cell suspension was laid over the nutrient agar plates supplemented with 2% tannic acid under sterile conditions. All the plates (20, 30, 40, 50, 60 and 70 min) were processed in the same manner. After keeping all the plates in dark for 30 minutes, they were incubated for 48 hours at 37°C. Subsequently, the survival percentage was determined over the control (plate containing unheated cell suspension).

UV INDUCED MUTAGENESIS

For the induction of UV induced mutagenesis, 1.0 ml of the appropriately diluted cell suspension was taken separately in different Petri plates. All of these plates were exposed to UV radiations for different periods ranging from 10 to 60 minutes by maintaining a distance of about 10 cm from the source of UV radiations. After the desired time period, the plates were given dark treatment for 30 minutes, plated on nutrient agar plates provided with 2% tannic acid and incubated for 48 hours at 37°C. The survival percentage of bacterial cells was calculated over the untreated control plate.

NTG (N-METHYL N-NITRO N-NITROSOGUANIDINE) AND MMS (METHYL METHANE SULFONATE) INDUCED MUTAGENESIS

To observe the effect of NTG and MMS mutagens, the bacterial cell suspension and NTG (1 mg/ml) and MMS (100 µl/ml) solutions were mixed separately in a ratio of 1:1 in corresponding test tubes excluding the control tube. This mixture was incubated at 37 °C for different time periods ranging from 10-60 min. After the desired period of treatment, mixture solution containing treated bacterial cells was centrifuged at 8000 x g for 10 min at 4 °C. The pellet obtained was washed twice with sterilized normal saline and plated on nutrient agar plates supplemented with 2% tannic acid. The plates were given dark treatment for 2 hours and then incubated at 37 °C for 48 hours. The cell survival percentage was determined using the plate containing the untreated cell suspension as control.

COMPARISON OF TANNASE PRODUCTION BETWEEN MUTANT STRAINS FROM EACH TREATMENT

For the isolation and identification of hyper tannase producer strain, two colonies from around 5% survival rate were selected for each treatment. The selected isolates were used for the production of extracellular tannase in submerged conditions. Tannase production was carried out in 250 ml Erlenmeyer's flask with 50 ml of fermentation medium(0.5 g/l K_2HPO_4, 0.5 g/l KH_2PO_4, 2.0 g/l $MgSO_4$, 1.0 g/l $CaCl_2$ and 3.0 g/l NH_4Cl) enriched with 1% tannic acid under optimized conditions. After regular intervals of 15, 30, 45, 60, 75, 90 and 105 hours, 1.0 ml of the fermented medium was aseptically removed and centrifuged at 10,000 rpm for 20 min at 4°C. The obtained supernatant (crude enzyme) was used for the estimation of tannase activity.

RESULTS AND DISCUSSION

ISOLATION AND SCREENING OF BACTERIA

A total of 13 pure isolates out of 20 were able to show significant growth on nutrient agar plates supplemented with 1% tannic acid. Out of these 13 isolates, only 6 isolates were found to be positive for visual detection method. However, only TAH 10 was able to exhibit distinct zone of hydrolysis on the agar plates (Fig. 1) with maximum tannase activity of 0.02 U/ml amongst all 6 tested strains (Table 1). Tannase production from this wild type strain was maximized by optimizing the various culture conditions. Under these optimum conditions (5.2 pH, 34.97 °C temperature, 103.34 rpm agitation speed and 91.34 hours of incubation time) this strain exhibited 0.065 U/ml of tannase in comparison to 0.025 U/ml obtained under un-optimized conditions (Kumar *et al.*, 2015a).

Table 1. Tannase activity of the positive isolates

Isolate number	Enzyme activity (U/ml)*
TAH 3	0.015±0.002
TAH 4	0.012±0.003
TAH 7	0.016±0.004
TAH 8	0.015±0.004
TAH 9	0.018±0.006
TAH 10	0.02±0.001

*Values are mean of three replicates; ± Standard deviation

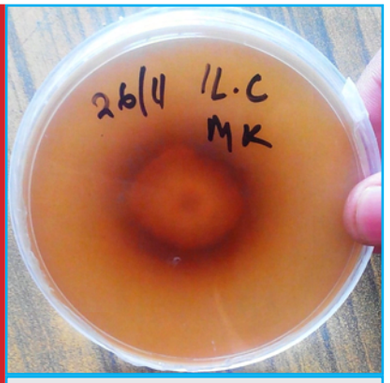

FIGURE 1. Nutrient agar plate showing tannase-producing bacterium TAH 10 after 4 days incubation

IDENTIFICATION OF BACTERIAL ISOLATE

On the basis of morphological characterization, the bacterial strain TAH 10 was found to be a gram negative, non-motile, rod shaped bacterium. Amplification of 16S rDNA and its subsequent gene sequence was used to construct the phylogenetic tree (Fig. 2). The 16S rDNA sequence of the strain TAH 10 has been deposited in the NCBI GeneBank (Accession Number KP715242).

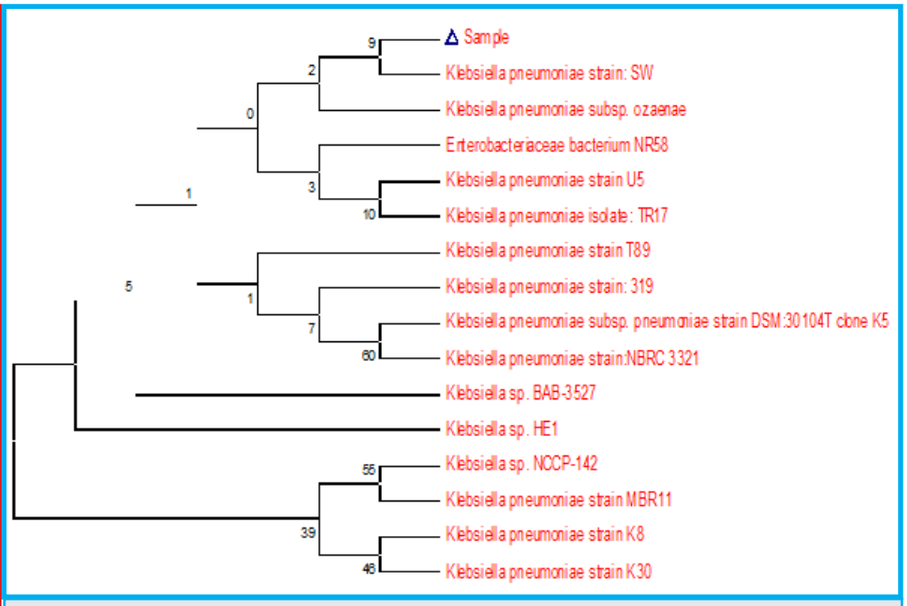

FIGURE 2. Neighbor-joining tree showing the position of isolate *Klebsiella pneumoniae* KP715242 shown as sample (Kumar *et al.*, 2015a).

DEVELOPMENT OF EFFICIENT TANNASE PRODUCING BACTERIAL STRAIN THROUGH MUTAGENESIS

For the development of hyper tannase producing bacterial strain, the parental isolate *Klebsiella pneumoniae* was subjected to various mutagenic treatments like heat treatment, ultra-violet (UV) radiation, N-methyl N-nitro N-nitrosoguanidine (NTG) treatment and methyl methane sulfonate (MMS) treatment. The action of such kind of mutagenic treatments is random in nature that may also lead to mutations in the desired genes resulting in the impairment of essential functions culminating in the death of the cells.

INFLUENCE OF HEAT ON THE SURVIVABILITY OF KLEBSIELLA PNEUMONIAE

The heat treatment (60°C) associated survival percentage of the bacterial cells is depicted in figure 3. The survival percentage declined to 32.20% after initial 20 minutes of heat treatment. There was a progressive decrease in the survival rate with the passage of time and the culture was almost lost after 50 minutes of treatment. The mechanism of heat action involves generation of an oxidative stress in the cells and such heat generated stress has been reported to be lethal at 50°C in *Saccharomyces cerevisiae* (Davidson and Schiestl, 2000). The other heat associated deleterious effects include mutations, recombination, and mitochondrial membrane disruption which are thought to cause decreased sulfhydryl content. Similarly, the co-culture of *Aspergillus foetidus* and *Rhizopus oryzae* was completely eliminated after 60 minute exposure of heat treatment (Purohit *et al.*, 2006). Zakipour *et al.* (2013) reported enhanced production of tannase from *Penicillium* sp. EZ-ZH190 through induced mutation. It was observed that after 10 minute exposure of heat treatment at 60°C, 8.5×10^4 colonies (17% of the initial number) were obtained that declined gradually with the increase in exposure time and became nil after exposure of 40, 50, and 60 minutes.

INFLUENCE OF UV RADIATIONS ON THE SURVIVABILITY OF *KLEBSIELLA PNEUMONIAE*

Extended exposure to UV radiations can alter the genetic makeup of a cell, resulting in deleterious mutations and the possible cell death. Most of the mutations are in the form of thymine dimers produced due to the fusion of two adjacent thymine bases. Thymine dimers negatively influence the structural organization of the DNA, subsequently mutating the genetic material of the cell. In the present study, the percent survival of *Klebsiella pneumoniae* culture after UV treatment is shown in figure 4. A survival rate of 43.1% was obtained after initial 10 minute exposure which declined progressively

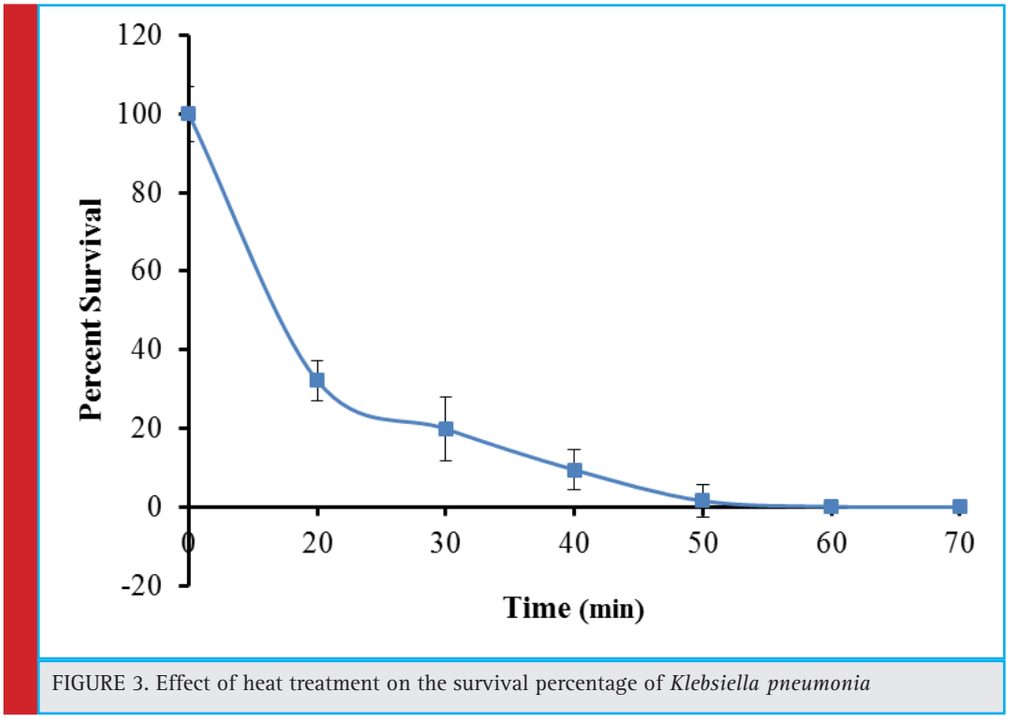

FIGURE 3. Effect of heat treatment on the survival percentage of *Klebsiella pneumonia*

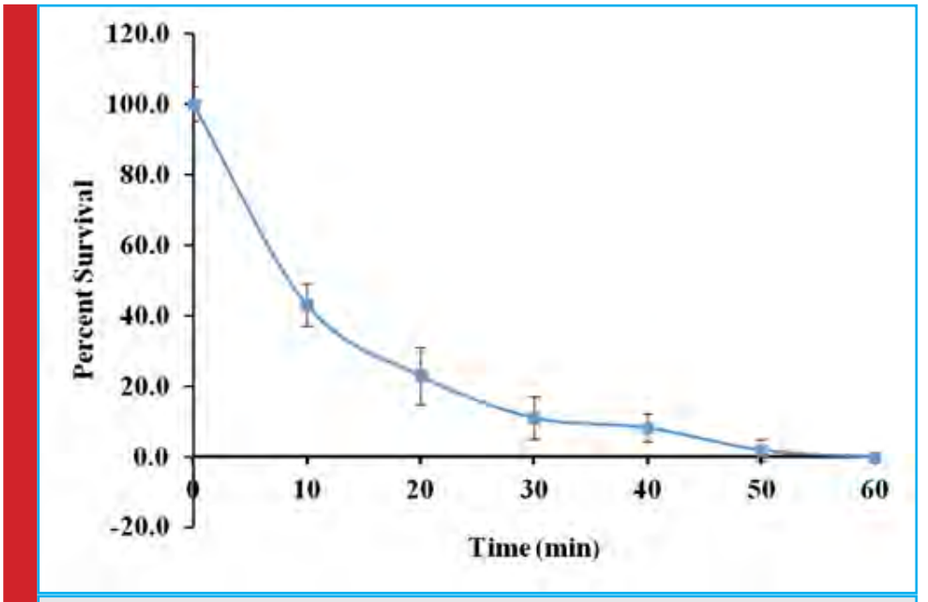

FIGURE 4. Effect of UV treatment on the survival percentage of *Klebsiella pneumoniae*

as the exposure time increased. The culture was virtually lost after exposure of 50 minutes. Similar impact of UV radiations has been observed in case of co-culture of *Aspergillus foetidus* and *Rhizopus oryzae* (Purohit *et al.*, 2006). Countless colonies were observed after the initial 10 minutes of treatment, however, the cell number decreased with further increase in time and became nil after exposure of 60 minutes.

INFLUENCE OF NTG (N-METHYL N-NITRO N-NITROSOGUANIDINE) MUTAGENS ON THE SURVIVABILITY OF *KLEBSIELLA PNEUMONIAE*

NTG mutagen induces repetitive mutations and strongly increase their frequency. It precisely interacts with DNA and is considered as UV-mimetic agent. In addition, NTG may also form nitrosoguanidine group containing reac-

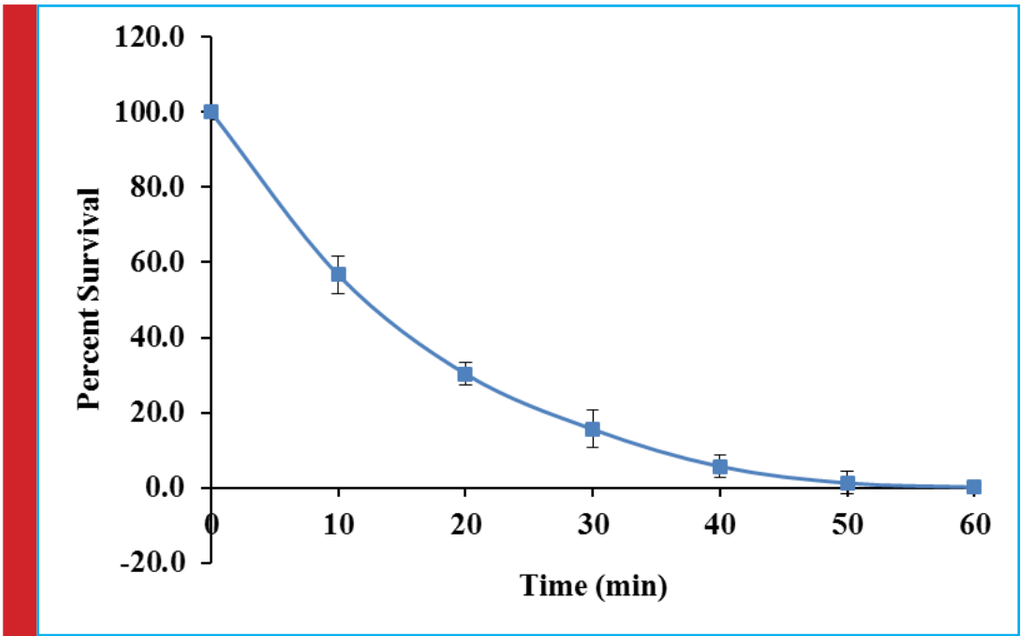

FIGURE 5. Effect of NTG treatment on the survival percentage of *Klebsiella pneumoniae*

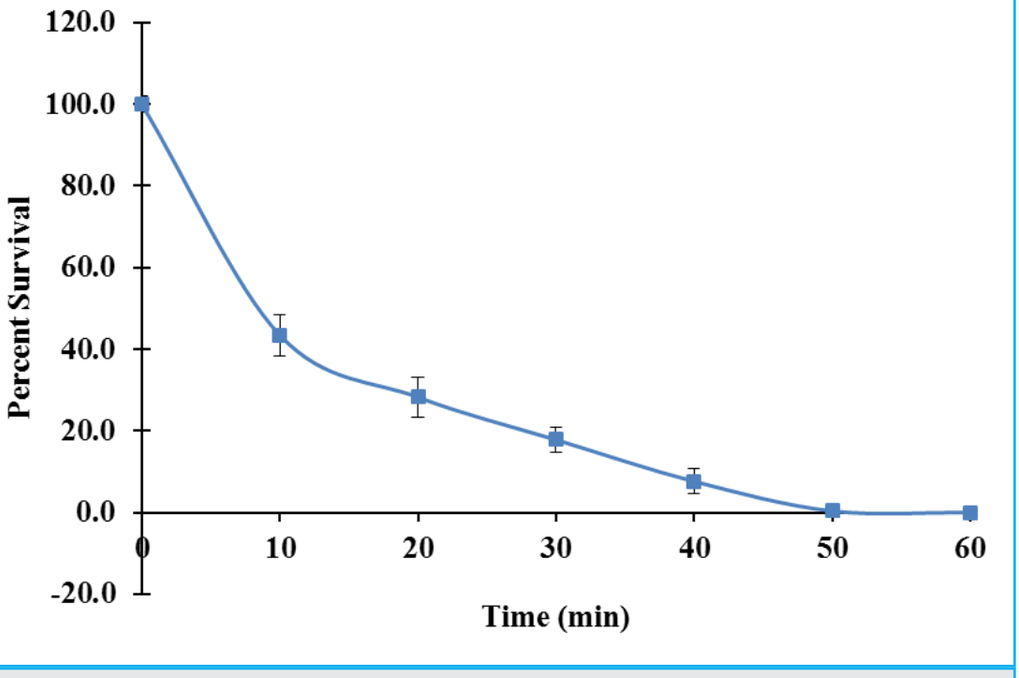

FIGURE 6. Effect of MMS treatment on the survival percentage of *Klebsiella pneumoniae*

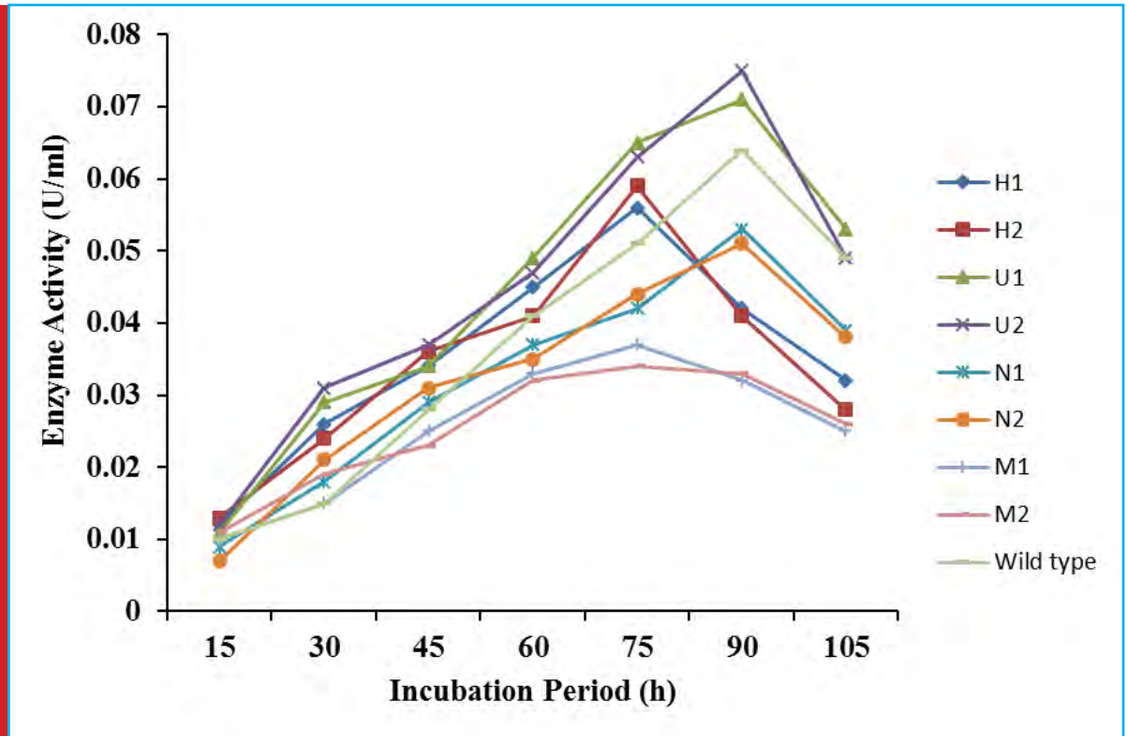

FIGURE 7. Effect of incubation period on the enzyme activity of different mutant strains of *Klebsiella pneumonia*

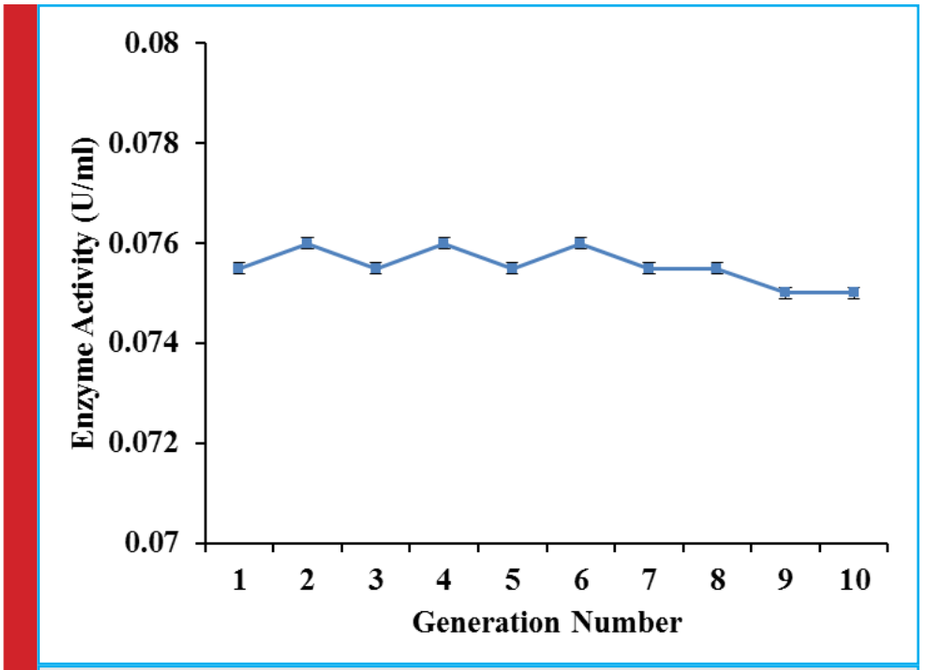

FIGURE 8. Stability test of most efficient mutant strain of *Klebsiella pneumoniae* for tannase production

tion products upon reaction with organic ions. It may inhibit the synthesis of functional proteins or could affect protein synthesis by causing mistakes during translation (Vorobjeva, 2013). These inhibitory effects of NTG have also been observed in the present study. After initial exposure of 10 minutes, the percent survival rate of *Klebsiella pneumoniae* was reduced to 56.7%. The survival rate declined steadily with increase in the exposure time and the culture was nearly eliminated after 50 minutes of treatment (Fig. 5). A similar trend has been observed in case of co-culture of *Aspergillus foetidus* and *Rhizopus oryzae* where 60 minute exposure to NTG completely eliminated the culture (Purohit *et al.*, 2006).

EFFECT OF MMS (METHYL METHANE SULFONATE) TREATMENT ON THE SURVIVABILITY OF *KLEBSIELLA PNEUMONIAE*

Methylmethane sulphonate (MMS), is a type of alkylating agent and possess cytotoxic and mutagenic properties. It primarily methylates purine bases leading to various adduct formation in the DNA. Most of the methylated bases are toxic to the cell, hamper DNA replication and can also be a source of base pair substitutions mutations. In this report, initial 10 minute exposure to MMS resulted in 43.4% survival rate which declined gradually as the exposure time increased and was practically lost as the exposure time reached 50 minutes (Fig. 6).

SELECTION OF MOST EFFICIENT TANNASE PRODUCING MUTANT STRAIN

From each mutagenic treatments, two most efficiently growing colonies per treatment were selected from 5–10% survival rate from the nutrient agar plates. These bacterial colonies were carefully chosen from the plates having 40-minute exposure to heat (H1 and H2), UV (UV1 and UV2), NTG (N1 and N2) and MMS (M1 and M2) treatments.

For the isolation and selection of most efficient tannase producing mutant strains, these mutants were further assessed for enzyme production under submerged fermentation at preoptimized culture conditions i.e. 5.2 pH, 34.97°C temperature, 103.34 rpm agitation speed and 91.34 hour of incubation time as reported in our previous study (Kumar *et al.*, 2015a). Among these, the maximum tannase production (0.075 U/ml) was witnessed in mutant U2 followed by U1, H2, and H1, producing 0.065, 0.059 and 0.056 U/ml, respectively (Fig. 7). It was found that the U2 was the most efficient tannase producing mutant, giving approximately 1.15 fold more enzyme over the wild type strain (0.065 U/ml) after 90 hours of incubation time under similar culture conditions. The maximum tannase in this mutant strain was 0.065 U/mL

with an incubation period of 75 hours as compared to wild strain where the incubation period was 90 hours in order to exhibit the same enzyme activity. Moreover, for the mutant strain U2 generated by 40 minute UV treatment, the incubation time lowered from decreased 90 hours to 75 hours to exhibit the same enzyme activity (0.065 U/mL) as obtained in case of wild culture.

The present results are in accordance to the previous report of enhanced tannase production through mutagenesis highlighting 1.21 fold increase in tannase production from mutant SCPR 337, produced by 60-minute heat treatment (Purohit *et al.*, 2006). In addition, the incubation period also decreased to 30 hours from 48 hours for maximum enzyme production as compared to the wild co-culture of *Aspergillus foetidus* and *Rhizopus oryzae*. Similarly, Zakipour *et al.* (2013) also observed that the incubation time of the mutant B named *Penicillium* sp. EZ-ZH290 (generated by 30 minute heat treatment at 60 °C) for maximum tannase production, decreased from 96 hours to 84 hours retaining the same tannase activity of 4.3 U/ml in comparison to the wild culture.

The best performing mutant strain U2 was assessed for its tannase producing capability for 10 generations. Figure 8 shows that this mutant maintained the production efficiency endorsing the stability and heritability of the mutation.

CONCLUSION

The tannase producer bacterium *K. pneumoniae* (GenBank Accession Number KP715242) used in the present study was isolated from soil and was subsequently identified at the molecular level through 16S ribosomal RNA gene sequence. Induction of mutations through various mutagenic agents and screening of commercially significant microorganisms are crucial processes for the efficacious development of various microbial strains required for fermentation industry. Enhanced tannase production through mutagenesis has been reported in case of fungi but till date, there is no report on strain improvement in case of bacteria. Therefore, mutagenesis was induced for the first time in the bacterial parent strain *Klebsiella pneumoniae* through various mutagenic treatments in an attempt for the development of more efficient tannase producing mutant bacterial strain. Amongst different mutagenic agents, UV-radiations were found to be most effective in generating more efficient tannase producer mutant strain. In comparison to the wild type strain, the improved mutated strain delivered enhanced tannase production coupled with reduced incubation period. Moreover, the most efficient mutant strain retained its tannase production efficacy for 10 generations reflecting the stability and inheritability of the mutation. Such desirable properties of this mutant strain could be exploited for commercial production of tannase at large scale with reduced cost.

ACKNOWLEDGEMENTS

The authors thank Chairperson, Department of Biotechnology, Chaudhary Devi Lal University, Sirsa, Haryana, India for providing necessary laboratory facilities to carry out this work.

FUNDING

This research did not receive any specific grant from funding agencies in the public, commercial, or not-for-profit sectors.

REFERENCES

Aguilar C.N., Rodríguez R., Gutiérrez-Sánchez G., Augur C., Favela-Torres E., Prado-Barragan L.A., Ramírez-Coronel A., Contreras-Esquivel J.C. (2007) Microbial tannases: advances and perspectives. Applied Microbiology and Biotechnology 6: 47–59.

Aguilar C.N., Sanchez G.G. (2001) Review: Sources properties, applications and potential uses of tannin acyl hydrolase. International Journal of Food Science & Technology 7(5): 373–382.

Aharwar A., Parihar D.K. (2018) Tannases: Production, Properties, Applications. Biocatalysis and Agricultural Biotechnology 15: 322-334.

Banerjee D., Mahapatra S. (2012) Fungal tannase: a journey from strain isolation to enzyme applications. Dynamic Biochemistry, Process Biotechnology and Molecular Biology 6: 49–60.

Belmares R., Contreras-Esquivel J.C., Rodriguez-Herrera R., Coronel A.R., Aguilar C.N. (2004) Microbial production of tannase: an enzyme with potential use in food industry. Lebensmittel-Wissenschaft und -Technologie 37: 857-864.

Bhat T.K., Singh B. Sharma O.P. (1998) Microbial degradation of tannins – a current perspective. Biodegradation 9: 343–57.

Chavez-Gonzalez M., Rodrigues-Durán L.V., Balagurusamy N., PradoBarragán A., Rodrigues R., Conheras J.C., Aguilar G.N. (2012) Biotechnological advances and challenges of tannase: an overview. Food and Bioprocess Technology 5(2): 445-459.

Chhokar V., Seema, Beniwal V., Salar R.K., Nehra K.S., Kumar A., Rana J.S. (2010) Purification and characterization of extracellular tannin acylhydrolase from *Aspergillus heteromorphus* MTCC 8818. Biotechnology and Bioprocess Engineering 15: 793–799.

Curiel J.A., Rodriguez H., Acebron I., Mancheno J.M., Rivas de las B., Munoz R.)2009) Production and physicochemical properties of recombinant *Lactobacillus plantarum* tannase. Journal of Agricultural and Food Chemistry 57: 6224–6230.

Davidson J.F., Schiestl R.H. (2000) Mis-targeting of multiple gene disruption constructs containing hisG. Current Genetics 38(4): 188-90.

Deschamps A.M., Otuk G., Lebeault J.M. (1983) Production of tannase and degradation of chestnut tannin by bacteria. Journal of Fermentation Technology, 61: 55–59.

Fathy S.A., Mahmoud A.E., Rashad M.M., Ezz M.K., Mohammed A.T. (2018) Improving the nutritive value of olive pomace by solid state fermentation of *Kluyveromyces marxianus* with simultaneous production of gallic acid. International Journal of Recycling of Organic Waste in Agriculture 7(2): 135-141.

Ghosh K., Mandal S. (2015) Nutritional evaluation of groundnut oil cake in formulated diets for rohu, *Labeo rohita* (Hamilton) fingerlings after solid state fermentation with a tannase producing yeast, *Pichia kudriavzevii* (GU939629) isolated from fish gut. Aquaculture Reports 2: 82–90.

Govindarajan R.K., Mathivanan K., Rameshkumar N., Shyu D.J.H., Kayalvizhi N. (2019) Purification, structural characterization and biotechnological potential of tannase enzyme produced by *Enterobacter cloacae* strain 41 Process Biochemistry. 77: 37-47.

Haslam E., Stangroom J.E. (1996) The esterase and depsidase activities of tannase. Journal of Biochemistry 99(1): 28–31.

Jana A, Halder S.K., Banerjee A, Paul T, Pati B.R., Mondal K.C., Mohapatra P.K.D. (2014) Biosynthesis, structural architecture and biotechnological potential of bacterial tannase: A molecular advancement, Bioresource Technology 157: 327–340.

Jana A., Maity C., Halder S.K., Das A., Pati B.R., Mondal K.C., Mohapatra P.K.D. (2013) Structural characterization of thermostable, solvent tolerant, cytosafe tannase from *Bacillus subtilis* PAB2. Biochemical Engineering Journal 77: 161–170.

Kumar M., Amrinder S., Beniwal V., Salar R.K. (2016) Improved production of tannase by *Klebsiella pneumoniae* using Indian gooseberry leaves under submerged fermentation using Taguchi approach. AMB Express 6: 46.

Kumar M., Beniwal V., Salar R.K. (2015) Purification and characterization of a thermophilic tannase from *Klebsiella pneumoniae* KP715242. Biocatalysis and Agricultural Biotechnology 4: 745–751.

Kumar M., Rana S., Beniwal V., Salar R.K. (2015a)Optimization of tannase production by a novel *Klebsiella pneumoniae* KP715242 using central composite design. Biotechnology Reports 7: 128–134.

Liu F., Wang B., Ye Y., Pan L. (2018) High level expression and characterization of tannase tan7 using *Aspergillus niger* SH-2 with low-background endogenous secretory proteins as the host. Protein Expression and Purification 144: 71–75.

Madeira J.J.V., Macedo J.A., Macedo G.A. (2011) Detoxification of castor bean residues and the simultaneous production of tannase and phytase by solid-state fermentation using *Paecilomyces variotii*. Bioresource Technology 102: 7343–7348.

Mahapatra K., Nanda R.K., Bag S.S., Banerjee R., Pandey A., Szakacs G. (2005) Purification, characterization and some studies on secondary structure of tannase from *Aspergillus awamori nakazawaI*. Process Biochemistry 40(10): 3251–3254.

Mahapatra S., Banerjee D. (2009) Extracellular tannase production by endophytic *Hyalopus* sp. The Journal of General and Applied Microbiology 55(3): 255-259.

Mohapatra P.K.D., Maity C., Rao R.S., Pati B.R., Mondal K.C. (2009) Tannase production by *Bacillus licheniformis* KBR6: Optimization of submerged culture conditions by Taguchi DOE methodology. Food Research International 42: 430–435.

Mondal K.C., Banerjee D., Jana M., Pati B.R. (2001) Colorimetric assay for determination of tannin acyl hydrolase (E.C.3.1.1.20) activity. Analytical Biochemistry 295: 168–171.

Osawa R. (1990) Formation of a clear zone on tannin-treated brain heart infusion agar by a *Streptococcus* sp. isolated from feces of koalas. Applied and Environmental Microbiology 56: 829-831.

Purohit J.S., Dutta J.R., Nanda R.K., Banerjee R. (2006) Strain improvement for tannase production from co-culture of *Aspergillus foetidus* and *Rhizopus oryzae*. Bioresource Technology 97: 795-801.

Raaman N., Mahendran B., Jaganathan C., Sukumar S., Chandrasekaran V. (2010) Optimisation of extracellular tannase production from *Paecilomyces variotii*. World Journal of Microbiology and Biotechnology 26: 1033–1039.

Vorobjeva L. (2013) Propionibacteria. Springer Science & Business Media.

Zakipour M.E., Hamidi-Esfahani Z., Sahari M.A., Azizi M.H. (2013) Improvement of strain *Penicillium* sp. EZZH 190 for tannase production by induced mutation. Applied Biochemistry and Biotechnology 17(6): 1376-1389.

Biotechnological Communication

Biosci. Biotech. Res. Comm. 12(1): 124-133 (2019)

BBRC Bioscience Biotechnology Research Communications

Synteny analysis of *Glycine max* and *Phaseolus vulgaris* revealing conserved regions of NBS-LRR coding genes

Gaurav Singh* and Anil Kumar

School of Biotechnology, Devi Ahilya University, Khandwa Rd., Indore-452001, India

ABSTRACT

Soybean (*Glycine max*) and common bean (*Phaseolus vulgaris*) are the two important of the leguminous family, Phaseoleae. Synteny gives a framework in which preservation of genes and gene order is determine between genomes of various species. The syntenic relationship between *G. max* and *P. vulgaris* is important to determine the potential for comparative genomic analysis. Here, synteny analysis has been performed between *G. max* and *P. vulgaris* by using the tool 'SATSUMA'. Genome data of these two legume species were retrieved from NCBI database, gene synteny alignment was then performed and comparatively analysed. Result was visualized by developing custom script in BioPython software version 3.7. The soybean chromosome 13 was aligned with whole genome of common bean as it contains genes which code for nucleotide binding site and leucine rich repeats (NBS-LRR) protein. The NBS-LRR genes play a major role in defense against pathogens. On alignment, a set of genes linked with disease resistant proteins (NBS-LRR) in *G. max* showed synteny with the different chromosomes of *P. vulgaris*. The data supported the theory that in legumes, genes are highly conserved, as extensive regions of synteny exist between these two species. The present study will be helpful to use both genomic resources as well as genetic data for crucial agronomic traits for the improvement of these two species.

KEY WORDS: DISEASE RESISTANCE GENES, *GLYCINE MAX*, NBS-LRR, *PHASEOLUS VULGARIS*, SYNTENY

INTRODUCTION

Synteny word came from greek where 'syn' means together and 'taenia' means ribbon. When gene order is conserved between the organism is commonly refered as Synteny. It is of two different type's viz. macrosynteny when many genes or large chromosomal segments of different organisms are syntenic; and microsynteny when only few genes are conserved in different species (Zhu et al., 2005 and Passoupathy, 2016). Relationship between plants, pathogens and pests have been currently discussed in different models (Andolfo and Ercol-

ARTICLE INFORMATION:

Corresponding Author: singhgauravbiotech@gmail.com
Received 12th Jan, 2019
Accepted after revision 2nd March, 2019
BBRC Print ISSN: 0974-6455
Online ISSN: 2321-4007 CODEN: USA BBRCBA
Thomson Reuters ISI ESC / Clarivate Analytics USA
NAAS Journal Score 2019: 4.31 SJIF: 4.196

Online Contents Available at: http//www.bbrc.in/
DOI: 10.21786/bbrc/12.1/16

ano, 2015). This models mainly include proteins which are coded by clustered disease-resistance (*R*) genes in plant genomes (Hulbert et. al., 2001). In earlier study, the *R* gene-encoded proteins were divided into eight major group on the basis of amino acid motif organization and localization in the cell (Gururani et. al., 2012). Among these group two main *R* gene proteins are (CC) NBS-LRR or CNL proteins and TNL proteins. NBS-LRR genes have been grouped into three classes (TNL, CNL and *R* NLs) (Shao et. al., 2016 Neupane et. al., 2018).

The legumes are extremely diverse and can be distributed into 3 subfamilies viz. *Caesalpinioideae, Mimosoideae* and *Papilionoideae* (Doyle and Luckow, 2003). The subfamily, Papilionoideae consists of almost all commercially important legumes like *Arachis hypogaea* (peanut), *Cicer arietinum* (chick pea), *Glycine max* (soybean), *Phaseolus vulgaris* (common bean), *Medicago sativa* (alfalfa), *Vigna radiata* (mungbean), *Lens culinaris* (lentil) and *Pisum sativum* (pea). Although these crop legumes have close phylogenetic relationship but differ extremely in their chromosome number, genome size and ploidy level (Table 1). However, previous studies on comparative genetic mapping suggested that the Papilionoideae subfamily members showed broad genome conservation (Weeden et al., 1992; Zhu et al., 2005). Young et al (2003) showed that legumes form a systematic taxonomic group with ubiquitous and prevailing macro- and micro- synteny. There are reports indicating that closely related species contain genomes having various genes with same map positions (Bennetzen, 2000; Devos and Gale, 2000; Paterson et al., 2000; Schmidt, 2000; Gualtieri et al., 2002).

Earlier, in plants, synteny analyses were aimed only on the species belonging to the families *Poaceae* and *Brassicaceae*. In recent time, such studies are being extended on other plants especially legumes (Gualtieri et al., 2002). It has been shown that sequence based tools help to study the evolution, organization and syntenic relationships of genomes. Macro- and micro- synteny of various species can be compared using linkage maps (Mc Connell et al., 2010). The studies indicated that level of synteny is found high in closely related species, and it decreases with growing phylogenetic distance (Choi et al., 2004). Recently, a linkage map for *Apios Americana* (a tuberous perennial legume in phaseolae tribe) has been reported and it showed synteny with selected warm-seasoned legumes. It also revealed a translocation event in *Glycine max* and common bean against *Apios* and *Vigna* species (Singh et al., 2018).

The two most important members of legume family Phaseoleae are soybean and common bean. These two species are commercially valuable legumes, common bean as a nutritional crop for poor population and soybean for its various human and animal uses (Mc Clean et al., 2010). Common bean has been diverged from soybean 19 million years ago. Considering syntenic relationship between two species is crucial to determine the potential for comparative genomic analysis. Whole genome duplication is one of the most salient characteristics of the soybean genome (Cannon and Shoemaker, 2012).

The RFLP mapping (Shoemaker et al., 1996) and EST Ks analysis have provided substantial evidences that whole genome duplication (WGD) in soybean has occurred about 13 million years ago (Schmutz et al., 2010 and Schlueter et al., 2004). Boutin et al (1995) have reported a number of syntenic linkage blocks between common bean and soybean by exploiting shared RFLP markers. They used using low density RFLP mapping, they showed that these two species share a high degree of homology in sequence, however, synteny has been found over short blocks of genomes. A clear one to two relationship between common bean and soybean genomes was shown by Lee et al (2001). A few synteny analyses have been reported between soybean and common bean. Mc Clean et al., (2010) studied the synteny

Table 1. Genomic information of nine legume species.

Species name	Common name	Genome size (Mbp)	Chr. No.	Gene number	Remark	Reference
Medicago truncatula	Barrel medic	470	2n = 2x = 16	50,894	WGS	Young et al. 2011
Medicago sativa	Alfafa	830–860	2n = 4x = 32	NA	–	Bauchan and Hossain2001
Pisum sativum	Pea	4300	2n = 2x = 14	NA	–	Franssen et al. 2011
Cicer arietinum	Chickpea	864	2n = 2x = 16	28,269	WGS	Varshney et al. 2013
Lotus japonicas	Bird's-foot trefoil	471	2n = 2x = 12	39,735	WGS	Sato et al. 2008
Vigna radiata	Mung bean	333	2n = 2x = 22	22,368	WGS	Kang et al. 2014
Glycine max	Soybean	1115	2n = 2x = 40	56,044	WGS	Schmutz et al. 2010
Phaseolus vulgaris	Common bean	625	2n = 2x = 22	38,482	WGS	Schmutz et al. 2014
Arachis hypogaea	Pea nut, ground nut	2,800	2n = 4x = 40	50,324	WGS	Chen et al. 2016

*NA- Not available, WGS - Whole genome sequencing completed.

between soybean and common bean on the basis of 300 gene base loci. Synteny blocks of averaging 32 cM in common bean and 4.9 Mb in soybean were found for all 11 common bean linkage groups which were mapped to all soybean linkage groups. A total 55 syntenic blocks each having 7 loci were observed between the common bean and soybean. By analysing the location of these blocks, it was revealed that each locus of common bean genome mapped to two loci of soybean genome (Mc Clean et al., 2010).

In 2014, Schmutz and co-workers observed considerable synteny between *Phaseolus vulgaris* and *Glycine max*, except in pericentromeric regions, where due to genomic expansion in one or both genomes micro- colinearity was much extended and due to that was lesser dense. Conservation of genome macrostructure has been reported between the soybean and other legumes including *Phaseolus vulgaris* (Lee et al., 2017). Studies showed the correlation between *Phaseolus* linkage group Pv01 and *Glycine max* chromosomes Gm06 and Gm04 (Cannon and Shoemaker 2012). It is also reported that Gm5 and Gm8 chromosomes share synteny to common bean Pv2 (Mc Clean et al., 2010). In another study, nearly 63% of common bean unigenes were shown to have homology to soybean (Kalavacharla et al., 2011). Microsynteny analysis was also reported between common bean and soybean where 6 BAC clones were sequenced and analyzed for microsynteny (Yadegari, 2013). Recently the genomes of *G.max* and *P. vulgaris* were analyzed for investigating synteny. Syntenic blocks were found between chromosomes Gm03 and Pv10, Gm10 and Pv07 as well as Gm14 and Pv01. A large number of present research make use of whole genome sequences to study *R* genes in legumes (Anderson 2016, Christie et. al., 2016 and Neupane et. al., 2018).

Earlier many research were done on NBS-LRR genes in *Glycine max* and other legumes by using bioinformatics approach (Benson 2014, Shao et. al., 2016 and Neupane et. al., 2018). Nepal and Benson (2015) showed the complete evolutionary relationship of the CNL- *R* genes in soybean and common bean. In the present study, synteny analysis between chromosome 13 of soybean having NBS-LRR enriched sequences and whole genome of common bean have been carried out since common bean has been reported to have NBS-LRR enriched regions which help in disease resistance. The results from our study will be helpful in understanding evolutionary relationships of NBS-LRR genes with potential implication in crop improvement.

MATERIALS AND METHODS

The gene synteny alignment, and genomic linkage analyses between the chromosome 13 of *G. max* and whole genome of *P. vulgaris* was performed by using 'SATSUMA version 3.1.0 freely available on the website, http://satsuma.sourceforge.net/. All the data in FASTA and GFF files required for genome sequence and annotation of soybean and common bean were downloaded from the NCBI database (https://www.ncbi.nlm.nih.gov/genome/). For synteny analysis, only sequence alignments of more than 200 bp and percent identity of more than 85% were considered and rest were filtered out. The results were visualized by developing custom script in Biopython module of BioPython, version 3.7 freely available on the website, http://biopython.org/DIST/docs/install/Installation.html.

RESULTS AND DISCUSSION

Comparison of orthologous regions of soybean and common bean

The syntenic analysis between soybean and common bean showed many conserved regions between the two as shown in Fig. 1. Twenty one genes mentioned in Table 2, which were screened on the basis of few parameters of our interest as highest, lowest percent similarity, protein kinase, diseases resistance protein, NBS-LRR proteins represent less than 1/4th of the genes we have obtained after synteny mapping. These genes were mentioned with their gene id, locus tag along with the product formed as shown in table 2. Soybean chromosome 13 region having start from 22449055 bp and up to 22449570 bp showed gene homology with the sequence starting from 31929662 to 31930177 of *Phaseolus vulgaris*. This genomic region in both the species codes for guanine nucleotide binding protein subunit gamma 3-like isoform X1. The guanine nucleotide binding protein is important for signalling pathway. It is to be noted that the Rpg1b genes in soybean mainly codes for NB and LRR proteins. Various NB-LRR protein coding genes which are present on chromosome 13 of *G. max* are also showing synteny with *P. vulgaris*. For instance, F-box/LRR-repeat protein 4-like (LOC100816140) is located at 27041793 bp to 27042286 bp in *Phaseolus vulgaris*. A mitogen-activated protein kinase2 (LOC100789734) located on chromosome 13 of *Glycine max* is showing homology with *Phaseolus vulgaris*.

A G type lectin S-receptors like serine/threonine-protein kinase coding gene located at chromosome 13 in *Glycine max* is also present in *Phaseolus vulgaris* genomic region having starts from 30144768 bp to 30146245 bp. It is having several molecular function like ATP binding, Calmodulin binding and protein serine/threonine kinase activity and few biological functions like protein phosphorylation and recognition of pollen. Glycogen phosphorylase 1-like isoform X1 coding gene which is present

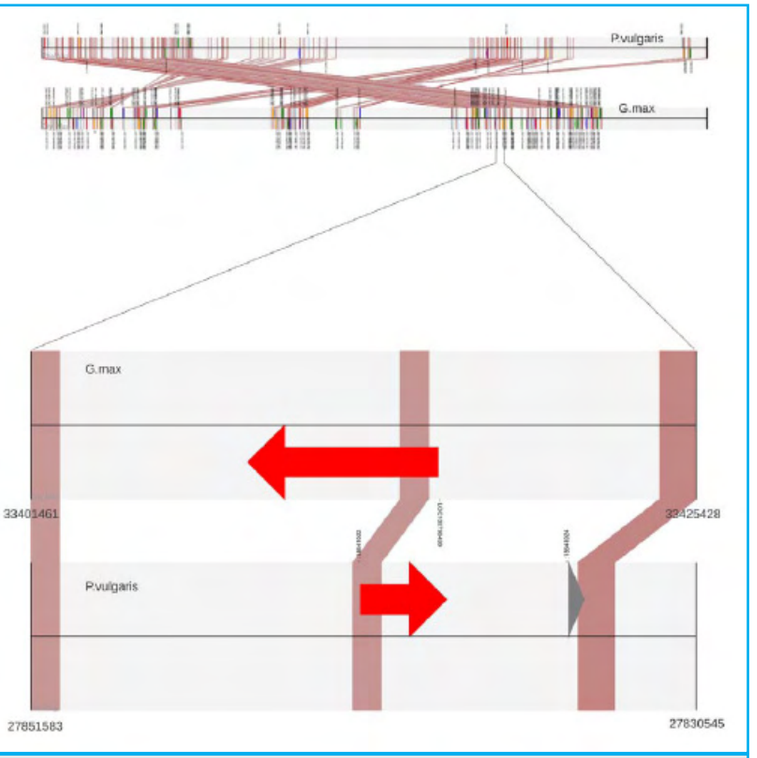

FIGURE 1. Syntenic regions between *Glycine max* and *Phaseolus vulgaris*. A synteny region has been amplified where synteny length has been indicated using colors. The colors of the links are based on the magnitude of synteny length (Light grey color indicates minimum synteny length whereas red brick color maximum synteny length).

at locus LOC100779066 on *Glycine max* chromosome 13 is present in *Phaseolus vulgaris*. Uncharacterized ATP-dependent helicase C23E6.02-like (LOC100792901) and B3 domain-containing protein Os07g0563300-like both were conserved in these legumes namely *Glycine max* and *Phaseolus vulgaris*. Highest synteny was found to be 91.794 % similarity between *Glycine max* and *Phaseolus vulgaris* for a region which codes for an uncharacterized protein LOC100775655 in both the legume. Similarly, lowest synteny was found to be 85.049 % similarity at loci LOC102661544 of *Glycine max*.

Various syntenic regions were found between the two legumes, which codes for different proteins like MAP Kinase kinase2, Guanine nucleotide binding protein, 1-phosphatidylinositol-3-Phosphate 5-kinase and several Serine threonine kinases. All the proteins have different molecular and biological functions like ATP and ADP binding, Kinase activity, Metal and Calcium Ion binding, signal transduction, defense responses respectively. Different gene functions and their position in soybean and common bean are described with details in Table 3.

In the present study, a different approach has been used for comparison of soybean genome with common bean. Advantage of synteny analysis is based on the concept that the species which are evolutionary related are diverged from their common ancestor and conserved genome synteny can be efficiently interpreted from a well-studied species to another less characterized genomes. Synteny is found to be higher between the closely related species (Lee et. al., 2017) and this concept is confirmed in this study. The outcome from the analysis identifies the best match to the *Glycine max* genome. Here focus was done only on chromosome 13 of *Glycine max*. We selected this chromosome because in *Glycine max,* diseases resistance coding genes are known to be found mostly on this region (Chr. 13). By the comparison of both the legumes sequences we get NB-LRR protein coding genes, which are responsible for disease resistance in *Glycine max* and *Phaseolus vulgaris*.

Identification of conserved synteny has noticeable advantage in understanding the legumes genetics. Large region of synteny occurs between *Glycine max* and *Phaseolus vulgaris* (Mc Clean et. al., 2010), our results also

Table 2. Comparison of Soybean (*Glycine_max* cultivar_Williams_82 chromosome_13, *Glycine_max*_v2.0, whole_genome shotgun sequence) with *Phaseolus vulgaris*.

Taregt_ID	Target Start	Target End	Query ID	Query Start	Query End	Identity	Strand	Synteny Length	Gene Start	Gene End	Gene and Locus tag	Product
Glycine max and Phaseolus vulgaris												
NC_016100.2_ Glycine_max cultivar_ Williams_82 chromosome_13, Glycine_max_v2.0, whole_genome shotgun_sequence	22120404	22121394	PhaVulg_2	32502275	32503260	86.3636	-	986	22121113	22121337	LOC100789734 GLYMA_13G106900	mitogen-activated protein kinase kinase 2
	22449055	22449570	PhaVulg_2	31929662	31930177	85.2427	-	516	22449124	22449517	LOC100787066 GLYMA_13G110900	guanine nucleotide-binding protein subunit gamma 3-like isoform X1
	22847546	22849062	PhaVulg_2	30908984	30910502	87.7309	-	1519	22848615	22848943	LOC100811146 GLYMA_13G114800	1-phosphatidylinositol-3-phosphate 5-kinase FAB1B-like%2C transcript variant X1
	22847546	22849062	PhaVulg_2	30908984	30910502	87.7309	-	1519	22847654	22848520	LOC100811146 GLYMA_13G114800	1-phosphatidylinositol-3-phosphate 5-kinase FAB1B-like isoform X1
	23222659	23223739	PhaVulg_2	30060722	30061802	87.037	-	1081	23222716	23223648	LOC100778006 GLYMA_13G119600	probable GTP diphosphokinase CRSH%2C chloroplastic
	22110388	22111570	PhaVulg_2	32514048	32515233	91.794	-	1186	22110445	22111163	LOC100775655 GLYMA_13G106700	uncharacterized protein LOC100775655
	24110505	24111213	PhaVulg_6	37793082	37793792	87.0056	+	711	24110547	24110936	LOC100784243 GLYMA_13G128200	receptor-like serine/threonine-protein kinase ALE2%2C transcript variant X1
	24110505	24111213	PhaVulg_6	37793082	37793792	87.0056	+	711	24110547	24110936	LOC100784243 GLYMA_13G128200	receptor-like serine/threonine-protein kinase ALE2 isoform X1
	24933885	24934843	PhaVulg_6	39244442	39245400	85.2818	+	959	24934259	24934787	LOC100798007 GLYMA_13G136700	probable LRR receptor-like serine/threonine-protein kinase At1g67720
	27466724	27467253	PhaVulg_2	37761025	37761551	88.6578	+	527	27466879	27467198	LOC100305441 GLYMA_13G159400	protein kinase

	NC_016100.2_ Glycine_max cultivar_ Williams_82 chromosome_13, Glycine_max_ v2.0, whole_genome shotgun_ sequence	32416131	32416981	PhaVulg_5	26826933	26827782	85.7647	+	850	32416429	32416584	LOC100814013 GLYMA_13G210300	mitogen-activated protein kinase 15-like
		32523009	32523502	PhaVulg_5	27041793	27042286	86.4097	+	494	32523037	32523443	LOC100816140 GLYMA_13G211600	F-box/LRR-repeat protein 4-like%2C transcript variant X1
		32779883	32782745	PhaVulg_5	27246593	27249457	89.4479	+	2865	32779922	32781577	LOC100777288 GLYMA_13G214400	serine/threonine-protein kinase RUNKEL-like
		32848947	32850530	PhaVulg_5	27294165	27295744	88.0606	+	1580	32850020	32850505	LOC100778885 GLYMA_13G215000	inactive beta-amylase 9
		34551754	34552841	PhaVulg_5	29104549	29105630	87.3965	+	1082	34551796	34552806	LOC100792540 GLYMA_13G234800	serine/threonine-protein kinase-like protein ACR4
		34706927	34708223	PhaVulg_5	29239944	29241240	86.6512	+	1297	34707002	34708057	LOC100798896 GLYMA_13G236700	putative leucine-rich repeat receptor-like serine/threonine-protein kinase At2g14440%2C transcript variant X2
		34706927	34708223	PhaVulg_5	29239944	29241240	86.6512	+	1297	34707002	34708057	LOC100798896 GLYMA_13G236700	putative leucine-rich repeat receptor-like serine/threonine-protein kinase At2g 14440 isoform X1
		35582629	35584126	PhaVulg_5	30027808	30029305	90.314	+	1498	35582677	35584018	LOC100785128 GLYMA_13G247300	probable serine/ threonine-protein kinase abkC isoform X1
		35582629	35584126	PhaVulg_5	30027808	30029305	90.314	+	1498	35582677	35584018	LOC100785128 GLYMA_13G247300	probable serine/ threonine-protein kinase abkC%2C transcript variant X4
		35712009	35713485	PhaVulg_5	30144768	30146245	89.0244	+	1478	35712083	35713370	LOC100804024 GLYMA_13G249300	G-type lectin S-receptor-like serine/ threonine-protein kinase At4g27290 isoform X1
		31895480	31897607	PhaVulg_5	26318633	26320755	85.049	+	2123	31895602	31895959	LOC102661544 GLYMA_13G204900	uncharacterized protein LOC102661544

Table 3. Different functions of gene products of *Glycine max* and *Phaseolus vulgaris*.

Gene Location in *Glycine max*	Gene products	Functions	
		Molecular	Biological
LOC100789734	mitogen-activated protein kinase kinase 2	ATP binding, MAP kinase kinase activity and protein serine/threonine kinase activity	Activation of MAPK activity, activation of protein kinase activity, auxin transport, cold acclimation, defense response, incompatible interaction, response to cold, response to salt stress, signal transduction by protein phosphorylation, stress-activated protein kinase signalling cascade and xylem and phloem pattern formation
LOC100787066	guanine nucleotide-binding protein subunit gamma 3-like isoform X1	-	G protein-coupled receptor signalling pathway
LOC100811146	1-phosphatidylinositol-3-phosphate 5-kinase FAB1B-like%2C transcript variant X1	ATP binding, metal ion binding and phosphatidylinositol phosphate kinase activity	-
LOC100778006	probable GTP diphospho kinase CRSH%2C chloroplastic	Calcium ion binding and kinase activity	Guanosine tetra phosphate metabolic process
LOC100775655	uncharacterized protein LOC100775655		
LOC100784243	receptor-like serine/threonine-protein kinase ALE2%2C transcript variant X1	ATP binding and protein kinase activity	-
LOC100798007	probable LRR receptor-like serine/threonine-protein kinase At1g67720	ATP binding and protein kinase activity	-
LOC100814013	mitogen-activated protein kinase 15-like	ATP binding and protein kinase activity	-

LOC100816140	F-box/LRR-repeat protein 4-like%2C transcript variant X1	Peptidyl-prolyl cis-trans isomerase activity and unfolded protein binding	-
LOC100777288	serine/threonine-protein kinase RUNKEL-like	ATP binding and protein kinase activity	-
LOC100778885	inactive beta-amylase 9	Beta-amylase activity	Polysaccharide catabolic process
LOC100792540	serine/threonine-protein kinase-like protein ACR4	ATP binding and protein kinase activity	-
LOC100798896	putative leucine-rich repeat receptor-like serine/threonine-protein kinase At2g14440%2C transcript variant X2	Kinase activity	-
LOC100785128	probable serine/threonine-protein kinase abkC%2C transcript variant X4	Kinase activity	-
LOC100809556	homeobox-leucine zipper protein HDG2	DNA-binding transcription factor activity, lipid binding and sequence-specific DNA binding	Maintenance of floral organ identity and trichome-morphogenesis
LOC100801911	putative E3 ubiquitin-protein ligase RING1a	Metal ion binding and transferase activity	Cell fate determination, chromatin organization, maintenance of floral meristem identity, maintenance of inflorescence meristem identity, maintenance of shoot apical meristem identity, negative regulation of gene expression, epigenetic, negative regulation of transcription, DNA-templated and protein ubiquitination
LOC100776037	V-type proton ATPase subunit a1-like isoform X2	ATPase binding, proton-transporting ATPase activity and rotational mechanism	ATP hydrolysis coupled proton transport, proton-transporting V-type ATPase complex assembly and vacuolar acidification
LOC100792901	uncharacterized ATP-dependent helicase C23E6.02-like%2C transcript variant X2	ATP binding, helicase activity and metal ion binding	-
LOC100782114	B3 domain-containing protein Os07g0563300-like	DNA binding and zinc ion binding	Regulation of transcription, DNA-templated transcription, and DNA-templated
Source: InterPro, UniProtKB-UniRule,UniProtKB-KW, GO_Central, TAIR.			

showed the gene conservation between both the legumes. Studies of the NBS-LRR gene family in legume plants can provide knowledge on the genomic and molecular mechanism that form the basis of gene regulation and protein functions. In this study, various NBS-LRR proteins (as mentioned in table 3 showing different functions of gene products) were found to be conserved in *Glycine max* and *Phaseolus vulgaris*. Now a day's gene cloning approach is advancing to make disease resistance varieties of legumes as in *Medicago sativa* cloning of a disease resistance gene was done by utilizing *Medicago truncatula* gene information through synteny (Yang et. at., 2008). In the same way this synteny analysis result will be useful for evolutionary studies that help in long term planning, breeding and developing disease resistance varieties of legumes.

ACKNOWLEDGEMENTS

Authors acknowledge the facilities of the Department of Biotechnology, Ministry of Science and Technology, Government of India, New Delhi (DBT) under the Bioinformatics Sub Centre as well as the golden jubilee research fellowship (GJRF) provided by School of Biotechnology, Devi Ahilya University Indore. M.P. India.

Conflict of Interest

The authors confirm that they have no conflict of interest.

REFERENCES

Andersen, E. J., Ali, S., Reese, R. N., Yen, Y., Neupane, S., & Nepal, M. P. (2016). Diversity and evolution of disease resistance genes in barley (*Hordeum vulgare* L.). Evolutionary Bioinformatics, 12, EBO-S38085.

Andolfo, G., & Ercolano, M. R. (2015). Plant innate immunity multicomponent model. Frontiers in plant science, 6, 987.

Bauchan, G. R., & Hossain, M. A. (2001). Distribution and characterization of heterochromatic DNA in the tetraploid African population alfalfa genome. Crop science, 41(6), 1921-1926.

Bennetzen, J. L. (2000). Comparative sequence analysis of plant nuclear genomes: microcolinearity and its many exceptions. The Plant Cell, 12(7), 1021-1029.

Benson, B. V. (2014). Disease resistance genes and their evolutionary history in six plant species.

Boutin, S. R., Young, N. D., Olson, T., Yu, Z. H., Vallejos, C. E., & Shoemaker, R. C. (1995). Genome conservation among three legume genera detected with DNA markers. Genome, 38(5), 928-937.

Cannon, S. B., & Shoemaker, R. C. (2012). Evolutionary and comparative analyses of the soybean genome. Breeding science, 61(5), 437-444.

Chen, X., Li, H., Pandey, M. K., Yang, Q., Wang, X., Garg, V., ... & Upadhyaya, H. (2016). Draft genome of the peanut A-genome progenitor (*Arachis duranensis*) provides insights into geocarpy, oil biosynthesis, and allergens. Proceedings of the National Academy of Sciences, 113(24), 6785-6790.

Choi, H. K., Mun, J. H., Kim, D. J., Zhu, H., Baek, J. M., Mudge, J., ... & Young, N. D. (2004). Estimating genome conservation between crop and model legume species. Proceedings of the National Academy of Sciences, 101(43), 15289-15294.

Christie, N., Tobias, P. A., Naidoo, S., & Külheim, C. (2016). The *Eucalyptus grandis* NBS-LRR gene family: physical clustering and expression hotspots. Frontiers in plant science, 6, 1238.

Devos, K. M., & Gale, M. D. (2000). Genome relationships: the grass model in current research. The Plant Cell, 12(5), 637-646.

Doyle, J. J., & Luckow, M. A. (2003). The rest of the iceberg. Legume diversity and evolution in a phylogenetic context. Plant Physiology, 131(3), 900-910.

Franssen, S. U., Shrestha, R. P., Bräutigam, A., Bornberg-Bauer, E., & Weber, A. P. (2011). Comprehensive transcriptome analysis of the highly complex *Pisum sativum* genome using next generation sequencing. BMC genomics, 12(1), 227.

Gualtieri, G., Kulikova, O., Limpens, E., Kim, D. J., Cook, D. R., Bisseling, T., & Geurts, R. (2002). Microsynteny between pea and *Medicago truncatula* in the SYM2 region. Plant molecular biology, 50(2), 225-235.

Gururani, M. A., Venkatesh, J., Upadhyaya, C. P., Nookaraju, A., Pandey, S. K., & Park, S. W. (2012). Plant disease resistance genes: current status and future directions. Physiological and molecular plant pathology, 78, 51-65.

Hulbert, S. H., Webb, C. A., Smith, S. M., & Sun, Q. (2001). Resistance gene complexes: evolution and utilization. Annual review of phytopathology, 39(1), 285-312.

Kalavacharla, V., Liu, Z., Meyers, B. C., Thimmapuram, J., & Melmaiee, K. (2011). Identification and analysis of common bean (*Phaseolus vulgaris* L.) transcriptomes by massively parallel pyrosequencing. BMC plant biology, 11(1), 135.

Kang, Y. J., Kim, S. K., Kim, M. Y., Lestari, P., Kim, K. H., Ha, B. K., ... & Shim, S. (2014). Genome sequence of mungbean and insights into evolution within *Vigna* species. Nature communications, 5, ncomms6443.

Lee, C., Yu, D., Choi, H. K., & Kim, R. W. (2017). Reconstruction of a composite comparative map composed of ten legume genomes. Genes & Genomics, 39(1), 111-119.

Lee, J. M., Grant, D., Vallejos, C. E., & Shoemaker, R. C. (2001). Genome organization in dicots. II. Arabidopsis as a'bridging species' to resolve genome evolution events among legumes. Theoretical and Applied Genetics, 103(5), 765-773.

McClean, P. E., Mamidi, S., McConnell, M., Chikara, S., & Lee, R. (2010). Synteny mapping between common bean and soybean reveals extensive blocks of shared loci. BMC genomics, 11(1), 184.

McConnell, M., Mamidi, S., Lee, R., Chikara, S., Rossi, M., Papa, R., & McClean, P. (2010). Syntenic relationships among

legumes revealed using a gene-based genetic linkage map of common bean (*Phaseolus vulgaris* L.). Theoretical and Applied Genetics, 121(6), 1103-1116.

Nepal, M. P., & Benson, B. V. (2015). CNL disease resistance genes in soybean and their evolutionary divergence. Evolutionary Bioinformatics, 11, EBO-S21782.

Neupane, S., Ma, Q., Mathew, F. M., Varenhorst, A. J., Andersen, E. J., & Nepal, M. P. (2018). Evolutionary Divergence of TNL Disease-Resistant Proteins in Soybean (*Glycine max*) and Common Bean (*Phaseolus vulgaris*). Biochemical genetics, 1-26.

Passoupathy, R. (2016). Synteny with Allied and Model Genomes. 10.1007/978-3-319-47789-3_6.

Paterson, A. H., Bowers, J. E., Burow, M. D., Draye, X., Elsik, C. G., Jiang, C. X., ... & Wright, R. J. (2000). Comparative genomics of plant chromosomes. The Plant Cell, 12(9), 1523-1539.

Sato, S., Nakamura, Y., Kaneko, T., Asamizu, E., Kato, T., Nakao, M., & Fujishiro, T. (2008). Genome structure of the legume, Lotus japonicus. DNA research, 15(4), 227-239.

Schlueter, J. A., Dixon, P., Granger, C., & Shoemaker, R. C. (2005). Mining the EST databases to determine evolutionary events in the legumes and grasses. In Genome Exploitation (pp. 163-181). Springer, Boston, MA.

Schmidt, R. (2000). Synteny: recent advances and future prospects. Current opinion in plant biology, 3(2), 97-102.

Schmutz, J., Cannon, S. B., Schlueter, J., Ma, J., Mitros, T., Nelson, W., ... & Xu, D. (2010). Genome sequence of the palaeopolyploid soybean. Nature, 463(7278), 178.

Schmutz, J., McClean, P. E., Mamidi, S., Wu, G. A., Cannon, S. B., Grimwood, J., ... & Torres-Torres, M. (2014). A reference genome for common bean and genome-wide analysis of dual domestications. Nature genetics, 46(7), 707.

Shao, Z. Q., Xue, J. Y., Wu, P., Zhang, Y. M., Wu, Y., Hang, Y. Y., ... & Chen, J. Q. (2016). Large-scale analyses of angiosperm nucleotide-binding site-leucine-rich repeat (NBS-LRR) genes reveal three anciently diverged classes with distinct evolutionary patterns. Plant Physiology, pp-01487.

Shoemaker, R. C., Polzin, K., Labate, J., Specht, J., Brummer, E. C., Olson, T., ... & Kochert, G. (1996). Genome duplication in soybean (*Glycine subgenus soja*). Genetics, 144(1), 329-338.

Singh, J., Kalberer, S. R., Belamkar, V., Assefa, T., Nelson, M. N., Farmer, A. D., ... & Cannon, S. B. (2018). A transcriptome-SNP-derived linkage map of *Apios americana* (potato bean) provides insights about genome re-organization and synteny conservation in the phaseoloid legumes. Theoretical and Applied Genetics, 131(2), 333-351.

Varshney, R. K., Song, C., Saxena, R. K., Azam, S., Yu, S., Sharpe, A. G., ... & Millan, T. (2013). Draft genome sequence of chickpea *(Cicer arietinum*) provides a resource for trait improvement. Nature biotechnology, 31(3), 240.

Weeden, N. F., Muehlbauer, F. J., & Ladizinsky, G. (1992). Extensive conservation of linkage relationships between pea and lentil genetic maps. Journal of Heredity, 83(2), 123-129.

Yadegari, Z. (2013). Molecular mapping and characterization of phenylpropanoid pathway genes in common bean (*Phaseolus vulgaris* L.) (Doctoral dissertation).

Young, N. D., Debellé, F., Oldroyd, G. E., Geurts, R., Cannon, S. B., Udvardi, M. K., ... & Van de Peer, Y. (2011). The Medicago genome provides insight into the evolution of rhizobial symbioses. Nature, 480(7378), 520.

Young, N. D., Mudge, J., & Ellis, T. N. (2003). Legume genomes: more than peas in a pod. Current opinion in plant biology, 6(2), 199-204.

Zhu, H., Choi, H. K., Cook, D. R., & Shoemaker, R. C. (2005). Bridging model and crop legumes through comparative genomics. Plant physiology, 137(4), 1189-1196.

Biotechnological Communication

Biosci. Biotech. Res. Comm. 12(1): 134-139 (2019)

BBRC Bioscience Biotechnology Research Communications

Biological eco-friendly synthesis of nanoparticles and their applications

Vivek Singh, Divya Bhatia, Sunita Khatak, Tarun Kumar and Deepak Kumar Malik*

Department of Biotechnology, U.I.E.T, Kurukshetra University Kurukshetra, Kurukshetra, Haryana, India-136119

ABSTRACT

The use, formation and manipulation of materials at nanoscale level is known as Nanotechnology, which change their properties at nanoscale. The nanoscale materials can be synthesized by using physical and chemical processes. Size, shape, morphology, stability and properties of nanoparticles can have direct impact on their potential applications. The design of an eco-friendly, time effective and economic synthesis method with easy control over their essential properties has become a leading area of research. Now a days, the biological entities are employed to improve nanoparticles production without the use of any harsh chemicals. The biological synthesis of nanoparticles is an eco-friendly method. Nanoparticles have broad range of applications such as optical, electronics, electrical, medical, environment, textile, energy science, optoelectronics, catalysis, single electron transistors, light emitters, nonlinear optical devices, photo-electrochemical applications, cosmetics and food industries owing to their unique physiochemical properties. The aim of this critical review is to provide an insight into the ecofriendly synthesis of nanoparticles with significant applications in various fields.

INTRODUCTION

The mechanical, magnetic, electrical and optical properties of materials having particle size between 0.1 and 100 nm can be different from the same materials at larger size. Now scientists are changing the form and size of materials at nano scale level to recognize the uncommon properties of the material. Metal nanoparticles like gold, titanium, titanium oxide, zinc oxide, iron, copper, silver and platinum are widely used in various domestic and commercial products. Silver nanoparticles are of interest owing to the distinctive properties which may be assimilated into antimicrobial applications, cosmetic products, biosensor materials, refrigerant super-conducting materials, composite fibres and electronic components. Gold nanoparticles are presently under intensive study for

ARTICLE INFORMATION:

Corresponding Author: deepmolbio@rediffmail.com
Received 18th Jan, 2019
Accepted after revision 20th March, 2019
BBRC Print ISSN: 0974-6455
Online ISSN: 2321-4007 CODEN: USA BBRCBA
Thomson Reuters ISI ESC / Clarivate Analytics USA
NAAS Journal Score 2019: 4.31 SJIF: 4.196

Online Contents Available at: http//www.bbrc.in/
DOI: 10.21786/bbrc/12.1/17

applications in ultrasensitive chemical, optoelectronic devices and biological sensors and as catalysts, (Perez *et al*., 2012 Khoei *et al*., 2017 Xu *et al*., 2018).

Evaporation-condensation and optical device ablation are the leading physical approaches for the synthesis of nanoparticles. However, Physical-chemical techniques of synthesis have many difficulty in scaling-up the process, separation and purification of nanoparticles. Microorganisms have been utilized in biotechnology implementations like bioremediation and bioleaching (Stephen *et al*., 1999). Microorganisms are able to carry out a range of oxidoreduction mechanisms and promote biochemical translation (Sastry *et al*., 2004). The biological methods are responsible for the synthesis of mono-dispersed silver nanoparticles starting from 5 to 15 nm in size (Karthik *et al*., 2014, Hassan *et al.,* 2018). Now a days, biological methods are used for the synthesis of nanoparticles, to construct the sustainable processes, which do not produce any harmful chemicals in to the environment. The plants and microorganisms used for the synthesis of nanoparticles are listed in Table 1.

Actinomycetes and Algae

Biogenesis of metal nanoparticles by using actinomycetes and algae is seeking attention since decade due to their unique property of intra and extra cellular synthesis of nanoparticles (Abdeen *et al.,* 2014). Reduction of metal ions may be due to interacting enzymes being released from the cell membrane and cell wall. Actinomycetes mediated synthesis of copper oxide nanoparticles and study for its antibacterial activity against selected human and fish pathogens was reported by Nabila *et al.,* (2018). In algae mediated synthesized nanoparticles decahedral, polyhedron and tetrahedral structure were observed (Luangpipat *et al*., 2011). Rajasulochana *et al.* (2010) reported the synthesis of silver nanoparticles by using *Kappaphycus alvarezii*. Senapati *et al.* (2012) reported the intracellular synthesis of silver nanoparticles via *Tetraselmis kochinensis*. Castro *et al.* (2013) reported the use of red *Chondrus crispus* and green algae *Spirogyra insignis* for the synthesis of gold and silver nanoparticles.

Bacteria and Fungi

Ability of bacteria to survive in diverse and sometimes extreme environmental situations renders them a suitable candidate for nanoparticles synthesis. Survival in these harsh conditions ultimately depends on their ability to resist the effects of environmental stresses. Bacteria are able to synthesize metallic nanoparticles by either intracellular or extracellular mechanisms. The various bacterial species were reported to synthesize the nanoparticles such as *Actinobacter* sp., *Escherichia coli, Klebsiella pneumonia, Lactobacillus* sp., *Bacillus cereus, Corynebacterium* sp. and *Pseudomonas* sp. (Mohanpuria *et al*., 2008; Iravani *et al*., 2014; Sunkar *et al*., 2014; Tollamadugu *et al*., 2011). The silver nanoparticles were synthesized by *Pseudomonas stutzeri* AG259 by reduction of Ag ions (Ahmad *et al*., 2003). Husseiny *et al.* (2007) reported extracellular synthesis of silver nanoparticles by using *Pseudomonas*. Sneha *et al.* (2010) reported that *Corynebacterium* sp. shows a non-enzymatic reduction mechanism in nanoparticle synthesis. The dried biomass

Table 1. Various bacterial entities responsible for the synthesis of nanoparticles

Biological entity	Size of nanoparticles	Type of Nanoparticle	Extracellular/ intracellular	References
Bacteria				
Pseudomonas aeruginosa	30-40nm	Silver	Extracellular	Jeevan *et al*., (2012)
Lysinibacillus varians.	10-20nm	Silver	Extracellular	Bhatia *et al*., (2018)
Burkholderia fungorum	95-100nm	Gold	Extracellular	Khoei *et al*., (2017)
Lactobacillus casei	50-80nm	Silver	Intracellular	Xu *et al*., (2018)
Fungi				
Aspergillus niger	15-80nm	Silver	Extracellular	Elegbede *et al*., (2018)
Helminthosporium sp.	15-20nm	Silver	Extracelluler	Lachmapure *et al*., (2017)
Cladosporium cladosporioides	10-20nm	Gold	Extracellular	Joshi *et al*.,(2017)
Pestalotiopsis microspora	2-10nm	Gold	Extracellular	Netala *et al*., (2016)
Plants				
Viburnum lantana	2- 80 nm	Silver	Leaves	Shafaghat (2015)
Tinospora cordifolia	60nm	Silver	Stem	Selvam *et al*., (2017)
Vitis viniera	10-80 nm	Silver	Fruit	Ahmed *et al*., (2016)

of *Lactobacillus* sp. and *Bacillus megaterium* reduced silver ions using interaction of molecules present on the cytomembrane to produce silver nanoparticles (Fu *et al.*, 2000).

Fungi being able to secrete large amounts of enzymes and proteins per unit of biomass can be utilized for synthesis of huge amounts of nanoparticles (Narayanan *et al.*, 2010). The *Aspergillus* sp., *Fusarium* sp. and *Penicillium* sp. have been reported for their biosynthetic ability of silver and gold nanoparticles (Vigneshwaran *et al.*, 2007; Shankar *et al.*, 2003; Philip *et al.*, 2009). The extracellular synthesis of silver nanoparticles by using *Aspergillus fumigatus* has been reported (Bhainsa and D'Souza, 2006). The biological synthesis of Au nanoparticles was carried out by reduction of Au ions by using *Trichothecium* sp. biomass (Ahmad *et al.*, 2005). The extracellular synthesis of nanoparticles due to its proteins discharged by fungal biomass was reported (Macdonald *et al.*, 1996). Bansal *et al.* (2007) reported that *Fusarium oxysporum* synthesized silica and titanium nanoparticles from binary compound solutions of SiO_6^{2-} and TiF_6^{2-} respectively.

Viruses, Yeast and Plants

The virus capsid proteins make an extremely reactive surface able to interact with metallic ions (Makarov *et al.*, 2014). The selection of proteins will act as attachment area for the deposition of materials (Kobayashi *et al.*, 2012). In virus mediated synthesis, size was significantly reduced along with increase in their numbers as compared to non viral mediated synthesis (Makarov *et al.,* 2014). The low concentrations of TMV's were supplementary to silver or gold salts before adding plant extracts of *Nicotiana benthamiana* or *Hordeum vulgare*.

Yeasts can absorb and accumulate significant amounts of toxic metals from their surrounding environment (Mandel *et al.*, 2006). Due to this property, yeast has been exploited for synthesis of metal nanoparticlesn. Yeasts use different mechanism for the synthesis and stability of nanoparticles which leads to variation in particle size, location and properties (Hulkoti *et al.*, 2014). Dameron *et al.* (1989) reported *Candida glabrata* mediated intracellular synthesis of CdS quantum dots. *Schizosaccharomyces pombe* cells were used for the synthesis of CdS quantum dots (Reese *et al.*, 1998). The intracellular synthesis of PbS quantum dots was carried out by *Torulopsis* sp. when exposed to Pb^{2-} ions (Kowshik *et al.*, 2002).

Plants mediated synthesis is a relatively simple, less time consuming, cost effective and an ecofriendly process. The process begins by mixing a sample of plant extract with a metal salt solution. In plants mediated synthesis of nanoparticles, metal ions changed from mono or divalent oxidation states to zero-valent states. As growth progresses nanoparticles combine to form different morphologies (Akhtar *et al.*, 2013; Malik *et al.*, 2014). The plants extract properties and incubation temperature significantly influence the synthesis of nanoparticles (Dwivedi *et al.*, 2010). The plant mediated nanoparticles synthesis are to be safe, less synthesis time and lesser cultivation value as compare to biological systems (Mittal *et al.*, 2013).

Applications of nanoparticles

One of the major applications of nanotechnology is in biology and medicine. Nanoparticles are used for detection of pathogens (Edelstein *et al.*, 2000), detection of proteins (Nam *et al.*, 2003), analysis of DNA structure (Mahtab *et al.*, 1995), Tissue engineering (Ma *et al.*, 20039, de la isla *et al.*, 2003). Now days, superbugs with multi drug resistance are major threat to human being. Nanotechnology can be a solution to combat antimicrobial drug resistance. Nanotechnology provides synthesis and design strategies to develop antimicrobial nanotherapeutics to fight the trouble of antimicrobial resistance. The large surface area-to-volume ratio at nanoscale may be the reason of antimicrobial mechanism against a broad spectrum of microorganisms. Nanoparticles can also be manipulated for effective and targeted delivery of drugs and imaging labels by overcoming the many biological, biophysical, and biomedical barriers. Nanoparticles has been also employed for targeted drug delivery at the tumor site or a certain group of cells without affecting non target cells (Huang, *et al.*, 2015 Shen *et al.*, 2016, Escarcega *et al.*, 2018).

The silver nanoparticles accumulate in tumours and their distinctive optical and chemical properties may be utilized in thermal treatment procedures (Hirsch *et al.*, 2003). Nanoparticles have been used in anti-odour clothes, furnishings textiles, kitchen cloths, sponges, towels, antibacterial drugs, patient dresses, reusable surgical gloves, protecting face masks, suits against biohazards, cosmetic products, toothbrushes, ultra hydrophobic materials with potential applications within the production of extremely water repellent materials, bactericide material to coat hospital instrumentation, antitumor medication, active wear, food packaging and waste water treatments (Pissuwan *et al.*, 2009, Cheng *et al.*, 2010, Lee *et al.* 2007, Ramaratnam *et al.* 2008, Hassan *et al.*, 2012). TiO_2 nanoparticles, as a result of their antibacterial activity, are utilized in antibacterial coatings and effluent disinfection processes (Miller *et al.*, 2012).

REFERENCES

Abdeen, S.; Geo, S.; Sukanya, S.; Praseetha, P.K.; Dhanya, R.P. Biosynthesis of Silver nanoparticles from Actinomycetes for therapeutic applications. Int. J. Nano Dimens. 2014, 5, 155–162.

Ahmad A., Senapati S., Khan M. I., Kumar R., Ramani R., Srinivas V., and Sastry M., (2003) Intracellular synthesis of gold nanoparticles by a novel alkalotolerant actinomycete *Rhodococcus* species. Nanotechnology. Vol. 14: Pages 824–828.

Edelstein R. L., Tamanaha C .R., Sheehan P. E., Miller M. M., Baselt D. R., Whit- man L. J., Colton R. J. (2000) The BARC biosensor applied to the detection of biological warfare agents. Biosensors Bioelectron Vol.14: Pages 805-813.

Nam J. M., Thaxton C. C., Mirkin C. A. (2003) Nanoparticles-based bio-bar codes for the ultrasensitive detection of proteins. Science Vol. 301: Pages 1884-1886.

Mahtab R., Rogers J. P., Murphy C. J. (1995) Protein-sized quantum dot luminescence can distinguish between "straight", "bent", and "kinked" oligonucleotides. J. Am. Chem. Soc. Vol. 117: Pages9099-9100.

Ma J., Wong H., Kong L. B., Peng K. W. (2003) Biomimetic processing of nanocrystallite bioactive ap atite coating on titanium. Nanotechnol. Vol. 14: Pages 619-623.

de la Isla A., Brostow W., Bujard B., Estevez M., Rodriguez J. R., Vargas S., Castano V.M. (2003) Nanohybrid scratch resistant coating for teeth and bone viscoelasticity manifested in tribology. Mat. Resr. Innovat. Vol. 7: Pages107-114

Ahmad A., Senapati S., Khan M. I., Kumar R., and Sastry M., (2005) Extra-/intracellular, biosynthesis of gold nanoparticles by an alkalotolerant fungus, *Trichothecium* sp. J. Biomed. Nanotechnol. Vol. 1: Pages 47–53.

Ahmed S. M., Ahmad B. L., Swami., and Ikram S., (2016) A review on plants extract mediated synthesis of silver nanoparticles for antimicrobial applications: A green expertise, J. Adv. Res. Vol. 7: Pages 17–28.

Akhtar M. S., Panwar J., and Yun Y. S. (2013) Biogenic synthesis of metallic nanoparticles by plant extracts. ACS Sustain. Chem. Eng. Vol. 1: Pages 591–602.

Bansal V., Syed A., Bhargava S. K., Ahmad A., and Sastry M. (2007). Zirconia enrichment in zircon sand by selective fungus-mediated bioleaching of silica. Langmuir. Vol. 23(9): Pages 4993-4998.

Bhainsa C.K. and D'Souza, F. S., (2006). Extracellular biosynthesis of silver nanoparticles using the fungus *Aspergillus fumigatus*, Colloids Surfaces B; Biointerfaces. Vol. 47: Pages 160-164.

Shen B., Ma Y., (2016). Smart multifunctional magnetic nanoparticle-based drug delivery system for cancer thermo-chemotherapy and intracellular imaging. (2016) ACS Appl. Mater Interf. Vol. 8(37): Pages 24502–24508.

Huang B., Abraham W. D., *et al.*, (2015) Active targeting of chemotherapy to disseminated tumors using nanoparticle-carrying T cells. Sci. Trans. Med. 7, 291ra94

Bhatia D., Mittal A., and Malik D. K., (2016). Antimicrobial activity of PVP coated silver nanoparticles synthesized by *Lysinibacillus varians*. 3 Biotech. Vol. 6(2): Pages 196.

Castro L., Blazquez M. L., Munoz J. A., Gonzalez F., and Ballester A., (2013) Biological synthesis of metallic nanoparticles using algae. IET Nanobiotechnol. Vol. 7: Pages 109–116.

Cheng, Y., Samia A. C., Li J., Kenney M E., Resnick A., and Burda C., (2010) Delivery and efficacy of a cancer drug as a function of the bond to the gold nanoparticle surface. Langmuir. Vol. 26: Pages 2248–2255.

Dwivedi A. D., and Gopal K., (2010) Biosynthesis of silver and gold nanoparticles using *Chenopodium album* leaf extract. Colloids Surf. A. Vol. 369: Pages 27–33.

Elegbede J. A., Lateef A., Azeez, M. A., Asafa T. B., Yekeen T. A., Oladipo I. C., and Gueguim-Kana E. B. (2018) Fungal xylanases-mediated synthesis of silver nanoparticles for catalytic and biomedical applications. IET Nanobiotechnology. Vol.12(6): Pages 857-863.

Escarcega-Gonzaez C. E., Garza-Cervantes J. A., Vazquez-Rodriguez A., Montelongo-Peralta L. Z., Trevino-Gonzalez M. T., Castro E. D. B., and Rosales J. C. (2018). In vivo antimicrobial activity of silver nanoparticles produced via a green chemistry synthesis using *Acacia rigidula* as a reducing and capping agent. International journal of nanomedicine. Vol. 13: Pages 2349.

Fu J. K., Liu Y. Y., Gu P. Y., Liang S. D., Yu L. Z., Xin Y. B., and Zhou W.S., (2000) Spectroscopic characterization on the biosorption and bioreduction of Ag(I) by *Lactobacillus* sp A09. Acta Phys. Chim. Sin. Vol. 16: Pages 779–782.

Hassan H. S., Elkady M. F., El-Sayed E. M., Hamed A. M., Hussein A. M., and Mahmoud I. M., (2018). Synthesis and Characterization of Zinc Oxide Nanoparticles using Green and Chemical Synthesis Techniques for phenol decontamination. International Journal of Nanoelectronics and Materials. Vol. 11(2): Pages 179-194.

Hassan M.S., Amna T., Yang O.B., El-Newehy M. H., Al-Deyab S. S., and Khil M. S., (2012) Smart copper oxide nanocrystals: Synthesis, characterization, electrochemical and potent antibacterial activity. Colloids Surf. B Biointerfaces. Vol. 97: Pages 201–206.

Hirsch L. R., Stafford R. J., Bankson J. A., Sershen S. R., Rivera B., Price R. E., and West J. L., (2003). Nanoshell-mediated near-infrared thermal therapy of tumours under magnetic resonance guidance. Proceedings of the National Academy of Sciences. Vol. 100 (23): Pages 13549-13554.

Hulkoti N. I., and Taranath T. C., (2014). Biosynthesis of nanoparticles using microbes—a review. Colloids and Surfaces B: Biointerfaces. Vol. 121: Pages 474-483.

Husseiny M.I., El-Aziz M.A., Badr Y., and Mahmoud, M. A., (2007) Biosynthesis of gold nanoparticles using *Pseudomonas aeruginosa*. Spectrochim. Acta A. Vol. 67: Pages 1003–1006.

Iravani S., (2014) Bacteria in nanoparticle synthesis: Current status and future prospects. Int. Sch. Res. Not. Vol. 2014: Pages 359-316.

Jeevan P., Ramya K., and Rena A. E., (2012). Extracellular biosynthesis of silver nanoparticles by culture supernatant of *Pseudomonas aeruginosa*. Indian Journal of Biotehnology. Vol. 11: Pages 72-76.

Joshi C. G., Danagoudar A., Poyya J., Kudva A. K., and Dhananjaya B. L. (2017) Biogenic synthesis of gold nanoparticles by marine endophytic fungus-*Cladosporium cladosporioides* iso-

lated from seaweed and evaluation of their antioxidant and antimicrobial properties. Process Biochemistry. Vol. 63: Pages 137-144.

Karthik L., Kumar G., Vishnu-Kirthi A., Rahuman A. A., Rao V. B., (2014) *Streptomyces* sp. LK3 mediated synthesis of silver nanoparticles and its biomedical application. Bioprocess. Biosyst. Eng. Vol. 37: Pages 261–267.

Khoei N. S., Lampis S., Zonaro E., Yrjala K., Bernardi P., and Vallini G., (2017). Insights into selenite reduction and biogenesis of elemental selenium nanoparticles by two environmental isolates of *Burkholderia fungorum*. New biotechnology. Vol. 34: Pages 1-11.

Kobayashi M., Tomita S., Sawada K., Shiba K., Yanagi H., Yamashita I., and Uraoka Y., (2012) Chiralmeta-molecules consisting of gold nanoparticles and genetically engineered tobacco mosaic virus. Opt. Express. Vol. 20: Pages 24856–24863.

Kowshik M., Vogel W., Urban J., Kulkarni S. K., and Paknikar K. M., (2002) Microbial synthesis of semiconductor PbS nanocrystallites. Adv. Mater. Vol. 14: Pages 815–818.

Lachmapure M., Paralikar P., Palanisamy M., Alves M., and Rai, M., (2017). Efficacy of biogenic silver nanoparticles against clinical isolates of fungi causing mycotic keratitis in humans. IET Nanobiotechnology. Vol. 11(7): Pages 809-814.

Lee H. Y., Park Y. K., Lee Y. M, Kim K., and Park S.B., (2007) A practical procedure for producing silver nanocoated fabric and its antibacterial evaluation for biomedical applications. Chem Commun. Pages 2959–2961.

Luangpipat T., Beattie I.R., Chisti Y., and Haverkamp R.G., (2011) Gold nanoparticles produced in a microalga. J. Nano part. Res. Vol. 13: Pages 6439–6445.

Macdonald I.D.G., and Smith W.E., (1996) Orientation of cytochrome c adsorbed on a citrate-reduced silver colloid surface. Langmuir. Vol. 12: Pages 706–713.

Makarov V. V., Love A.J., Sinitsyna O. V., Makarova S. S., Yaminsky I. V., Taliansky M. E., Kalinina, N. O. (2014) Green nanotechnologies: Synthesis of metal nanoparticles using plants. Acta Naturae. Vol. 6: Pages 35–44.

Malik P., Shankar R., Malik V., Sharma N., and Mukherjee T. K, (2014) Green chemistry based benign routes for nanoparticle synthesis. J. Nanopart. Vol. 2014: Pages 302-429.

Miller R. J., Bennett S., Keller, A. A., and Pease, S., Lenihan, H. S., (2012) TiO_2 nanoparticles are phototoxic to marine phytoplankton. PLOS Biol. Vol. 7: Pages 1–7.

Mittal A. K., Chisti Y., and Banerjee U. C., (2013) Synthesis of metallic nanoparticles using plants. Biotechnol. Adv. Vol. 31: Pages 346–356.

Mohanpuria P., Rana N. K., and Yadav S. K., (2008) Biosynthesis of nanoparticles: Technological concepts and future applications. J. Nanopart. Res. Vol. 10: Pages 507–517.

Mandel, C. R., Gebauer, D., Zhang, H., & Tong, L. (2006). A serendipitous discovery that in situ proteolysis is essential for the crystallization of yeast CPSF-100 (Ydh1p). Acta Crystallographica Section F: Structural Biology and Crystallization Communications, 62(10), 1041-1045.

Nabila M. I., and Kannabiran K., (2018). Biosynthesis, characterization and antibacterial activity of copper oxide nanoparticles (CuO NPs) from actinomycetes. Biocatalysis and Agricultural Biotechnology. Vol. 15: Pages 56-62.

Narayanan K. B., and Sakthivel N., (2010) Biological synthesis of metal nanoparticles by microbes. Adv. Colloid Interface Sci. Vol. 156: Pages 1–13.

Netala V. R., Bethu M. S., Pushpalatha B., Baki V. B., Aishwarya S., Rao J. V., and Tartte V., (2016). Biogenesis of silver nanoparticles using endophytic fungus *Pestalotiopsis microspora* and evaluation of their antioxidant and anticancer activities. International journal of nanomedicine. Vol. 11: Pages 56-83.

Perez-Espitia P.J., Ferreira-Soares N. F., Dos Reis Coimbra J. S., De Andrade N. J., Cruz, R. S., and Medeiros, E. A. A., (2012) Zinc oxide nanoparticles: Synthesis, antimicrobial activity and food packaging applications. Food Bioprocess Technol. Vol. 5: Pages 1447–1464.

Philip, D., (2009) Biosynthesis of Au, Ag and Au-Ag nanoparticles using edible mushroom extract. Spectrochim. Acta A. Vol. 73: Pages 374–381.

Pissuwan D., Cortie C. H. Valenzuela S. M., and Cortie M. B., (2009) Functionalised gold nanoparticles for controlling pathogenic bacteria. Trends Biotechnol. Vol. 28: Pages 207–213.

Rajasulochana P., Dhamotharan R., Murugakoothan P., Murugesan S., and Krishnamoorthy P., (2010) Biosynthesis and characterization of gold nanoparticles using the alga *Kappaphycus alvarezii*. Int. J. Nanosci. Vol. 9: Pages 511–516.

Ramaratnam K., Iyer S. K., Kinnan M. K., Chumanov G., Brown P. J., and Luzinov I., (2008) Ultra hydrophobic textiles using nanoparticles: lotus approach. J Eng Fibers Fabrics. Vol. 3: Pages 1–14.

Reese R. N., and Winge D. R., (1998) Sulfide stabilization of the cadmium-γ-glutamyl peptide complex of *Schizosaccharomyces pombe*. J. Biol. Chem. Vol. 263: Pages 12832–12835.

Sastry M., Ahmad A., Khan M. I., and Kumar R., (2004) Microbial nanoparticle production. Nanotechnology, (Wiley-VCH, 2004).

Selvam K., (2017) Eco-friendly biosynthesis and characterization of silver nanoparticles using *Tinospora cordifolia* (Thunb.) Miers and evaluate its antibacterial, antioxidant potential, J. Radiat. Res. Appl. Sci. Vol. 10: Pages 6–12.

Senapati S., Syed A., Moeez S., Kumar A., and Ahmad, A. (2012) Intracellular synthesis of gold nanoparticles using alga *Tetraselmis kochinensis*. Mater. Lett. Vol. 79: Pages 116–118.

Shafaghat A., (2015) Synthesis and Characterization of Silver Nanoparticles by Phytosynthesis Method and Their Biological Activity, Synth. React. Inorganic, Met. Nano-Metal Chem. Vol. 45(3): Pages 381–387.

Shankar S. S., Ahmad A., Pasricha R., and Sastry M., (2003) Bio reduction of chloroaurate ions by *Geranium* leaves and its endophytic fungus yields gold nanoparticles of different shapes. J. Mater. Chem. Vol.13: Pages 1822–1826.

Sneha K., Sathish K. M., Mao J., Kwak I. S., and Yun Y. S., (2010) *Corynebacterium glutamicum*-mediated crystallization

of silver ions through sorption and reduction processes. Chem. Eng. J. Vol. 162: Pages 989–996.

Stephen J. R., and Macnaughton S. J., (1999) Developments in terrestrial bacterial remediation of metals. Curr. Opin. Biotechnol. Vol. 10: Pages 230–233.

Sunkar S., and Nachiyar C. V., (2014) Biogenesis of antibacterial silver nanoparticles using the endophytic bacterium *Bacillus cereus* isolated from *Garcinia xanthochymu*. Asian Pac. J. Trop. Biomed. Vol. 12: Pages 953–959.

Tollamadugu N. V. K. V., Prasad T., Kambala V. S. R., and Naidu R., (2011) A critical review on biogenic silver nanoparticles and their antimicrobial activity. Curr. Nanosci. Vol. 7: Pages 531–544.

Vigneshwaran N., Ashtaputre N. M., Varadarajan P.V., Nachane R.P., Paralikar K.M., and Balasubramanya R. H., (2007) Biological synthesis of silver nanoparticles using the fungus *Aspergillus flavus*. Mater. Lett. Vol. 61: Pages 1413–1418.

Xu C., Guo Y., Qiao L., Ma L., Cheng Y., and Roman, A., (2018). Biogenic synthesis of novel functionalized selenium nanoparticles by *Lactobacillus casei* ATCC 393 and its protective effects on intestinal barrier dysfunction caused by Enterotoxigenic E. coli K88. Frontiers in microbiology. Vol. 9: Pages 11-29.

Biotechnological Communication

Biosci. Biotech. Res. Comm. 12(1): 140-146 (2019)

BBRC Bioscience Biotechnology Research Communications

Biotechnological management of water quality: A mini review

Lakhan Kumar, Rajkumar Bidlan, Jaigopal Sharma and Navneeta Bharadvaja*

Department of Biotechnology, Delhi Technological University, Shahbad Daulatpur, Delhi-110042, India

ABSTRACT

Since eighteenth century onwards, with the advent of industrial revolution, petrochemical and chemical industries have seen tremendous growth. Wastewater is an essential raw material as well as a by-product of modern day industries and the magnitude of wastewater generation depends upon the level of technological progress of the particular industry of a particular country. It has been observed that least developed and developing countries generate a huge volume of wastewater as compared to the developed ones. This paper discusses the chemistry of water and wastewater, parameters of water for application in drinking water, wildlife and fisheries, irrigation and industrial cooling purpose. Various methods based on physical, chemical and biological treatment available for treatment of wastewater to make it reusable and less harmful to the environment on discharge. Several biological methods of waste treatment and treatment process including trickling filter, activated sludge, aerated lagoon, and waste stabilisation ponds to reduce or degrade some pollutants have been presented in this study. New approaches incorporate natural processes instead of conventional chemical treatment. The role of various microbes has been also discussed to treat various organic pollutants present in wastewater. Applications of genetic engineered microbes as well as certain metabolic engineering mediated interventions have shown significant degradation and reduction of pollutants concentration. Research on wastewater treatment suggests treatment of wastewater must be designed specifically for the particular type of effluent produced. Nevertheless, strategies can be developed for multipollutant targets using biotechnological approaches.

KEY WORDS: BIOLOGICAL TREATMENT, DDT, METABOLIC ENGINEERING, ORGANOCHLORINE, WASTEWATER

ARTICLE INFORMATION:

Corresponding Author: navneetab@dce.ac.in
Received 15th Dec, 2018
Accepted after revision 21st March, 2019
BBRC Print ISSN: 0974-6455
Online ISSN: 2321-4007 CODEN: USA BBRCBA
Thomson Reuters ISI ESC / Clarivate Analytics USA
NAAS Journal Score 2019: 4.31 SJIF: 4.196

Online Contents Available at: http//www.bbrc.in/
DOI: 10.21786/bbrc/12.1/18

INTRODUCTION

Waste is defined as the unwanted or the discarded material which has no further known application and can be divided into three categories-solid, liquid and gaseous. When any undesired agent mixes with water it makes it impure and unacceptable for further use. Wastewater has been defined as water which has some impurities. Generally, it is pure water and various polluting agents in different proportion. Chemistry of pure water elaborating the physical and chemical properties of water and how its peculiar structure makes it a universal solvent has been discussed in detail later section. Wastewater is an essential a by-product of modern day industries (Buljan & Kral 2011, Shi Hanchang 2011, Miksch et al., 2015, González-Camejo et al., 2017).

From agriculture to domestic to anindustrial level, water is extensively used as a raw material. Agriculture and public health practices add many pesticides to the water making it unfit for use. From oil, food, dairy& beverages to textile & leather to pharmaceutical & chemical to paper & pulp to metal and power generating industries, each and every industry needs ahuge amount of water for its operation and is a major contributor of wastewater production. Nuclear, mining and quarries also produce agreat volume of wastewater as a by-product. For example, agricultural nitrate is one of the major reasons for groundwater pollution, (Shukla et al. 2013) (Miksch et al., 2015) (González-Camejo et al., 2017). After use of water, it is discharged as wastewater. Composition of wastewater varies to reference to its production site. Major characteristics include total organic content, solid content present in it, pH, temperature, colour, presence of heavy metals and their concentration, presence of microbes and their population etc. For reuse of this water, government agencies and various international bodies dealing with water and health have graded water into different categories. In India, Central Pollution Control Board has classified water into five classes depending upon their end use and passing the standards set by it. It is very important to know the standard parameters of water quality before its application towards human and animal consumption and for watering plants. Scientific progress in each sector contributed to exhaustion of water resources and waste generation. The amount of wastewater generation depends on the level of technological process development to the particular industry in a particular country and it will be reduced with the improvement of industrial technology. (Hammer 2001, Gogate and Pandit, 2004, Rastogi, 2010 Shi, Hanchang 2011 Rawat et al., 2011, Veerakumari, 2015, Ansari et al., 2017).

It has been observed that least developed and developing countries generate a huge volume of wastewater as compared to the developed ones. In the present review, a detailed account of water chemistry, wastewater characteristics, and wastewater treatment methods has been summarized. Also, the role of various biological methods in the treatment of a range of organic pollutants has been discussed.

Chemistry of water

Water is composed of one oxygen atom and two hydrogen atoms that form covalent bonds with the unpaired electrons of oxygen. The hydrogen atoms are placed at 0.958Å from oxygen. The angle between the two hydrogen (bond angle) is 104.5° making it a bent molecule with partial positive charges on each hydrogen and a partial negative charge on the oxygen atom. Thus, it is a polar molecule. This helps water molecules to form hydrogen bonds with other molecules, including water, (Némethy et al., 1962, Devangee Shukla, et al 2013, Veerakumari, 2015, Emiliano et al. 2017).

It is termed as a universal solvent for the ability to effect many chemical reactions and facilitating the hydrolysis, breaking the bigger molecules into their simpler forms. It possesses certain peculiar and unique physiochemical properties vital for the maintenance of life activities. It solubilises a large number of organic and inorganic compounds. Therefore, it might have been the primary resource for the origin of life. Almost all living organisms possess >70% of their mass comprising water. It is important for many biochemical reactions. It has a high affinity for salts. Physical properties of water are as follows: heat capacity 1 cal/g, heat of vaporization 540 cal/g at 0°C, latent heat of fusion 97.7 cal/g at 0°C, surface tension 76 erg/cm^2, dielectric constant 79, melting point 0°C, boiling point 100°C and viscosity 1.14 x 10^{-3} g/cm-s (Rastogi Smita, 2010 Devangee Shukla, et al 2013, Veerakumari 2015).

Parameters of water for various uses

Central Pollution Control Board (CPCB) of India has proposed various classes of water as 'A to E' about their end use. Drinking Water Source without conventional treatment but after disinfection has been categorised under Class "A" of water and possess the following characteristics: i) Total Coliforms Organisms MPN/100mL shall be 50 or less ii) pH between 6.5 and 8.5 iii) Dissolved Oxygen 6mg/L or more and iv) Biochemical Oxygen Demand (BOD_5^{20}) of 5 days at 20°C 2mg/L or less. Bureau of Indian Standards has defined Indian Standard Specifications for Drinking Water, under IS: 10500, 1992. This report provides information on the permissible and desirable limits of various parameters in drinking water. Rahmanian et al. (2015) have discussed the determination of parameters for drinking water. Class B water is designated best for organised outdoor bathing. The coli-

forms MPN/100 mL in this class is ≤500 and pH 6.5-8.5. The dissolved oxygen and the BOD_5^{20} levels are set at ≥5 ppm and ≤3 ppm respectively. Class C water is a drinking water source that is available after conventional treatment and disinfection process. The MPN for coliforms is set at ≤5000 per mL with pH 6-9 and dissolved oxygen level of ≥ 4 ppm while the BOD_5^{20} is recommended at ≤ 5 ppm. Class D water is useful for wildlife and fisheries. Its free ammonia -N is ≤ 1.2 ppm. The pH ranges between 6.5-8.5 while the dissolved oxygen is ≥ 4 ppm. Water for Irrigation, Industrial Cooling, Controlled Waste disposal comes under class "E" of water and it shall have the pH between 6 and 8.5. Additionally, the boron content shall not be more than 2mg/L and maximum Electrical Conductivity at 25°C (mhos/cm) is capped on 2250 (Ansari et al., 2009) for the purpose of proper treatment and dilution of effluent before discharge in water stream or on land. Physico-chemical characteristics of distillery effluent samples such as colour, odour, Total Solids, Total dissolved solids, Total Suspended Solids, pH, Electrical Conductivity, Total hardness, Calcium, Magnesium, Alkalinity, Chloride, Dissolved Oxygen, Biological Oxygen Demand, Chemical Oxygen Demand, Ammonical Nitrogen, Total Phosphorus, and Total Potassium were analysed and it was observed that the characteristics of spent wash and PTDE (primary treated distillery effluent.

The composition of wastewater

Wastewater is simply that part of the water supply to the community or to the industry which has been used for different purposes and has been mixed with solids, either suspended or dissolved. Wastewater is 99.9% water and 0.1% solids. The main task of treating the wastewater is to remove most or all of this 0.1% of solids (Spellman, 2013) toxic chemical products formed as secondary metabolites by a few fungal species that readily colonise crops and contaminate them with toxins in the field or after harvest. Ochratoxins and Aflatoxins are mycotoxins of major significance and hence there has been significant research on broad range of analytical and detection techniques that could be useful and practical. Due to the variety of structures of these toxins, it is impossible to use one standard technique for analysis and/or detection. Practical requirements for high-sensitivity analysis and the need for a specialist laboratory setting create challenges for routine analysis. Several existing analytical techniques, which offer flexible and broad-based methods of analysis and in some cases detection, have been discussed in this manuscript. There are a number of methods used, of which many are lab-based, but to our knowledge there seems to be no single technique that stands out above the rest, although analytical liquid chromatography, commonly linked with mass spectroscopy is likely to be popular. This review manuscript discusses (a.The composition of wastewater varies according to the primary use of water. It gives a reflection of the lifestyle and technologies enjoyed by this progressive world. Two major constituents are organic and inorganic compounds, (Rastogi, 2010, Ansari et al., 2017).

Carbohydrate, protein, fats, amino acids and volatile acids etc. come under the organic compounds while sodium, calcium, chlorine, potassium, sulphur, magnesium, bicarbonate ammonium salts and heavy metals etc. are listed as inorganic compounds by various researchers (Abdel-Raouf et al., 2012). Hydrocarbons, fats, oils, waxes and high molecular weight fatty acids are collectively referred to as oil and grease come under organic substances (Hammer 2001). Biological components constitute bacteria, fungi, virus and algae etc. Eutrophication is a common phenomenon worldwide due to the discharge of industrial wastes into open water resources which includes vast amounts of nitrogen andphosphorous (Rawat et al., 2011, González-Camejo et al., 2017). Characteristics of wastewater from various industries

Characteristics and compositions of wastewater vary from industry to industry. Wastewater characterisation depends upon changes in colour, odour, total dissolved solids (TDS), total suspended solids (TSS), pH, conductivity, temperature, biochemical oxygen demand (BOD), chemical oxygen demand (COD) and volatile organic compounds (VOCs)etc. The physical characteristics of distillery effluent samples and observed spent wash colour to be dark brown, odour unpleasant, total solids 42400.2 ± 6.4 (CPCB: 90000-120000), total dissolve solids 38200.2 ± 4.8, total suspended solids 4200.0 ± 0.0, pH 4.2 ± 1.2 (CPCB: 3.7-4.5), electrical conductivity (µmho/cm) 16450.8 ± 8.2, total hardness 2432.4 ± 5.4 calcium 2070.0 ± 2.6 (CPCB: 2000-3500), magnesium 2260.5 ± 6.7, alkalinity 2864.5 ± 8.0, chloride 8530.2 ± 8.3(CPCB: 5000-6000), dissolve oxygen Nil, biochemical oxygen demand 32300.8 ± 10.8 (CPCB: 45000-50000), chemical oxygen demand 57164.6 ± 12.9 (CPCB: 80000-100000), ammonical nitrogen 1254.4 ± 2.4 (CPCB: 1000-2000), total phosphorus 44.4 ± 5.6 (CPCB: 200-300), total potassium 7440.2 ± 3.8 (CPCB: 8000-12000). All values given here are in mg/litre(Central Pollution Control Board, 2008) (Ansari et al., 2009)for the purpose of proper treatment and dilution of effluent before discharge in water stream or on land. Physico-chemical characteristics of distillery effluent samples such as colour, odour, Total Solids, Total dissolved solids, Total Suspended Solids, pH, Electrical Conductivity, Total hardness, Calcium, Magnesium, Alkalinity, Chloride, Dissolved Oxygen, Biological Oxygen Demand, Chemical Oxygen Demand, Ammonical Nitrogen, Total Phosphorus, and Total Potassium were analysed and it was

Table 1. Various methods of biological treatment. (Cheremisinoff, 1996) (Hoffmann, 1998) (Tchobanoglous et al., 2003) (Von Sperling, 2007) (Mara, 2009) (Butler et al., 2017)

S. No.	Process	Treatment Agents	Waste treated
1	Trickling filters (attached growth)	Packed bed covered by the microbial film	Acetaldehyde, benzene, chlorinated hydrocarbons, nylon, rocket fuel
2	Activated sludge (suspended growth)	Aerobic microorganisms suspended in wastewater	Refinery, petrochemical and biodegradable organic wastewaters
3	Aerated lagoon	Surface impoundment plus mechanical agitation	Biodegradable organic chemicals
4	Waste stabilization ponds	Shallow surface impoundments plus aeration to promote the growth of algae and bacteria and algae symbiosis	Biodegradable organic chemicals

observed that the characteristics of spent wash and PTDE (primary treated distillery effluent (Devangee Shukla, et al. 2013).

Wastewater treatment

Wastewater treatment refers to the application of various treatment methods on wastewater to make it reusable or less harmful to the environment when discharged. Methods of treatment used for removal of contaminants using physical, chemical and biological reactions are known as unit operations, and they are categorized as primary, secondary and tertiary treatment methods. Primary treatments involve physical operations such as screening and sedimentation for removal of floating and settle able solids found in wastewater. Secondary treatments involve chemical and biological processes to remove most of the organic and inorganic matters present in the wastewater. Then comes the tertiary treatment methods or advanced techniques. Treatment of wastewater must be designed specifically for the specific effluent produced (Gogate and Pandit, 2004, a review of oxidation processes operating at ambient conditions was presented. It has been observed that none of the methods can be used individually in wastewater treatment applications with good economics and high degree of energy efficiency. Moreover, the knowledge required for the large-scale design and application is perhaps lacking. In the present work, an overview of hybrid methods (the majority are a combination of advanced oxidation processes Central Pollution Control Board, 2008, Shi, Hanchang 2011).

Biological treatments of wastewater

Biological treatments of wastewater facilitate the removal of all the settleable colloidal solids and degrade or reduce the present organic as well as inorganic matters (Rawat et al., 2011). Microorganisms utilize the organic/inorganic sources present in the wastewater as a nutrient or food for growth. The process of nutrient utilisation significantly reduces the organic and inorganic loads of the wastewater. Several microorganisms including bacteria, fungus and algae (Table-2) or symposium of algae and bacteria or fungal and bacterial have been explored for wastewater remediation across the globe, (Cheremisinoff, 1996, Butler et al., 2017). Various methods have been devised to date for remediation of wastewater and they include aerobic, anaerobic and the combination of both. They are further subdivided as per their growth system into attached or suspended growth systems. Some of them are listed in Table 1 & 2.

Metabolic engineering to treat wastewater

Metabolic engineering stands for a branch of molecular biology where alternation in the genome of an organism is carried out to achieve a specific purpose of bringing specific genotypic or phenotypic changes in the concerned microorganism. Metabolic engineering is exercised to achieve many objectives such as to reduce or stop the production of by-products to optimise the yield, to increase the rate of thebiochemical process, reduce the energy consumption and ultimately to develop a strain with resistance to biotic as well abiotic stress (Yang & Liu, 2007) (Kumar and Prasad, 2011). The purpose of metabolic engineering is to obtain a robust strain of microorganism to gain optimum productivity, in the case of wastewater remediation, optimum nutrient removal to decrease the organic and inorganic loads. Mutant bacteria have also been introduced for wastewater treatment (Ostergaard et al., 2000) (Siejen & Macro 2008) (Naidoo & Adimola 2014).

Although for metabolic overproduction, very often the strains of the microorganisms are subjected to mutation and selection for yield improvement, the prospect to introduce heterologous genes and regulatory elements makes metabolic engineering, a promising area of research (Soda et al., 1999). The use of a floc-forming bacterium as the host for a recombinant plasmid was proposed. The floc-forming and phenol-degrading GEM Sphingomonas paucimobilis 551 (pS10-45. Bioaugmentation engineered bacteria have a unique position

Table 2. Microbial degradation of various organic pollutants. (Bush et al., 1961) (McCLURE et al., 1991) (Rochkind et al., 1986) (Cheremisinoff, 1996) (Smidt et al., 2000) (Wang et al., 2000) (Tchobanoglous et al., 2003) (Bidlan R, Manonmani H. K., 2007) (Seo et al., 2009) (Mandal and Mallick, 2011) (Renuka et al., 2013) (Saxena et al., 2016) (Gong et al., 2017) (Kumar et al., 2017) (Singh et al., 2017)

S. No.	Organic Pollutant	Microbes involved
1	Petroleum hydrocarbons,	*Acinetobacter, Arthrobacter, Mycobacteria, Actinomycetes, Pseudomonas etcamongbacteria; Scolecobasidium and Cladosporium among yeasts.*
2	Pesticides,herbicides, like Aldrin, Dieldrin and organophosphates like Parathion and Malathion	*Zylerionxylestrix (fungus)*
3	2, 4-D, 1,2,3-trichloropropane (TCP)	*Pseudomonas, Arthrobacter*
4	Diichlorodiphenyltrichloro ethane(DDT)	*Penicillium (fungus), Serratia marcescens (Bacteria)*
5	Kepone, piperonylic acid, Lignocellulosic wastes, Pentachlorophenol	*Pseudomonas*
6	Ethyl benzene	*Nocardiatartaricans (Bacteria)*
	Wastewater	*Calothrix sp., Lyngbya sp., Ulothrix sp, and Chlorella sp. Chlamydomonasrenhardtii, Parachlorellakessleri-I, Nannochloropsisgaditana Scenedesmussp.(Algae)*
7	Heavy metals like cadmium	*Genetically modified E. coli*
8	Chlorinated aromatic compounds	*Desulfomonile tiedjei (bacteria)*
9	Lignins from Paper mills	*Aspergillustrichosporon (Yeast), arthrobacter, Chromobacter, Pseudomonas, Xanthomonas (Bacteria)*

in the treatment of effluent from printing and dyeing industries because of its various advantages, including powerful treatment capability, good decolourisation effect, and modest impact on the surrounding of the original processing system and so on (Xie et al., 2014). McClure *et al*. discussed the role of genetic engineering in improving wastewater treatment with a focus on the degradation of recalcitrant compounds especially chlorinated aromatic compounds. They also investigated the survival and function of natural and genetically modified bacteria when inoculated into laboratory-scale activated sludge units, (McClure et al., 1991). Research on wastewater treatment suggests treatment of wastewater must be explicitly designed for the particular type of effluent produced. Banerjee *et al*. studied various aspects to increase the lipid accumulation in microalgae *Chlamydomonas reinhardtii* and stressed on metabolic engineering associated with other factors to get the desired result (Banerjee et al., 2016).

Trained microorganisms to treat wastewater

Raju *et al*. investigated the role of a consortium of microorganisms to degrade or reduce the concentration of lindane and DDT present in pesticide water. They reported enhanced green gram seed germination upon reduction of Lindane and DDT concentration when the microbial consortium was used (Raju et al., 2017). The strain of *Serratia marcescens* was found to have profound DDT degrading potential Organochlorine which was considered recalcitrant compounds were shown to degrade at enhanced rates in the presence of non-ionic surfactants such as tweens and specificdead-end metabolites of Dichlorodiphenyltrichloroethane (DDT) like Dichlorodiphenyldichloroethylene (DDE) and Dichlorodiphenyldichloroethane (DDD) have also been shown to get metabolised by indeed trained microbes (Bidlan 2007a) (Bidlan 2007b) (Bidlan 2009) (Bharadvaja et al., 2016).

CONCLUSION

Wastewater is generated from various activities in the community and also through natural processes. There are various strategies developed to reduce the levels of various contaminants in the wastewater. Most of the treatment plants use microbial remediation from the microbes already exixtinng in the sludge. Latest trend is to shift from the conventional chemical treatments to the biological treatments as these are more ecofriendly. Research is being carried out around the globe by various groups and a lot of funds are being pushed into this by many countries so that the best possible treatment methods can be implemented for facilitating clean and healthy water for a better, green and robust environment.

REFERENCES

Abdel-Raouf, N., Al-Homaidan, A.A. and Ibraheem, I.B.M. (2012), Microalgae and wastewater treatment Saudi Journal of Biological Sciences, Elsevier, 1 July.

Ansari, A.A., Khoja, A.H., Nawar, A., Qayyum, M. and Ali, E. (2017), Wastewater treatment by local microalgae strains for CO2 sequestration and biofuel production Applied Water Science, Springer Berlin Heidelberg, Vol. 7 No. 7, pp. 4151–4158.

Ansari, F., Awasthi, A.K. and Srivastava, B.P. (2009), Physico-chemical Characterization of Distillery Effluent and its Dilution Effect at Different Levels Archives of Applied Science Research, Scholars Research Library, Vol. 4 No. 4, pp. 1705–1715.

Banerjee, C., Dubey, K.K. and Shukla, P. (2016), Metabolic Engineering of Microalgal Based Biofuel Production: Prospects and Challenges, Frontiers in Microbiology, Vol. 7, p. 432.

Bidlan R, Manonmani HK, Kunhi AAM. (2007) Indian Patents. 209454:A Process For Degration Of Dichloro Dipheny Ltrichloro Ethane (Ddt) Using An Improved Strain Of *Serratia marcescens*.

Bidlan R., Manonmani HK. (2007a), A Process For Enhanced Degradation Of Dichloro-Dip Henyl-Trichloroethane (DDT) Indian patent.

Bidlan R., Manonmani HK. (2007b), A Process For The Preparation Of Biocatalysts Useful For The Degradation Of Dichlorodiphenyldichloroethylene (Dde) Indian patent.

Bidlan Rajkumar, Manonmani HK. (2009), A Process For The Preparation Of Biocatalysts For The Remediation Of Dichlorodiphenyldichlo Roethane (Ddd /Tde) Containing Industrial Effluents Indian patent.

Brini, Emiliano, Brini, E., Fennell, C.J., Fernandez-Serra, M., Hribar-Lee et al (2017) How water's properties are encoded in its molecular structure and energies Chemical reviews, Vol. 117, No. 19, pp. 12385-12414.

Buljan J. and I. Kral (2011), Introduction To Treatment of Tannery Effluents United Nations Industrial Development Organization, p. 10.

Bush, A.F., Isherwood, J.D. and Rodgi, S. (1961) Dissolved Solids Removal from Waste Water by Algae Journal of the Sanitary Engineering Division, ASCE, Vol. 87 No. 3, pp. 39–60.

Butler, E., Hung, Y.-T., Suleiman Al Ahmad, M., Yeh, R.Y.-L., Liu, R.L.-H. and Fu, Y.-P. (2017), Oxidation pond for municipal wastewater treatment Applied Water Science, Springer Berlin Heidelberg, Vol. 7 No. 1, pp. 31–51.

Central Pollution Control Board. (2008), Guidelines for Water Quality Management CPCB, available at:https://doi.org/10.1074/jbc.M002965200.

Cheremisinoff, N.P. (1996), Biotechnology for Waste and Wastewater Treatment, Noyes Publications.

Devangee Shukla, et al (2013) Physicochemical Analysis of Water from Various Sources and Their Comparative Studies IOSR Journal of Environmental Science, Toxicology, and Food Technology , Vol. 5, No. 3, pp. 2319-2402.

Gogate, P.R. and Pandit, A.B. (2004) A review of imperative technologies for wastewater treatment II: hybrid methods Advances in Environmental Research, Pergamon, Vol. 8 No. 3–4, pp. 553–597.

Gong, T., Xu, X., Che, Y., Liu, R., Gao, W., Zhao, F., Yu, H., et al. (2017), Combinatorial metabolic engineering of *Pseudomonas putida* KT2440 for efficient mineralization of 1,2,3-trichloropropane Scientific Reports, Vol. 7 No. 1, p. 7064.

González-Camejo, J., Serna-García, R., Viruela, A., Pachés, M., Durán, F., Robles, A., Ruano, M.V., et al. (2017), Short and long-term experiments on the effect of sulphide on microalgae cultivation in tertiary sewage treatment Bioresource Technology, Vol. 244 No. Pt 1, pp. 15–22.

Hammer MJ, J.H.M. (2001), Water and Wastewater Technology / Mark J. Hammer, Mark J. Hammer, Jr. - Version Details - Trove.

Hoffmann, J.P. (1998) Wastewater Treatment With Suspended And Nonsuspended Algae Journal of Phycology, Vol. 34 No. 5, pp. 757–763.

Indian Standard Specifications for Drinking Water, under IS: 10500, 1992 by Bureau of Indian Standards.

Kumar L, Roy A, Saxena G, Kundu K, Bharadvaja N. (2017) Isolation , Identification and biomass productivity analysis of microalga *Scenedesmus rubescens* from DTU Lake Vol. 8 No. July, pp. 56–67.

Kumar, R.R. and Prasad, S. (2011) Metabolic Engineering of Bacteria Indian Journal of Microbiology, Springer, July.

Mandal, S. and Mallick, N. (2011) Utilization and biodiesel production by the green microalga *Scenedesmus obliquus* Applied and Environmental Microbiology, Vol. 77 No. 1, pp. 374–377.

Mara, D. (2009) Waste stabilization ponds: Past, present and future Desalination and Water Treatment, Taylor & Francis Group, Vol. 4 No. 1–3, pp. 85–88.

McClure, N.C., Fry, J.C. and Weightman, A.J. (1991) Genetic Engineering for Wastewater Treatment Water and Environment Journal, John Wiley & Sons, Ltd, Vol. 5 No. 6, pp. 608–616.

Miksch, K., Cema, G., Corvini, P.F.-X., Felis, E., Sochacki, A., Surmacz-Górska, J., Wiszniowski, J., et al. (2015) R&D priorities in the field of sustainable remediation and purification of agro-industrial and municipal wastewater New Biotechnology, Vol. 32 No. 1, pp. 128–132.

Naidoo Shalinee and Ademola Olaniran (2014) Treated wastewater effluent as a source of microbial pollution of surface water resources International journal of environmental research and public health, Vol. 11, No.1, pp. 249-270.

Némethy, George, and Harold A. Scheraga (1962) Structure of water and hydrophobic bonding in proteins. I. A model for the thermodynamic properties of liquid water The Journal of Chemical Physics , Vol. 36, No. 12, pp. 3382-3400.

Ostergaard, S., Olsson, L. and Nielsen, J. (2000) Metabolic engineering of Saccharomyces cerevisiae. Microbiology and Molecular Biology Reviews : MMBR, American Society for Microbiology (ASM), Vol. 64 No. 1, pp. 34–50.

Raju, S.M., Bashambu, D., Bidlan, R., Sharma, J.G. and Kumar, S. (2017), Enhancement In Seed Germination Through Simultaneous Degradation Of Organochlorine Pesticides (Lindane And Ddt) By A Novel Microbial Consortium International

Journal of Advance Research in Science and Engineering, Vol. 6, pp. 707–13.

Rahmanian, Nejat, et al. (2015), Analysis of physiochemical parameters to evaluate the drinking water quality in the State of Perak, Malaysia Journal of Chemistry, Hindawi publications, pp. 1-10.

Rastogi, S.C. (2010), Biochemistry, 3rd ed., Tata McGraw-Hill Education.

Rawat, I., Ranjith Kumar, R., Mutanda, T. and Bux, F. (2011), Dual role of microalgae: Phycoremediation of domestic wastewater and biomass production for sustainable biofuels production Applied Energy, Elsevier, Vol. 88 No. 10, pp. 3411–3424.

Renuka, N., Sood, A., Ratha, S.K., Prasanna, R. and Ahluwalia, A.S. (2013), "Nutrient Sequestration, Biomass Production By Microalgae And Phytoremediation Of Sewage Water International Journal of Phytoremediation, Vol. 15 No. 8, pp. 789–800.

Rochkind, M.L., Blackburn, J.W. and Sayler, G.S. (1986), Microbial decomposition of chlorinates aromatic compounds.

Saxena G, Kumar L, Hariri SM, Bhardvaja N (2016) Identification of Potential Culture Conditions for Enhancing the Biomass Production of Microalga *Chlorella minutissima* Expert Opinion on Environmental Biology, SciTechnol, Vol. s1.

Seo, J.-S., Keum, Y.-S. and Li, Q.X. (2009) Bacterial Degradation of Aromatic Hydrocarbons Int. J. Environ. Res. Public Health, Multidisciplinary Digital Publishing Institute (MDPI), Vol. 6 No. 1, pp. 278–309.

Shi, Hanchang (2011) Industrial wastewater-types, amounts and effects Encyclopedia of Life Support Systems, Vol. 1, pp. 191–204.

Siezen, RJ, and Marco Galardini (2008) Genomics of biological wastewater treatment Microbial biotechnology, Vol. 1, No. 5, pp. 333.

Singh, A.K., Sharma, N., Farooqi, H., Abdin, M.Z., Mock, T. and Kumar, S. (2017), Phycoremediation of municipal wastewater by microalgae to produce biofuel International Journal of Phytoremediation, Vol. 19 No. 9, pp. 805–812.

Smidt, H., Akkermans, A.D.., Van Der Oost, J. and De Vos, W.M. (2000) Halorespiring bacteria-molecular characterization and detection Enzyme and Microbial Technology, Vol. 27, Elsevier, pp. 812–820.

Soda, S., Uesugi, K., Ike, M. and Fujita, M. (1999) Application of a floc-forming genetically engineered microorganism to a sequencing batch reactor for phenolic wastewater treatment Journal of Bioscience and Bioengineering, Elsevier, Vol. 88 No. 1, pp. 85–91.

Spellman, F.R. (2013), Handbook of Water and Wastewater Treatment Plant Operations, Springer, Vol. 23, CRC Press, available at:https://doi.org/10.1007/s13398-014-0173-7.2.

von Sperling, M. (2007), Wastewater Characteristics, Treatment and Disposal, Iwa Publishing. London.

Tchobanoglous, G., Burton, F.L. (Franklin L., Stensel, H.D. and Metcalf & Eddy. (2003), Wastewater Engineering : Treatment and Reuse, McGraw-Hill. Veerakumari, L. (2015), Biochemistry, MJP Publ.

Wang, C.L., Maratukulam, P.D., Lum, A.M., Clark, D.S. and Keasling, J.D. (2000), "Metabolic engineering of an aerobic sulfate reduction pathway and its application to precipitation of cadmium on the cell surface", Applied and Environmental Microbiology, Vol. 66 No. 10, pp. 4497–4502.

Xie, X.H., Liu, N., Jiang, H. and Zhu, L.Y. (2014) Construction and Application of Engineered Bacteria for Bioaugmentation Decolorization of Dyeing Wastewater: A Review Journal of Geoscience and Environment Protection, Scientific Research Publishing, Vol. 02 No. 02, pp. 84–88.

Yang ST, Liu X, Z.Y. (2007) Metabolic Engineering - Applications, Methods, and Challenges Bioprocessing for Value-Added Products from Renewable Resources - New Technologies and Applications - Elsevier Publications.

Biochemical
Communication

Biosci. Biotech. Res. Comm. 12(1): 147-155 (2019)

BBRC
Bioscience Biotechnology
Research Communications

Bile salt hydrolase, a potent enzyme capable of removing cholesterol present in bacteria: A review

Akhila. B. Rajan, Abhini K N and Fathimathu Zuhara K*

Department of Life Sciences, University of Calicut, Kerala, India 673635

ABSTRACT

Bile salt hydrolase (BSH) is a highly significant enzyme involved in bile acid alteration in the gastrointestinal tract of humans and animals. Bile salt hydrolase belongs to the chologlycine hydrolase enzyme family and is normally associated with the gastrointestinal bacteria of both human and animals. This enzyme is responsible for the hydrolysis of conjugated bile acids into free bile acid and amino acid residue. Today, BSH is considered as an upcoming pharmacologically important enzyme since it has the ability to lower cholesterol levels in hypercholesterolemic patients because high cholesterol levels are found as an important reason of atherosclerosis which results in cardiovascular diseases (CVD's). This review discusses about the incidence of BSH enzyme among bacteria and the role and potential application of this highly significant enzymes on the host.

INTODUCTION

Cholesterol, though is regarded as an important substance in human body, high levels of serum cholesterol may lead to atherosclerosis which in turn can end in cardiovascular diseases (CVD's) (Jones *et al*., 2004, Tsai *et al*., 2014). There is tremendous increase in the number of people suffering from cardiovascular diseases in the developing countries like India. During the past five decades, rate of coronary artery diseases among urban population have risen from 4% to 11% due to modernization and stressful life styles. Many clinical and epidemiological studies indicate that a correlation exists between the elevated serum cholesterol levels and coronary heart disease (Pereira & Gibson, 2002). According to the recent reports of World Health Organization (WHO), the CVD's are regarded as number 1 cause of death globally and responsible for 31% of all global deaths (WHO, 2017). On 22 September, 2016 WHO has launched "Global Hearts", a new initiative to beat back the global threat of cardiovascular diseases.

ARTICLE INFORMATION:

Corresponding Author: kfzuhra@gmail.com
Received 3rd Jan, 2019
Accepted after revision 26th March, 2019
BBRC Print ISSN: 0974-6455
Online ISSN: 2321-4007 CODEN: USA BBRCBA
Thomson Reuters ISI ESC / Clarivate Analytics USA
Crossref Clarivate Analytics
NAAS Journal Score 2019: 4.31 SJIF: 4.196

Online Contents Available at: http//www.bbrc.in/
DOI: 10.21786/bbrc/12.1/19

Nowadays, a number of non-pharmacologic methodologies such as dietary management, regular exercise and drug therapies are commonly used for lowering cholesterol levels (Dunn-Emke *et al*., 2001). But most of the drugs in use, though may effectively reduce the cholesterol level, are expensive and known to have side effects (Bliznakov, 2002). Hence the importance of using enzymatic deconjugation by bile salt hydrolase (BSH), both to lower serum cholesterol levels in hypercholesteremic patients and to prevent hypercholesteremia in normal people is increasing day by day (Sridevi *et al*., 2009). In this regard, bile salt hydrolase can be considered as an alternative therapy for lowering serum cholesterol levels. Bile salt hydrolase, a highly biologically significant enzyme, belongs to the family chologlycine hydrolase (EC 3.5.1.11). This enzyme has been classified as N-terminal nucleophilic (Ntn) hydrolase which is involved in the deconjugation of conjugated bile acids resulting in the formation of free bile acids and amino acids (Kumar *et al*., 2006, Chand *et al*., 2017).

Bile

Bile is a yellow-green aqueous solution which typically consists of bile acids, cholesterol, phospholipids and the pigment biliverdin. In addition to the trace amounts of mucus, tocopherol and immunoglobulin A (IgA) are also present which prevent the bacterial growth and oxidative damage to the epithelium (De Smet *et al*., 1998, Schiff *et al*., 2002) . Bile is synthesized in the pericentral hepatocytes of the liver in many mammals and is stored and concentrated in gallbladder followed by the release of this into the duodenum just after the food intake.The bile acids play important role as a biological detergent which emulsifies and solubilizes lipids, thereby enhancing the absorption and digestion of fats. Under normal conditions, the conservation of bile acids are done by a process called enterohepatic recirculation (Ridlon *et al*., 2006, Russell, 2009).

Enterohepatic circulation

The cholesterol metabolism, in humans and animals, leads the formation of C24 acid steriods possessing a carboxyl group at the end of the side chain called as bile acids. The synthesis of C24 acid steriods in liver from cholesterol is followed by their conjugation with amino acids such as taurine or glycine at the C24 position of the steroid nucleus, catalysed by the enzyme N-acyltransferase (Appleby and waters 2014, Schapp *et al* 2014, Camilleri & Gores 2015). The ratio of conjugation of bile acids with the amino acids glycine or taurine, depends upon the relative abundance of these amino acids, which may not have any functional or regulatory consequences (Ridlon, 2006). These conjugated bile salts are amphipathic in nature with enhanced solubility which makes them impermeable to cell membranes. At physiological pH, the carbon at the terminal position of glycocholic acid or oxygen atom of taurocholic acid bonded with sulphur gets ionized. The ionized oxygen atom along with planar structure of bile acids and the hydroxyl groups present in their rings make them highly amphipathic in nature. In the case of glycocholic acid, the conjugation of aminoacid glycine with cholic acid results in the reduction of pKa of cholic acid from 6.4 to 4.4 units thereby enhancing the bile acids to get completely ionized and highly soluble (Alrefai *et al*., 2007).

The intake of lipids initiates the secretion of bile salts through the common duct into the duodenum, hence results in the association with dietary lipids and various digestive products (Begley, 2005). The conjugated bile acids are ionized molecules which are resistant to deamidation by pancreatic and mucosal carboxypeptidases. Instead they move to the distal ileum, where they get absorbed by an active transport system known as ileum bile acid transporter (IBAT) and the members of the ATP binding cassette (ABC) family of transporters (Lack & Weiner, 1966, Nicoloau *et al*., 2012). About 95% of the bile salt mixture is re-absorbed and returns back to the liver by hepatic portal circulation and this process is known as enterohepatic circulation (fig.1).

Approximately 600 to 800 ml of bile is being produced daily and the total circulating bile acid pool is about 1.7 to 40 g. The recirculation of entire bile acid pool is about 6 to 15 times per day and a total of 0.2 to 0.5 g is excreted via feces thereby enhancing the synthesis of bile acid by de novo pathway (Kumar *et al*., 2012). The bile acid that eludes the absorption is subjected to bacterial metabolism including reduction and epimerization of their OH groups from α to β conformation (Chiang, 2009). One such important transformation by indigenous intestinal bacteria is deconjugation of bile acids which is catalyzed by the enzyme called bile salt hydrolase (BSH) (Kim and Lee, 2005)

Role of BSH

The function of BSH still remains unclear and several hypotheses have been put forward regarding the expression and function of the BSH gene present in the bacteria of the human gastrointestinal tract.

Nutritional role

BSH confer nutritional advantage for the BSH positive strains as they utilize the hydrolysed amino acid moieties (Begley *et al*., 2005). The deconjugation process results in the release of two amino acids such as glycine, which may be further metabolized to ammonia and carbon dioxide and taurine, which may be metabolized to ammonia, carbon dioxide and sulphate. Evidences supporting these hypotheses, proposed by Huijghebaert *et*

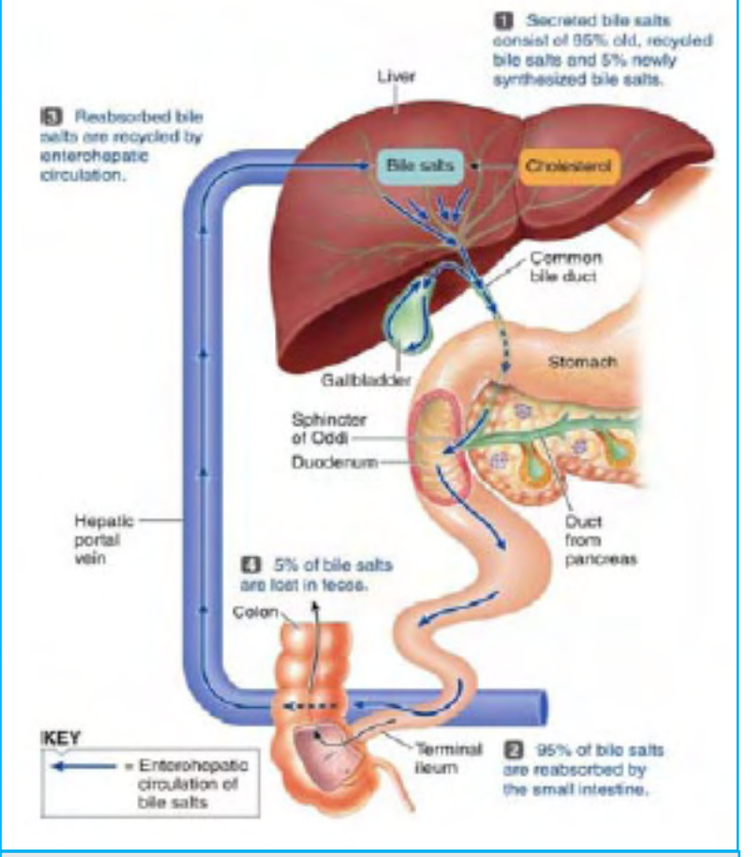

FIGURE 1. Enterohepatic circulation of Bile acids. (Adapted from http://www.gestaltreality.com/2013/09/21/metabolic-cholestatic-pruritus/)

al. in 1982 and Van Eldere *et al.* in 1996, stated that certain bile salt deconjugating *Clostridium* strains were able to utilize the released taurine as an electron acceptor and the growth rates of these strains were improved in the presence of taurine and taurine-conjugated bile salts (Huijghebaert *et al.*,1982; Van Eldere *et al.*, 1996).

Modification of Membrane characteristics

Most of the friendly intestinal bacteria play a crucial role in maintaining host gut health. The hydrolytic enzymes, lysozyme, phospholipase A2 and α-defensins, produced by these bacteria in host gut provide a defense mechanism in the intestine. The extent of damage by host defenses on these bacterial membranes is determined by the composition, fluidity, permeability, hydrophobicity and net charge of the membrane (Peschel, 2002). Studies have revealed that the cholesterol or bile incorporation into the bacterial membranes has been facilitated by BSHs (Dambekodi & Gilliland, 1998; Taranto *et al.*, 2003; Taranto *et al.*, 1997), which may increase the membrane potency by forming BSH- mediated lipid intermolecular hydrogen bonding (Boggs, 1987) or could change its fluidity or charge. The resultant cell surface modification by BSH activity could offer safety against perturbation of the structure and bacterial membranes integrity by the immune system and such resistance mechanisms ensures in establishing prolonged persistence. This mechanism may strongly confer commensals, possessing BSH enzyme, the capacity to dominate over the BSH- negative pathogens or other transients (Patel *et al.*, 2010)

Bile detoxification

BSH activity of microorganisms might be detoxification action and these enzymes make the strains bile tolerant, thereby making positive environment in the gastrointestinal tract for survival. Many investigators have disproved this hypothesis of correlation between bile tolerance and BSH activity (Ahn *et al,* 2003; Moser & Savage, 2001;). Although ambiguity exists between the correlation of bile salt hydrolase and bile tolerance, several studies have been undertaken to study this relation.

Studies by four independent groups using wild-type and bsh mutant combinations provide a connection between BSH activity and bile tolerance. The study using *Lactobacillus amylovorus* mutant, with partly reduced BSH activity, displayed reduced growth rates in the presence of bile salts (Grill *et al*., 2000). Also BSH mutated *Listeria monocytogenes* made the cells more sensitive to bile and bile salts (Begley *et al*., 2005; Dussurget *et al*., 2002) and *Lactobacillus plantarum* (De Smet *et al*., 1995). The actual mechanism by which BSH positive strains exhibit bile tolerance is not yet fully known. However it was proposed that the toxicity may be exhibited through the intercellular interface by the protonated form of bile salts and BSH positive cells may protect themselves by the weaker unconjugated counterparts. Hence this mechanism helps in dropping the pH and making suitable environment for bringing back and exporting the co-transported proton (De Smet *et al*., 1995). The unconjugated bile acids resulting from the enzymatic deconjugation of BSH active strains have an inhibitory effect on bacteria but the study of De Smeth *et al* suggested that the BSH active strains may be capable of detoxifying these effects or they may be associated with 7α-dehydroxylating bacteria which will dehydroxylate unconjugated bile acids (De Boever & Verstraete, 1999).

Application of Bile Salt Hydrolase enzyme

Hypocholesterolemic effect

An elevated level of cholesterol in blood can lead to hypercholesterolemia which in turn becomes a threat for the development of coronary heart diseases. Pharmacologic agents such as statins, bile acid sequestrants etc. and food products are being formulated continuously to control the serum cholesterol levels in these patients. Recently many studies have shown that probiotics with bile salt hydrolase activity have the ability of cholesterol lowering. These have given much attention of using BSH positive probiotic strains in animal models and human subjects. In 1995 De Smet *et al* proposed that the BSH active probiotic strains or cultured products containing them result in the reduction of serum cholesterol levels by interacting with the bile salt mechanism of the host. The studies of Sukling *et al* in 1991 revealed that the proposed mechanism of cholesterol lowering effect by De Smet *et al* (1995) is comparable with pharmacological agents (sequestrants) which prevent the bile salts from being reabsorbed by binding with them (Suckling *et al*., 1991). In addition to this Liong and shah (2005) and Parvez *et al* (2005) found that the strains Bifidobacterium and Bifidobacterium bifidum NRRL 1976 was also able to remove cholesterol by bacterial assimilation and precipitation. Studies of Dong *et al* (2012) has also demonstrated that bsh positive *Lactobacillus plantarum* BBE7 was capable of removing cholesterol *in vitro*.

Human studies

The hypocholesterolemic effects of probiotic strain, first discovered by Mann and Spoerry in 1974, showed that the Maasai tribes in Africa who consumed large amount of milk fermented by *Lactobacillus* sps resulted in the reduction of serum cholesterol levels (Mann & Spoerry, 1974). In 1979 Hepner reported that the consumption of either pasteurized or non-pasteurized milk showed an effective reduction of serum cholesterol levels which was higher than that expressed by those who consumed 2% butterfat milk after 1 week (Hepner *et al*.,1979). Moreover, the studies of Sarkar in 2003 revealed that the cholesterol reducing abilities of six strains of *L. acidophilus* was either due to the assimilation of cholesterol or attachment of cholesterol to the surface of *L. acidophilus* cells. Since this bacterium is a natural inhabitant of intestine with bile salt hydrolase activity, they can be utilized for the production of acidophilus milk which can bring out hypocholesterolemic effect. As part of the study he has also proposed that the efficacy of acidophilus milk to lower serum cholesterol level can be influenced by a number factors such as the milk type employed for the manufacture and also the age, sex, food habits and initial cholesterol concentration of the tested subjects (Sarkar, 2003).

Lactobacillus sps have been most widely used since there are several reports supporting the hypocholesterolemic effects of this strain. It was in 1989 Lin *et al* experimented with 23 human subjects, who received tablets containing 3x107 CFU *L. acidophilus* (ATCC 4962) and *Lactobacillus delbrueckii* ssp *bulgaricus* (ATCC 33409) daily for 16 weeks, which resulted in reduction of serum cholesterol level in an experimental group from 5.7 to 5.4 mmol/L, while the control group remained the same (Lin *et al*., 1989). Another study with the consumption of buffalo milk, fermented with specific strain of *L. acidophilus*, for a month resulted in the reduction of serum cholesterol by 12 to 20% (Khedkar *et al*.,1993). Even a small reduction in serum cholesterol of 1% can reduce risk of coronary heart disease by 2-3% (Gilliland, Nelson, & Maxwell, 1985; Manson *et al*., 1992). A number of placebo controlled studies have been carried out to study these effects. In one such study 30 volunteers consumed yoghurt enriched with specific strain *L. acidophilus* and it resulted in lowering of cholesterol levels in serum by 0.23 mmol/L (Schaafsma *et al*, 1998).

Another study with *L. Plantarum* 229 from the food product Pro-Viva has revealed that the cholesterol levels were affected in humans with moderately elevated serum cholesterol. For this study Bukowska *et al*., 2001 utilized a randomized-placebo design where 30 healthy men who consumed 200 mL/day of Pro-viva for 6 weeks showed a significant decrease in total cholesterol, LDL cholesterol and fibrinogen levels(Bukowska *et al*.,1998).

The findings of Harrison and Peat, 1975 stated that a decrease in serum cholesterol level was visible in bottle-fed babies whereas the count of *L. acidophilus* in their stool was increased (Harrison & Peat, 1975). Similarly the consumption of yogurt has also resulted in the reduction of serum cholesterol levels in humans (Hepner *et al*., 1979; Mann, 1977).

Studies with *Bifidobacterium* sp have also shown potential hypocholesterolemia effects. Rasic *et al* in 1992 had found that consumption of *B. bifidum* can lead to the assimilation of cholesterol by in vitro experiments (Rašić *et al*., 1992). It was also able to reduce the serum cholesterol concentration in human subjects with hypercholesterolemia. In 2003 Xiao *et al* proposed that milk fermented with *B. longum* BL1 resulted in the reduction of serum total cholesterol, LDL cholesterol and triglycerides in hypercholesterolemia patients as well as in rats (Xiao *et al*., 2003).

Animal studies

Animal models such as rats, mice, hamsters, guinea pigs and pigs have been widely used due to their similarities with respect to digestive anatomy and physiology, nutritional requirements and various other metabolic processes including cholesterol and bile acid metabolism, distribution of plasma lipoprotein and regulation of hepatic cholesterol enzymes. Several studies have been conducted to compare the effect of milk and milk products on cholesterol concentrations in animal models.

Gilliland *et al* in 1975 showed that *L. acidophilus* RP32, capable of assimilating cholesterol in vitro, was able to inhibit the increase of serum cholesterol levels of pigs fed on a high-cholesterol diet (Gilliland, Speck, & Morgan, 1975). In addition, the same author in 1985 had also reported the cholesterol lowering capability of *L. casei* P47 in pigs (Gilliland *et al*., 1985). Another study conducted by Mahrous *et al*., 2011 reported that consumption of yogurt, fermented by *L. acidophilus*, by mice significantly decreased the cholesterol content in the serum and increased bile acid content in the feces (Mahrous, Shaalan, & Ibrahim, 2011). Chiu *et al*., 2006 had showed that intake of probiotic fermented foods results in the reduction of total serum cholesterol levels in hamsters with high blood cholesterol levels (Chiu, Lu, Tseng, & Pan, 2006). Moreover, Sindhu and Khetarpaul in 2003 had studied the effect of probiotic fermented foods in 20 young Swiss mice, where there was reduction in the total serum cholesterol (Sindhu & Khetarpaul, 2003).

Studies with *L. plantarum* PH04 from infant feces showed a significant reduction in the serum cholesterol level and triglycericides when compared with the control (Nguyen, Kang, & Lee, 2007). The efficacy of buffalo milk-yogurts containing *B. longum* Bb-46 was determined by administering it to 48 hypercholesterolemic male albino rats for 35 days and significant reduction of total cholesterol, LDL cholesterol and triglycerides were obtained when compared to the control (El-Gawad *et al*., 2005). *L. acidophilus* fermented rice bran showed significant improvement of lipid profile in hypercholesterolemic male Fischer rats (Fukushima *et al*., 1999). In a study by Lee 2007, on the anti-obesity activity of Trans-10, cis-12 conjugated linoleic acid produced by *L. plantarum* PL62, an observable reduction was obtained in the weight of epididymal, inguinal, mesenteric and perirenal white adipose tissues in mice (Lee *et al*., 2007). Similarly the intake of *L. gasseri* BNR17 also exhibited a reduction in weight, hip and waist circumference without any change in behavior or diet (Jung *et al*., 2013).

Until now, several studies have been conducted to evaluate the effects of consumption of probiotics or fermented products and they have given variable data (Taylor and Williams, 1998). In most of the cases cholesterol lowering effect was observed only during the intake of very high doses of the product whereas the normal consumption of probiotics failed to deliver such effects. Such contradictory results obtained may be due to the design of the experiment, lack of statistical power, inadequate sample sizes, improper nutrient intake and expenditure of energy during the experiments and variation in the baseline levels of blood lipids (Pereira & Gibson, 2002).

BSH a desirable trait in probiotics

In 2002 World Health Organization (WHO) has recommended BSH activity as one of the main characteristics for considering the strains *Lactobacillus* and *Bifidobacteria* as probiotics, along with their ability to resist the harsh environment of the gut and to colonize in gastrointestinal epithelia (WHO, 2002). Overall, several studies have strongly supported the hypothesis that BSH positive strains are capable of detoxifying bile salts there by increasing the intestinal survival. Hence BSH activity can be considered as a desirable factor for the probiotics. The BSH activity may result in the accumulation of large amounts of deconjugated bile salts and hence cause undesirable effects in the human host which may arise concerns over the safety administration of BSH positive strains. However, the probiotic strains *Lactobacillius* and *Bifidobacterium* are not capable of dehydroxylating deconjugated bile salts (Ahn *et al*., 2003; Gilliland & Speck, 1977; Takahashi & Morotomi, 1994) and hence majority of the breakdown products may be precipitated or excreted through feces which may vary from person to person depending upon the colonic pH and intestinal transit time (Thomas *et al*., 2000; Thomas *et al*., 2001).

Studies by two other groups have proposed that the intestinal bacteria, except certain strains of *Clostridium*

and *Eubacterium*, the only strains that possess dehydroxylating activity, (Dawson *et al*., 1996; Doerner *et al*, 1997) inhibit further modification of deconjugated products. First, Kurdi *et al* in 2003 proposed that BSH positive probiotic strains *Lactobacillus* and *Bifidobacterium* are able to accumulate cholic acid, the main free bile acid produced in the intestine by BSH activity, as long as the bacteria were energized (Kurdi *et al*., 2003). Second, studies by Jones *et al* in 2004 revealed that microencapsulated BSH positive *L. plantarum* can hydrolyze bile salts in vitro and the deconjugated products were trapped within the membrane which makes these products less bioavailable. In addition to this the encapsulation of strain would protect them from the harsh gut environment and persistence of the strain (Jones *et al*., 2004)

Present scenario

Various studies have been carried out with BSH positive probiotics to illustrate the cholesterol lowering capacity with the same concept based on the interruption of enterohepatic circulation. So far the hypocholesterolemic effects of probiotics have been confirmed in both humans (Anderson & Gilliland, 1999) as well as animals(Gilliland *et al*., 1975; Mahrous *et al*., 2011; Sridevi *et al*., 2009). It was observed and reported that Bile salt hydrolase enzyme was associated with only microbiota in gastrointestinal tract and autochthous intestinal bacteria such as *Listeria monocytogenes* (Dussurget *et al*., 2002) and *Xanthomonas maltophila* (Dean *et al*., 2002).

Future perspectives

Recently this enzyme is reported to be present in thermophilic bacteria, *Brevibacillus borstelensis* isolated from hot water springs, near Konkan, Maharashtra, India (Sridevi & Prabhune, 2009). Also, a potent producer of BSH, *Staphylococcus saprophyticus* ZABR2, was isolated from the soil samples collected from the dumping sites of fish waste (Rajan & Fathimathu Zuhara, 2018). These findings reveal that microorganisms from other sources may also possess the highly significant enzyme BSH and hence it needs to be explored more for the isolation of the potent producers

REFERENCES

Ahn, Y. T., Kim, G. B., Lim, K. S., Baek, Y. J., & Kim, H. U. (2003). Deconjugation of bile salts by *Lactobacillus acidophilus* isolates. International Dairy Journal, 13(4), 303–311.

Alrefai, W. A., and R. K. Gill. 2007. Bile acid transporters: structure, function, regulation and pathophysiological implications. Pharmaceutical Research 24: 1803-1823.

Anderson, J. W., & Gilliland, S. E. (1999). Effect of Fermented Milk (Yogurt) Containing Lactobacillus Acidophilus L1 on Serum Cholesterol in Hypercholesterolemic Humans. Journal of the American College of Nutrition, 18(1), 43–50.

Appleby, RN and Walters, JR (2014). The role of bile acids in functional GI disorders. Neurogastroenterology & Motility **26**: 1057–1069

Begley, M., Sleator, R. D., Gahan, C. G. M., & Hill, C. (2005). Contribution of Three Bile-Associated Loci, bsh, pva, and btlB,to Gastrointestinal Persistence and Bile Tolerance of *Listeria monocytogenes*. Infection and Immunity, 73(2), 894–904.

Beher, W. T., Lin, G. J., & Bajraszewski, F. (1984). The determination and excretion of individual human fecal bile acids. Steroids, 44(6), 539–547.

Bliznakov, E. G. (2002). Lipid-lowering drugs (statins), cholesterol, and coenzyme Q10. The Baycol case--a modern Pandora's box. Biomedicine & Pharmacotherapy= Biomedecine & Pharmacotherapie, 56(1), 56–59.

Boggs, J. M. (1987). Lipid intermolecular hydrogen bonding: influence on structural organization and membrane function. BBA - Reviews on Biomembranes, 906(3), 353–404.

Bortolini, O., Medici, A., & Poli, S. (1997). Biotransformations on steroid nucleus of bile acids. Steroids, 62(8–9), 564–577.

Bukowska, H., Pieczul-Mroz, J., Jastrzebska, M., Chelstowski, K., & Naruszewicz, M. (1998). Decrease in fibrinogen and LDL-cholesterol levels upon supplementation of diet with *Lactobacillus plantarum* in subjects with moderately elevated cholesterol [1]. Atherosclerosis, 137(2), 437–438.

Camilleri, M and Gores, GJ (2015). Therapeutic targeting of bile acids. American Journal of Physiology-Gastrointestinal and Liver Physiology **309**:G209–G215

Chand, D., Avinash, V. S., Yadav, Y., Pundle, A. V., Suresh, C. G., & Ramasamy, S. (2017). Molecular features of bile salt hydrolases and relevance in human health. Biochimica et Biophysica Acta (BBA)-General Subjects, 1861(1), 2981-2991.

Chiu, C. H., Lu, T. Y., Tseng, Y. Y., & Pan, T. M. (2006). The effects of Lactobacillus-fermented milk on lipid metabolism in hamsters fed on high-cholesterol diet. Applied Microbiology and Biotechnology, 71(2), 238–245. https://doi.org/10.1007/s00253-005-0145-0

Dambekodi, P. C., & Gilliland, S. E. (1998). Incorporation of Cholesterol into the Cellular Membrane of *Bifidobacterium longum*. Journal of Dairy Science, 81(7), 1818–1824.

Dawson, J. A., Mallonee, D. H., Bjorkhem, I., & B, P. (1996). 4 bile acid 12708 in *Escherichia coli* k &. Journal Of Lipid Research, 37, 1258–1267.

De Boever, P., & Verstraete, W. (1999). Bile salt deconjugation by *Lactobacillus plantarum* 80 and its implication for bacterial toxicity. Journal of Applied Microbiology, 87(3), 345–352.

De Smet, I., De Boever, P., & Verstraete, W. (1998). Cholesterol lowering in pigs through enhanced bacterial bile salt hydrolase activity. British Journal of Nutrition, 79, 185–194.

De Smet, I., Van Hoorde, L., Vande Woestyne, M., Christiaens, H., & Verstraete, W. (1995). Significance of bile salt hydrolytic activities of *Lactobacilli*. Journal of Applied Bacteriology, 79(3), 292–301.

Dean, M., Cervellati, C., Casanova, E., Squerzanti, M., Lanzara, V., Medici, A., ... Bergamini, C. M. (2002). Characterization of cholylglycine hydrolase from a bile-adapted strain of *Xanthomonas maltophilia* and its application for quantitative hydrolysis of conjugated bile salts. Applied and Environmental Microbiology, 68(6), 3126–3128.

Doerner, K. C., Takamine, F., LaVoie, C. P., Mallonee, D. H., & Hylemon, P. B. (1997). Assessment of fecal bacteria with bile acid 7α-dehydroxylating activity for the presence of bai-like genes. Applied and Environmental Microbiology, 63(3), 1185–1188.

Dong, Z., Zhang, J., Lee, B., Li, H., Du, G., & Chen, J. (2012). A bile salt hydrolase gene of *Lactobacillus plantarum* BBE7 with high cholesterol-removing activity. European Food Research and Technology, 235(3), 419-427.

Dunn-Emke, S., Weidner, G., & Ornish, D. (2001). Benefits of a Low-Fat Plant-Based Diet. Obesity Research, 9(11), 731.

Dussurget, O., Cabanes, D., Dehoux, P., Lecuit, M., Buchrieser, C., Glaser, P., & Cossart, P. (2002). Listeria monocytogenes bile salt hydrolase is a PrfA-regulated virulence factor involved in the intestinal and hepatic phases of listeriosis. Molecular Microbiology, 45(4), 1095–1106.

El-Gawad, I. A. A., El-Sayed, E. M., Hafez, S. A., El-Zeini, H. M., & Saleh, F. A. (2005). The hypocholesterolaemic effect of milk yoghurt and soy-yoghurt containing bifidobacteria in rats fed on a cholesterol-enriched diet. International Dairy Journal, 15(1), 37–44.

Franklund, C. V, de Prada, P., & Hylemon, P. B. (1990). Purification and characterization of a microbial, NADP-dependent bile acid 7 alpha-hydroxysteroid dehydrogenase. Journal of Biological Chemistry, 265(17), 9842–9849.

Fukushima, M., Yamada, A., Endo, T., & Nakano, M. (1999). Effects of a mixture of organisms, Lactobacillus acidophilus or Streptococcus faecalis on δ6-desaturase activity in the livers of rats fed a fat-and cholesterol-enriched diet. Nutrition, 15(5), 373–378.

Gilliland, S. E., Nelson, C. R., & Maxwell, C. (1985). Assimilation of cholesterol by Lactobacillus acidophilus. Applied and Environmental Microbiology, 49(2), 377–381.

Gilliland, S. E., & Speck, M. J. (1977). Deconjugation of bile acids by human intestinal bacteria. Applied and Environmental Microbiolog, 33, 15–18.

Gilliland, S. E., Speck, M. L., & Morgan, C. G. (1975). Detection of Lactobacillus acidophilus in feces of humans, pigs, and chickens. Applied Microbiology, 30(4), 541–5.

Grill, J. P., Cayuela, C., Antoine, J. M., & Schneider, F. (2000). Isolation and characterization of a Lactobacillus amylovorus mutant depleted in conjugated bile salt hydrolase activity: Relation between activity and bile salt resistance. Journal of Applied Microbiology, 89(4), 553–563.

Harrison, V. C., & Peat, G. (1975). Serum cholesterol and bowel flora in the newborn. The American Journal of Clinical Nutrition, 28(12), 1351–1355.

Hepner, G., Fried, R., St Jeor, S., Fusetti, L., & Morin, R. (1979). Hypocholesterolemic effect of yogurt and milk. The American Journal of Clinical Nutrition, 32(1), 19–24. Retrieved from

Huijghebaert, S. M., Mertens, J. a, & Eyssen, H. J. (1982). Isolation of a bile salt sulfatase-producing *Clostridium* strain from rat intestinal microflora. Applied and Environmental Microbiology, 43(1), 185–192.

Jones, M. L., Chen, H., Ouyang, W., Metz, T., & Prakash, S. (2004). Microencapsulated genetically engineered Lactobacillus plantarum 80 (pCBH1) for bile acid deconjugation and its implication in lowering cholesterol. Journal of Biomedicine and Biotechnology, 2004(1), 61–69.

Jung, S. P., Lee, K. M., Kang, J. H., Yun, S. Il, Park, H. O., Moon, Y., & Kim, J. Y. (2013). Effect of Lactobacillus gasseri BNR17 on overweight and obese adults: A randomized, double-blind clinical trial. Korean Journal of Family Medicine, 34(2), 80–89.

Khedkar, C. D., Garge, R. D., Mantri, J. M., Kulkarni, S. A., & Khedkar, G. D. (1993). Effect of feeding acidophilus milk on serum cholesterol in human volunteers. J Dairy Foods Home Sci, 12, 33–38.

Kim, G and Lee, BH (2005) Biochemical and molecular insights into bile salt hydrolase in the gastrointestinal microflora-a review. Asian Australasian Journal of Animal Sciences **18**: 1505

Kumar, R. S., Brannigan, J. A., Prabhune, A. A., Pundle, A. V., Dodson, G. G., Dodson, E. J., & Suresh, C. G. (2006). Structural and functional analysis of a conjugated bile salt hydrolase from *Bifidobacterium longum* reveals an evolutionary relationship with penicillin V acylase. Journal of Biological Chemistry.

M. Kumar, R. Nagpal, R. Kumar (2012). Cholesterol-lowering probiotics as potential biotherapeutics for metabolic diseases, Experimental Diabetes Research, vol. 2012, Article ID 902917, 14 pages, 2012.

Kurdi, P., Tanaka, H., van Veen, H. W., Asano, K., Tomita, F., & Yokota, A. (2003). Cholic acid accumulation and its diminution by short-chain fatty acids in bifidobacteria. Microbiology, 149(8).

Lack, L., & Weiner, I. M. (1966). Intestinal bile salt transport: structure-activity relationships and other properties. American Journal of Physiology-Legacy Content, 210(5), 1142–1152.

Lee, K., Paek, K., Lee, H. Y., Park, J. H., & Lee, Y. (2007). Antiobesity effect of trans-10, cis-12-conjugated linoleic acid-producing *Lactobacillus plantarum* PL62 on diet-induced obese mice. Journal of Applied Microbiology, 103(4), 1140–1146.

Liong, M.T. and Shah, N.P. (2005). Bile salt deconjugation ability, bile salt hydrolase activity and cholesterol co-precipitation ability of lactobacilli strains. International Dairy Journal 15, 391-398

Lin, S. Y., Ayres, J. W., Winkler, W., & Sandine, W. E. (1989). *Lactobacillus* Effects on Cholesterol: In Vitro and In Vivo Results1. Journal of Dairy Science, 72(11), 2885–2899.

Macdonald, I. A., Bokkenheuser, V. D., Winter, J., McLernon, A. M., & Mosbach, E. H. (1983). Degradation of steroids in the human gut. Journal of Lipid Research, 24(6), 675–700.

Mahrous, H., Shaalan, U. F., & Ibrahim, A. M. (2011b). The role of some probiotic lactic acid bacteria in the reduction of cho-

lesterol on mice. International Research Journal of Microbiology, 2(7), 242–248.

Mann, G. V., & Spoerry, A. (1974). Studies of a surfactant and cholesteremia in the Maasai. American Journal of Clinical Nutrition, 27(May), 464–469.

Mann, G. V. (1977). A factor in yogurt which lowers cholesteremia in man. Atherosclerosis, 26(3), 335–340.

Manson, J. E., Tosteson, H., Paul M, R., Satterfield, S., Herbert, P., O'Conner, G. T. &Hennekens, C. H. (1992). The Primary prevention of Myocardial infraction. The New England Journal of Medicine, 326, 1406–1416.

Moser, S. A., & Savage, D. C. (2001). Bile Salt Hydrolase Activity and Resistance to Toxicity of Conjugated Bile Salts are Unrelated Properties in *Lactobacilli*. Applied and Environmental Microbiology, 67(8), 3476–3480. https://doi.org/10.1128/AEM.67.8.3476-3480.2001

Nicolaou, M., Andress, E. J., Zolnerciks, J. K., Dixon, P. H., Williamson, C., & Linton, K. J. (2012). Canalicular ABC transporters and liver disease. The Journal of pathology, 226(2), 300- 315.

Nguyen, T. D. T., Kang, J. H., & Lee, M. S. (2007). Characterization of Lactobacillus plantarum PH04, a potential probiotic bacterium with cholesterol-lowering effects. International Journal of Food Microbiology, 113(3), 358–361.

Owen, R. W., Thompson, M. H., & Hill, M. J. (1984). Analysis of metabolic profiles of steroids in faeces of healthy subjects undergoing chenodeoxycholic acid treatment by liquid-gel chromatography and gas-liquid chromatography-mass spectrometry. Journal of Steroid Biochemistry, 21(5), 593–600.

Parvez, S., Malik, K.A., Kang, S.AH. & Kim, H.K. (2005). Probiotics and their fermented food products are beneficial for health. Journal of Applied Microbiology ISSN 1364-5072.

Patel, A. K., Singhania, R. R., Pandey, A., & Chincholkar, S. B. (2010). Probiotic bile salt hydrolase: Current developments and perspectives. Applied Biochemistry and Biotechnology.

Pereira, D. I. A., & Gibson, G. R. (2002). Cholesterol Assimilation by Lactic Acid Bacteria and Bifidobacteria Isolated from the Human Gut. Applied and Environmental Microbiology, 68(9), 4689–4693.

Peschel, A. (2002). How do bacteria resist human antimicrobial peptides? Trends in Microbiology.

Rajan, A. B., & Fathimathu Zuhara, K. (2018). Isolation screening and identification of bile salt hydrolase producing bacteria from waste samples, 11(1), 104–108.

Rašić, J. L., Vujičić, I. F., Škrinjar, M., & Vulić, M. (1992). Assimilation of cholesterol by some cultures of lactic acid bacteria and bifidobacteria. Biotechnology Letters, 14(1), 39–44.

Ridlon, JM, Kang, D-J and Hylemon, PB (2006). Bile salt biotransformations by human intestinal bacteria. Journal of Lipid Research **47**: 241–259.

Russell, DW (2009). Fifty years of advances in bile acid synthesis and metabolism. Journal of Lipid Research **50**: S120–S125

Sarkar, S. (2003). Potential of acidophilus milk to lower cholesterol. Nutrition & Food Science, 33(6), 273–277

Schaafsma, G., Meuling, W. J., van Dokkum, W., & Bouley, C. (1998). Effects of a milk product, fermented by Lactobacillus acidophilus and with fructo-oligosaccharides added, on blood lipids in male volunteers. European Journal of Clinical Nutrition, 52(6), 436–40.

Schaap, FG, Trauner, M and Jansen, PL (2014). Bile acid receptors as targets for drug development. Nature Reviews Gastroenterology & Hepatology **11**: 55–67

Schiff ER, Sorrell MF, Maddrey WC, editors. Schiff's Diseases of the Liver. Philadelphia: Lippincott, Williams & Wilkins; 2002. pp. 135–165.

Sindhu, S. C., & Khetarpaul, N. (2003). Effect of feeding probiotic fermented indigenous food mixture on serum cholesterol levels in mice. Nutrition Research, 23(8), 1071–1080.

Smet, I. De, Hoorde, L. Van, Saeyer, N. De, Woestyne, M. Vande, & Verstraete, W. (1994). in vitro study of bile salt hydrolase (BSH) activity of BSH isogenic *Lactobacillus plantarum* 80 strains and estimation of cholesterol lowering through enhanced BSH activity. Microbial Ecology in Health and Disease, 7(6), 315–329.

Sridevi, N., & Prabhune, A. A. (2009). Brevibacillus sp: A novel thermophilic source for the production of bile salt hydrolase. Applied Biochemistry and Biotechnology, 157(2), 254–262.

Sridevi, N., Pradnya, V., & Prabhune, A. (2009). Hypocholesteremic effect of bile salt hydrolase from Lactobacillus buchneri ATCC 4005. Food Research International, (42), 516–520.

Suckling, K. E., Benson, G. M., Bond, B., Gee, A., Glen, A., Haynes, C., & Jackson, B. (1991). Cholesterol lowering and bile acid excretion in the hamster with cholestyramine treatment. Atherosclerosis, 89(2–3), 183–190.

Takahashi, T., & Morotomi, M. (1994). Absence of cholic acid 7 alpha-dehydroxylase activity in the strains of *Lactobacillus* and *Bifidobacterium*. J Dairy Sci, 77(11), 3275–3286.

Taranto, M. P., Fernandez Murga, M. L., Lorca, G., & De Valdez, G. F. (2003). Bile salts and cholesterol induce changes in the lipid cell membrane of *Lactobacillus reuteri*. Journal of Applied Microbiology, 95(1), 86–91.

Taranto, M. P., Sesma, F., Pesce De Ruiz Holgado, A., & De Valdez, G. F. (1997). Bile salts hydrolase plays a key role on cholesterol removal by *Lactobacillus reuteri*. Biotechnology Letters, 19(9), 845–847.

Thomas, L. A., Veysey, M. J., Bathgate, T., King, A., French, G., Smeeton, N. C. & Dowling, R. H. (2000). Mechanism for the transit-induced increase in colonic deoxycholic acid formation in cholesterol cholelithiasis. Gastroenterology, 119(3), 806–815.

Thomas, L. A., Veysey, M. J., Murphy, G. M., & Dowling, R. H. (2001). Influence of pH on the phase distribution of nascent deoxycholic acid in fresh human cecal aspirates. American Journal of Physiology-Gastrointestinal and Liver Physiology, 281, G371–G374.

Tsai, C.-C., Lin, P.-P., Hsieh, Y.-M., Zhang, Z., Wu, H.-C., & Huang, C.-C. (2014). Cholesterol-lowering potentials of lactic acid bacteria based on bile-salt hydrolase activity and effect of potent strains on cholesterol metabolism in vitro and in vivo. The Scientific World Journal, 2014.

Van Eldere, J., Celis, P., De Pauw, G., Lesaffre, E., & Eyssen, H. (1996). Tauroconjugation of cholic acid stimulates 7 alpha-dehydroxylation by fecal bacteria. Applied and Environmental Microbiology, 62(2), 656–61.

Xiao, J. Z., Kondo, S., Takahashi, N., Miyaji, K., Oshida, K., Hiramatsu, A &tHosono, A. (2003). Effects of Milk Products Fermented by *Bifidobacterium longum* on Blood Lipids in Rats and Healthy Adult Male Volunteers. Journal of Dairy Science, 86(7), 2452–2461.

Medical
Communication

Biosci. Biotech. Res. Comm. 12(1): 156-161 (2019)

BBRC
Bioscience Biotechnology
Research Communications

Detection of poly cystic ovarian syndrome (PCOS) using follicle recognition techniques

T. Abirami* and S. Palanivel Rajan

Department of Electronics and Communication Engineering, M. Kumarasamy College of Engineering, Karur, Tamilnadu, India

ABSTRACT

Now a days most of the females are facing the problems of infertility in the age group of 22 to 35. In order to analyze and classify the problems, one can start with making the decision of comparing the normal ovary and affected ovary structurally using advanced techniques. The two images have to be taken and can be compared using the accurate images for detecting the affected ovary or its areas. Using the feature extraction method, the image can be further diagnostically extracted. Then the image can be processed by segmentation and finally it can be detected and subjected to a diseased degree classification. The method used here is Support Vector Machine (SVM) with Fuzzy Logic. SVM algorithm is used to classify and regression analysis. It works on the concept of partial truth, where the given value might range between absolutely true and absolutely false. Histogram adjustment calculation is connected to get a complexity improved picture. The wiener channel is the greatest appropriate decision for diminishment of clamor in ovarian using the ultrasound picture. The results are distinguished and then taken for physical request from the experts. Exactness of system can be approximately 95%. Subsequently, this figuring can be customized by screening of Poly Cystic Ovarian Syndrome problems.

KEY WORDS: POLYCYSTIC OVARIAN DETECTION (PCOD), BODY MASS INDEX (BMI), FOLLICLE-STIMULATING HORMONE (FSH) AND LUTEINIZING HORMONE (LH)

ARTICLE INFORMATION:

Corresponding Author: abiramit.ece@mkce.ac.in
Received 22nd Dec 2018
Accepted after revision 3rd March 2019
BBRC Print ISSN: 0974-6455
Online ISSN: 2321-4007 CODEN: USA BBRCBA
Thomson Reuters ISI ESC / Clarivate Analytics USA
NAAS Journal Score 2019: 4.31 SJIF: 4.196

Online Contents Available at: http//www.bbrc.in/
DOI: 10.21786/bbrc/12.1/20

Many females of reproductive age suffer with the disorders Polycystic Ovarion Syndrome commonly known as PCOS. It is a heterogenous endocrine disorder and is most common among the young generation. Though the exact cause for this disorder is unknown factors, like hormonal imbalance, central or overall obesity and having Body Mass Index greater than 24 can be considered as some of its causes (Abirami et al. 2018). This may result is abnormal ovulation, with absence of or irregular menstrual cycle, infertility conditions called as called as amenorrhea, (Vijayprasath et al. 2015). It also results in release of additional quantity of androgenic hormones and it's effects are frustrating. This leads to acne and insulin resistance which is often accompanied by obesity, high cholesterol levels and type 2 diabetes. The diagnosis procedures usually followed are the ovarian ultrasound images which show ovaries with the disorder having multiple cysts. But it cannot be stated as the only symptom for the disorder. Huge variety in the side effects and seriousness of the problem has been seen in some females, (Annakamatchi et al. 2018).

Few methodologies are used to identify the PCOD problems. These are medical, biological, and the ovarian ultrasound imaging which are used to find the problem. A patient can be examined as affliction from PCOD or not, if the any of two from the three situations are given below: (1) Prolonged ovulation or portrayed by sporadic menses series, (2) Additional measures which are caused by membrane breakdown, besides raised serum chemicals and (3) Occurrence of polycystic ovaries realized by the image of gynecologic ultrasounds, (Choudhary et al. 2015).

For an ordinary and sound ovary just a single follicle develops in a size of 20mm in width, develops and is prepared for ovulation, under right levels of FSH and LH hormones[1]. But in the case of PCOS affected ovary many small follicles of size 12 or more than that and about 2-9 mm in diameter is found dispersed along the periphery of the ovary which is medically termed as 'necklace formation'. Hence the volume of ovary will raise above 10 cm3 in PCOS affected patients (Dinesh et al. 2015a). Figure 1 indicates ultrasound picture of typical ovary demonstrating just a single follicle prepared for ovulation and figure 2 depicts the scenario in which various little follicles are found in the edge of ovary (Dinesh et al. 2015b).

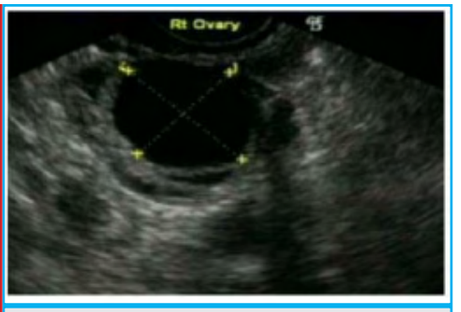

FIGURE 1. Normal ovary

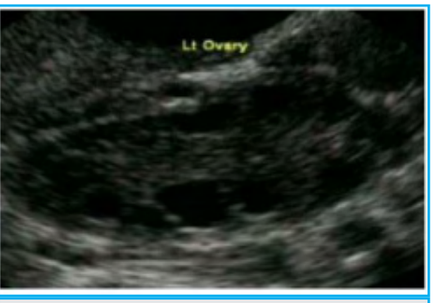

FIGURE 2. PCOD affected ovary

In this paper, the images have been tested and affected by PCOS tended to by all the three techniques. Ovarian ultrasound pictures have been gathered for around 20 patients either with or without PCOS side effect alongside values for the measuring parameters of PCOS (Essam et al. 2018). This process is carried out with a 6MHz ultrasound transducer. Techniques such as enhancement of contrast and then filters are used to increase the excellence of the images can be obtained. Highlight extraction incorporates were done by removing dull or splendid highlights from the first picture. Divisional identification was carried from which the coveted areas are chosen utilizing qualities such as size, area, compactness and so forth, (Kavitha et al. 2017). The facts were utilized for the compactness which was constructed from the count of follicles acquired in the overhead process and medical and biological information was gathered from specialists, characterization was completed by the algorithm following the method of Keerthi et al. (2018).The Process Flow of PCOS detection is shown in figure.3

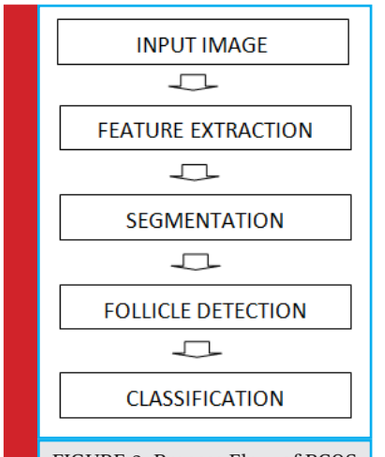

FIGURE 3. Process Flow of PCOS detection

The outcomes are noted and it is contrasted with finding the manual location with figure exactness of the proposed calculation. The stream of process is given beneath in the figure.3. Medical ultrasonography produces poor quality images of high noise content and low contrast. For upcoming processes such as feature extraction, segmentation and follicle detection high quality images are required (Vijayprasath et al. 2012). Hence it is necessary to remove the noise and improve the contrast of images (Rajan 2014). The preprocessing technique involves improving the quality of images with the help out of distinction improvement and filtering methodologies. Contrast enhancement which was the first step in preprocessing improves the contrast of ovarian ultrasound images using different global and local techniques (Rajan 2015). This paper focuses to contrast enhanced image and performances are calculated based on Signal-to-Noise ratio (SNR) given in equation 1 where is the variance of original image and is the variance of enhanced image.

$$SNR(in\ decibels = 10 \log_{10} \frac{\sigma^2}{\sigma_{\hat{i}}^2} \quad (1)$$

Table 1. SNR value of different filtering techniques

Image/filtered image	Signal-to-noise ratio (SNR) in dB
Original image	1.935
Averaging filter	4.0058
Median filter	4.247
Gaussian filter	4.1546
Wiener filter	4.2597

In table 1, the signal to noise ratio of different filtering methods are illustrated. From the table original image is a ultrasound image. If processing of original image may give wrong results. So that the original image can be processed for filtering to remove the noise and enhance the contrast for further processing. Here different filtering methods are carried out. Signal to Noise Ratio (SNR) is calculated for various methods of filtering. Examples Median Filtering, Averaging Filtering, Gaussian Filtering, Wiener Filtering. The output of preprocessing stage is given the figure

In the ovarian image using the ultrasound picture, aside since follicles, endometrial veins, lymph hubs, nerve strands and stroma is seen (Ramakrishnan et al. 2018). Hence, it is to be reduced the incorrect discovery, include removals are finished through utilizing Multistage morphological method, for the situation Top-cap change. White and Dull highlights dismiss be removed after the picture and later the subsequent picture is deducted from

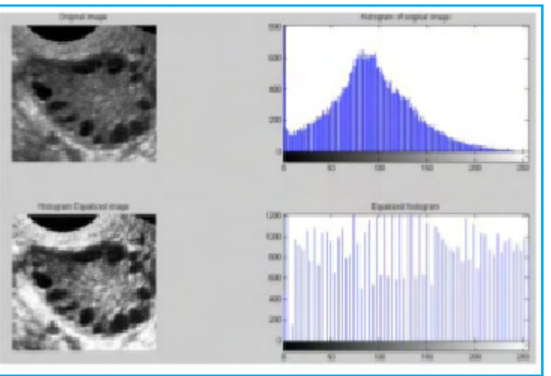

FIGURE 4. Output image of pre-processing stage

sole picture to become differentiate improved picture on (Sukanesh et al. 2013). In the calculation the change assistances by the extraction of brilliant highlights since the foundation by means of utilizing morphological initial and finish task in an organizing component individually[5]. The organizing component utilized as a part of this case is a plate organizing component (Ramesh et al. 2018). The splendid best cap change is characterized as the contrast between the information picture and its opening by the basic component. Then again, dark best cap change is characterized as the contrast between shutting by same basic component and information picture[6]. On the off chance that is an organizing component, at that point splendid and dull best cap changes can be given as in equation 2 and 3 individually (Rajan et al. 2013).

$$T_w^{(f)} = f - f \circ b(x) \quad (2)$$

$$T_b^{(f)} = f \bullet b(x) - f \quad (3)$$

Picture division is utilized to distinguish wanted highlights with the goal that the consequential picture being less demanding to investigate[7] (Ribana et al. 2018). The different methodologies have been suggested and second-hand for picture division like edge area, edge, etc., various edge distinguishing proof practices can be utilized for the division of ovarian picture. In the edge identification method, focuses in picture are documented where picture brilliance changes pointedly or consumes discontinuities, in the picture, get after linearization[8]. In binaries picture, pixel esteems at all the specific focuses or the areas alteration all of a sudden from 0 to 255 (i.e. dull to brilliant) and the other way around. Every one of these focuses is sorted out into an arrangement of bended line sections to recognize the edges (Rajan et al. 2012).

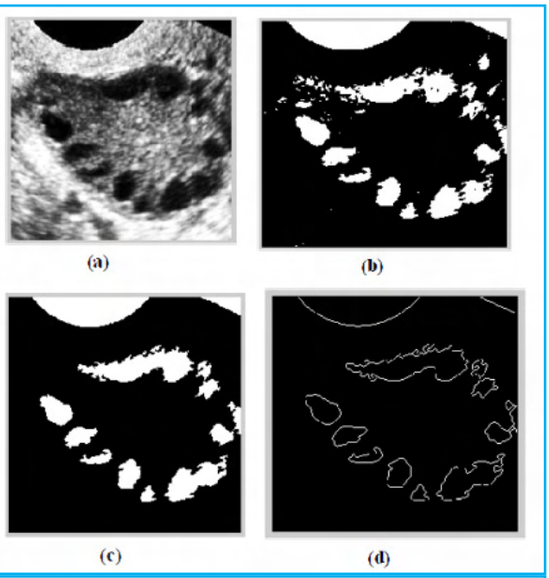

FIGURE 5. (a) Image obtained after feature extraction(b) Image obtained after linearization (c) Image obtained for important follicle detection (c) Follicular boundaries detected after canny edge detection

Table 2. Parameters taken for classification of PCOS

Parameters	PCOS Affected	Normal (Not affected by PCOS)
No. of follicle	>8-10	1 Dominant
BMI (kg/mL)	> 24	<=24
Menstrual cycle	>32	28-32
LH (lU/L)	>8	2-8
FSH (lU/L)	>5	2-5

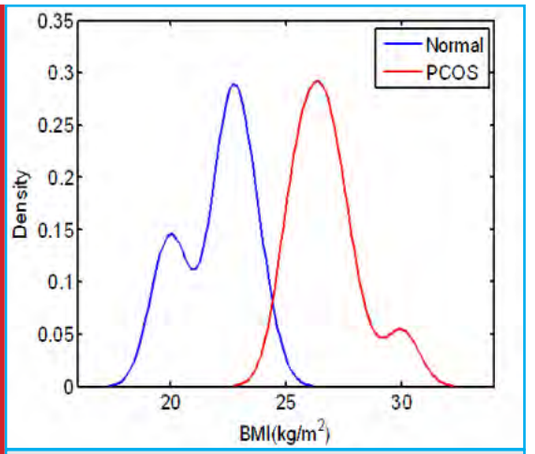

FIGURE 6. Plot Vs Density and BMI

Vast number of highlights is recognized after binarization what's more, edge identification (Sivagurunathan et al. 2018). To isolate out imperative follicles from identified highlights, criterion for example highest and lowest amount of follicles, zone, eroticism as well as smallness must be additionally taken for the calculation. Consider the follicles are round fit as a fiddle, isolate locales will associate with 4-80 mm^2 for PCOS ovary and around 314 mm^2 for common place ovarian follicle. Although it is accredited with the purpose of the follicles are circuitous alive and well, whim is generally comparable to 1 (Sivaranjani et al. 2018). Thinking about every one of these qualities for edge, region of each identified area or highlight is figured and number of essential follicles identified is discovered. In Figure 4, the Image can be obtained after all the process image extraction (Sukanesh et al. 2010a).

The number of ovarian follicles is not an only matter for the problem of PCOS and also it has to measure the parameters of BMI, cycle length, post menstrual FSH and LH10 (Sukanesh et al. 2010b). In every image of the parameter is close at hand of number of follicles is measured and it shown patients are having the problem otherwise it is not showing it to the maximum level[14]. Here comparing the parameters of Normal Patient with the PCOS affected patients are given in table 1. The parameters were No. of follicle, BMI (kg/mL), Period Cycle, LH (lU/L), FSH (lU/L). The follicle may present in normal patient also but the number should be only one, and value of BMI (Body Mass Index) is about to be less than or equal to 24[15]. The menstrual cycle also taken as 28 days to 32 days if it is more than 32 days three will be a problem of PCOS. The value of LH and also FSH

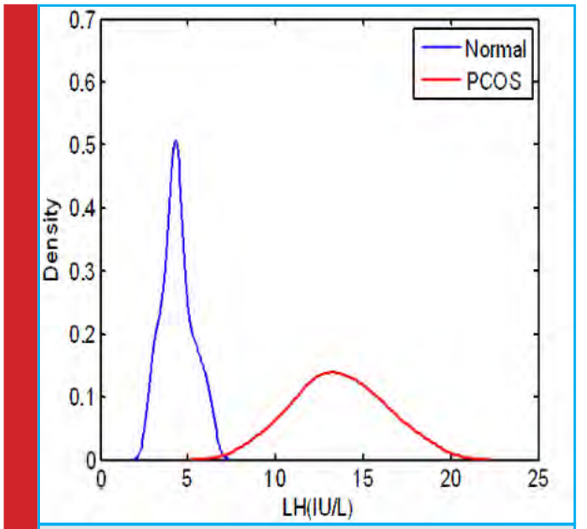

FIGURE 7. Kernel Density plot for LH

Table 3. Classification of PCOS and Normal patients

Data Sets	BMI	Cycle Length	FSH	LH	Follicles	Result
Data Set A	25.03-26.87	38	5.76	13.08	7	PCOS
Data Set B	20.47-22.04	26	3.4	4.4	1	Normal
Data Set C	24.67-26.34	32	3.98	3.18	2	Normal
Data Set D	25.09-25.39	36	6.07	15.66	10	PCOS
Data Set E	21.94-22.69	28	1.78	4.28	1	Normal

are also compared with PCOs and the Normal patients. With these above parameters are helped to classify the problems to be taken[16].

The different set of images are monitored and preliminary 15 number of data's is used for setting up for computation, course of action of subsequently 5 instructive lists is finished. The system is frequently for instructive record of the impressive number of patients. It is used for planning the data sets and gathering of all the information. Outcomes acquired be contrasted and individuals gotten by physical grouping and commencing to specialists. In the figure 6, it shows the graph between BMI vs density. It is used to predict PCOS ovary or normal ovary.

The both information's are taken into account and number of follicles are identified and in the above process are utilized for order utilizing in SVM calculation. Motion to-commotion proportions (SNR) are computed for unique picture and for each separated picture and outcomes are gotten by way of appeared in the table 1. From this, it can be derived that wiener channel is the greatest appropriate decision for diminishment of clamor in ovarian using the ultrasound picture.

In the figure 7, it shows the graph between kernel densities with LH. The Wiener sifted picture is utilized for additional processing.

In the given table 3, already the parameter taken for classification of PCOS illustrated in Table 2. 5 different data sets are taken to find the values of BMI, Menstrual Cycle, FSH, LH, No of Follicles. After finding the values of all the parameters comparing with the table No:2 and it will help to decide or classify the Normal patient or PCOS affected patients. Training sets are available to make decision of PCOS affected or not.

At last it has been concluded with a robotized procedure for Polycystic Ovarian Syndrome area using follicle affirmation as well as portrayal by means of Support Vector Machine. Picture is to be preprocessed and it is (differentiate upgrade and sifting) utilized for enhancing nature of the picture. Highlights are removed utilizing Multiscale morphological approach and brilliant best cap change. The picture is binarized and portioned utilizing watchful edge discovery method. Critical follicles are isolated from different areas utilizing region and unpredictability limit. Grouping of the considerable number of information is finished utilizing the SVM algorithm for calculation. The results have been achieved and the accuracy is about 95%. In the same way, this estimation has been done by enough number of modified screenings of PCOS.

REFERENCES

Abirami T,Ramesh L (2018) Bio-Nano Things: Organically stimulated Bio-Cyber Interface Architecture, International Journal of Pure and Applied Mathematics 119(15), 3257-3262

Annakamatchi M, Keralshalini V (2018) Design of Spiral Shaped Patch Antenna for Bio-Medical Applications. International Journal of Pure and Applied Mathematics 118(11): Pages 131-135.

Choudhary, J. Chowdhary, M.L. Swarankar, et al., (2015) Predictive value of subendometrial–endometrial blood flow assessment by transvaginal 3D power doppler on the day of HCG on clinical outcome of IVF cycles, Int. J. Res. Med. Sci. 3 3114.

Dinesh T, Palanivel S (2015a) Systematic Review on Wearable Driver Vigilance System with Future Research Directions. International Journal of Applied Engineering Research 2(2): Pages 627-632.

Dinesh T, Palanivel S (2015b) Statistical Investigation of EEG Based Abnormal Fatigue Detection using LabVIEW. International Journal of Applied Engineering Research 10(43): Pages 30426-30431

Essam R. Othman, Karim S.Abdullah, Ahmed M.Abbas, Mostafa Hussein(2018), Elwany Elsnosy, Ihab H.EI-Nashar, "Evaluation of endometrial and subendrometrial vascularity in obese women with polycystic ovarian disease" Middle East Fertility Society Journal 23, pages 324–330

Kavitha V, Palanivel Rajan S (2017) Diagnosis of Cardiovascular Diseases using Retinal Images through Vessel Segmentation Graph. Current Medical Imaging Reviews 13(4).

Keerthi S, Dhivya S (2017) Comparison of RVM and SVM Classifier Performance in Analysing the Tuberculosis in Chest X Ray. International Journal of Control theory and Applications 10(36): Pages 269-276.

Palanivel Rajan S (2014) A Significant and Vital Glance on "Stress and Fitness Monitoring Embedded on a Modern Telematics Platform. Telemedicine and e-Health Journal 20(8): Pages 757-758.

Palanivel Rajan S (2015) Review and Investigations on Future Research Directions of Mobile Based Tele care System for Cardiac Surveillance. Journal of Applied Research and Technology 13(4): Pages 454-460.

Ramakrishnan P, Sivagurunathan P T (2018) Wireless Patient Monitoring systems. International Journal of Pure and Applied Mathematics 118(11): Pages 761- 766.

Ramesh L, Abirami T (2018) Segmentation of Liver Images Based on Optimization Method. International Journal of Pure and Applied Mathematics 118 (8) : Pages 401-405.

Rajan S P, Sukanesh R (2013) Viable Investigations and Real Time Recitation of Enhanced ECG Based Cardiac Tele-Monitoring System for Home-Care Applications: A Systematic Evaluation. Telemedicine and e-Health Journal 19(4): Pages 278-286.

Rajan S P, Sukanesh R, Vijayprasath S (2012) Performance Evaluation of Mobile Phone Radiation Minimization through Characteristic Impedance Measurement for Health-Care Applications. IEEE Digital Library Xplore.

Ribana K, Pradeep S (2018) Contrast Enhancement Techniques for Medical Images. International Journal of Pure and Applied Mathematics 118: Pages 695-700.

Sivagurunathan P T, Ramakrishnan P (2018) A Survey on Wearable health Sensor– Based System Design. International Journal of Pure and Applied Mathematics 118(08): Pages 383 -385.

Sivaranjani S, Kaarthik K (2018) Medical Imaging Technique to Detect Tumor Cells. International Journal of Pure and Applied Mathematics, 118(11): Pages 399 – 404.

Sukanesh R, Gautham P, Rajan S P, Vijayprasath S (2010a) Cellular Phone based Biomedical System for Health Care. IEEE Digital Library Xplore: Pages 550-553.

Sukanesh R, Palanivel Rajan S (2013) Experimental Studies on Intelligent, Wearable and Automated Wireless Mobile Tele-Alert System for Continuous Cardiac Surveillance. Journal of Applied Research and Technology 11(1): Pages 133-143.

Sukanesh R, Rajan S P, Vijayprasath S (2010b) Intelligent Wireless Mobile Patient Monitoring System. IEEE Digital Library Xplore: Pages 540-543.

Vijayprasath S, Sukanesh R, Rajan S P (2012) Experimental Explorations on EOG Signal Processing for Real Time Applications in LabVIEW. IEEE Digital Library Xplore.

Vijayprasath S, Rajan S P (2015) Performance Investigation of an Implicit Instrumentation Tool for Deadened Patients Using Common Eye Developments as a Paradigm. International Journal of Applied Engineering Research 10(1): Pages 925-929.

Medical
Communication

Biosci. Biotech. Res. Comm. 12(1): 162-168 (2019)

BBRC
Bioscience Biotechnology
Research Communications

Annexin A2 mediated posttranscriptional destabilization of BRCA1 mRNA in sporadic breast cancer

Anil Bapu Bargale[1,3,4], Jayarama Shetty K[2], Suchetha Kumari N[5], Vidya S Patil[4], R D Kulkarni[6], Rajesh Kumar Manne[7], Sarath Kumar E[3] and Praveenkumar Shetty[3,4]

[1]Ph D Scholar, K S Hegde Medical Academy, NITTE University, Mangalore, India
[2]Department of Radiotherapy & Oncology, K S Hegde Medical Academy, NITTE University, Mangalore
[3]Central Research Laboratory, SDM College of Medical Sciences & Hospital, Dharwad, India
[4]Department of Biochemistry, SDM College of Medical Sciences & Hospital, Dharwad, India
[5]Department of Biochemistry, K S Hegde Medical Academy, Mangalore, NITTE University, Mangalore
[6]Department of Microbiology, SDM College of Medical Sciences & Hospital, Dharwad, India
[7]Cancer Biology division, National Centre for Cell Science, Pune

ABSTRACT

BRCA1 is a nuclear phosphoprotein involved in genome integrity by regulating cell cycle checkpoints, DNA repair and apoptosis. BRCA1 down regulation occurs in sporadic breast cancer (BC). Posttranscriptional regulation of gene expression has evolved as a means of fine-tuning of protein levels. There are several posttranscriptional regulatory motifs, including CU-rich, U-rich and AU-rich elements, which are usually located in the 5' and 3' UTR's. Post-transcriptional regulation of BRCA1 is poorly characterized and underappreciated. To elucidate the molecular mechanism of AnxA2 mediated posttranscriptional regulation of BRCA1 mRNA in sporadic breast cancer. In order to investigate BRCA1 mRNA levels in MDAMB-231 & MCF-7 cells, we conducted DRB chase experiment. The BRCA1 mRNA destabilization is significantly increased upon AnxA2 induction in MCF-7 cells. Further we knocked down AnxA2 in MDAMB-231 cells we found, BRCA1 mRNA stabilization which proves AnxA2 destabilizes BRCA1 mRNA. In RIP-CHIP experiment we found BRCA1 immunoprecipitated with AnxA2. This supports our finding that AnxA2 has role in the regulation of BRCA1 at mRNA level. Luciferase reporter assay showed decrease in luciferase activity with BRCA1 3'UTR. On treating with AnxA2 binding oligo from BRCA1 3'UTR showed decrease in cell viability.

KEY WORDS: ANXA2, BRCA1, RNA BINDING PROTEIN, RENILLA LUCIFERASE

ARTICLE INFORMATION:

Corresponding Author: anymh9832@rediffmail.com
Received 12th Jan 2019
Accepted after revision 27th March 2019
BBRC Print ISSN: 0974-6455
Online ISSN: 2321-4007 CODEN: USA BBRCBA
Thomson Reuters ISI ESC / Clarivate Analytics USA
NAAS Journal Score 2019: 4.31 SJIF: 4.196

Online Contents Available at: http//www.bbrc.in/
DOI: 10.21786/bbrc/12.1/21

INTRODUCTION

Breast Cancer (BC) is one of the leading causes of death among women and has 10% life time risk of developing malignancies in many countries in the western world (Newman 1988). Hereditary BC Syndrome accounts for 5-10% of all BC cases, while the other 90-95% of BC is "Sporadic. According to Population Based Cancer Registry (PBCR); In India, Breast cancer accounts for 25 - 35% of all female cancers in metro cities like; Mumbai, Delhi, Bengaluru, Kolkata, Chennai, Ahmadabad, Bhopal, etc. and it is second common cancer in rural areas. This implies, practically, one fourth of all female cancer cases are breast cancers, (Adnan 2018). Several studies have been reported the evidences, suggesting involvement of BRCA1 in the etiology of sporadic breast and ovarian cancer through reduced expression. Decreased levels of BRCA1 mRNA are frequently observed in breast tumors, (George 1998, Adnan, 2018, Nicolas 2018, Harahap 2018, Huszno 2019).

Lower or undetectable levels of expression of the BRCA1 protein have been observed in sporadic BC (McCoy 2003). Different mechanisms have been shown to be responsible for the reduced expression of BRCA1; epigenetic silencing of the BRCA1 gene at the transcriptional level by means of promoter methylation is another mechanism involved (Das 2004, Choic 2009, Robertson 2002, Baylin 2006). The BRCA1 gene was identified and cloned in 1994. BRCA1 known for its multiple vital functions such as tumor suppressor activity, including roles in cell cycle progression, DNA damage repair processes DNA damage responsive cell cycle check point regulation of a set of specific transcriptional pathways and apoptosis (Rice 1998). Since, BRCA1 gene is rarely mutated in sporadic breast cancer. It has been suggested that, dysregulation of BRCA1 expression causes reduced mRNA or protein levels in BC (Thompson 2011).

Post-transcriptional regulation of gene expression has evolved as a mean of fine tuning protein levels and generating rapid temporal or spatial changes in protein expression following an environmental stimulus (Saunus 2008). Regulation of the dynamics of mRNA molecule is a wide spread phenomenon and there are many such examples of genes regulated in this way including tumor suppressor genes (Rosen 2003, Maity 1997). The mechanisms often involve RNA-binding proteins and non-coding RNAs (transacting factors) which recognizes sequence motif in their target transcripts and 'tag' them for recognition by macromolecular complexes involved in RNA metabolism such as mRNA transport granules, RNA induced silencing complexes (RISC), the exosome, GW bodies and stress granules(Thanin 2018, Cok 2001, Fu 1997, anderson 2006). There are many examples of post-transcriptional regulatory motifs, including CU-rich, U-rich and AU-rich elements which are usually located regions of regulated transcripts (Moore 2005, Kedeersha 2002, Engels 2006). It can be difficult to predict the regulatory functions of individual motif based on primary sequence alone, as they often associate with multiple transacting factors with different and sometimes opposing activities.

BRCA1 is post-transcriptionally regulated by mRNA binding proteins, the identity of which is unknown. HuR is an RNA binding protein already proven to play role in the event of post-transcriptional regulation of BRCA1 by Jodi M Saunus et al. HuR is ubiquitously expressed RNA binding protein that regulates the stability and translation of transcripts that function in multiple cellular pathways, such as p21WAFI, COX, TP24, Cyclin A and B and P27. As like HuR other mRNA binding proteins like Annexin A2 (AnxA2) expression increases in basal breast cancer where BRCA1 expression is very less or null. AnxA2 is a multifunctional calcium dependent phospholipid binding protein. AnxA2 shows functional diversity like it regulates membrane traffic and cytoskeleton organization, extracellular activities and targeted gene disruption (Lopez 2005). AnxA2 is highly expressed in the surface of human tumor cells and promotes cell migration and invasion by activating plasminogen and cleaving extracellular matrix[25]. AnxA2 stimulates cell proliferation, angiogenesis and invasion (Wein 2003, Wiklund 2002, Maji 2016, Volker 2002). This study demonstrates the hypothesis of AnxA2 mediated post-transcriptional regulation of tumor suppressor BRCA1 gene contributes to the development and progression of sporadic breast cancer.

MATERIALS & METHODS

Cell Culture

Human breast cancer cell lines, MDA-MB-231 and MCF-7 were obtained from National Center for cell Sciences (NCCS), Pune and grown in respective media as prescribed by the supplier.

Real Time RT-PCR

Total RNA was isolated using TRIZOL (Invitrogen). cDNA was synthesized using RevertAid First strand cDNA synthesis kit by Thermo Fischer scientific with following primers; For BRCA1 (F: 5'-GGTTCTGATGACTCACATGATGGG-3'&R: 5'-TCTGTGGCTCAGTAACAAATGCTC-3'),AnxA2(5'TAACTTTGATGCTGAGCGGG-3'&R:5'-TAATTTCCTGCAGCTCCTGG-3') and for GAPDH (5'-GAGCGAGATCCCTCCAAA-3' & R: 5'-ACTGTGGTCATGAGTCCTTC-3'. BRCA1, AnxA2 & GAPDH were amplified by DyNAmo Color Flash SYBR Green q-PCR kit (Thermo Fischer scientific) on Cepheid Smart cycler. PCR set up for

BRCA1 was 2 minutes for 95^0 C for one cycle, followed by 30 second 94^{0}C, 55^{0}C & 72^{0}C for 35 cycles. PCR reaction set up for AnxA2 & GAPDH used was 2 minutes at 95^{0}C and 40 cycles of 30 s at 95^{0}C, 30 s at 54^{0}C, and 30 s at 68^{0}C. The comparative ΔCt method was used to determine relative BRCA1, AnxA2 mRNA expression.

RNA stability:

RNA stability was analyzed by transcription-chase experiment. The cells were stimulated to over express BRCA1 & AnxA2 by selected agonists respectively and then treated with DRB to inhibit ongoing transcription, after which total RNA was isolated at selected time points and cDNA was synthesized and amplified as described earlier.

RNA Immunoprecipitation: Formaldehyde was added to cosslink protein-RNAs in MDAMB-231 Cells grown in specific medium, at RT after 15 minutes stopped by addition of 2M glycine and incubated for 5 minutes. Cells were collected in 500µl of RIPA lysis buffer containing RNase inhibitor. The lysate was centrifuged at 12000g. Annexin A2 specific primary antibody added and incubated at 4^{o}C overnight on shaker. 50 µl of Protein A/G beads added to the lysate and incubated at 4^{o}C for 4 hours. The lysate was washed twice with RIPA lysis buffer. The crosslinking reversed by 6µl of 5M NaCl and 20 µg of proteinase k added to the lysate and incubated 1 hour at 42^{o}C and 1 hour at 65^{o}C. RNA was extracted by following TRIZOL RNA extraction protocol. RNA was reverse transcribed and amplified for BRCA1 by specific primers as described earlier. PCR products were resolved on ethidium bromide–stained 1.5% agarose gel.

Luciferase reporter assays

Luciferase reporter used was BRCA1 3'UTR luciferase reporter construct, made by ligating the full-length BRCA1 3'UTR downstream of the luciferase of pLuc. MDAMB-231 cells in 12 well plates were transiently transfected with equimolar amounts of luciferase reporter constructs. After 24 h of luciferase expression, Firefly luciferase reporter activity was determined relative to Renilla using a Dual Luciferase Reporter Assay kit (Promega) and Promega Luminometer.

MTT assay:

The MTT (3-(4, 5-dimethyl-2-thiazolyl)-2,5-diphenyl-2H-tetrazolium bromide) assay conducted to check cell proliferation by transfecting the MDAMB-231 cells by 50 oligo nucleotide specific binding to BRCA1 3'UTR analyzed by NCBI BLAST software and read by Epoch analyzer.

RESULTS & DISCUSSION

A detailed understanding of the mechanisms regulating BRCA1 expression is very much essential to identify the regulatory abnormalities in breast cancer (Diaz 2004, Blasi 1999). Reduction in BRCA1 expression in sporadic breast cancer is well documented (Tarui 2002). In our earlier data, we have demonstrated that the expressions of BRCA1 and AnxA2 protein are reciprocally regulated, which indicate the possibility of AnxA2 involvement in BRCA1 posttranscriptional regulation. The posttranscriptional regulation of BRCA1 in the sporadic breast cancer is underappreciated and poorly studied. This study suggests BRCA1 mRNA stability is regulated by AnxA2 in sporadic breast cancer (Wein 2003, Wiklund 2002, Huszno 2019).

BRCA1 & AnxA2 mRNA expression in different cells

Levels of BRCA1 & AnxA2 mRNA were analyzed in BT-549, MCF-7 & MDAMB-231 cells. We found abundant AnxA2 mRNA in MDAMB-231 & BT-549 cells than MCF-7. On the other hand MCF-7 cells showed abundant BRCA1 mRNA as compared to BT-549 & MDAMB-231 (Figure 1).

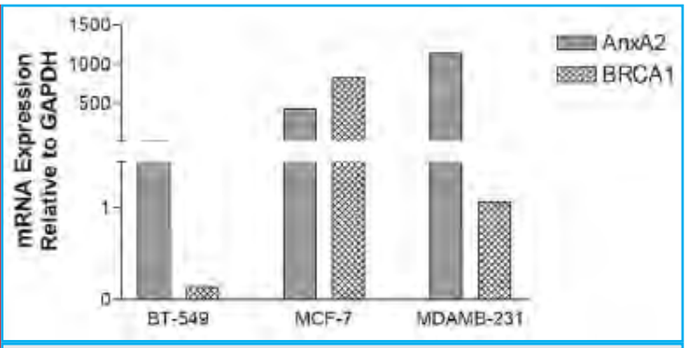

FIGURE 1. BRCA1 & AnxA2 mRNA expression in BT-549, MCF-7 & MDAMB-231 cells

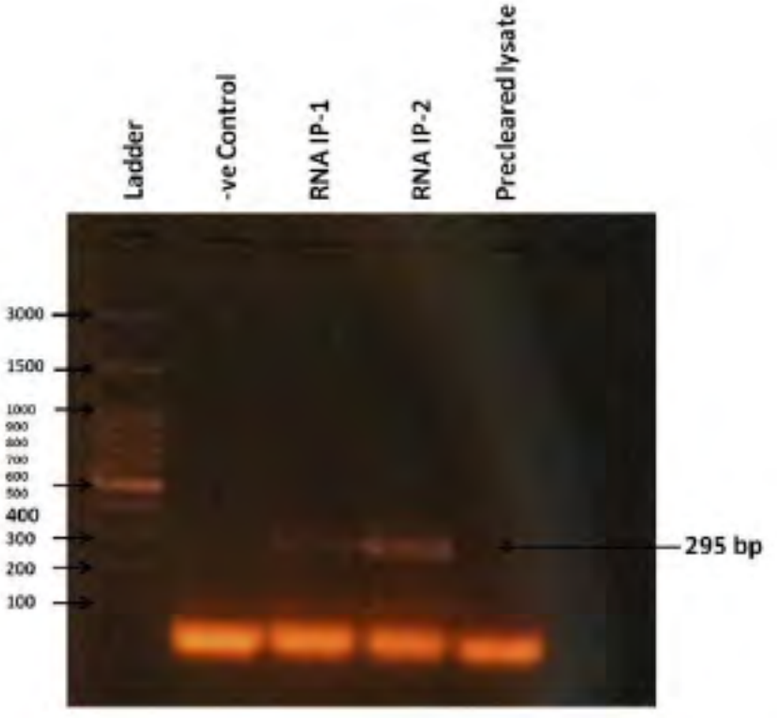

FIGURE 2. RNA Immunoprecipitation assay - anti AnxA2 antibody and BRCA1 specific primers. AnxA2 coimmunoprecipitates with BRCA1 mRNA in MDAMB-231 breast cancer cells. BRCA1 PCR products were undetectable without anti AnxA2 antibody. Lane -1 without AnxA2 antibody, Lane-2 & 3 with AnxA2 antibody and Lane - 4 Pre-cleared cell lysate.

Endogenous AnxA2 and BRCA1 mRNA are binding partners

To determine the association between endogenous AnxA2 and BRCA1 mRNA transcripts, we performed an IP-RT-PCR assay using an anti AnxA2 antibody and BRCA1 specific primers. We are able to show that AnxA2 coimmunoprecipitates with BRCA1 mRNA in MDAMB-231 breast cancer cells (figure 2). Conversely, BRCA1 PCR products were undetectable without anti AnxA2 antibody. The results provide clear evidence that AnxA2 associates with BRCA1 mRNA TNBC cells.

AnxA2 Regulates BRCA1 Post-transcriptionally

To address AnxA2 associated with BRCA1 mRNA, we investigated the effect of AnxA2 over expression on the regulation of BRCA1 mRNA stability. MCF-7 cells were induced to over express AnxA2 and studied the effect on BRCA1 mRNA stability. We observed decreased BRCA1 mRNA stability with time dependent manner, which shows AnxA2 overexpression degrades BRCA1 mRNA. To validate, AnxA2 associated in the regulation of BRCA1 mRNA. We knocked down AnxA2 by specific siRNA in MDAMB-231 cells and analyzed for BRCA1 mRNA stability. We found increase in BRCA1 mRNA stability in time dependent manner (figure 3). This shows AnxA2 is involved in regulation of BRCA1 mRNA. To study whether post-transcriptional regulation of BRCA1 occurs in sporadic breast cancer, we investigated BRCA1 expression and mRNA stability by DRB chase experiment. BRCA1 mRNA was normalized to control mRNA. We observed decrease in BRCA1 mRNA stability when we over expressed AnxA2 in TNBC cells. Interestingly, when we knocked down AnxA2 by AnxA2 specific siRNA we found increase in BRCA1 mRNA stability (figure 3). This data suggests that AnxA2 may be involved in the post transcriptional processes as well as in the destabilization of BRCA1 mRNA (Tali 2017, Harahap 2018, Zhang 2018).

To investigate, AnxA2 is involved in the regulation of BRCA1 mRNA through the binding of BRCA1 3'UTR region. We designed pLuc vector having multiple cloning site downstream to a luciferase reporter gene in the coding region. The cloning of BRCA1 3'UTR construct

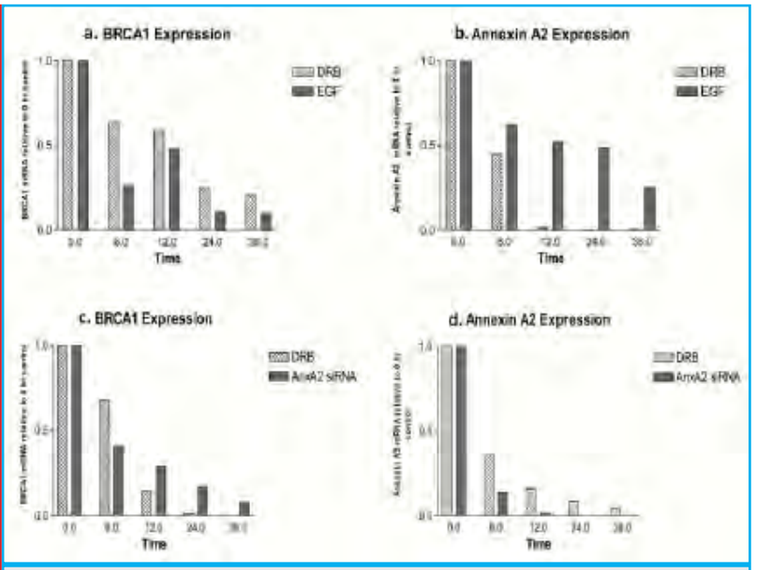

FIGURE 3. DRB Chase experiment –a) BRCA1 mRNA stability decreased on EGF induced MCF-7 cells. b) AnxA2 mRNA stability increased on EGF induction in MCF-7 cells. c) BRCA1 mRNA stability increased on AnxA2 knock down. d) AnxA2 knock down caused decrease in AnxA2 mRNA stability.

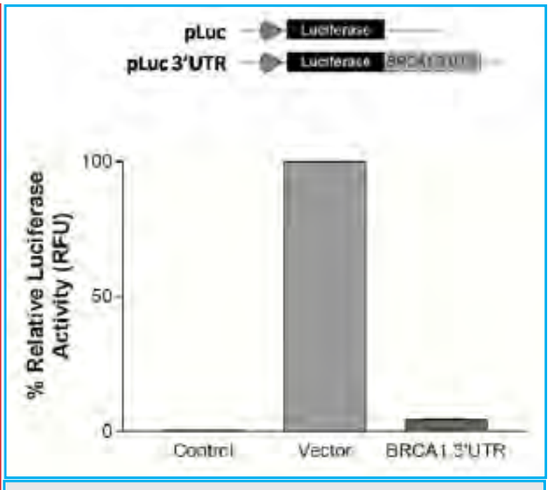

FIGURE 4. Luciferase Reporter Assay - BRCA1 3'UTR construct allows the luciferase reporter expression that mimic putative AnxA2 target in the 3' UTR of BRCA1 gene. As a control, firefly luciferas construct having targeted sequence. In each well, the transfection mixture included a Renilla luciferase reporter vector, allowing readout for normalizing the transfection efficiency at 24 hours after transfection in MDAMB-231 cells. The lysate was collected and analyzed firefly luciferase activity, which was normalized to Renilla luciferase activity.

allows the luciferase reporter expression that mimic putative AnxA2 target in the 3' UTR of BRCA1 gene. As a control, firefly luciferase construct having targeted sequence was tested. In each well, the transfection mixture included a Renilla luciferase reporter vector, allowing readout for normalizing the transfection efficiency at 24 hours after transfection in MDAMB-231 cells. The lysate was collected and analyzed firefly luciferase activity, which was normalized to Renilla luciferase activity. We found reduced luciferase expression containing BRCA1 3' UTR as compared to the control and pLuc vector control (figure 4). We identified that AnxA2 interacts with BRCA1 3'UTR, leading to decreased luciferase activity (Maji 2016).

Effect of AnxA2 putative binding oligo on cell viability

To study the similarity or association of AnxA2 protein sequence with BRCA1 3'UTR, with the help of Vienna RNA web service for secondary structure prediction and BLAST of NCBI software we selected 50 nucleotide oligo having affinity of AnxA2 to bind BRCA1 3'UTR. We transfected MDAMB-231 cells with 50 oligo nucleotides and analyzed cell viability by MTT experiment. We found decrease in cell viability of oligo treated cells than without treatment (Figure 5). Finally, putative 50 oligo nucleotide transfected MDAMB-231 cells showed increased apoptosis upon performing cell viability assay. This suggests that, putative oligo nucleotide spares BRCA1 3'UTR from AnxA2 to accelerate tumor suppres-

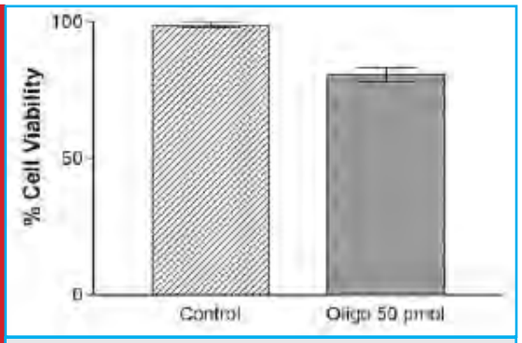

FIGURE 5. MDAMB-231 cells with 50 oligo nucleotides putative binding sequence and analyzed the cell viability by MTT.

sor activity in turn promoting the cells to undergo apoptosis (Shetty 2012).

In summary, we demonstrate that AnxA2 is involved in BRCA1 gene expression at the posttranscriptional level as well as destabilization on BRCA1 in sporadic breast cancer.

CONCLUSION

In the present study, we demonstrate that AnxA2 has a role in posttranscriptional regulation of BRCA1 expression.

ACKNOWLEDGEMENT

The authors would like to acknowledge the help of Harikrishna Ellanki, Avinash Kedari, Clinton D'Souza & Vishwas Kaveeshwar, SDM college of Medical Sciences & Hospital, Dharwad, Karnataka for their help.

RFERENCES

Adnan M, Saldanha E, Palatty PL, Naik T, Monteiro AD, Manjeshwar, et al. (2018) Incidence of Breast Cancer in Women from Agriculture based Areas of Costal Karnataka, India: A Twenty Year Observations from a Tertiary Care Hospital. 3: ClinOncol.; 3: 1437

Anderson, P. and Kedersha, N. (2006). RNA granules. J. Cell. Biol. 172 (6): 803–808.

Baylin SB, Ohm JE. (2006). Epigenetic gene silencing in cancer-a mechanism for early oncogenic pathway addiction. Nat Rev Cancer. 6:107–116. doi: 10.1038/nrc1799.

Blasi F, Stoppelli MP. (1999).Proteases and cancer invasion: From belief to certainty. AACR meeting on proteases and protease inhibitors in cancer, nyborg, denmark, BiochimBiophysActa. 1423(1):R35-44.

Choi JY, James SR, Link PA, et al. (2009). Association between global DNA hypomethylation in leukocytes and risk of breast cancer. Carcinogenesis. 30:1889–1897. doi: 10.1093/carcin/bgp143.

Cok, S.J. and Morrison, A.R. (2001). The 30-untranslated region of murine cyclooxygenase-2 contains multiple regulatory elements that alter message stability and translational efficiency. J. Biol. Chem. 276 (25): 23179–23185

Das PM, Singal R. (2004). DNA methylation and cancer. J Clin Oncol., 22: 4632–4642. doi: 10.1200/JCO.2004.07.151.

Diaz VM, Hurtado M, Thomson TM, Reventos J, Paciucci R. (2004).Specific interaction of tissue-type plasminogen activator (t-PA) with annexin II on the membrane of pancreatic cancer cells activates plasminogen and promotes invasion in vitro. Gut.;53(7):993-1000.

Engels, B.M. and Hutvagner, G.(2006). Principles and effects of microRNA-mediated post-transcriptional gene regulation. Oncogene 25 (46): 6163–6169.

Fu, L. and Benchimol, S. (1997). Participation of the human p53 30UTR in translational repression and activation following gamma-irradiation. EMBO J. 16 (13): 4117–4125

Harahap, W. A., Sudji, I. R., &tNindrea, R. D. (2018). BRCA1 Promoter Methylation and Clinicopathological Characteristics in Sporadic Breast Cancer Patients in Indonesia. Asian Pacific journal of cancer prevention: APJCP, 19(9), 2643-2649. doi:10.22034/APJCP.2018.19.9.2643

Huszno, J., Kołosza, Z., &tGrzybowska, E. (2019). BRCA1 mutation in breast cancer patients: Analysis of prognostic factors and survival. Oncology Letters, 17, 1986-1995.

Jodi M Saunus, Juliet D Freanch et al, (2008). post-transcriptional regulation of the breast cancer susceptibility gene BRCA1 by the RNA binding protein HuR. Cancer Res; 68(22); 9469-9478

Kedersha, N. and Anderson, P. (2002). Stress granules: sites of mRNA triage that regulate mRNA stability and translatability. Biochem. Soc. Trans. 30 (6): 963–969.

Lopez-de-Silanes, I. et al. (2005).Identification and functional outcome of mRNAs associated with RNA-binding protein TIA-1. Mol. Cell. Biol. 25 (21):9520–9531.

Maity, A., McKenna, W.G. and Muschel, R.J. (1997). Cyclin A message stability varies with the cell cycle. Cell Growth Differ. 8 (3):311–318.

Maji Sayantan, Pankaj Chaudhary, Irina Akopova, et al. (2016). ExosomalAnnexin A2 Promotes Angiogenesis and Breast Cancer Metastasis. Mol Cancer Res, DOI:101158/1541-7786.MCR-160163.

McCoy, M. L., Mueller, C. R., & Roskelley, C. D. (2003). The role of the breast cancer susceptibility gene 1 (BRCA1) in sporadic epithelial ovarian cancer. Reproductive biology and endocrinology: RB&E, 1, 72. doi:10.1186/1477-7827-1-72

Moore, M.J. (2005). From birth to death: the complex lives of eukaryotic mRNAs. Science 309 (5740):1514–1518

Newman Beth, A Melissa. Austin, Lee Ming and KingMary-Claire. (1988). Inheritance of human breast cancer: evidence for autosomal dominant transmission in high-risk families. 85(9): 3044-3048

Nicolas, E., Bertucci, F., Sabatier, R., &tGonçalves, A. (2018). Targeting BRCADeficiency in Breast Cancer: What are the Clinical Evidences and the Next Perspectives?. Cancers, 10(12), 506. doi:10.3390/cancers10120506

Rice, J. C., Massey-Brown, K. S., and Futscher, B. W. (1998). Oncogene 17: 1807–1812

Robertson KD. (2002). DNA methylation and chromatin-unraveling the tangled web. Oncogene. 21:5361–5379. doi: 10.1038/sj.onc.1205609.

Rosen, E.M., Fan, S.J., Pestell, R.G. and Goldberg, I.D. (2003). BRCA1 gene in breast cancer. J. Cell. Physiol. 196 (1):19–41.

Shetty PK, Thamake SI, Biswas S, Johansson SL, Vishwanatha JK. (2012). Reciprocal regulation of annexin A2 and EGFR with Her-2 in Her-2 negative and herceptin-resistant breast cancer. PLoS ONE. 7(9): e44299. DOI10.1371/journal.pone.0044299

Spiros Miyakis George, Sourvinos Demetrios A. Spandidos. (1998). Differential Expression and Mutation of the ras Family Genes in Human Breast Cancer. Biochem. Biophys. Res. Commun, 20(2), Pages 609-612

Tali Cohen Sinai, Zoya Cohen, Haim Werner, Raanan Berger. (2017). Identification of BRCA1 as a potential Biomarker for Insulin like growth factor-1 receptor targeted therapy in breast cancer. Front Endocrinol. 8:10.3389/Fendo.2017.00148

Tarui T, Majumdar M, Miles LA, Ruf W, Takada Y. (2002).Plasmin-induced migration of endothelial cells. A potential target for the anti-angiogenic action of angiostatin. J Biol Chem. 277(37): 33564-70.

Thanin Chantarachot and Julia Bailey-Serres. (2018). Polysomes, Stress Granules, and Processing Bodies: A Dynamic Triumvirate Controlling Cytoplasmic mRNA Fate and Function. Plant Physiology. Vol. 176, pp. 254–269

Thompson, C., MacDonald, G., & Mueller, C. R. (2011). Decreased expression of BRCA1 in SK-BR-3 cells is the result of aberrant activation of the GABP Beta promoter by an NRF-1-containing complex. Molecular cancer, 10, 62. doi:10.1186/1476-4598-10-62

Volker Gerke, Stephen E, (2002).Annexins: From structure to function. Physiol Rev: 82; :331-371.

Wein, G., Rossler, M., Klug, R. and Herget, T. (2003).The 30-UTR of the mRNA coding for the major protein kinase C substrate MARCKS contains a novel CU-rich element interacting with the mRNA stabilizing factors HuD and HuR. Eur. J.Biochem. 270 (2): 350–365.

Wiklund, L., Sokolowski, M., Carlsson, A., Rush, M. and Schwartz, S. (2002).Inhibition of translation by UAUUUAU and UAUUUUUAU motifs of the AU-rich RNA instability element in the HPV-1 late 30 untranslated region. J. Biol. Chem. 277 (43): 40462–40471.

Zhang Y, Meng L, Xiao L, Liu R, Li Z, Wang Y: (2018). The RNA-Binding Protein PCBP1 Functions as a Tumor Suppressor in Prostate Cancer by Inhibiting Mitogen Activated Protein Kinase 1. Cell Physiol Biochem. 48:1747-1754. doi: 10.1159/000492315

Biotechnological Communication

Biosci. Biotech. Res. Comm. 12(1): 169-173 (2019)

BBRC Bioscience Biotechnology Research Communications

A low energy based event driven and secure node deployment protocol for Wireless Medical Sensor Network

Sandip Mandal and Rama Sushil

DIT University Dehradun, India

ABSTRACT

A wireless sensor network consists of a huge number of sensor nodes associated via wireless medium. Nodes in a WMSN(Wireless Medical Sensor Network) are organized with limited battery energy and thus improvement on network lifetime by reducing energy-usage is of extreme important. One of the solutions to minimize such energy-usage is associate clustering of network nodes. In this paper an associate clustering scheme in WMSN is proposed where cluster heads are formed by creating a probable associate list is in descending order in which cluster heads are organized according to their residual energy. We have conducted simulation-based evaluations to compare the performance of EEACPSC against Energy Aware Coverage Preservation and Lifetime Enhancement Protocol (EACPLEP) and Enhanced-Energy Efficient Protocol with Static Clustering (E3PSC). Our experiment results show that the performance of present scheme is much better than the previous one. And it provides better result. 40.3% gain of EEACPSC over E3PSC and 25.3% gain over EACPLEP in terms of number of nodes alive in the network.

KEY WORDS: CLUSTER HEAD, NETWORK LIFETIME, ENERGY EFFICIENCY, WIRELESS MEDICAL SENSOR NETWORK

INTRODUCTION

Innovations in industrial, home and automation in transportation represent smart environments. Data for smart environments are obtained through Wireless Medical Sensor Networks (WMSN), where thousands of sensors are deployed at different locations operating in different modes, (Cook et al, 2004). A sensor network is capable of sensing, processing and communicating which helps the base station or command node to observe and react according to the condition in a particular environment (physical, battle field, biological) (Sohraby et al, 2007). Sensor network protocols have a unique self-organizing capability. Another interesting feature of WMSNs is

ARTICLE INFORMATION:

Corresponding Author: sandy06.gcect@gmail.com
Received 22nd Dec 2018
Accepted after revision 27th Feb 2019
BBRC Print ISSN: 0974-6455
Online ISSN: 2321-4007 CODEN: USA BBRCBA
Thomson Reuters ISI ESC / Clarivate Analytics USA
Crossref Clarivate Analytics
NAAS Journal Score 2019: 4.31 SJIF: 4.196

Online Contents Available at: http//www.bbrc.in/
DOI: 10.21786/bbrc/12.1/22

that the sensor nodes cooperate with each other. Sensor nodes have an in-built processor, using which raw data are processed before transmission. These features facilitate wide range of applications of WMSNs ranging from biomedical, environmental, military, event detection and vehicular telematics, (Akyildizet al, 2002). In this paper we assume a sensor network model, similar to those used in (Mandal et al, 2018), with the following properties:

- All sensor nodes are immobile and homogeneous with a limited stored energy.
- The nodes are equipped with power control capabilities to vary their transmitted power.
- None of the nodes know their location in the network.
- Each node senses the environment at a fixed rate and always has data to send to the base station.
- Base station is fixed and not located between sensor nodes.

In this paper, we propose EEACPSC (An Enhanced Energy Aware Coverage Preservation with Static Clustering), a hierarchical static clustering based protocol, which eliminates the overhead of dynamic clustering and as a result prolongs the network lifetime. In this scheme, cluster heads are selected by creating a probable associate list where cluster heads are organized according to their residual energy and all the rounds are divided into iteration. The rest of paper is organized as follows. Section 2 describes the proposed scheme followed by the supporting algorithm. Performance-evaluation (Mandal et al, 2019) and simulation results are presented in section 3. The entire work is concluded in section 4 and 5.

PROPOSED SCHEME

This section contains the proposed scheme, An Enhanced Energy Aware Coverage Preservation with Static Clustering (EEACPSC) followed by the algorithm of the proposed scheme. The present scheme is a modification of an existing scheme, An Enhanced Energy-Efficient protocol with Static Clustering (E3PSC) [Loscri V et al, 2005] and Energy Aware Coverage Preservation and Lifetime Enhancement Protocol (EACPLEP) [Junepei et al, 2004]

In the present work, cluster heads are choose by creating a probable associate list for next n number of rounds and the entire cluster heads are organized according to their residual energy.

Algorithm (EEACPSC)

1. BEGIN
/* Setup Phase (tasks are performed by the base station) */
2. Form*k* clusters taking n randomly distributed nodes based on distance
/* Same as EACPLEP*/
3. For i ← 1 to k
4. Compute mean position of node distribution, mean in $cluster_i$
5. for j ← 1 to m_i
/* m_i → No. of nodes in $cluster_i$ */
6. Compute distance of $node_j$ from $P_{mean\ i}$, $d_{mean\ i}$
7. End For
8. Select Temporary Cluster Head (TCH_i) randomly for $cluster_i$
9. Create TDMA schedule for the nodes of $cluster_i$
10. for j ← 1 to m_i
11. Send 3-tuple (TCH_i, $TDMA_i$, $d_{mean\ i}^{j}$) data to $node_j$
12. End For
13. End For
/* End of Setup Phase */
14. For v ← 1 to round
/* round → Total no. of rounds
/* Responsible Node Selection Phase */
15. For i ← 1 to k
16. For Alive_node ← 1 to m_i
/* Alive_node → Nodes whose residual energy is greater than or equal to threshold energy (Eth)
17. Send 2-tuple ($d_{mean\ i}^{j}$, $E_{residual\ i}^{j}$) information to TCH_i
18. End For
/* TCH_i performs the following tasks */
19. Call Responsible_Node_Selection()
/* Select CH_i for the current round Select TCH_i for the next round */
20. End For
/* Steady-State Phase */
21. For i ← 1 to k
22. For Alive_node ← 1 to m_i
23. Send data to CH_i
/*Data transmission by Alive_node(s) */
24. End For
25. Send aggregated data to the base station /* Data transmission by CH_i */
26. End For
27. End For /* End of rounds */
28. END /* End of Algorithm */

Responsible_Node_Selection( )

1. BEGIN
2. For i ← k /* Creating a list of probable CH_i. */ /*k=length (Cluster.nodes)*/
3. RGroup=[ ]; /*R denotes Right*/
4. LGroup=[ ]; /*L denotes Left*/
5. if ~isempty([Cluster.TCH])
6. for i=1:k
7. if $R_{energy} > L_{energy}$
8.[C,T]=ISelection(Anode,RGroup,Eth); /* Select the node from right group*/
9. else
10. [C,T]=ISelection(Anode,LGroup,Eth); /* Select the node from left group*/
11. End
12. CH_i=C;
13. TCH_i=T;
14. Else
15. CH_i=[ ];
16. TCH_i=[ ];
17. end
/*End of Algorithm */

PERFORMANCE COMPARISON

Qualitative Analysis

The network lifetime is defined in terms of energy-usage. The associate list is determined in such a manner that presence of cluster head within a list is sufficient and further, to keep the network alive, probable list needs to be associated. To declare the network alive, we can say that for every round the cluster head with maximum energy among all the pre-decided cluster heads within that list should be greater than a threshold energy level $E_{threshold}$ beyond which the node is considered as a dead. Since this must hold for every round, we can easily considered that only the minimum of these energies should be above $E_{threshold}$ thereby guarantees that each round has sufficient energy to keep the network alive.

Quantitative Analysis

Simulation Environment

To evaluate the performance of EEACPSC, MATLAB 7.1 is used as a simulation tool. We consider that the sensor nodes are deployed randomly across in plain area of (x_m = 100m X y_m = 100m) and the base station is located (x=50, y=175). Each node is equipped with equal amount of initial energy (2J) at the beginning of the simulation. Further we assume that WMSN is working in continuous data flow application domain. Table 1 represents various parameters and their values used in simulation.

Simulation Metric

The performance of the scheme is evaluated considering network lifetime as a parameter which is defined as the time until the last node dies in the network. Network lifetime is measured using following yard-stick.

- Number of nodes alive in the network : more number of nodes alive involves network lifetime last longer.
- 3D result: results are in 3D format which outperforms better performance as compare to E3PSC and EACPLEP.

Table 1. Parameters and Corresponding Values used in Network Simulation for Medical Sensor Network

Parameter	Parameter's Name
Network Area	100m X 100m
Base Station's Position	(50m, 175m)
Initial Energy for Nodes	2 Joule
Number of Deployed Nodes	100
Size of Data Message	4000 bits
Energy Consumed in Data Aggregation(EDA)	5nJ/bit/signal
Energy Consumed by Transceiver's Circuitry (Eelec)	50nJ/bit
Energy Expenditure in Transmit-Amplification in free-space model(efs)	10pJ/bit/m2
Energy Expenditure Transmit-Amplification in multipath fading model (Emp)	0.0013pJ/bit/m4

RESULTS AND DISCUSSION

A set of experiments is conducted to compare the performance of present scheme EEACPSC with E3PSC (Zahmati et al, 2007) and EACPLEP (Lindsay et al, 2002).

Fig.1 shows that, after 26 seconds, only 67 nodes are alive over the network.

Fig. 2 shows that, after 26 seconds, only 75 nodes are alive over the network.

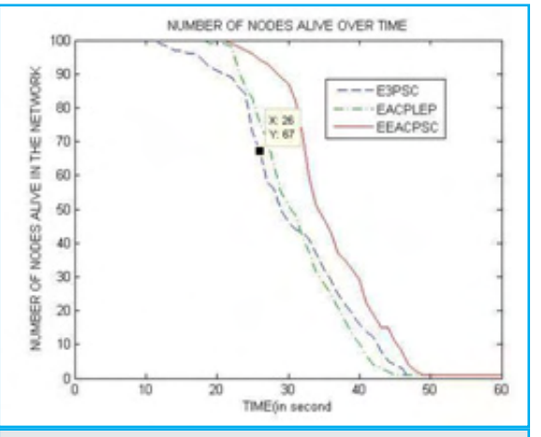

FIGURE 1. Comparison of EEACPSC with E3PSC in terms of number of nodes alive in the network over time

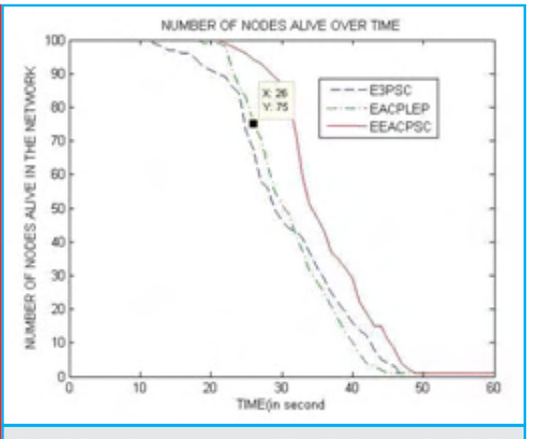

FIGURE 2. Comparison of EEACPSC with EACPLEP in terms of number of nodes alive in the network over time

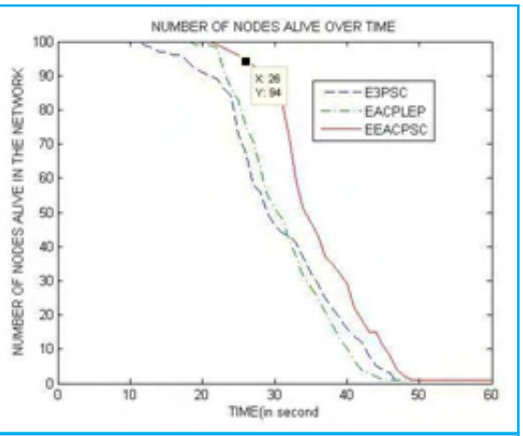

FIGURE 3. Number of nodes alive in the network over time in EEACPSC

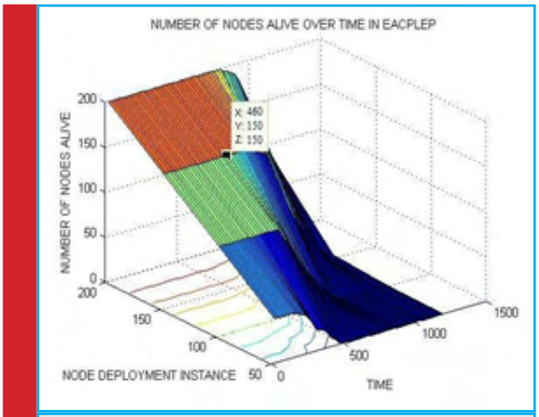

FIGURE 5. Number of nodes alive over time in EACPLEP (3D)

Fig. 3 shows that, after 26 seconds, 94 nodes are alive over the network.

After comparing these 3 graphs we conclude that the performance of present scheme is much better than the previous one. And it provides better result. 40.3% gain of EEACPSC over E3PSC and 25.3% gain over EACPLEP in terms of number of nodes alive in the network. Following are the representation of 3D graphs.

In fig 4, there is a deployment of 150 nodes instantly and after 460 seconds there are 145 nodes alive in the network.

Fig.5 indicates that, after 460 seconds, there are 150 nodes alive over the network.

Fig.6 shows that, after 460 seconds, 155 nodes are alive over the network.

After comparing these 3D graphs, we conclude that the performance of present scheme is better as compare to previous scheme. 6.89% gain of EEACPSC over E3PSC and 3.33% gain over EACPLEP in terms of number of nodes alive in the network.

In this paper an energy-efficient routing scheme EEACPSC for WMSN is proposed. The EEACPSC is developed by modifying an existing routing scheme E3PSC and EACPLEP with an objective to prolong network lifetime further (more number of nodes alive in the network). With the results of simulation, we can conclude that in the case of EACPLEP, the intra-cluster communication is increased, which is removed in the EEACPSC, because the cluster head will be choose on the basis of creating a probable list of nodes.

So the energy dissipated in the node to cluster head is less than the EACPLEP. And it organizes by the 3D graph also. So we can say that EEACPSC is more energy efficient and coverage preserving as compare to E3PSC and EACPLEP and spatial allocation of nodes plays a vital role in the election of cluster-heads for network opera-

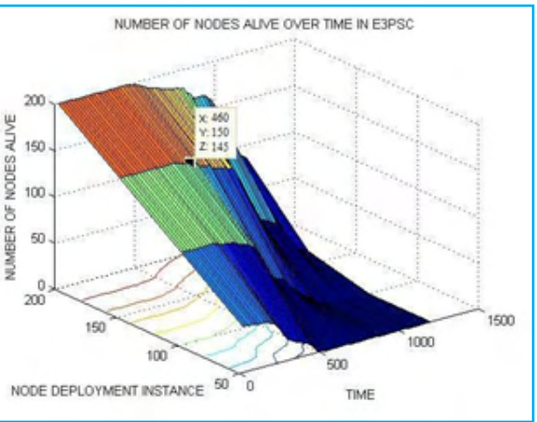

FIGURE 4. Number of nodes alive over time in E3PSC (3D)

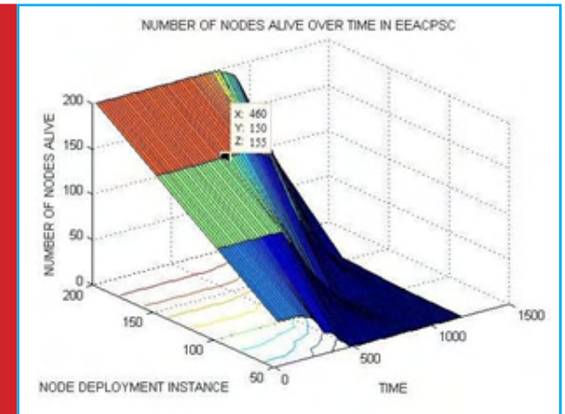

FIGURE 6. Number of nodes alive over time in EEACPSC(3D)

tion. As per the quantitative results, EEACPSC proves to be better performer than EACPLEP and E3PSC.

As future work, we intend to study more complicated situations, like coverage problems in case of mobile nodes, heterogeneous sensor networks consisting nodes of different capabilities, and other non-disk coverage models.

REFERENCES

Akyildiz I.F., Su W, Sankarasubramaniam Y, and Cayirci E (2002), Wireless sensor networks: A survey

Amir SepasiZahmati and Bahman Abolhassani (2007), EPM-PLCS: An Efficient Power Management Protocol with Limited Cluster Size for Wireless Sensor Networks Proc. 27th International Conference on Distributed Computing Systems (ICDCS 2007)Computer Networks, vol. 38, pp. 393-422

Cook D. J. and Das S. K. (2004), Smart environments: technologies, protocols and applications New York:John Wiley, pp. 13-15

Heinzelman W.R. Chandrakasan A.P, and Balakrishnan H. (2000), Energy- Efficient Communication Protocol for Wireless Microsensor Networks, Proc. 33rd Hawaii Int'l. Conf. Sys. Sci., Jan 2000.

JunpeiKamimura and Naoki Wakamiya and Masayuki Murata (2004)Energy-efficient clustering method for data gathering in sensor networks," in Proceedings of First Workshop ON Broadband Advanced Sensor Networks

Lindsey S, Raghavendra C and Sivalingam K. M (2002), Data-Gathering Algorithms in Sensor Networks using Energy Metrics, IEEE Trans. Parallel and Distrib. Sys., vol. 13, no. 9, Sept., pp. 924–35.

Loscri' V. Marano S. ,Morabito G. (2005) A Two-Level Hierarchy for Low-Energy Adaptive Clustering Hierarchy (TL-LEACH). Proceedings VTC2005 Dallas (USA), pp. 1809-1813.

Mandal, Sandip and Sushil, Rama (2018) Adaptive Modelling and Simulation of Wireless Sensor Radio Energy depends On Probabilistic and Stochastic Analysis, Institute of Integrative Omics and Applied Biotechnology Vol. 9 No. 2 pp. 129-135

Mandal, Sandip and Sushil, Rama (2018) Detection and Mitigation from Wormhole Based Protocol Deviation depends on Neighbor Discovery Approach In WSN, International Journal of Engineering and Technology Vol.7 No. 4 pp. 62-65

Mandal, Sandip and Sushil, Rama (2018) Energy Saving Dynamic Clustering Protocol for Wireless Sensor Network , International Journal of Engineering Applied and Management Sciences Paradigms Vol, 53 No. 03 pp. 25-28

Mandal, Sandip and Sushil, Rama (2018) Enhanced Energy-Balanced Lifetime Enhancing Clustering for WSN (EEBLEC), International Journal of Applied Engineering Research Vol 13 No. 16 pp. 12911—12916

Mandal, Sandip and Sushil, Rama (2018) Real time deployments of sensors and sensing patients vital parameters using secure autonomous WSN for medical applications, Bioscience Biotechnology Research Communications Vol. 11 No. 3 pp. 523-534

Mandal, Sandip and Sushil, Rama (2019) Security Enhancement Approach in WSN to Recovering from Various Wormhole-Based DDoS Attacks, Innovations in Soft Computing and Information Technology pp.179—190, Springer, Singapore

Sohraby K., Minoli D., and Znati T. (2007)Wireless sensor networks: technology, protocols and applications,NewJersey: John Wiley, pp. 38-71

Yongcai Wang, Qianchuan Zhao and Dazhong Zheng (2004), Energy-Driven Adaptive Clustering Data Collection Protocol in Wireless Sensor Networks Proceedings of the 2004 International Conference on Intelligent Mechatronics and Automation, Chengdu, China.

Medical
Communication

Biosci. Biotech. Res. Comm. 12(1): 174-180 (2019)

BBRC
Bioscience Biotechnology
Research Communications

Proposed model for the detection of breast cancer using mammogram images

M. Manikandan* and A. Nithya

Department of Electronics and Communication Engineering, M. Kumarasamy College of Engineering, Karur, Tamilnadu, India

ABSTRACT

In the modern world the technology is growing day by day and at the same time the biological pathology is also growing in a proportional rate, wherewomen are diagnosed more than men for various types of dreadful cancers like the breast and ovarian. The technology will never fail to address the biomedical aspects including a specific diagnosis. In this communication, we have tried to present our approach towards a possible early detection of breast cancer using mammogram image in 3 dimensional views. The purpose of the presentlyproposed analysis is to recognize the level of calcification or calcification deposits in breast tissues. Usual method for the image analysis is preprocessing followed by segmented results. In this paper we propose to develop the traditional mechanisms with Graphical User Interface, in order to estimate the level of the calcification formed in the breast tissuecontent, which can become an easy way of diagnosis, thus using a 3D analysis as one of the easiest ways for precise future analysis and early treatment of breast cancer, whichcan save the lives of many women.

KEY WORDS: MAMMOGRAM, PREPROCESSING, 3D, CALCIFICATION, GUI, CANNY EDGE DETECTOR

Bosom Tomosynthesis or 3D mammography is the most recent development in advanced mammography (Mohanapriya et al. 2013). The favorable circumstances over customary mammography comprise of better tumor location at a prior arena and less go back break for extra pictures and consequently less nervousness and more noteworthy practicality for ladies experiencing mammography (Sukanesh et al. 2010b). 3D mammography is basically like conventional 2D mammography from various perspective (Vijayprasath et al. 2012). The

ARTICLE INFORMATION:

Corresponding Author: manikandanm.ece@mkce.ac.in
Received 19th Dec 2018
Accepted after revision 22nd Feb 2019
BBRC Print ISSN: 0974-6455
Online ISSN: 2321-4007 CODEN: USA BBRCBA
Thomson Reuters ISI ESC / Clarivate Analytics USA
NAAS Journal Score 2019: 4.31 SJIF: 4.196

Online Contents Available at: http//www.bbrc.in/
DOI: 10.21786/bbrc/12.1/23

machine appears to be identical and each bosom has pictures taken in two positions (Dinesh et al. 2015a). Be that as it may, rather than taking a solitary picture while the bosom is compacted, every 3D picture is a 4-second sweep of the bosom. These outcomes in a progression of 1 mm thick pictures or cuts of the bosom (Dinesh et al. 2015b). There are roughly 50 picture cuts for each position. This enables the radiologist to see the bosom at different points and to isolate covering typical tissue that can appear like growth or make tumor hard to distinguish on a conventional mammogram (Sukanesh et al. 2010a). Consider it similar to a volume when you glance down at the book, everything you can see is the cover. This resembles customary mammography. Be that as it may, you can see every one of the pages (Dhivya et al. 2018). This resembles 3D mammography. The 3D check likewise creates an extra picture that resembles a customary mammogram, or, in other words combination with the picture cuts and can be contrasted and your earlier mammograms (Manikandan et al. 2014). The emission dose from a 2D mammogram image and a 3D scan is almost the identical (Kavitha et al. 2017).

Earlier, datahave been provided with the details of usingsensitive markersfor the detection of myocardial deformation, where strained cardiac rates were measured in left ventricle before the measure of the general parameters like left ventricle ejection, fractions in breast cancer also forms the mammogram imaging sequences (Keerthi et al. 2017). In addition, the use of 3Dimensional echocardiography as a more susceptible and reproducible calculation of left ventricle ejection fraction was not consistent to distinguish these changes (Shapiro et al. 1982). Left ventricular ejection fraction was calculated by 2 and 3 dimensional echocardiography, and myocardial twist was evaluated by means of tissue Doppler imaging and 2D based injures and strain rate. Revolutionized over- time was measured up to every 3 months as reported by Manikandan et al. (2018).

In various imaging laboratories, mammography is an important testing aid for breast cancer identification, combined with reference data which results from the other estimations, (Rajan 2014). The mechanism for breast cancer in dark breast parenchyma is not fast developed due to the masking of real time cancers that are rejected on testing mammograms (Sukanesh et al. 2013). These discoveries additionally recommend that the option of mammographic screening in patients with thick bosom parenchyma is likely not to increment analytic yield in the identification of bosom growths, (Rajan 2015a). In theprevious work, the detection of the cancer from the mammogram image using the canny edge vector was identified and shown in the figure 1. From this extraction the cancer level was furtheridentified (Rajan et al. 2013a). Here we havediscussed the same for the comparison. In this paper we havediscussed the proposed method to identify the cancer depth in 3 dimensional views (Dengler et al. 1993). The previous work was to identify the cancer affecting areas.Here the depth will be taken in to 3 dimensional aspects for further clinical and specific examination, (Rajan et al. 2015b).

FIGURE 1. Canny Edge Identifier for the Breast cancer

The proposed methods have the ability to get the input image, and then it will be taken into preprocessing techniques(Rajan et al. 2015d). The preprocessing technique involves the conversion of the gray scale domain form the RGB domain. In order to satisfies the exact analysis of the cancer detection, (Rajan 2015c). Followed by the filtering methods. The role of the filters is to remove the unwanted noise in the input image and the unwanted transition may present during the RGB to Gray scale conversion (Rajan et al. 2013b). The third Role in the method is to segment the state of significance form the filtered image. All process put in the single module is the way in which to create the GUI(Graphical User Interface). Parameters have to select in such way to identify the appropriate region of interest, (Rajan et al. 2015e).

The estimated parameters are as follows: Growing: 0.1 Per Gray, Noise Level: 0.9 Per Gray, Cut Level: 0.0.5 Per Gray N Volume: 2. After carrying out the preprocessing, the post processing will be evaluated. The evaluation will be done with the segmented region in to the segmented volume (Rajan et al. 2012). On the other hand genetic algorithm with various clustering hasbeen used for the cancer detection for breast cancer form mammogram image. Here comes the discussion about various clusters with best and mean fitness of the mammogram inputs. The following table shows the same.

Furthermore the sample cluster and their representation are show below.

Here wehave discussed the result of the breast cancer detection from the mammogram image sequences in 3

Table 1. Comparison of Various clusters with fitness values

No of Clusters	Best Fitness	Mean Fitness
1	3821.97	3821.97
2	1037.34	1037.34
3	377.21	377.405
4	211.563	216.063
5	116.189	116.208
6	118.19	118.218
7	55.8693	55.8693
8	45.3636	45.3788
9	54.5532	56.0221
10	29.7613	29.7769

dimensional views. The GUI was loaded to observe the input sequence and the input image was displayed in the input panel.

After displaying the input mammogram image in the GUI tool, then set the parameters have been discussed in the section II. Select the region which will cover the region of the interest.

Selection of ROI is done then the segmentation will be estimated. Segmented ROI is evaluated in two ways.

The extracted areas are needed to be highlighted with the help of GUI for the accurate computation of cancer cell,as well as estimation of distribution of cancer cells in mammogram.

Finally with the help of all relevant source and findings to develop the 3 dimensional projections the cancer

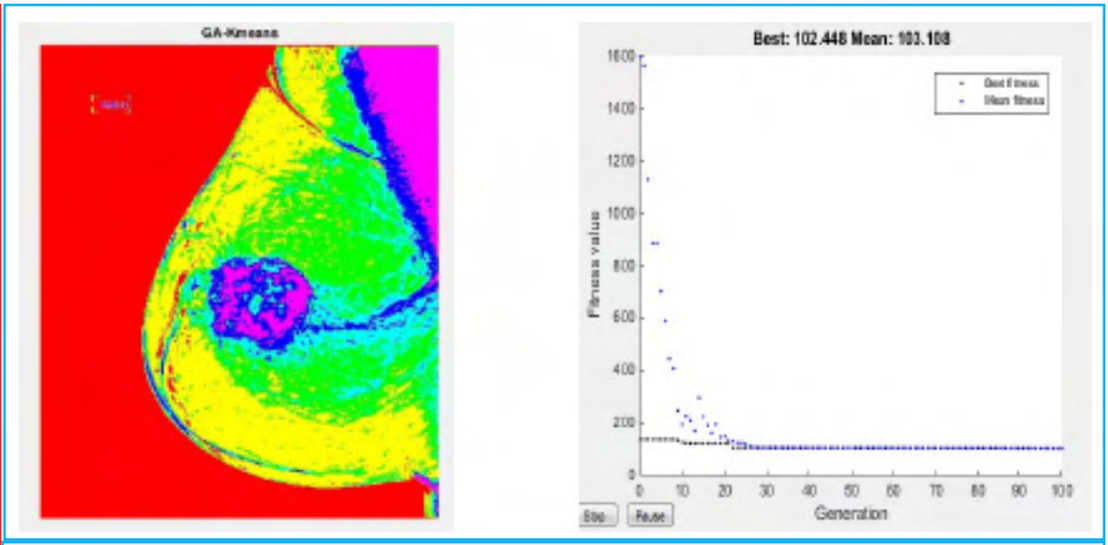

FIGURE 2. Cluster Number=6 and associated extracted image with fitness values

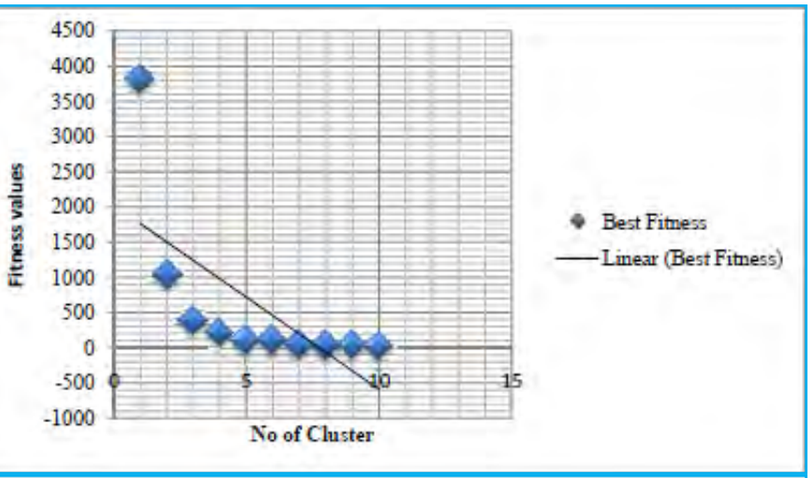

FIGURE 3. Best fitness Values Vs No of Clusters

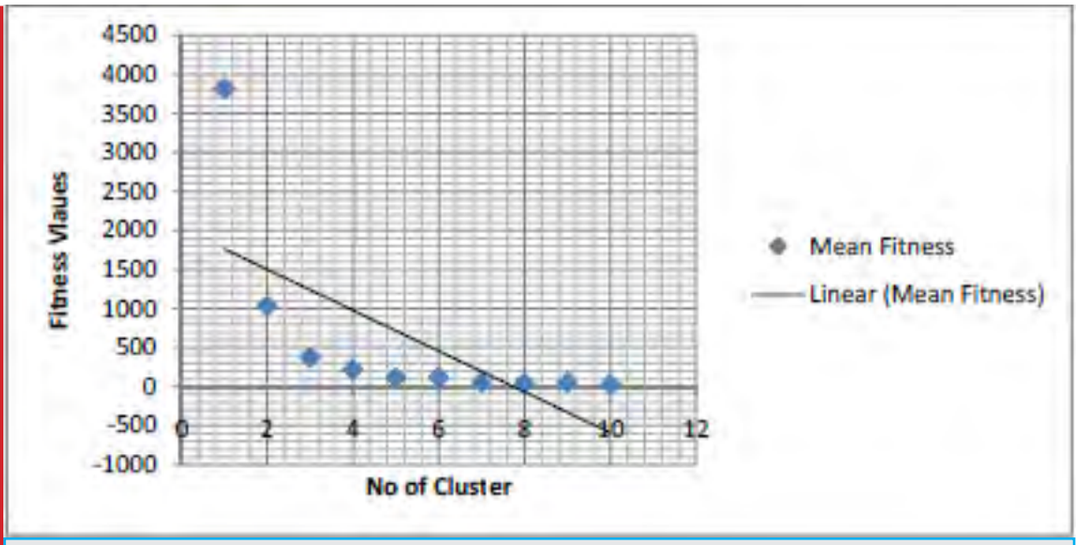

FIGURE 4. Mean fitness Values Vs No of Clusters

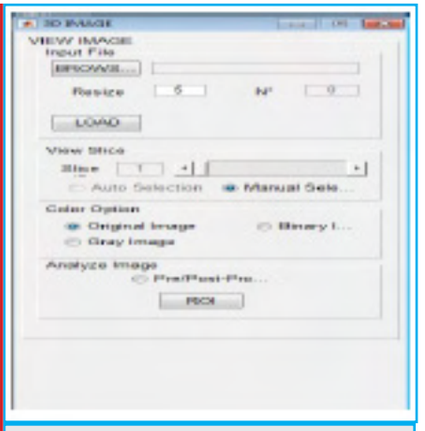

FIGURE 5. GUI front look

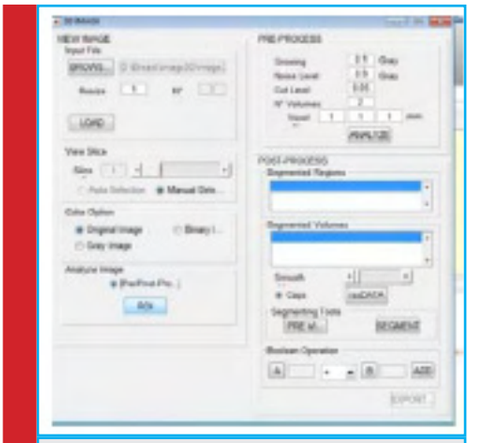

FIGURE 7. Loading of input image

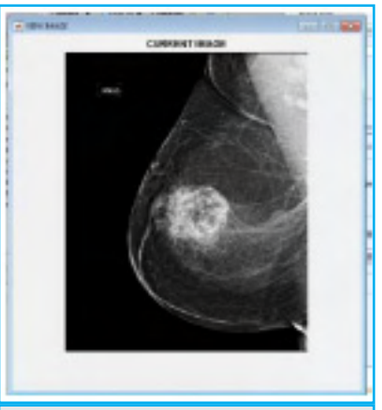

FIGURE 6. Input image of the Breast mammogram image Sequence

affected areas. That will help to the doctors to examination the root and cause of the cancer in breast.

In existing systems there are more complex mathematical calculationsthat are used and it is very difficult to understand for the users. There is more complexity to provide the accurate results in the specified areas and also there may be chance to show many false images which may not be actually affected by cancer cells. Canny edge detector can estimate the amount of affected cells. These algorithms are used to find the segmented regions accurately and it is very useful to find the different stages of patients. Early stage of a person can be cured easily and if a patient is affected severely immediate action should be needed. Another method for estimation of the breast cancer is Genetic Algorithm with suitable fitness values, population identity, stand-

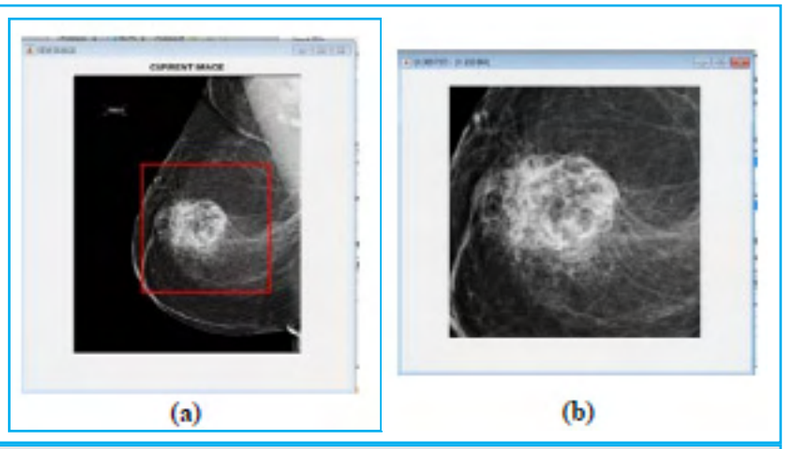

FIGURE 8. (a) Selection of ROI (b) Segmented ROI

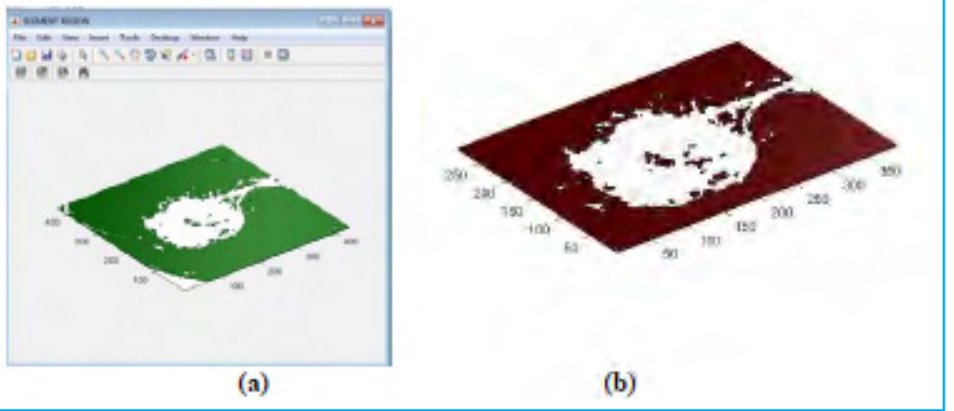

FIGURE 9. Segmented ROI (a) Volume 1 (b) Volume 2

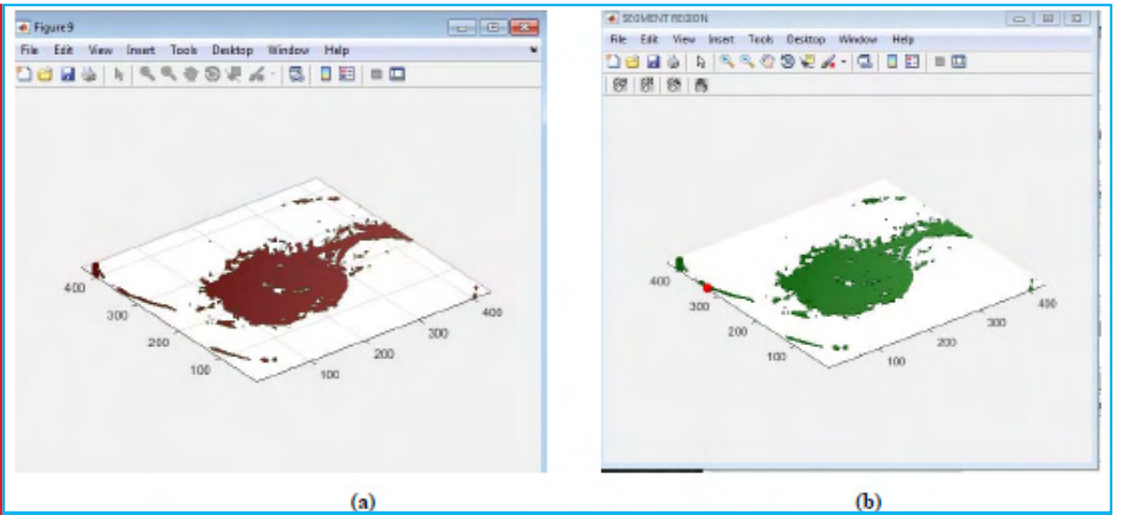

FIGURE 10. Highlighted Segmented ROI (a) Volume 1 (b) Volume 2

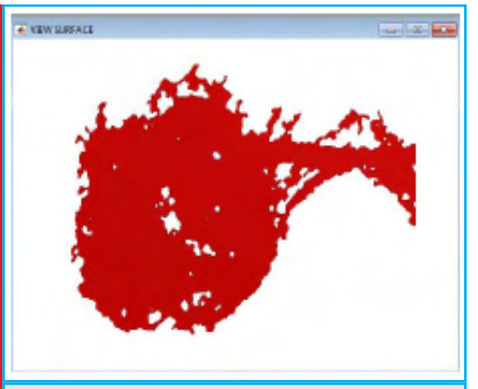

FIGURE 11. Estimated 3D Surface of the Cancer affected Area

ard mutation procedures are evaluated. And the results were discussed but the accurate examination was not up to the level. The added way of the existing methods is 3 Dimensional of projection of cancer identified areas. This gives easy for the doctors to examine the cancer patient in easiest way. Further this can be improved by the help of 3 dimensional projection will able to answer the root cause and correspondence of cancer tissues, this may be described in medical terms a diagnostic need to be studied in future.

REFERENCES

Dengler J, Behrens S, Desaga JF(1993) Segmentation of micro calcifications in mammograms. IEEE Transactions on Medical Imaging. 1993, 12 (4), pp. 634-642.

Dhivya, Nithya, Abirami, (2018) Mamogram Image Classification Using Extreme Learning Machine", Indian Journal of Science and Technology, 11 (17), pp.1-4.

Dinesh T, Palanivel S (2015a) Statistical Investigation of EEG Based Abnormal Fatigue Detection using LabVIEW. International Journal of Applied Engineering Research 10(43): Pages 30426-30431.

Dinesh T, Palanivel S (2015b) Systematic Review on Wearable Driver Vigilance System with Future Research Directions. International Journal of Applied Engineering Research 2(2): Pages 627-632.

Kavitha V, PalanivelRajan S (2017) Diagnosis of Cardiovascular Diseases using Retinal Images through Vessel Segmentation Graph. Current Medical Imaging Reviews 13(4).

Keerthi S, Dhivya S (2017) Comparison of RVM and SVM Classifier Performance in Analysing the Tuberculosis in Chest X Ray. International Journal of Control theory and Applications 10(36): Pages 269-276.

Manikandan M, Prabakar S (2014) Active Cardiac Model and its Application on Structure Revealing from Fetal Ultrasound Sequence. International Journal of Engineering Research and General Science. (2014), 2 (4), pp. 6-11.

Manikandan, Paranthaman, NeeththiAadithiya, (2018), Detection of Calcification form Mammogram Image using Canny Edge Detector Indian Journal of Science and Technology, Vol 11(20).

Mohanapriya S, Vadivel M (2013) Automatic retrival of MRI brain image using multiqueries system. International Conference on Information Communication and Embedded Systems (ICICES): Pages 1099-1103.

PalanivelRajan S (2014) A Significant and Vital Glance on Stress and Fitness Monitoring Embedded on a Modern Telematics Platform. Telemedicine and e-Health Journal 20(8): Pages 757-758.

PalanivelRajan S (2015a) Review and Investigations on Future Research Directions of Mobile Based Tele care System for Cardiac Surveillance. Journal of Applied Research and Technology 13(4): Pages 454-460.

PalaniveRajan S, (2015c) Review and Investigations on Future Research Directions of Mobile Based Telecare System for Cardiac Surveillance Journal of Applied Research and Technology, ISSN No.: 1665–6423, 13(4), pp. 454- 460.

PalanivelRajan S,(2015b) Visual and tag-based social image search based on hypergraph ranking method IEEE Digital Library Xplore, ISBN : 978-1-4799-3835-3, INSPEC Accession Number : 14916051, DOI : 10.1109/ICICES.2014.7034079.

PalanivelRajan S, Sheik Davood, (2015d) Performance evaluation on automatic follicles detection in the ovary", International Journal of Applied Engineering Research, 10(55), pp.1-5.

Rajan S P, Sukanesh R (2013a) Viable Investigations and Real Time Recitation of Enhanced ECG Based Cardiac Tele-Monitoring System for Home-Care Applications: A Systematic Evaluation. Telemedicine and e-Health Journal 19(4): Pages 278-286.

Rajan S P, Sukanesh R, Vijayprasath S (2012) Performance Evaluation of Mobile Phone Radiation Minimization through Characteristic Impedance Measurement for Health-Care Applications. IEEE Digital Library Xplore.

Rajan S P, Vijayprasath S (2015e) Performance Investigation of an Implicit Instrumentation Tool for Deadened Patients Using Common Eye Developments as a Paradigm. International Journal of Applied Engineering Research 10(1): Pages 925-929.

Palanivel S Rajan, R.Sukanesh, (2013b) Experimental Studies on Intelligent, Wearable and Automated Wireless Mobile Tele-Alert System for Continuous Cardiac Surveillance Journal of Applied Research and Technology, ELSEVIER, ISSN No.: 1665–6423, Vol. No. 11, Issue No.: 1, pp.133-143, (2013).

Shapiro S, Venet W, Strax P, Venet L, Roeser R (1982). Ten to 14-year effect of screening on breast cancer mortality. J Natl Cancer Inst 1982;69: 349-55.

Sukanesh R, Gautham P, Rajan S P, Vijayprasath S (2010a) Cellular Phone based Biomedical System for Health Care. IEEE Digital Library Xplore: Pages 550-553.

Sukanesh R, PalanivelRajan S (2013) Experimental Studies on Intelligent, Wearable and Automated Wireless Mobile Tele-Alert System for Continuous Cardiac Surveillance. Journal of Applied Research and Technology 11(1): Pages 133-143.

Sukanesh R, Rajan S P, Vijayprasath S (2010b) Intelligent Wireless Mobile Patient Monitoring System. IEEE Digital Library Xplore: Pages 540-543.

Vijayprasath S, Sukanesh R, Rajan S P (2012) Experimental Explorations on EOG Signal Processing for Real Time Applications in LabVIEW. IEEE Digital Library Xplore.

Agricultural Communication

Biosci. Biotech. Res. Comm. 12(1): 181-185 (2019)

BBRC Bioscience Biotechnology Research Communications

Studies of geo-gravimetric properties of polished rice, *Oryza sativus*, (Pusa Sugandha-1)

V.K. Tiwari*, Nikhat Parveen Ansari, Astha Asati and Madhusudhan

Department of Post-Harvest Process and Food Engineering, Jawaharlal Nehru Krishi Vishawa Vidhyalaya, Jabalpur (M.P.) India

ABSTRACT

Geometric and gravimetric properties of grain are necessary for designing the equipment for processing, sorting, sizing and other post-harvest operations. The aim of this study is to determine the geometric and gravimetric properties of polished rice, (Pusa Sugandha-1).The geometric properties i.e. length, breadth, thickness, sphericity, size, L/B ratio and the gravimetric properties i.e. bulk density, true density, porosity and test weight were measured. The experiments were conducted at fourteen percent moisture content (wb). The average kernel length, breadth and thickness were observed as 8.17, 1.60 and 1.54 mm respectively. The size and volume were recorded as 2.77 mm and 10.53 mm3 respectively. The sphericity was found 33.90. Bulk density, true density and porosity were observed as 798 kg/m3, 1412.56 kg/m3 and 43.4 percent respectively. Test weight of polished rice was recorded as 16.82 grams. The L/B ratio was found 5.10. This rice will be characterized as extra-long (>7 mm), slender shape (L/B> 3) in an international market.

KEY WORDS: POLISHED RICE, GEOMETRIC, GRAVIMETRIC, AND DEHUSKING

INTRODUCTION

Rice (*Oryzasativa L.*) is the most important and extensively grown food crop in the world (Agriculture Statistics 2016). As a cereal grains, it is the most widely consumed staple food for a large part of the world's human population, especially in Asia. India is the second largest rice producer, exporter and consumer after China. Rice is the main food approximately for sixty per cent of the Indian population. Milling consists of the removal of husk and bran to obtain the edible portion (endosperm) to a level that is acceptable and _t for human consumption (Singh et al., 2015). Determining geo-gravimetric properties of rice can facilitate design of machinery for planting, harvesting, storing and processing operations such as threshing, handling, cleaning and drying (Ash-

ARTICLE INFORMATION:

Corresponding Author: iitkgp84@gmail.com
Received 22nd Jan 2019
Accepted after revision 24th March 2019
BBRC Print ISSN: 0974-6455
Online ISSN: 2321-4007 CODEN: USA BBRCBA
Thomson Reuters ISI ESC / Clarivate Analytics USA
NAAS Journal Score 2019: 4.31 SJIF: 4.196

Online Contents Available at: http//www.bbrc.in/
DOI: 10.21786/bbrc/12.1/24

tiani et al., 2010; Ghasemlou et al., 2010). Milling consists of the removal of husk and bran to obtain the edible portion (endosperm) to a level that is acceptable and _t for human consumption (Singh et al., 2015). Rice not only supplies the energy (calorie) need but also fulfil much of the requirement of proteins, vitamins and other nutrients. Total nutrient contents of rice are carbohydrate (77.8 g), protein (6.8 g), fiber (1.4 g), fat (0.6 g) and energy 344 Kcal (Verma and Shukla, 2011, Rather et. al. 2016, Tiwari et al., 2017 Sahu et al 2018).

Paddy consists of 18-24 % husk, 8-12 % bran depending on the milling degree and 68-72 % white rice depending on the variety (IRRI Rice Knowledge Bank, 2017). Rice is also available in the form of brown rice, white rice, sweet rice, jasmine bhutanese red rice and forbidden rice. Rice is obtained after dehusking the paddy and is termed as brown rice. When outer layer bran is removed, the rice is termed as polished rice. The process is known as whitening or polishing.

MATERIAL AND METHODS

All the experiments were carried out in the rice milling laboratory of Post-Harvest Process and Food Engineering Department, College of Agricultural Engineering, JNKVV, Jabalpur.

Determination of moisture content:According to the standard procedure of AOAC (1980), weighed samples of kernel is kept in a Petri dish and dried in a hot air oven at 105 ^{0}C for 24 hours. The moisture content was determined by following formula

$$\text{Moisture \% (wb)} = \frac{\text{Weight of moisture}}{\text{Weight of sample}} \times 100$$

Cleaning and grading

The Pusa sugandha-1 variety of rice was cleaned and graded by laboratory model air screen cleaner (Model – Delux, S.No: T.S.G. 135). The clean paddy was shelled by rubber roll sheller (Indosaw Industrial Products Pvt. Ltd.) and polished by friction polisher (Osaw Industrial Products Pvt Ltd).

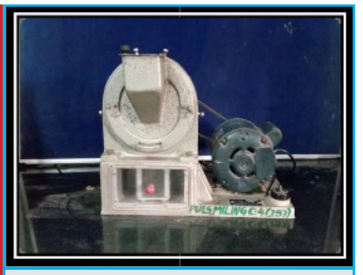

PLATE 1. Polisher

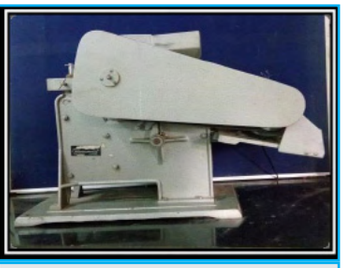

PLATE 2. Rubber roll Sheller

Geometric properties

Hundred kernels were randomly selected for measurement of length, breadth and thickness. These parameters were determined by using a digital dial gauge (least count 0.01 mm). Length was taken as the largest intercept of the kernel at resting position, breadth was taken as the largest intercept perpendicular to the length and thickness was measured as the largest intercept perpendicular to the length and breadth.

Size: Size and shape are important physical properties and are used to describe the object. Size measurement analysedbehavior of grain during handling, processing, storage and designing the machinery using following expression.

$$\text{Size} = (\text{length} \times \text{breadth} \times \text{thickness})^{1/3}$$

$$\text{Size} = (l \times b \times t)^{1/3}$$

L/B ratio

In India, most of the rice varieties are long (more than 7 mm) and slender in shape (L/B >2.5 and < 3). The shape of the grain influenced volume and weight. Slender varieties of paddy or rice occupy more volume than round varieties. Therefore, one ton of a slender variety of paddy will need more storage space than the same weight of round variety of paddy. Size and shape of rice affects many other properties, namely, sieving, dehusking, polishing, storage as well as cooking (Rather et. al. 2016).

Sphericity: Sphericity is defined as the ratio of the diameter of a sphere of same volume as that of the sphere particle and the largest diameter of the sphere. This parameter shows the shape character of the particle relative to the sphere having the same volume. The sphericity (φ) of the kernels was calculated as (Curray et al. 1951).

$$\text{Sphericity} = \frac{(l \times b \times t)^{1/3}}{l}$$

Volume:The unit volume of the rice kernels was calculated by the following relationship (Varnamkhasti et al., 2007).

$$\text{Volume, } V = \frac{\pi}{6} \times (l \times b \times t)$$

Where,

V = unit volume (mm^3). l, b and t = length, breadth and thickness of grain (mm)

Gravimetric properties: Bulk Density*:* The density of the grains is used in the design of storage bins and silos, separation of desirable materials from impurities, cleaning and grading, evaluation of the grain maturity etc. The bulk density of the rice kernels is the density of whole grains (including the voids). It was determined by filling a 100 ml cylindrical vessel with rice kernels, tapping it twice to cover the extra space between the kernels and then weighing the contents of the vessel using a weighing balance. The volume of the vessel taken as the volume of the rice kernels. Bulk density is the ratio of the mass of the sample to its total volume.

$$\text{Bulk density} = \frac{\text{Mass of sample (kg)}}{\text{Total volume } (m^3)}$$

True Density: The true density of the rice kernels is the density of grains excluding the voids. This was determined by the toluene ($C_6H_5CH_3$) displacement method. In this method, toluene was filled in a 100 ml measuring cylinder and then same mass of sample that was taken for bulk density was put into the vessel containing toluene. The displacement of toluene level in the vessel on putting rice kernels was noted down. The ratio of the mass of rice kernels to the volume of displaced toluene gave the true density.

$$\text{True density} = \frac{\text{Mass of sample (kg)}}{\text{Volume displaced } (m^3)}$$

Porosity: The porosity of rice grains refers to the fraction of the pore spaces in the bulk grain that is not occupied by the grain. It is calculated from the values of true density and bulk density by the following relationship

$$\text{Porosity} = \frac{\text{(True density - Bulk density)}}{\text{True density}} \times 100$$

Test weight: Thousand grain weights of different rice samples was determined by counting one hundred rice kernels, weighing them on a weighing balance and then multiplying it with the factor of 10 (Varnamkhasti et al., 2008).

RESULTS AND DISCUSSION

The length, breadth and thickness are very important geometric characteristics for deciding the size of opening of air screen cleaners. A summary of the results of the geogravimetric properties of polished rice (Pusa Sugandha-1) is shown in Table 1 and 2. The average length, breadth and thickness were 8.17, 1.60 and 1.64 mm respectively. The ratio of length and breadth was obtained as 5.10. Tiwari et al. (2017) conducted a study to evaluate of physical properties of brown rice (MTU 1010) and reported average values of length, breadth and thickness as 6.39, 2.14 and 1.9 mm. Similar results were observed by Sahu et. al (2018) while studying some physical properties of Madhuraj, Hanthipanjra and Mahamayavarieties.The shape and L/B ratio are very important for designing the indents of disc and cylindrical separator. Shape is very important for design of helices of spiral separator also. Extra-long (> 7 mm) rice gets high price in national and international market. Rice is also grouped in three grades i.e. super fine (L/B >3), fine (L/B > 2.5) and common (L/B<2.5) on the basis of above ratio, (Araullo et al., 1985).

Size of polished rice was observed in the range of 2.52-2.89 mm. The size of the grain is useful in estimation of the projected area of a particle moving in the turbulent or near- turbulent region of an air steam (Omobuwajo *et al*., 1999). The sphericity of polished rice was observed as 33.9, which indicates elongated shape of the grains and makes it difficult to roll on surface. This was lower than corresponding value of sphericity (35.72) reported by Tiwari et al (2010) for Sugandha-3 variety of rice. While the value of sphericity of paddy (var. Sazandegi) was 39.88% (Varnamkhasti et al., 2007). Paddy grains with lower sphericity will likely be more difficulty to roll freely on a flat surface, Sanusiet. al (2017). The ability to either roll or slide is necessary in the design of hoppers for milling process. Sphericity values (44.36, 38.82, and 41.47 %) were reported bySahuet.al (2018) for Madhuraj, Hanthipanjra and Mahamaya varieties respectively.

The bulk density, true density, and porosity of polished rice were observed as 798.60 kg/$m^{3,}$ 1412.56 kg/m^3, and 43.4 percent respectively. Varnamkhasti et al. (2007) studied true density, bulk density, and porosity of rough rice (Sazandegi) and reported the values as 798.60 kg/m^3,1193.38 kg/m^3 and 60.3 percent respectively. The similar results 592.50 kg/m^3, 1145.88 kg/m^3 and 48.09 percent respectively, were also observed by Tiwari and Sharma (2012) for brown rice (WGL 32100). These properties are used for designing the size of opening of screen.Thousand grain weight is commercially very important as it characterized various grades like extra heavy, heavy and moderately heavy, which decides the export price. Thousand-grain weight of polished rice

PLATE 3. Paddy

PLATE 4. Polished rice

Table 1. Geometric properties of polished rice (Pusa Sugandha-1)

Properties	Number of observations	Mean value	Minimum value	Maximum value
Length (mm)	100	8.17	7.43	8.24
Breadth (mm)	100	1.60	1.59	1.76
Thickness (mm)	100	1.54	1.36	1.68
Size (mm)	100	2.77	2.52	2.89
L/B ratio	100	5.10	4.67	5.29
Volume (mm^3)	100	10.53	8.40	12.75
Sphericity	100	33.90	33.64	35.18

Table 2. Gravi metric properties of polished rice (Pusa Sugandha -1)

Properties	Number of observations	Mean value	Minimum value	Maximum value
True density (Kg/m^3) Bulk density (Kg/m^3)	5 5	1412.56 798.60	1289.14 756.43	1506.23 812.12
Porosity (%)	5	43.46	41.32	46.08
Test weight (g)	5	16.82	15.58	17.43

was recorded as 16.82 grams. Since the weight of polished rice is less than 20 grams it will be characterized in *moderately heavy* group.

CONCLUSION

The results of geometric and gravimetric properties of Pusa Sugandha-1 at fourteen percent moisture content (wb) are shown in Table 1 and 2 respectively. The average

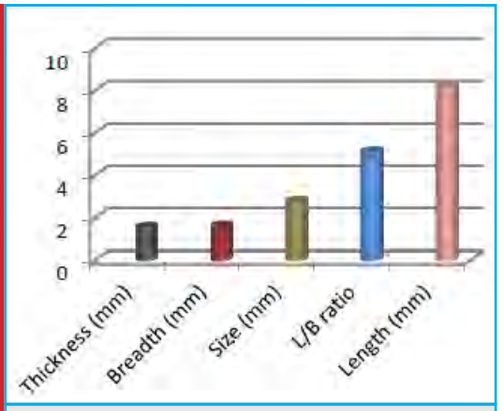

FIGURE 1. Geometric properties of polished rice

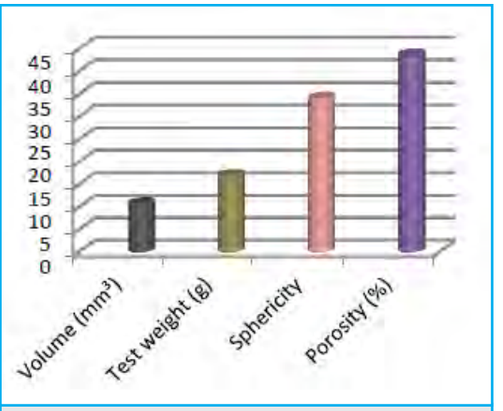

FIGURE 2. Gravimetric properties of polished rice

length, breadth and thickness were observed as 8.17, 1.60 and 1.54 mm respectively. The average size, L/B ratio and volume were determined 2.77 mm, 5.10 and 10.53 mm^3. The bulk density true density, and porosity were observed 798.6 kg/m^3, 1412.56 kg/m^3 and 43.46 percent. The sphericity of rice was 33.90 percent which shows that rice is elongated and will create friction in rolling.

REFERENCES

Agriculture Statistics at a Glance, http://eands.dacnet.nic.in/PDF/Glance-2016.pdf, (2016).

AOAC. 1980. Association of Analytical Chemists, Official methods of analysis, 13th Edition, Washington, D.C

Araullo EU, Padua DBD and Graham M. 1985. Rice post-harvest technology. International Development Research Centre.

Ashtiani AH, Sadeghi M, Hemmat A. 2010. Physical properties of two rough rice varieties affected by moisture content. International Agrophysics 24: 205-207.

BhupendraSahu, D. Khokhar, S. Patel, N. K. Mishra and Girish Chandel (2018). Some Engineering Properties of Selected Paddy Varieties.

Department of the Agricultural Processing and Food Engineering, Faculty of Agricultural Engineering, IGKV, Raipur, Chhattisgarh. Int. J. Pure App. Biosci.6 (2): 1337-1342 (2018).

Curray JR. 1951. Analysis of sphericity drying of food grains. Int Res Journal 22 15-20.

Dipti, S. S., Bari, M. N., &tKabir, K. A. (2003). Grain quality characteristics of some beruin rice varieties of Bangladesh. Pakistan Journal Nutrition, 2 (4), 242-245.

Ghasemlou M, Khodaiyan F, Gharibzahedi SMT, Moayedi A, Keshavarz B. 2010. Study on postharvest physico-mechanical and aerodynamic properties of mungbean [*Vigna radiate* (L.) Wilczek] seeds. International Journal of Food Engineering 6: 122.

IRRI Rice Knowledge Bank. 2017. (www.knowledgebank.irri.org/.../postharvest/milling).

IRRI, 2013. Trends in global rice consumption: Rice Today. International Rice Research Institute, Manila, Philippines. 12:1.

Mayowa S. Sanusia, Rahman Akinosoa, and NahemiahDanbabab (2017). Evaluation of Physical, Milling and Cooking Properties of Four New Rice (*Oryzasativa* L.)

Varieties in Nigeria). International Journal of Food Studies.

Department of Food Technology, Faculty of Technology, University of Ibadan, Nigeria. October 2017 Volume 6 page 245-

256.

Omobuwajo TO, Akanda EA and Sanni LA. 1999. Selected physical, mechanical and aerodynamic properties of African breadfruit (Treculla Africana) seeds. J. Food Engg 40: 241–4.

Rather, T. A., Malik, M. A., & Dar, A. H. (2016). Physical, milling, cooking, and pasting characteristics of different rice varieties grown in the valley of Kashmir india. Cogent Food & Agriculture, 2 (1), 1178694.

Tiwari VK and Sharma N. 2012. Varietal influence on physical characteristics of brown rice. JNKVV Res J 46(1): 90-93.

Tiwari VK, Dayma V, and Sharma HL note on the studies of physical properties of brown rice. International Journal of Scientific Development and Research 2.

Tiwari VK. 2010. Investigations on physical and engineering properties of rice variety Sugandha-3 grain at Jabalpur, Madhya Pradesh. JNKVV Res J 44(2): 213-216.

Varnamkhasti MG, Mobli H, Jafari A, Rafiee S, Heidarysoltanabadi M and KheiralipouR K..2007. Some Engineering Properties of Paddy (var. Sazandegi).International Journal of Agriculture & Biology 5:763–766.

Varnamkhasti MG, Mobli H, Jafari A, Key-hani AR, Soltanabadi MH, Raee S and Kheiralipour, K. 2008. Some physical properties of rough rice (*Oryzasativa*.) grain. Journal of Cereal Science 47 (3):496.

Verma DK, and Shukla K. 2011. Nutritional value of rice and their importance. Indian Farmers' Digest.

Soil Science Communication

Biosci. Biotech. Res. Comm. 12(1): 186-193 (2019)

BBRC Bioscience Biotechnology Research Communications

Distribution of nitrogen fractions under long term fertilizer and manure application in a vertisol

A. Khandagle[1,2*], B. S. Dwivedi[1], S. B. Aher[2], A. K. Dwivedi[1], D. S. Yashona[2], S. Mohbe[2] and S. Panwar[2]

[1]*Jawaharlal Nehru Krishi Vishwa Vidyalaya, Jabalpur 482004, Madhya Pradesh, India*
[2]*ICAR-Indian Institute of Soil Science, Bhopal 462038, Madhya Pradesh, India*

ABSTRACT

A field experiment was conducted under Long Term Fertilizer Experiment during 2016-17 at Research Farm, College of Agriculture, JNKVV, Jabalpur. The eight treatments were applied in comprising of different doses of fertilizers viz. 50% NPK, 100% NPK, 150% NPK, 100% NP, 100% N, 100% NPK+FYM, 100% NPK-S and Control, replicated four times in a randomized block design. The application of 100% NPK+FYM showed higher content of all the fractions of N viz. Total hydrolysable-N, Hydrolysable ammonical-N, inorganic–N, hexose amine & hydro.ammo.-N, hexose amine-N, amino acid-N, unidentified hydrolysable-N, non-hydrolysable-N and total N and lower content was recorded in treatment 50%NPK followed by 100% N. The result also revealed that the N fractions were significantly decreased with increasing depth of soil.

KEY WORDS: LONG TERM FERTILIZER ADDITION, ASSESSMENT OF SOIL FERTILITY, NITROGEN FRACTIONS

INTRODUCTION

Nitrogen is the key element among the major nutrients and without N plant can neither complete a normal reproductive process nor reach its yield potential. It is a constituent of ADP and ATP to most substance in life process, thereby, N nutrient play key role in protein synthesis, oxidation reduction and energy transfer reaction of cell metabolism. It has been established that there are two major sources accounts for the availability viz. inherently from soil source and secondly supplementation through fertilizers and manures. Prolonged application of fertilizers and organic manures differentially influenced mineral N (NO_3^--N and NH_4^+-N), organic N fractions, and total N in soils. Organic N fractions constituted about 94.2% of total N as compared with 5.8%

ARTICLE INFORMATION:

Corresponding Author: abhishekkhandagle13@gmail.com
Received 27th Dec 2018
Accepted after revision 23rd March 2019
BBRC Print ISSN: 0974-6455
Online ISSN: 2321-4007 CODEN: USA BBRCBA
Thomson Reuters ISI ESC / Clarivate Analytics USA
NAAS Journal Score 2019: 4.31 SJIF: 4.196

Online Contents Available at: http//www.bbrc.in/
DOI: 10.21786/bbrc/12.1/25

share of mineral N. Nitrate N was the dominant mineral N fraction in the soil, which was 4.4 times higher than NH_4^+-N fractions. Application of fertilizers improved available N in soil. Hydrolyzable-N increased with the application of organic manures. Of the total hydrolyzable-N fractions in soils, ammonia-N was 25%, amino sugar-N 9.9%, amino acid-N 25.2%, and hydrolyzable unknown-N 39.8%. A significant positive correlation was recorded between crop yield and N uptake. Amino acid-N and amino sugar-N explained 82.9% of the variation in rice yield and 73.4% of the variation in wheat yield. Integrated use of organic manures and inorganic fertilizers improved the N fractions in the soil, which should help increase rice and wheat production (Durani et al. 2016).

Mineralization of organic nitrogen fraction may play a major role in the N supply of plants. Nitrogen mineralization is of great importance because it converts organic N into NH_4^+ which is available for plant uptake and microbial processes, Mineralization of soil organic N must be taken in to account if N fertilizers are to be used efficiently, Unfortunately, little progress has been made in identifying and measuring an easily mineralizable fraction, or dealing with year to year variability in net mineralization under field conditions, which arises from the effects of temperature and moisture supply on N-cycle process Hence N-fertilizer recommendations have often been made on the basis of cropping or economics factor rather than soil testing (Mulvaney et al., 2001) However, N mineralization studies have largely been confined to the top soil, although plants also utilize N from deeper horizons. The topsoil has the largest contents of crop residues, easily decomposable organic matter, the greatest microbial biomass and activity, and therefore N Mineralization (Soudi et al., 1990). However, other studies have shown that a significant proportion of N mineralization occurs in sub soil (Patra et al., 1999).

MATERIALS AND METHODS

Experimental site, climate and soil characteristics: Present investigation was conducted in an ongoing scheme All India Coordinated Research Project (AICRP) on Long Term Fertilizers Experiment (LTFE) of Indian Council of Agricultural Research (ICAR). The LTFE is laid out on a permanent site at the Experimental field Department of Soil Science and Agricultural Chemistry, Jawaharlal Nehru Krishi Vishwa Vidyalaya. Jabalpur (M.P.). The experimental site is situated in 'Kymore Plateau and Satpura Hills' agro climatic region of M.P. It falls on 23.9° N latitude and 79.6° E longitudes with an altitude of 411.8 m above the mean sea level. Jabalpur is situated in the semi-arid region having sub-tropical climate with hot dry summer, and cold winter. The average rainfall is about 1350 mm, which is mainly distributed from mid June to October. The maximum and minimum temperature ranges between 35.1°C and 5.3°C. The average annual relative humidity is 62%.

Table 1. Initial characteristics of experimental soil

Soil properties	Value
Sand (%)	25.5
Silt (%)	17.6
Clay (%)	56.9
Texture class	Clay
Bulk density (Mg m^{-3})	1.30
pH (1:2.5)	7.60
EC (1:2.5) (dSm^{-1})	0.18
OC (%)	0.57
Available nitrogen (kg ha^{-1})	193
Available phosphorus (kg ha^{-1})	7.60
Available potassium (kg ha^{-1})	370
Available sulphur (mg kg^{-1})	7.80

The experiment was started with maize fodder as the first crop in summer season of 1972; since then Soybean (Kharif)-Wheat (Rabi)-Maize fodder (summer) crop rotation was adopted till 1994.However, since 1994 the cultivation of maize fodder was left and presently the cropping sequence being followed is soybean (Kharif) and wheat (Rabi). The soil of the experimental field is medium black belonging to Kheri series of fine montmorillonitic hyperthermic family of Typic Haplustert. At the beginning of this experiment in 1972, initial soil samples was collected before application of the treatments and analyzed for different soil properties (Table 1).

Treatments detail: The experiment has been in continuance since 1972 with 10 different treatments, however in present experiment following 8 set of treatments was selected. The selected treatments involve 50% NPK; 100% NPK; 150% NPK; 100% NP; 100% N; 100% NPK+FYM; 100% NPK-S and Control. The 100% optimal NPK doses based on initial (1972) soil test values were 120:80:40 and 20:80:20 ($N:P_2O_5:K_2O$) for wheat and soybean respectively. Nitrogen was applied through urea, phosphorus through single super phosphate and potassium was applied through murate of potash. The farm yard manure in FYM treatment was applied @ 5 ton ha^{-1} $year^{-1}$ to soybean crop only. Due to build of Zn content in soil. The application of Zn as $ZnSO_4$@ 20 Kg ha^{-1} in alternate year to wheat crop was discontinued since, 1987.

Soil sampling and analysis : The representative soil samples were collected from two depths viz. 0-15 and 15-30 cm from each plot with the help of soil auger after

44 year of continuous cropping. The composite soil samples were prepared by quartering technique. The composite soil samples were air dried, crushed by wooden pestle and mortar then passed through 2 mm sieve and finally the processed samples were used for analysis of different physical and chemical properties.

The soil pH and electrical conductivity (EC) was measured by glass electrode pH meter and EC meter in 1:2.5 soil: water suspension (Piper, 1950). For determination of the soil organic carbon, a suitable quantity of the soil was digested with chromic acid and sulphuric acid. Excess of chromic acid left over unreduced by the organic matter of the soil was determined by a titration with Ferrous Ammonium Sulphate solution using diphenylamine indicator (Walkley and Black, 1934). Available nitrogen in soil sample was determined by using alkaline permanganate method (Subbiah and Asija, 1956) in which soil was mixed with excess of alkaline permanganate and distilled. Organic matter present in soils was oxidized by the nascent oxygen liberated by KMnO4 in the presence of NaOH and thus ammonia was released. The released ammonia was absorbed in the boric acid (2%) containing mixed indicator and converted to ammonium borate. The formed ammonium borate was back titrated with standard sulphuric acid. The soil available phosphorus content was estimated by extracting the soil with 0.5 M NaHCO3 (pH 8.5) and determination was done by ascorbic acid method on spectrophotometer (Olsen et al., 1954). The available potassium in soil was extracted by neutral 1N ammonium acetate and it was estimated using flame photometer (Muhr et al., 1963). Soil available sulphur was extracted with 0.15% solution of CaCl2 and determined by turbidimetric method (Chesin and Yien, 1951). The total nitrogen and various nitrogen fractions were determined by following standard methods (Table 2).

Statistical analysis: The data obtained was compiled and analyzed for its significance (p=0.05) by statistical procedure appropriate for randomized block design as outlined by Gomez and Gomez (1985).

Table 2. Standard methods employed for determination of different soil parameters

Soil properties	Standard method	Reference
pH(1:2.5)	Glass electrode pH meter	Piper (1967).
Electrical conductivity (1:2.5)	Conductivity meter	Black (1965).
Organic carbon	Dichromate oxidation	Walkley and Black (1934)
Available Nitrogen	Alkaline potassium permanganate method	Subbiah and Asija (1956)
Available Phosphorus	Spectrophotometer	Olsen et al (1954)
Available Potassium	Flame photometer	Muhr et al (1965)
Available Sulphur	Spectrophotometer	Chesin and Yien (1951)
Total Nitrogen	Steam distillation method	Page and Bremmer (1965)
Nitrogen fractions	Steam distillation method	Bremmer (1965)

RESULTS AND DISCUSSION

Distribution of total nitrogen and nitrogen fractions: Total N

The total N content in soil (0-15 cm) increased successively from 1463 to 1621 and 1723 kg ha^{-1} as the dose of fertilizer increased from 50%, 100% and 150% NPK, respectively. The highest value of total N was 1818 kg ha^{-1} recorded with 100% NPK+FYM treatment. While, the lowest value of total N was observed in control (1306 kg ha^{-1}). It is equal to sum of total hydrolysable-N and non-hydrolysable-N (Table 3). The total N content in soil decreased with depth. The highest total N content 1687 kg ha^{-1} in 15-30 cm soil depth was recorded in 100% NPK+FYM, whereas the lowest value was noticed as 1132 kg ha^{-1} in control followed by 50% NPK (1437 kg ha^{-1}). Slightly higher value of total N content was noticed in 150% NPK (1572 kg ha^{-1}) as compared to 100% NPK (Table 4).

The total N content as influenced by various treatments indicated that higher values of N content was obtained from surface soil could be due to the presence of residues after the harvest of crop as suggested by Meints and Peterson, (1977). The total N in soils at various depths differed significantly by application of manure and fertilizer with respect soil depths. Interaction of treatment levels with soil depth was found to be significant on total N. These finding are in accordance with those of Aggarwal et at. (1990) and Singh and Singh (2007). It has also been noted that higher status of total N was obtained on the surface while it progressively declined with depth (Kushwaha, 2011). The increase in fertilizer application rate, the amount of total nitrogen was also found increased significantly. The present results are also in conformity with the findings of Babita (2010) and Nayak et al. (2013).

Inorganic N: The inorganic N content in soil (0-15 cm) increased successively from 141 to 152 and 173 kg ha^{-1} as the dose of fertilizer increased from 50%, 100% and 150% NPK, respectively. The lowest value of inorganic-N was observed in control (122 kg ha^{-1}). While, the high-

Table 3. Effect of long term application of fertilizers and manure on total nitrogen and nitrogen fractions in 0-15 cm soil depth

Treatments	Total N	Inorganic-N (NH_4-N+NO_3-N)	Total Hydrolysable-N	Hydrolysable Ammonical-N
50 % NPK	1463.4	141.8	1010.8	274.4
100% NPK	1621.3	152.0	1208.0	293.4
150% NPK	1723.4	173.8	1288.4	307.4
100 %NP	1540.1	148.3	1131.3	288.0
100 % N	1513.3	142.6	1087.9	281.4
100% NPK+FYM	1818.6	188.5	1371.4	341.1
100 % NPK-S	1568.2	150.8	1164.7	290.9
Control	1306.1	122.2	939.2	259.0
SEm±	55.6	3.2	38.0	14.4
CD (5%)	181.2	10.5	123.8	46.9
(Values in kg ha^{-1})				

est value of inorganic-N 188 kg ha^{-1} was recorded with 100% NPK+FYM treatment (Table 3). The inorganic N content of soil decreased with soil depth (Table 4). Significantly higher value of inorganic-N content in 15-30 cm soil depth was noticed in 150% NPK (163 kg ha^{-1}) as compared to 100% NPK (143 kg ha^{-1}). The highest inorganic N content of 172 kg ha^{-1} was recorded in 100% NPK+FYM whereas the lowest value was noticed as 109 kg ha^{-1} in control followed by 50% NPK (130 kg ha^{-1}). The inorganic N content was significantly influenced by various treatments due to addition of fertilizer doses suboptimal, optimal and super optimal, N content was correspondingly improved enrichment in Inorganic-N as a result of fertilizer application in these treatments in surface and subsurface soil positive effect of FYM (Kushwaha, 2011). Application of FYM also increased NH_4^+ - N and NO_3^- N content in soil over the control throughout the incubation period and this was attributed to increase microbial population and N content (Duhan et al. 2005).

Total hydrolysable N: The highest value of total hydrolysable-N in 0-15 cm soil depth was recorded with 100% NPK+FYM treatment (Table 3). While, the lowest value 939 kg ha^{-1} of total hydrolysable-N was noticed in control. Total hydrolysable-N content in soil increased successively from 1010 to 1208 and 1288 kg ha^{-1} as the dose of fertilizer increased from 50%, 100% and 150% NPK, respectively. The data presented in Table 4 showed that the total hydrolysable N content of soil decreased with soil depth. The highest total hydrolysable N content 1215 kg ha^{-1} was recorded in 100% NPK+FYM, whereas the lowest value was noticed as 712 kg ha^{-1} in control followed by 50% NPK (913 kg ha^{-1}). Slightly higher value of total hydrolysable N content was obtained in 150% NPK (1132 kg ha^{-1}) as compared to 100% NPK (1048 kg ha^{-1}).

Table 4. Effect of long term application of fertilizers and manure on total nitrogen and nitrogen fractions in 15-30 cm soil depth

Treatments	Total N	Inorganic-N (NH_4-N+NO_3-N)	Total Hydrolysable-N	Hydrolysable Ammonical-N
50 % NPK	1437.0	130.2	913.4	259.6
100% NPK	1519.6	143.5	1048.5	285.1
150% NPK	1572.5	163.0	1132.0	297.5
100 %NP	1449.7	138.3	1005.4	279.8
100 % N	1439.3	131.0	998.3	271.7
100% NPK+FYM	1687.3	172.8	1215.2	332.6
100 % NPK-S	1510.8	141.3	1020.4	282.3
Control	1132.9	109.4	712.5	227.8
SEm±	46.8	2.9	28.7	10.7
CD (5%)	152.5	9.5	92.3	34.9
(Values in kg ha^{-1})				

It has been observed that higher status of total hydrolysable N was obtained on the surface while progressively decreased with depth but the rate of depletion was more apparent from surface to subsurface soil. This could be attributed to higher root biomass in the rhizospheric upper soil layer and which decreased with increasing soil depth. It supports the view that total hydrolysable N is more susceptible to mineralization than non-hydrolysable N (Rao and Ghosh, 1981; Reddy et al., 2003). The content of the total hydrolysable N were maximum in surface soil and thereafter decreased with the depth reported by Reddy et al. (2003), Kushwaha (2011) and Rai (2013).

Hydrolysable ammonical N: The Hydrolysable ammonical-N content in soil (0-15 cm) increased successively from 274 to 293 and 307 kg ha^{-1} as the dose of fertilizer increased from 50%, 100% and 150% NPK, respectively. The lowest value of hydrolysable ammonical-N was noticed in control 259 kg ha^{-1}.While, the highest value of hydrolysable ammonical-N 341 kg ha^{-1} was recorded with 100% NPK+FYM treatment (Table 3). The hydrolysable ammonical N content of soil decreased with soil depth (Table 4). The higher value of hydrolysable ammonical-N content was noticed in 150% NPK (297 kg ha^{-1}) as compared to 100% NPK (285 kg ha^{-1}). Maximum hydrolysable ammonical-N content 332 kg ha^{-1} was recorded in 100% NPK+FYM, whereas the minimum value was noticed as 227 kg ha^{-1} in control followed by 50% NPK (259 kg ha^{-1}). The highest hydrolysable ammonical N content was found with 100% NPK+FYM (341 kg ha^{-1}), which could be due to organic matter build up which facilitates N accumulation in soil. Rai (2013) reported that hydrolysable ammonium N content was highest in the surface soil and decreased down the profile. Sub surface soil layer recorded 5% reduction in hydrolysable ammonical–N as compared to surface layer in all the treatment, the increase in hydrolysable ammonical–N in surface layer might be due to carry over effect of continuous use of organic residue (Sepehya et al., 2012).

Hexose amine and hydrolysable ammonical-N: The maximum value of hexose amine and hydrolysable ammonical-N 378 kg ha^{-1} in 0-15 cm soil depth was recorded with 100% NPK+FYM treatment (Table 5). While, the minimum value of hexose amine and hydrolysable ammonical-N 277 kg ha^{-1} was observed in control. Hexose amine and hydrolysable ammonical N content in soil increased successively from 297 to 323 and 341 kg ha^{-1} as the dose of fertilizer increased from 50%, 100% and 150% NPK, respectively. The highest hexose amine and hydrolysable ammonical-N content in 15-30 cm soil depth (366 kg ha^{-1}) was recorded in 100% NPK+FYM, whereas the lowest value 240 kg ha^{-1} was noticed in control followed by 50% NPK (278 kg ha^{-1}). Slightly higher value of hexose amine and hydrolysable ammonical-N content was recorded in 150% NPK (327 kg ha^{-1}) as compared to 100% NPK (305 kg ha^{-1}) (Table 6). The data showed that higher values of Hexose amine and hydrolysable ammonical-N content were recorded at surface soil as compare to sub surface soil which could be resulted due to FYM build up hydrolysable ammonical and hexose amine and chemical fertilizers may enhance hexose amine + hydrolysable ammonical-N content in soil (Broabdent 1965). Similar results have been reported by Kushwaha (2011).

Hexose amine-N: Hexose amine-N content in soil (0-15 cm) increased successively from 23.0 to 29.6 and 34.5 kg ha^{-1} as the dose of fertilizer increased from 50%, 100% and 150% NPK, respectively. The highest value of

Table 5. Effect of long term of fertilizers and manure on N-fractions in 0-15 cm soil depth

Treatments	Hexose amine and hydrolysable Ammonical N	Hexose amine N	Amino acid N	Unidentified Hydrolysable N	Non-hydrolysable N
50 % NPK	297.3	23.0	279.0	434.5	452.7
100 % NPK	323.1	29.6	295.7	589.3	413.3
150% NPK	341.5	34.6	328.5	618.0	435.0
100 %NP	315.3	27.4	294.8	521.1	408.8
100 % N	310.3	29.1	288.5	488.9	425.5
100 % NPK+FYM	378.3	37.2	356.5	636.6	447.3
100 % NPK-S	319.3	29.3	299.7	544.9	403.5
Control	277.0	18.2	241.0	420.4	367.0
SEm±	13.9	1.7	13.8	15.8	44.9
CD (5%)	45.2	5.5	44.3	45.7	NS

(Values in kg ha^{-1})

Table 6. Effect of long term of fertilizers and manure on N-fractions in 15-30 cm soil depth

Treatments	Hexose amine and hydrolysable Ammonical N	Hexose amine N	Amino acid N	Unidentified Hydrolysable N	Non-hydrolysable N
50 % NPK	278.1	18.5	261.6	373.8	523.6
100 % NPK	305.1	20.0	280.0	463.4	471.2
150% NPK	327.1	29.6	316.2	488.7	440.5
100 %NP	301.3	21.5	278.8	425.4	444.2
100 % N	297.8	26.2	273.1	427.3	441.0
100 % NPK+FYM	366.3	32.8	326.8	522.1	472.1
100 % NPK-S	307.3	25.0	280.1	433.0	490.4
Control	240.8	13.0	223.6	248.1	420.4
SEm±	11.3	1.1	10.7	14.8	20.8
CD (5%)	36.8	3.6	34.8	43.0	60.4

(Values in kg ha^{-1})

hexose amine-N 37.2 kg ha^{-1} was recorded with 100% NPK+FYM treatment. While, the lowest value of hexose amine-N was observed in control 18.2 kg ha^{-1} (Table 5). The data in Table 6 showed that the hexose amine N content of soil decreased with soil depth. Slightly higher value of hexose amine-N content (15-30 cm) was obtained in 150% NPK (29.5 kg ha^{-1}) than 100% NPK (20.0 kg ha^{-1}). The maximum hexose amine N content 32.7 kg ha^{-1} was recorded in 100% NPK+FYM, whereas minimum value was noticed as 13.0 kg ha^{-1} in control followed by 50% NPK (18.4 kg ha^{-1}). The continuous addition of nitrogen through organic and inorganic sources contributed directly to the enrichment of this pool of organic nitrogen, similar build up in this fraction under same set of agro climatic condition has been reported by Kumar (2003) and Kushwaha (2011). Similar results have also been reported by Swapana et al. (2012).

Amino acid-N: Amino acid-N content in soil (0-15 cm) increased successively from 279 to 295 and 328 kg ha^{-1} as the dose of fertilizer increased from 50%, 100% and 150% NPK, respectively. The minimum value of amino acid-N was observed in control 241 kg ha^{-1}. While, the maximum value of amino acid-N 356 kg ha^{-1} was recorded with 100% NPK+FYM treatment (Table 5). The highest amino acid-N content (15-30 cm soil depth) of 326 kg ha^{-1} was recorded in 100% NPK+FYM, whereas the lowest value was noticed as 223 kg ha^{-1} in control followed by 50% NPK (261 kg ha^{-1}). Non-significantly higher value of amino acid-N content was obtained in 150% NPK (316 kg ha^{-1}) than 100% NPK (Table 6).

The content of the amino acid N was maximum in surface soil and thereafter decreased with the depth reported by Reddy et al. (2003), Sammy et al. (2003) and Sepehya et al (2012). However, due to addition of fertilizer doses suboptimal, optimal and super optimal, Amino acid N content was correspondingly improved indicating an impact of fertilizer application on enrichment of N pools (Keeney and Bremner 1964). The small decrease in amino acid-N fraction as compared to Hexose amine N and Hydrolysable ammonica-N in control plot could be due to inclusion of legume crop (soybean) in the rotation which has been found to promote the buildup of amino acid-N (Stevension, 1956).

Unidentified hydrolysable-N: Unidentified hydrolysable-N content in 0-15 cm soil increased successively from 434 to 589 and 617 kg ha^{-1} as the dose of fertilizer increased from 50%, 100% and 150% NPK, respectively. The value of unidentified hydrolysable-N was slightly higher in 100% NP than 100% N. The highest value of unidentified hydrolysable-N 636 kg ha^{-1} was recorded with 100% NPK+FYM treatment. While, the lowest value of unidentified hydrolysable-N was observed in control 421 kg ha^{-1} (Table 5). The data further showed that the unidentified hydrolysable-N content of soil (15-30 cm) decreased with soil depth (Table 6). Higher value of unidentified hydrolysable-N content was observed in 150% NPK (489 kg ha^{-1}) as compared to 100% NPK (463 kg ha^{-1}). The highest unidentified hydrolysable-N content 522 kg ha^{-1} was recorded in 100%NPK+FYM, whereas the lowest value was noticed as 216 kg ha^{-1} in control followed by 50% NPK (373 kg ha^{-1}).

The higher value of unidentified hydrolysable-N content was obtained from surface soil compare to sub surface soil. Highest Unidentified hydrolysable N content was registered with 100% NPK+FYM (636 kg ha^{-1}). Further lower content was found in control (421 kg ha^{-1}) attributed due to no fertilizers application which directly or indirectly affected normal biological activi-

ties Rao and Ghosh, (1981). The treatment wise pattern was almost same as that was observed in case of surface soil. Positive effect on build up of unidentified-N fraction with the application of organic along with chemical fertilizers might be attributed to the movement of applied nitrogen from upper layer been reported Sepehya et al. (2012). It has also been noted that higher status of Unidentified hydrolysable N was obtained on the surface while progressively declined with depth but the rate of depletion was more apparent from surface to subsurface soil while, it was stabilized below 30 cm. Thus, it could be attributed to higher root biomass in the rhizospheric upper soil layer and which declined with increasing soil depth (Kushwaha, 2011).

Non-hydrolysable-N: Non-hydrolysable-N content in 0-15 cm soil depth varied from 452, 414 and 436 kg ha^{-1} as levels of fertilizer increased from 50%, 100% and 150% NPK, respectively (Table 5). The maximum value of non-hydrolysable N 458 kg ha^{-1} was recorded with 100% NPK+FYM treatment. While, the lowest value of non- hydrolysable-N was observed control 366 kg ha^{-1}. Similarly, the highest non-hydrolysable N content (15-30 cm soil depth) of 524 kg ha^{-1} was recorded with 50% NPK, whereas the lowest value was noticed as 420 kg ha^{-1} in control followed by 100% NP (428 kg ha^{-1}) (Table 6).

The data indicated lower values of Non-hydrolysable-N content in surface soil. The addition of fertilizer doses suboptimal, optimal and super optimal did not showed any significant improvement in N-pool. The application of fertilizers N even up to its highest level did not show any improvement in non hydrolysable N content in soil. Further, it has also been noted that lower status of Non-hydrolysable N was obtained on the surface while progressively increased with depth. The similar results have been reported by Reddy et al. (2003) and Kushwaha (2011).

CONCLUSION

The results from Long Term Fertilizer Experiment revealed that the application of 100% NPK+FYM showed higher content of studied N-fractions viz. Total hydrolysable-N, Hydrolysable ammonical-N, inorganic–N, hexose amine & hydro.ammo.-N, hexose amine-N, amino acid-N, unidentified hydrolysable-N, non-hydrolysable-N and total N, whereas lower content was recorded in treatment 50%NPK followed by 100% N. The result also revealed that the N fractions were significantly decreased with increasing depth of soil.

REFERENCES

Aggarwal, R. K., Kumar, P. and Sharma, B. K. 1990. Distribution of nitrogen in some arid soils. J. Indian Soc. Soil Sci., 38: 430-433.

Babita B. 2013. Dynamics of organic and inorganic fractions of nitrogen in an acid alfisol after long-term addition of chemical fertilizers and amendments in maize-wheat cropping system. International Journal of Agricultural Science and Research, 3(3): 179-184.

Black, C. A., 1965, Methods of Soil Analysis – Part II, Agronomy Monograph, American Society of Agronomy Madison, Wisconsin, USA.

Bremner J.M. (1965a). Total nitrogen. In 'Methods of Soil Analysis, Part 2, (Ed CA Black) Am. Soc. Agron Madison, WI pp. 1149-1178.

Bremner JM. 1965b. Organic forms of nitrogen. In 'Methods of Soil Analysis, Part 2 (Ed CA Black) Am. Soc. Agron. Madison, WI pp. 1238-1255.

Broadbent FE. 1965. Effect of fertilizer nitrogen on the release of soil nitrogen. Soil Sc. Soc. Am. Proc. 29: 692-696.

Chesin, L. and C. H. Yien, 1951. Turbidmetric determination of available sulphur in soil. Soil. Sci. Soc. Am. Proc. **15**: 149-157.

Duhan BS, Katarai D, Singh JP, Kuhad MS and Dahiya SS. 2005. Effect of nitrogen, FYM and metribuzin on nitrogen transformation. J. Indian Soc. Soil Sci., 53(2): 184-187.

Durani A, Brar BS and Dheri GS. 2016. Soil Nitrogen Fractions in Relation to Rice-Wheat Productivity: Effects of Long-Term Application of Mineral Fertilizers and Organic Manures. Journal of Crop Improvement, 30 (4): 399–420.

Gomez, K. A. and A. Gomez, 1984. Statistical Procedures for Agricultural Research (2nd edition), John Willey and Sons, New York, 1-680.

Keeney DR and Bremner JM. 1964. Effect of cultivation on the nitrogen distribution in soils. Proc., Soil Sci. Soc. Am. J. 28: 653-656.

Kumar V. 2003. Integrated effect of chemical fertilizers and green manure on forms of nitrogen and their availability under rice-wheat cropping system in Calciorthents. Journal of the Indian Society of Soil Science 51:561-564.

Kushwaha satybhan. 2011. Effect of long term application of fertilizers and manure on nitrogen fractions in a Vertisol. M.Sc. thesis JNKVV, Jabalpur.

Muhr, G. R., N. P. Datta, H. S. Subrsmany, V. K. Leley and R. L. Dunahue, 1965. Soil testing in India. Asia Press, New Delhi.

Mulvaney, R.L. , S.A. Khan, R.G.Hoeft, and H.M. Brown 2001. A soil organic nitrogen fraction that reduce the need for nitrogen fertilization. Soil Science Society of American Journals 65:1164-1172

Nayak VN, Gatav GK and Bhagat RK. 2013. Different N fractions and their relationship with available Nitrogen, yield and nutrient uptake in safflower, (*Carthanmus tinctoroius*) in vertisol. Current Advances in Agriculture Science 5(1): 135-137

Olsen, S. R., C. V. Cole, F. S. Watanbe and L. A. Dean, 1954. Estimation of available phosphorus in soils by extraction with sodium bicarbonate. USDA circ. **939:** 19-33.

Patra A, Jarvis SC and Hatch DJ. 1999. Nitrogen mineralization in soil layers, soil particles and macro-organic matter under grassland. Bio. Fertil. Soils 29: 38-45.

Piper, C. S. 1966. Soil and Plant Analysis. Hans Publisher, Bombay. 85-102.

Rai Suraj Kumar 2013. Influence of long term use of fertilizers and manure on nitrogen dynamics in a Vertisol in wheat under rice-wheat cropping system. Msc. Thesis IGKVV, Raipur

Rao SA and Ghosh AB. 1981. Effect of continuous cropping and fertilizer use on the organic nitrogen fractions in a Typic Ustochepret Soil. Plant and Soil, 62:377-383.

Reddy SK, Singh M, Tripathi AK. Singh MV and Saha MN. 2003. Changes in amount of organic and inorganic fractions of nitrogen in an Eutrochrept soil after long-term cropping with different fertilizer and organic manure inputs. J. Plant Nutri. Soil Sci. 166: 232-¬238.

Sepehya S and Subehia SK 2012, Nitrogen dynamic as influenced by long- term fertilization and amendments under rice – wheat system in a north- western Himalaya soil. Depatment of Soil Science CSK Himalaya Pradesh Krishi Vishvavidyalaya, Palampur

Singh, K. K., and Singh, R. 2007. Distribution of nitrogen and sulphur forms in profiles of mid-western Utter Pradesh. J. Indian Soc. Soil Sci., 55 (4): 476-480

Soudi BA, Sbai and Chiang CN. 1990. Nitrogen mineralization in semi arid soils of Morocco: rate constant variation with depth. Soil Sci. Soc. Am. J. 54: 756-761.

Stevenson FJ. 1956. Effect of some long time rotations of the amino acid composition of the soil. Proc, Soil Sci. Soc. Am. J. 20: 204-208.

Subbiah, B. V. and G. L. Asija, 1956. A rapid procedure for estimation of available nitrogen in soils. Curr. Sci. 25: 259-260.

Swapana S. and Subehia SK. 2012. Nitrogen dynamic as influenced by long term fertilization and amendments under rice wheat system in a North- western Himalayan soil. CSK Himachal Pradesh Krishi Vishvavidyalaya, Palampur – 176062 (H.P.),India

Swapana S. and Subehia SK. 2012. Nitrogen dynamic as influenced by long term fertilization and amendments under rice wheat system in a North- western Himalayan soil. CSK Himachal Pradesh Krishi Vishvavidyalaya, Palampur – 176062 (H.P.), India

Walkley, I. A. and C. A. Black, 1934. An examination of the Degtozeff methods for determining the soil organic matter and nitrogen in the soil and a proposed modification of the chromic acid titration method. Soil Sci. 37: 29-38.

Environmental Communication

Biosci. Biotech. Res. Comm. 12(1): 194-202 (2019)

BBRC Bioscience Biotechnology Research Communications

Biological monitoring of riverine ecosystem and its correlation with water quality

D. D. Bhutekar[1] and S. B. Aher[2]*

[1]*Department of Environmental Science, Arts, Commerce and Science College, Ambad, Maharashtra-431204, India*
[2]*ICAR-Indian Institute of Soil Science, Bhopal, Madhya Pradesh–462038, India*

ABSTRACT

The River Godavari serves as a source of water for drinking and domestic use, agricultural irrigation and industries in Ambad stretch. The anthropogenic activities in the stretch caused ecological disturbance through water pollution. In present study, the spatial variation in water quality parameters was studied with respect to the fish population and diversity. The fish diversity and water quality of Godavari River at Ambad Stretch (16 km length) was studied at five identified sampling sites viz. Paithan (R), Balegaon (A), Gandhari (B), Shahagad-A (C) and Shahagad-B (D). The results revealed that the water quality followed the trend: R>D>B>A>C. The fish diversity index was observed between 2.35 and 3.03 among different sampling sites with highest at site R. The correlation study showed significant correlation between water quality parameters viz. total dissolved solids, phosphate, nitrate, dissolved oxygen, biological oxygen demand and chemical oxygen demand and fish population and diversity. The pollution tolerant fish species *Oreochromic mossumbicus* population showed significant positive correlation with water quality parameters except dissolved oxygen where it was found negatively correlated.

KEY WORDS: GODAVARI RIVER, FISH DIVERSITY, WATER QUALITY, SHANNON DIVERSITY INDEX, AMBAD STRETCH

INTRODUCTION

The water is the most essential and precious resource and is the elixir of life. Water resources comprising of surface water (river and lakes), ground water, and marine and coastal waters support all living things including human beings. Surface Rivers have always been the lifelines of development but the freshwater habitats receiving the highest levels of human disturbance. Recent studies on the status of inland water ecosystems showed that the river catchments in the Indian subcontinent are globally most threatened. Therefore, it is essential to identify, monitor and conserve the riverine ecosystems. Biological assessment of the freshwater habitats aims at char-

ARTICLE INFORMATION:

Corresponding Author: satishbaher@yahoo.com
Received 10th Dec, 2018
Accepted after revision 25th Feb, 2019
BBRC Print ISSN: 0974-6455
Online ISSN: 2321-4007 CODEN: USA BBRCBA
Thomson Reuters ISI ESC / Clarivate Analytics USA
NAAS Journal Score 2019: 4.31 SJIF: 4.196

Online Contents Available at: http//www.bbrc.in/
DOI: 10.21786/bbrc/12.1/26

acterizing and monitoring the conditions of the aquatic resources. The assessments are commonly associated with human impact (Saunders et al., 2002; Resh, 2008; Bhutekar et al., 2015, Bhutekar et al., 2018a).

In India various studies have presented spatial and temporal trends in diversity or biotic index of streams, rivers and lakes (Bhat, 2002). But still relatively little information is available on the correlation between water quality parameters and population and diversity of the aquatic animals (Rai et al., 2013). The river Godavari is considered to be one of the very sacred rivers of India. But being the ultimate sink of anything and everything drained through surface runoff, the river has been subjected to considerable stress. As a result, the ecology and water quality has suffered. In India some studies have presented spatial and temporal trends in diversity or biotic index of streams, rivers and lakes (Bhat, 2002). The biomonitoring system developed for the temperate streams was tested and found useful. However, biomonitoring can not entirely replace standard physic-chemical water quality methods. Standard physico-chemical water quality measures provide information on water quality at a particular spatial unit during the time of sampling. It cannot provide historical information on water quality (Bhutekar et al., 2018b). On the other hand, by knowing the ecology of aquatic insect community, biomonitoring tools provide some historic insights into the water quality. Standard physico-chemical water quality methods need to be carried out in conjunction with biomonitoring tools to comprehensively evaluate the health of freshwater ecosystems (Glorian et al., 2018).

River Godavari serves as a source of water for drinking and domestic use, agricultural irrigation and industries in Ambad stretch. Therefore, it was felt appropriate to evaluate, monitor and improve water quality and ecological conditions of river Godavari at Ambad stretch. The attempt was made to study the correlation between the water quality parameters and fish population and diversity.

MATERIALS AND METHODS

Sampling site

Present work was carried out on Godavari River water at Ambad Stretch. The total length of the study stretch was around 16 km. The five different locations were identified and fish diversity was studied by conducting seasonal fish sampling. Fishes of this river system were sampled seasonally over a period of two years i.e. July 2012 to May 2014 at 5 sampling sites. The sites were selected on the basis of depth and availability of water. The distance between two sampling sites was approximately 3 km. The five sampling sites were Paithan, Balegaon, Gandhari, Shahagad-A and Shahagad-B (Table 1).

Fish sampling, identification and diversity computation

Before starting the sampling, a thematic map was developed denoting the sampling sites where GIS based information was used. On basis of the map a pilot survey was carried out prior to actual sampling. Depending on the suitability and participatory appraisal with local fisherman community the sampling station were decided. Sampling efforts i.e. a single gill net operation or cast net operation for one hour was conducted and a species accumulation curve was obtained which was used to calculate the minimum sampling efforts vs. sampling effort plot.Based on such pilot survey carried out at many sampling sites, a sampling effort for 3 hours by gill net and drag net operation was used as standard for the sampling of fishes at all sites under this study.Fish samples were collected seasonally viz. monsoon, winter and summer for both years at each sampling station using different nets and gears of local fisherman. Sampling was carried out using a variety of fishing nets traditionally used by local fisherman comprising varying mesh sizes of gill, cast nets and drag nets.The fishes were identified and some representative specimens were collected and preserved in (4% formaldehyde solution) in glass jars. The identification of the fish specimens from various stations of the river Godavari was carried out with standard methods given by Mishra (1962), Jayaram (1981; 1999; 2006), Fischer and Bianchi (1984) and Jhingran (1997). In addition to this, electronic database like catalogue of life (2005), fishebase (2004) and FAO fish identification sheets were also used during fish identification.The identified fishes were grouped as per standard chronology of standard classification and Shannon Index was computed (Shannon, 1948) as follows:

$$H' = -\sum_{i=1}^{R} pi \ln pi$$

Table 1. Details of sampling sites

Sampling site	Code	Geographical Position	Water depth (m)	River width (m)
Paithan	R	19°29'083" N, 75°22'408" E	6-7	700-900
Balegaon	A	19°23'17.5"N,75°36'54.0"E	2-3	600-650
Gandhari	B	19°22'05.4"N,75°40'21.5"E	2-4	550-650
Shahagad-A	C	19°22'32.3"N,75°43'21.0"E	3-4	600-700
Shahagad-B	D	19°22'35.4"N,75°43'29.5"E	6-8	550-600

Where

H'- Shannon Index

ρi - proportion of individuals belonging to the ith species in the dataset of interest.

Water sampling and analysis

Water samples were collected from each sampling stations (Table 1) in first week of every month during June 2012 to May 2014 in morning hours (between 7.00 to 10.00 am). Water temperature was recorded and dissolved oxygen was fixed at sampling site. The collected water samples were analyzed in laboratory for different physical and chemical parameters as per the standard methods (APHA, 2005; Trivedi and Goel, 1984). The parameters studied were temperature, turbidity, pH, total dissolved solids, total alkalinity, total hardness, phosphate, nitrate, chlorides, dissolved oxygen, biological oxygen demand and chemical oxygen demand.

Statistical analysis

The collected data was compiled and subjected to statistical analysis for computation ofcoefficient of determination (r^2) and correlation coefficient (r) as follows and the relationship between two parameters was studied.

$$\text{Coefficient of determination } (r^2)=\frac{[n(\sum xy)-(\sum x)(\sum y)]^2}{[n\sum x^2-(\sum x)^2][n\sum y^2-(\sum y)^2]}$$

$$\text{Correlation coefficient } (r)=\frac{n(\sum xy)-(\sum x)(\sum y)}{\sqrt{[n\sum x^2-(\sum x)^2][n\sum y^2-(\sum y)^2]}}$$

RESULTS AND DISCUSSION

Fish diversity and population

During the study period, the fishes belonging to ten different families viz. Notopteridae, Cyprinidae, Bagridae, Siluridae, Heteropneustidae, Mugilidae, Beonidae, Mastacembelidae, Cichlidae and Channidae were observed

Table 2. Spatial variation in occurrence of fish species of Godavari River at Ambad stretch

Family	Name of species (CODE)	Sampling site				
		R	A	B	C	D
Notopteridae	*Notopterus notopterus (NN)*	43	21	21	15	26
	Chitala chitala (CH)	36	23	26	19	31
Cyprinidae	*Hypothalmicthys molitrix (HM)*	17	4	2	0	13
	Salmostoma navacula (SN)	51	16	32	12	34
	Chela laubuca (CL)	24	0	7	0	13
	Cyprinus carpio carpio (CY)	17	13	13	3	24
	Thynicthys sandkhol (TS)	11	0	0	0	5
	Osteobrama vigorsii (OV)	45	0	9	0	41
	Puntius ticto (PT)	49	0	7	0	30
	Cirrhinus mirgala (CM)	15	0	10	5	14
	Catla catla (CC)	29	3	22	0	26
	Labeo rohita (LR)	28	5	17	0	23
	Garra mullya (GM)	10	0	0	0	0
Bagridae	*Mystus aor =Sperata aor (SA)*	64	22	36	11	43
Siluridae	*Ompak bimaculatus(OB)*	32	15	20	9	20
	Wallago attu (WA)	21	6	16	0	13
Heteropneustidae	*Heteropneustes fossilis (HF)*	25	0	23	0	19
Mugilidae	*Rhinomugil carsula (RC)*	66	0	52	0	48
Beonidae	*Xanthodon cansula (ST)*	88	0	64	0	70
Mastacembelidae	*Mastacembelus armatus(MA)*	55	8	24	15	33
	Mascrognathus pancalus (MP)	74	0	47	0	54
Cichlidae	*Oreochromis mossambicus (OM)*	4	15	13	22	7
Channidae	*Channa muralius(MU)*	30	10	13	7	25
	Channa straita (CS)	16	12	20	6	20
	Chanda nama (CN)	38	15	16	12	24

(R- Paithan; A- Balegaon; B- Gandhari; C- Shahagad A and D- Shahagad B).

in Godavari River at Ambad stretch (Table 2). Similarly, during the study period, total 25 fish species were identified in River Godavari at Ambad stretch at different sampling sites viz., R- Paithan, A-Balegaon, B-Gandhari, C-Sahagad A and D-Sahagad B. The identified fish species were Notopterus notopterus, Chitala chitala, Hypothalmicthys molitrix, Salmostoma novacula, Chela laubuca, Cyprinus carpio carpio, Thynicthys sandkhol, Osteobrama vigorsii, Puntius ticto, Cirrhinus mirgala, Catla catla, Labeo rohita, Garra mullya, Aorichthys aor, Ompak bimaculatus, Wallago attu, Heteropneustes fossilis, Rhinomugil corsula Xanthodon cansula, Mastacembelus armatus, Mascrognathus pancalus, Oreochromis mossambicus, Channa muralius, Channa straita and Chanda nama. (Table 2)

The fish population at different sampling sites ranged 133-881 individuals. The highest and lowest fish population was found at site R and site C, respectively. The fish population at study sites followed the trend: R>D>B>A>C (Table 3). The family wise distribution of fish population at different sites revealed that, species from all families were observed at all sites except the species of family Heteropneustidae, Mugilidae and Beonidae which was not observed at site A and site C (Table 2). The total fish families and species reported at sampling sites R, A, B, C and D was 10 and 25, 7 and 15, 10 and 23, 7 and 12; and 10 and 24, respectively (Table 3). The pollution tolerant fish species *Oreochromis mossambicus* was found dominant at site C followed by site A and B. The species was least dominant at site R and D.

The Shannon diversity index value observed between 2.35 and 3.03 among different sampling sites of Godavari River at Ambad stretch. The lowest value of 2.35 was observed at site C.The results clearly indicated that the maximum Shannon Index value was found at reference and at site D (3.03). The diversity index of site A and B were 2.56 and 2.93 respectively. The higher diversity index at site R might be due to the undisturbed habitat whereas the dilution and self purification process of the river water resulted in higher value of fish diversityat site D. The water quality at site R and D was found suitable for fish growth. The higher degree of the pollution and habitat disturbance made the water quality unsuitable for the growth of the fish community which can be evidenced from lower diversity index value at site C (2.35) and site A (2.56).

Physico-chemical properties of Godavari River water

Temperature, turbidity and pH

The spatial variation in water quality of the Godavari River is presented in Table 4. The average water temperature was observed between 23.3 and 23.6°C among different sampling locations. Temperature plays very important role in the physiological behavior and distribution of aquatic organisms. The variation in river water temperature usually depends on the season, geographic location, ambient air temperature and chemical reaction in a water body (Ahipathi and Puttaiah, 2006). However, no significant difference in site specific temperature was observed during the investigation.

Turbidity measures water clarity or the ability of light to pass through water. In present investigation water turbidity was observed between 7.0 and 23.4 NTU among different sampling sites (Table 4). The lowest average turbidity was observed at reference location (R) followed by B and D site. The highest turbidity was recorded for site C (23.4 NTU) followed by site A (17.1 NTU). Surface-runoff, stream flow and overland flow in natural waters increase the turbidity levels in water. The higher level of pollutants in water also imparts turbidity to water. Yadav and Kumar (2011); Medudhula et al. (2012); Dhawde et al. (2018) and Bhutekar et al. (2018a) reported the similar observations.

The pH of the water was found slightly basic at all the sampling sites during the study period (Table 4). The mild alkaline nature of river water attributed to the presence of CO_2 in water as bicarbonate (Azeez et al., 2000). The leaching of basic rock material by rainwater and carried by surface runoff to river stream attributed to the higher values of water pH during rainy season (Lalparmawii, 2007).

Table 3. Fish population and diversity of Godavari River at various sites

Sampling site	No. of fish families observed	No. of fish species observed	Total fish individuals observed	Oreochromis mossambicus population	Shannon Diversity Index
R	10	25	881	4	3.03
A	7	15	184	15	2.56
B	10	23	505	13	2.93
C	5	12	133	22	2.35
D	10	24	652	7	3.03

(R- Paithan; A- Balegaon; B- Gandhari; C- Shahagad A and D- Shahagad B).

Table 4. Physico-chemical properties of Godavari River water at different sampling site

Parameter	Sampling site				
	R	A	B	C	D
Temperature (°C)	23.3	23.5	23.4	23.6	23.6
Turbidity (NTU)	7	17.1	9.6	23.4	9.6
pH	7.55	7.77	7.64	7.85	7.53
Total dissolved solids (mg lit^{-1})	288.7	622.8	434.9	674.4	305.9
Total alkalinity (mg lit^{-1})	202.9	300.2	231.7	485.9	201
Total hardness (mg lit^{-1})	133.6	194	185.9	316.2	167.4
Phosphate (PO_4^{-3}) (mg lit^{-1})	0.19	3.12	3.1	4.67	0.49
Nitrate (NO_3^-) (mg lit^{-1})	5.31	19.5	19.5	39.1	3.35
Chlorides (Cl^-) (mg lit^{-1})	27.1	92.4	45.7	109.2	28.6
Dissolved oxygen (mg lit^{-1})	6.7	4.9	5.8	4.2	6.4
Biological oxygen demand (mg lit^{-1})	4.3	20.9	12.3	37.8	4.4
Chemical oxygen demand (mg lit^{-1})	12.2	136.9	108.5	215.0	20.1

(R- Paithan; A- Balegaon; B- Gandhari; C- Shahagad A and D- Shahagad B).

Dissolved solids, alkalinity and hardness

In the present investigation TDS showed variation at all the sites during study period. The TDS ranged between 288.7 mg l^{-1} and 674.4 mg l^{-1} among different sampling locations (Table 4). The highest value of TDS was observed at site C followed by site A (622.8 mg l^{-1}). Total dissolved solids (TDS) are a measure, of the amount of dissolved materials in the water and are mainly contains minerals (Senthilnathan et al., 2011).

Alkalinity is the measure of buffering capacity of the water. It is generally imparted by the salts of carbonates, bicarbonates, phosphate, nitrates etc. (Yellavarthi, 2002). In present investigation the TA ranged from 201.0 mg l^{-1} (site D) to 485.9 mg l^{-1} (site C) among different sampling sites (Table 4). The increase in total alkalinity due to various religious activities, domestic waste and especially due to soaps and detergents was earlier reported by Patil (2003); Mithani et al. (2012) and Dhawde et al. (2018).

The total hardness ranged from 133.6 mg l^{-1} at site R to 316.2 mg l^{-1} at site C (Table 4). Hardness of water is a measure of its capacity to produce lather with soap (Garnaik et al., 2013). Total Hardness is an important parameter of water quality whether it is used for domestic, industrial or agricultural purposes (Jothivenkatachalam et al., 2010). The cations of calcium, magnesium, iron and manganese contribute to the hardness of water (Shrivastava and Patil, 2002). The widespread abundance of these metals in rock formations leads often to very considerable hardness levels in surface and ground waters (EPA, 2001). Similarly, the Ca and Mg that enter the water bodies through residues of soaps, detergents and parent bed rock materials made up of Ca, Mg and other metal ions also significantly contributes to total hardness of water (Nanda, 2005).

Phosphate, nitrate and chlorides

The phosphate concentration in Godavari River water at different sampling location was ranged between 0.19 mg l^{-1} and 4.67 mg l^{-1} (Table 4). The highest phosphate concentration was found at site C followed by site A and site B. The animal waste, agriculture waste and detergent in domestic wastewater may have contributed towards the observed increment in phosphates (Anda et al., 2001). Sinha et al. (1998) have also reported higher phosphate content in lower stretch of Ganga River.

Nitrate concentration in Godavari River water sampled at different locations was ranged between 3.35 mg l^{-1} and 39.1 mg l^{-1} with mean value of 17.3 mg l^{-1} (Table 4). The highest concentration of nitrate was found at site C followed by site A and B (19.5 mg l^{-1}). The lowest concentration of nitrate was observed at site D (3.35 mg l^{-1}). Nitrate in surface water is an important factor for water quality assessment (Jhones and Burt, 1993) which is mainly contributed waste discharges and artificial nitrogenous fertilizers.

The chloride in Godavari River water was ranged from 60.6 mg l^{-1} to 109.2 mg l^{-1} at various sampling locations (Table 4). The highest concentration of chlorides was observed at site C followed by site A and site B. Venkatesharaju et al. (2010) and Bhutekar et al. (2018a) also observed similar results with respect to chloride contents of the river water.

Table 5. Correlation between water quality parameters and fish population and diversity

Parameter	TFF	TFS	TFP	OMP	SDI
TDS	-0.928*	-0.974*	-0.973*	0.947*	-0.973*
PO_4^{-3}	-0.805	-0.852	-0.911*	0.980*	-0.872
NO^{-3}	-0.872	-0.871	-0.848	0.970*	-0.904*
DO	0.949*	0.978*	0.971*	-0.977*	0.981*
BOD	-0.963*	-0.955*	-0.893*	0.964*	-0.974*
COD	-0.893*	-0.921*	-0.931*	0.993*	-0.939*

*(TFF-Total fish family; TFS-Total fish species; TFP-Total fish population; OMP-Oreochrimos mossumbicus population; TDS-Total dissolved solids; SDI-Shannon diversity index; PO_4^{3}-Phosphates; NO_3-Nitrates; DO-Dissolved oxygen; BOD-Biological oxygen demand; COD-Chemical oxygen demand;*Significant at 5% level as per Students T test; T table value – 3.182)*

Dissolved oxygen, Biological oxygen demand and Chemical oxygen demand

The sampling station wise mean dissolved oxygen data showed that, DO ranged between 4.2 mg l^{-1} to 6.7 mg l^{-1}. The highest DO values was recorded for sampling site R followed by D and B. The mean monthly DO concentration showed that, it was ranged between 4.7 mg l^{-1} and 7.0 mg l^{-1} (Table 4). Dissolved oxygen is one of the important parameter in water quality assessment as it regulates and governs metabolic activities and metabolism of the biological community as a whole, respectively and also acts as an indicator of trophic status of the water body (Saksena and Kaushik, 1994). Its presence is essential to maintain variety of forms of biological life in water. Similar observations were also recorded by Singh and Gupta (2010) and Bhutekar et al. (2018a).

The biological oxygen demand of Godavari River water was observed between 4.3 mg l^{-1} and 37.8 mg l^{-1} among different sampling sites (Table 4). The highest BOD was observed at site C followed by site A (20.9 mg l^{-1}). The lowest BOD was observed at site R (4.3 mg l^{-1}) followed by site D (4.4 mg l^{-1}). Biodegradation of organic materials exerts oxygen tension in the water and increases the biochemical oxygen demand (Abida, 2008). BOD increases with organic matter addition, wastewater or urban storm water runoff took place at the river water. The higher BOD in polluted water was reported earlier by Garg et al. (2006); Zainudin et al. (2010); Glorian et al. (2018).

The COD is a measure of oxygen equivalent to the organic matter content of the water susceptible to oxidation and thus is an index of organic pollution in river (Khaiwal and Anubha, 2003).In present investigation the COD was observed 12.2 and 215.0 mg l^{-1} among different sampling sites (Table 4). The highest value of COD was observed at site C followed by site A (136.9 mg l^{-1}) and site B (108.5 mg l^{-1}). The lowest value of COD was observed for site R (12.2 mg l^{-1}) followed by site D (20.1 mg l^{-1}). Highest COD at site C indicated the higher pollution of water while lower level of COD indicated low level of pollution of water at the study area (Waziri and Ogugbuaja, 2010).Similar result was also reported by Bamniya et al. (2011); Bhutekar et al. (2018b) and Dhawde et al. (2018).

Correlation between water quality and fish population and diversity

The water quality of a water body is determined by measuring the physic-chemical properties of the water. Among the criteria parameters, dissolved oxygen, biological oxygen demand, total dissolved solids, chemical oxygen demand, nitrate and phosphate are considered as key parameters. The correlation between these parameters and fish diversity/population was studied and its significance was interpreted using Student's T Test (Table 5).

The fish population, fish diversity, number of fish families observed, number of fish species observed and the population of pollution tolerant fish species *Oreochromis mossumbicus* was studied in relation with the water quality parameters. The data showed significant negative correlation between total fish families observed and total dissolved solids (*r=-0.928*), biological oxygen demand (*r= -0.963*) and chemical oxygen demand *(r= -0.893)* whereas significant positive correlation with dissolved oxygen (*r=0.949*). The similar type of relationship was also existed with total fish species observed and total fish population recorded. The total fish population showed significant positive correlation with dissolved oxygen (*r= 0.971*; Fig. 1-A) and significant negative correlation with biological oxygen demand (*r= -0.893*) and chemical oxygen demand (*r= -0.993*; Fig. 1-B). The nitrate content did not show significant correlation with total fish families, species and population. The phosphate content also did not shown correlation with TFF and TFS but showed significant negative correlation with total fish population. It is interesting to note that, the pollution tolerant fish species *Oreochromis mossumbicus* showed significant positive correlation with TDS (*r= 0.947*); phosphate (*r= 0.980*); nitrate (*r= 0.970*); BOD (*r= 0.964*) (Fig. 1-F) and COD (*r= 0.993*). The *Oreochromis mossumbicus* showed significant negative correlation with dissolved oxygen (*r= -0.977*) (Fig.1-E). The Shannon diversity index showed significant positive correlation with dissolved oxygen (*r= 0.981*; Fig. 1- C) whereas significant negative correlation with TDS (*r= -0.973*); nitrate (*r= -0.904*); BOD (*r= -0.974*; Fig. 1-D) and COD (*r= -0.939*).

The aquatic biodiversity of world is changing and getting depleted alarmingly fast as a result of extinctions caused by habitat loss, pollution, introduction of exotic

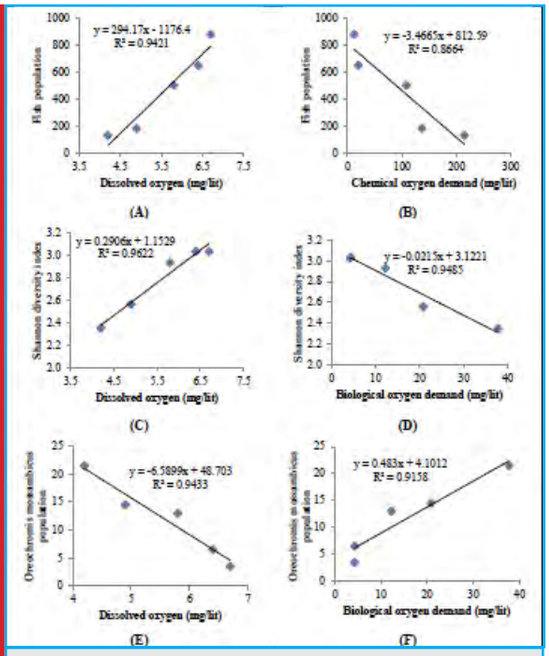

FIGURE 1. Linear regression coefficient between water quality parameters and fish population and diversity (A-Fish population Vs Dissolved oxygen; B- Fish population Vs Chemical oxygen demand; C- Shannon diversity index Vs Dissolved oxygen; D- Shannon diversity index Vs Biological oxygen demand; E- *Oreochronis mossumbicus* population Vs Dissolved oxygen; F- *Oreochronis mossumbicus* population Vs Biological oxygen demand).

species, over exploitation and other anthropogenic activities. Fishes are the keystone species which determine the distribution and abundance of other organisms in the ecosystem they represent and are good indicators of water quality and aquatic ecosystem. The fresh water fishes are one of the most threatened taxonomic groups (Darwall and Vie 2005) because of their high sensitivity to the quantitative and qualitative alteration of aquatic habits (Laffaille et al., 2005; Kang et al., 2009; Sarkar et al., 2008). Therefore, fishes are often used as bioindicator for the assessment of water quality, river network connectivity or flow regime (Chovance et al., 2003; Matta et al., 2018). Present investigation, clearly indicated a significant correlation of water quality parameters and fish diversity. The higher population of *Oreochromis mossambicus* at site C and B indicated it is a pollution tolerant species and favors such habitat (Murugan and Prabaharan, 2012). The healthy population of remaining species at site R, site D and site B may be attributed to the favorable water quality as evidenced from the data on water quality parameters (Table 4). The observed dominant species at site R and D are fresh water fishes (Munshi and Srivastava, 2006; Teta et al., 2017).

CONCLUSION

The results of the present investigation revealed that, the water quality followed the trend: R>D>B>A>C. The fish diversity index was observed between 2.35 and 3.03 among different sampling sites with highest at site R. The correlation study showed significant correlation between water quality parameters viz. total dissolved solids, phosphate, nitrate, dissolved oxygen, biological oxygen demand and chemical oxygen demand and fish population and diversity. The pollution tolerant fish species *Oreochromic mossumbicus* population showed significant positive correlation with water quality parameters except dissolved oxygen where it was found negatively correlated.

REFERENCES

Abida, B. (2008). Study on the quality of water in some streams of Cauvery River. e-Journal of Chemistry, 5(2): 377-384.

Ahipathi, M.V. and Puttaiah, E.T. (2006). Ecological characteristics of Vrishabhavathi river in Bangalore (India). Environmental Geology, 49: 1217-1222.

Anda, J., Shear, H., Maniak, U. and Riedel, G. (2001). Lakes & Reservoirs: Research and Management, 6: 313–321.

APHA. (2005). Standard Methods of Water and Wastewater. 21st Edn., American Public Health Association, Washington, DC. 2-61.

Azeez, P.A., Nadarajan, N.R. and Mittal, D.D. (2000). The impact of monsoonal wetland on ground water chemistry. Pollution Research, 19(2): 249–255.

Bamniya, B.R., Mahecha, G.S., Kapoor, C.S. and Kapasya, V. (2011). Water quality status of two water reservoirs of Thar desert city, Jaisalmer. Indian Journal Environment and Eco planning, 18(1): 113-116.

Bhat, A. (2002). A study of the diversity and ecology of the freshwater fishes of four river systems of Uttara Kannada District, Karnataka, India. Ph.D. Thesis submitted to Indian Institute of Science, Bangalore, Pp. 178.

Bhutekar, D.D., Aher, S.B. and Babare, M.G. (2018a) Spatial and seasonal variation in physico-chemical properties of Godavari River water at Ambad region, Maharashtra. Journal of Environment and Biosciences, 32(1):15-23.

Bhutekar, D.D., Aher, S.B. and Babare, M.G. (2018b) Status of water quality and strategies for conservation of Pushkarni reservoir, Ambad. International Journal of Recent Trends in Science and Technology, Special Issue, ACAEE: 2018, 110-113.

Chovance, A., Hoffer, R. and Schiemer, F. (2003). Fish as bioindicators. In: Market, B.A., Breure, A.M. and Zechmeiser, H.G. (eds) Bioindicatos and biomonitors, Pp. 639–675.

Darwall, W.R.T. and Vie, J.C. (2005). Identifying important sites for conservation of freshwater biodiversity: extending the species- based approach. Fisheries Management Ecology, 12: 287-293.

Dhawde, R., Surve, N., Macaden, R., Wennberg, A., Seifert-Dähnn, I., Ghadge, A. and Birdi, T. (2018). Physicochemical and Bacteriological Analysis of Water Quality in Drought Prone Areas of Pune and Satara Districts of Maharashtra., India. Environments, 5(61): 1-20.

EPA (2001). Parameters of Water Quality, Interpretation and Standards, Environmental Protection Agency, Ireland.

Fischer, W. and Bianchi, G. (1984). FAO Species Identification Sheets for Fishery Purposes: Western Indian Ocean Fishing Area. Food and Agriculture Organisation of the United Nations, Rome. Pp. 51

Garg, R.K., Saksena, D.N. and Rao, R.J. (2006). Assessment of physic-chemical water quality of Harsi Reservoir, district Gwalior, Madhya Pradesh. Journal of Ecophysiology and Occupational Health, 6: 33-40.

Garnaik, B., Panda, S., Tripathy, S. and Tripathy, U. (2013). Seasonal Variation of Nagavali River Water Quality at the Vicinity of Paper Mill near Jaykaypur, Odisha, India. International Research Journal of Environment Sciences, 2(5): 46-52.

Glorian, H., Börnick, H., Sandhu, C. and Grischek, T. (2018). Water Quality Monitoring in Northern India for an Evaluation of the Efficiency of Bank Filtration Sites. Water, 10 (1804): 1-15.

Jayaram, K.C. (1981). The freshwater Fishes of India, Pakistan, Bangladesh, Burma and Sri Lanka. Hand Book of Zoological Survey of India, Calcutta, Pp. 475.

Jayaram, K.C. (1999). The fresh water fishes of the Indian region. Narendra Publishing House, Delhi, Pp. 551.

Jayaram, K.C. (2006). Catfishes of India. Narendra Publishing House, Delhi, Pp.386.

Jhingran, V.G. (1997). Fish and Fisheries of India, 3rd edition, corrected reprint. Hindustan Publishing Corporation, Delhi, India. Pp. 727.

Jones, P.J. and Burt, P.T. (1993). Nitrate in Surface Waters. In: Burt, T.P., Heathwaite, A.L. and Trudgill, S.T. eds. Nitrate: Processes, Patterns and Management. John Wiley & Sons, Chichester, 269-317.

Jothivenkatachalam, K., Nithya, A. and Chandra, M.S. (2010). Correlation analysis of drinking water quality in and around Perur block of Coimbatore district, Tamil Nadu, India. Rasayan Journal of Chemistry, 3(4): 649-654.

Kang, B., He, D., Perrett, L., Wang, H., Hu, W., Deng, W. and Wu, Y. (2009). Fish and fisheries in the Upper Mekong: current assessment of the fish community, threats and conservation. Reviews in Fish Biology and Fisheries, 19: 465–480.

Khaiwal, R. and Anubha, K. (2003). Seasonal variations in physicochemical characteristics of River Yamuna in Haryana and its ecological best-designated use. Journal of Environmental Monitoring, 5: 419-426.

Laffaille, P., Acou, A., Guillouet, J. and Legult, A. (2005). Temporal change in European eel, *Anguilla anguilla,* stock in a small catchment after installation of fish passes. Fisheries Management Ecology, 12: 123–129.

Lalparmawii, S. (2007). Analysis of water quality and Biomonitoring of Tuirial River in vicinity of the Hydel Project in Mizoram. Ph.D Thesis. Mizoram University, Aizawl.

Matta, G., Gjyli, L., Kumar, A. and Machel, J. (2018). Hydrochemical characteristics and planktonic composition assessment of River Henwal in Himalayan Region of Uttarakhand using CPI, Simpson's and Shannon-Weaver Index. Journal of Chemical and Pharmaceutical Sciences, 11(1): 122-130.

Medudhula, T., Samatha, C. and Sammaiah, C. (2012). Analysis of water quality using physico-chemical parameters in lower manair reservoir of Karimnagar district, Andhra Pradesh. International Journal of Environmental Sciences, 3(1): 22-25.

Mishra, K.S. (1962). An aid to the identification of the common commercial fishes of India and Pakistan. Records of the Indian Museum, 57(1-4): 320.

Mithani, I., Dahegaonkar, N.R., Shinde, J.S. and Tummawar, S.D. (2012). Preliminary studies on physico-chemical parameters of river Wardha, District Chandrapur, Maharashtra. Journal of Research in Ecology, 1: 14-18.

Munshi, D. and Srivastava, J.S. (2006). Natural History of Fishes and Systematics of Freshwater Fishes of India. Narandra Publishing House, Delhi. Pp. 423.

Nanda, S.P. (2005). Environmental management plan (EMP) for Bhubaneswar, India.

Patil, D.S. (2003). Ecological studies in some lentic water bodies of Kolhapur city. Ph.D. Thesis, Shivaji University, Kolhapur.

Rai, A.K., Diba, F. and Paul, B. (2013). A study on the seasonal variations of different physic-chemical water quality parameters of Indrapuri Dam Rohtas District Bihar. International Journal of Environmental Sciences, 2(3): 125-129.

Resh, V.H. (2008). Which group is best? Attributes of different biological assemblages used in freshwater biomonitoring programs. Environmental Monitoring and Assessment, 138: 131-138.

Saksena, D.N. and Kaushik, S. (1994). Trophic status and habitat ecology of entomo fauna of three water bodies at Gwalior, Madhya Pradesh. In: Agrawal, O.P. Eds, Perspective in entomological research Scientific Publishers, Jodhpur.

Sarkar, U.K., Pathak, A.K. and Lakra, W.S. (2008). Conservation of freshwater fish resources of India: new approaches, assessment and challenges. Biodiversity Conservation, 17: 2495–2511.

Saunders, D.L., Meeuwig, J.J. and Vincent, A.C.J. (2002). Freshwater protected areas: Strategies for Conservation. Conservation Biology, 16(1): 30-41.

Senthilnathan, T., Parvathavarthini, K.V. and George, S.M. (2011). Assessment of ground water quality of Maraimalai Nagar town near Chennai, India. Journal of Environmental Research and Development, 5(4): 943-955.

Shannon, C.E. (1948). A mathematical theory of communication. The Bell System Technical Journal, 27: 379–423.

Shrivastava, V.S. and Patil, P.R. (2002). Tapti river water pollution by industrial wastes: A statistical approach. Nature, Environment, Pollution and Technology, 1: 279-283.

Singh, M.R. and Gupta, A. (2010). Seasonal variation in certain physicochemical parameters of Imphal, Iril and Thoubal rivers from Manipur river system, India. Ecology, Environment and Conservation, 16(2): 197-207.

Sinha, M., De, D.K. and Jha, B.C. (1998). The Ganga environment and fisheries. Central Inland fisheries Institute, Barrackpore. pp.142

Teta, C., Ncube, M. and Naik, Y. S. (2017). Heavy metal contamination of water and fish in peri-urban dams around Bulawayo, Zimbabwe. African Journal of Aquatic Science, 42(4): 351-358.

Trivedy, R.K. and Goel, P.K. (1984). Chemical and biological methods for water pollution studies, Environmental publication Media, Karad, India. 1-251.

Venkatesharaju, K., Ravikumar, P., Somashekar, R.K. and Prakash, K.L. (2010). Physicochemical and bacteriological investigation on the river Cauvery of Kollegal stretch in Karnataka. Karnataka University Journal of Science, Engineering and Technology, 6(1): 50-59.

Waziri, M. and Ogugbuaja, V.O. (2010). Interrelationship between physicochemical water pollution indicators: A case study of River Yobe-Nigeria. American Journal of Science and Industrial Research,1: 76-80.

Yadav, S.S. and Kumar, R. (2011). Monitoring Water quality of Kosi River in Rampur District, Uttar Pradesh, India. Advances in Applied Science Research, 2(2): 197-201.

Yellavarthi, E. (2002). Hydrobiological studies of Red hills Reservoir, North Chennai, Tamilnadu. Journal of Aquatic Biology, 17(1): 13-16.

Zainudin, Z., Rahman, N.A., Abdullah, N. and Mazlan, N.F. (2010). Development of water quality model for Sungai tebrau using QUAL2K. Journal of Applied Sciences, 10: 2748-2750.

Join Society For Science & Nature and Avail Multiple Benefits

1. Life members and fellows of Society of Science & Nature (MSSN/FSSN), Bhopal, India will be entitled to receive free early on line issues of BBRC for life. They will get substantial waivers for publication of their research papers.
2. Selected life members on the basis of their academic and research contributions will be conferred with Honorary Fellowship of SSN (FSSN), who will be instrumental in scientific awareness programmes particularly encouragement and popularisation of Science. These members will be appointed reviewers of the Journal in different subject areas.
3. Life members will be invited to attend society sponsored conferences and seminars on invitation.

Subscription Form For MSSN Life (Fellow Member Society For Science & Nature, along with BBRC):
Kindly complete the form and send it, together with the necessary payment to the Secretary of the Society on the address below (Photocopies will be accepted). Forms can also be downloaded from our website (http://www.bbrc.in/subscriptions.html).

(Crossed DD in favor of Treasurer, Society for Science and Nature, C-52, Housing Board Colony, Kohe-Fiza, Bhopal-462001, India, to be sent by Speed/Regd. Post.) Life Membership One Time Subscription (MSSN) including Life Member-ship of BBRC is Rs. 5000/- Direct NEFT can be also made on contacting the Managing Editor. Foreign Members will have to obtain separate invoices for making payment to the Society for Fellowship.

Name: Dr./Prof. (In capital letters):_____

Designation & Organization: _____

Qualification & Specialization of Research: _____

Present and Past Academic Positions: _____

Research Publications Experience Enclose Biodata with full publications list:_____

Academic Achievements Memberships of Societies etc.: _____

Mailing Address (With tel./Mob./Email id): _____

I wish to become life Member / Fellow of Society for Science And Nature Bhopal, India. I have read the details and agree to abide by them.

Signature
Details of Accompanying Payment _____ DD No. _____ Date _____

JOIN AS LIFE MEMBER BIOSCIENCE BIOTECHNOLOGY RESEARCH COMMUNICATIONS

SUBSCRIPTION FORM FOR BBRC (Only Journal)

Kindly complete this form if you want to become life member/annual member of BBRC only (Individual Life Member BBRC Rs. 4000/-)

I wish to subscribe to Early On Line Copy of Bioscience Biotechnology Research Communications.

Name: _____

Address: _____

E-mail: _____ Signature: _____ Date: _____

Subscription: Annual/Life..... Amount Rs. _____

*DD No. _____ enclosed.

All payments by Demand draft should be made in favour of Treasurer, Bioscience Biotechnology Research Communications and sent to: *Treasurer, C-52, Housing Board Colony, Kohe-Fiza, Bhopal-462001, India*, by registered Post. Direct NEFT can be also made on contacting the Managing Editor
E-mail: drshariqalibbrc@gmail.com or editor@bbrc.in Telephone No. +91-0755-4241662, +919893015818
Website: www.bbrc.in

BBRC SUBCRIPTION RATES	(INR)
1. Life Member (BBRC)	INR 4000/-
2. Institutional Annual Member Libraries for Hard Copy issues	INR 6000/-

Declaration about the ownership of
Bioscience Biotechnology Research Communications
Form (IV) [See Rule 3]

1. Place of Publication	:	Bhopal, India
2. Periodicity of its Publication	:	Six Monthly
3. Printer's Name	:	Ayesha S. Ali On behalf of Society For Science & Nature
(Whether Citizen of India)	:	Yes
Address	:	H. No. C-52, H.B. Colony, Kohefiza Bhopal-462001, India
4. Publisher's Name	:	Ayesha S. Ali on Behalf of Society For Science & Nature
(Whether Citizen of India)	:	Yes
Address	:	H. No. C-52, H.B. Colony, Kohefiza Bhopal-462001, India
5. Editor's Name	:	Dr. Sharique Ali
(Whether Citizen of India)	:	Yes
Address	:	H. No. C-52, H.B. Colony, Kohefiza Bhopal-462001, India
6. Name & Address of the individual/	:	Ayesha S. Ali
who own the newspaper & partners or share holders holding more than one percent of the total capital	:	H. No. C-52, H.B.Colony, Kohefiza, Bhopal-462001, India
(Whether Citizen of India)	:	Yes

I, Ayesha S. Ali hereby declare that the particulars given above are true to the best of my knowledge and belief.

Date : 31st Mar 2019
Place : Bhopal

Detailed instructions to authors for preparing and submitting manuscripts to *Bioscience Biotechnology Research Communications (BBRC)* Please see journal sample manuscript

Bioscience Biotechnology Research Communications (BBRC) is a broad based peer reviewed international open access journal that publishes original research papers, short communications and exciting reviews in all basic and applied fields of Life Sciences, including Biology & Medicine on a fast track. **The journal is indexed in leading citation agencies of the world such as Thomson Reuters, Clarivate Analytics (ESCI) USA Research Gate, CAS (USA), Uhrlich, Biobase, EBSCO, Copernicus Indicus, NISCAIR, NAAS, and many others and has a NAAS 2019 journal score of 4.31. It has recently got an Impact Factor of 4.006 and has been approved by University Grants Commission (UGC New Delhi) Ministry of HRD, Government of India, Journal No. 42929 www.ugc.ac.in.**

On Ethical and Animal Welfare Issues: Bioscience Biotechnology Research Communications requires that the experimental conditions under which human and animal assays and tests are performed are as per standard protocols used worldwide. Studies on animals must comply with the prevailing standards of animal welfare according to Indian Council of Medical Research Guidelines in India and likewise following similar conditions elsewhere. Authors must make it clear that the procedures they used were as humane as possible and have been complied with the guidelines for animal care of their institutions or with national/ international guidelines. Studies involving human subjects/animals must be carried out with the formal approval of the relevant Ethical Committee and evidence of such approval must be provided as and when needed.

Submission Of Manuscript: Manuscripts should be in 12 point size, Times New Roman Font with one and half space on A4 size paper in MS Word in the given format and must be sent by e-mail as attachment to the editor (editor@bbrc.in and a copy to drshariqalibbrc@gmail.com). A cover letter signed by author(s) must be enclosed with the manuscript stating that the work is their own and has not been published earlier. Only online MS should be sent by email

Length of contributions: Papers should be ideally be no longer than 08 pages for short communications and 20 pages for full length papers, although we can publish longer papers.

SUBMISSION GUIDELINES: PLEASE PREPARE YOUR MS AS BELOW PLEASE SEE THE JOURNALS ANY SAMPLE MANUSCRIPT

• Abstract: All Manuscripts should have an abstract and keywords with the following in the mind but without any sub heads: Objectives, Methods, Results and Conclusion of no more than 200 words. Key words: Up to five key words should be included in italics in alphabetical order.

• Introduction: It should be concise, with what has been done and why, giving in brief the background, latest work done in the area with existing lacunae /controversies/contradictions and valid reasons for taking up the research problem. Review of literature should be brief pertinent and up-to-date. Recent references till-date be added. All references should be checked minutely, for their appearance in text as well as in References/Bibliography section. MS with incomplete references will not be accepted. Reference style of BBRC is Harvard Style ie author last name with year in bracket in the text.

• Material & Methods: Brief description of standard procedures adopted worldwide with standard references.

• Results & Discussion: Should be combined to avoid repetition. Sub-headings may be provided in this section if they improve the clarity. Latest references are a must with interpretational significance in introduction and discussion.

• References: **All references used in the text must be arranged alphabetically in the last section of References. Last names of authors with initials should be written with year of publication in bracket ( ) followed by full title of the article, the name of the journal, volume number, and the first and last page numbers (see 1 below). Journal title should be given in full, or abbreviated according to the style of Index Medicus. Title of book should be followed by author(s), year of publication, the publisher and place. THERE SHOULD BE NO USE OF ITALICS IN THE REFERENCE, IE LAST SECTION EXCEPT FOR SCIENTIFIC/ZOOLOGICAL/BOTANICAL NAMES Examples of References in BBRC are as:**

(1) Ali S.A., S. Salim, T. Sahni, Peter J. and Ali A. S. (2012c). Serotinergic receptors as novel target for optimizing skin pigmentary responses in Indian bull frog *Hoplobatrachus tigerinus*. British J. of Pharmacol. John Wiley The British Pharmacological Society Vol. 165, Issue 5, 1515-1525.
(2) Book: Falconer DC (1960) Introduction to Quantitative Genetics. Oliver & Boyd, Edinburgh 165-185.
(3) References to article in book: Simonsen B. (1989). In: Processing of poultry. Pp 221 250 (Ed) G. C. Mead, Elsevier Applied Science, London.
(6) Tables and illustrations: Tables and figures should be numbered in Arabic numerals and given in separate pages with due reference in the text. Units of measurement should be metric units. Graphs and other line drawings should be drawn in India ink and individually identified by Arabic numerals. Photographs should have good contrast with numbers and explanation of figures. **Please note that the figures/illustrations should be of minimum 300dpi (printable resolution with inside letters or captions clear in reproducible size.).**

Peer review: All papers submitted to *BBRC* undergo a quick internal and external double blind peer review process. On the basis of the referees' responses, papers will be rejected, accepted subject to minor or major revisions, or accepted unconditionally.

Acceptance of submission: On acceptance, the editors retain the right to make stylistic changes, decide on the date of publication and shorten material, as necessary.

Proofs: Authors will be sent an online copy of the galley on request. Corrections should be confined to typographical errors or matters of accuracy. Authors should return proofs within two days of receipt, along with a signed copy-right form downloaded from journals website.

Article Processing Charges (APC): **Indian authors will have to bear the article processing cost of INR 4000/- per manuscript submitted, (US$ 300 per manuscript submitted for foreign authors).** In order to meet the rigorous academic standards on a fast track, the open access journal has some expenses, and for these reasons we charge a very modest article processing fee. Nevertheless, as we believe that lack of funds should not be a barrier to open access publication, Biosc. Biotech Res.Comm. has a policy to provide waivers to deserving authors from middle and low income countries. Authors can request for a waiver in such cases.

Note: For any hard copies of journals and reprints additional amount will be charged. Please contact the Managing Editor for details.

Copyright: All materials received by *Biosc.Biotech Res.Comm.* are assumed to be submitted exclusively. It is understood that contributions have not been and will not be published elsewhere. A copy right letter downloaded from journals website duly, signed by all authors is to be submitted after acceptance of the MS.

Accuracy and liability: A contribution is accepted on the strict understanding that its author(s) is/are responsible for accuracy of all information contained in it. BBRC condemns the malice of plagiarism and strongly advocates the policy of out rightly condemning and reporting of any academic malpractice with regard to manipulation, copying, pilfering or pirating of any research material or data in practice and writing thereof.

On Plagiarism and Retraction Policy: Articles found with plagiarized material will be liable for immediate retraction from the issue and action will be taken against such authors as per standard norms.

For any information please contact: Managing Editor, *BBRC*, C-52, HOUSING BOARD COLONY, KOHE FIZA, Bhopal, (MP) 462001, India.
Tel: +91-755-4241662 Mob: +919893015818
A soft copy (MS Word file) of the manuscript as attachment with a cover letter declaring originality of the research work and statement of no conflict of the authors, should be sent to: editor@bbrc.in with a copy to drshariqalibbrc@gmail.com Journals Website: www.bbrc.in

New Delhi Office: Dr. Mohd. Miraj, AIHMS
Gautam Nagar, Behind AIIMS New Delhi , LL: +91-11-41030907 Mob: +09560407405, Website: www.aihms.in

Name of Fellow/Member	Life Member, Fellow Society Science & Nature and Member BBRC	Designation and Address
Dr. Sharique A. Ali	SSN and BBRC	Professor and Head, Department of Biotechnology Saifia Science College, Bhopal
Dr. Ayesha S. Ali	SSN and BBRC	Professor, Department of Biotechnology & Zoology Saifia Science College, Bhopal
Dr. J. Peter	SSN and BBRC	Associate Professor, RKDF University, Bhopal
Dr. M. Miraj	SSN and BBRC	Director, Institute of Health & Management Studies, New Delhi
Dr. Z.H. Khan	SSN and BBRC	Professor & Head Department of Biochemistry Shri Shivaji College of Science, Akola
Dr. G.N. Wankhede	SSN and BBRC	Professor & Head, Department of Zoology, SGB UniversityAmrawati (MS)
Dr. S. Shrivastava	BBRC	Professor of Chemistry, MVM, Bhopal
Dr. P.M. Makode	BBRC	Associate Professor of Zoology, Venue, Park, Shegaon Naka VMV Road, Amravati (MS)
Dr. S. Yadav	BBRC	Assistant Department of Zoology, Satya Sai College for Women BHEL, Bhopal
Dr. R. Singh	BBRC	Associate Professor,Department of Zoology, MLB Girls College, Bhopal
Dr. A. D. Lakha	BBRC	Associate Professor of Zoology, Nagazari Area, MIT Road, Ambajogai, Beed (MS) 431517
Dr. R. S. Virani	BBRC	Associate Professor Karimabad Society, Pandhar Kawada, District, Yeobtmal (MS)
Dr. M. Pal	BBRC	Assistant Professor, Department of Biotechnology Sadhu Vaswani College Bhopal
Dr. V.R. Wankhede	BBRC	Assistant Professor, Department of Zoology, Deccan College, Pune
Dr. Mrs. V. Ingole	BBRC	Department of Zoology Vidya Bharti Mahavidyalaya, Amravati
Dr. U.N. Bhale	BBRC	Associate Professor RTM University, Nagpur
Dr. A.P. Sawane	BBRC	Associate Professor RTM University, Nagpur
Dr. A.D. Bobde	BBRC	Associate Professor RTM University, Nagpur
Dr. R.G. Jadhaw	BBRC	SGB University, Amravati
Dr. O.N. Tiwari	FSSN	DBT Imphal, Manipur
Dr. R. K. Singh	BBRC	USDA Washington, USA
Dr. V. Meitei	BBRC	Jaipur University, Jaipur
Dr. T. Sultan	BBRC	Medical Genetics Department, Riyadh University, KSA
Dr. N. Qayyumi	BBRC	Assistant Professor of Zoology, Bhopal
Dr. M. Sajid	BBRC	Head Department of Biotechnology Bonnifie College, Bhopal
Dr. L. Jakkala	BBRC	Director Macrocare, Macrocare Towers, Hyderabad, AP
Dr. V. Jaiswal	BBRC	Research Scholar, SGB University, Amravati
Dr. A. Kumar	BBRC	Associate Professor, Department of Biotechnology, SMD Teerth University, Haryana
Dr. A.S. Dighde	BBRC	SGB University, Amravati
Dr. P Babu	BBRC	Professor of Pomology, Horticulture University of Horticulture Science, Bagalkot
Dr. (Smt) S. Sinha	BBRC	Plot-18, Street-1, Ashish Nagar (East) Risalt, Bhilai, Durg, CG
Dr. R. Khalique	BBRC	Department of Zoology, University of Kashmir, Srinagar
Dr. A. Siddiqui	FSSN	Department of Zoology Holkar Science Colege, Indore
Dr. MM. Shrivastava	FSSN	Department of Biotechnology Holkar Science College, Indore
Dr. A. Eberle	FSSN	Basel Switzerland
Dr. S. Newton	FSSN	University of Virginia, USA
Dr. J Galgut	BBRC	Department of Biomedicine, Qatar
Dr. S. Salim	BBRC	Maryland, USA
Dr. Ruchi Shivle	MSSN	DAVV, Indore
Dr. Kirti Dubey	MSSN	DAVV, Indore
Dr. AT Kalse	FSSN	NEM University, Jalgaon (MS)
Dr. F Kabinwar	FSSN	University of California, Los Angeles, USA
Dr. Arjun Deb	FSSN	Professor of Zoology Lumding College Lumding Assam
Dr. Z.Pir	FSSN	University of Kashmir, Srinagar
Dr. Razia Sultan	FSSN	DAVV, Indore
Dr. Thingujam I. Devi	FSSN	Institute of Bioresources and Sustainable Development, Imphal, Manipur
Dr. I Onyesom	FSSN	Professor Abraska, Delta State Nigeria
Dr. K. Sudhakar	FSSN	Assistant Professor Energy Centre,Maulana Azad National Institute of Technology Bhopal, India.

Bioscience Biotechnology Research Communications
Society For Science & Nature Bhopal, C-52 Housing Board Colony, Kohe – Fiza,
Bhopal 462001 INDIA, Phone no.: +91-755-4241662
Website:www.bbrc.in Email:editor@bbrc.in

COPYRIGHT TRANSFER FORM:

(This form is signed by all the authors or by the corresponding author on behalf of all of them)

1) I / (We) confirm that the enclosed article entitled:

_____

_____

_____

Authored by: 1._____ 2._____

3._____ 4._____

has not previously been published in whole or in part, is not currently being considered elsewhere for publication, and, if accepted for publication in the above Journal, will not be published elsewhere in any language, without the consent of the editor and the publisher.

2) I/We acknowledge that it is a condition of acceptance by the editor that the publisher, Society for Science & Nature/Biosc. Biotech.Res.Comm. acquires automatically the copyright in the manuscript throughout the world.
3) I/We confirm that I have obtained all the necessary permissions to include in the paper items such as quotations, figures, and the results of government sponsored research.
4) I/We enclose where necessary written permission of authors and publishers to use any copyright material (e.g.previously published figures and tables).

We also certify that the research work carried out is original, and does not contain any plagiarized material. All due permissions / ethical clearances have been taken from concerned authorities.

We also understand that if our article is found with plagiarized material, it will be liable for immediate retraction from the issue and due action can be taken as per standard norms.

Author 1

Signature: _____ Name: _____ Date: _____
Institution:_____ Dept:_____
Street:_____ City:_____ State:_____
Zip:_____ Country: _____ Country Code: _____
Phone:_____ Fax: _____ Email: _____

Author 2

Signature:_____ Name: _____ Date: _____
Institution: _____ Dept: _____
Street:_____ City: _____ State: _____
Zip:_____ Country: _____ Country Code: _____
Phone:_____ Fax: _____ Email: _____

Author 3

Signature: _____ Name: _____ Date: _____
Institution:_____ Dept:_____
Street:_____ City: _____ State: _____
Zip:_____ Country: _____ Country Code: _____
Phone: _____ Fax: _____ Email: _____

Author 4

Signature: _____ Name: _____ Date: _____
Institution:_____ Dept:_____
Street:_____ City: _____ State:_____
Zip:_____ Country: _____ Country Code: _____
Phone:_____ Fax: _____ Email: _____